

Unclassified

ESC-TR-96-062

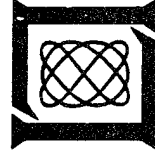
Project Report
ASAP-4
Volume 1

Proceedings of the Adaptive Sensor Array Processing (ASAP) Workshop 13-15 March 1996

P.A. Netishen
Editor

29 April 1996

Lincoln Laboratory
MASSACHUSETTS INSTITUTE OF TECHNOLOGY
LEXINGTON, MASSACHUSETTS



Prepared for the Advanced Research Projects Agency and the U.S. Air Force under Contract F19628-95-C-0002.

Approved for public release; distribution is unlimited.

19960621 109

DTIC QUALITY INSPECTED 1


Unclassified

This report is based on a workshop that was held at Lincoln Laboratory, a center for research operated by Massachusetts Institute of Technology. The work was sponsored in part by the Advanced Research Projects Agency and in part by the U.S. Air Force under Contract F19628-95-C-0002.

This report may be reproduced to satisfy needs of U.S. Government agencies.

The ESC Public Affairs Office has reviewed this report, and it is releasable to the National Technical Information Service, where it will be available to the general public, including foreign nationals.

This technical report has been reviewed and is approved for publication.
FOR THE COMMANDER

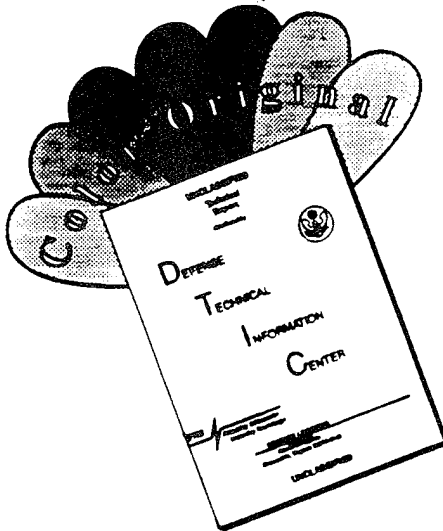

Gary Pittungian
Administrative Contracting Officer
Contracted Support Management

Non-Lincoln Recipients

PLEASE DO NOT RETURN

Permission is given to destroy this document
when it is no longer needed.

DISCLAIMER NOTICE



THIS DOCUMENT IS BEST QUALITY AVAILABLE. THE COPY FURNISHED TO DTIC CONTAINED A SIGNIFICANT NUMBER OF COLOR PAGES WHICH DO NOT REPRODUCE LEGIBLY ON BLACK AND WHITE MICROFICHE.

Unclassified

MASSACHUSETTS INSTITUTE OF TECHNOLOGY
LINCOLN LABORATORY

**PROCEEDINGS OF THE ADAPTIVE SENSOR ARRAY
PROCESSING (ASAP) WORKSHOP
13-15 MARCH 1996**

P.A. NETISHEN
EDITOR
Division 10

PROJECT REPORT ASAP-4, VOLUME 1

29 APRIL 1996

Approved for public release; distribution is unlimited.

LEXINGTON

MASSACHUSETTS

Unclassified

1996 ASAP Workshop Theme

The first Adaptive Sensor Array Processing (ASAP) workshop was held in 1993. The workshop charter has been and remains the fostering of multidisciplinary investigations into adaptive sensor array processing. Each year we have selected a timely theme to focus our efforts and render a coherent set of presentations. The first workshop in 1993 was focused on synergism among the diverse applications within the defense community for adaptive array processing. A noteworthy feature was extensive theoretical coverage of the fundamental challenges arising from joint spatial and temporal adaptation in active sensor arrays. In 1994 the application focus specialized to AEW (Airborne Early Warning) radars, and in particular on novel techniques applied to the newly available Mountaintop testbed. Significant discussion surrounded measured experimental improvements in sensitivity in strong jammer/clutter environments using recent space-time ASAP techniques, such as those unveiled the previous year. In 1995 a concerted effort was made to foster interaction with commercial applications and university researchers. For the first time the workshop was wholly unclassified and featured special sessions on sonar and wireless applications.

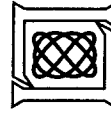
ASAP is now a maturing discipline. The ARPA (Advanced Research Projects Agency) Mountaintop test environment has been operational for three years, both at White Sands, New Mexico, and Kauai, Hawaii. Documented data sets have been made available through the Internet, and diverse industrial and university researchers have presented research findings at international conferences and in journals.

This brings us to the focus of this year's workshop in which we return to the uses of ASAP for advanced military radar systems, from a more developed perspective, with an emphasis on end-to-end systems issues and the user's perspective. New topics include the target detection and parameter estimation steps that typically follow clutter and jammer nulling. Several papers that describe algorithm mapping to parallel processors will also be presented. In classified sessions on adaptive seekers and SAR (Synthetic Aperture Radar) we explore connections between AEW and alternate radar systems which are potential beneficiaries of multichannel adaptivity.

We appreciate your participation in the fourth annual ASAP workshop.



Gene Bal
ARPA/STO
Advanced Signal Processing
Program Manager



Kenneth D. Senne
MIT Lincoln Laboratory
Workshop Chairman

Steering Committee

Kenneth D. Senne / MIT Lincoln Laboratory
Lloyd J. Griffiths / University of Colorado
Frederick Lee / Naval Research Laboratory
Jay Loomis / U.S. Army MICOM

ADAPTIVE SENSOR ARRAY PROCESSING WORKSHOP

13-15 March 1996

SPEAKER PRESENTATIONS

VOLUME I

SPEAKER	TITLE	PAGES
Irving S. Reed University of Southern California	A Multidisciplinary Perspective on Adaptive Sensor Array Processing	1-29
Pamela Kove and Jack Li MIT Lincoln Laboratory	Terrain-Scattered Interference Visualization	53-63
Yaron Seliktar, Douglas B. Williams, and James McClellan Georgia Institute of Technology	A Mountaintop MATLAB Toolbox	65-70
Edward J. Baranoski MIT Lincoln Laboratory	Constraint Optimization for Pre-Doppler STAP Algorithms	71-95
James McClellan, Greg Showman, and Ali Saidi Georgia Institute of Technology	Direct Clutter Cancellation for STAP	97-123

SPEAKER PRESENTATIONS (Continued)

SPEAKER	TITLE	PAGES
Daniel J. Rabideau and Allan O. Steinhart MIT Lincoln Laboratory	Power Selected Training for False Alarm Mitigation in Airborne Radar	125-157
Anthony E. Filip and Stephen C. Pohl MIT Lincoln Laboratory	STAP Applied to Electro-Optical Sensors	159-192
Thomas W. Miller and Janet M. Ortiz Hughes Aircraft Company	An Overview of Issues in Hot Clutter Mitigation	193-239
Larry Brennan Larry Brennan and Associates	Cancellation of Terrain Scattered Jamming in Airborne Radars	241-260
Robert A. Gabel MIT Lincoln Laboratory	Signal Subspace Issues in TSI Mitigation	261-283
Daniel F. Marshall and Robert A. Gabel MIT Lincoln Laboratory	Simultaneous Mitigation of Multipath Jamming and Ground Clutter	285-313
Stephen M. Kogon, Douglas B. Williams, and E. Jeff Holder Georgia Institute of Technology	Hot Clutter Cancellation with Orthogonal Beamspace Transforms	315-341
Lloyd J. Griffiths University of Colorado	Adaptive Hot Clutter Mitigation Using Multiple Linear Constraints	343-372

SPEAKER PRESENTATIONS (Continued)

SPEAKER	TITLE	PAGES
Prashanth B. Bhat, Young W. Lim, and Viktor K. Prasanna University of Southern California	Scalable Portable Parallel Algorithms for STAP	401-427
Mark F. Skalarin and Thomas H. Einstein Mercury Computer Systems, Inc.	STAP Processing on a Multicomputer: Distribution of 3-D Data Sets and Processor Allocation for Optimum Interprocessor Communication	429-488
George A. Tsihrintzis and Chrysostomos L. Nikias University of Virginia	STAP Detection with Sub-Gaussian Distributions and Fractional Lower-Order Statistics for Airborne Radar	449-475
Christ D. Richmond Massachusetts Institute of Technology	Adaptive Array Processing in Non-Gaussian Environments	477-498
Ram Raghavan and Nick Pulsone Northeastern University	A Generalization of the Adaptive Matched Filter Receiver for Array Detection in a Class of Non-Gaussian Interference	499-517
Steven T. Smith MIT Lincoln Laboratory	Detection Performance with Combined Adaptive Filters	519-546

SPEAKER PRESENTATIONS (Continued)

SPEAKER	TITLE	PAGES
Kristine L. Bell, Yariv Ephraim, and Harry L. Van Trees George Mason University	Explicit Ziv-Zakai Lower Bound for Bearing Estimation Using Planar Arrays	547-568
James Ward MIT Lincoln Laboratory	Angle and Doppler Estimation with Space-Time Adaptive Processing Radar	569-595
Ralph T. Compton, Jr. Compton Research, Inc.	Radome Effects on Two-Dimensional Angle Estimation	597-620
Scott D. Coutts MIT Lincoln Laboratory	3-D Jammer Localization	621-648
Athina P. Petropulu and Haralambos Pozidis, Drexel University Kenneth Abend Gorca Systems, Inc.	Cross-Correlation Based Estimation of Multipath Propagation Channels	649-671
A. Lee Swindlehurst Brigham Young University	Exploiting Frequency Domain Models in Array Signal Processing	673-699

A MULTIDISCIPLINARY PERSPECTIVE ON ADAPTIVE SENSOR ARRAY PROCESSING

Irving S. Reed

University of Southern California
Los Angeles, CA 90089-2564
tel: (213) 740-7335

Abstract Space-Time Adaptive Processing (STAP) has been shown to be very effective in suppressing ground clutter in airborne MTI radars. Practical implementations of STAP are often further enabled by careful attention to rank reducing transformations prior to the STAP processing. A review of a number of different sensor applications reveals that an identical statistical detection framework can arise if the raw sensor data is appropriately preprocessed. We show how multi-spectral imaging, synthetic aperture radar, and non-coherent processing of infrared images of moving targets all can be transformed into similar STAP problems by very different preprocessing.

A MULTIDISCIPLINARY PERSPECTIVE ON ADAPTIVE SENSOR ARRAY PROCESSING

**PROFESSOR IRVING S. REED
UNIVERSITY OF SOUTHERN CALIFORNIA**

1996 ASAP WORKSHOP

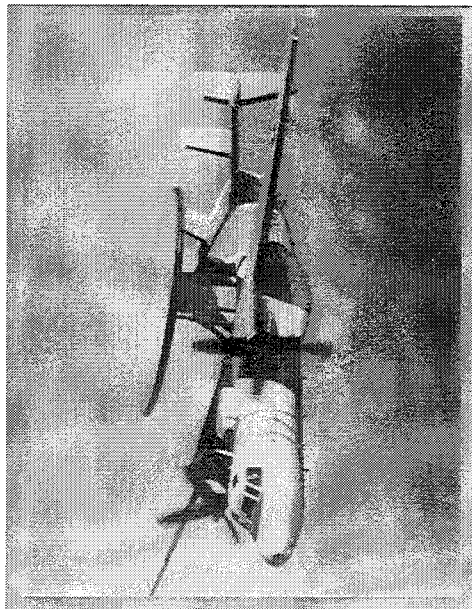
13 MARCH 1996

OUTLINE

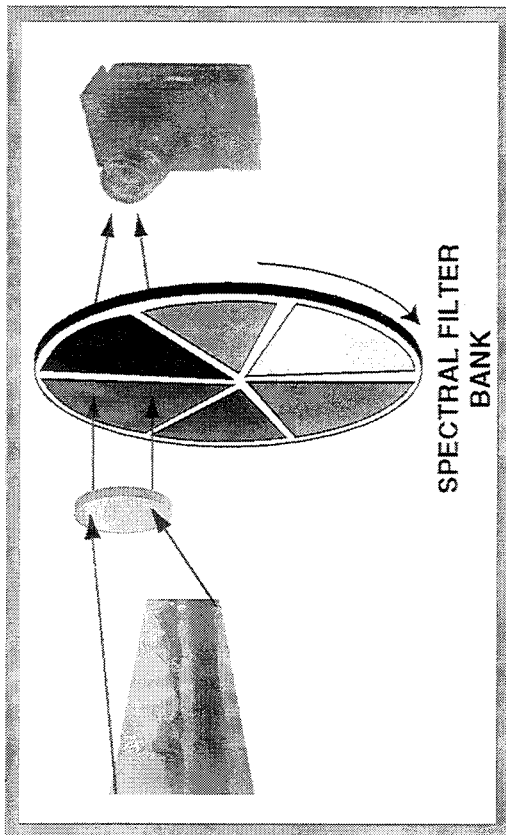
- **INTRODUCTION**
- **APPLICATION AREAS**
- **SUMMARY AND CONCLUSIONS**

ASAP APPLICATION AREAS

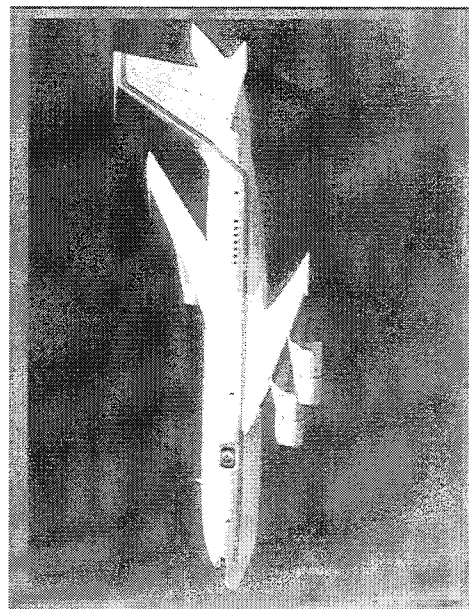
AEW RADAR



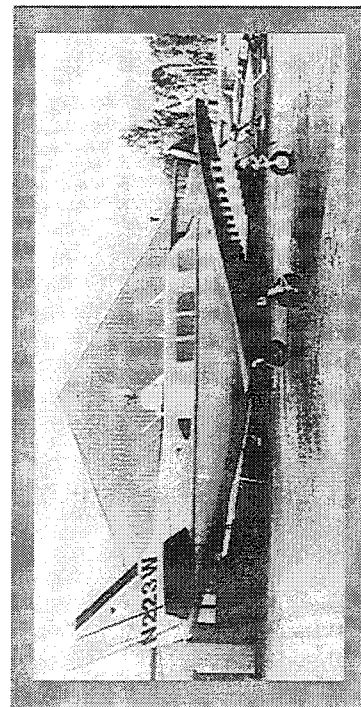
MULTISPECTRAL IMAGING



PASSIVE IR IMAGING



SAR



KS3496/1

PRINCIPLES OF ADAPTIVE SENSOR ARRAY PROCESSING

- **MODELLING ASSUMPTIONS**
 - LINEAR TARGET MODEL WITH UNKNOWN PARAMETERS
 - UNKNOWN INTERFERENCE CORRELATION “STRUCTURE” THAT IS LOCALLY HOMOGENEOUS AND GAUSSIAN (TYPICALLY)
- **ADAPTIVE MATCHED FILTERS**
 - ‘WHITENS’ THE INTERFERENCE DATA
 - INCREASES TARGET TO INTERFERENCE PLUS NOISE RATIO
- **ADAPTIVE MATCHED FILTER DETECTORS**
 - CONSTANT AND PREDICTABLE FALSE ALARM RATE

A TYPICAL ADAPTIVE DETECTOR

DATA MODEL:

$$x_0 = \begin{cases} \alpha s + n & ; \quad H_1 \\ n & ; \quad H_0 \end{cases} \quad \begin{array}{l} \text{TARGET PRESENT} \\ \text{TARGET ABSENT} \end{array}$$

x_1, x_2, \dots, x_K — TRAINING DATA

ADAPTIVE MATCHED FILTER (AMF) DETECTOR:

$$r(X) = \frac{|\hat{S}^H \hat{M}^{-1} x_0|^2}{\hat{S}^H \hat{M}^{-1} \hat{S}} \gtrless \rho$$

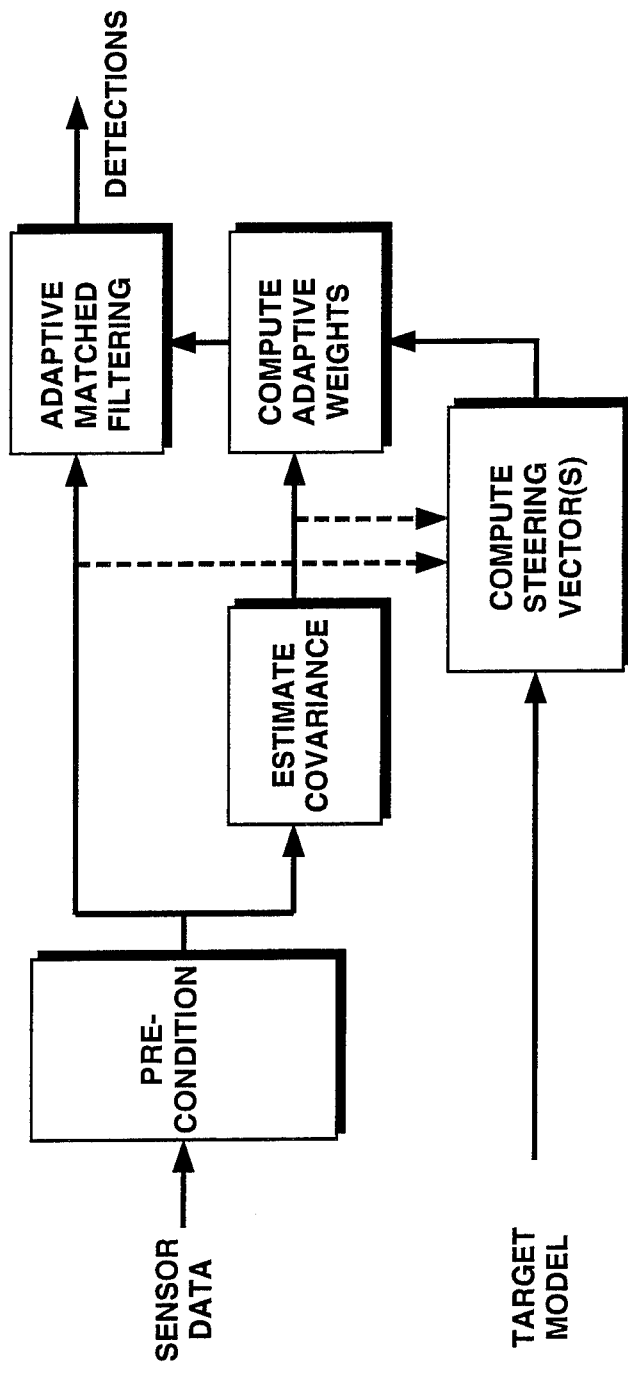
ADAPTIVE WEIGHTING (SMI)

STEERING VECTOR (KNOWN OR ESTIMATED)

INTERFERENCE COVARIANCE ESTIMATION

CFAR NORMALIZATION

GENERIC ADAPTIVE DETECTION ARCHITECTURE

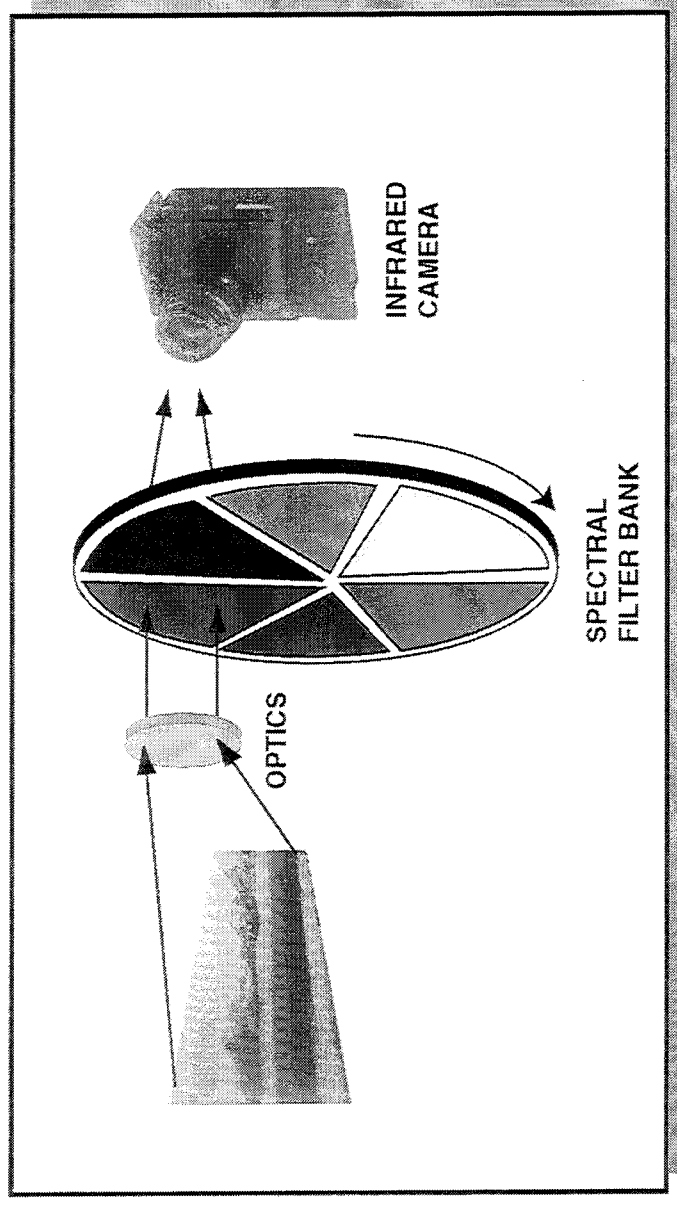


- ESTIMATE BACKGROUND INTERFERENCE FROM DATA
- TARGET MODEL (PLUS ESTIMATES OF UNKNOWN SIGNAL PARAMETERS) DETERMINE STEERING VECTORS
- SOLVE LINEAR SYSTEM FOR ADAPTIVE WEIGHTS
- DATA-DEPENDENT NORMALIZATION FOR EMBEDDED CFAR

OUTLINE

- **INTRODUCTION**
- **APPLICATION AREAS**
 - **MULTISPECTRAL IR IMAGING**
 - **PASSIVE IR MOVING TARGET DETECTION**
 - **SAR EXTENDED TARGET DETECTION**
- **SUMMARY AND CONCLUSIONS**

MULTISPECTRAL INFRARED IMAGING

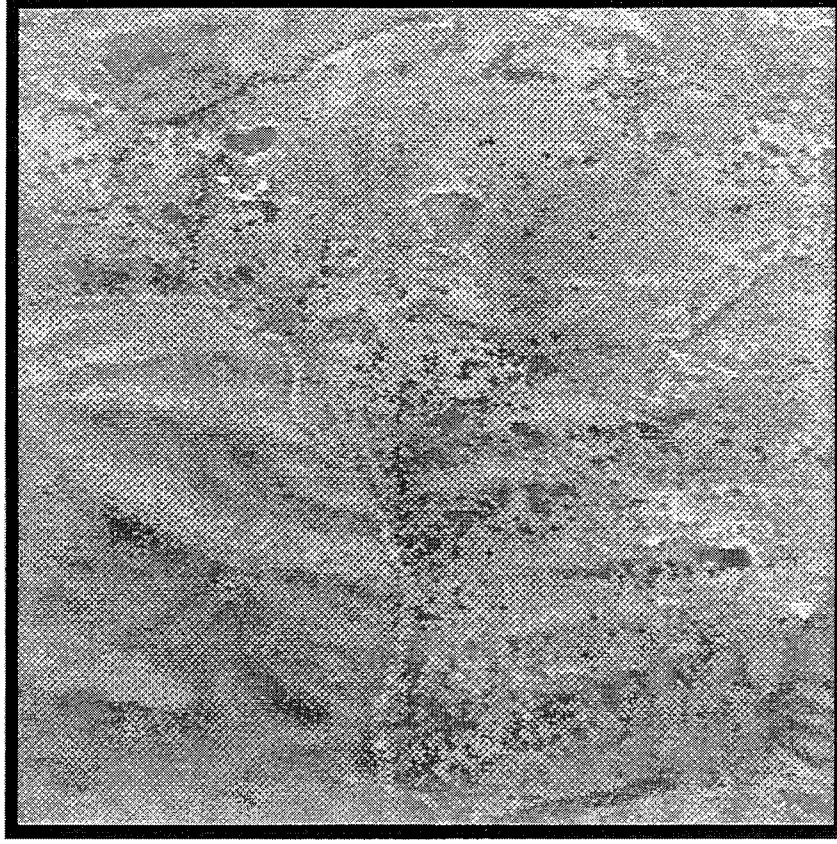


- SURFACE MAPPING
- DETECTION OF OBJECTS
SPECTRALLY DIFFERENT FROM BACKGROUND

KS3496/2

EXAMPLE IMAGE - SINGLE BAND

ADELAIDE,
AUSTRALIA



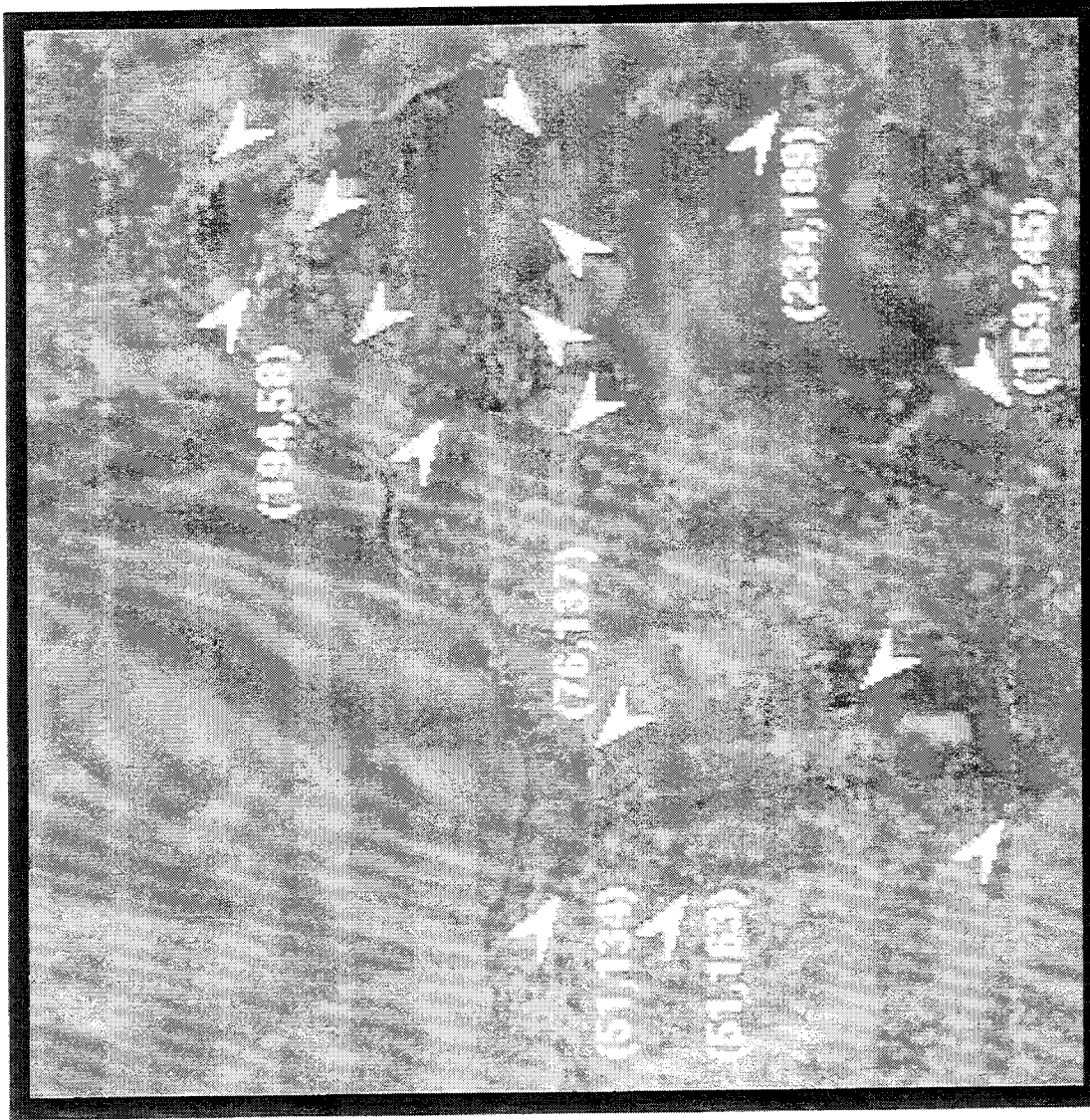
NASA THERMAL INFRARED MULTISPECTRAL SCANNER (TIMS)

- SIX BANDS FROM 8.2 - 12.2 μm

KS3496/6

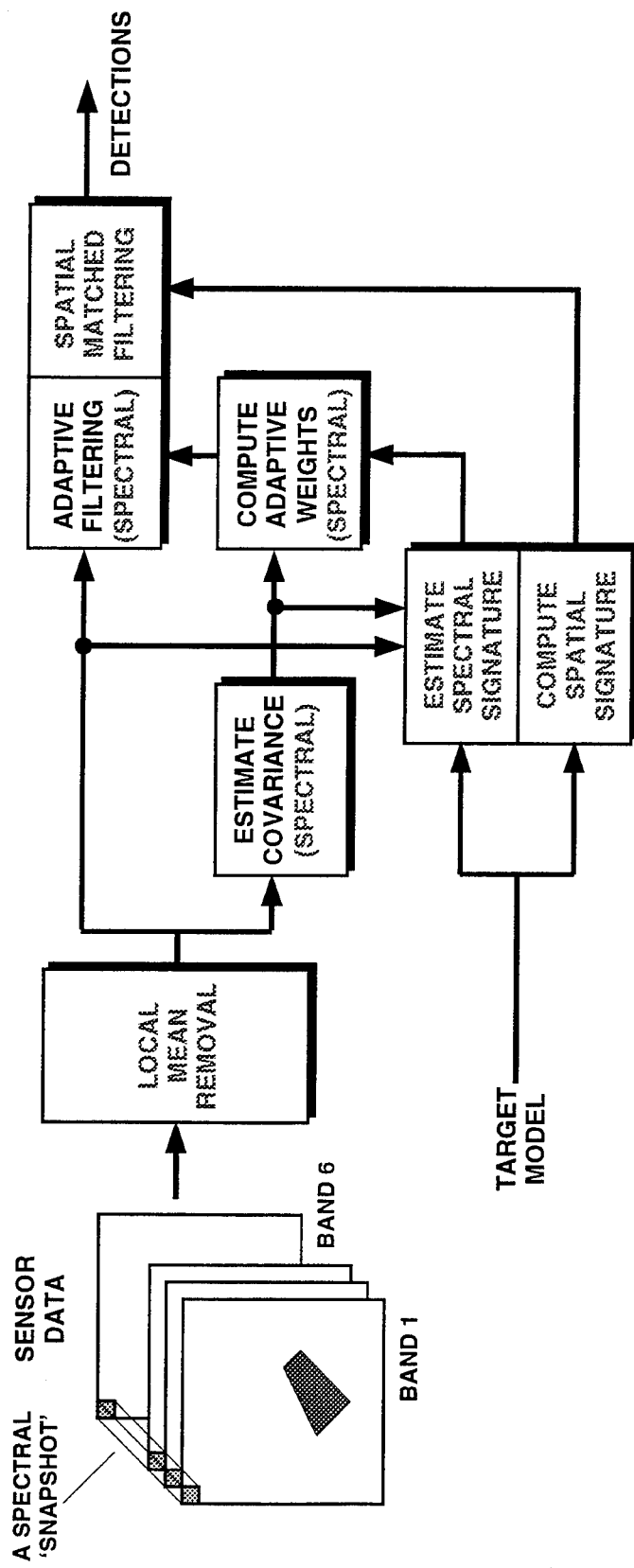
TEST IMAGE - MULTICOLOR COMPOSITE

ADELAIDE,
AUSTRALIA



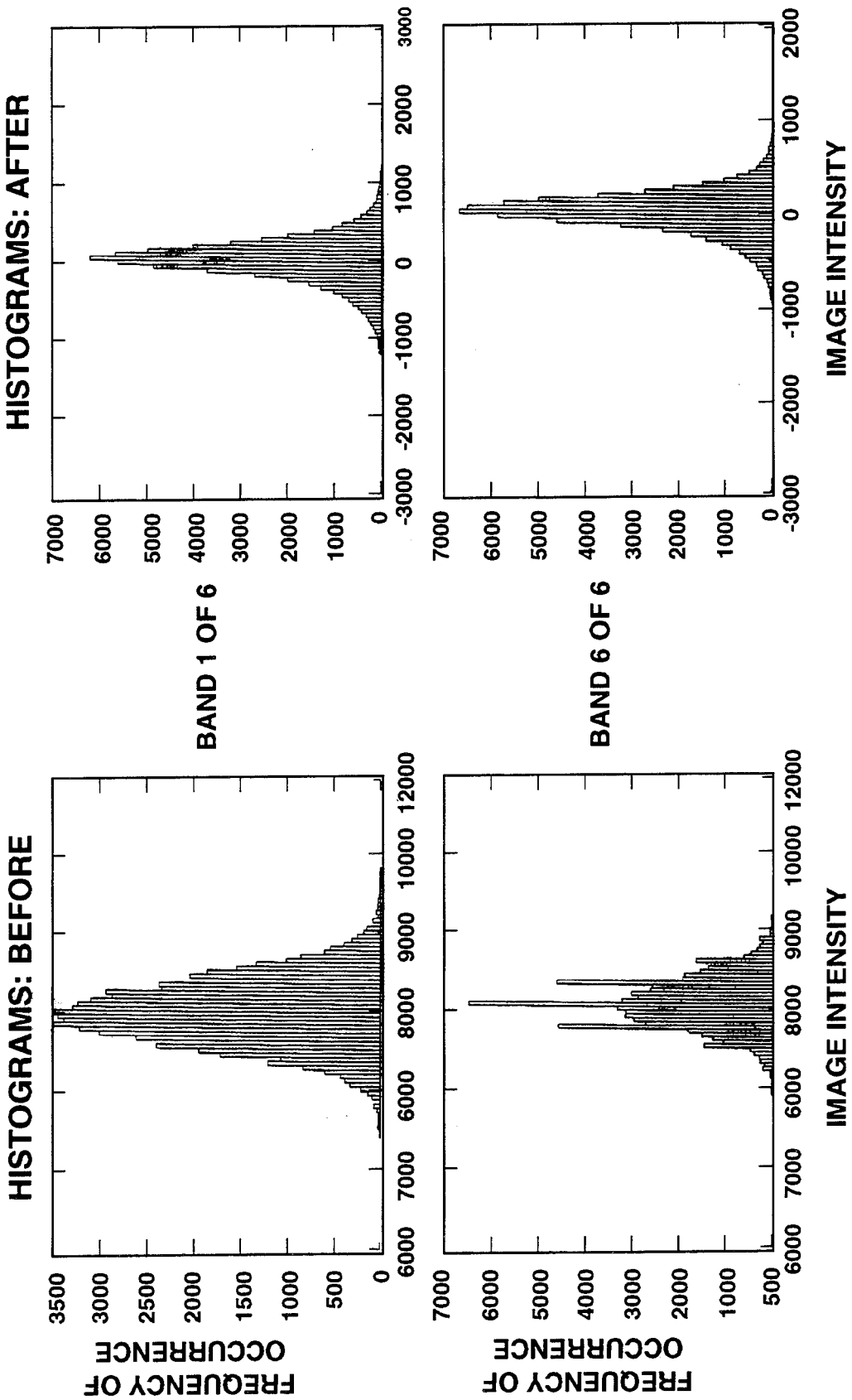
KS349677

MULTISPECTRAL IR ADAPTIVE DETECTOR ARCHITECTURE



- KNOWN SPATIAL SIGNATURE
- KNOWN OR UNKNOWN SPECTRAL SIGNATURE MODELS
- ONE-DIMENSIONAL SPECTRAL ADAPTATION

LOCAL MEAN REMOVAL



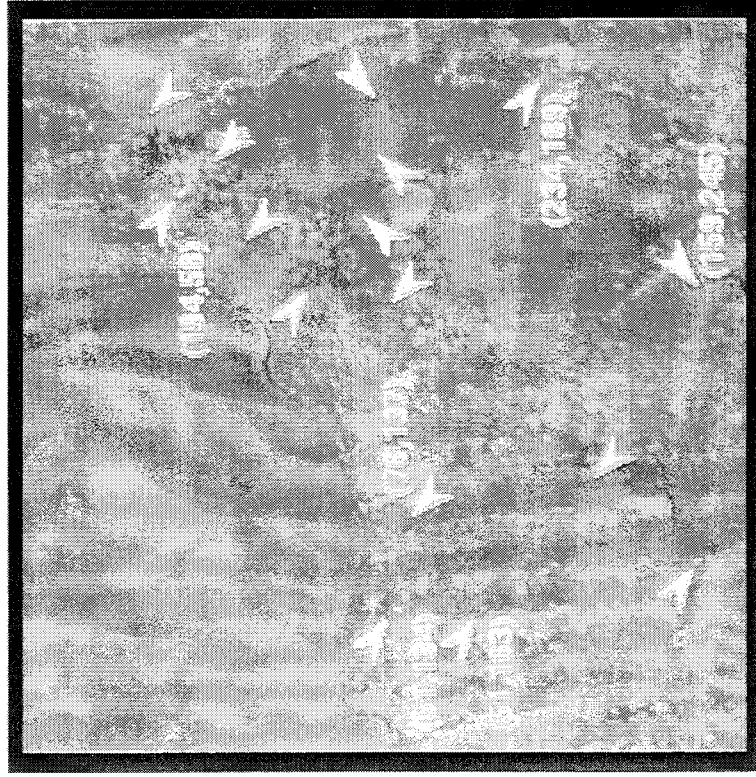
• PREPROCESSING MAKES PIXEL DATA:

- APPROXIMATELY GAUSSIAN
- APPROXIMATELY I.I.D.

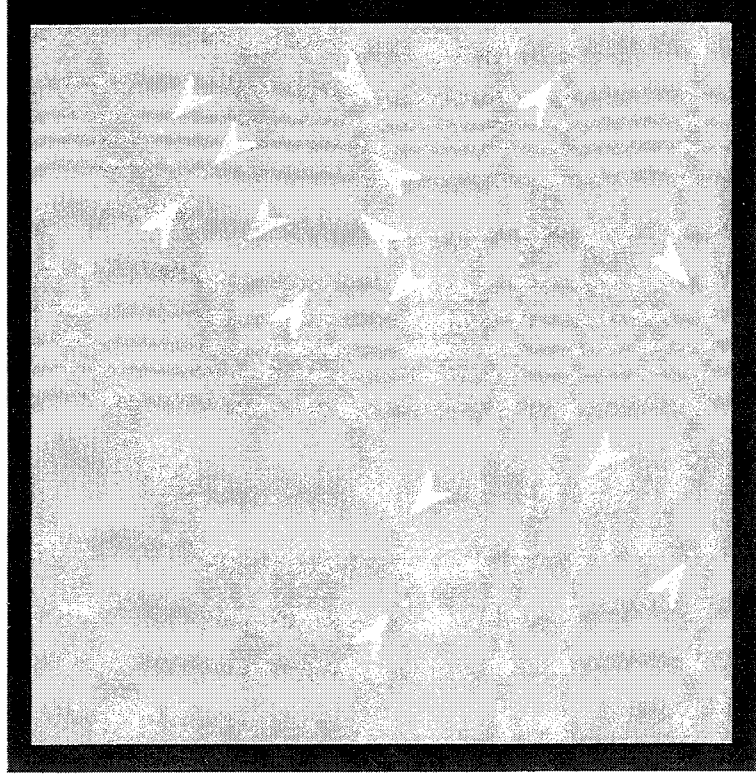
KS3496/10

EXAMPLE 1: UNKNOWN SPECTRAL RESPONSE

TEST IMAGE



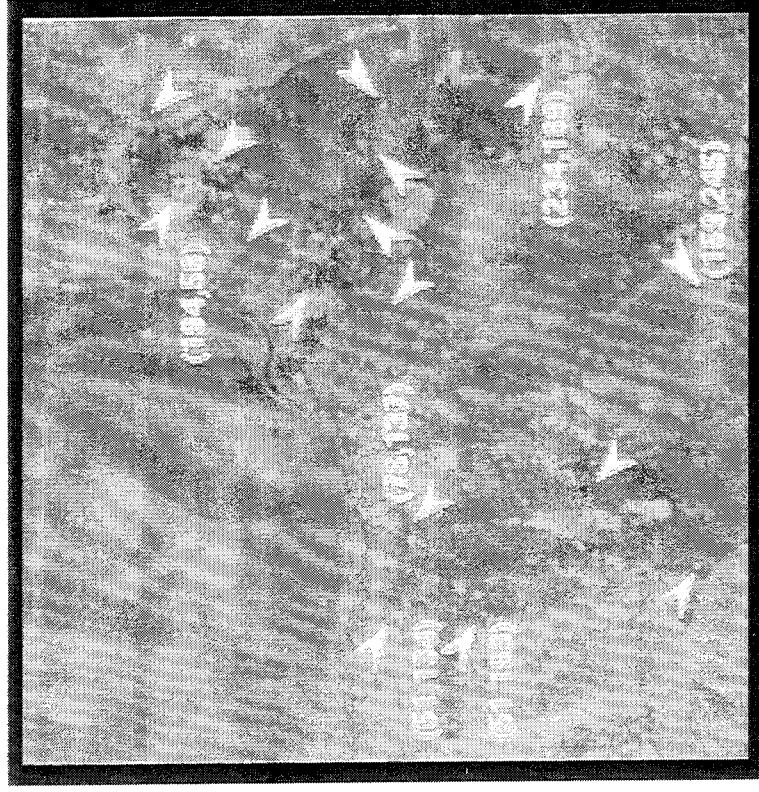
DETECTOR OUTPUT



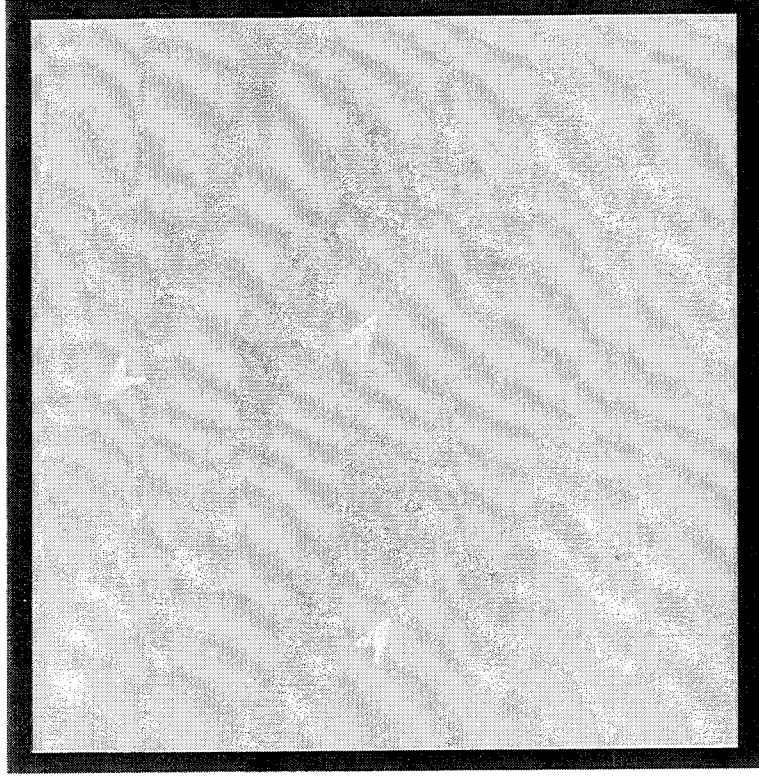
- DETECTS ALL TARGETS WITH SPECTRA DIFFERENT FROM LOCAL BACKGROUND

EXAMPLE 2: KNOWN SPECTRAL RESPONSE

TEST IMAGE

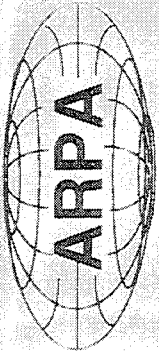


DETECTOR OUTPUT



- MOBILE HOME TRAILER USED AS KNOWN TARGET
- SPECTRAL RESPONSE MEASURED THEN ASSUMED KNOWN

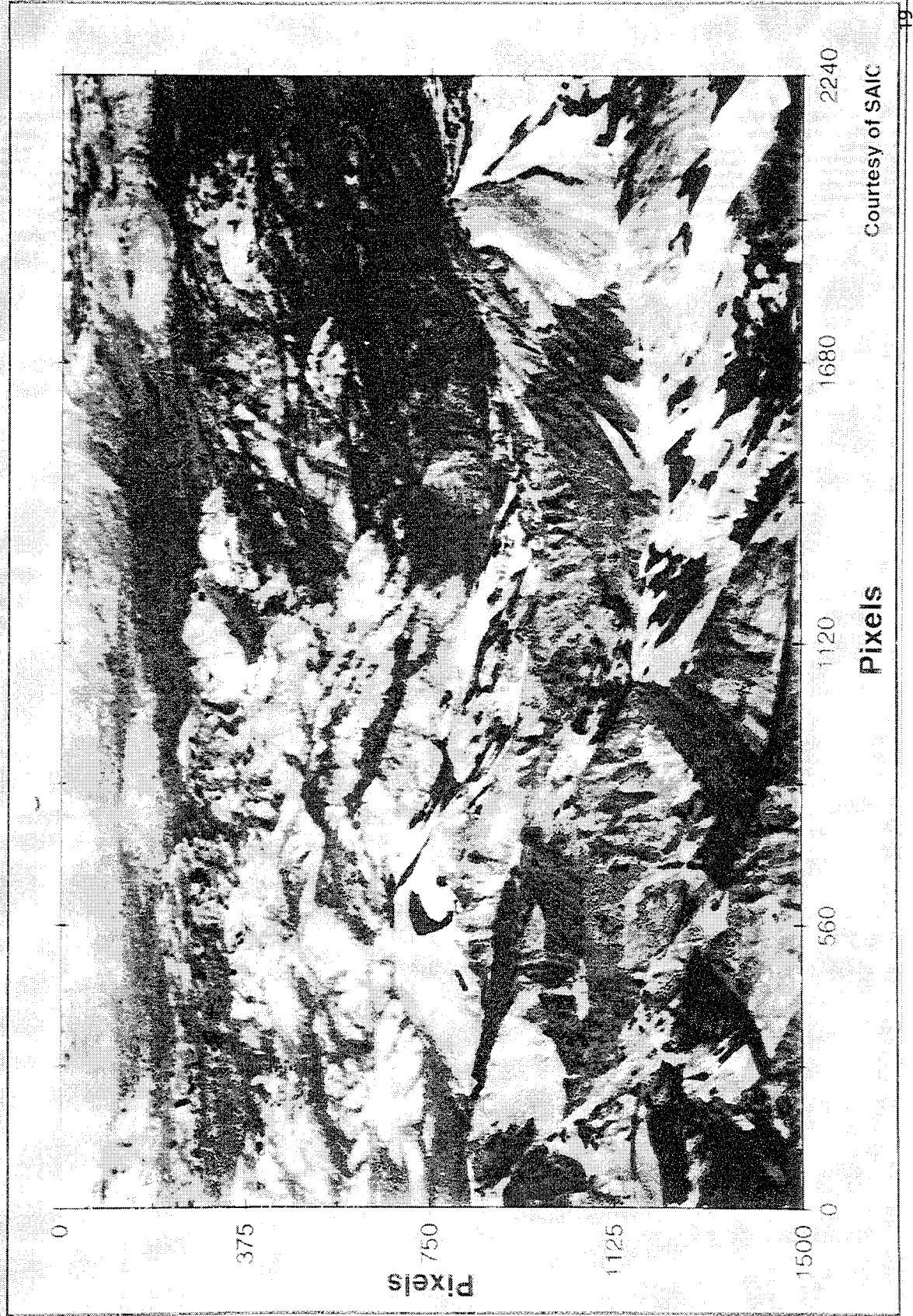
KS3496/9



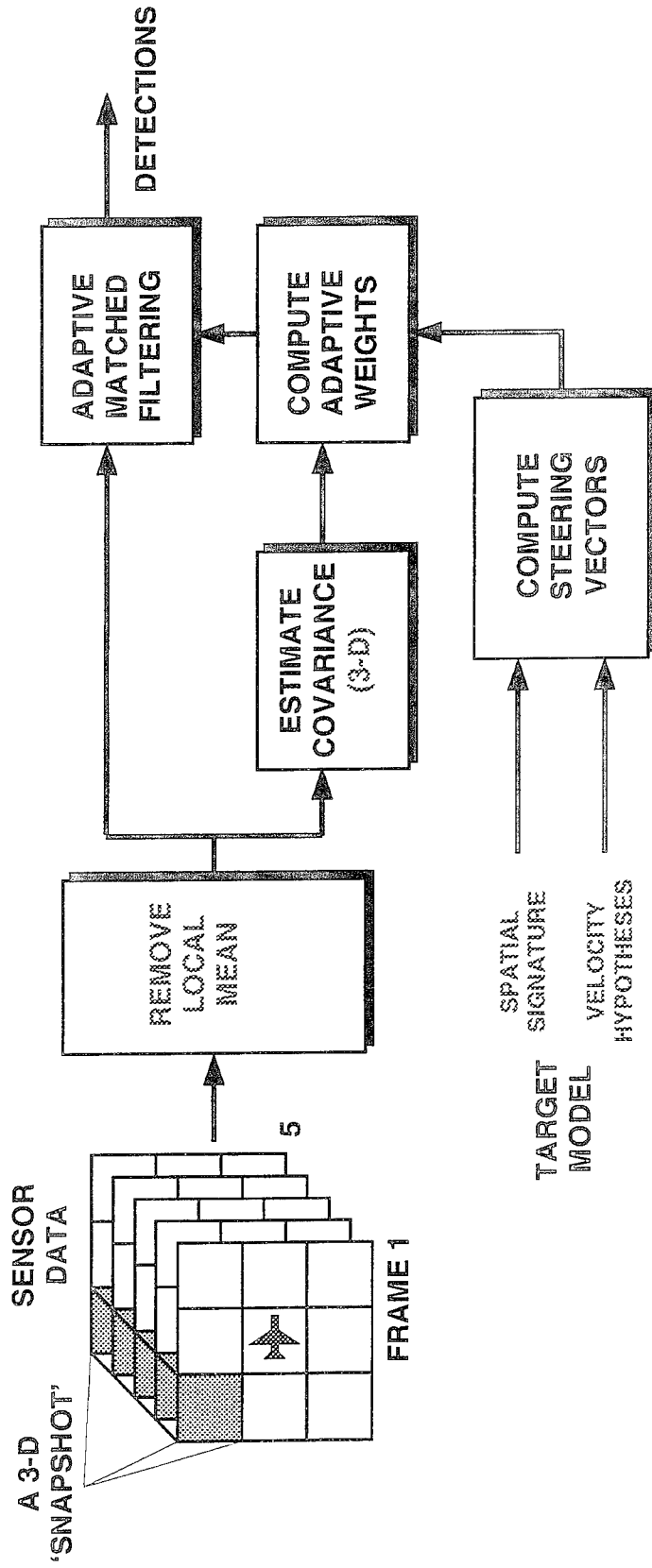
MAMMOTH MTN

FROM 39 KFT ALT. ~80 N. MI.

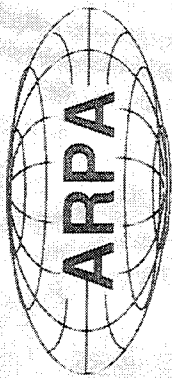
HUGHES
AIRCRAFT



PASSIVE IR ADAPTIVE DETECTOR



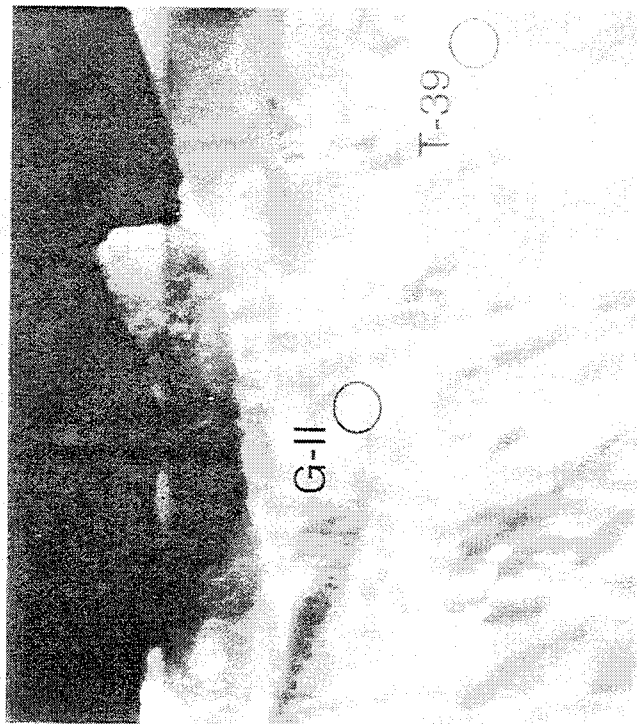
- SNAPSHOTS FORMED FROM MULTIFRAME SUBIMAGES
- A THREE-DIMENSIONAL (TWO SPATIAL PLUS FRAME TIME) ADAPTIVE PROCESSOR
- STEERING VECTOR SPATIALLY AND TEMPORALLY MATCHED TO CONSTANT VELOCITY TARGET
- ROBUST TO COMPENSATION JITTER AND REGISTRATION ERROR



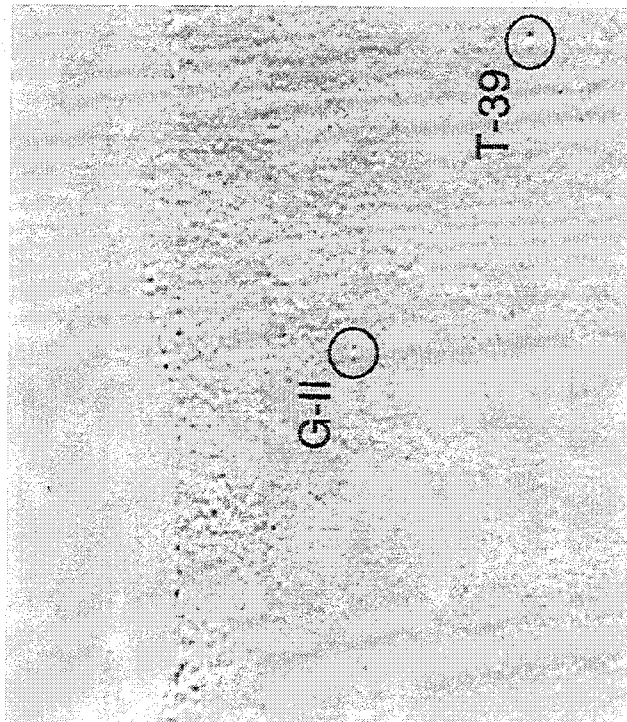
GULFSTREAM IIB & T-39 ~ 130 N. MI.

HUGHES
AIRCRAFT

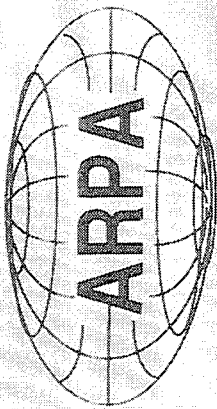
- Raw Image (Sierra Background)
(T39 SNR = + 5.3 dB)



- Filter Output
(T39 SNR = +27.8 dB)



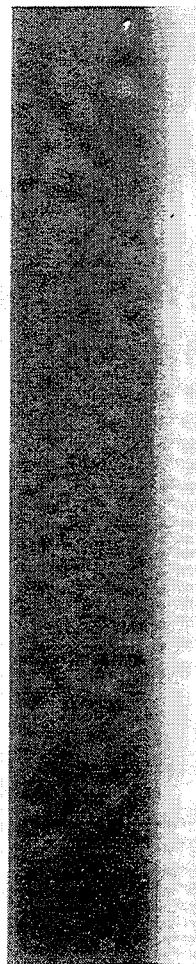
Courtesy of PAR



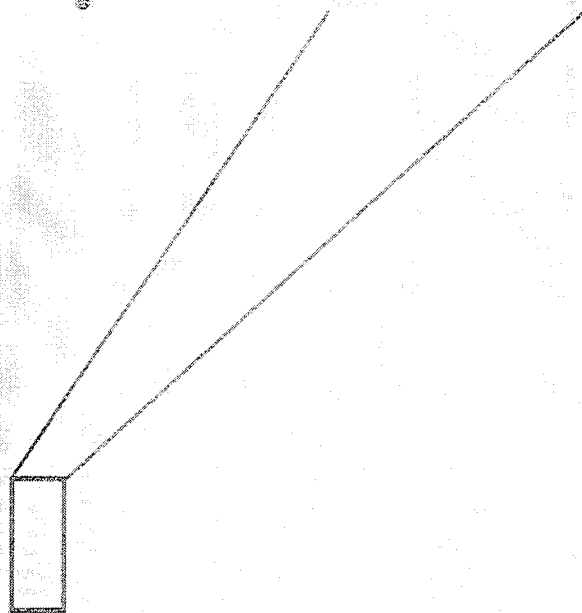
TWO F-4's
~ 150 N. MI.

HUGHES
AIRCRAFT

- Raw Image
w/ Two F-4G Aircraft



- Tracker Output
- F-4G Targets
Separated by 10
Pixels in Az and 5
Pixels in El

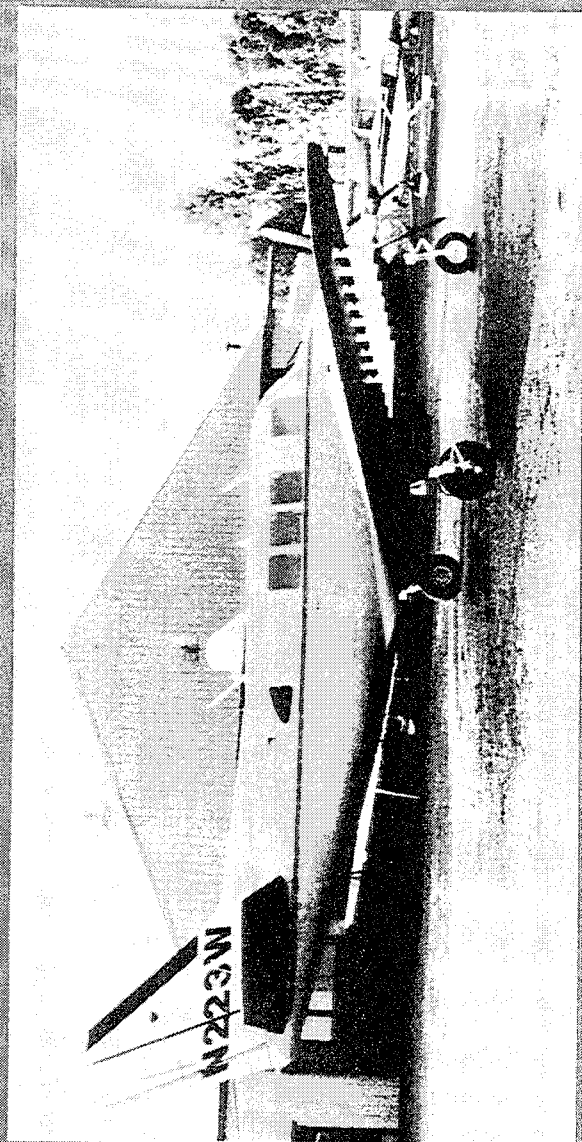


Courtesy of PAR

OUTLINE

- **INTRODUCTION**
- **APPLICATION AREAS**
 - **MULTISPECTRAL IR IMAGING**
 - **PASSIVE IR MOVING TARGET DETECTION**
 - **SAR EXTENDED TARGET DETECTION**
- **SUMMARY AND CONCLUSIONS**

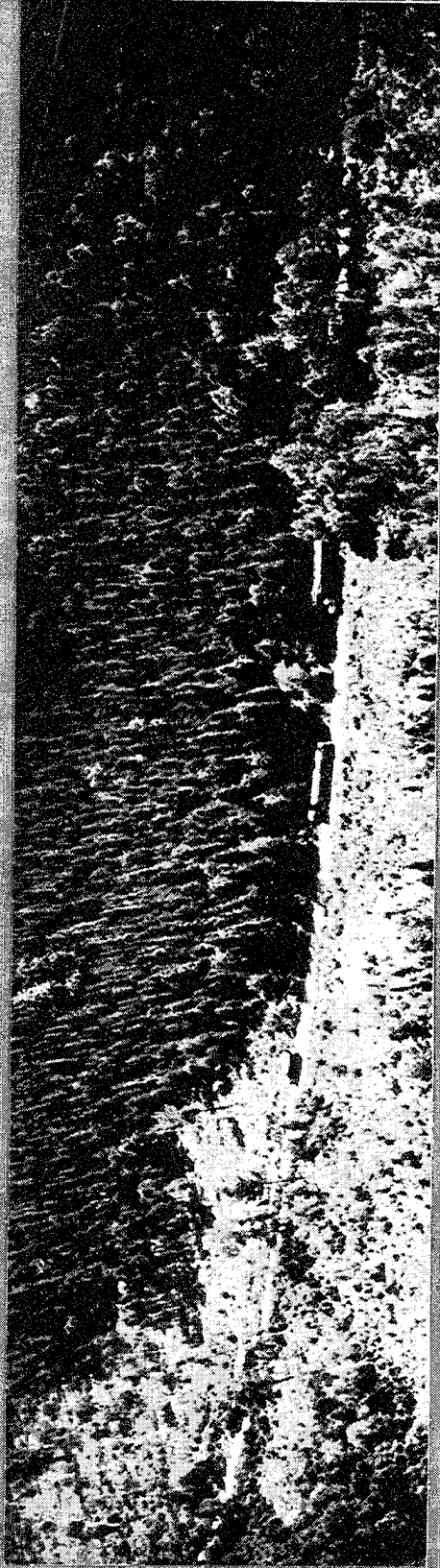
SRI INTERNATIONAL ULTRA-WIDEBAND SAR



RADAR PARAMETERS

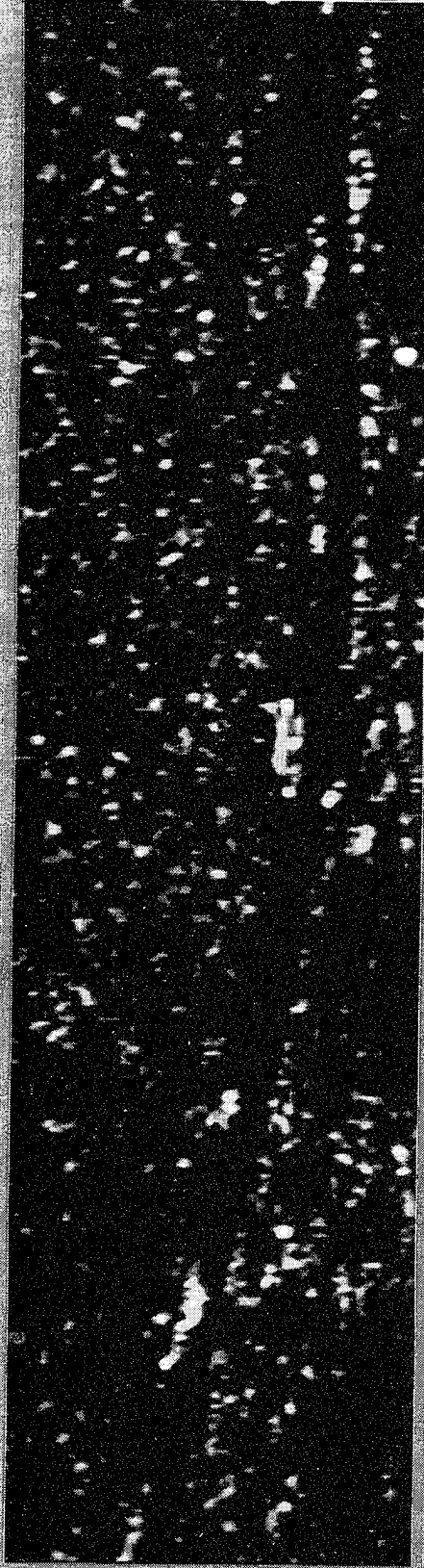
WAVEFORM	IMPULSE
BANDS	200-400 MHz 100-300 MHz
RESOLUTION	1 m \times 1 m
POLARIZATION	HH
POWER	50 kW PEAK 0.1 W AVERAGE

CEDAR SWAMP DEPLOYMENT



AERIAL PHOTO

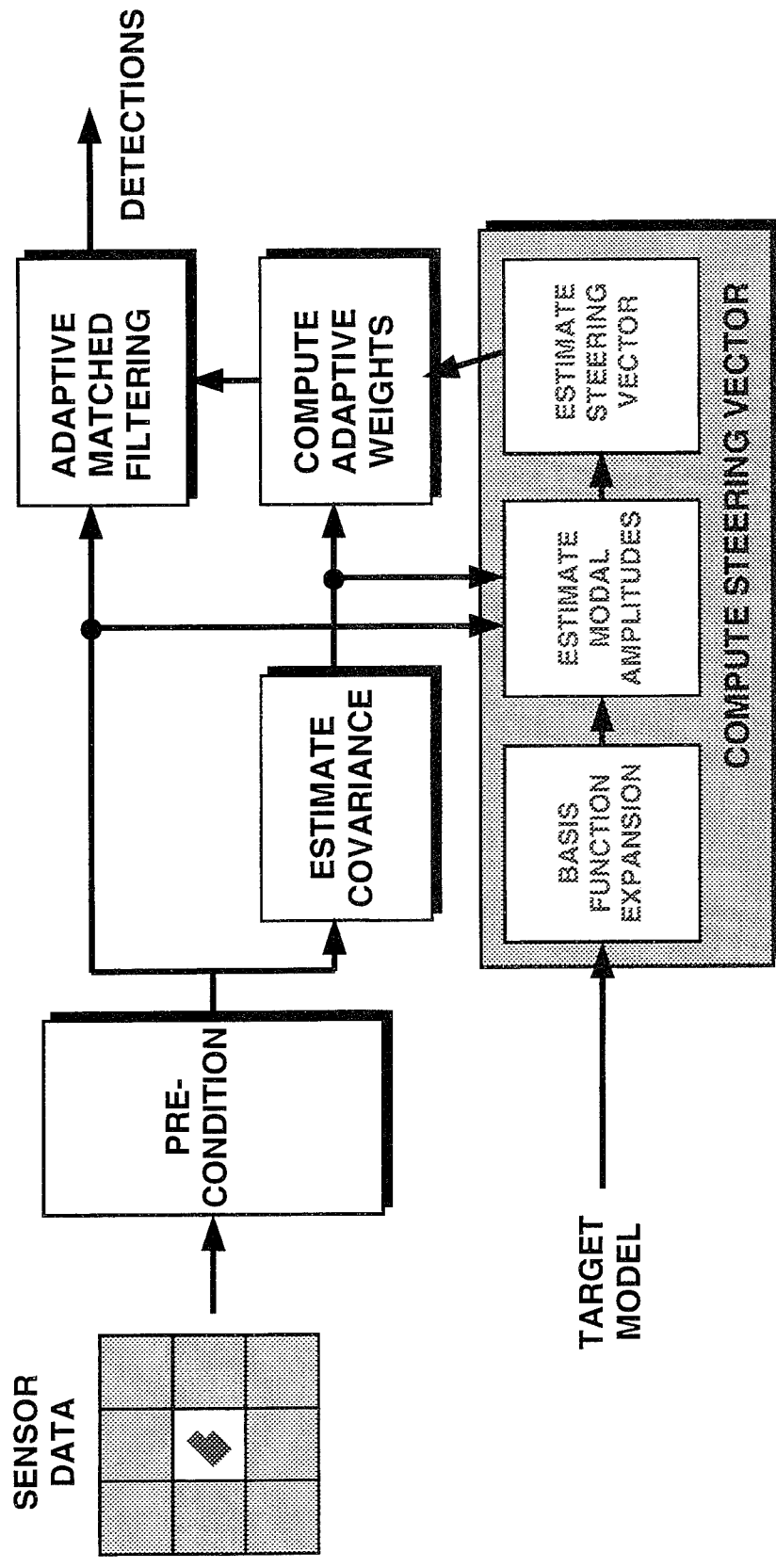
7/90



SRI HH 1m x 1m

8/92

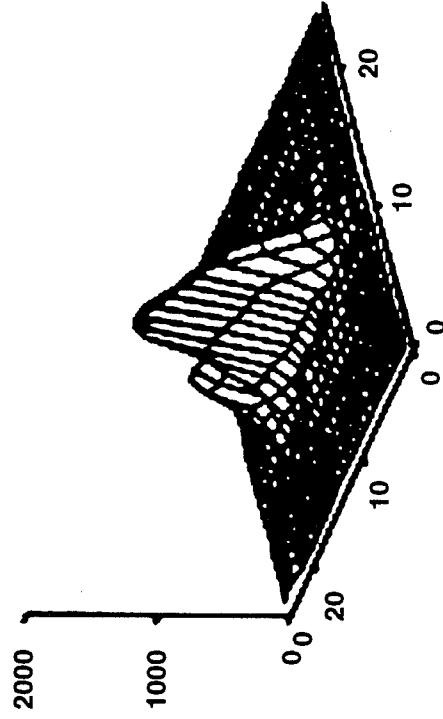
SAR ADAPTIVE DETECTOR ARCHITECTURE



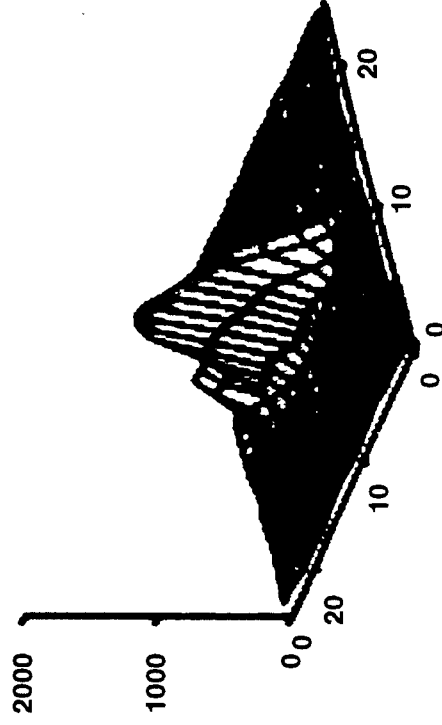
- LINEAR MODEL FOR TARGETS
- TARGET BASIS DETERMINED FROM DCT OF MEASURED IMAGE
- DETECTOR REDUCES TO AMF OR ENERGY DETECTOR
- A TWO-DIMENSIONAL SPATIAL ADAPTIVE PROCESS

DISCRETE COSINE TRANSFORM (DCT) FOR TARGET FEATURE MAPPING

RAW IMAGE



RECONSTRUCTED IMAGE

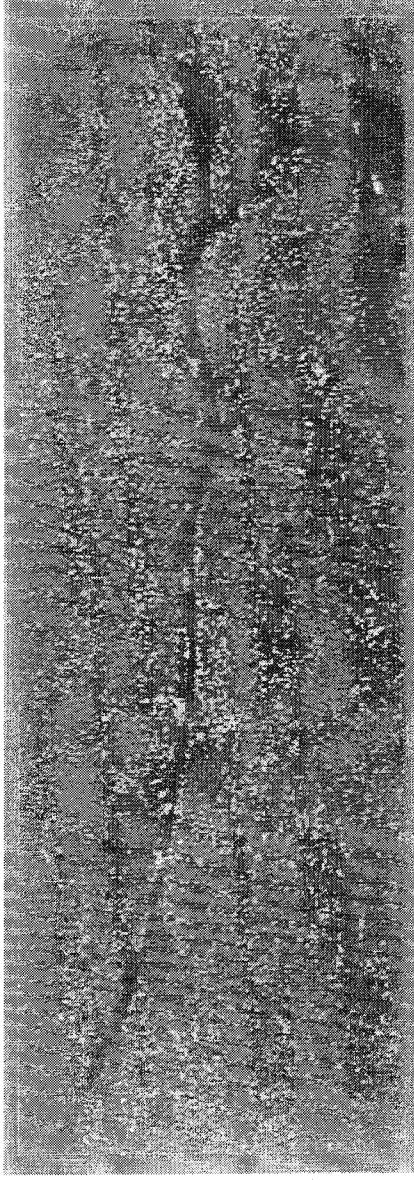


- HEMTT TRUCK
- RECONSTRUCTION 25% OF DCT COEFFICIENTS

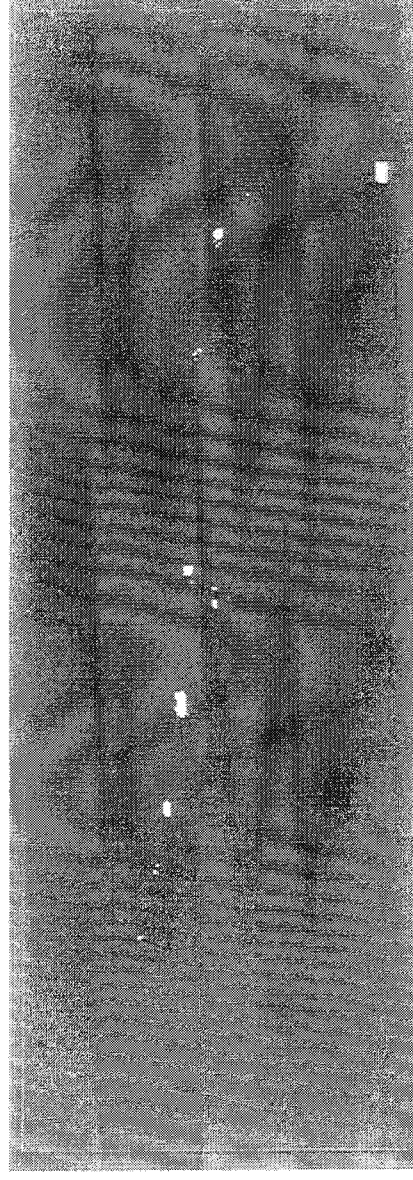
KS3496/3

SAR PROCESSING EXAMPLE: CEDAR SWAMP

INPUT IMAGE



DETECTOR OUTPUT



- TARGET BASIS MEASURED FROM HEMTT TARGET IN CLEAR
- SMALL VEHICLES NOT MATCHING MEASURED TARGET ARE UNDETECTED

KS3496/5

SUMMARY AND CONCLUSIONS

- **ADAPTIVE MATCHED FILTER DETECTION IS WIDELY APPLICABLE (FOR BOTH REAL AND COMPLEX DATA)**
- **CAREFUL ATTENTION TO ALGORITHM DESIGN IS REQUIRED**
 - **DESIGN OF TARGET MATCHED FILTERS**
 - **SELECTION OF SUITABLE DATA FOR ESTIMATING INTERFERENCE COVARIANCE**
 - **SMART PREPROCESSING SUCH AS LOCAL MEAN REMOVAL AND NORMALIZATION IS IMPORTANT IN SOME APPLICATIONS**
- **SUBSTANTIAL INCREASE IN PERFORMANCE POSSIBLE FOR MANY APPLICATIONS**

(Pages 31-51 have been intentionally omitted)

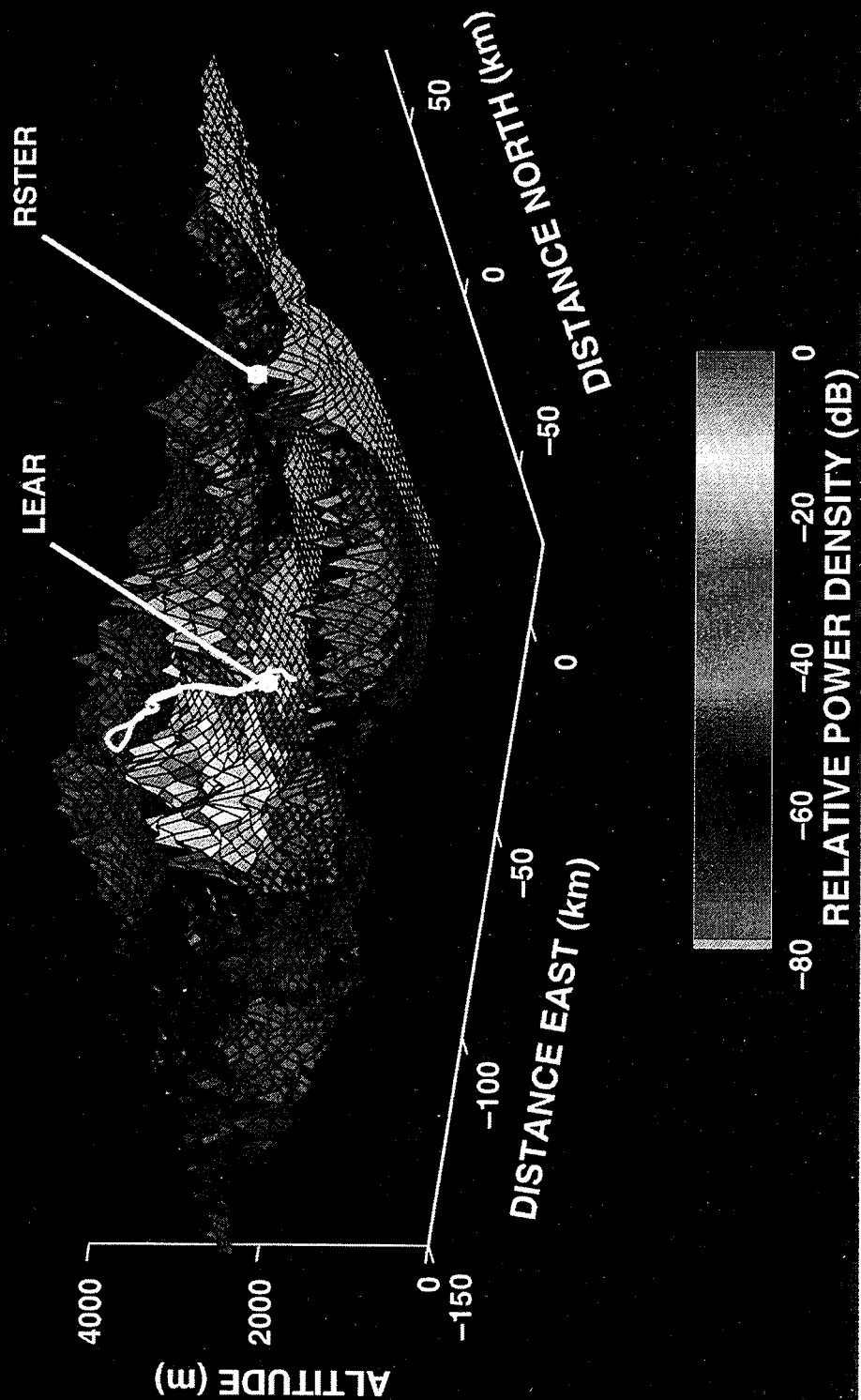
TERRAIN-SCATTERED INTERFERENCE VISUALIZATION

Pamela Kove and Jack Li

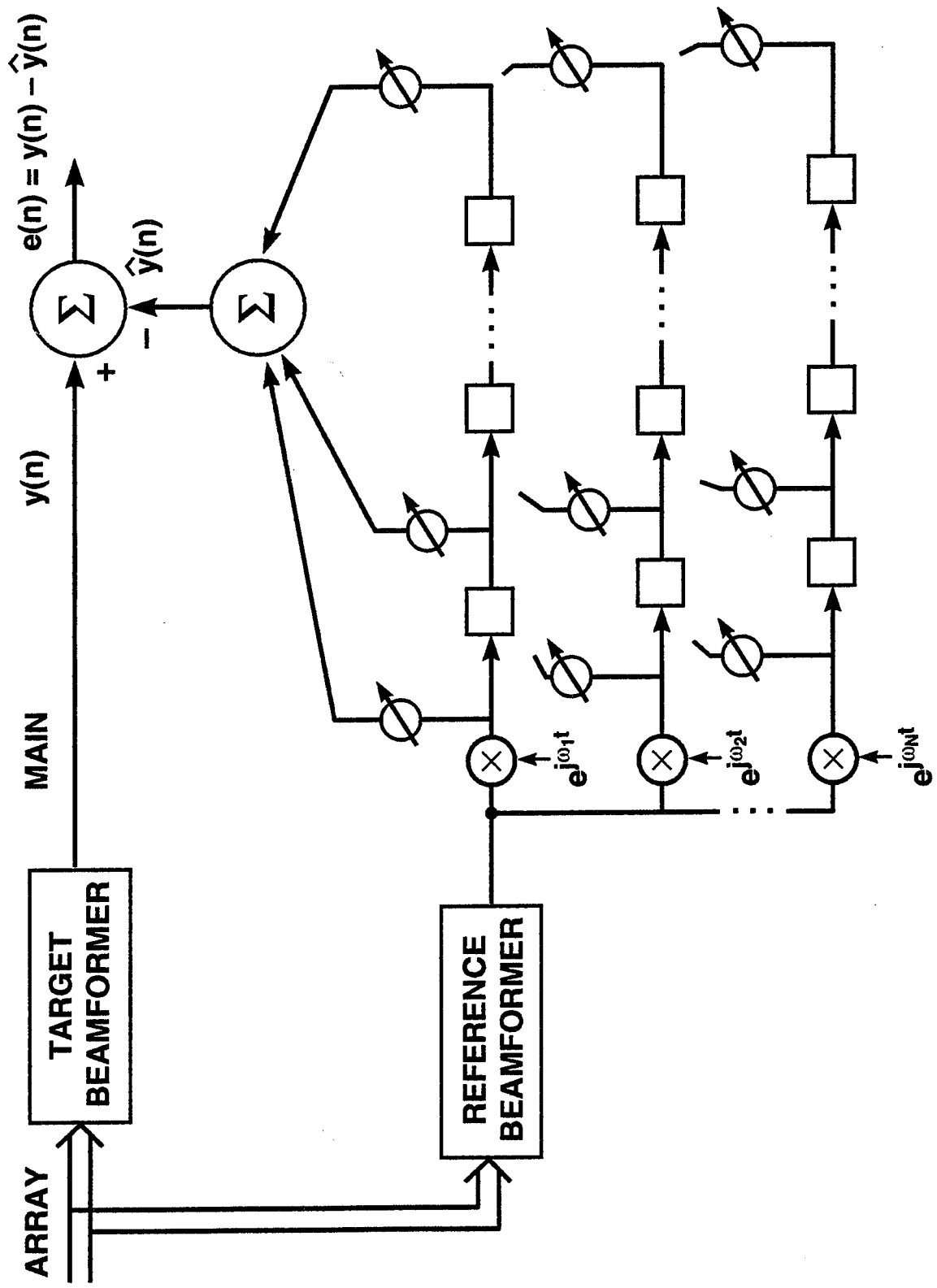
MIT Lincoln Laboratory
244 Wood Street
Lexington, MA 02173-9108
tel: (617) 981-4120
email: kove@ll.mit.edu
email: jackli@ll.mit.edu

Abstract This demonstration presents the visualization of the terrain-scattered interference (TSI) that can arise from aircraft-based jammers. Field data collected under the Mountaintop program was used to evaluate the crosscorrelation between direct-path and multipath jamming signals in the reference and target beams of a TSI mitigation structure. Following spectral analysis across each data set, we obtain a portrait of the corresponding TSI in terms of its arrival azimuth, bistatic delay, and relative Doppler. This portrait may be viewed in an interactive manner to expose interesting features of the TSI energy distribution that bear directly on the selection of TSI mitigation parameters, such as number of taps, Doppler compensation, and required weight update rate. The energy distribution is seen to compare favorably with predictions based on the aircraft's trajectory. From a series of data files collected along the aircraft flight path, we view the time dependence of this energy distribution.

MILLIGAN GULCH BISTATIC SCATTERING

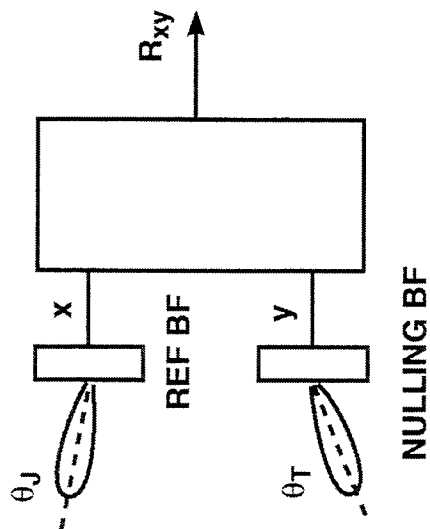
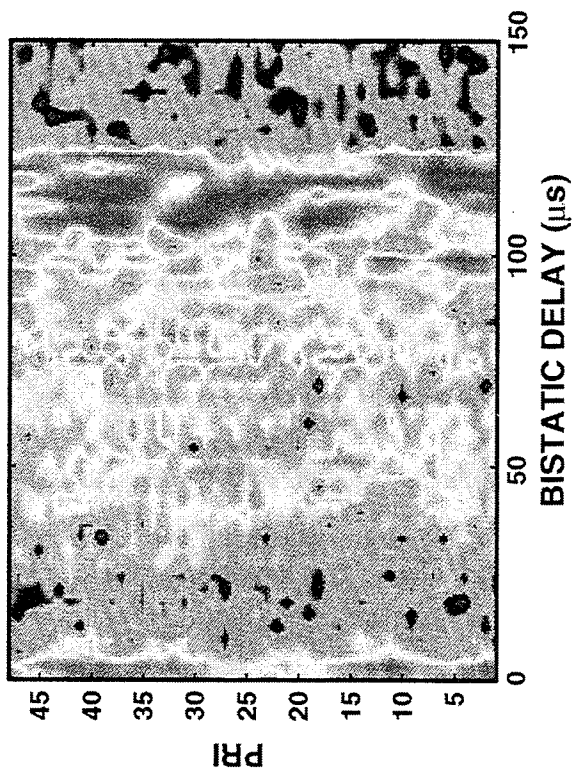


JAMMER MULTIPATH CANCELLATION

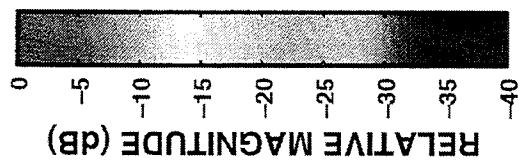
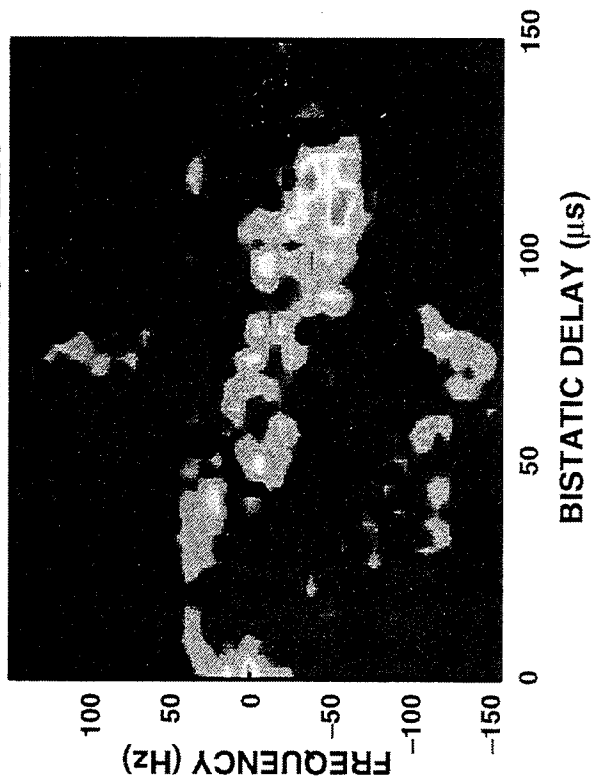


TSI CROSS-COVARIANCE PORTRAITS

CROSS-COVARIANCE MAGNITUDE

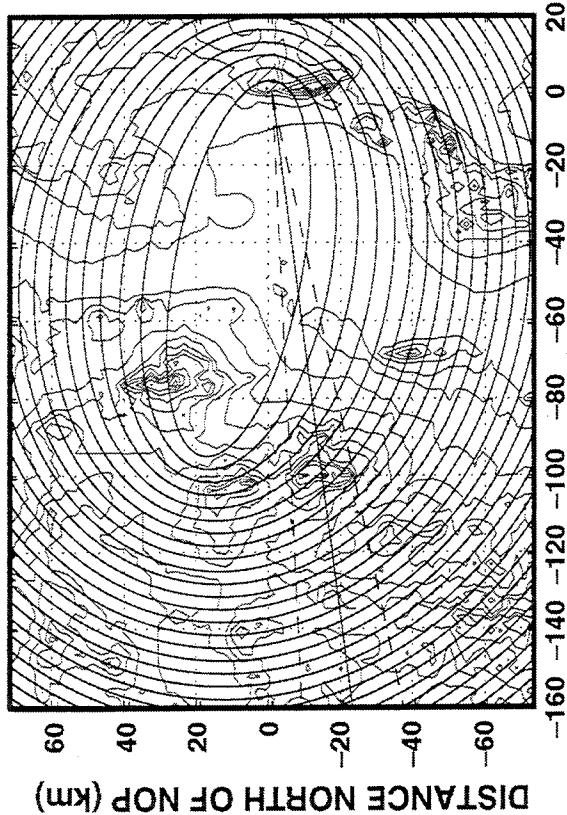


CROSS-COVARIANCE MAGNITUDE
vs DELAY AND DOPPLER

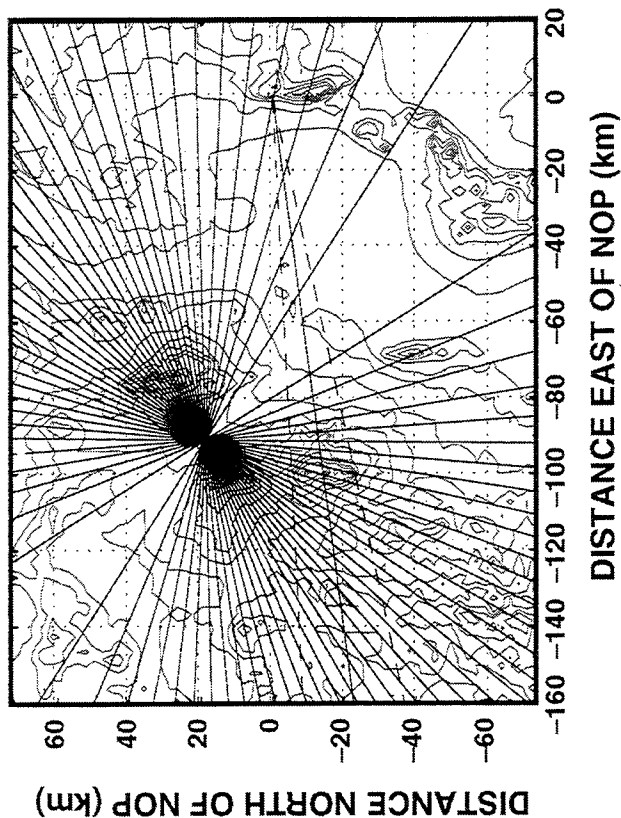


TSI CROSS-COVARIANCE ENERGY DISTRIBUTION

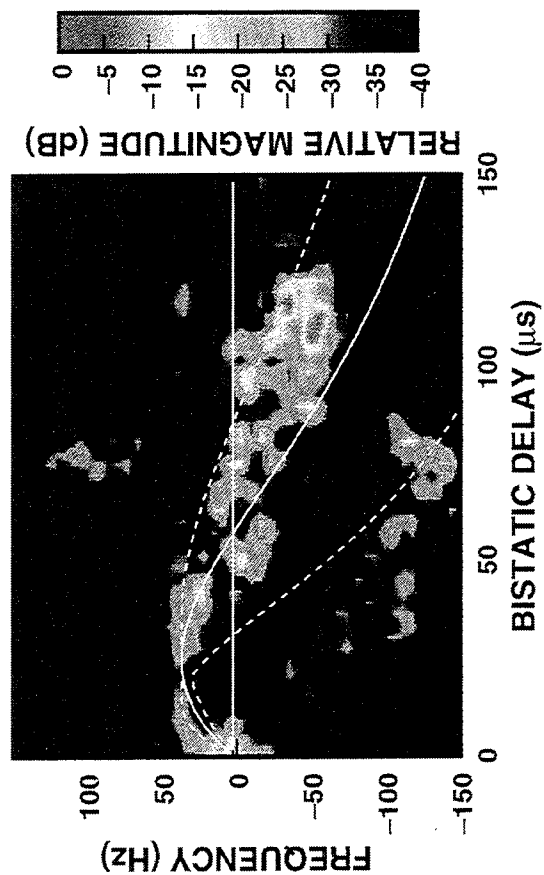
ISO-DELAY CONTOURS



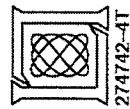
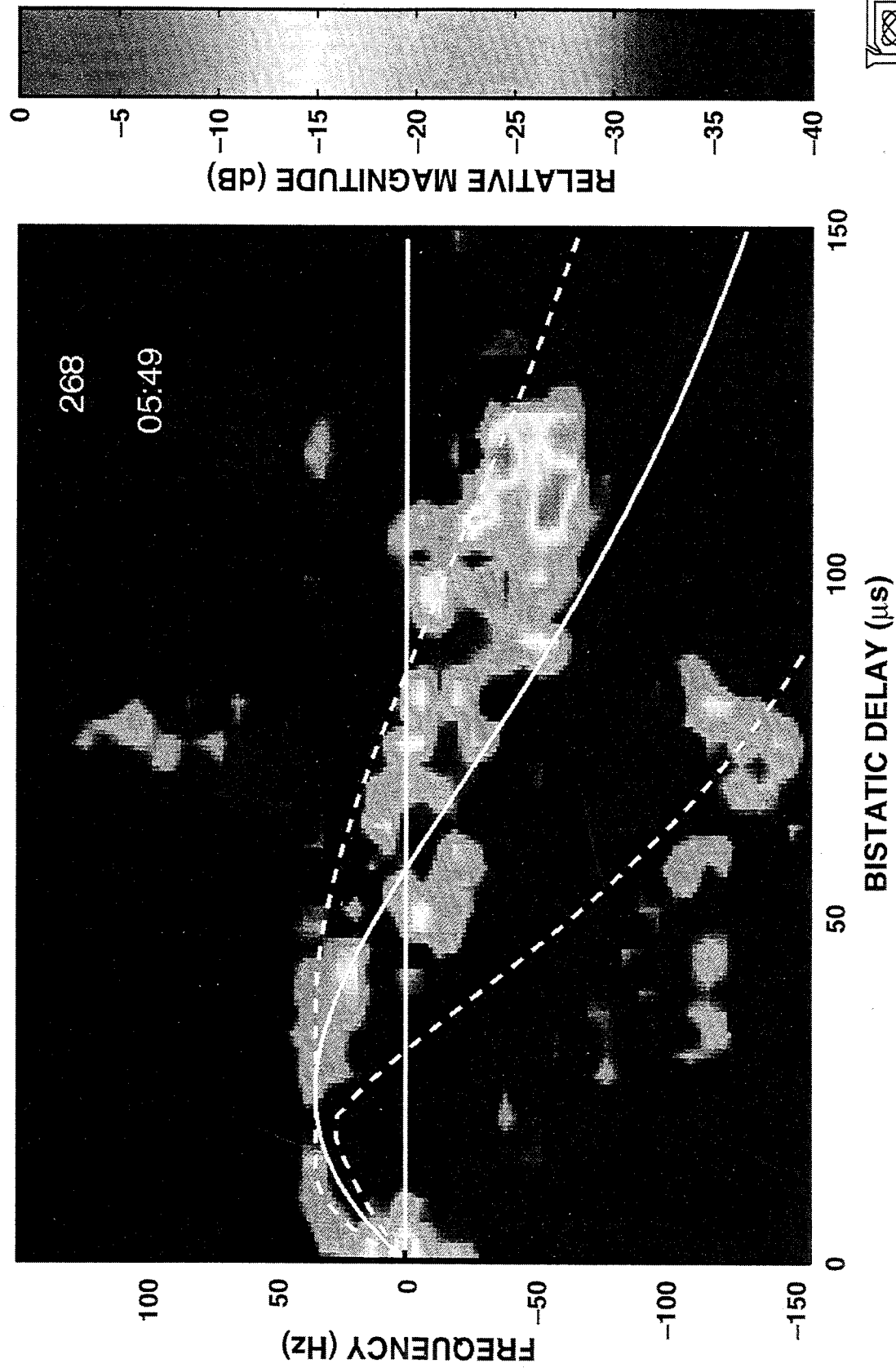
ISO-DOPPLER CONTOURS

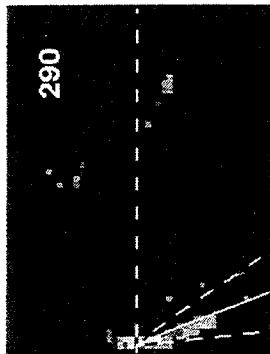
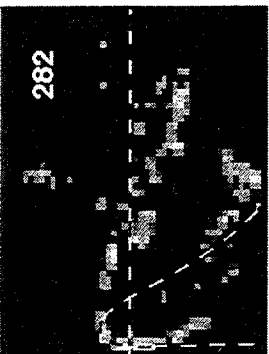
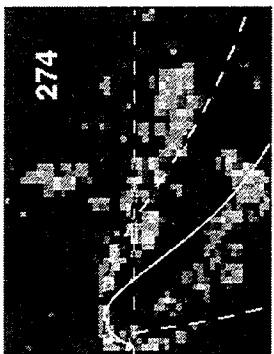
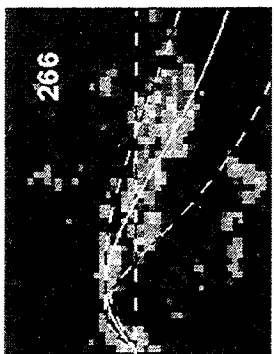
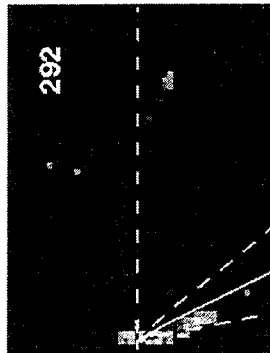
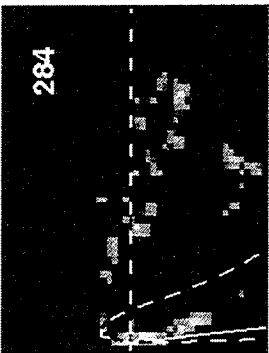
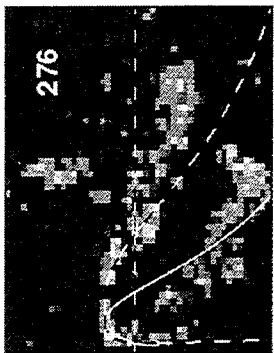
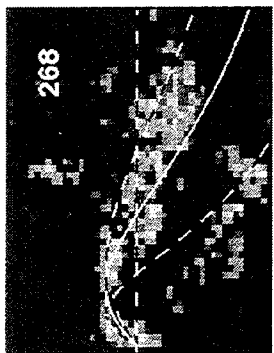
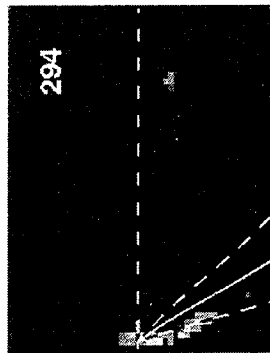
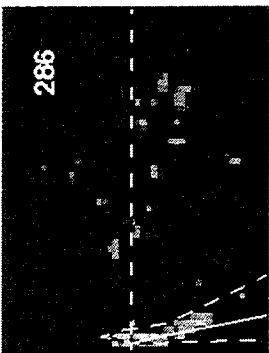
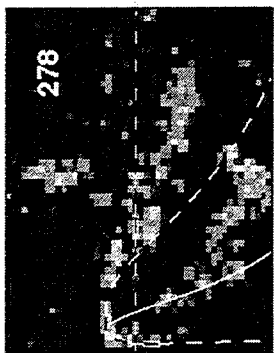
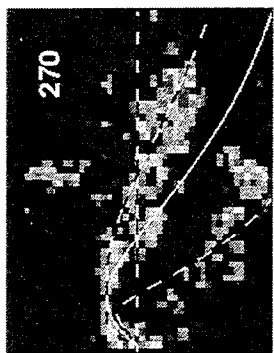
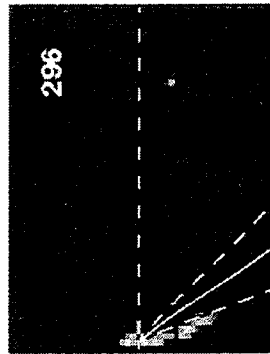
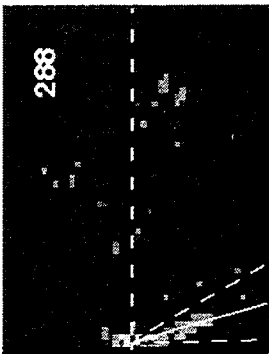
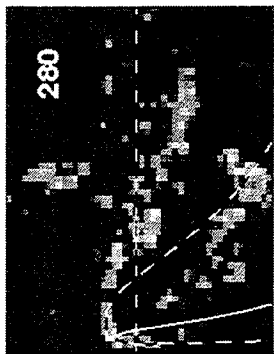
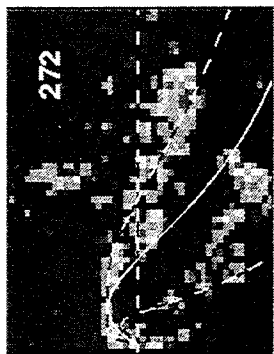


CROSS-COVARIANCE vs DELAY AND DOPPLER



CROSS-COVARIANCE MAGNITUDE vs DELAY AND DOPPLER



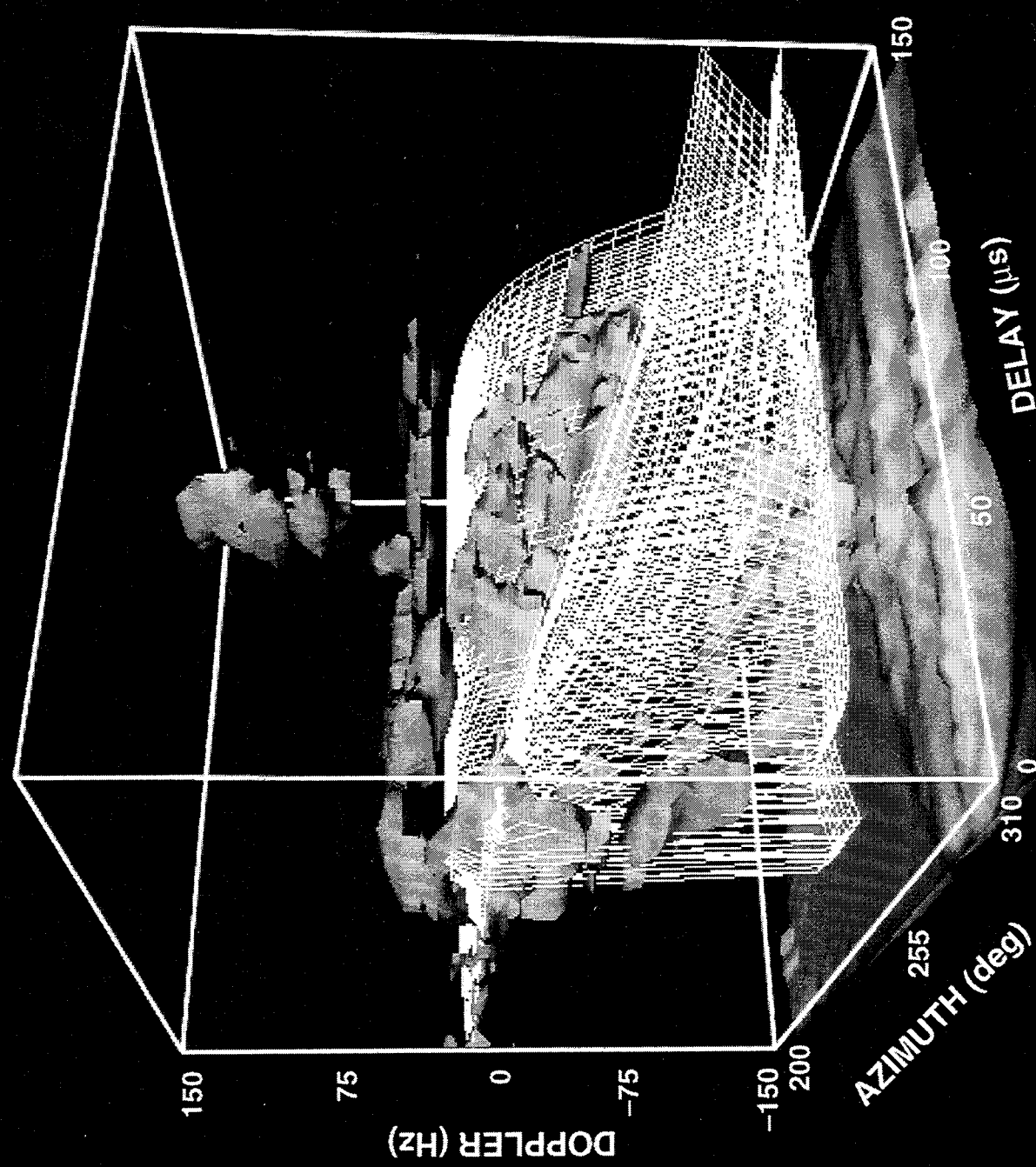


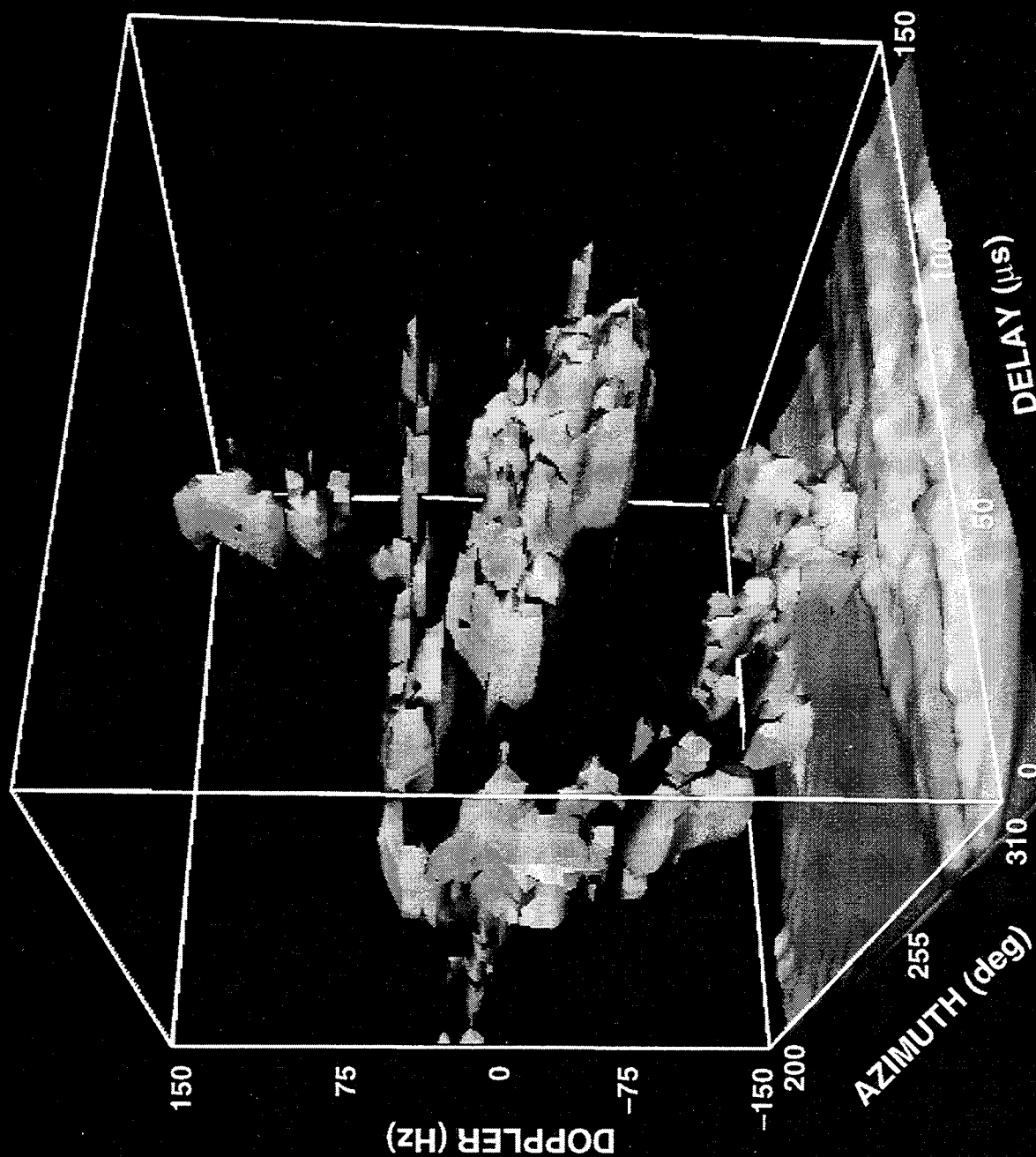
05:49

DOPPLER

AZIMUTH

DELAY





A MOUNTAINTOP MATLAB TOOLBOX

Yaron Seliktar, Douglas B. Williams, and James McClellan

Georgia Institute of Technology

777 Atlantic Drive

Digital Signal Processing Laboratory

Atlanta, GA 30332-0250

tel: (404) 854-9832

fax: (404) 894-8363

email: dbw@eedsp.gatech.edu

Abstract In order to facilitate use of the Mountain Top (MT) data set, we offer a toolbox of MATLAB routines for processing, synthesizing, and visualizing radar data. The first set of routines implement some common adaptive and non-adaptive techniques for processing both synthetic and MT data under a common framework. Additional algorithms can be incorporated into this general format in the future. The second set of routines are used to synthesize interference and target data having the same data format as the MT data sets. A third set of routines provides useful display tools for visualizing data and the processed results. Each of the three sets comes with a graphical interface to facilitate usage. All MATLAB code and accompanying documentation can be obtained through anonymous ftp at [ftp.ee.gatech.edu](ftp://ftp.ee.gatech.edu) (130.207.224.30) in directory "pub/users/yaron".

ASAP Workshop 1996

(MIT)² Mountain Top MATLAB Toolbox

Yaron Seliktar

yaron@eedsp.gatech.edu

Prof. Douglas B. Williams

dbw@eedsp.gatech.edu

Prof. James H. McClellan

mcclella@eedsp.gatech.edu

**Digital Signal Processing Laboratory
School of ECE
Georgia Institute of Technology**

Research sponsored in part by Air Force Rome Labs/ARPA contract number F03602-94-1-0014. Computing facilities sponsored in part by the National Science Foundation under Grant MIP-9295853 and the Hewlett-Packard Company.

Software Features

- A collection of MATLAB routines used for generating synthetic radar data, processing synthetic and Mountain Top (MT) data, and displaying the results.
- Mountain Top compatible - may be used with RLSTAP.
- Script based - certain simulation and processing tasks can be automated.
- Comes with a graphical interface demo.
- General structure for Space-Time Adaptive Processor (STAP) (ICASSP-96 paper).
- Written entirely in MATLAB - easy to add new processing algorithms.
- Available through anonymous FTP with online documentation (<ftp.eedsp.gatech.edu/pub/users/yaron>).

Example (t38pre01v1 Mountain Top Data File)

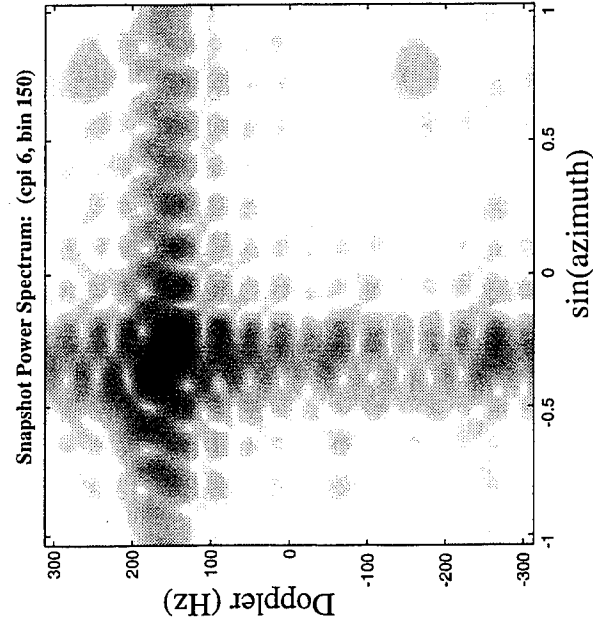
Processing Interface

PROCIT GRAPHICAL INTERFACE	
Processing Specifications	Control Unit
Target Information	File Names
Target Angle 30 deg	Output Script File proct.txt
Doppler 143 Hz	Input Data File tn2
Target Range (optional) 150 bin	Output Weight File weights
CPI (optional) 6	
Target Extraction Information	RUN
Scan From: 140 To: 150 Interval: 11 bin	EXTRACT TARGET
Guard Interval 10 bin	CONVOLVE
Algorithm Selection	
<input checked="" type="checkbox"/> Conventional Beamformer	
<input checked="" type="checkbox"/> Fully Adaptive Weight	
<input checked="" type="checkbox"/> Cross Spectral Subspace Selection	
<input checked="" type="checkbox"/> Principal Component Selection	
<input checked="" type="checkbox"/> Element Space Pre-Doppler STAP	
<input checked="" type="checkbox"/> Element Space Post-Doppler STAP	
<input checked="" type="checkbox"/> Beam Space Pre-Doppler STAP	
<input checked="" type="checkbox"/> Beam Space Post-Doppler STAP	
<input checked="" type="checkbox"/> Displaced Phase Center Antenna	
Temporal DOF (Kt) 3	

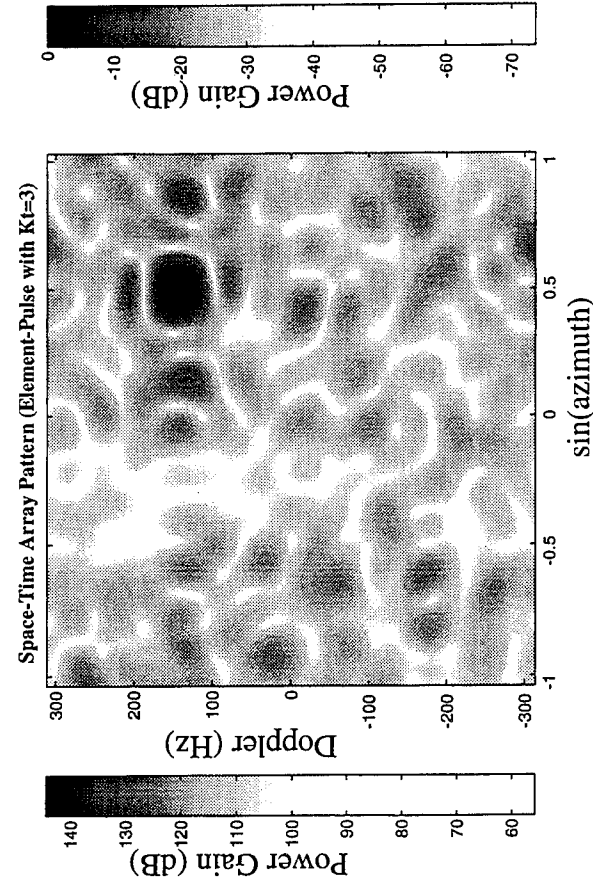
There are also simulation and display interfaces.

Resulting Plots

Snapshot Power Spectrum



Space-Time Array Pattern



CONSTRAINT OPTIMIZATION FOR PRE-DOPPLER STAP ALGORITHMS

Edward J. Baranoski

MIT Lincoln Laboratory
244 Wood Street
Lexington, MA 02173-9108
tel: (617) 981-0480
email: ejb@ll.mit.edu

Abstract Conventional pre-Doppler STAP algorithms perform adaptive clutter nulling for airborne radars over a portion of a coherent processing interval (CPI) and then non-adaptively combine the sub-CPI results using a Doppler constraint vector. This approach can be constructed as adaptively inflating the dimensionality of the problem followed by applying a non-adaptive constraint. Pre-Doppler algorithms have generally provided a decreased minimum detectable velocity (MDV) compared to post-Doppler algorithms since the pre-Doppler constraint is not optimal for the adapted sub-CPI outputs. Significant improvements in MDV can be obtained by allowing partial adaptivity in the constraint vector with only a fractional increase in computational complexity compared with conventional pre-Doppler techniques. This erases the performance improvement of post-Doppler over pre-Doppler algorithms. This presentation shows a subspace analysis of sub-CPI nulling which demonstrates how to minimize the computational complexity by optimally splitting the adaptivity between the clutter nulling and constraint vector optimization. This yields a multi-stage adaptive processing architecture employing low dimensionality nulling in each stage, allowing for greater parallelism and scalability.

CONSTRAINT OPTIMIZATION FOR PRE-DOPPLER STAP ALGORITHMS

**EDWARD J. BARANOSKI
MIT LINCOLN LABORATORY**

**ADAPTIVE SENSOR ARRAY PROCESSING WORKSHOP
MARCH 13, 1996**



960313-1

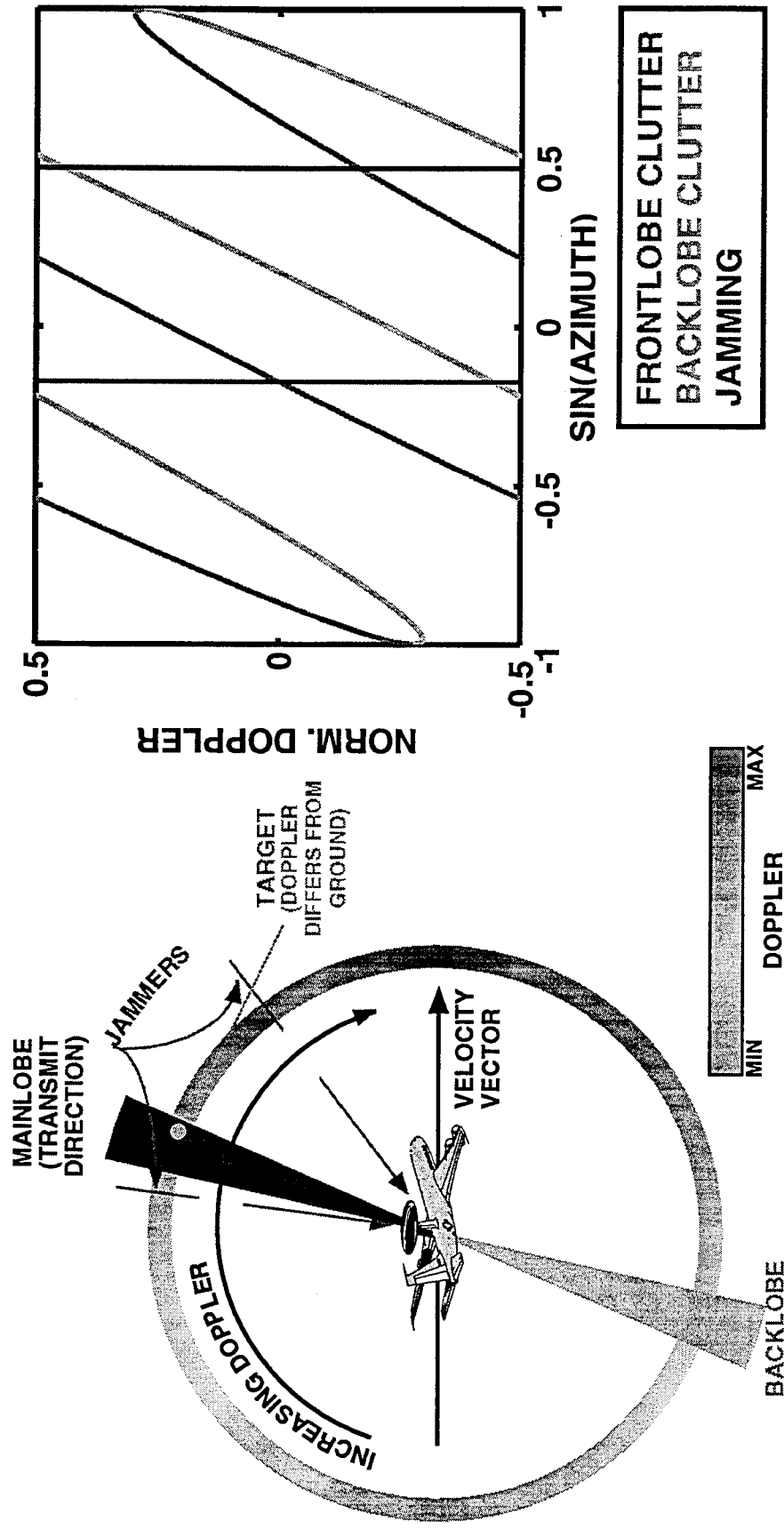
OUTLINE

- ➔ • INTRODUCTION
 - PRE-DOPPLER SPACE-TIME ADAPTIVE PROCESSING
- PRE-DOPPLER CONSTRAINT OPTIMIZATION
- PERFORMANCE COMPARISONS
- SUMMARY



960313-2

SPACE-TIME ADAPTIVE PROCESSING

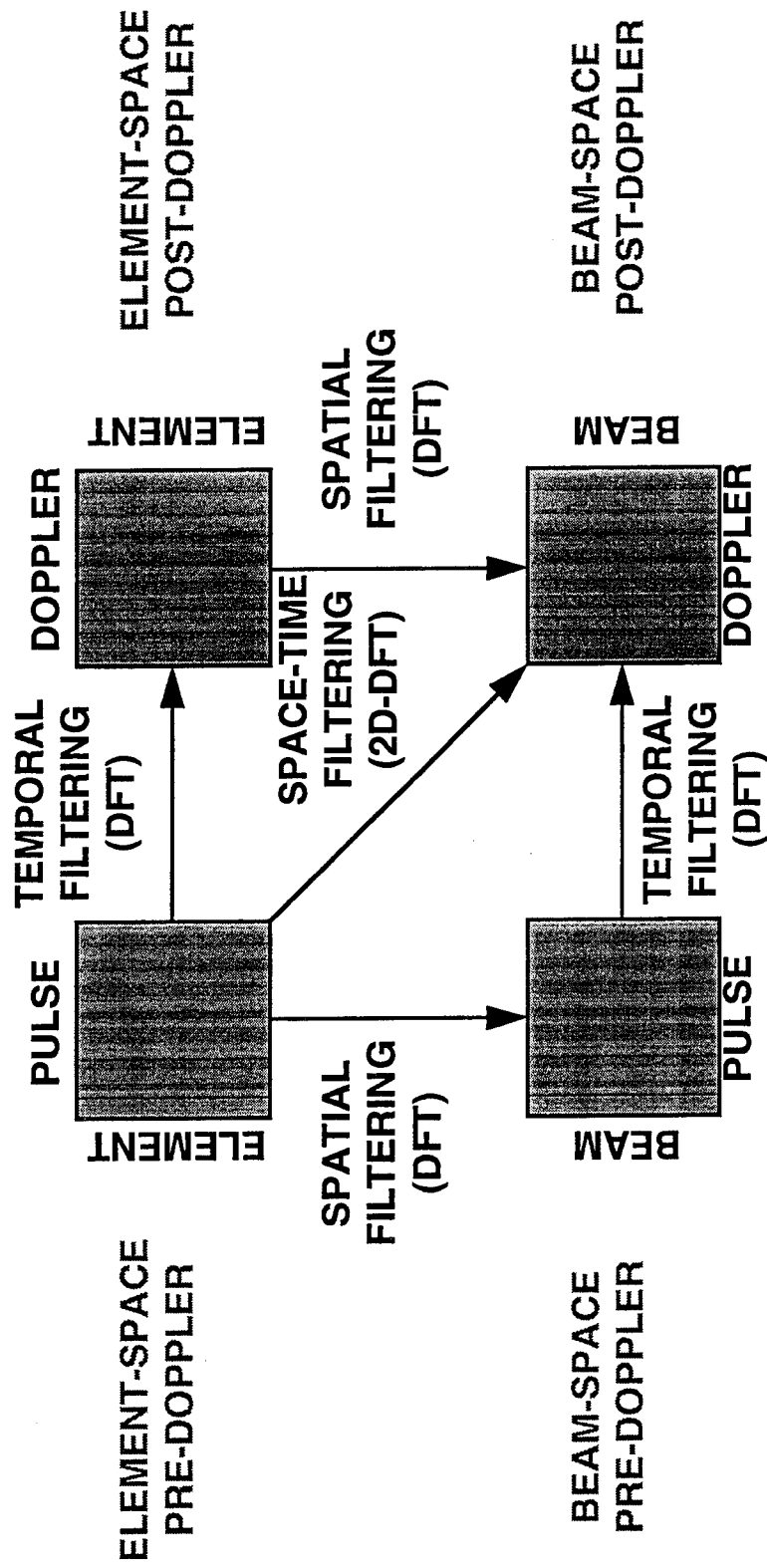


- SPATIAL NULLS FOR JAMMING
- SPACE-TIME NULLS FOR CLUTTER



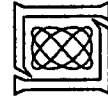
960313-3

A TAXONOMY OF STAP ARCHITECTURES



• ARCHITECTURES CLASSIFIED BY

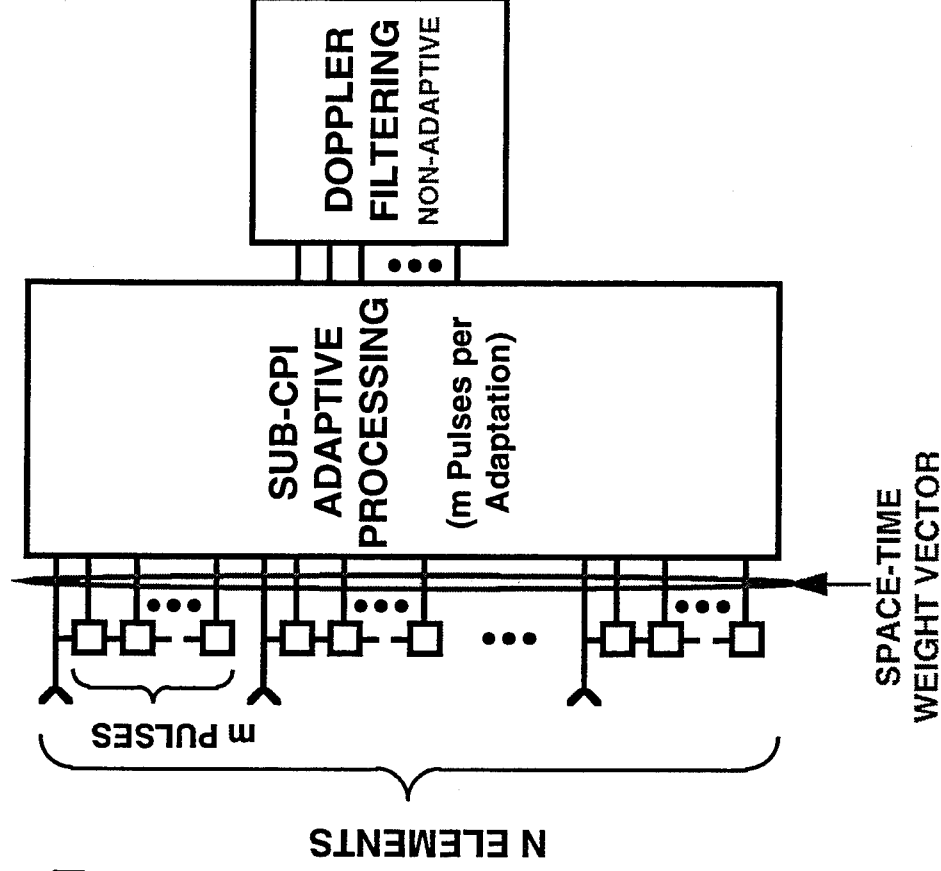
- TYPE OF PREPROCESSOR
- DOMAIN IN WHICH ADAPTIVE WEIGHTING OCCURS



960313-4

PRE-DOPPLER MOTIVATION

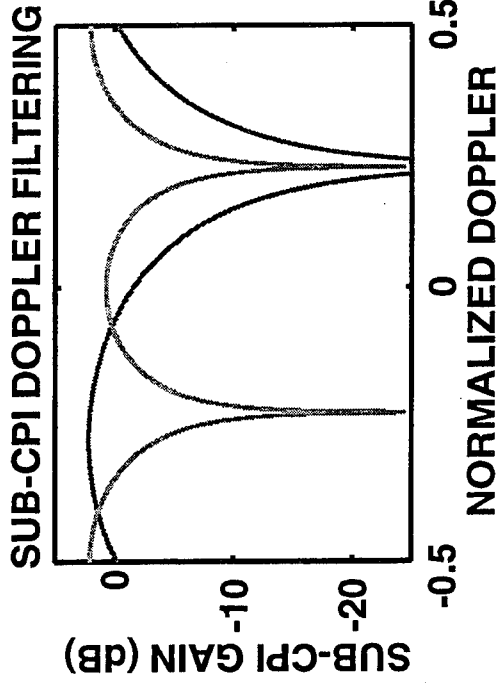
- ADAPT OVER m PULSE SUB-CPI
- MULTIPLE ADAPTATIONS PER CPI
- ALLOWS FOR CHANGING INTERFERENCE WITHIN CPI
 - NON-STATIONARY JAMMING
 - ROTATING ANTENNA
 - TERRAIN-SCATTERED INTERFERENCE
- FILTER ADAPTED OUTPUTS WITH NON-ADAPTIVE DOPPLER CONSTRAINT
- PERFORMANCE GENERALLY WORSE THAN POST-DOPPLER
- ARE NON-ADAPTIVE CONSTRAINTS SUFFICIENT?



960313-5

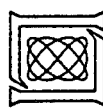
BINOMIAL PRE-DOPPLER

- SINGLE BEAMFORMER PER SUB-CPI
- SUB-CPI TEMPORAL CONSTRAINT NULLS FRONTLOBE CLUTTER
 - BINOMIAL TAPER USED, e.g. $m=3$
$$w_i = R_i^{-1} \begin{bmatrix} -e^{j2\pi d} \\ 2e^{j2\pi 2d} \\ -e^{j2\pi 3d} \end{bmatrix} \otimes \mathbf{v}$$
- APPLY SUB-CPI WEIGHTS TO EACH SUB-CPI VECTOR: $y_i = w_i^H x_i$
- DOPPLER COMBINE THE SUB-CPI OUTPUTS: $y = \sum_{i=1}^{M-2} y_i e^{j2\pi \phi_i}$



BINOMIAL TAPER
NULLS FRONTLOBE CLUTTER

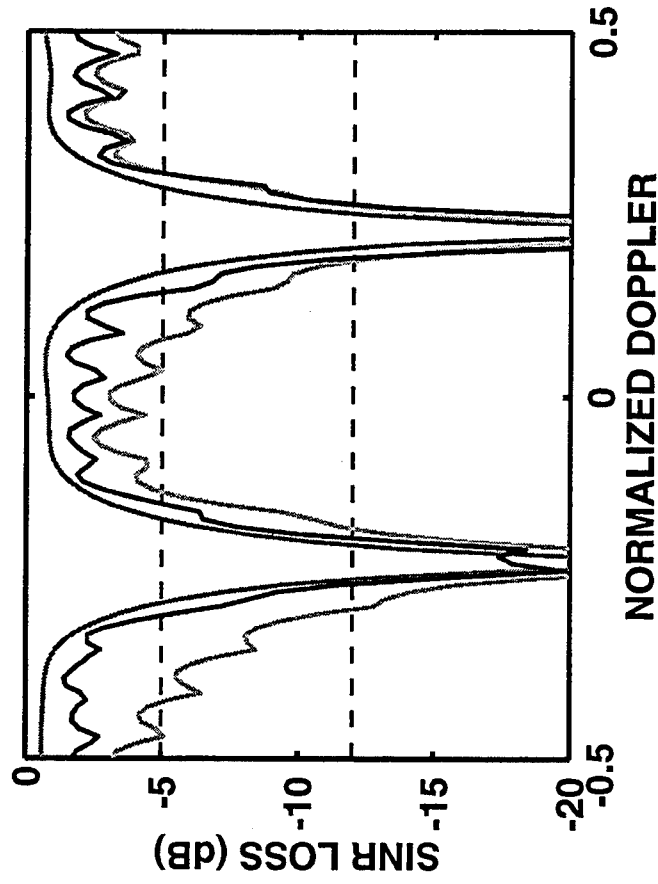
TWO-NULL TAPER
NULLS FRONT AND BACKLOBE CLUTTER



960313-6

PRE-DOPPLER PERFORMANCE BINOMIAL TAPER

- N = 18 ELEMENTS
- M = 18 PULSES
- CLUTTER FOLDOVER $\beta = 2.6$
- CNR = 50 dB (per ELEMENT per PULSE)
- 20 dB FRONT/BACK RATIO (TRANSMIT AND RECEIVE: -40 dB BACKLOBE/FRONTLOBE)
- 40 dB JAMMERS @ $-10^\circ, 30^\circ$
- 30 dB CHEBYSCHV TAPERS (AZIMUTH AND DOPPLER)



OPTIMAL TAPERED
PRI-STAG. POST-DOPPLER
BINOMIAL PRE-DOPPLER



960313-7

OUTLINE

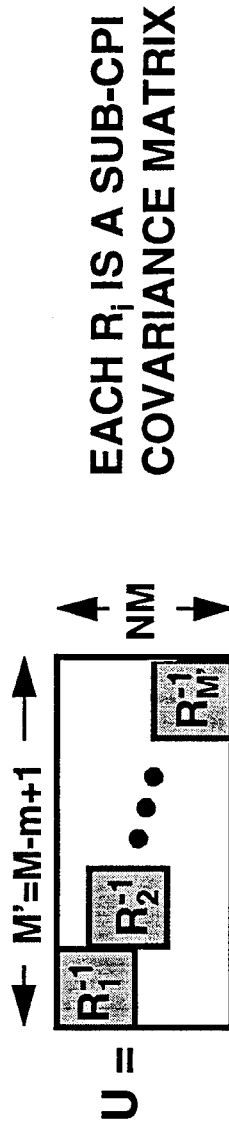
- INTRODUCTION
- ➡ • PRE-DOPPLER CONSTRAINT OPTIMIZATION
 - ADAPTIVE SUB-CPI TAPER
 - ADAPTIVE DOPPLER CONSTRAINT
- PERFORMANCE COMPARISONS
- SUMMARY

PRE-DOPPLER DATA TRANSFORMATION

- PREPROCESS WITH TRANSFORMATION MATRIX U : $w = U a$

$$\text{SINR} = \frac{|w^H(d \otimes v)|^2}{w^H R w} = \frac{|a^H U^H (d \otimes v)|^2}{a^H (U^H R U) a}$$

- UNDERCONSTRAINED: U HAS MORE COLUMNS THAN ROWS



- OPTIMAL SOLUTION POSSIBLE IF a IS UNCONSTRAINED
 - NEAR OPTIMAL SOLUTIONS WITH a CONSTRAINED



960313-9

SUB-CPI ADAPTIVITY

- MAXIMIZE SINR WITHIN THE i-th SUB-CPI

$$\text{SINR}_i = \frac{|a_i^H R_i^{-1} (d_i \otimes v)|^2}{a_i^H R_i^{-1} a_i} \Rightarrow a_i = R_i^{-1} (d_i \otimes v)$$

- OPTIMAL SUB-CPI WEIGHTS ARE MATCHED TO TARGET DOPPLER
- SINGLE SUB-CPI TAPER DESIRABLE COMPUTATIONALLY
 - USE $\tilde{a}_i = R_i^{-1} (t_i \otimes v)$ WHERE t_i MAXIMIZES SINR OVER DOPPLER SPACE
 - t_i IS MAXIMUM EIGENVECTOR OF $(m \times m)$ MATRIX $(I_m \otimes v)^H R_i^{-1} (I_m \otimes v)$
- ADAPTIVITY IN SUB-CPI COVARIANCE AND TEMPORAL TAPER

DOPPLER ADAPTIVITY

- PRE-DOPPLER USED NON-ADAPTIVE DOPPLER PROCESSING
 - VULNERABLE TO WEAK INTERFERENCE
 - CPI INTEGRATION NOT REFLECTED IN SUB-CPI ADAPTIVITY
- CORRELATION EXISTS IN SUB-CPI OUTPUTS
- ADAPT SUB-CPI OUTPUTS: $\mathbf{d}(\phi) = \mathbf{R}_s^{-1} \mathbf{u}(\phi)$
 - \mathbf{R}_s IS THE SUB-CPI COVARIANCE MATRIX
 - $\mathbf{u}(\phi)$ IS THE SUB-CPI FILTERED STEERING VECTOR CONSTRAINT

$$\mathbf{u}(\phi) = (\mathbf{I}_m \otimes \mathbf{t} \otimes \mathbf{v})^H \mathbf{U}^H (\mathbf{d} \otimes \mathbf{v})$$



PRE-DOPPLER ADAPTIVITY

FULL SPACE-TIME
PRE-DOPPLER
WEIGHT VECTOR

$$W = U (d \otimes t \otimes v)$$

LEVEL OF ADAPTIVITY

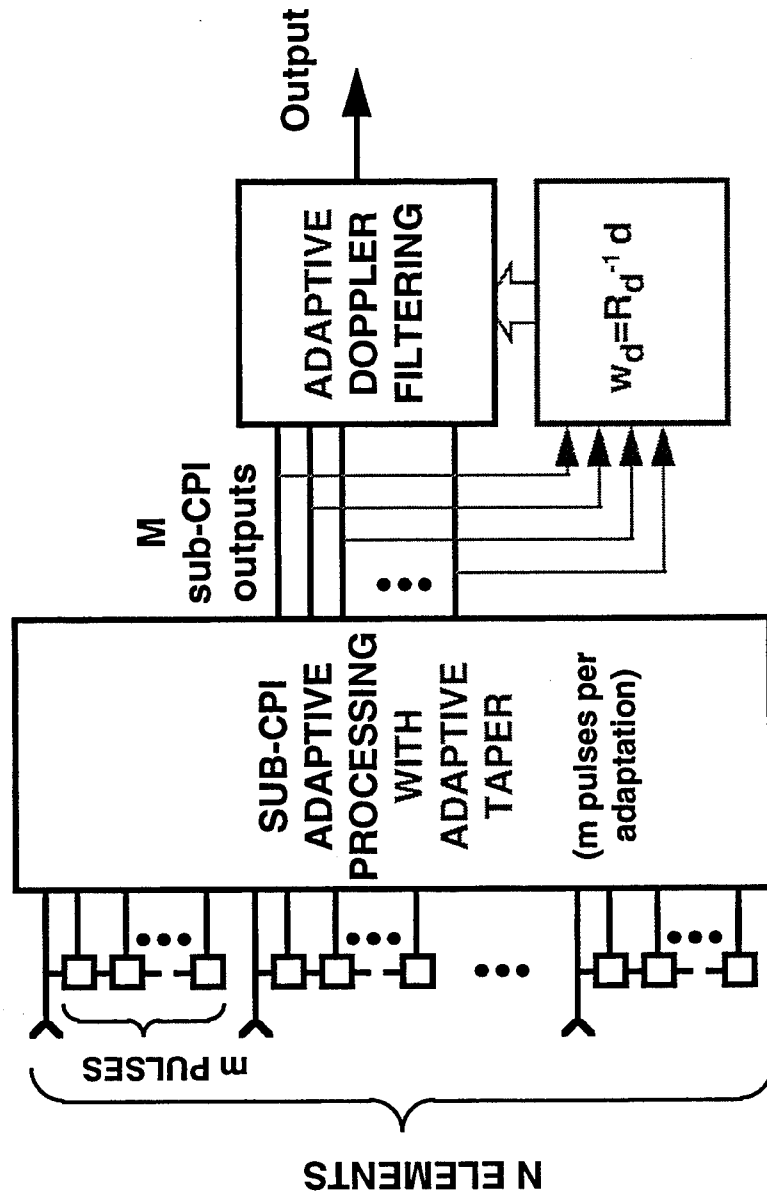
		LEVEL OF ADAPTIVITY	
		BINOMIAL	OPTIMALLY CONSTRAINED
	SPATIAL CONSTRAINT	FIXED	FIXED
	SUB-CPI TEMPORAL CONSTRAINT	FIXED	SUB-CPI
	DOPPLER CONSTRAINT	FIXED	CPI
DATA TRANSFORMATION MATRIX		SUB-CPI	SUB-CPI

- “FIXED” SPATIAL CONSTRAINT ALREADY OPTIMAL
- ADAPTIVE TEMPORAL CONSTRAINTS



960313- 12

OPTIMALLY CONSTRAINED PRE-DOPPLER



- SPACE-TIME PROCESSING EACH SUB-CPI WITH ADAPTIVE TAPER
- TEMPORAL ADAPTATION OF SUB-CPI LEVEL OUTPUTS
 - ADAPTATION COST NEGLIGIBLE
 - DOPPLER COST SMALL COMPARED TO BEAM APPLICATION



960313-13

COST OF OPTIMAL CONSTRAINT

	BINOMIAL PRE-DOPPLER	OPT. CONSTRAINED PRE-DOPPLER
ADAPTIVITY	$5 M (mN)^3$	$5M(mN)^3 + m^3 + 5M^3$
BEAMFORMING	$K(mNM + M \log_2 M)$	$K(mNM + M^2)$

SUB-CPI TEMP. CONSTRAINT
DOPPLER CONSTRAINT

- LARGEST INCREASE DUE TO NON-FFT DOPPLER FILTERING
 - ADAPTIVE COST NEGLIGIBLE
- EXAMPLE: LET $N=M=18$ AND $m=3$
 - ADAPTIVE PROCESSING INCREASES 0.2%
 - BEAMFORMING INCREASES 24%



960313- 14

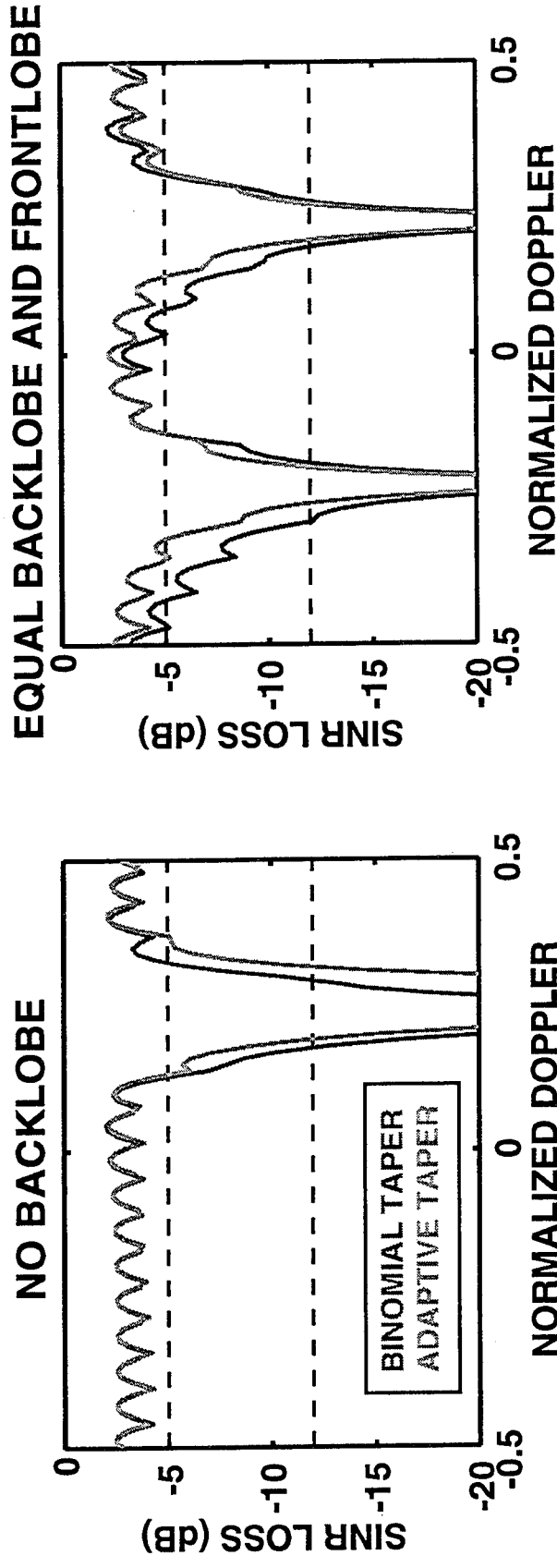
OUTLINE

- INTRODUCTION
- PRE-DOPPLER CONSTRAINT OPTIMIZATION
- ➡ • PERFORMANCE COMPARISONS
- SUMMARY



960313-15

COMPARISONS OF SUB-CPI TAPERS

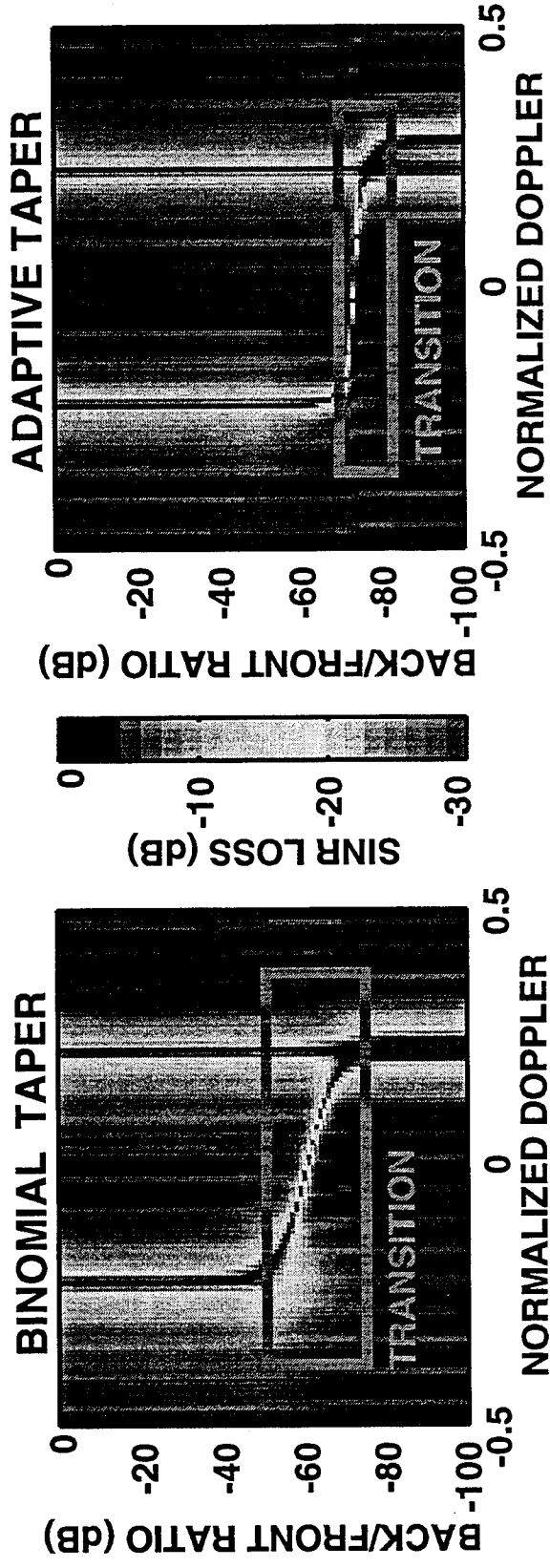


- WITH NO BACKLOBE, BINOMIAL TAPER IS BEST (A PRIORI)
 - ADAPTIVE TAPER SLIGHTLY BIASED DUE TO COVARIANCE EST.
- WITH BACKLOBE, ADAPTIVE TAPER BETTER SUITED



960313-16

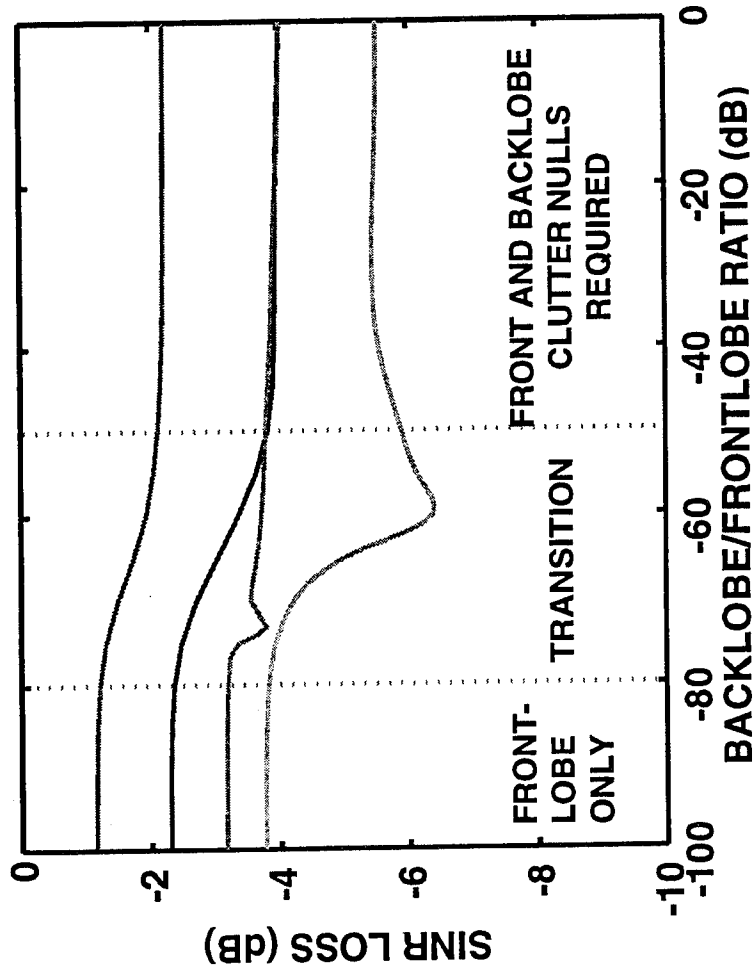
SUB-CPI TAPER EFFECTS ON SINR LOSS



- VERY LOW BACKLOBE: NULLING FOCUSES ON FRONTLOBE
- HIGH BACKLOBE: NULLING NULLS BOTH FRONT AND BACKLOBE
- TRANSITION: FRONTLOBE NULL SPLITS, MIGRATES TO BACK
 - SLOW MIGRATION OF BACKLOBE NULL WITH NON-ADAPTIVE TAPER



AVERAGE SINR LOSS vs. BACKLOBE POWER



OPTIMAL TAPERED
PRI-STAG. POST-DOPPLER
OPT. CONSTR. PRE-DOPPLER
BINOMIAL PRE-DOPPLER

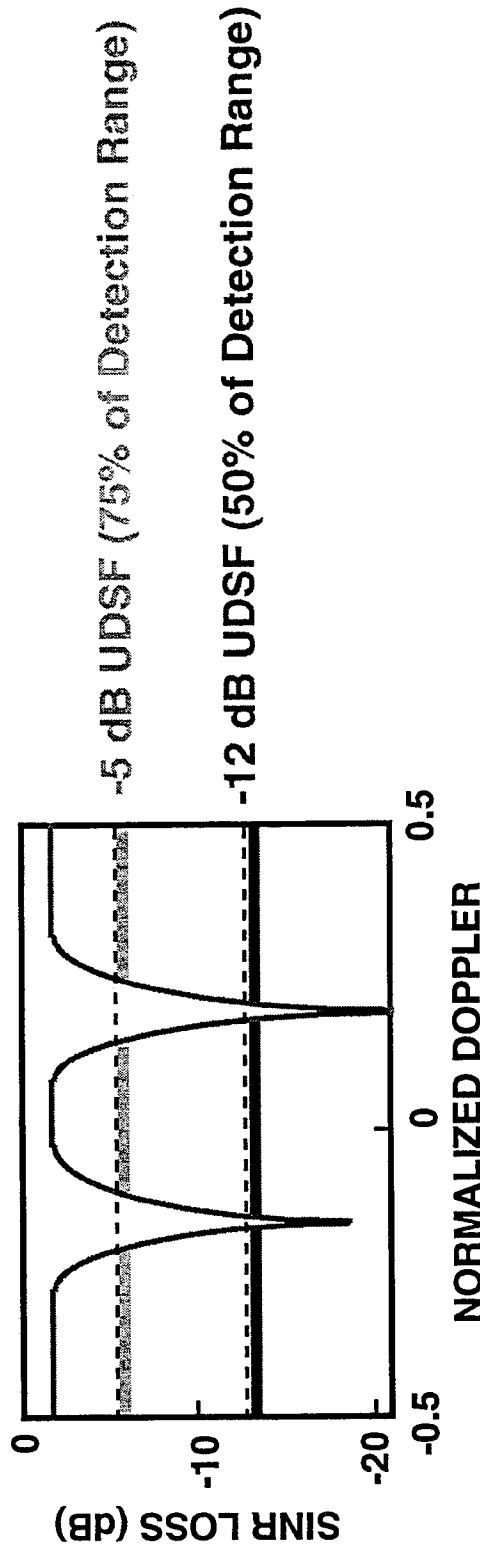
- OPTIMALLY CONSTRAINED PRE-DOPPLER PERFORMANCE COMPARABLE TO POST-DOPPLER



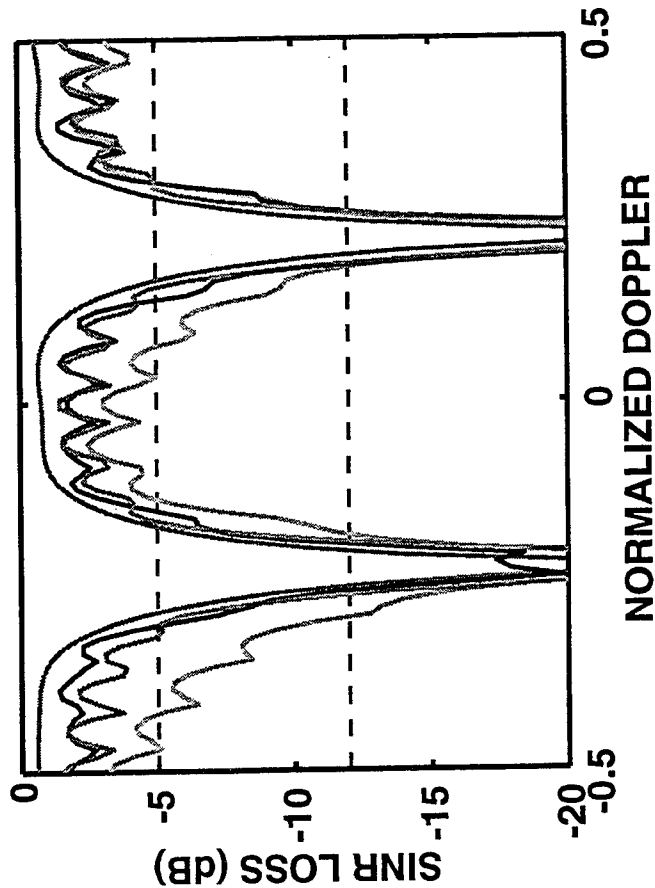
960313-18

PERFORMANCE METRICS

- SIGNAL TO INTERFERENCE PLUS NOISE RATIO (SINR)
- $\text{SINR LOSS} = \frac{\text{ADAPTIVE SINR}}{\text{INPUT SINR}}$
- AVERAGE SINR LOSS: MEAN SINR LOSS OVER DOPPLER
- USABLE DOPPLER SPACE FRACTION (UDSF):



OPTIMALLY CONSTRAINED PRE-DOPPLER PERFORMANCE

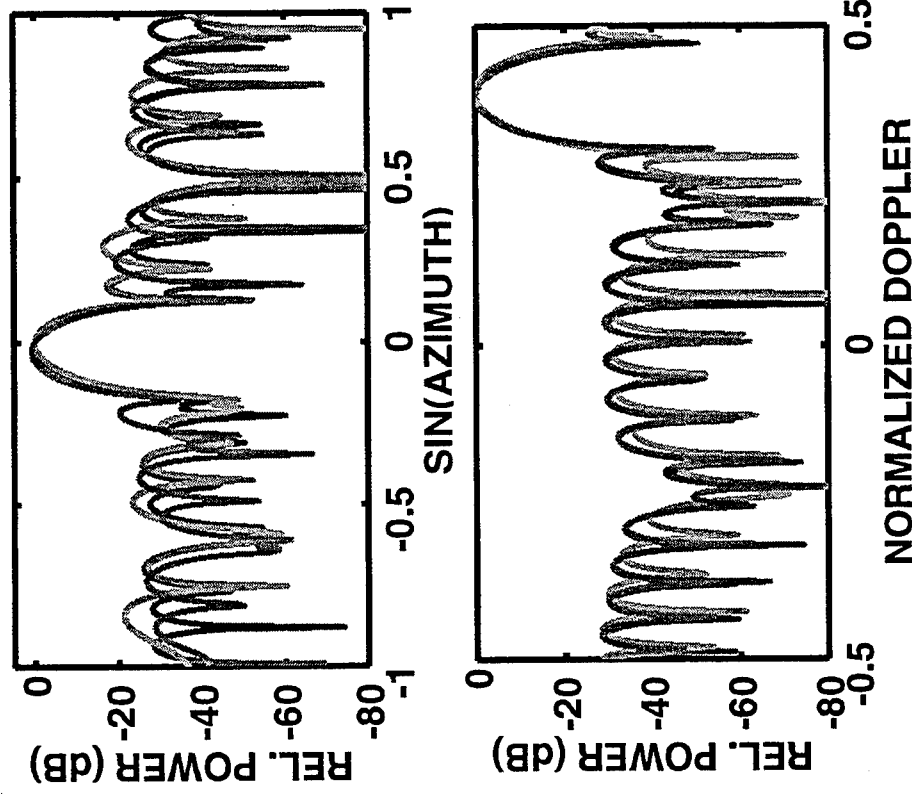
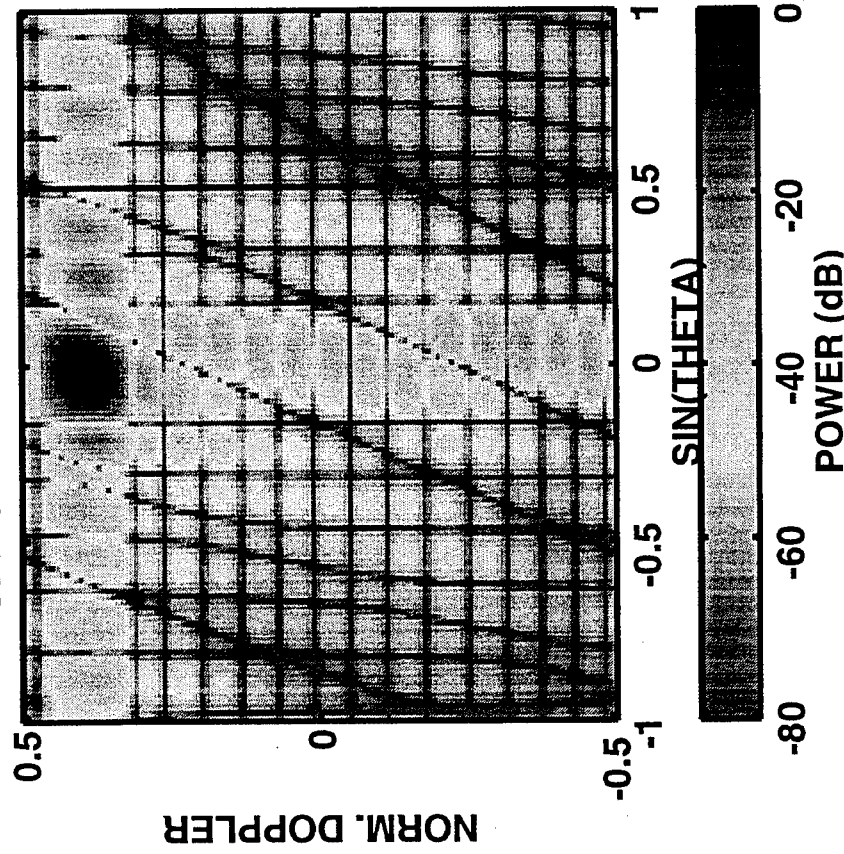


- OPTIMALLY CONSTRAINED PRE-DOPPLER CLOSES THE GAP WITH POST-DOPPLER

ALGORITHM	OPTIMAL TAPERED STAP	PRI-STAG. POST-DOPPLER	BINOMIAL PRE-DOPPLER	OPT. CONSTR. PRE-DOPPLER
AVG. SINR LOSS	-2.2 dB	-4.0 dB	-5.5 dB	-3.8 dB
UDSF (-5 dB)	78%	68%	48%	72%
UDSF (-12 dB)	90%	87%	81%	86%

ADAPTIVE PATTERNS

OPTIMALLY CONSTRAINED
PRE-DOPPLER
SPACE-TIME PATTERN



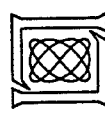
OPTIMUM TAPERED
BINOMIAL PRE-DOPPLER
OPT. CONST. PRE-DOPPLER



960313-21

OUTLINE

- INTRODUCTION
- PRE-DOPPLER CONSTRAINT OPTIMIZATION
- PERFORMANCE COMPARISONS
- ➡ • SUMMARY



9603 13- 22

SUMMARY

- **PRESENTED SYSTEMATIC FRAMEWORK FOR PRE-DOPPLER**
 - **MATCHED FILTER APPROACH USING CONSTRAINT OPTIMIZATION**
- **OPTIMALLY CONSTRAINED PRE-DOPPLER ALGORITHM**
 - **ADAPTIVE SUB-CPI TAPER**
 - **ADAPTIVELY COMBINE SUB-CPI OUTPUTS**
- **CLOSES PRE-DOPPLER PERFORMANCE GAP COMPARED WITH POST-DOPPLER**
- **USEFUL FOR ANY PARTIALLY ADAPTIVE ALGORITHM**



960313-23

DIRECT CLUTTER CANCELLATION FOR STAP

James McClellan, Greg Showman, and Ali Saidi

Georgia Institute of Technology

777 Atlantic Drive

School of Elec. and Comp. Engineering

Atlanta, GA 30332-0250

tel: (404) 894-8325

fax: (404) 853-9171

email: mclella@eedsp.gatech.edu

Abstract We have developed a two-dimensional FIR filtering method that can model signals with linear move-out. In the frequency domain, such signals have energy concentrated along a straight line. This method has recently been extended to the case where the signal energy lies along an approximate elliptical contour in frequency. In this presentation, we apply this method as a pre-processor for STAP, in which the 2-D filter would directly cancel clutter ridge energy present in airborne radar data prior to adaptive processing. This approach is the natural extension of two and three-point cancellers used in 1-D Doppler radars. The preprocessor is a low-order 2-D FIR filter whose coefficients can be parameterized in terms of the slope of a linear clutter ridge and/or the shape of an elliptical clutter ridge. The performance of this preprocessing approach in conjunction with adaptive processing are presented.

1996 ASAP WORKSHOP

DIRECT CLUTTER CANCELLATION for STAP

Georgia Tech / DSP

Prof. James H. McClellan

mcclella@eedsp.gatech.edu (404) 894-8325

Mr. Greg A. Showman

showman@eedsp.gatech.edu

Mr. Ali Saidi

saidi@eedsp.gatech.edu

Research sponsored in part by Air Force Rome Labs/ARPA contract # F03602-94-1-0014.
Computing facilities sponsored in part by NSF under Grant MIP-9295853 and the Hewlett-Packard Co.

Mar-1996 GT DSP Group

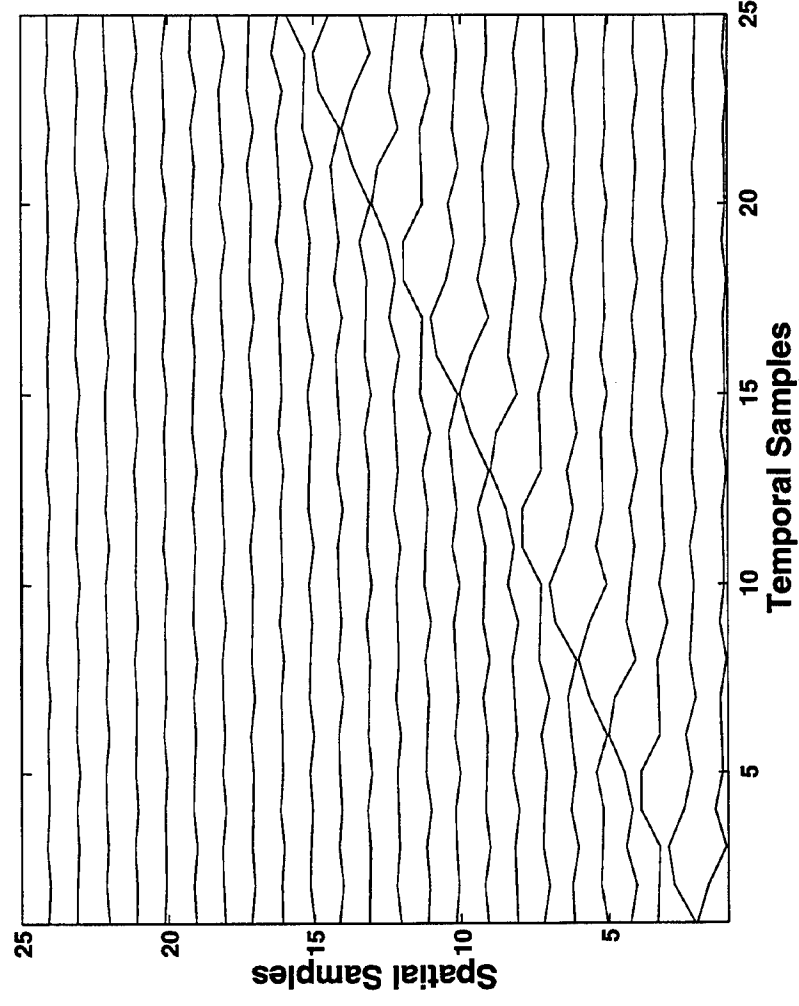
OUTLINE

- ZERO CONTOURS of MULTI-DIMENSIONAL FILTERS
 - FIR FILTERS of LOW ORDER
 - LINEAR MOVE-OUT
 - ELLIPTICAL CONTOURS
- CANCELLATION in DOPPLER/BEAM-SPACE
 - MOTIVATED by ONE-PULSE MTI CANCELLER
 - PRE-PROCESSING for FULLY ADAPTIVE STAP
- AUTOMATIC PARAMETER SELECTION for 2-D NULLING POLYNOMIALS
- SIMULATION EXAMPLE and PERFORMANCE STUDIES

LINEAR MOVEOUT – TIME

- 2-D SIGNAL WITH LINEAR MOVEOUT

- MOVEOUT SLOPE = $1/1.75$

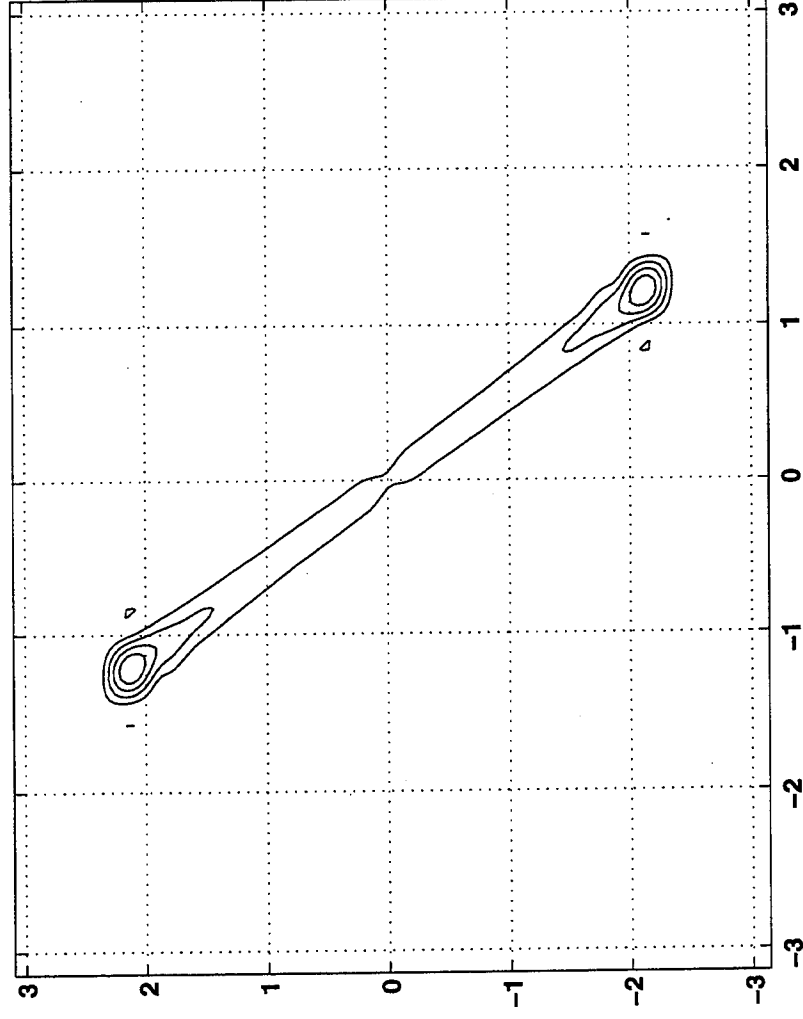


Mar-1996 GT DSP Group

LINEAR MOVEOUT – FREQUENCY

- FREQUENCY DOMAIN LINE: $\omega_2 = k\omega_1$

– SLOPE $k = -1.75$



2-D LINEAR PREDICTION

- 3×3 SUPPORT

$$a(n_1, n_2) = \begin{bmatrix} a(2,0) & a(2,1) & a(2,2) \\ a(1,0) & 2 & a(1,2) \\ a(0,0) & a(0,1) & a(0,2) \end{bmatrix}$$

- FREQUENCY RESPONSE:

$$A(e^{j\omega_1}, e^{j\omega_2}) = 1 + \sum_{(n_1, n_2) \in A} a(n_1, n_2) e^{-jn_1\omega_1} e^{-jn_2\omega_2}$$

- NULLING CONTOUR SATISFIES:

$$1 + a(0,0) \cos(\omega_1 + \omega_2) + a(1,0) \cos \omega_2 \\ + a(0,1) \cos \omega_1 + a(0,2) \cos(\omega_1 - \omega_2) = 0$$

- UNIT-CIRCLE ZEROS of $A(e^{j\omega_1}, e^{j\omega_2})$

NULLING CONTOUR

- LINEAR MOVEOUT:

$$x(n_1, n_2) = x_1(n_1 + kn_2)$$

- POWER SERIES EXPANSION LEADS TO QUADRATIC EQUATION:

$$(1 + a(0, 1))k^2 - 2(a(0, 0) - a(0, 2))k + (1 + a(1, 0)) = 0$$

- TWO DISTINCT SOLUTIONS FOR k

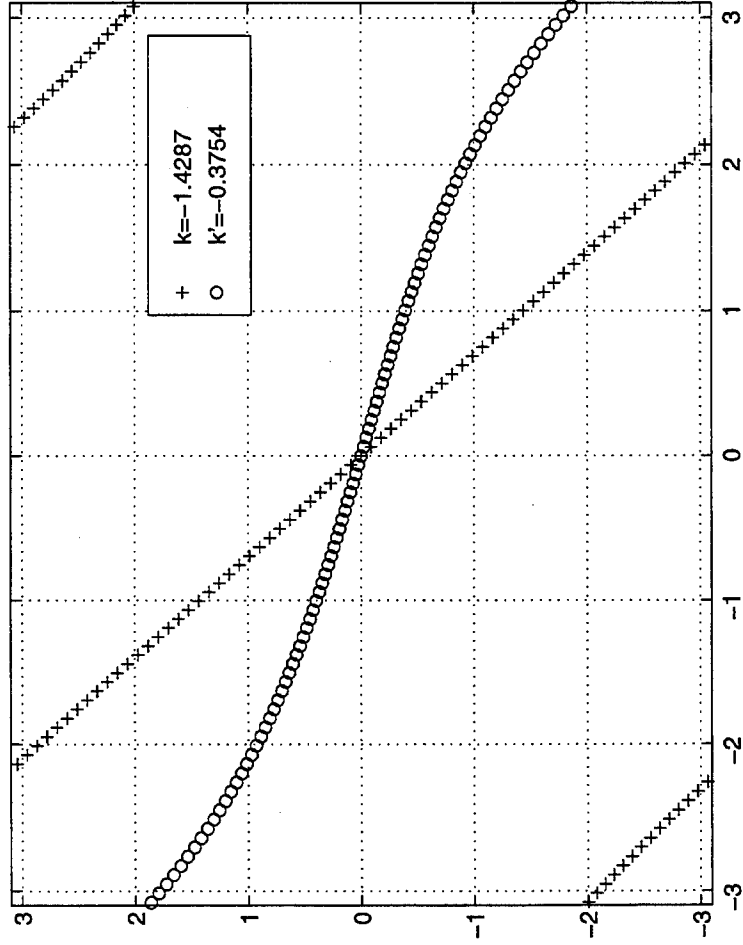
- PROPERTIES:

$$\begin{array}{llll} - |a(0, 0)| \gg |a(0, 2)| \approx 0 & \text{when} & k < 0 \\ - |a(0, 2)| \gg |a(0, 0)| \approx 0 & \text{when} & k > 0 \\ - |a(1, 0)| < |a(0, 1)| & \text{when} & |k| > 1 \\ - |a(1, 0)| > |a(0, 1)| & \text{when} & |k| < 1 \end{array}$$

ZEROS OF TYPICAL NULLING FILTER

- LINEAR MOVEOUT, 100 SCATTERERS

— TRUE SLOPE = -1.4287 via LINEAR PREDICTION



AUTOMATIC PARAMETER SELECTION

- GIVEN k , EVALUATE THE NULLING CONTOUR AT FOUR ARBITRARY VALUES OF (ω_1, ω_2) SUCH THAT $\omega_2 = k\omega_1$
- FOR EXAMPLE: CHOOSE $\omega_1 = 0, \frac{\pi}{2k}, \frac{\pi}{4k}, \frac{\pi}{8k}$
- SOLVE THE FOLLOWING SET OF EQUATIONS FOR $a(n_1, n_2)$:

$$\begin{bmatrix} 1 & 1 & 1 & 1 \\ \cos(\frac{(1+k)\pi}{2k}) & 0 & \cos(\frac{\pi}{2k}) & \cos(\frac{(1-k)\pi}{2k}) \\ \cos(\frac{(1+k)\pi}{4k}) & \cos(\frac{\pi}{4}) & \cos(\frac{\pi}{4k}) & \cos(\frac{(1-k)\pi}{4k}) \\ \cos(\frac{(1+k)\pi}{8k}) & \cos(\frac{\pi}{8}) & \cos(\frac{\pi}{8k}) & \cos(\frac{(1-k)\pi}{8k}) \end{bmatrix} \begin{bmatrix} a(0,0) \\ a(1,0) \\ a(0,1) \\ a(0,2) \end{bmatrix} = - \begin{bmatrix} 1 \\ 1 \\ 1 \\ 1 \end{bmatrix}$$

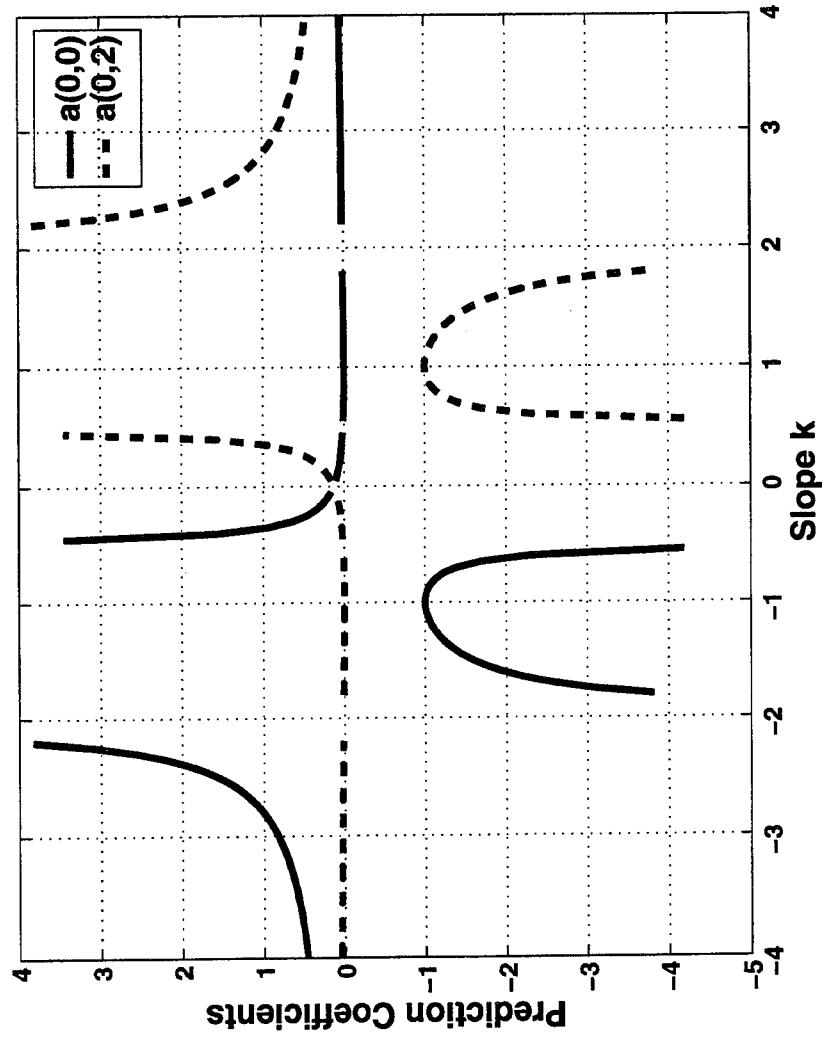
SLOPE \rightarrow FILTER COEFFS

- EXAMPLE: $k = -1.75$
- FIND THE FILTER COEFFICIENTS: $a(n_1, n_2)$

COEFF	TRUE	ESTIMATED
$a(0, 0)$	-3.0864	-3.0583
$a(0, 1)$	-0.2047	-0.1945
$a(1, 0)$	2.2801	2.2432
$a(0, 2)$	0.0110	0.0096
- COULD USE MORE THAN FOUR TIE DOWN POINTS
 - LEAST-SQUARES SOLUTION OF OVER-CONSTRAINED EQUATIONS
 - EQUIVALENT TO 2-D LINEAR PREDICTION

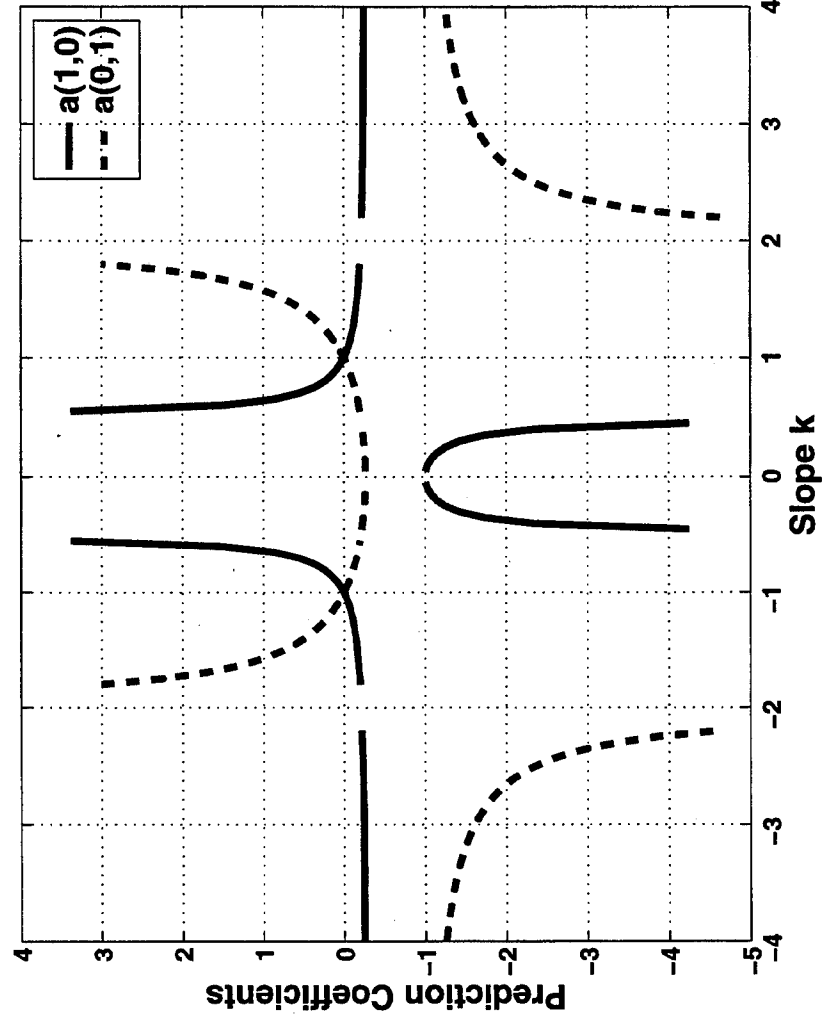
PREDICTION COEFFICIENTS – 1

- $a(0,0)$ and $a(0,2)$ VERSUS k



PREDICTION COEFFICIENTS – 2

- $a(1,0)$ and $a(0,1)$ VERSUS k



ELLIPTICAL CONTOUR

- ELLIPSE EQUATION:

$$\alpha\omega_1^2 + 2\beta\omega_1\omega_2 + \gamma\omega_2^2 = 1$$

- NULLING CONTOUR SATISFIES:

$$1 + a(0, 0) \cos(\omega_1 + \omega_2) + a(1, 0) \cos \omega_2 \\ + a(0, 1) \cos \omega_1 + a(0, 2) \cos(\omega_1 - \omega_2) = 0$$

- USE POWER SERIES EXPANSION:

$$\sigma - a(0, 0) \frac{(\omega_1 + \omega_2)^2}{2!} - a(1, 0) \frac{\omega_2^2}{2!} \\ - a(0, 1) \frac{\omega_1^2}{2!} - a(0, 2) \frac{(\omega_1 - \omega_2)^2}{2!} + \text{h.o.t} = 0$$

$$\text{WHERE } \sigma = 1 + a(0, 0) + a(1, 0) + a(0, 1) + a(0, 2)$$

ELLIPSE PARAMETER EVALUATION

- USE POWER SERIES TO FIND COEFFICIENTS:

$$\alpha = \frac{a(0,0) + a(0,1) + a(0,2)}{2\sigma}$$

$$\beta = \frac{(a(0,0) - a(0,2))}{2\sigma}$$

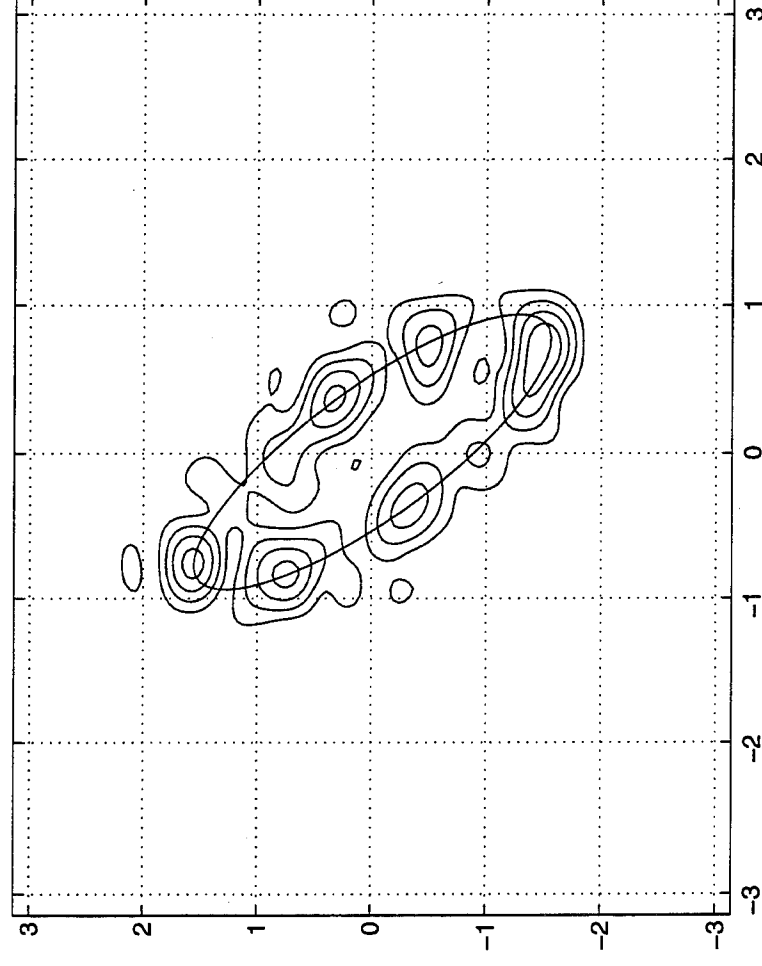
$$\gamma = \frac{a(0,0) + a(1,0) + a(0,2)}{2\sigma}$$

- EXAMPLE:
 - TRUE PARAMETERS: $\alpha = 3.5477$, $\beta = 1.7588$, $\gamma = 1.2772$
 - ESTIMATED PARAMETERS: $\alpha = 3.8444$, $\beta = 1.9100$ and $\gamma = 1.3390$
- EVALUATE THE ELLIPSE AT FOUR TIE DOWN POINTS
SOLVE LINEAR EQUATIONS TO FIND $a(n_1, n_2)$

ELLIPTICAL CONTOUR MATCH - 1

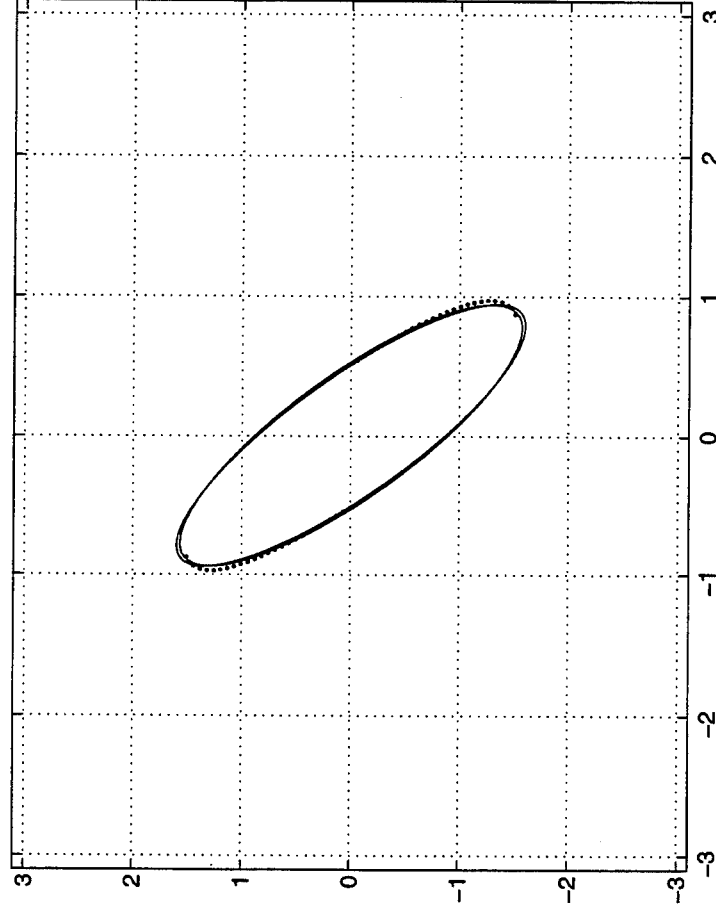
- 2-D DFT OF THE CLUTTER RIDGE SIGNAL

— $\alpha = 3.5477$, $\beta = 1.7588$, $\gamma = 1.2772$



ELLIPTICAL CONTOUR MATCH – 2

- ESTIMATED ELLIPSE FROM LINEAR PREDICTION
 - $\alpha = 3.8444$, $\beta = 1.9100$ and $\gamma = 1.3390$



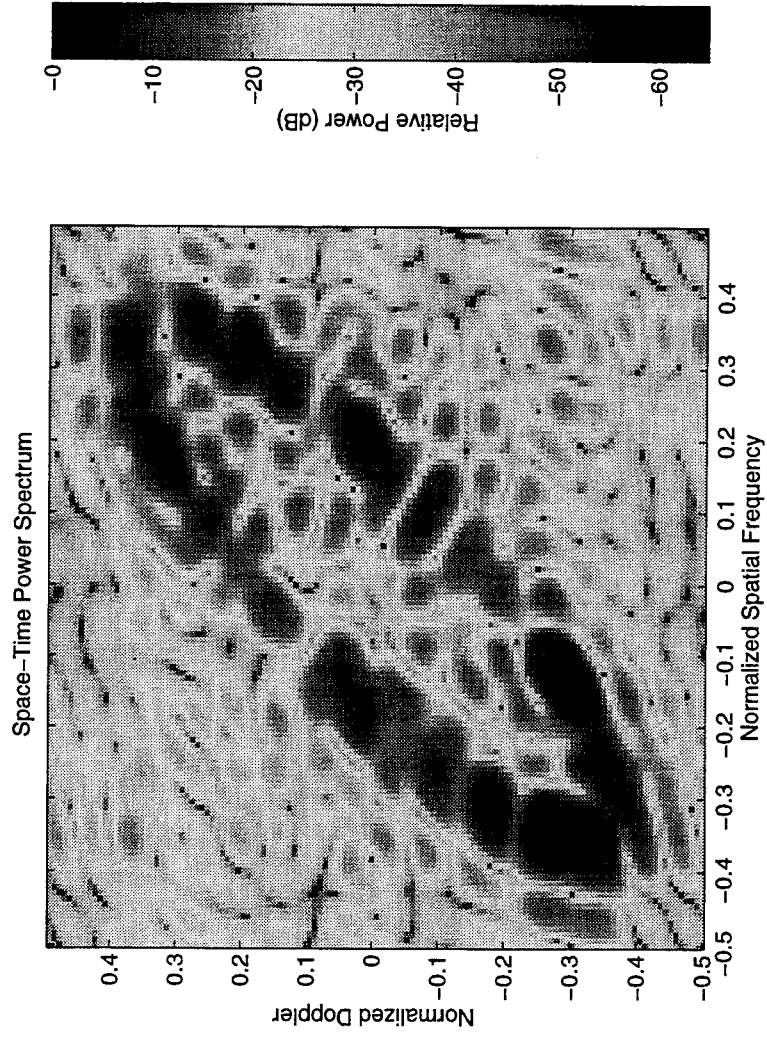
SAMPLE PROCESSING

- CLUTTER CANCELLATION
 - TWO PLOTS of DOPPLER-AZIMUTH SPECTRUM
 - SIGNAL PLUS ELLIPTICAL CLUTTER RIDGE
 - AFTER CANCELLATION with 3×3 FILTER
- PARAMETERS:
 - 14 ELEMENTS, 18 PRI SAMPLES
 - TARGET AT -20° , 150 Hz, $(f_1, f_2) = (-0.17, 0.24)$

	Case #1	Case #2 [†]
Element Separation ($\lambda/2$)	0.72	0.95
Ownship speed (1/unambig)	0.74	0.95
Array Rotation	30°	70°

TEST OF NULLING

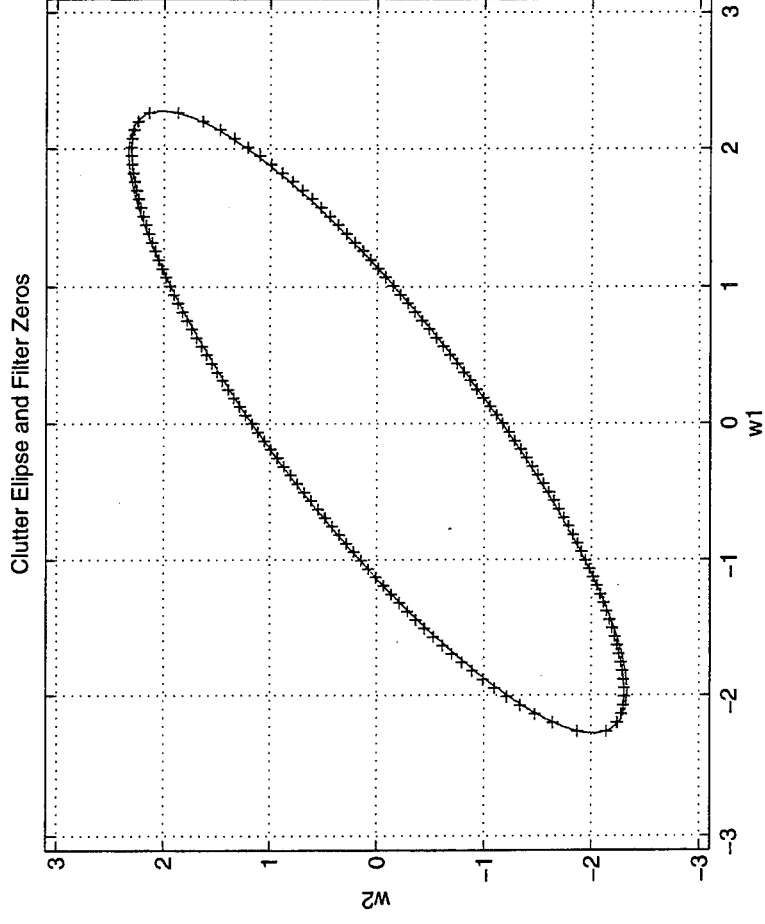
- TARGET PLUS CLUTTER ELLIPSE
 - SINGLE SPACE-TIME SNAPSHOT; SANDPAPER CLUTTER MODEL



NULLING CONTOUR

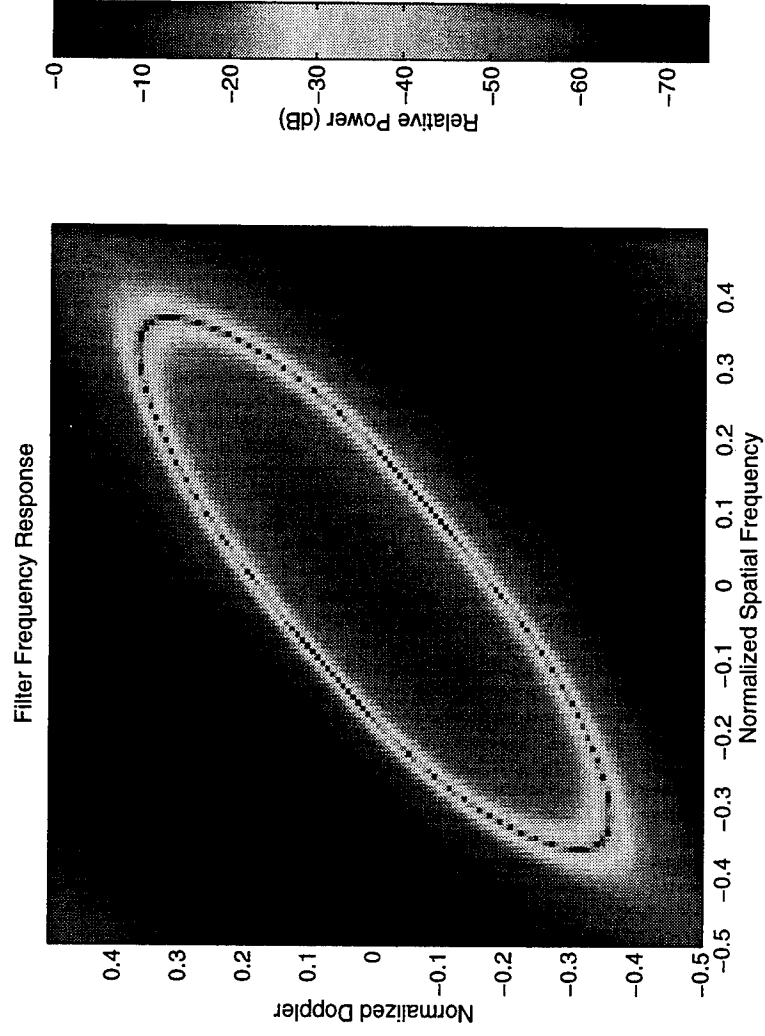
- COMPARED TO ELLIPSE

- IDEAL ELLIPSE (solid), FILTER ZEROS (+)



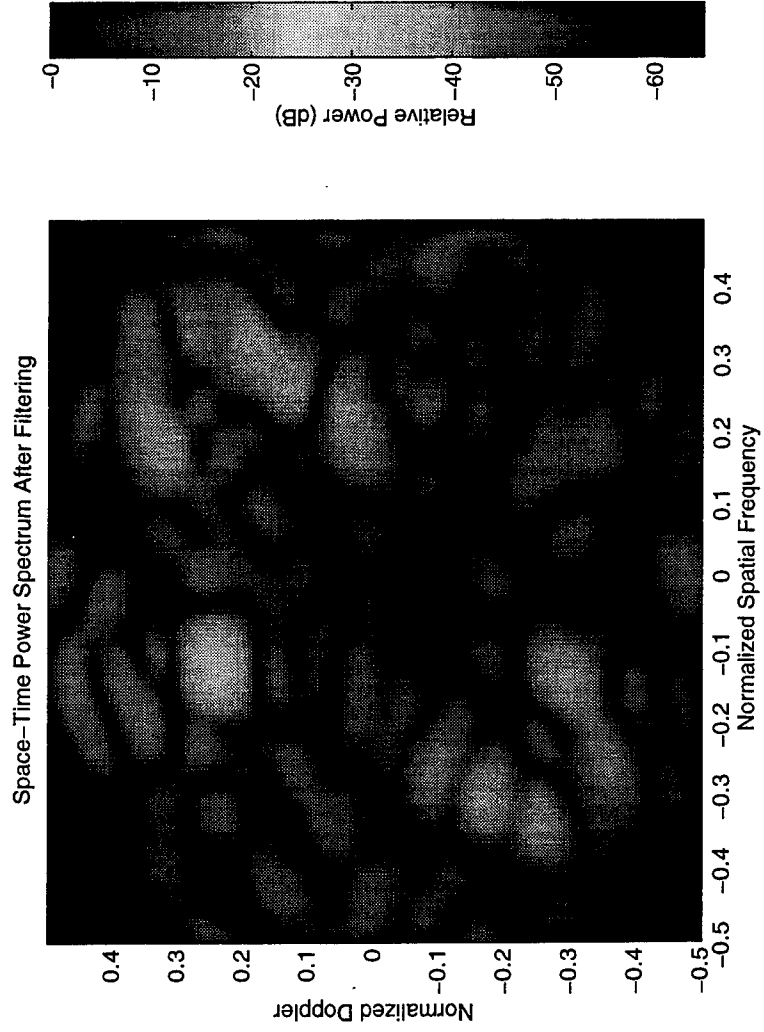
FREQUENCY RESPONSE

- ACTUAL NULLLING CONTOUR



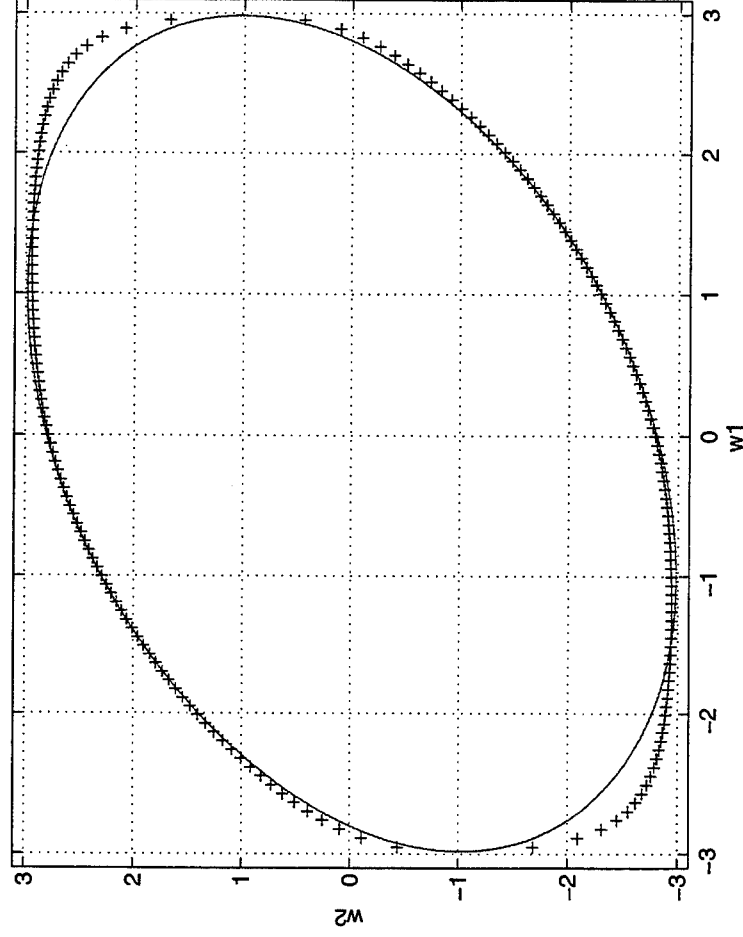
AFTER 2-D CANCELLER

- TARGET & CLUTTER RESIDUAL
 - TARGET AT $(-0.17, 0.24)$ EXCEEDS CLUTTER LEVEL



DEVIATION FROM ELLIPTICAL

- IF CLOSE TO NYQUIST IN ANGLE & DOPPLER
 - SPATIAL, DOPPLER EXTENTS = 0.95, MISALIGNMENT = 70°

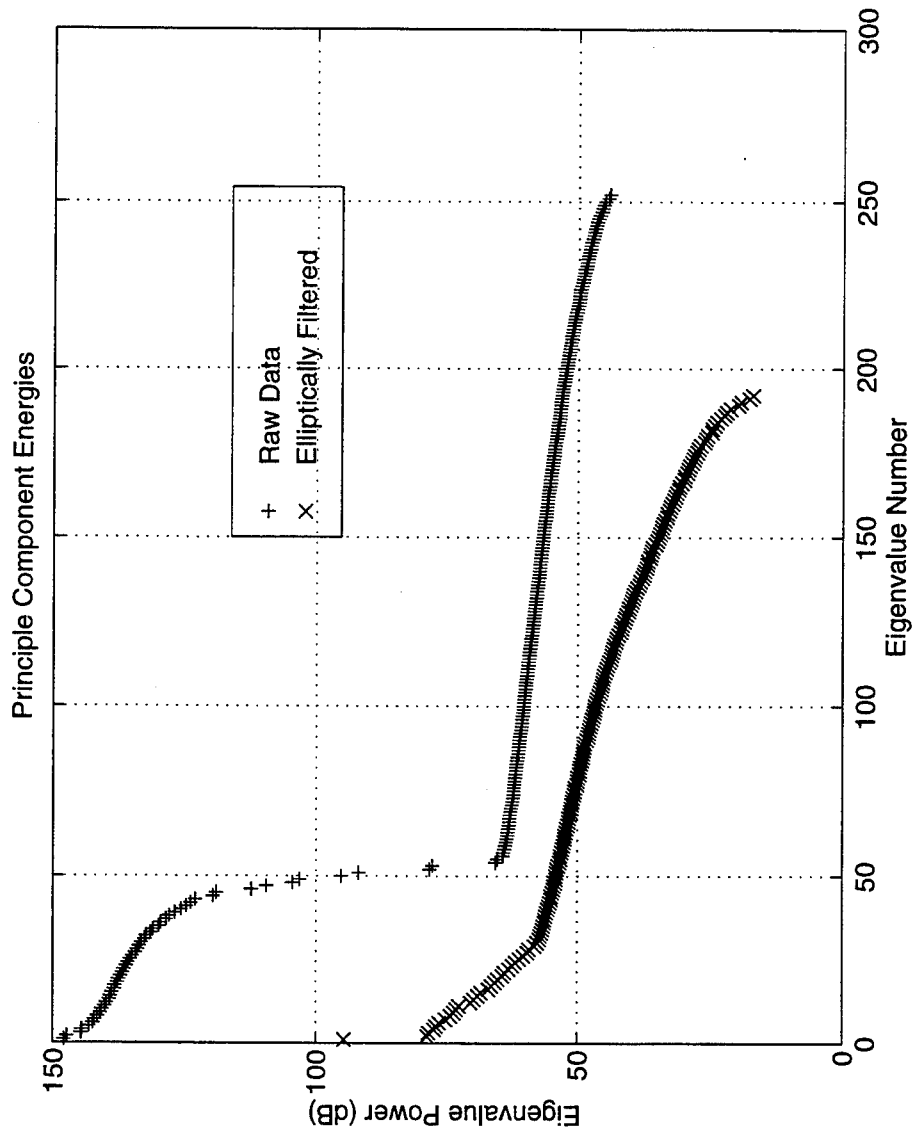


PERFORMANCE EXPERIMENTS

- PROCESSING SEQUENCE
 - CLUTTER NULLING IS NON-ADAPTIVE FRONT-END
 - FULLY ADAPTIVE STAP BACK-END
 - CAN WE SIMPLIFY ADAPTIVE BACK-END ?
- FIGURES OF MERIT
 - RANK OF SPACE-TIME DATA
 - * COMPARE EIGENVALUE SPREAD BEFORE & AFTER NULLING
 - SINR LOSS for SUB-OPTIMAL STAP
 - COMPARE 20 ALGORITHMS USING $(MT)^2$:
 - * BEAM-SPACE POST-DOPPLER (VARYING DOFs)
 - * ELEMENT-SPACE PRE-DOPPLER
 - * BEAMFORMING

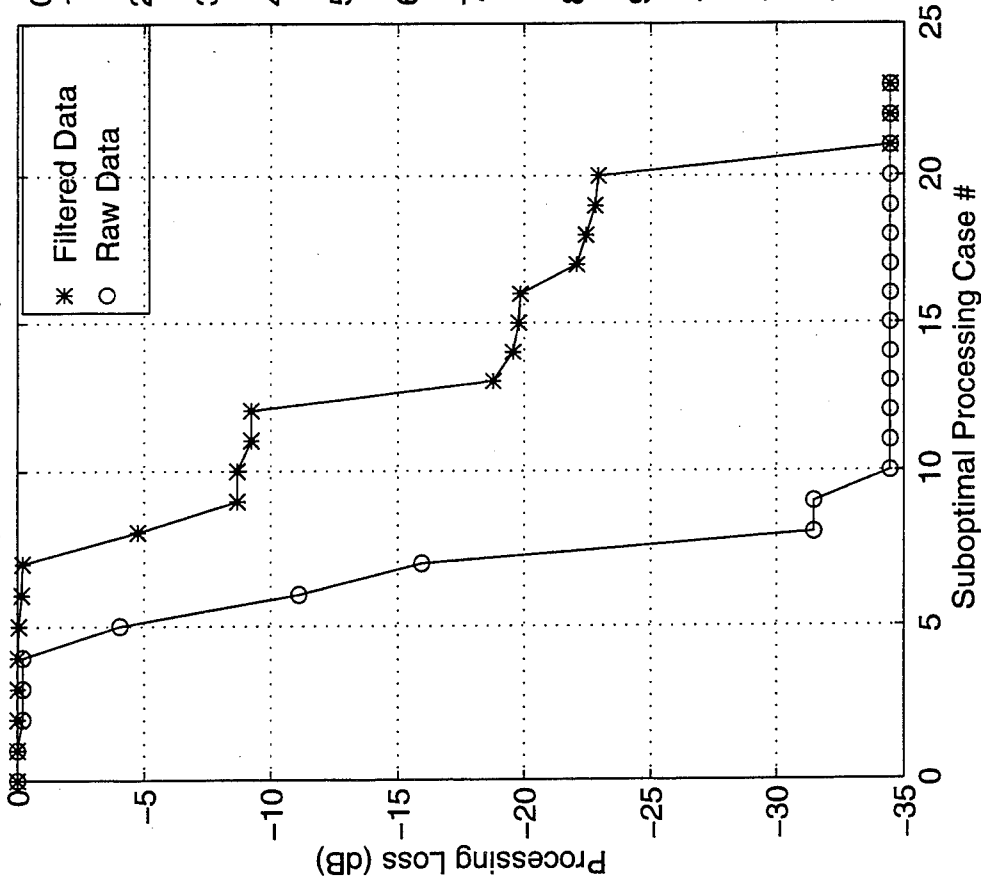
DOF AFTER NULLING

• EIGENVALUE BREAK AT APPROX 30



SUB-OPTIMAL PROCESSORS

Suboptimal Processing Losses



PROCESSING ALGORITHMS

0. Fully Adaptive STAP
1. Element-Space Pre-Doppler
DOF: 3 Temporal
2. Beam-Space Post-Doppler
DOF: 5 Spatial / 3 Temporal
3. Beam-Space Post-Doppler
DOF: 5 Spatial / 2 Temporal
4. Beam-Space Post-Doppler
DOF: 5 Spatial / 1 Temporal
5. Beam-Space Pre-Doppler
DOF: 5 Spatial / 3 Temporal
6. Beam-Space Pre-Doppler
DOF: 4 Spatial / 3 Temporal
7. Beam-Space Pre-Doppler
DOF: 3 Spatial / 3 Temporal
8. Conventional Beamforming
9. 2-D Hamming Windowing
10. Beam-Space Post-Doppler
DOF: 4 Spatial / 3 Temporal
11. Beam-Space Post-Doppler
DOF: 4 Spatial / 2 Temporal
12. Beam-Space Post-Doppler
DOF: 3 Spatial / 3 Temporal

CONCLUSIONS

- MULTI-DIMENSIONAL FILTERS HAVE WELL-DEFINED ZERO CONTOURS
- RELATE $a(n_1, n_2)$ TO ELLIPSE PARAMETERS
- 2-D CANCELLATION PROPOSED AS PRE-PROCESSOR FOR STAP
- SIMULATION EXAMPLE & PERFORMANCE STUDIES
- FUTURE WORK:
 - OTHER PERFORMANCE MEASURES
 - NOT SPATIALLY SHIFT INVARIANT: e.g., MUTUAL COUPLING

POWER SELECTED TRAINING FOR FALSE ALARM MITIGATION IN AIRBORNE RADAR

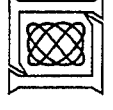
Daniel J. Rabideau and Allan O. Steinhardt

MIT Lincoln Laboratory
244 Wood Street
Lexington, MA 02173-9108
tel: (617) 981-2892
email: danr@ll.mit.edu

Abstract STAP algorithms have been shown to be very effective in localizing and nulling ground clutter in homogeneous environments. However, false alarms due to moderate and strong clutter disretes continue to be a problem. This is because the depth of the adaptive clutter null depends on the amount of representative clutter in the sample correlation matrix. Since clutter is often quite non-homogeneous (e.g., due to varying terrain), conventional training strategies may not select range gates containing enough clutter. This, in turn, may lead to weaker clutter nulls, clutter breakthrough, and ultimately false alarms. New techniques, such as Clutter Editing, can identify some of these false alarms during the detection stage. However, a complementary approach that works directly in the adaptive nulling stage would be desirable. This presentation shows a data-adaptive method for selecting the range gates used to form the sample correlation matrix. The technique, called Power Selected Training, results in deeper clutter nulls by choosing a subset of the most powerful range gates for training. Using the Mountaintop Data Library, we demonstrate the improved clutter nulling ability of Power Selected Training when compared with conventional training approaches. We also examine performance issues such as SINR and MDV, as well as computational aspects.

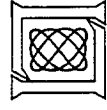
POWER SELECTED TRAINING FOR FALSE ALARM MITIGATION IN AIRBORNE RADAR

**Daniel Rabideau and Allan Steinhardt
MIT Lincoln Laboratory**

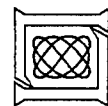
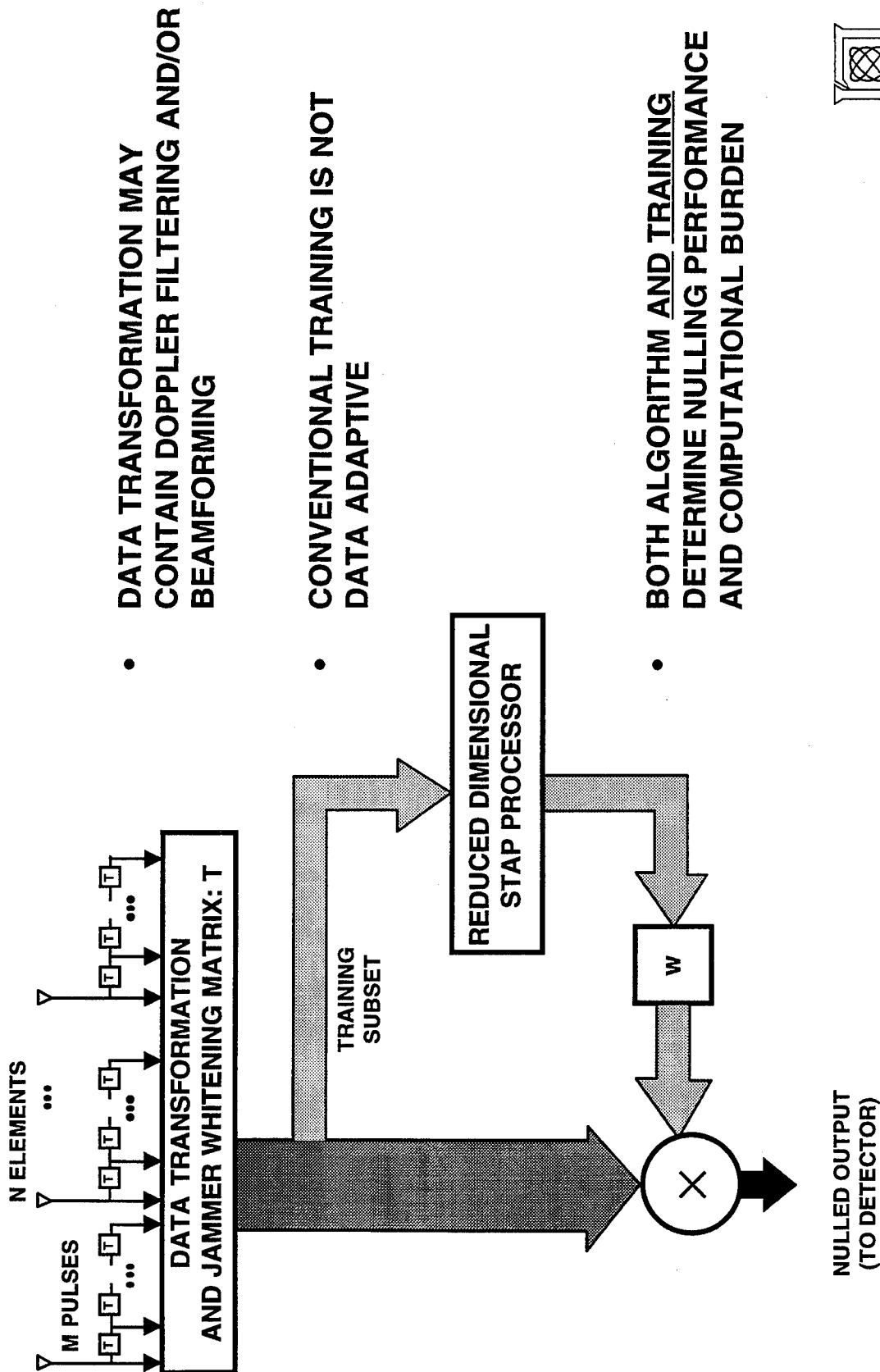


OUTLINE

- ➔ • INTRODUCTION
- POWER SELECTED TRAINING
- POWER SELECTED DE-EMPHASIS
- DATA ANALYSIS
- SUMMARY

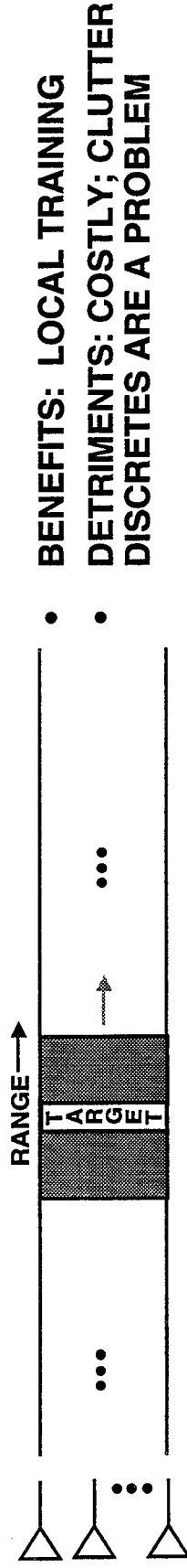


INTRODUCTION

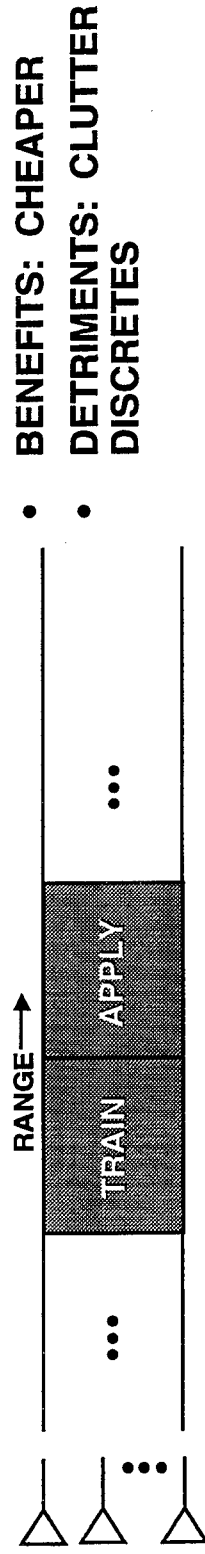


CONVENTIONAL TRAINING STRATEGIES

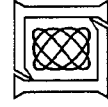
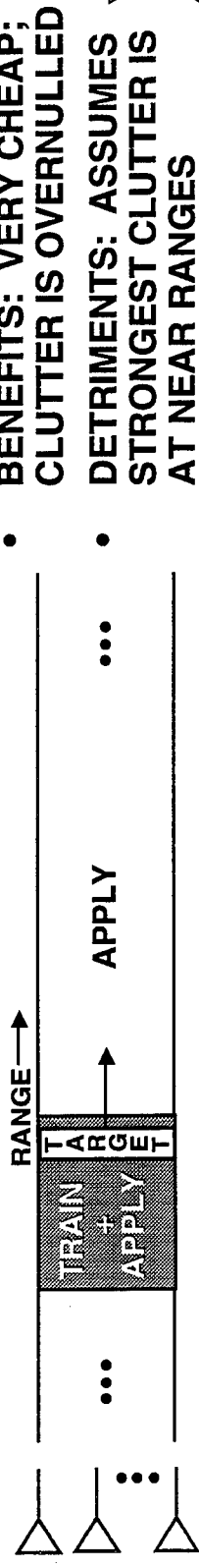
SLIDING WINDOW WEIGHT TRAINING



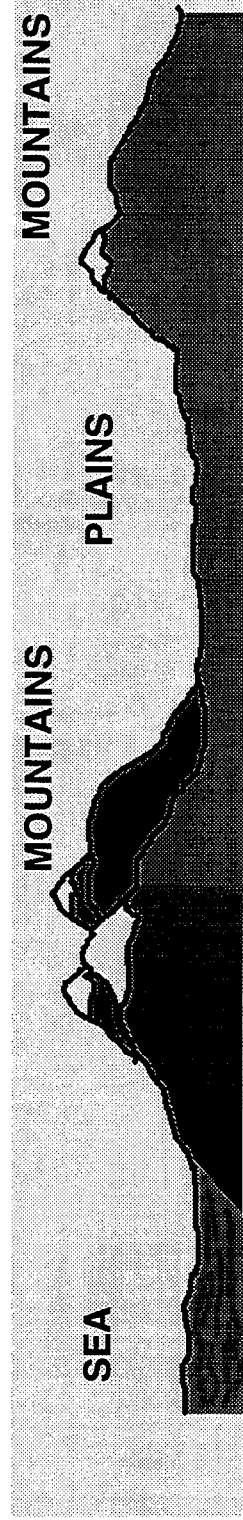
RANGE SEGMENTATION TRAINING



FIXED, SLIDE AND FREEZE TRAINING



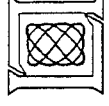
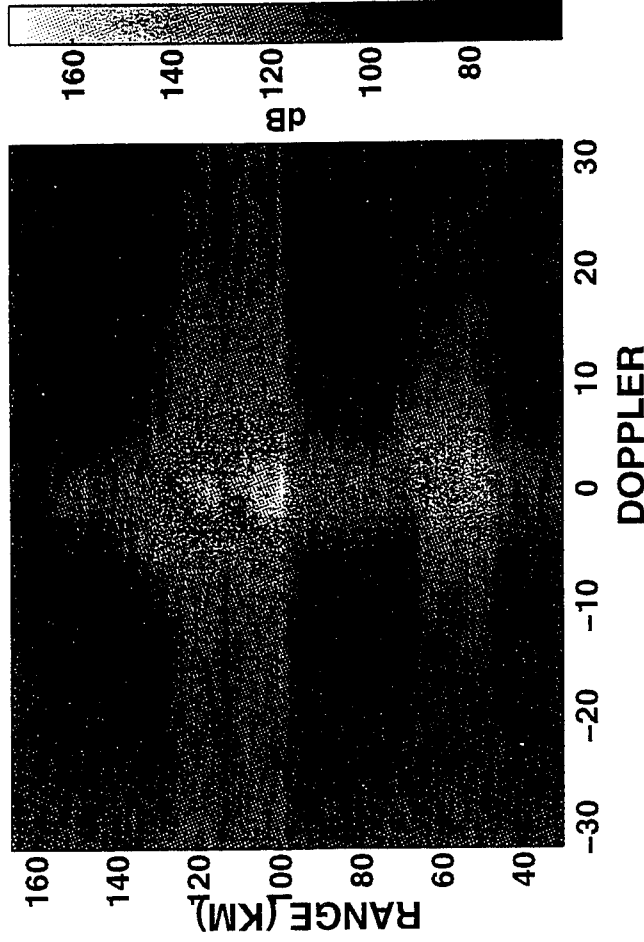
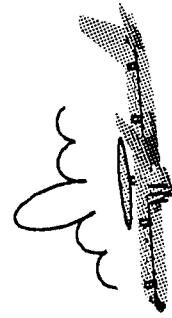
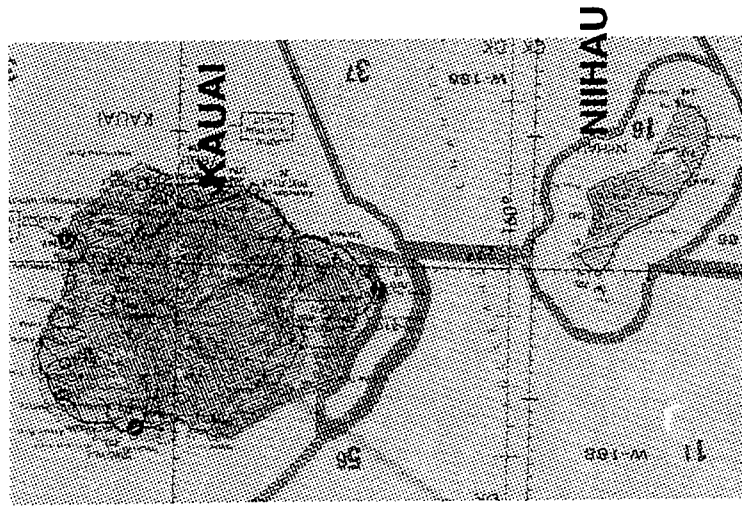
TERRAIN DIFFICULTIES: LAND/SEA DESERT/MOUNTAIN INTERFACES




- **HETEROGENEOUS TERRAIN <==> CLUTTER DISCRETES**
 - CONVENTIONAL TRAINING STRATEGIES ARE VULNERABLE
- **WE NEED A NEW TRAINING STRATEGY THAT:**
 - GENERATES NULLS DEEP ENOUGH FOR STRONG DISCRETES
 - HAS LOW COMPLEXITY, LIKE SLIDE & FREEZE TRAINING
- **WE ARE WILLING TO OVERNULL WEAKER CLUTTER**

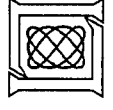


EXAMPLE: NONADAPTIVE RANGE-DOPPLER MAP (RLSTAP SIMULATED DATA)



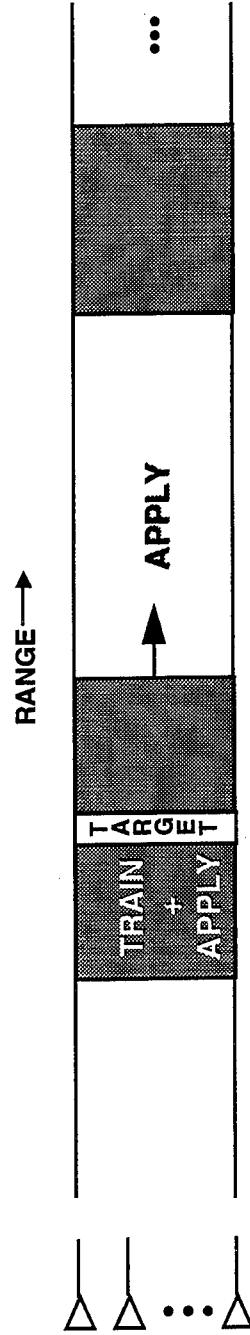
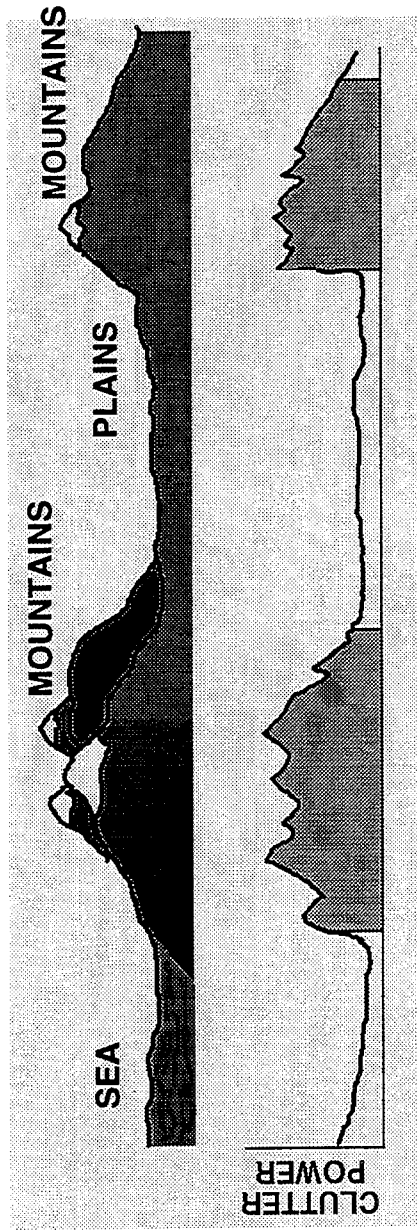
OUTLINE

- INTRODUCTION
-  POWER SELECTED TRAINING
- POWER SELECTED DE-EMPHASIS
- DATA ANALYSIS
- SUMMARY

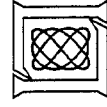




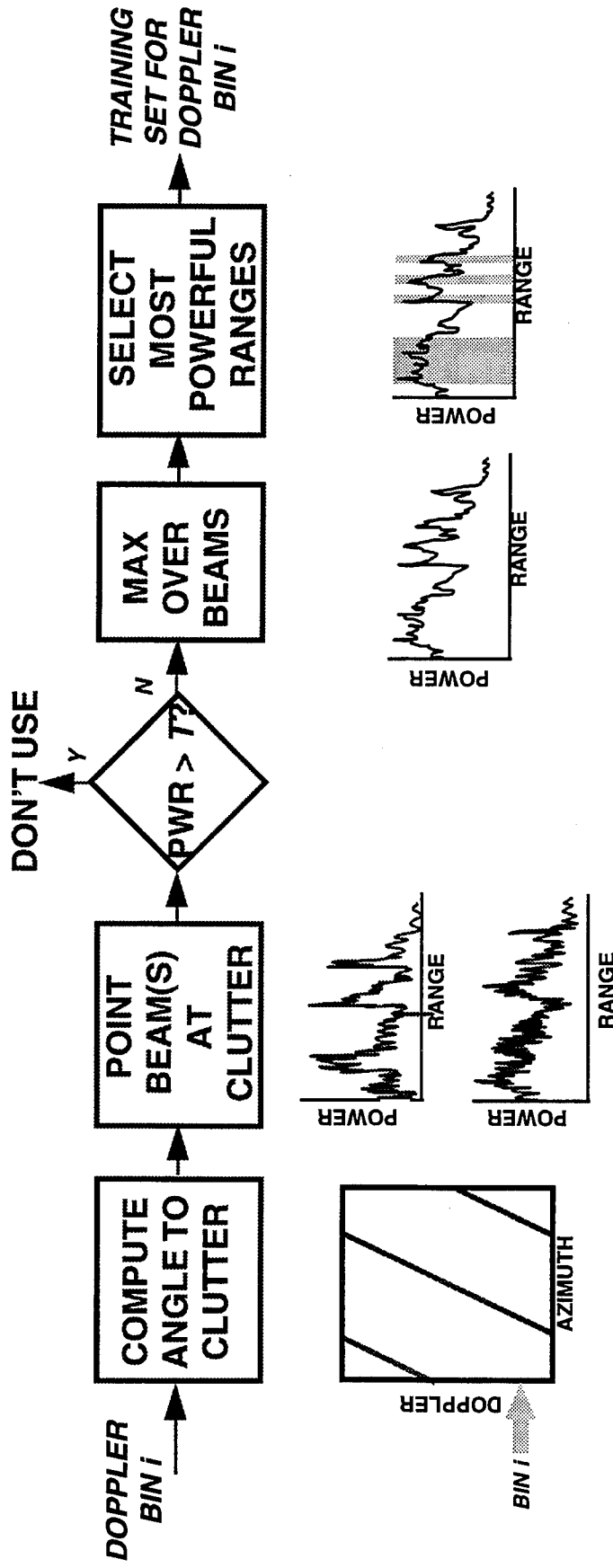
POWER SELECTED TRAINING



- NULL DEPTH \Leftrightarrow AVERAGE CLUTTER POWER IN TRAINING SET
- TRAINING ON STRONG CLUTTER WILL DRIVE DEEP NULLS



POWER SELECTED TRAINING (POST DOPPLER VERSION)



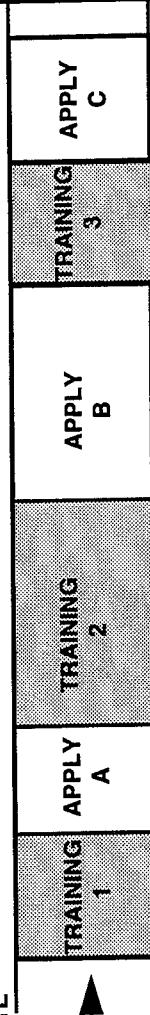
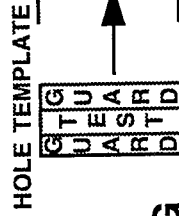
- THRESHOLD PREVENTS TRAINING ON GATES WHICH ARE A/D SATURATED OR EXCEED CANCELLATION RATIO
- USE MULTIPLE BEAMS FOR:
 - DOPPLER FOLDOVER OR BACKLOBE
 - NARROW BEAMWIDTH RELATIVE TO DOPPLER RESOLUTION (OR: USE A SPOILED BEAM).



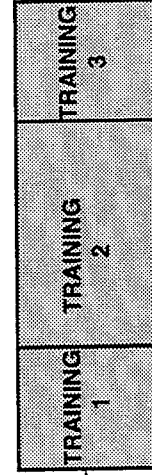
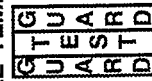
IMPLEMENTATION OF SLIDING HOLE WITH POWER SELECTED TRAINING

OPTION A:

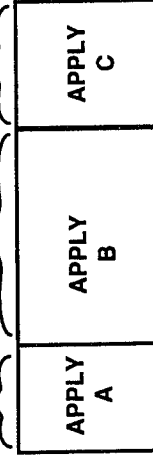
- HOLE SLIDES THROUGH DISCONNECTED TRAINING REGIONS
- LOCATION & SIZE OF DOWNDATA IS DATA DEPENDENT



HOLE TEMPLATE

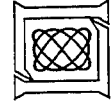


WEIGHTS:




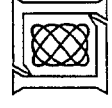
OPTION B:

- CONCATENATED TRAINING REGIONS
- SIMPLIFIED CONTROL-FLOW
- GUARD GATES MAY NOT BORDER TEST CELL



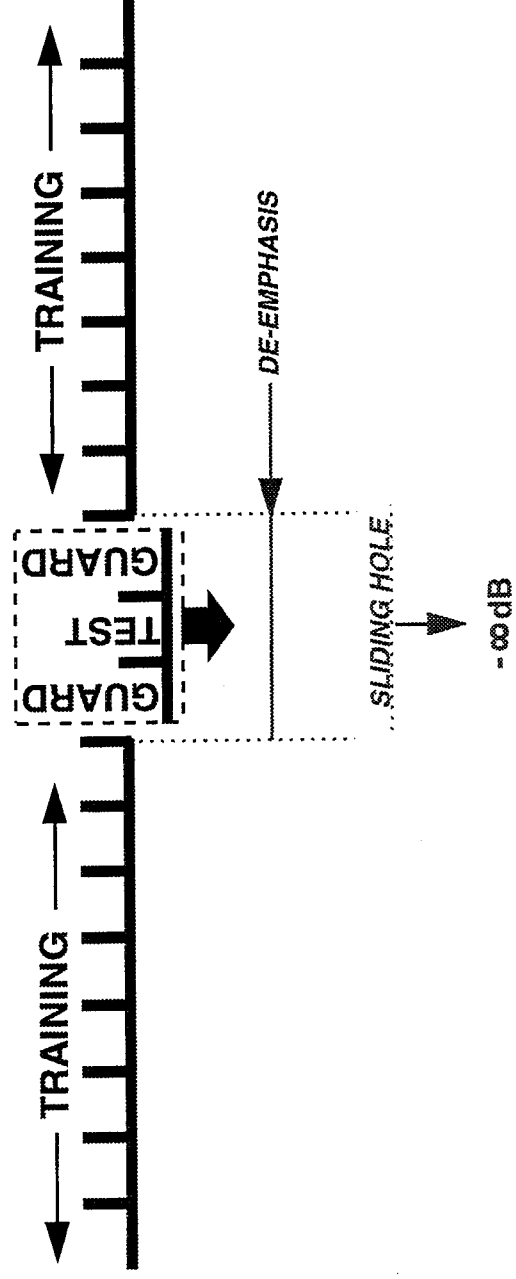
OUTLINE

- INTRODUCTION
- POWER SELECTED TRAINING
-  POWER SELECTED DE-EMPHASIS
- DATA ANALYSIS
- SUMMARY



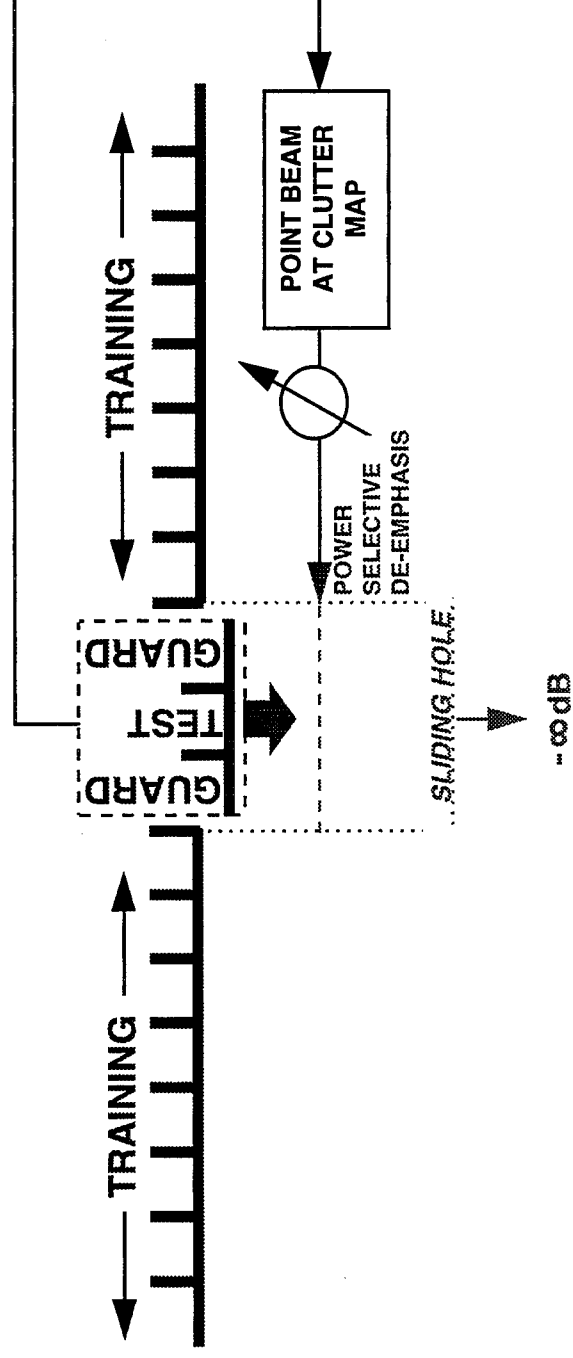
DE-EMPHASIS

- TRAINING SET RETAINS A FRACTION OF THE ENERGY FROM THE TEST CELL & GUARD GATES
 - SUPPRESSES CLUTTER AT TEST CELL
 - POTENTIAL FOR SINR LOSS ON STRONG TARGETS



POWER SELECTIVE DE-EMPHASIS

- THE FRACTION TO BE RETAINED IS CHOSEN ADAPTIVELY AFTER MEASURING THE CLUTTER'S STRENGTH
 - REDUCES POTENTIAL FOR SINR LOSS
 - » E.G., WEAKER CLUTTER => RETAIN LESS
- ADDED COMPLEXITY: INSIGNIFICANT
 - ALREADY MEASURING THE CLUTTER IN EACH BIN



EXAMPLE: MEDIAN DE-EMPHASIS

MEDIAN COMPUTATION

DOPPLER
BIN i

POINT BEAM(S)
AT CLUTTER

MAXIMIZE
OVER
BEAMS

COMPUTE
MEDIAN FOR
TRAINING SET

CLUTTER MAP, C

MEDIAN, M

ADAPTATION

RANGE
GATE r

YES
NO
 $C(r) > M?$

$R - XX^H$

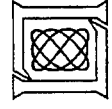
$R - \gamma XX^H$

NULLING

R = FULL TRAINING SET COVARIANCE ; X = TEST & GUARD CELLS

OUTLINE

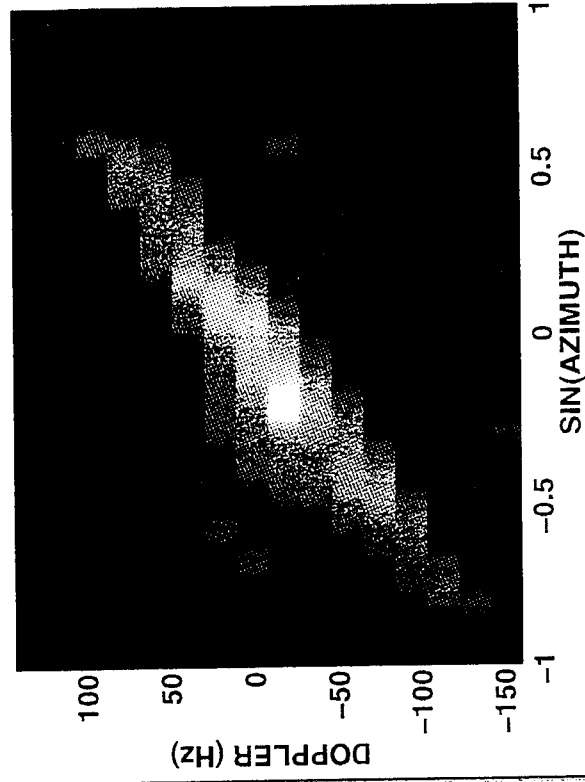
- INTRODUCTION
- POWER SELECTED TRAINING
- POWER SELECTED DE-EMPHASIS
- DATA ANALYSIS
- SUMMARY



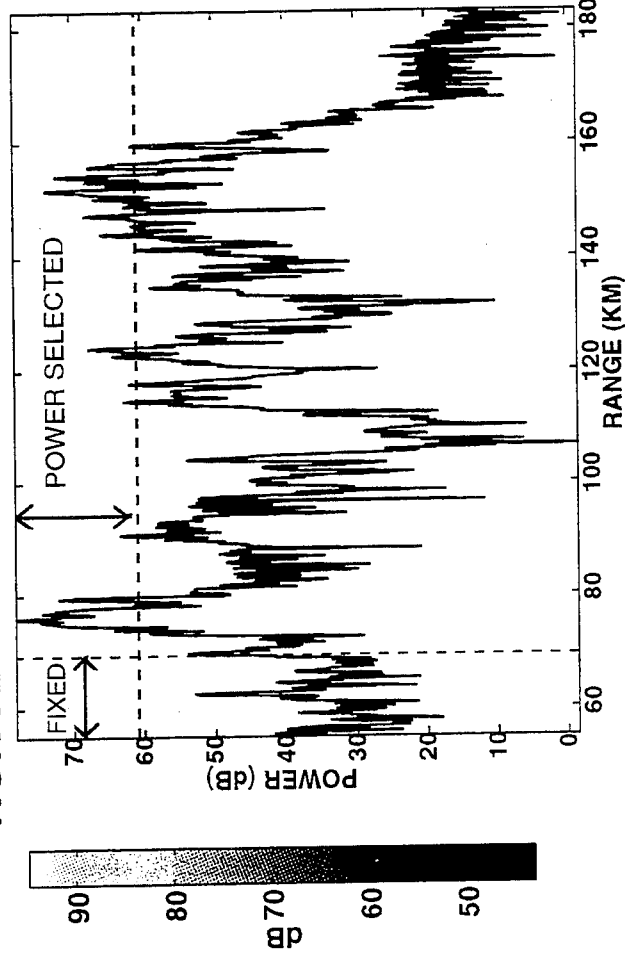
RSTER EXAMPLE

WSMR DATA, JAN 1994

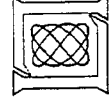
MVDR SPECTRUM



NON-ADAPTIVE BEAM ON 0HZ CLUTTER



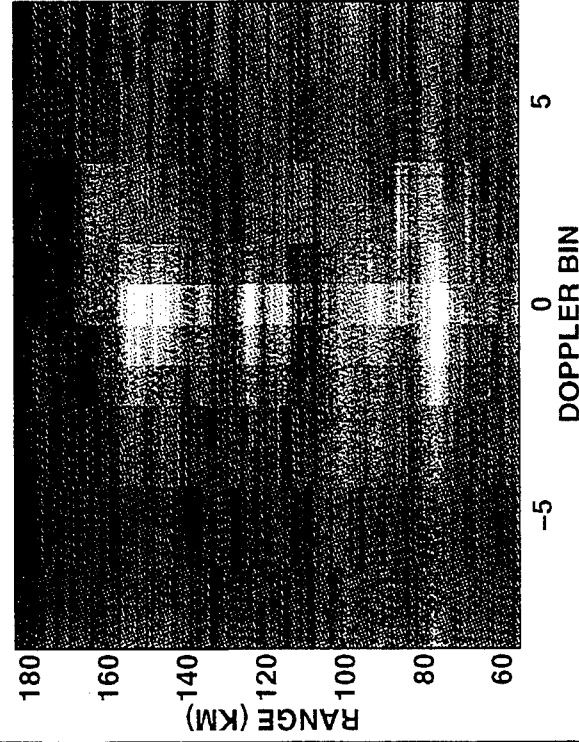
- FIXED: TRAINS ON WEAKER CLUTTER
- POWER SELECTED: ALWAYS TRAINS ON STRONG CLUTTER



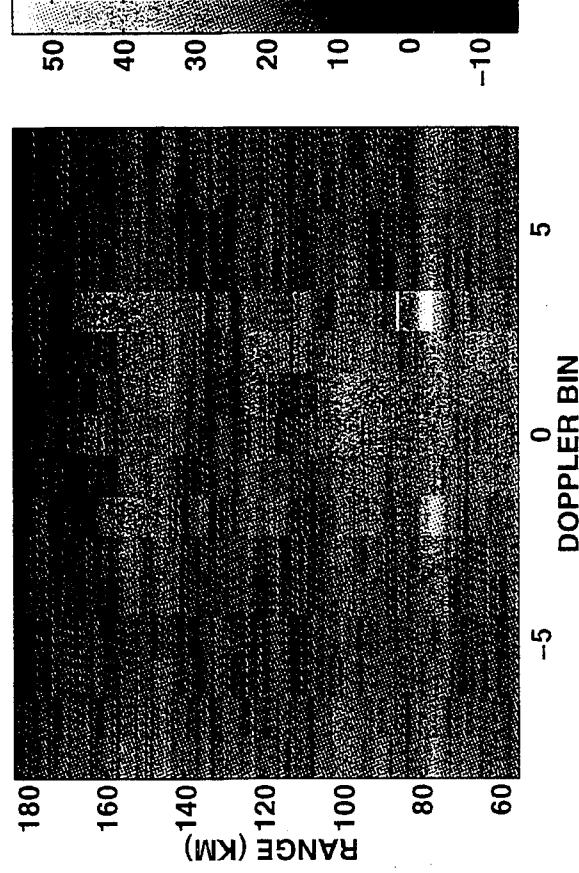
FIXED VS. POWER SELECTED TRAINING: ADAPTIVE RANGE DOPPLER MAPS

RSTER DATA, TWO-BIN POST DOPPLER

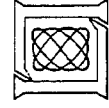
FIXED TRAINING



POWER SELECTED TRAINING



- POWER SELECTED: REDUCES CLUTTER BREAK-THROUGH

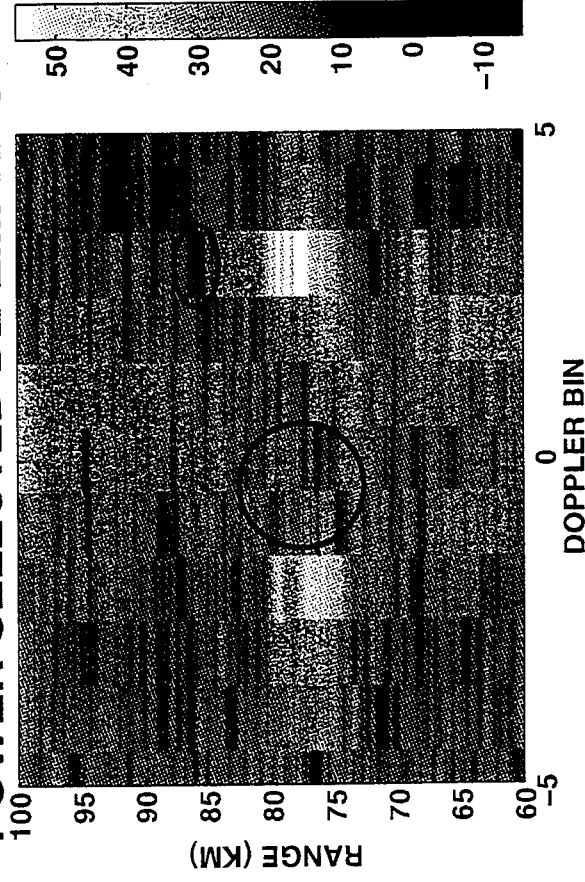
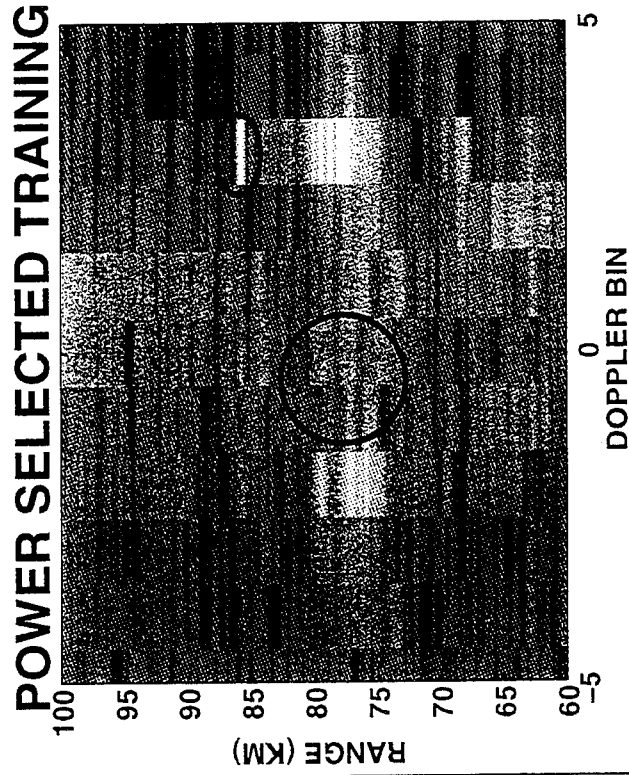


13 DOF
100 samples

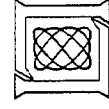
POWER SELECTED DE-EMPHASIS: ADAPTIVE RANGE DOPPLER MAPS

RSTER DATA, TWO-BIN POST DOPPLER

POWER SELECTED TRAINING AND
POWER SELECTED DE-EMPHASIS

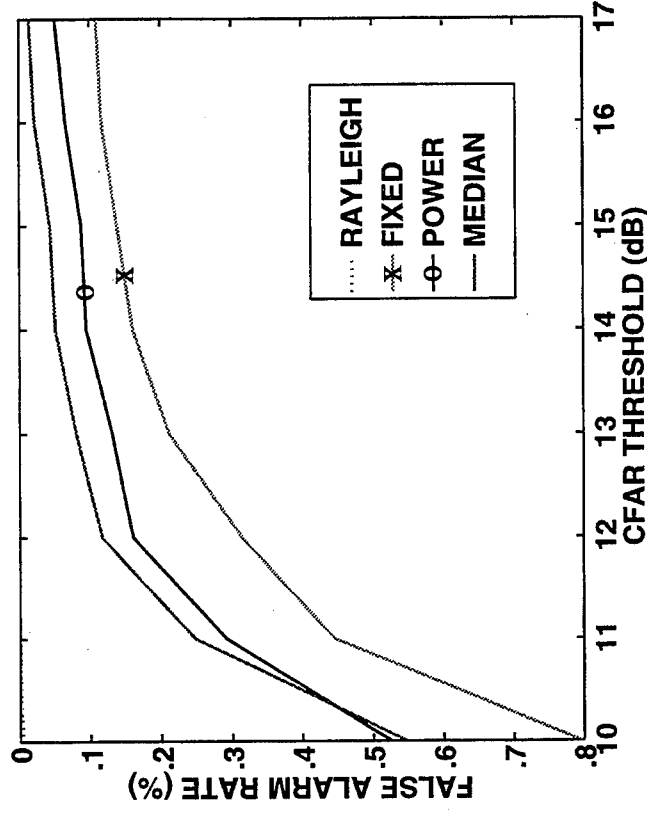
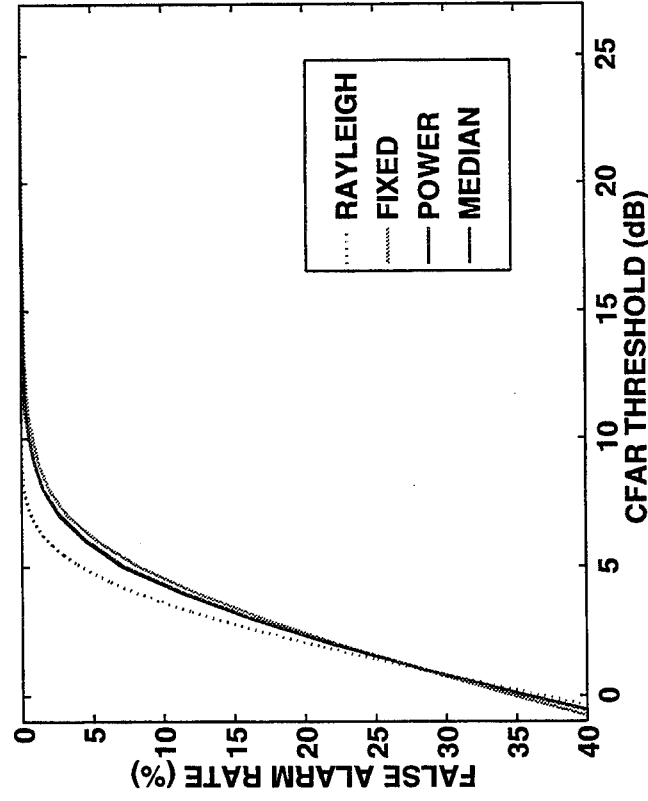


- POWER SELECTED DE-EMPHASIS REDUCES DISCRETES

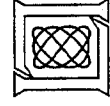


MEASURED CFAR FALSE ALARM RATES

RSTER DATA, TWO-BIN POST DOPPLER



- RAYLEIGH CURVE GIVES FUNDAMENTAL LIMIT
- NEW TRAINING METHODS MOVE TOWARD RAYLEIGH
 - FALSE ALARMS (RELATIVE TO FIXED TRAINING):
 - POWER: 38% FEWER
 - POWER/DE-EMPHASIS: 60% FEWER

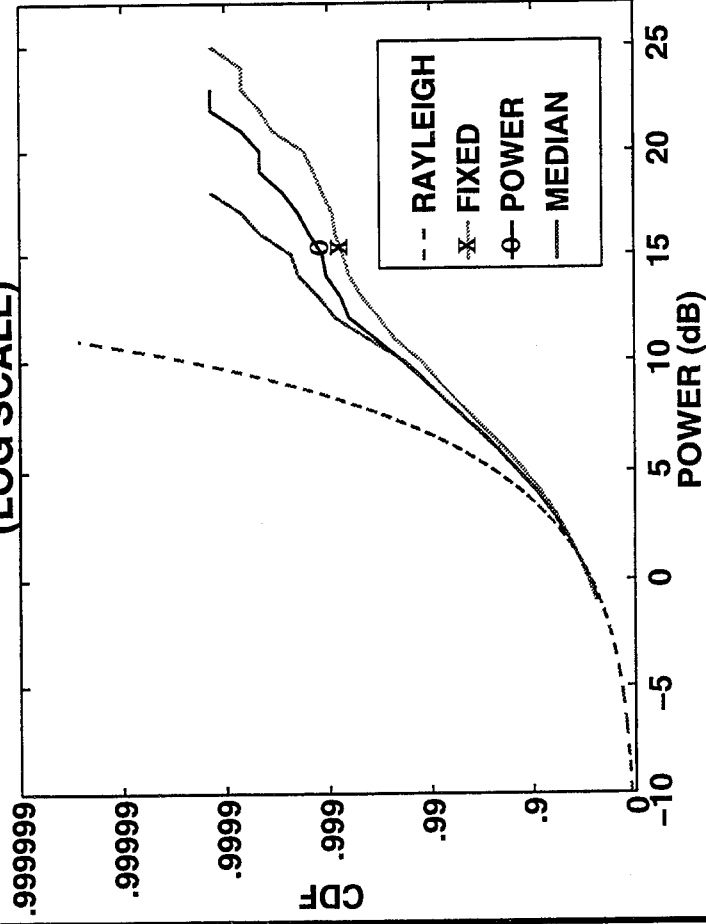


MEASURED DISTRIBUTIONS

RSTER DATA, TWO-BIN POST DOPPLER

CUMULATIVE DISTRIBUTION FUNCTION

(LOG SCALE)

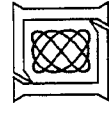


- UNDER-NULLED CLUTTER SHOWS IN TAILS

- NEW TRAINING METHODS MOVE TOWARD RAYLEIGH

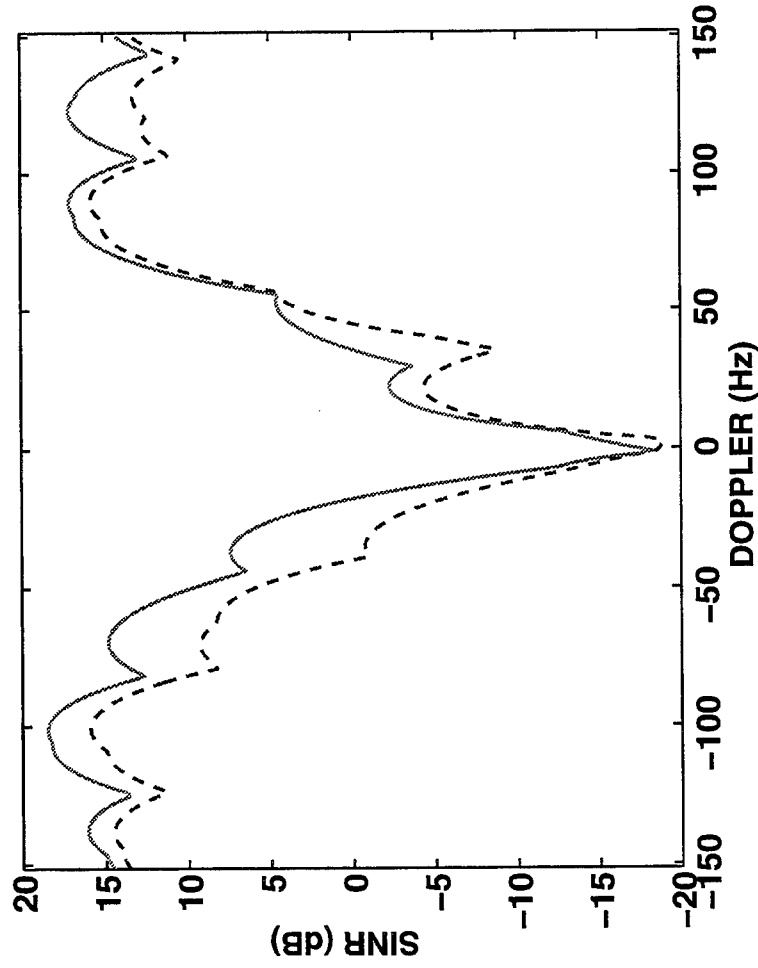
- MORE NEEDS TO BE DONE ...

- CLUTTER EDITING [KREITHEN '94]



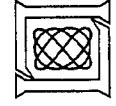
MEASURED SINR PERFORMANCE

RSTER DATA, TWO-BIN POST DOPPLER



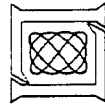
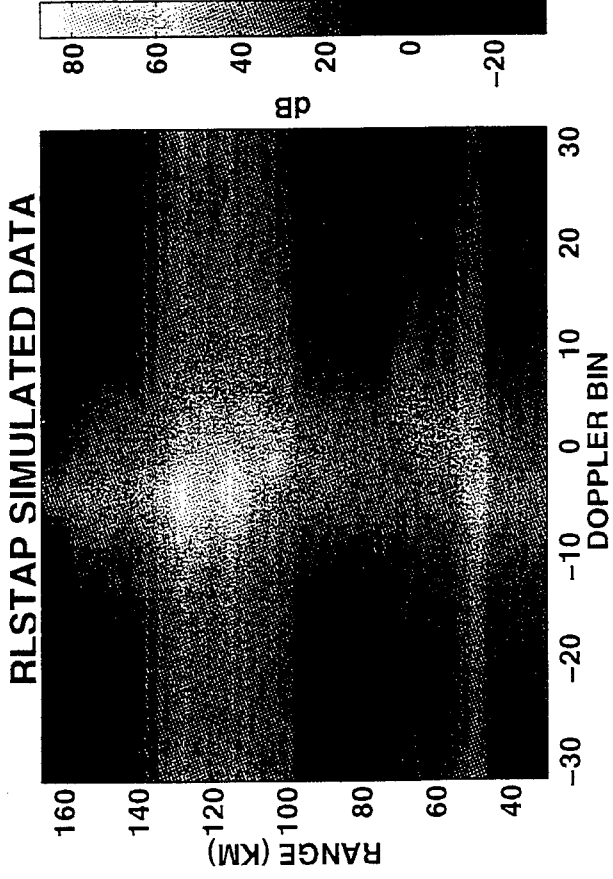
SOLID: POWER
SELECTED
DASH: FIXED

- BETTER TRAINING CAN MAINTAIN OR IMPROVE MDV



POINT BEAMS VS. ELEMENT RESPONSE

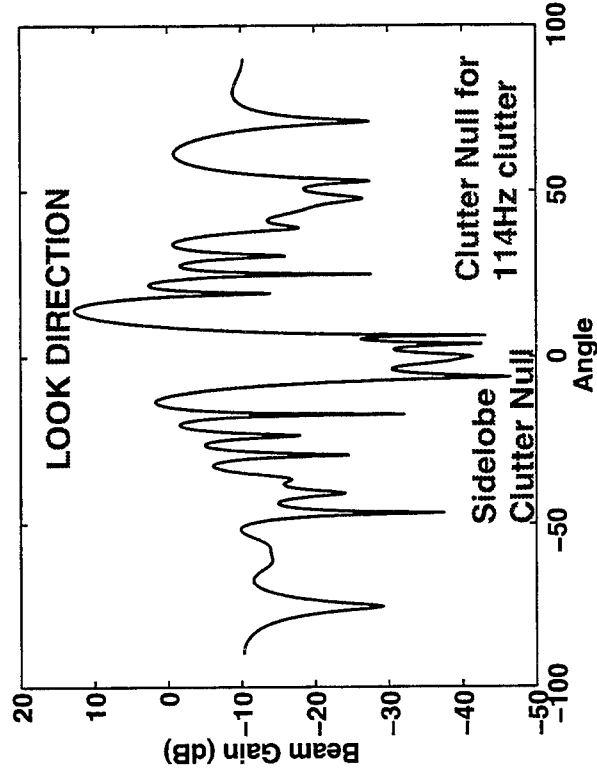
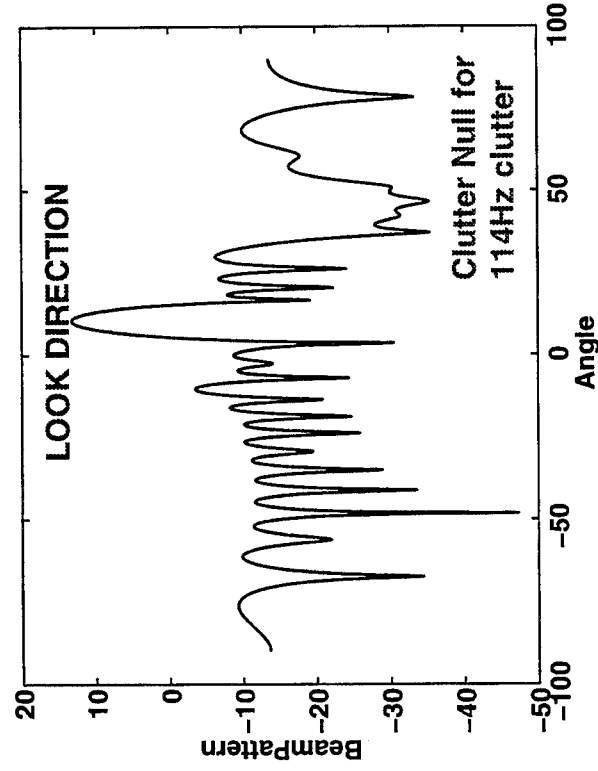
- “POINT BEAM AT CLUTTER” APPROACH IS WELL SUITED TO POST DOPPLER STAP (LOCALIZED CLUTTER)
- IF CLUTTER IS NOT WELL LOCALIZED IN DOPPLER, USE AN ELEMENT’S RESPONSE INSTEAD OF POINT BEAM
 - TARGETS MORE LIKELY TO APPEAR IN TRAINING SET (INCREASING POTENTIAL FOR NULLING TARGETS)



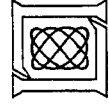
BEAMPATTERN COMPARISON

RLSTAP SIMULATED DATA PROCESSED USING
SINGLE BIN POST DOPPLER (WITH >90dB CLUTTER DISCRETES, 60dB DOPPLER TAPER)

POWER TRAINING USING POINT BEAMS POWER TRAINING USING ELEMENT RESPONSE



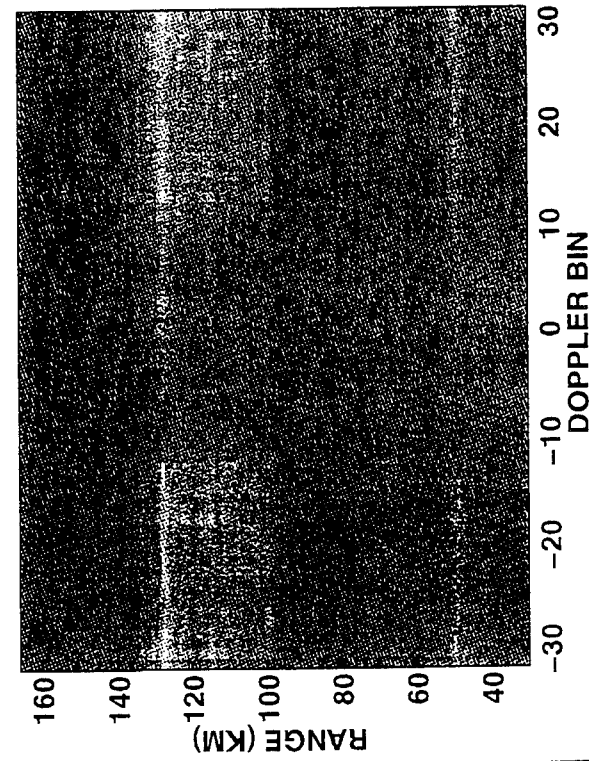
- ELEMENT APPROACH NULLS CLUTTER IN DOPPLER SIDELOBES



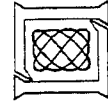
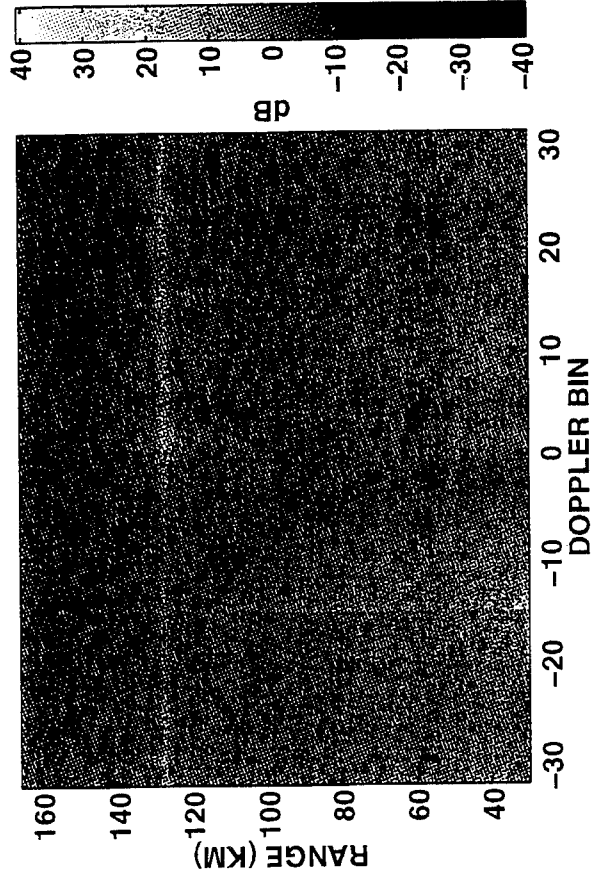
ADAPTIVE RANGE-DOPPLER MAPS

RLSTAP SIMULATED DATA PROCESSED USING
SINGLE BIN POST DOPPLER (WITH >90dB CLUTTER DISCRETES, 60dB DOPPLER TAPER)


POWER TRAINING USING POINT BEAMS

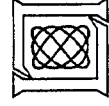


POWER TRAINING USING ELEMENT RESPONSE



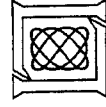
OUTLINE

- INTRODUCTION
- POWER SELECTED TRAINING
- POWER SELECTED DE-EMPHASIS
- DATA ANALYSIS
-  SUMMARY



SUMMARY

- REAL CLUTTER IS SEVERELY NONHOMOGENEOUS
- POWER SELECTED TRAINING:
 - FORMS DEEPER CLUTTER NULLS, MITIGATING FALSE ALARMS
 - NEGLIGIBLE ADDED COMPUTATIONAL COST OVER FIXED TRAINING
- POWER SELECTED DE-EMPHASIS
 - PERMITS CONTROLLED AMOUNTS OF “SELF NULLING”, MITIGATING THE STRONGEST CLUTTER DISCRETES
- THIS MAY BE JUST THE BEGINNING ...
 - ADAPTIVE TRAINING HAS THE POTENTIAL TO UNLEASH A NEW WAVE OF PERFORMANCE IMPROVEMENTS & COMPUTATIONAL REDUCTIONS



APPENDIX A

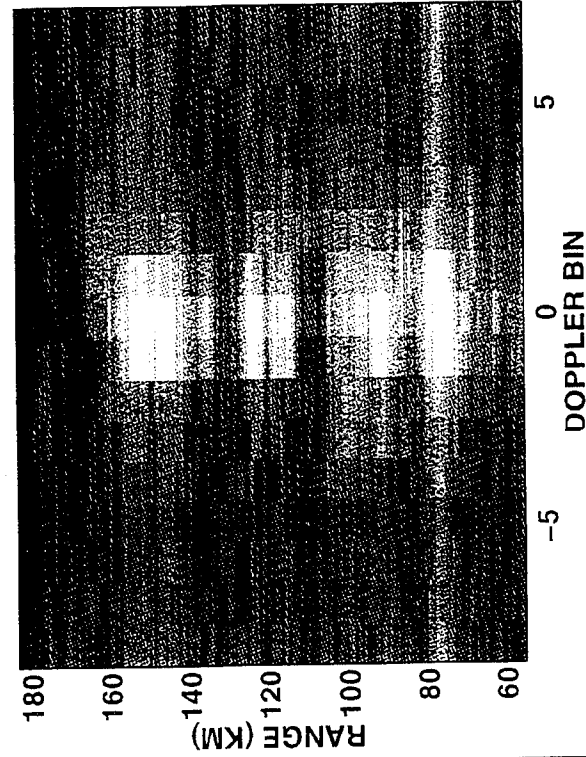
DATA ANALYSIS USING SINGLE BIN POST DOPPLER STAP (RSTER DATA)



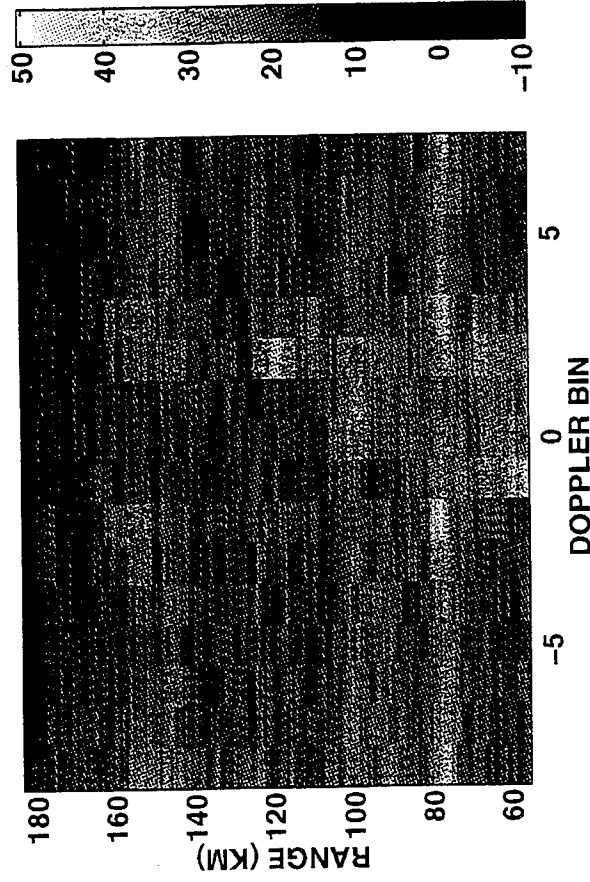
FIXED VS. POWER SELECTED TRAINING: ADAPTIVE RANGE DOPPLER MAPS

RSTER DATA, SINGLE BIN POST DOPPLER

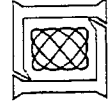
FIXED TRAINING



POWER SELECTED TRAINING



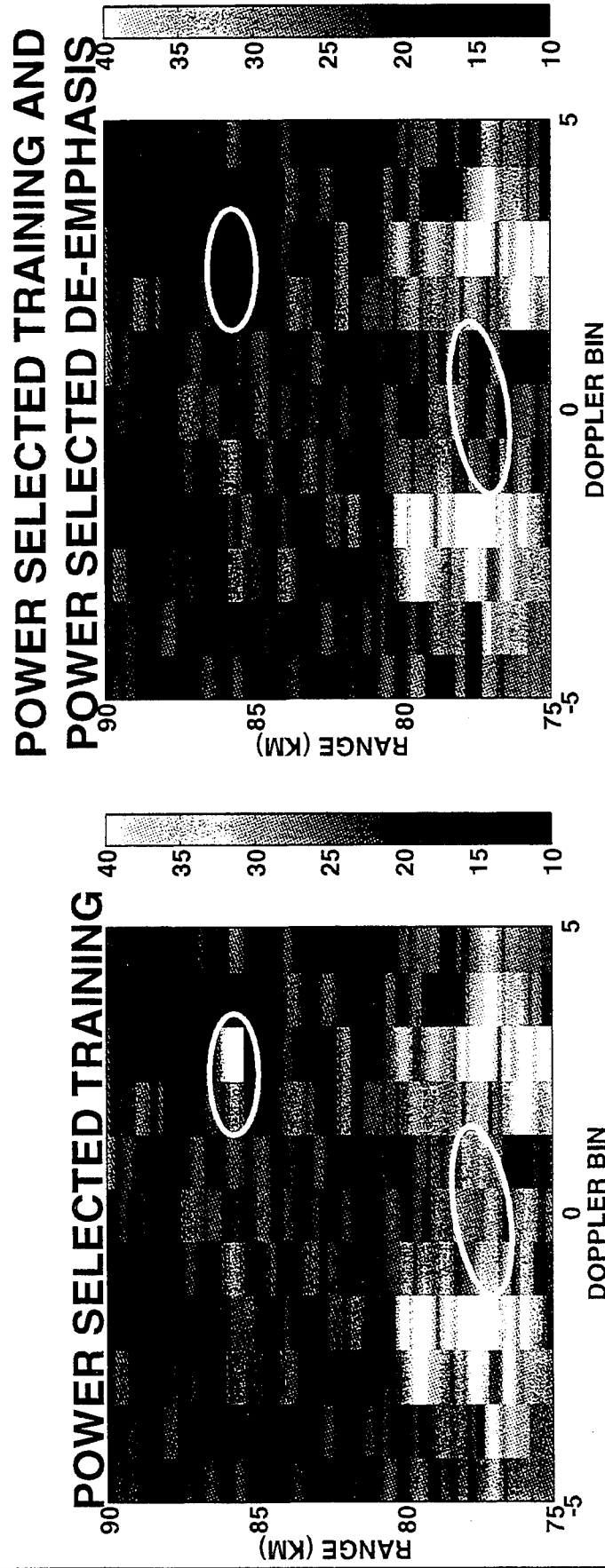
- POWER SELECTED: REDUCES CLUTTER BREAK-THROUGH



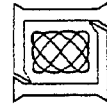
9 DOF
100 samples

POWER SELECTED DE-EMPHASIS: ADAPTIVE RANGE DOPPLER MAPS

RSTER DATA, SINGLE BIN POST DOPPLER



- POWER SELECTED DE-EMPHASIS REDUCES DISCRETES

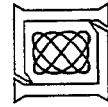


CFAR DETECTIONS

RSTER DATA, SINGLE BIN POST DOPPLER

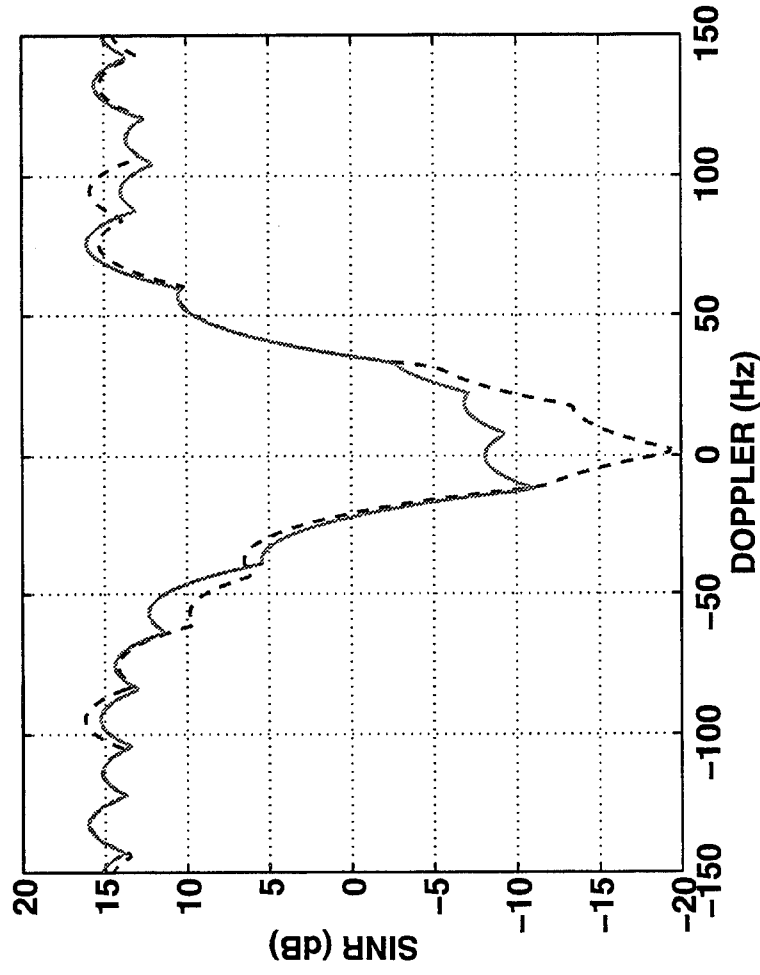
TRAINING METHOD	CFAR DETECTS 13 dB THRESHOLD	CFAR DETECTS 15 dB THRESHOLD
FIXED TRAINING	26	12
POWER SELECTED	15	9
POWER SELECTED WITH MEDIAN DE-EMPHASIS	10	5

- POWER SELECTED TRAINING REDUCES CFAR DETECTS BY 25% - 42%
- POWER SELECTED TRAINING/DE-EMPHASIS GIVES BETTER APPROX. 60% REDUCTION



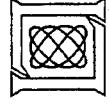
MEASURED SINR PERFORMANCE

RSTER DATA, SINGLE BIN POST DOPPLER



SOLID: POWER
SELECTED
DASH: FIXED

- BETTER TRAINING CAN MAINTAIN OR IMPROVE MDV



STAP APPLIED TO ELECTRO-OPTICAL SENSORS

Anthony E. Filip and Stephen C. Pohl

MIT Lincoln Laboratory
244 Wood Street
Lexington, MA 02173-9108
tel: (617) 981-7975
email: filip@ll.mit.edu
email: pohl@ll.mit.edu

Abstract In a general sense, the problem of detecting targets with an electro-optical (EO) sensor shares many elements with that of radar target detection. For example, targets are obscured by receiver noise and clutter in both radar and EO systems. Clutter statistics are generally non-Gaussian and non-stationary in both cases. Adaptive clutter mitigation for an array radar yields the STAP approach which has at its core the exploitation of a 3-D data cube consisting of element/pulse/range-cell samples. Its counterpart in the EO world uses large format 2-D focal plane arrays to create a 3-D data cube consisting of x/y/frame-number samples. It should not be surprising, therefore, that the EO community has evolved a signal processing approach which shares many features with STAP for radar. This presentation explores those techniques as applied to a variety of electro-optical sensor systems and attempts to stimulate synergism between the two sensor domains.

STAP APPLIED TO ELECTRO-OPTICAL SENSORS

13 MARCH 1996

A. E. FILIP & S. C. POHLIG

MIT LINCOLN LABORATORY



OUTLINE

- INTRODUCTION
- EO STAP THEORY
- EO STAP EXAMPLES
- HARDWARE IMPLEMENTATIONS
- FUTURE HYPERSPECTRAL SENSORS
- SUMMARY



UNPROCESSED DATA HARVARD (LOW SNR), LWIR



SINGLE UNPROCESSED FRAME, $6.2^\circ \times 2.15^\circ$ FOV

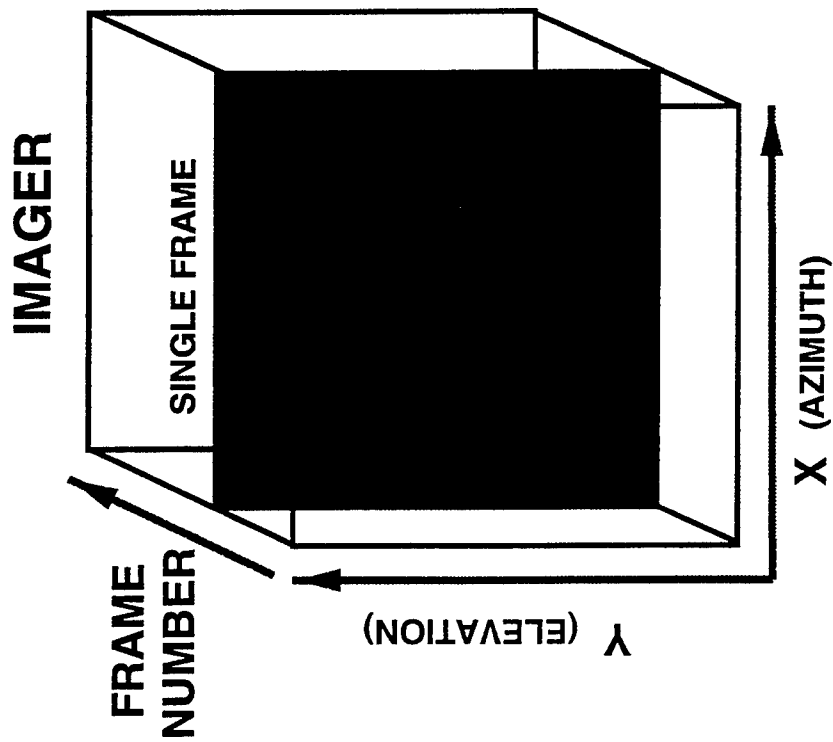
PROCESSING: 10 FRAME SLIDING TEMPORAL WINDOW

48 FRAMES

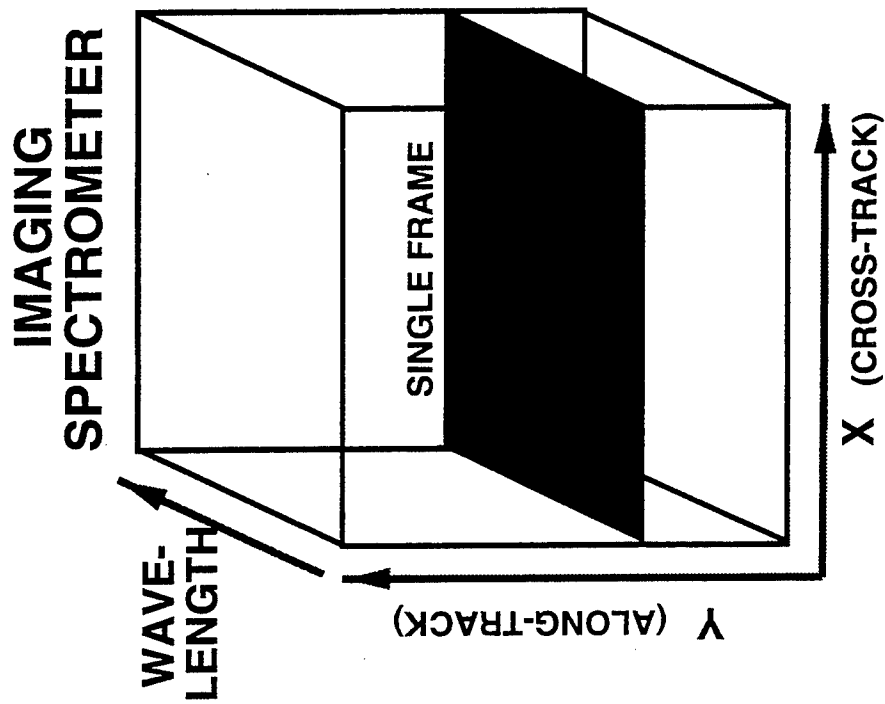
10^{-8} SINGLE HYPOTHESIS P_{FA}



ELECTRO-OPTICAL DATA CUBES



- LITTLE SPACE-TIME CORRELATION

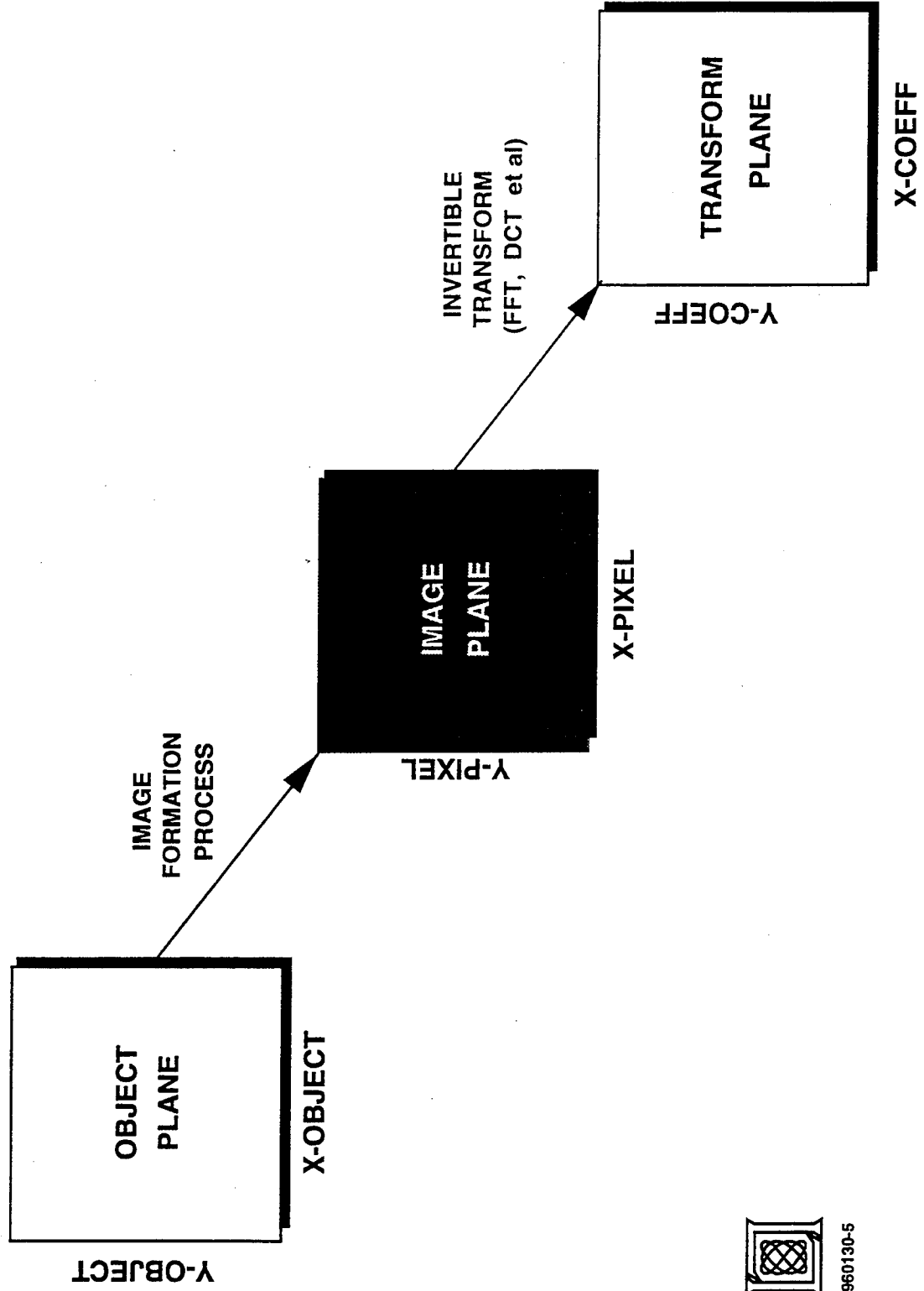


- HIGHLY CORRELATED IN WAVELENGTH



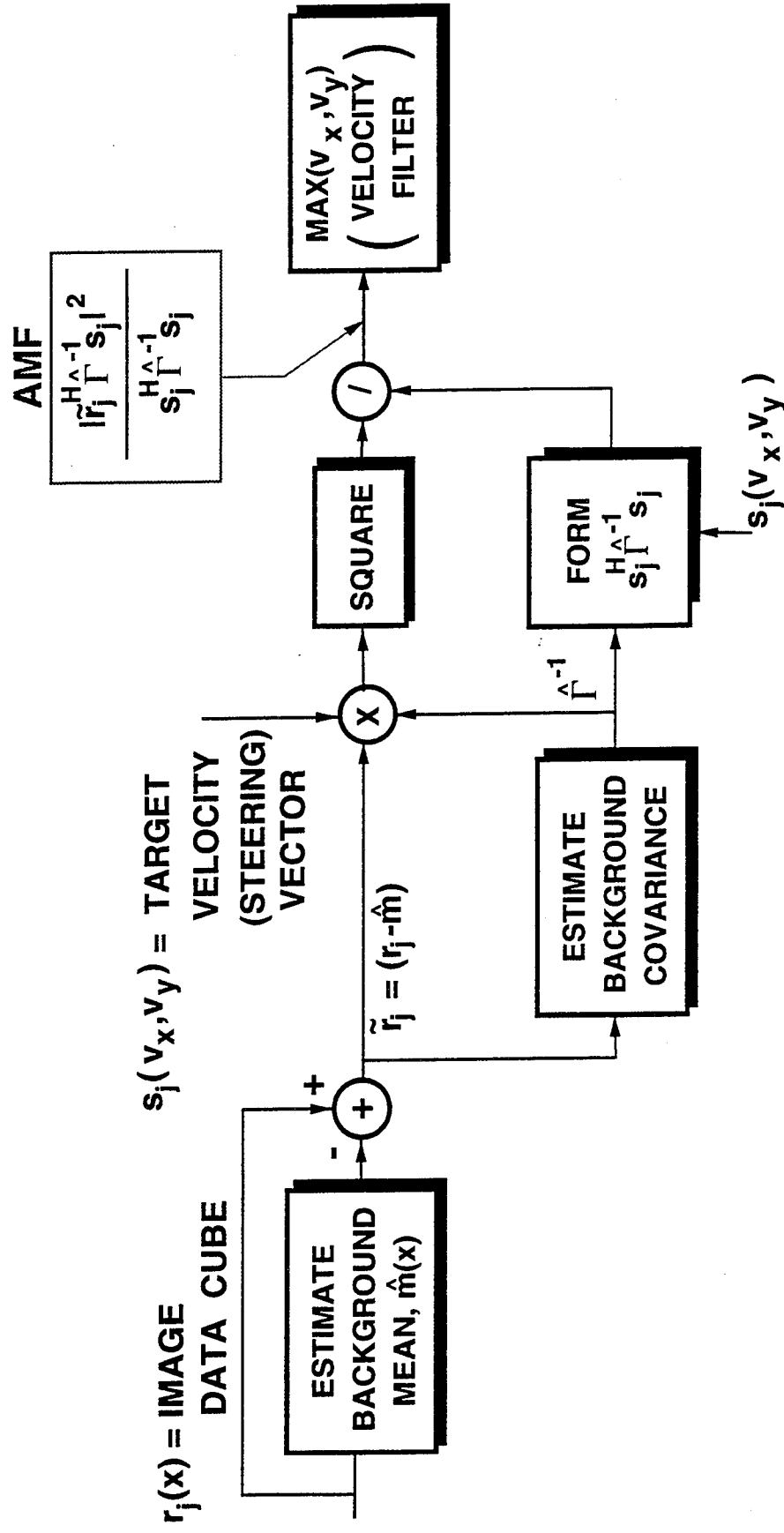
960130-6

STAP TAXONOMY FOR ELECTRO-OPTICS



960130-5

STAP IMAGE PROCESSING



QUALITATIVE COMPARISON OF RADAR AND EO STAP

RADAR

- COHERENT SIGNAL
PHASE VERY IMPORTANT
- STATIONARY, ZERO-MEAN GAUSSIAN
STATISTICS
- HIGH DEGREE OF BACKGROUND
CORRELATION
- MANY ($O(100)$) SAMPLES FOR PA-
RAMETER (COVARIANCE) ESTIMA-
TION

EO IMAGERS

- NONCOHERENT SIGNAL
PHASE NOT AVAILABLE
- NON-STATIONARY, NON-ZERO MEAN
GAUSSIAN (POISSON) STATISTICS
- VERY LITTLE BACKGROUND CORRE-
LATION
- FEW ($O(10)$) SAMPLES FOR PARAM-
ETER ESTIMATION



OUTLINE

- INTRODUCTION
- ⇒ • EO STAP THEORY
- EO STAP EXAMPLES
- HARDWARE IMPLEMENTATIONS
- FUTURE HYPERSPECTRAL SENSORS
- SUMMARY



MODELING ASSUMPTIONS

- BACKGROUND RADIANCE IS SPATIALLY NON-STATIONARY WITH UNKNOWN MEAN, VARIANCE
- EACH SPACE-TIME SAMPLE INDEPENDENT
- FLUCTUATING TARGET INTENSITY UNKNOWN
- STATISTICS ARE POISSON (or GAUSSIAN)
- REGISTERED FRAME SET



STAP SIMPLIFICATION

- GLRT RESULT WITH $\tilde{r}_j \equiv r_j - \hat{m}_j$,

$$l = \sum_j \frac{|s_j^T \hat{\Gamma}^{-1} \tilde{r}_j|^2}{(s_j^T \hat{\Gamma}^{-1} s_j)},$$

or

$$l = \sum_j \left\{ \left[\sum_i \frac{s_{ij} \tilde{r}_{ij}}{\hat{\sigma}_i^2} \right]^2 / \sum_i \frac{s_{ij}^2}{\hat{\sigma}_i^2} \right\}$$

- FOR POINT TARGETS MOVING AT VELOCITY, v , :

$$l = \sum_{\text{ALONG TRACK}} \frac{(r_{jv,j} - \hat{m}_{jv})^2}{\hat{\sigma}_{jv}^2}$$

MAX-LIKELIHOOD APPROXIMATION

$$l = \sum_{\text{AlongTrack}} \left[\frac{r_j(x) - \hat{m}(x)}{\hat{\sigma}_K(x)} \right]^2 \lesssim T$$

where

$r_j(x)$ = raw data in j th frame

$$\hat{m}(x) = \frac{1}{K} \sum r_j(x)$$

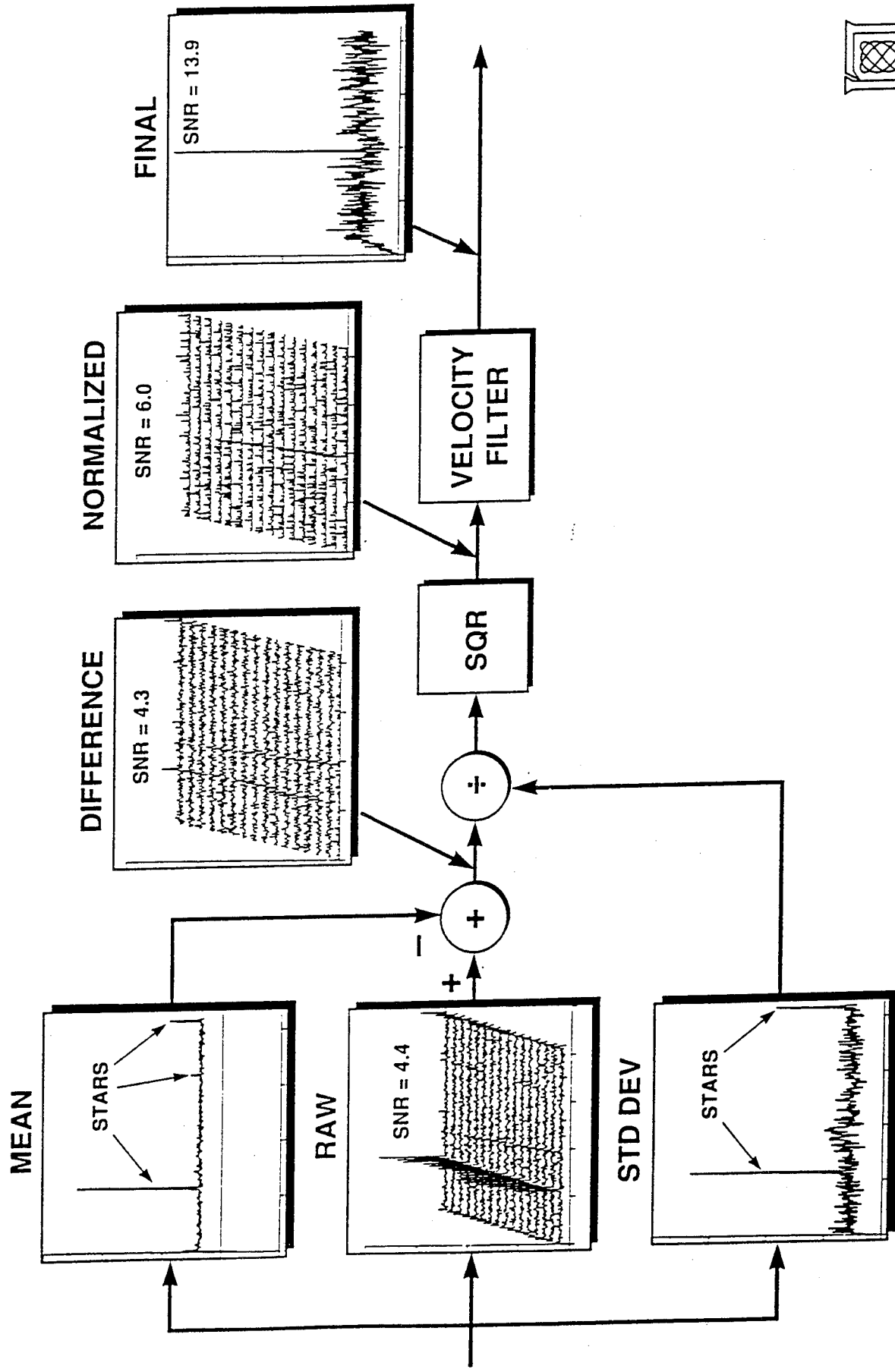
and

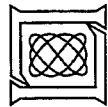
$$\hat{\sigma}_K^2(x) = \frac{1}{K} \sum [r_j(x) - \hat{m}(x)]^2$$

- PROCESSOR OFFERS CFAR PERFORMANCE



OPTIMUM PROCESSING FLOW

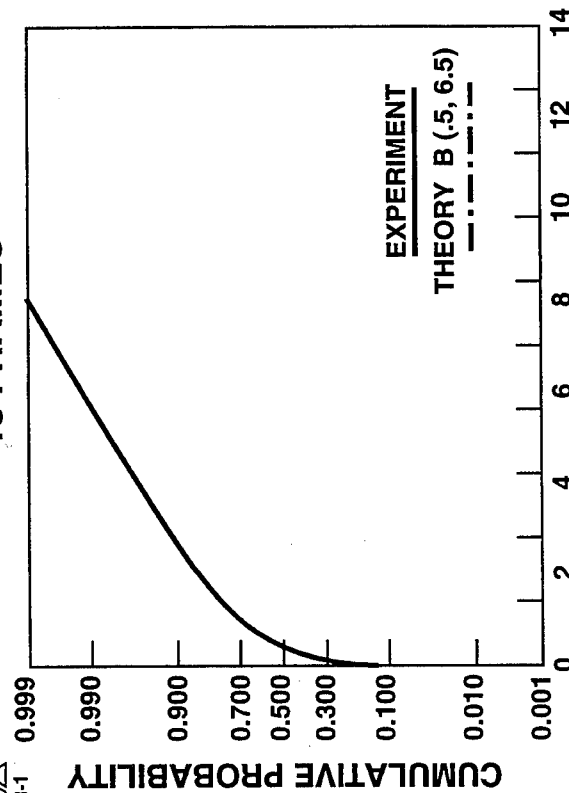




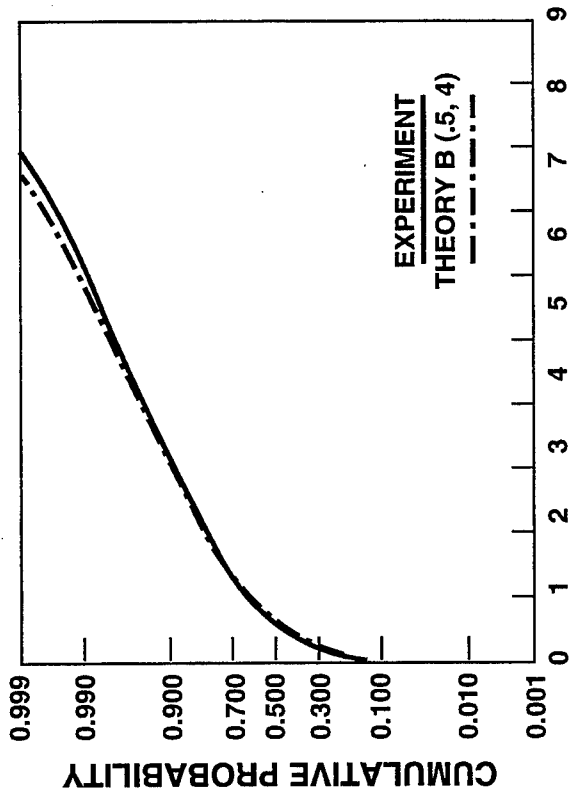
211203-1

NORMALIZER STATISTICS

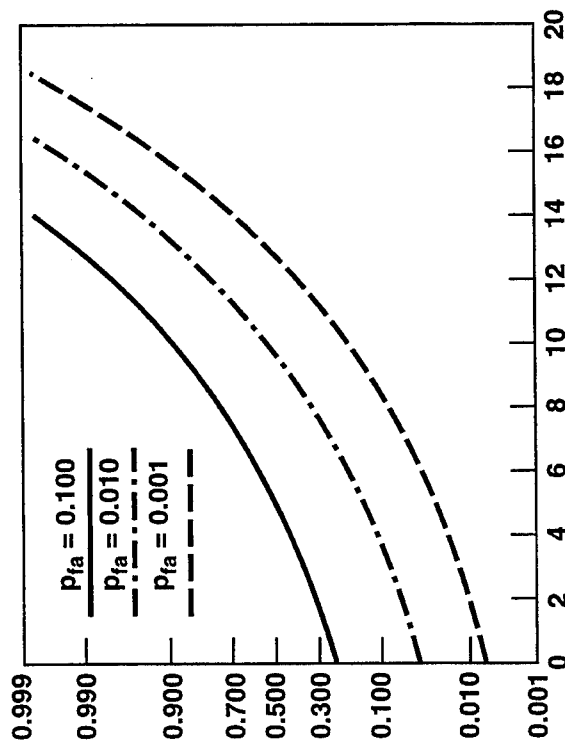
15 FRAMES



10 FRAMES

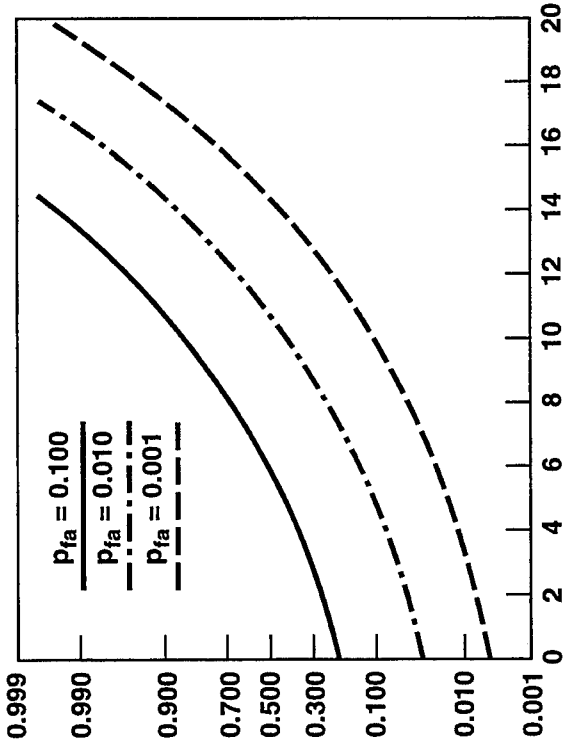


PROBABILITY OF DETECTION



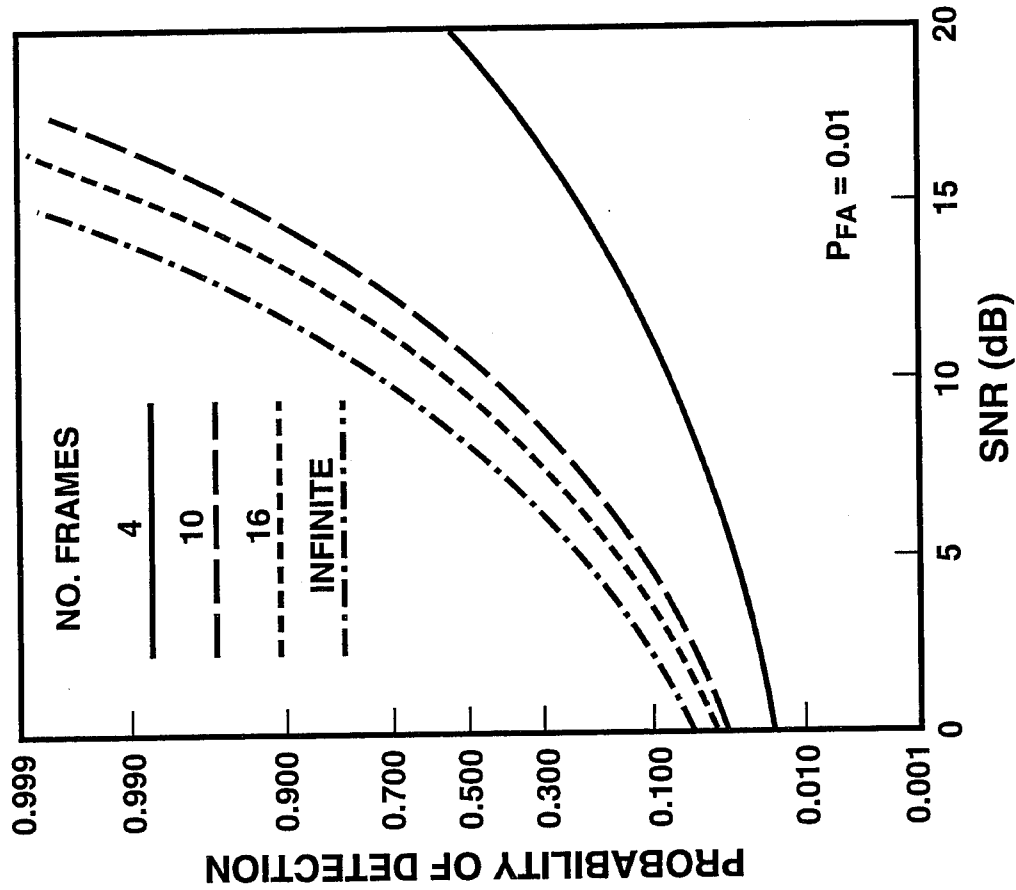
VISIBLE-BAND STARRER
STAR CLUTTER

PROBABILITY OF DETECTION

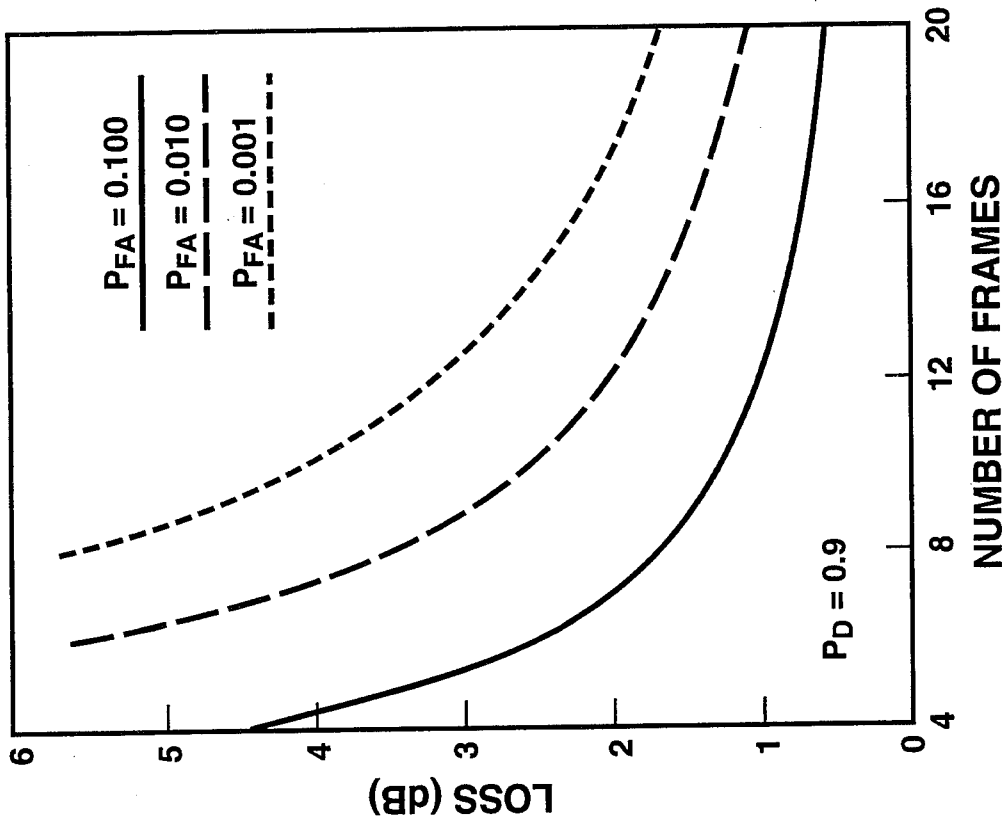


LWIR SCANNER
GROUND CLUTTER

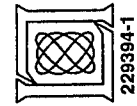
DETECTION PERFORMANCE



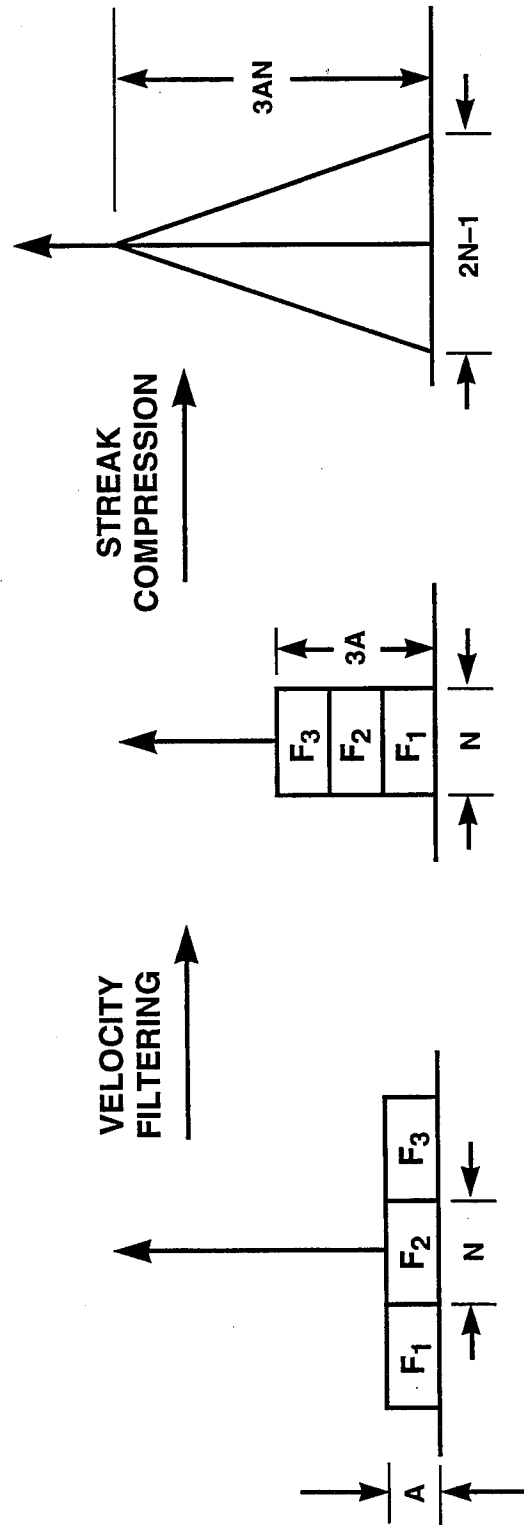
SINGLE FRAME P_D vs SNR



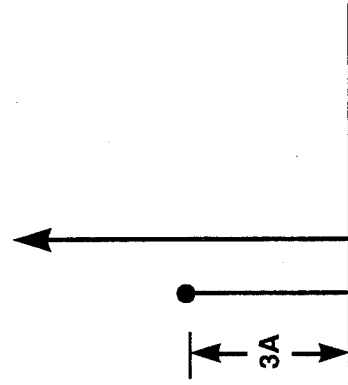
SINGLE FRAME CFAR LOSS



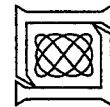
VELOCITY FILTER CONCEPT



STARING ARRAY

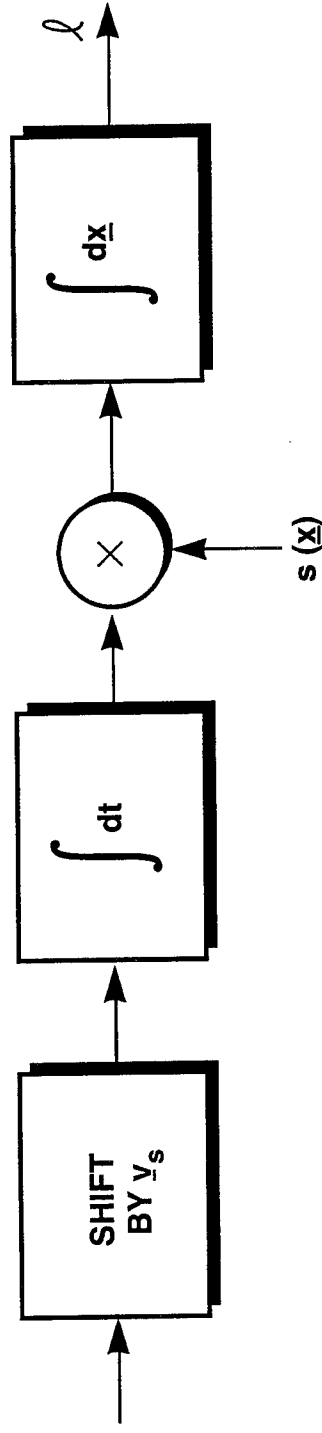


SCANNING ARRAY

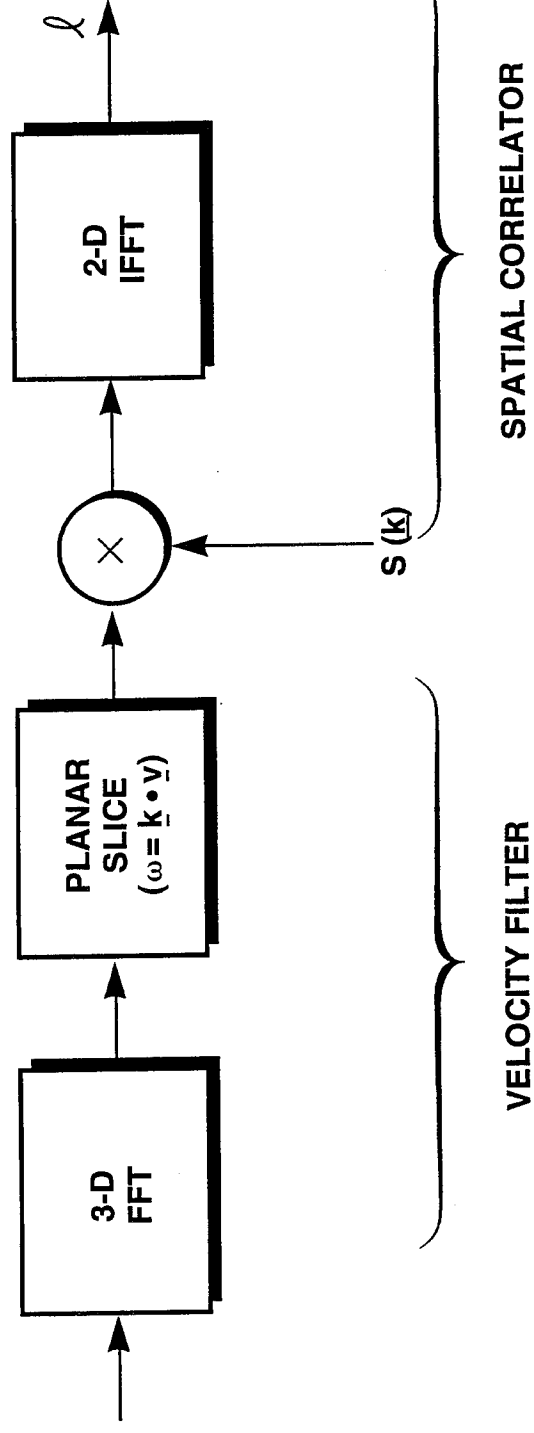


TWO IMPLEMENTATIONS OF VELOCITY FILTER AND CORRELATOR

SPACE-TIME DOMAIN



FREQUENCY DOMAIN



SIMPLIFICATIONS TO MAX-LIKELIHOOD RESULT

- BINARY DETECTION AFTER NORMALIZATION*
- USE OF MAX-VALUE FRAME ONLY*
- RECURSIVE ESTIMATION of BACKGROUND PARAMETERS:

$$\hat{m}_i(x) = (1 - a)r_i(x) + a\hat{m}_{i-1}(x)$$

and

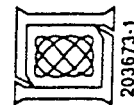
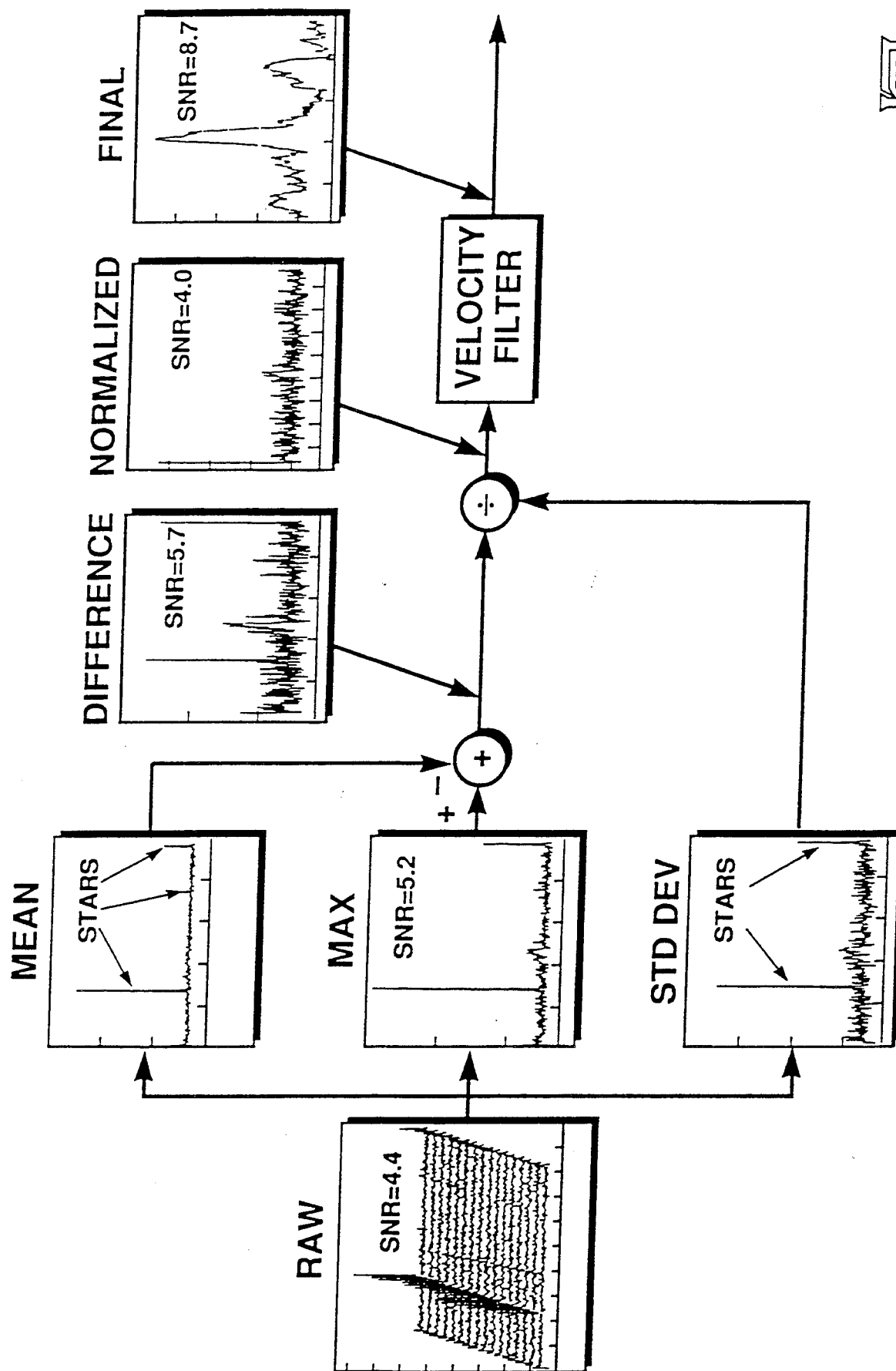
$$\hat{\sigma}_i^2(x) = (1 - a)[r_i(x) - \hat{m}_i(x)]^2 + a\hat{\sigma}_{i-1}^2(x)$$

- SIMPLIFIES REAL-TIME PROCESSOR IMPLEMENTATION VIA:
 - MEMORY REDUCTION
 - THROUGHPUT REDUCTION
 - LATENCY REDUCTION

*USED IN SPACE-BASED VISIBLE (SBV) INSTRUMENT

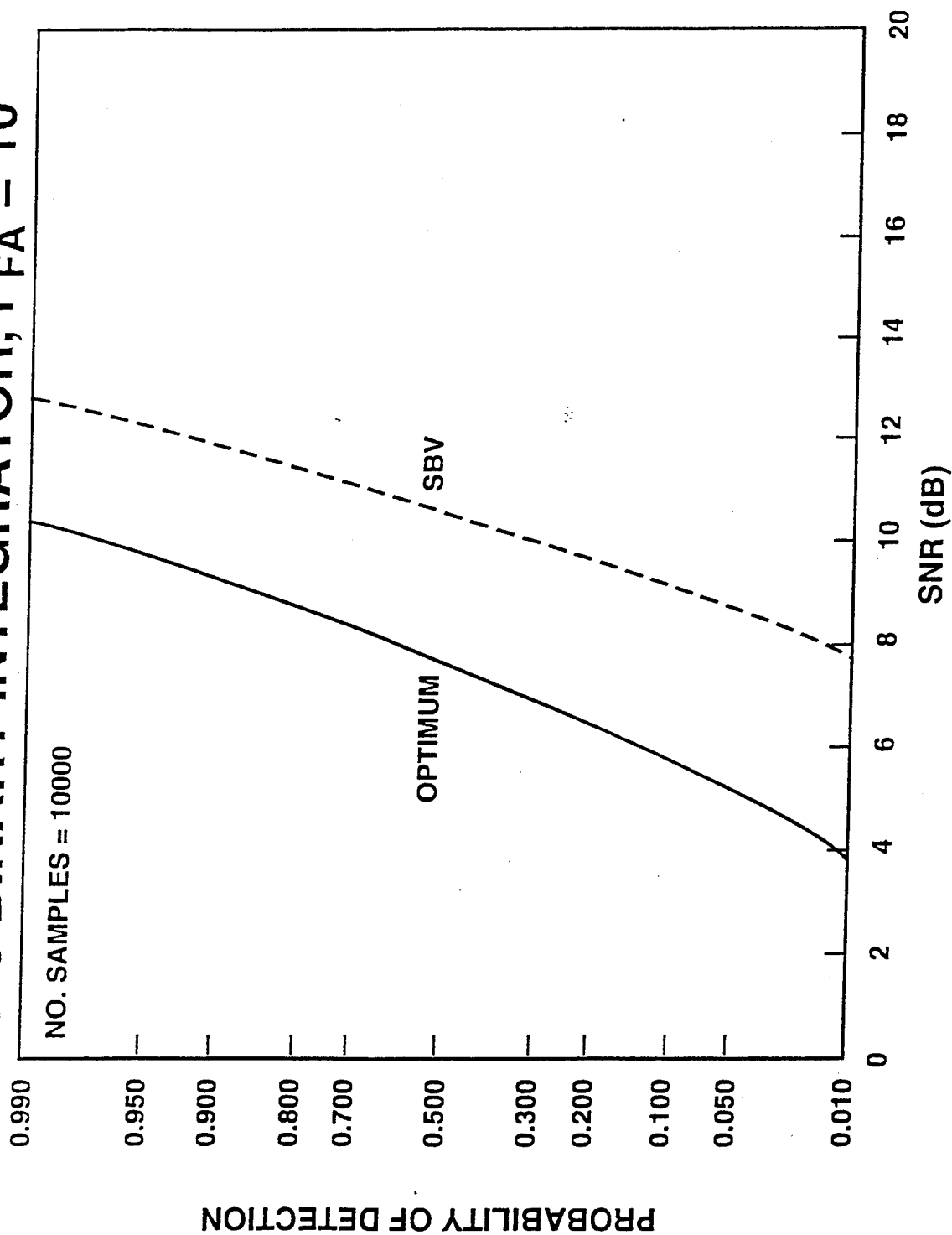


SBV PROCESSING FLOW



203673-1

COMPARISON OF SBV & OPTIMUM PROCESSOR 7/15 BINARY INTEGRATOR, $P_{FA} = 10^{-8}$



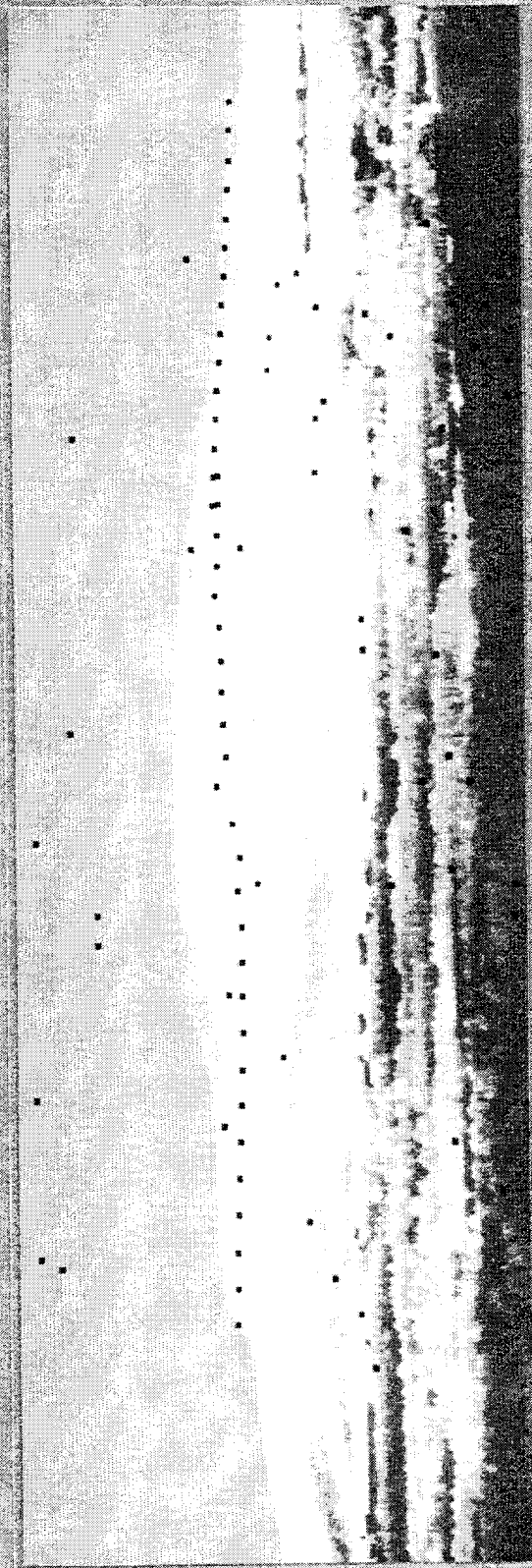
OUTLINE

- INTRODUCTION
- EO STAP THEORY
- ⇒ • EO STAP EXAMPLES
- HARDWARE IMPLEMENTATIONS
- FUTURE HYPERSPECTRAL SENSORS
- SUMMARY



TARGET DETECTION

HARVARD (Low SNR), LWR

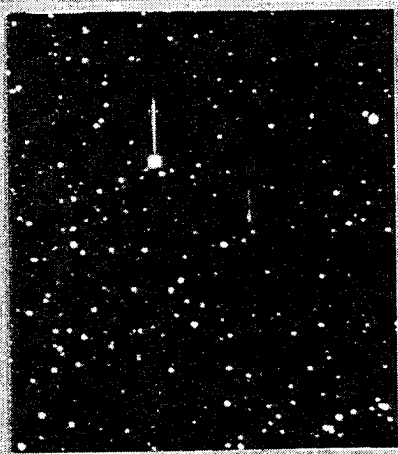


TEMPORAL WINDOW 10 FRAMES
ESTIMATED SNR_{dB} 9 - 12 dB
ESTIMATED SNRV 2.8 - 4



ROBUST TARGET DETECTION AND CLUTTER SUPPRESSION

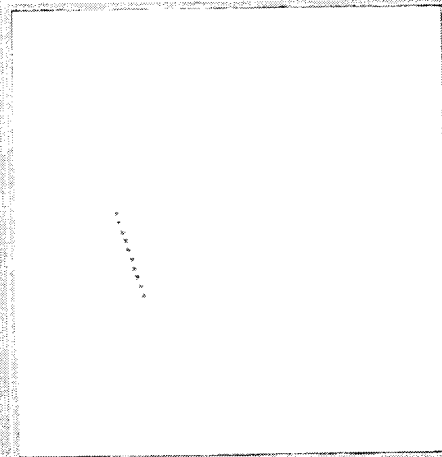
THREE EXAMPLES



VISUAL
STANDARD

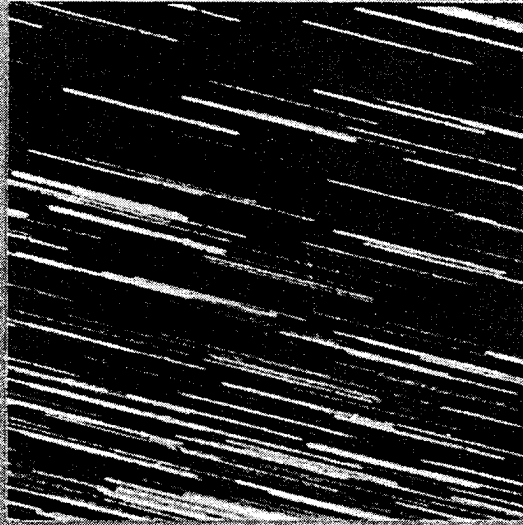


VISUAL
STANDARD

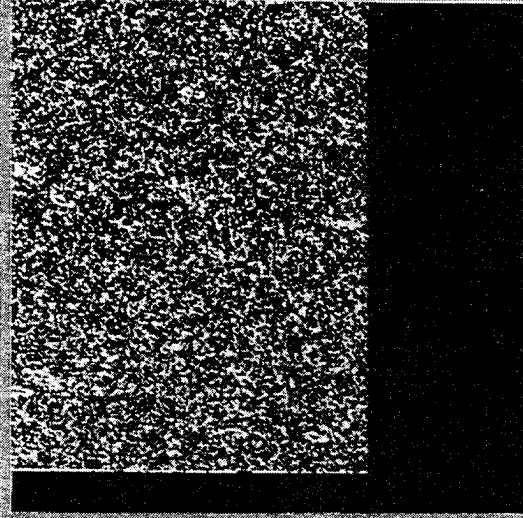


VISUAL
STANDARD

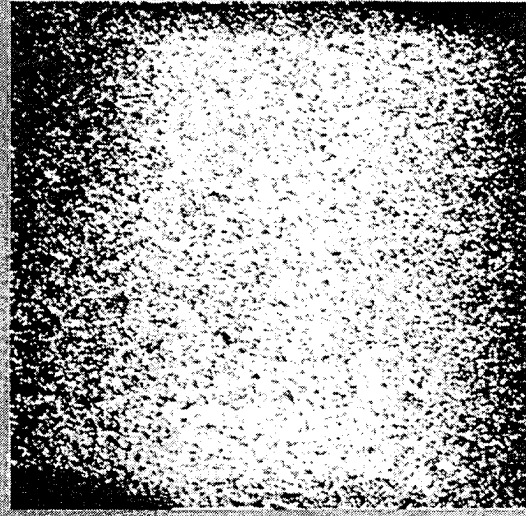
TARGET TRACK EXAMPLE 1 STATIONARY AND 1 MOVING TARGET



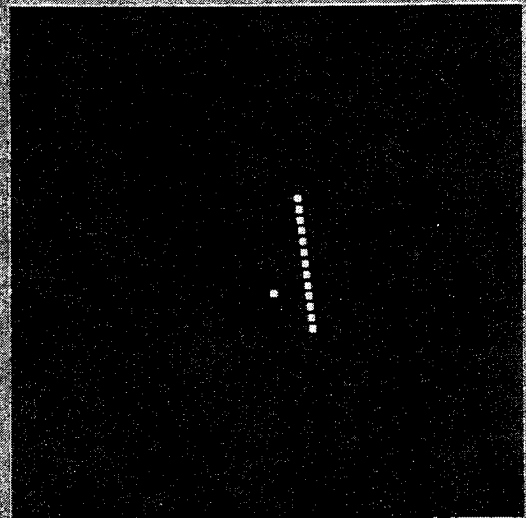
RAW DATA-16 FRAMES



DATA SHIFTED TO REMOVE
STARS AND NORMALIZED



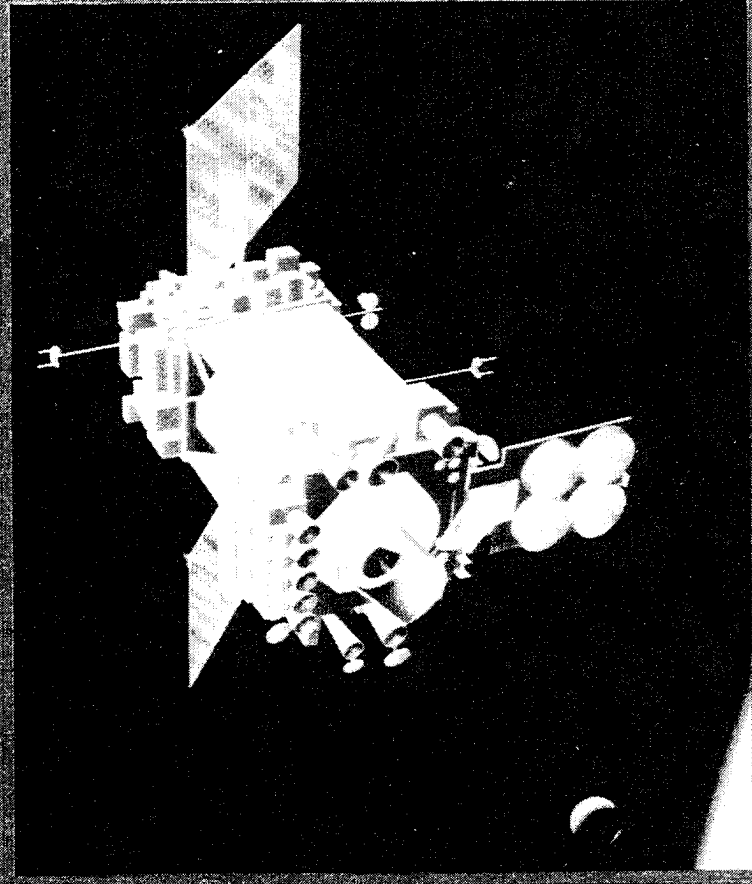
NORMALIZED DATA SHIFTED BACK



DETECTED TARGETS



MIDCOURSE SPACE EXPERIMENT (MSX) SATELLITE

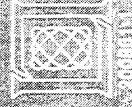


SENSOR SUITE

- SPIRIT III (Utah State Univ.)
- SBV (MIT/LL)
- UVISI (JHU/APL)
- CONTAMINATION CONTROL (JHU/APL)
- REFERENCE SPHERE (MIT/LL)

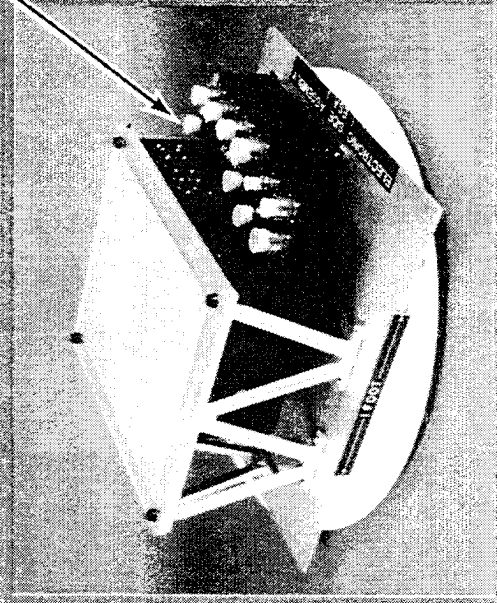
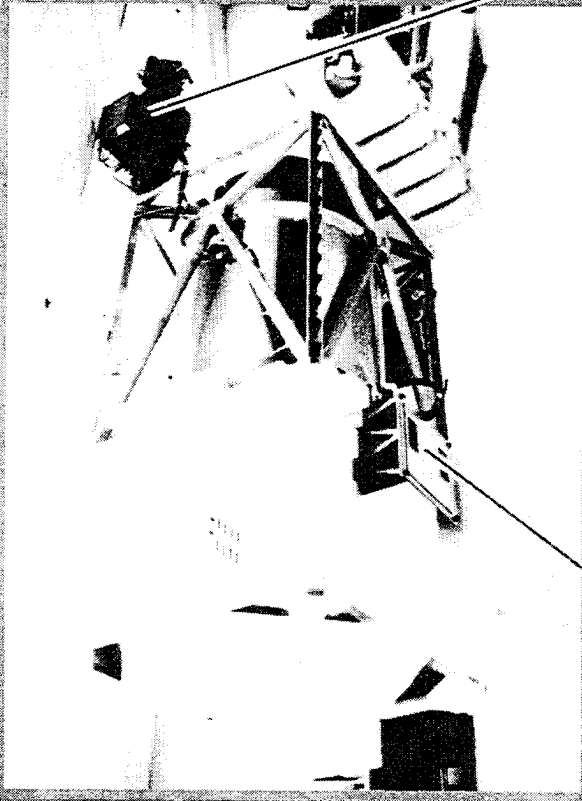
SPACECRAFT (JHU/APL)

- 888 km, 99° INCLINATION ORBIT
- DELTA II LAUNCH
- COMMAND AND TELEMETRY PROCESSORS
- ATTITUDE AND TRACK PROCESSORS
- TAPE RECORDERS
- 5700 lb AND 1.2 KW

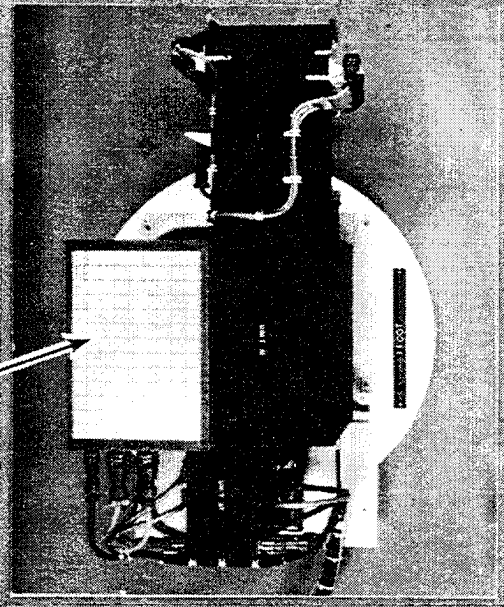


MSX SPACECRAFT WITH SBV PAYLOAD

(Mockup)



ELECTRONICS SIDE ASSEMBLY



TELESCOPE ASSEMBLY

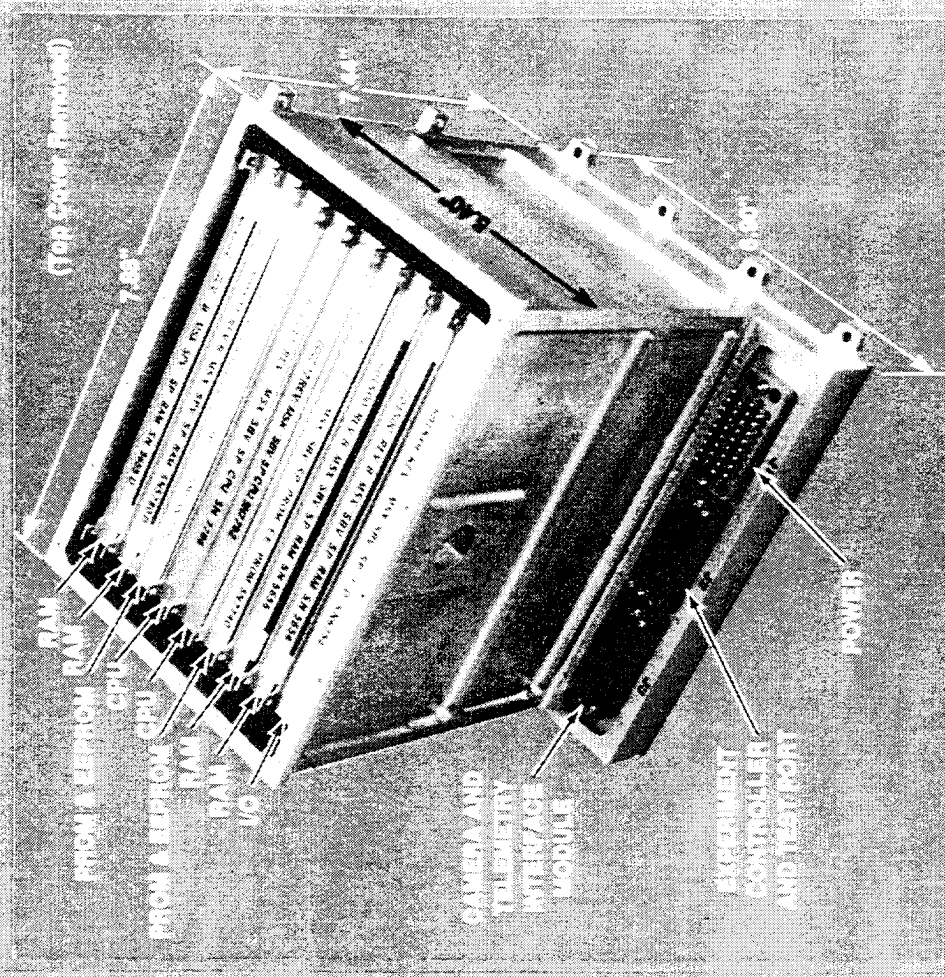
3BV SIGNAL PROCESSOR

• FUNCTIONS

- START DETECTION
- CLUTTER REJECTION
- TARGET DETECTION
- METRIC ESTIMATION
- SIGNATURE GENERATION
- REPORT FORMATTING

• FEATURES

- 2 REDUNDANT CHANNELS
- DSP6001 CPUs
- 10 MIPS PER CHANNEL
- 4 MEMONVOLATILE PROGRAM MEMORY PER CHANNEL
- 1.6 MB DATA RAM PER CHANNEL
- 10 W POWER PER CHANNEL
- 12 lb TOTAL WEIGHT



PACKAGING COMPARISON

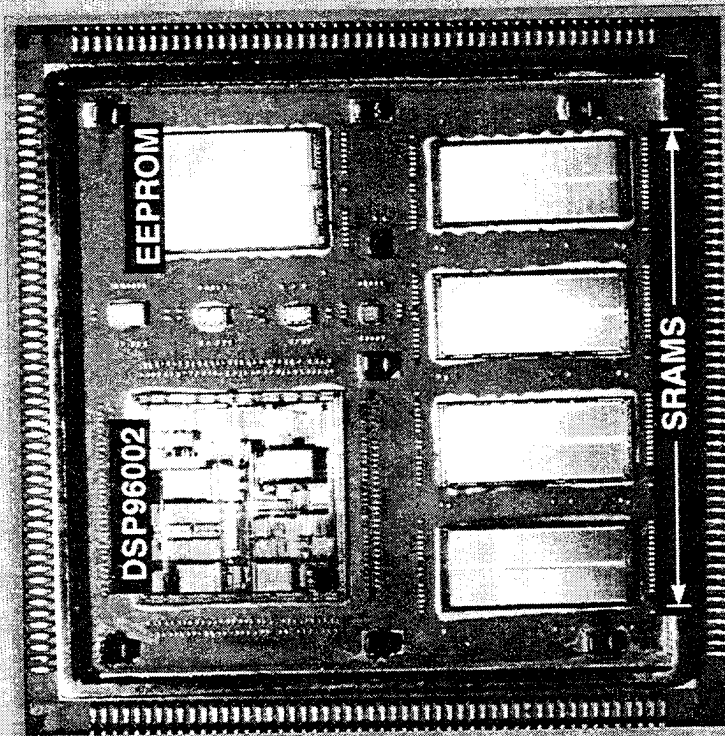
386V SIGNAL PROCESSOR



60 1989
20 MHz
1.5 Mbytes

2.5 kg (11 lb 5 oz)
7 W
2000 cm³

MULTI-CHIP MODULE PROCESSOR



2 INCHES

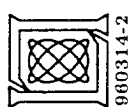
60 1989
60 MHz
0.5 Mbytes

0.5 kg (1 lb 5 oz)
3 W
500 cm³

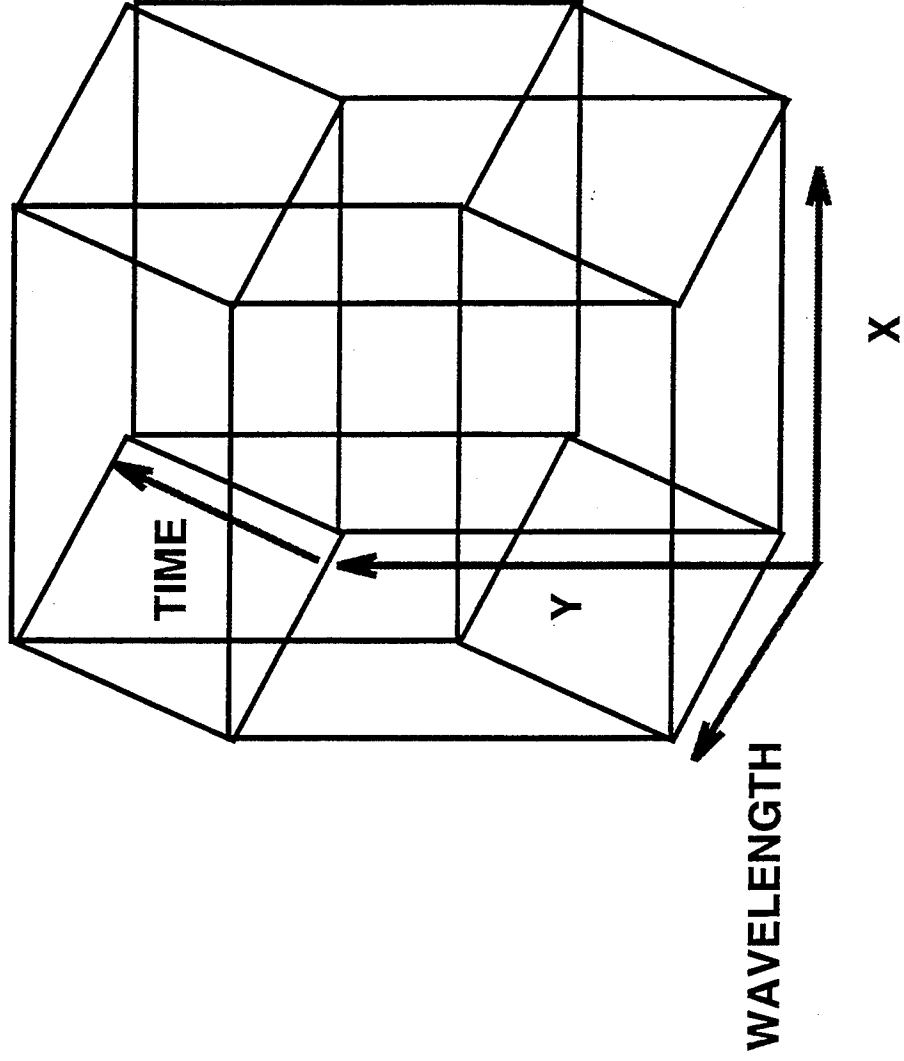


OUTLINE

- INTRODUCTION
- EO STAP THEORY
- EO STAP EXAMPLES
- HARDWARE IMPLEMENTATIONS
- ⇒ • FUTURE HYPERSPECTRAL SENSORS
- SUMMARY



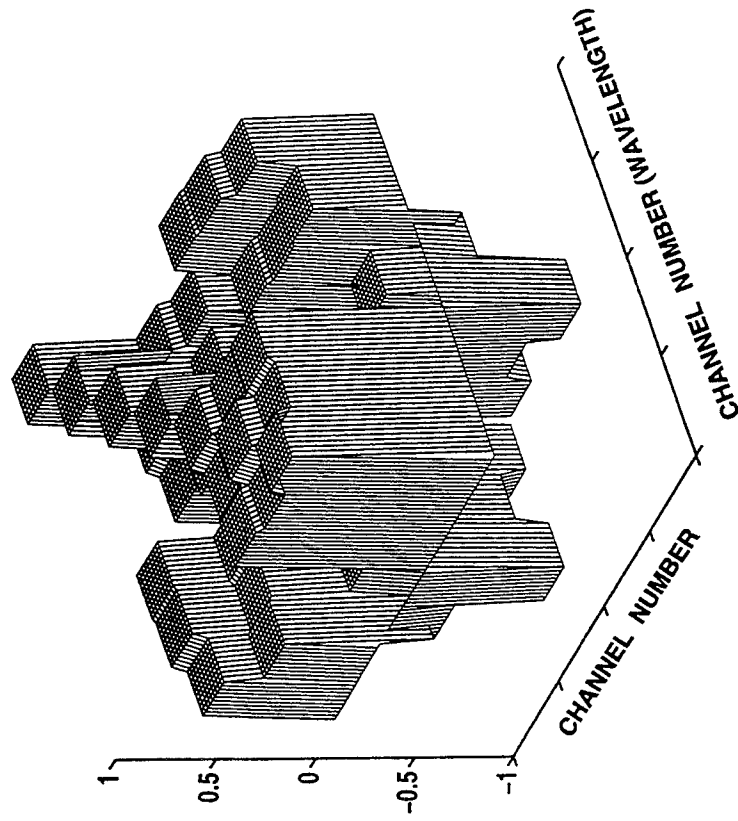
HYPERSPECTRAL HYPERCUBE



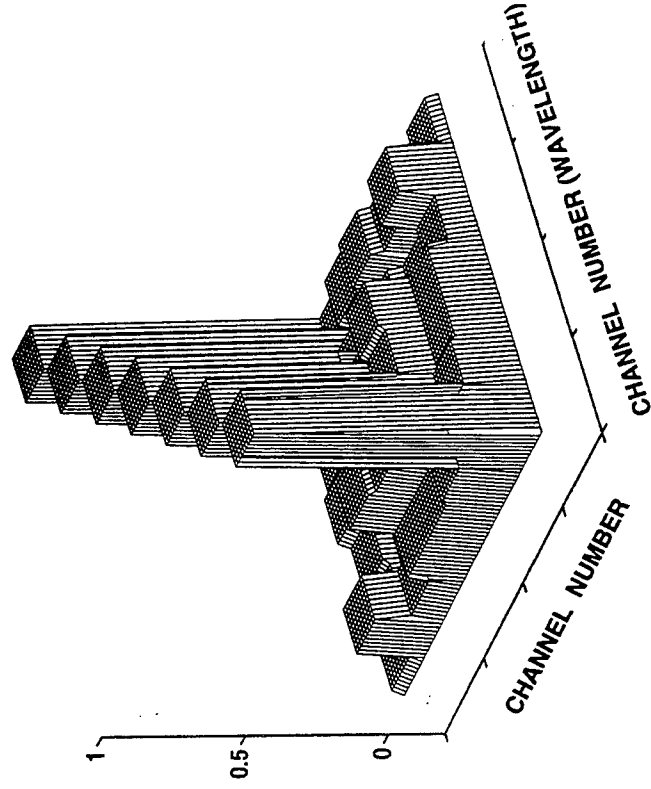
960130-4

LANDSAT MULTI-SPECTRAL (7-CHANNEL) CORRELATION

VEGETATION



WATER



OUTLINE

- INTRODUCTION
- EO STAP THEORY
- EO STAP EXAMPLES
- HARDWARE IMPLEMENTATIONS
- FUTURE HYPERSPECTRAL SENSORS
- ⇒ • SUMMARY



SUMMARY

- EO STAP THEORY SIMILAR TO RADAR STAP EXCEPT:
 - LITTLE OR NO BACKGROUND CORRELATION
 - IMPLEMENTATION OF VELOCITY FILTER
- EO STAP IS VERY ROBUST
 - SENSOR TYPES (STARING vs SCANNING)
 - WAVELENGTH (VIS, SWIR, MWIR, LWIR)
 - BACKGROUND (STELLAR, SKY, GROUND)
 - NON-UNIFORMITY IN SENSOR
- HARDWARE IMPLEMENTATION
 - SBV (SPACE-BASED VISIBLE) SENSOR TO LAUNCH 4/96



AN OVERVIEW OF ISSUES IN HOT CLUTTER MITIGATION

Thomas W. Miller and Janet M. Ortiz

Hughes Aircraft Company

P.O. Box 902

MS E1/J132

El Segundo, CA 90245

tel: (310) 616-8247

fax: (310) 355-6387

email: jortiz2@msmail2.hac.com

Abstract Because multipath jamming, or "hot clutter," consists of the coherent sum of weighted, time-delayed, Doppler-shifted versions of a common jammer waveform, mitigation techniques seek to exploit the commonality between the direct path waveform and the scattered signals. This is often done by obtaining a clean sample of the direct path jammer, then weighting it, through tapped delay lines and Doppler frequency weights, to cancel the scattered component. Other approaches exploit the commonality between separate areas on the ground to cancel the interference. In active radars, however, ground or "cold" clutter and target returns are also present, and the processing used to mitigate hot clutter can adversely affect standard STAP and radar signal processing. The five presentations in this session discuss issues in hot clutter mitigation, approaches to cancelling hot clutter including beam space, element space, and multiple linear constraint, and preliminary results in the simultaneous mitigation of hot clutter and ground clutter. In this overview, a brief discussion of the phenomenology of hot clutter is presented to motivate the development of alternate mitigation algorithms. Specific issues particular to the various mitigation approaches are presented, including general limitations on performance and the special requirements for simultaneous hot and cold clutter mitigation. Example performance using simulated data and selected Mountaintop samples is also shown. This presentation intends to summarize major work performed to date, introduce the subsequent current papers, and suggest areas that still remain to be studied.

**SESSION II:
MULTIPATH JAMMER MITIGATION**

**DR. THOMAS W. MILLER
SESSION CHAIR**

13 MARCH 1996

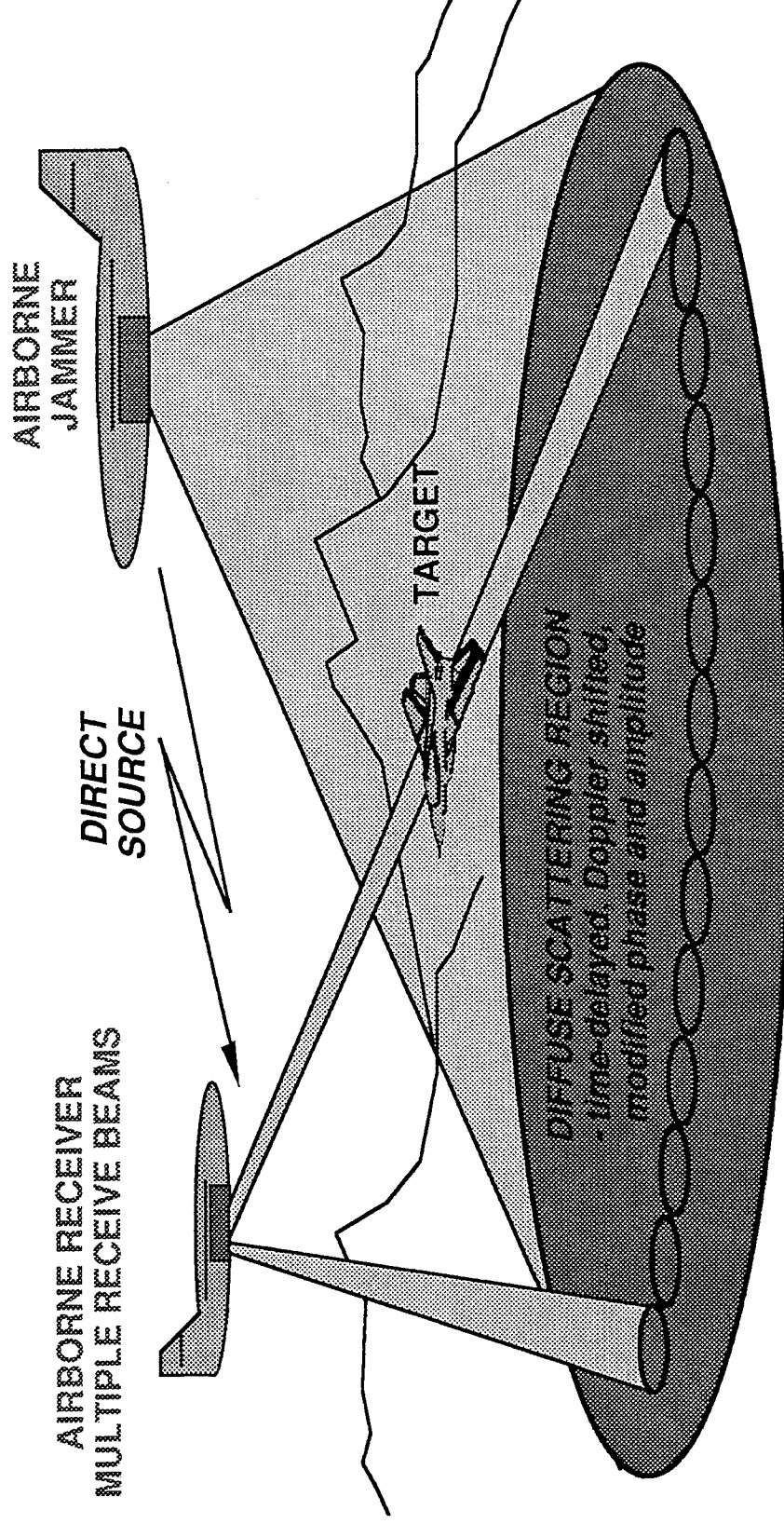
OUTLINE

HUGHES

- **PROBLEM DESCRIPTION**
- OVERVIEW OF PAPERS IN SESSION
- TSI PHENOMENOLOGY
- EFFECT OF TSI ON SYSTEM PERFORMANCE
- CONCEPTS FOR TSI MITIGATION
- PERFORMANCE EXAMPLES, MOUNTAINTOP SCENARIO
 - REFERENCE BEAM TECHNIQUES
 - ELEMENT SPACE TECHNIQUES
- MITIGATION OF COMBINED TSI AND RADAR CLUTTER
- CONCLUSIONS

JAMMER MULTIPATH SCENARIO

HUGHES



- direct path: $A(t)\cos(\omega t + \theta(t))$
- reflected path i : $\sigma_i A(t - \tau_i)\cos[(\omega + \omega_{di})(t - \tau_i) + \theta(t - \tau_i) + \phi_i]$

SO WHAT'S THE PROBLEM?

HUGHES

A HIGH POWER JAMMER OR INTERFERENCE SOURCE ILLUMINATES A LARGE SURFACE AREA

- Secondary sources of interference due to multipath
- Characterized by wide angular spread, time delay, and Doppler
- Difficult to eliminate by spatial adaptive array processing

ISSUES

- Cost-effective mitigation techniques are needed
- Problem of combined TSI and radar clutter mitigation
- Jammer multipath is highly terrain and scenario dependent
- Data collection for model verification can be difficult to obtain
- Accurate model of TSI to predict severity and to aid in design

DEFINITION OF TERMS

HUGHES

- **JAMMER MULTIPATH SCATTERED FROM THE EARTH'S SURFACE ALSO KNOWN AS**
 - Terrain Scattered Interference (TSI)
 - Hot Clutter
 - Usually contains direct path as well as multipath
- **GROUND BOUNCE JAMMING**
 - Deliberate illumination of the Earth's surface to mask a target
 - Direct path may not be present
- **RADAR CLUTTER**
 - Ground clutter returns in a pulsed or CW radar
 - Also known as "cold" clutter

GENERAL APPROACH TO MITIGATION OF JAMMER MULTIPATH

HUGHES

OBJECTIVE

Use adaptive processing to eliminate jamming and jammer multipath.

APPROACH

Add adaptive tapped delay-lines to the adaptive array to help equalize the multipath.

DESIGN METHOD

Characterize jammer multipath amplitude, time delay, Doppler shift.
Determine number of taps/channel required to eliminate only significant multipath.
Minimize interaction between jammer and radar clutter nulling.

SOLUTION

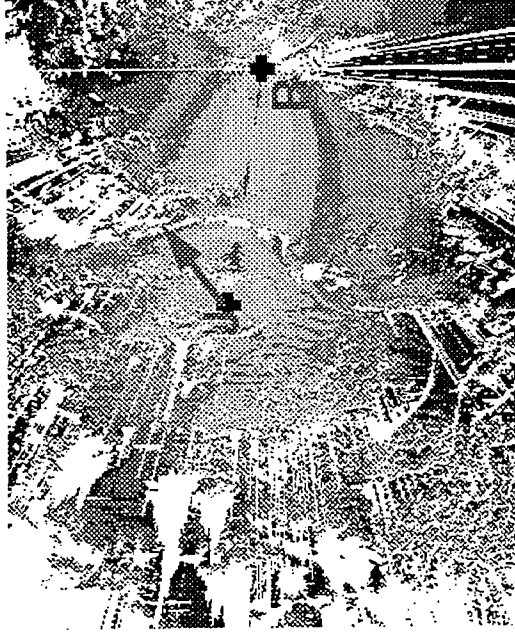
Complexity of adaptive processor will depend on bandwidth, jammer characteristics, and the selected adaptive processing method.

SUMMARY OF RESEARCH AREAS

HUGHES

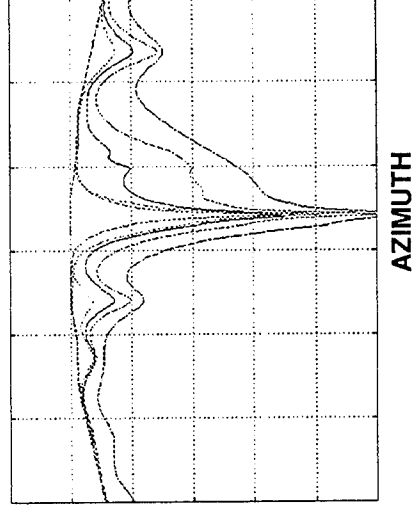
- PHENOMENOLOGY

- TSI CHARACTERIZATION
 - *amplitude, time delay, Doppler shift, polarization, angle of arrival*
- BISTATIC REFLECTIVITY MODELS
 - *constant γ*
 - *two scales of roughness*
- TERRAIN DATA AND MODELS
- COLLECTED TSI DATA (i.e., MOUNTAINTOP)



- TSI-ONLY MITIGATION

- REFERENCE BEAM APPROACH
- BEAM SPACE WITH TAPPED DELAYS
- ELEMENT SPACE WITH TAPPED DELAYS
- WITH/WITHOUT DOPPLER COMPENSATION ^{SINR}
- OTHER COMBINATIONS



- SIMULTANEOUS TSI AND RADAR CLUTTER MITIGATION

- CURRENT AREA OF EMPHASIS

OUTLINE

HUGHES

- PROBLEM DESCRIPTION
- OVERVIEW OF PAPERS IN SESSION
- TSI PHENOMENOLOGY
- EFFECT OF TSI ON SYSTEM PERFORMANCE
- CONCEPTS FOR TSI MITIGATION
- PERFORMANCE EXAMPLES, MOUNTAINTOP SCENARIO
 - REFERENCE BEAM TECHNIQUES
 - ELEMENT SPACE TECHNIQUES
- MITIGATION OF COMBINED TSI AND RADAR CLUTTER
- CONCLUSIONS

CURRENT SESSION PAPERS: 1

HUGHES

- Cancellation of Terrain Scattered Jamming in Airborne Radars

Larry Brennan

- Problem
 - Simultaneous hot and cold clutter nulling requires both:
 - *RAPID WEIGHT UPDATES*
 - *LONG COHERENT PROCESSING INTERVALS*
- Proposed Solution
 - 2- or 3-pulse MTI canceller in main beam, followed by scatter cancellation
 - Alternate: DFT Doppler processing over many PRIs for clutter removal, followed by scatter cancellation
 - Rotating scatter canceller weights compensate for the changing bistatic path lengths
- Tested with Collected Mountaintop Data

- Signal Subspace Issues in TSI Mitigation

Robert A. Gabel

- Problem
 - Computation costs of TSI mitigation configurations can be high
 - *MANY TAPS REQUIRED FOR LARGE DELAY AND DOPPLER DISPERSIONS*
- Proposed Solutions
 - Minimize cost of TSI mitigation weight training using:
 - *ALGORITHM MODIFICATIONS, WEIGHT PRUNING, TRADEOFFS IN DOPPLER TRACKING OF WEIGHTS ACROSS A CPI*
 - Use TSI parameters (delay, azimuth, Doppler and time) to select weights to be implemented
- Tested with Collected Mountaintop Data
 - Metrics: residual jammer power, system SINR, net array patterns

CURRENT SESSION PAPERS: 3

HUGHES

- Simultaneous Mitigation of Multipath Jamming and Ground Clutter

Daniel F. Marshall and Robert A. Gabel

- Problem
 - Current STAP algorithms do not effectively accommodate multipath jamming in the main beam
 - *POTENTIAL DEGRADED PERFORMANCE OVER A LARGE AREA*
 - Challenge to train for jammer mitigation in the presence of clutter
- Proposed Solutions
 - Combine existing STAP and multipath jamming mitigation techniques
 - *BEAMSPACE*
 - *ELEMENT SPACE*
- Performance Results Shown Using Simulated Data

CURRENT SESSION PAPERS: 4

HUGHES

- Hot Clutter Cancellation with Orthogonal Beamspace Transforms

Stephen M. Kogon, Douglas B. Williams, and E. Jeff Holder

- Problem
 - Conventional adaptive canceller with reference beam needs many temporal degrees of freedom
 - Hot clutter is not limited to mainbeam; present at many angles
- Proposed Solutions
 - Use orthogonal beamspace transformation to make use of entire angular spectrum
 - *REDUCES TEMPORAL WINDOW OF RESULTING CANCELLER*
 - *TRADES OFF SPATIAL FOR TEMPORAL DEGREES OF FREEDOM*
- Tested with Collected Mountaintop Data
 - Metrics: performance vs. total number of degrees of freedom

CURRENT SESSION PAPERS: 5

HUGHES

- Adaptive Hot Clutter Mitigation Using Multiple Linear Constraints

Lloyd J. Griffiths

- Problem
 - Simultaneous hot clutter adaptation in both space and time can adversely affect other radar functions, such as Doppler extraction
- Proposed Solution
 - Use multiple linear constraints in adaptive radar array processors
 - MAXIMIZE SNR OF DESIRED SIGNAL
 - PRODUCE DISTORTIONLESS TIME ESTIMATE OF THE SIGNAL
- Tested with Collected Mountaintop Data
 - Metrics: comparison with previous approaches

**AN OVERVIEW OF ISSUES
IN HOT CLUTTER MITIGATION**

DR. THOMAS W. MILLER

and

JANET M. ORTIZ

HUGHES AIRCRAFT COMPANY

OUTLINE

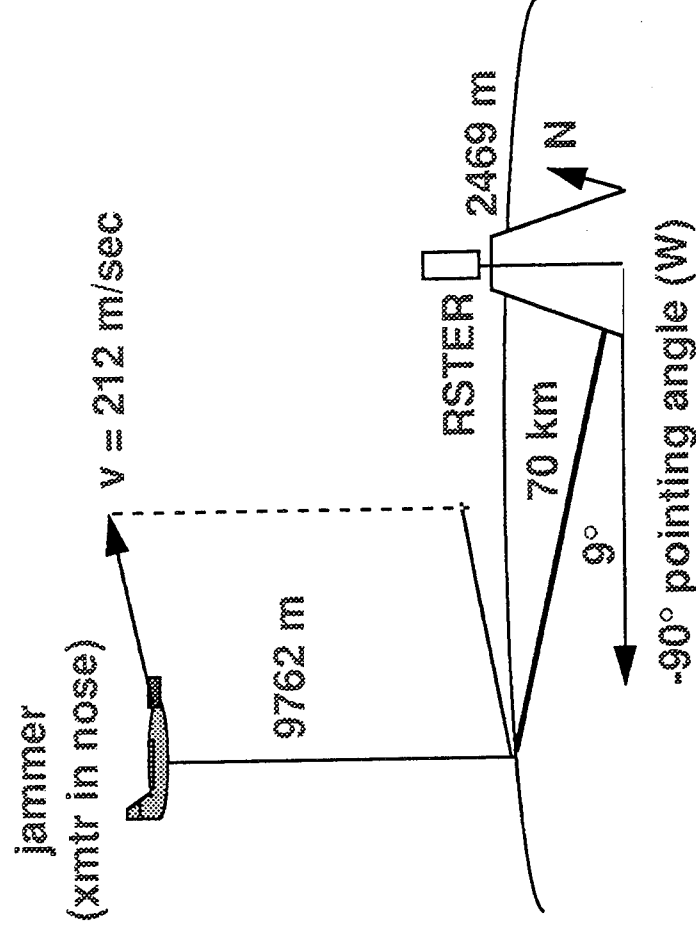
HUGHES

- PROBLEM DESCRIPTION
- OVERVIEW OF PAPERS IN SESSION
- TSI PHENOMENOLOGY
- EFFECT OF TSI ON SYSTEM PERFORMANCE
- CONCEPTS FOR TSI MITIGATION
- PERFORMANCE EXAMPLES, MOUNTAINTOP SCENARIO
 - REFERENCE BEAM TECHNIQUES
 - ELEMENT SPACE TECHNIQUES
- MITIGATION OF COMBINED TSI AND RADAR CLUTTER
- CONCLUSIONS

MOUNTAINTOP SCENARIO

HUGHES

- Radar (RSTER-90)
 - altitude = 2469 m above sea level
 - 14-channel antenna
 - sample rate = 1MHz
- Jammer
 - altitude = 9762 m above sea level
 - range = 70 km
 - azimuth = 9° from broadside
 - velocity = 212 m/sec towards NE (53°)
 - bandwidth = 200 KHz, Gaussian*
 - power = 48 dB into omni channel

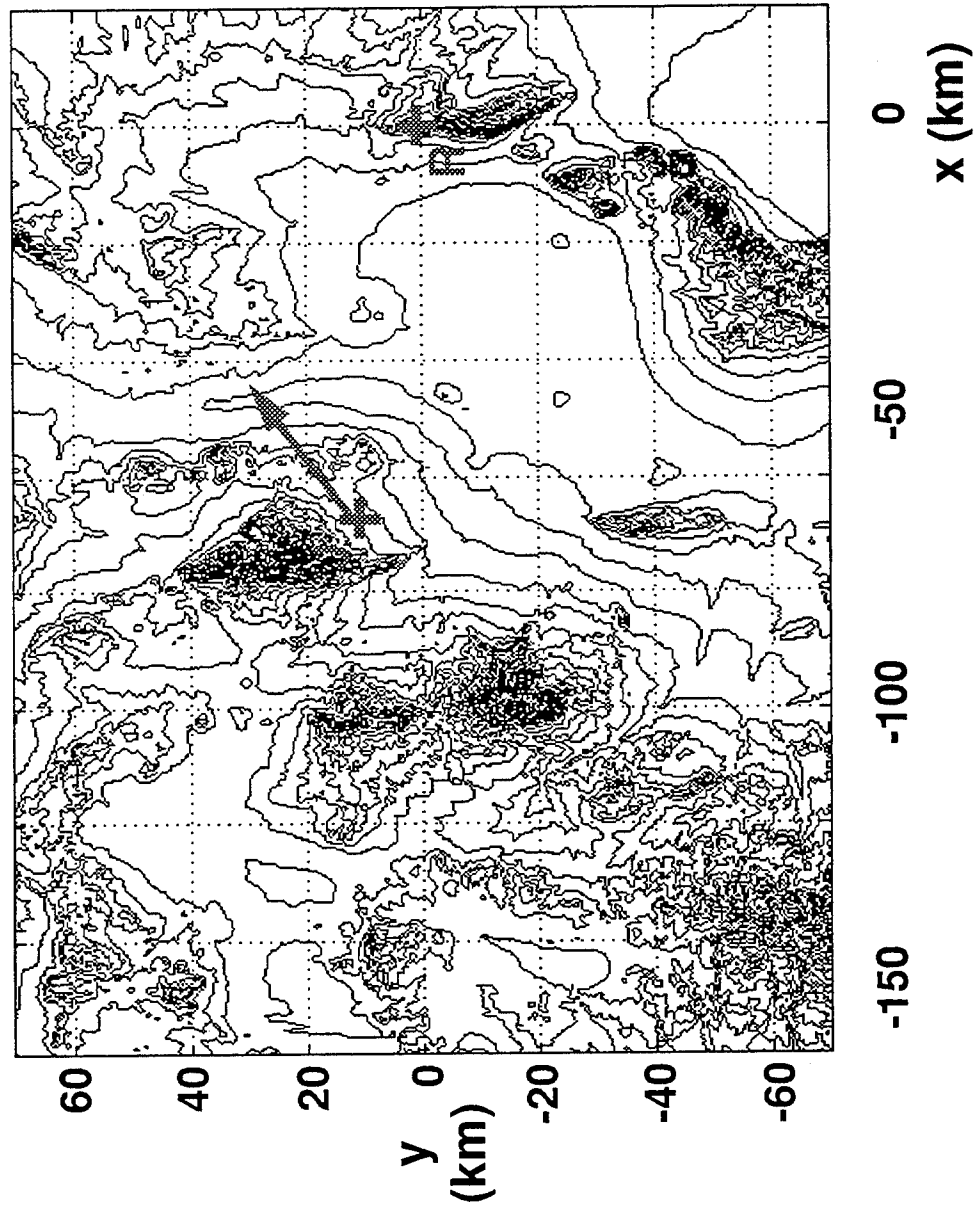


* for simplification of the analysis, bandwidth was reduced to 100 KHz with a sharper cut-off in frequency

TERRAIN CONTOURS

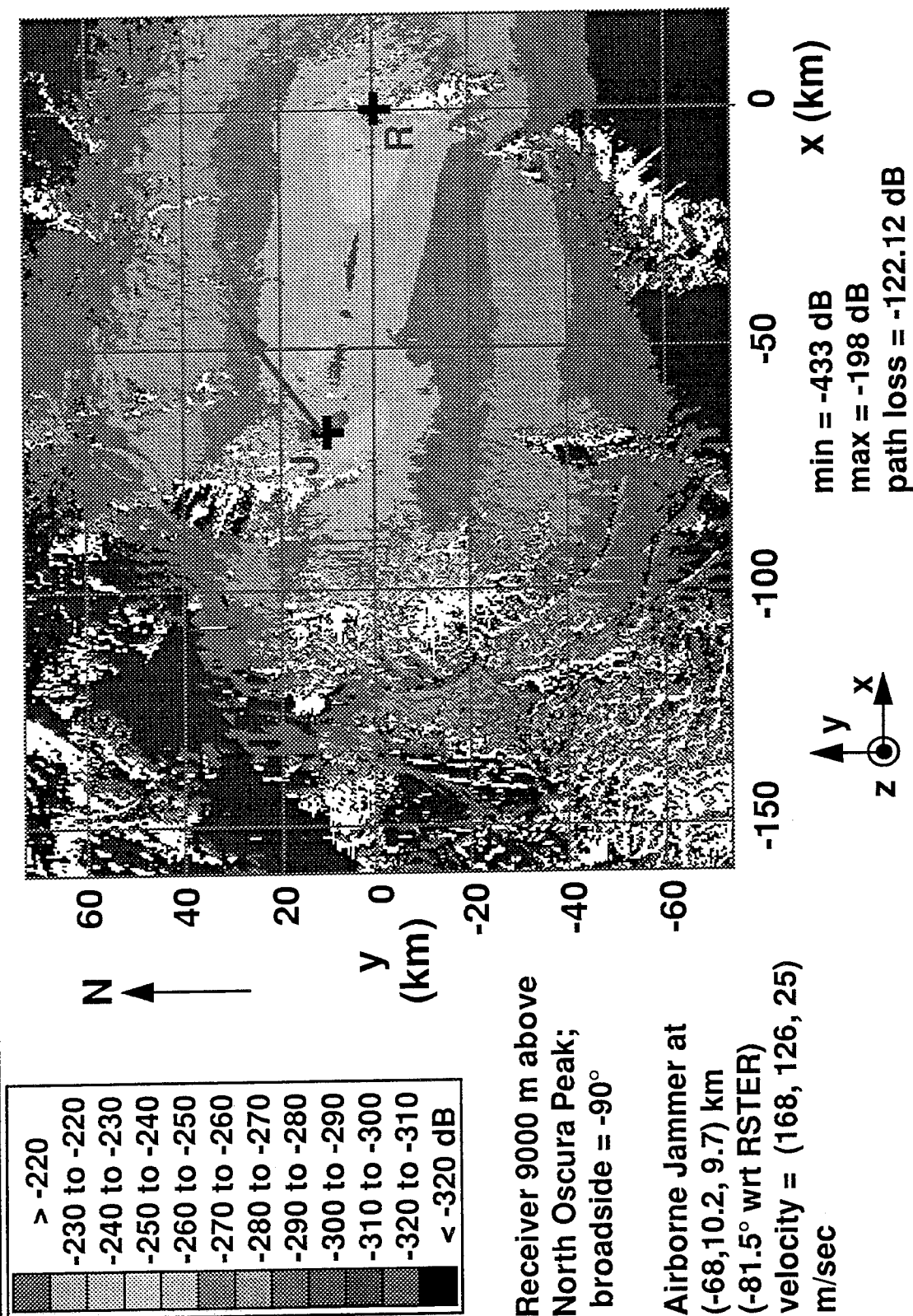
HUGHES

White Sands
Missile Range
(WSMR)
1200-3200 m
100 m contours



SIMULATED POWER RETURNS: AIRBORNE RECEIVER

HUGHES



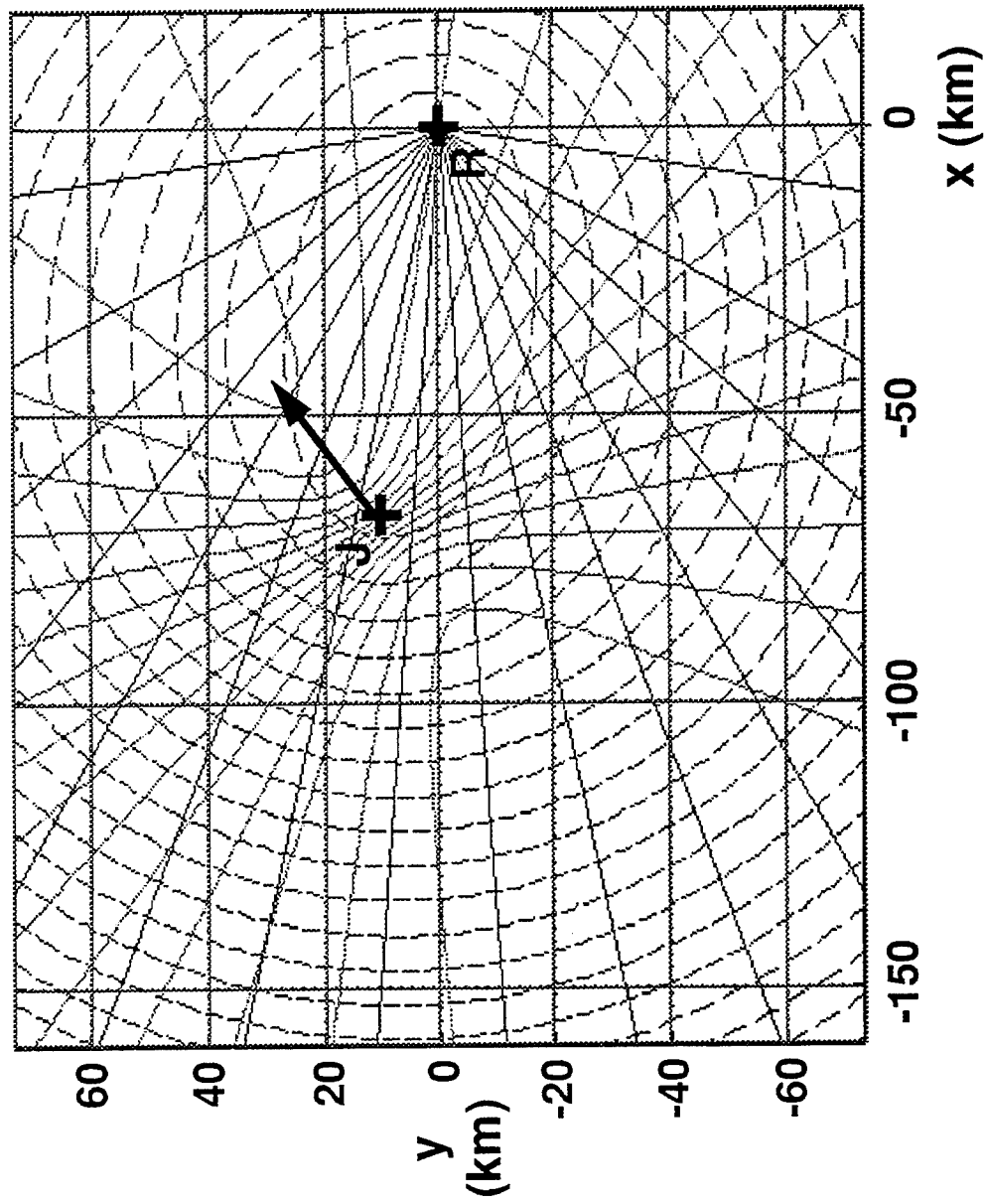
GEOMETRY CONSTANT CONTOURS

HUGHES

40 μ sec
Time Delay

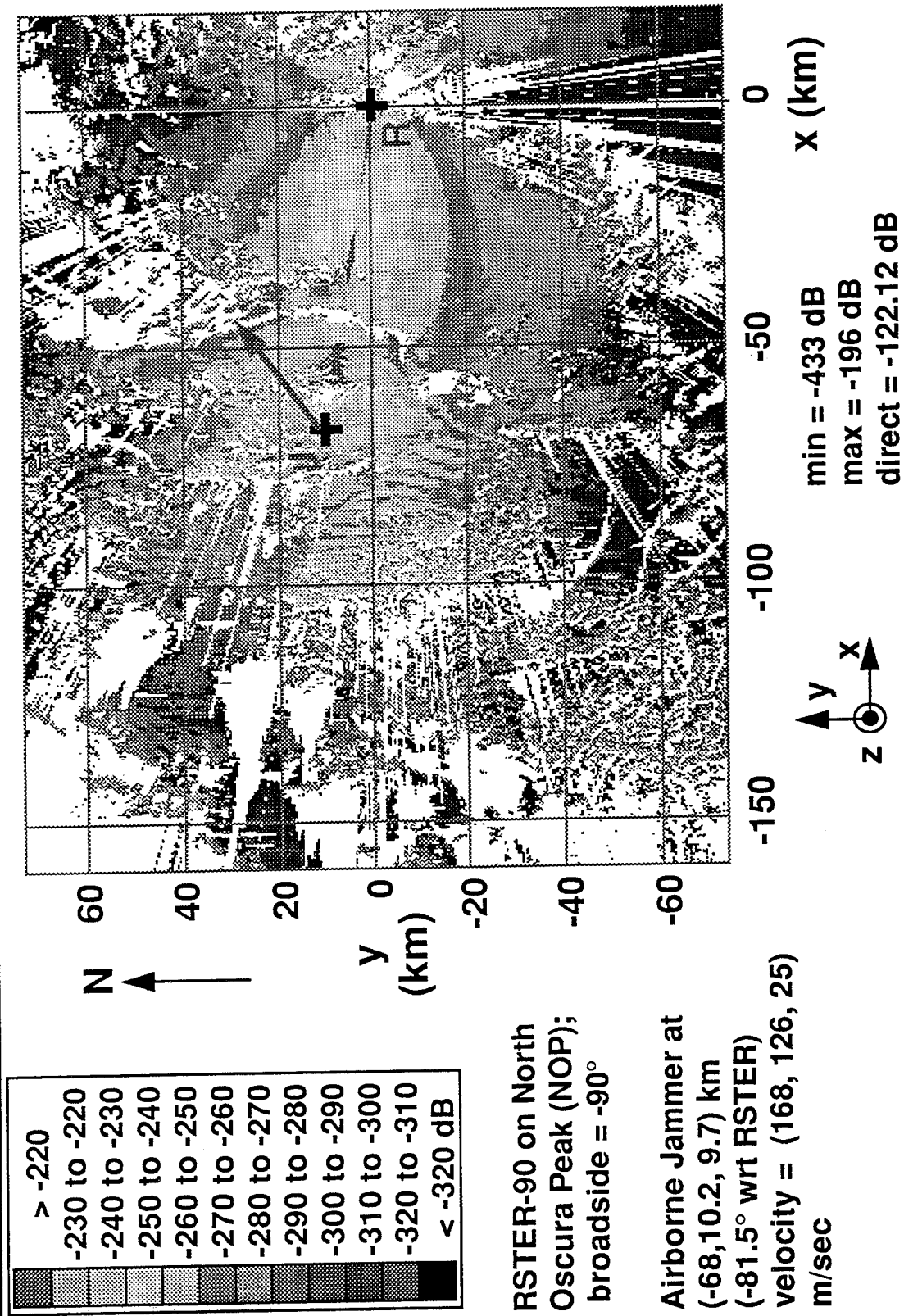
40 Hz
Doppler

8° Beams



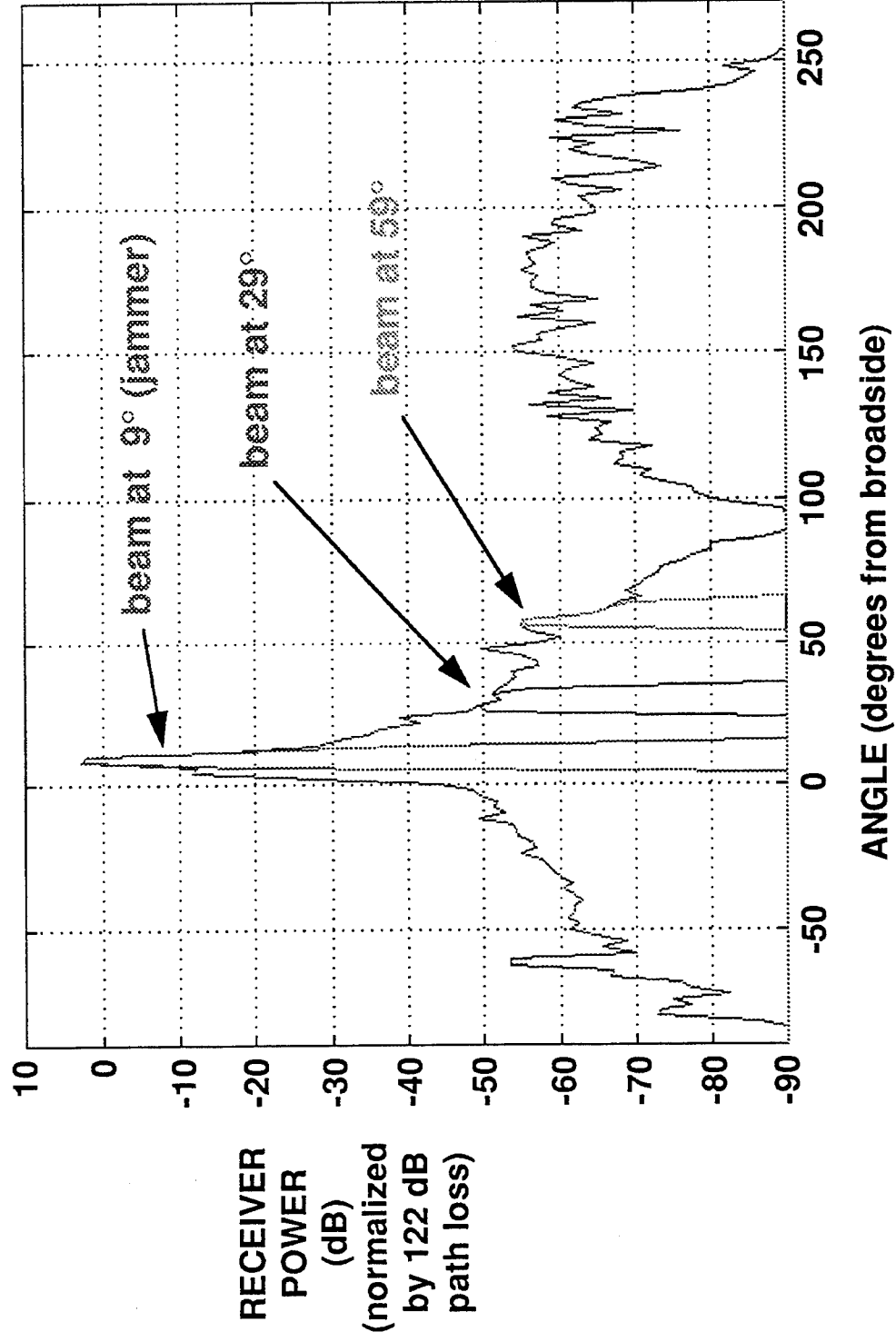
CALCULATED POWER RETURN FOR RIO042

HUGHES



RECEIVED POWER VS. AZIMUTH; SINGLE JAMMER AT 9°

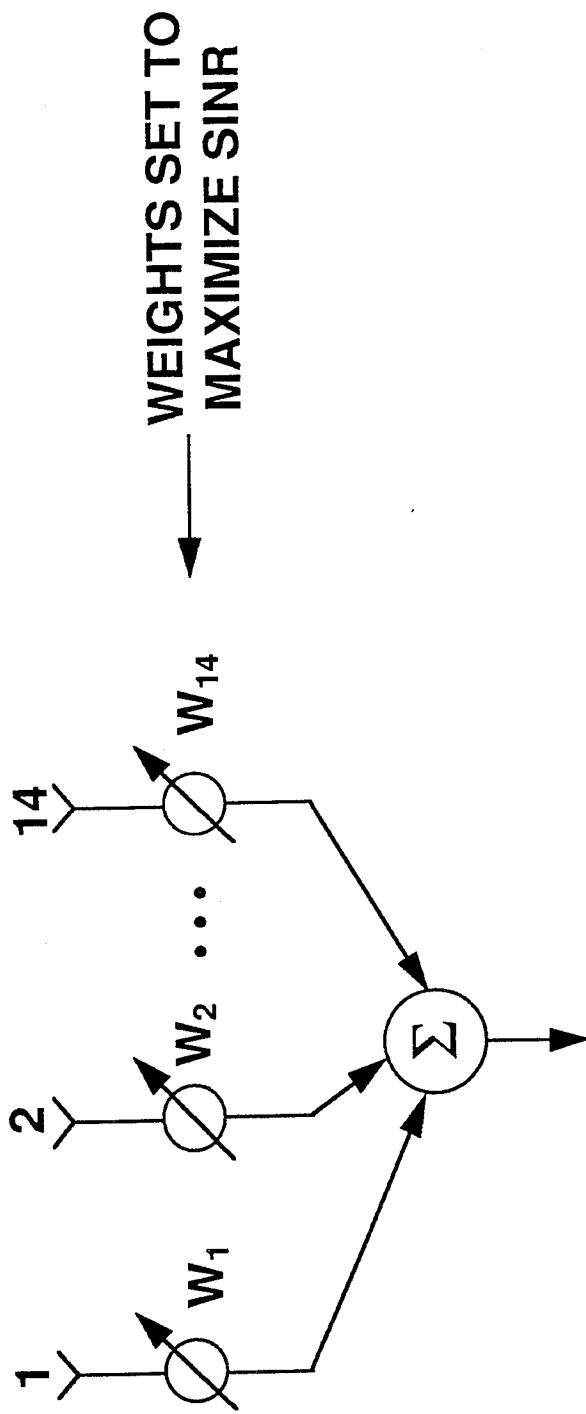
HUGHES



CONVENTIONAL SPATIAL ADAPTIVE PROCESSOR

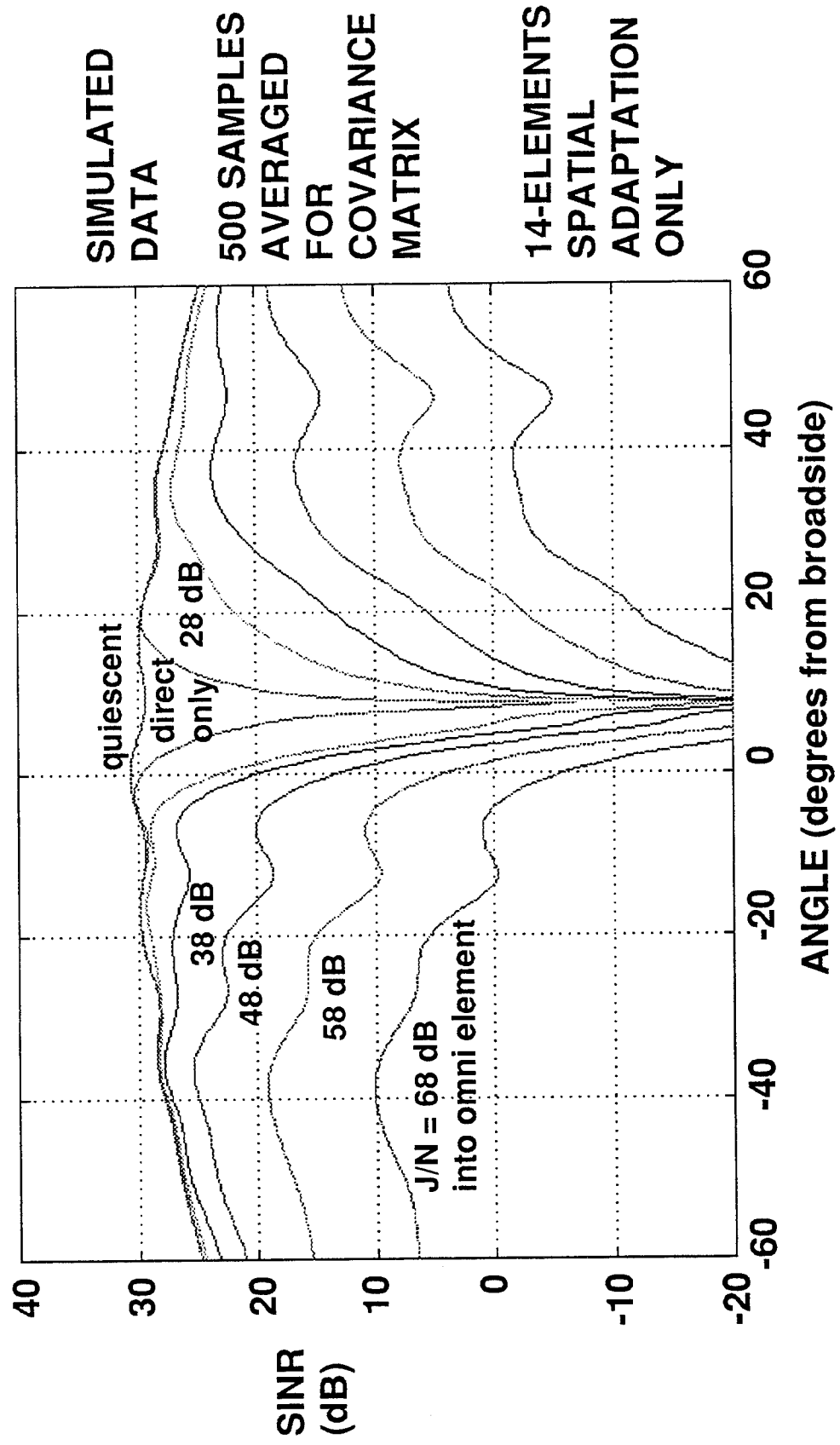
HUGHES

SUBARRAYS



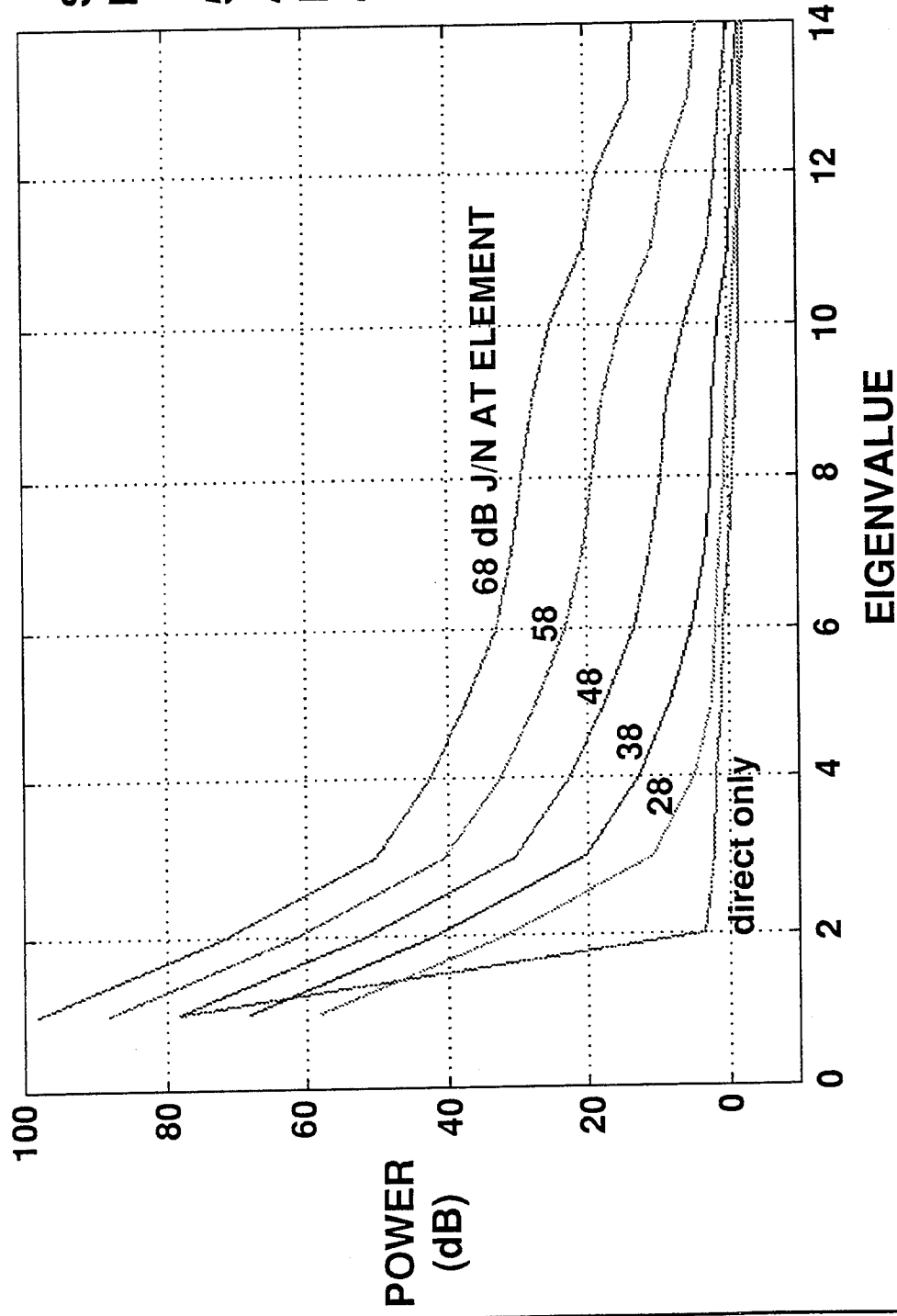
EFFECT OF TSI ON ADAPTIVE ARRAY PERFORMANCE

HUGHES



EIGENVALUES OF COVARIANCE MATRIX (500 SAMPLES AVERAGED)

HUGHES



ADAPTIVE ARRAY PERFORMANCE IS LIMITED DUE TO TSI

HUGHES

- Dispersion in angle
 - jammer nulling requires multiple degrees of freedom per jammer
 - potential degraded performance over a large area
- Primarily a main beam problem
 - TSI strongest in main beam
 - formation of broad spatial null in main beam degrades SINR
- Mitigation techniques take advantage of the time correlation between direct path and multipath
 - allows use of temporal (tapped delay line) processing
- Observation: Magnitude in wide angle regions varies widely according to terrain
 - mountainous generally produces strongest returns
 - much lower over water; depends on sea state

TOOLS FOR CHARACTERIZING TSI

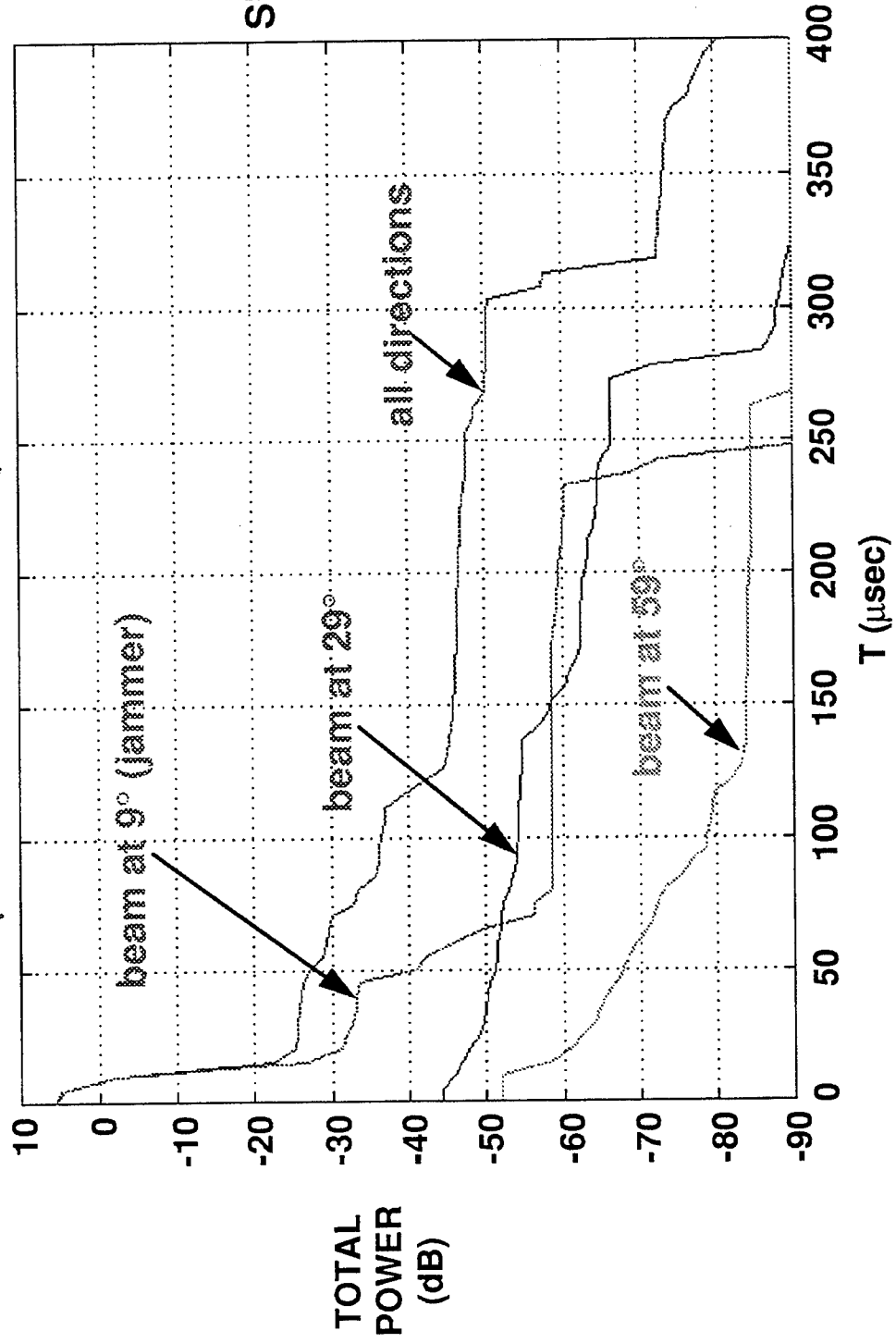
HUGHES

- Purpose is to design mitigation procedure
- Important parameters for designing adaptive processor
 - total time delay extent of significant jammer multipath
 - determines length of tapped delay line (number of taps)
 - total Doppler shift extent of jammer multipath
 - determines weight update rate
 - determines the number of Doppler compensation channels required
 - maximum bandwidth and band shape
 - determines maximum tap spacing
 - eigenvalues of covariance matrix
 - indicates number of adaptive degrees of freedom needed for particular adaptive processing configuration
 - required cancellation ratio
 - determines extent of “significant” time delay / Doppler shift

TIME DELAY CHARACTERIZATION OF TSI (RIO042)

HUGHES

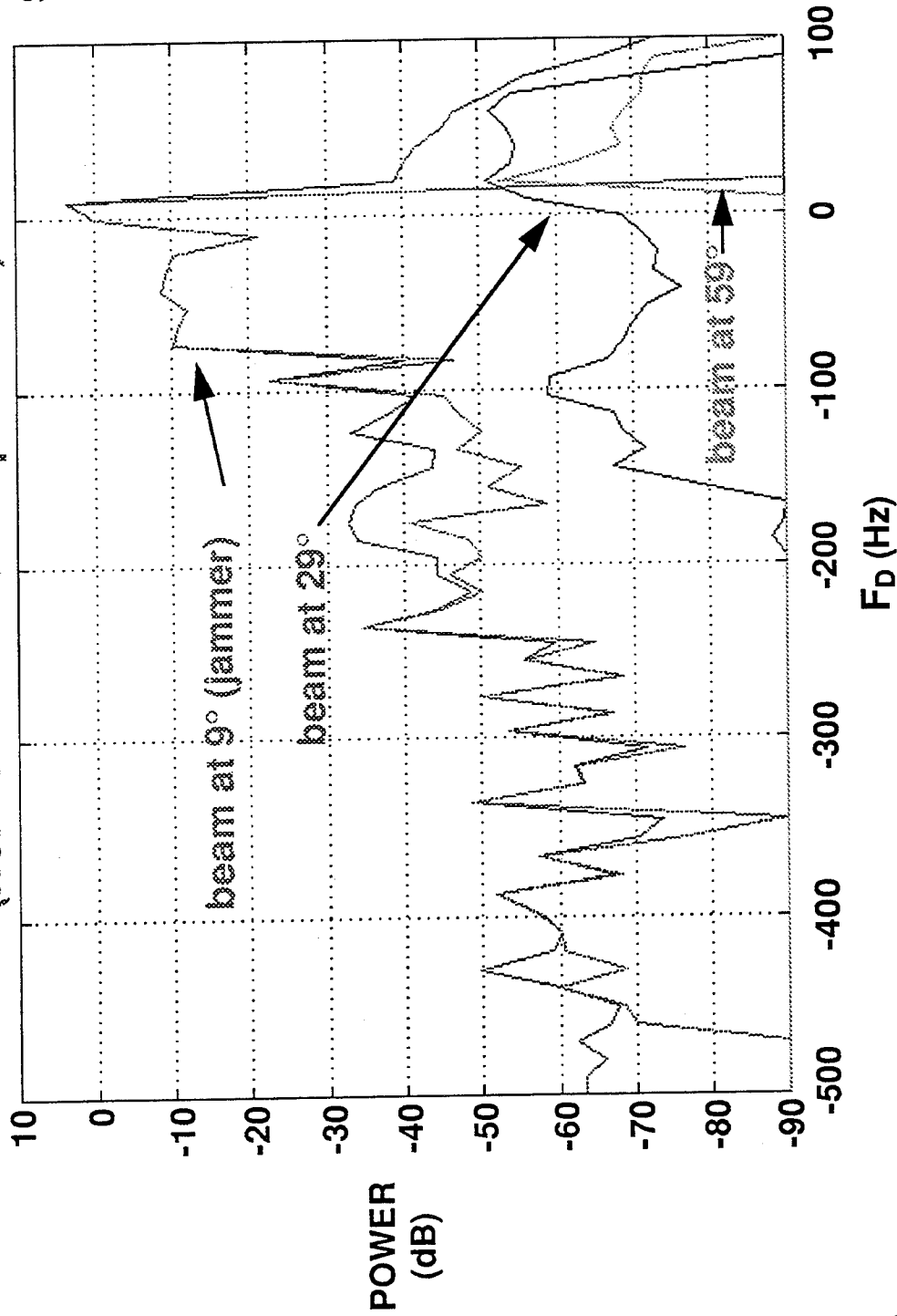
TOTAL POWER WITH TIME DELAY GREATER THAN T
(normalized to direct path loss)



DOPPLER CHARACTERIZATION

HUGHES

POWER AT DOPPLER FREQUENCY F_D
(normalized to direct path loss)



SIMULATED
DATA

Note:
Returns
with
highest
Doppler are
in beams
pointed
near
jammer.

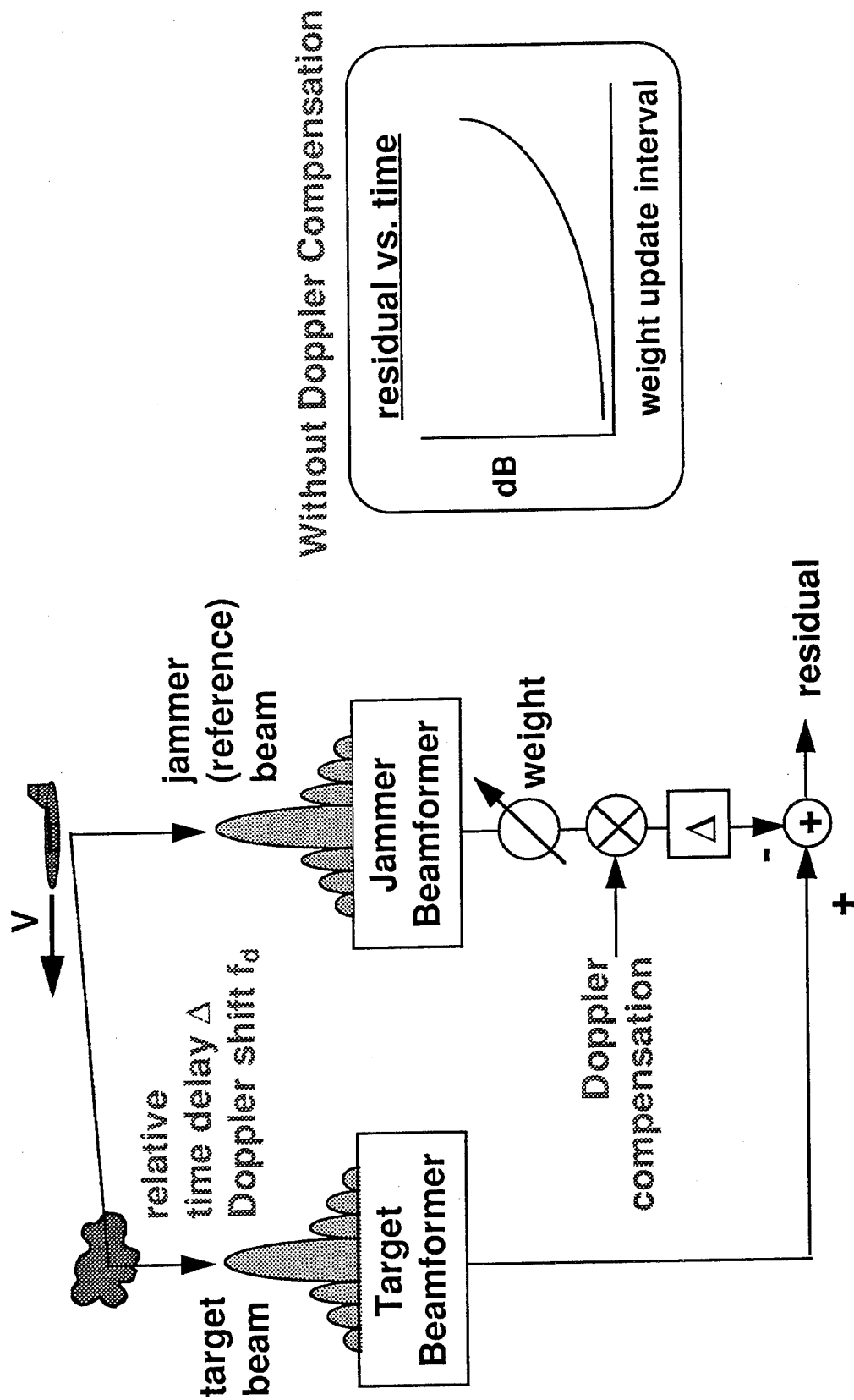
OUTLINE

HUGHES

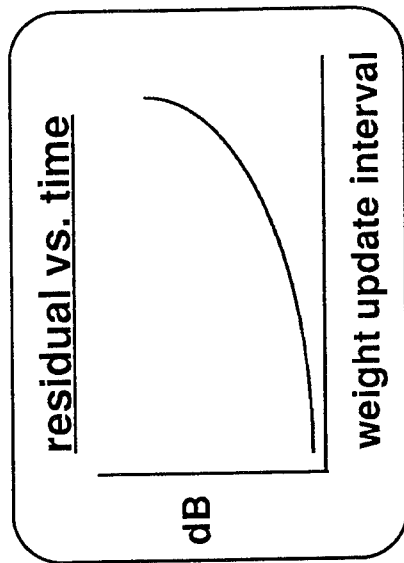
- PROBLEM DESCRIPTION
- OVERVIEW OF PAPERS IN SESSION
- TSI PHENOMENOLOGY
- EFFECT OF TSI ON SYSTEM PERFORMANCE
- CONCEPTS FOR TSI MITIGATION
- PERFORMANCE EXAMPLES, MOUNTAINTOP SCENARIO
 - REFERENCE BEAM TECHNIQUES
 - ELEMENT SPACE TECHNIQUES
- MITIGATION OF COMBINED TSI AND RADAR CLUTTER
- CONCLUSIONS

ONE MITIGATION APPROACH: REFERENCE BEAM CONCEPT

HUGHES

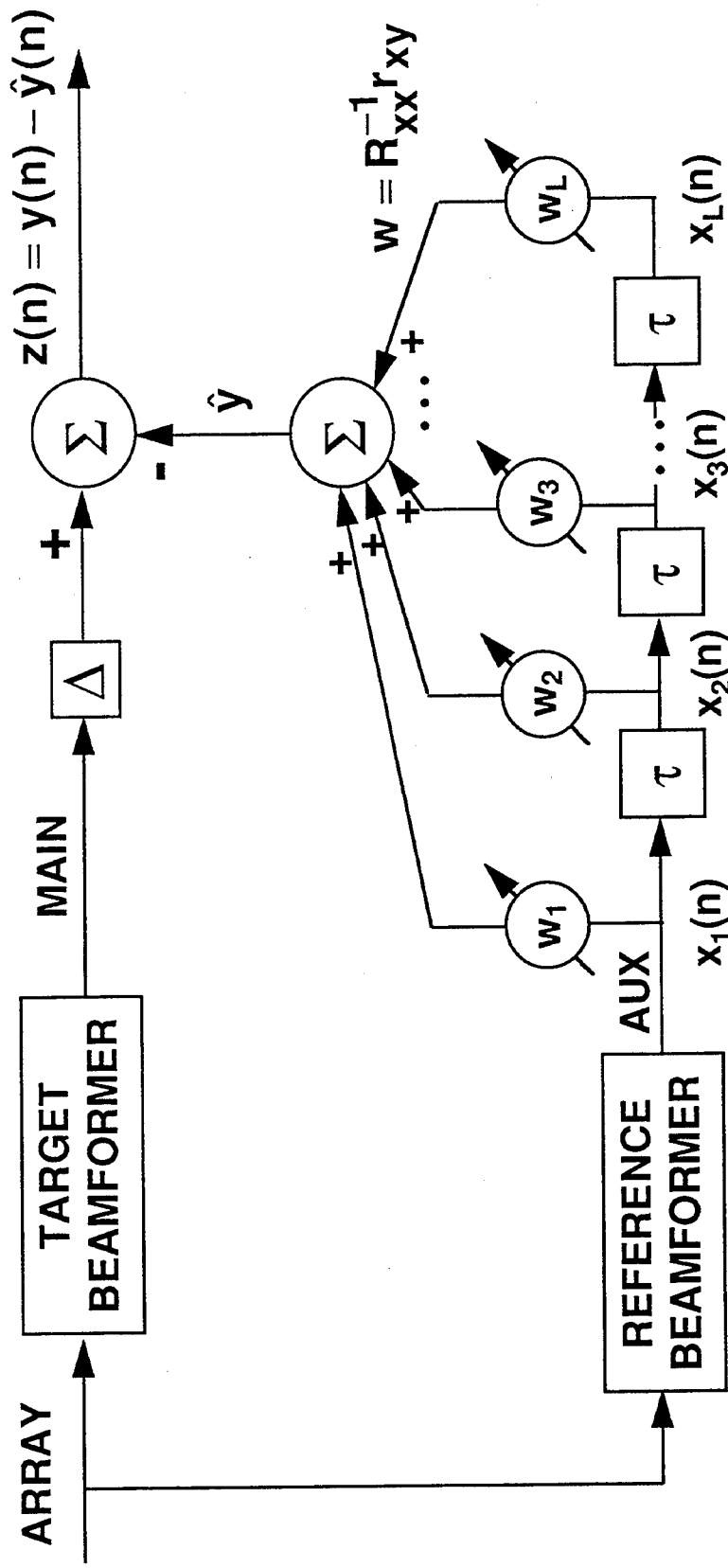


Without Doppler Compensation



JAMMER MITIGATION: REFERENCE BEAM APPROACH *

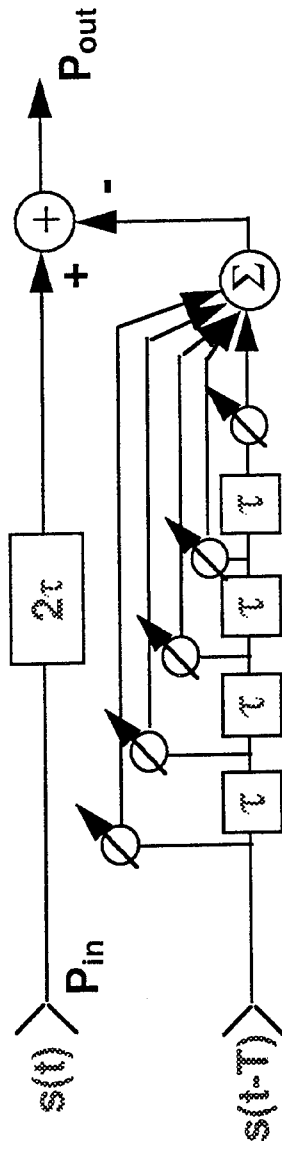
HUGHES



* COURTESY OF BOB GABEL, MIT/LL

CANCELLATION RATIO VS. TIME DELAY FOR 5-TAP TAPPED DELAY LINE

HUGHES

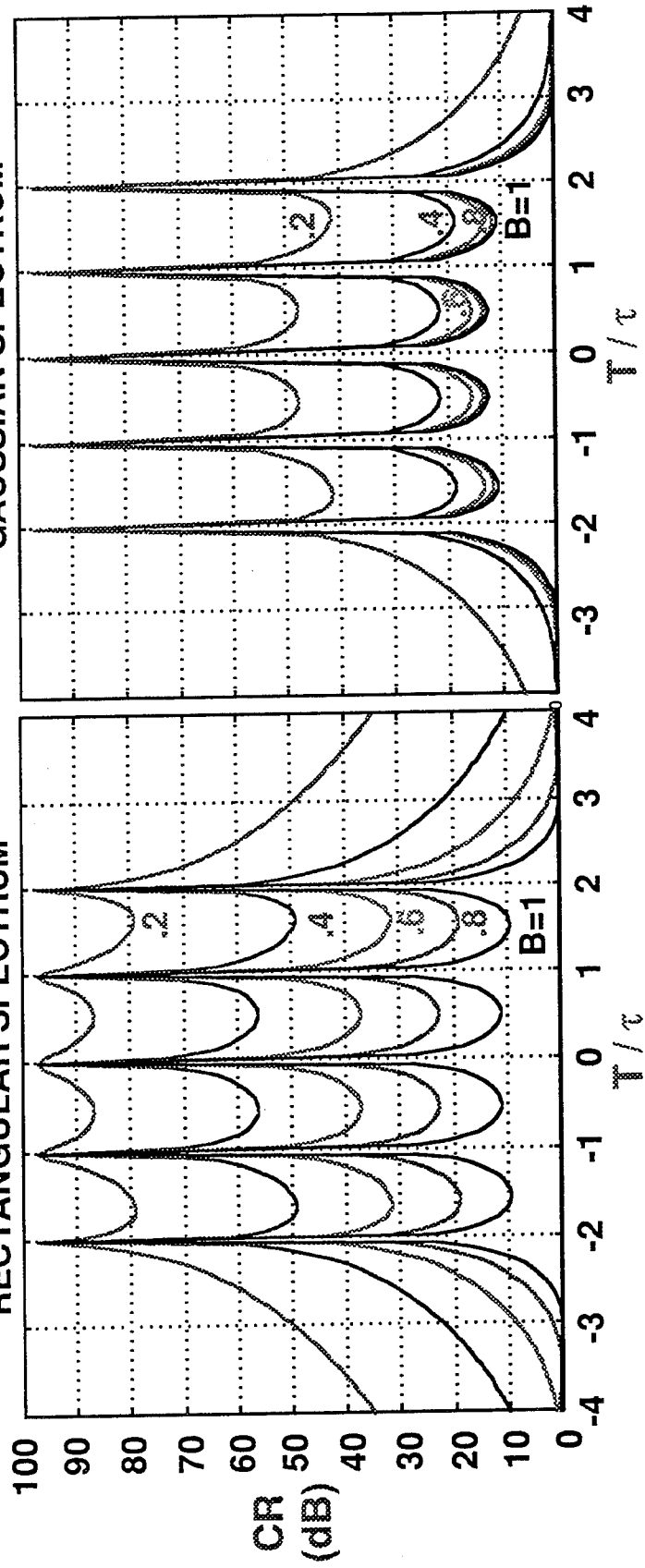


$$CR = \frac{P_{in}}{P_{out}}$$

$B = \text{bandwidth} \cdot \tau$

RECTANGULAR SPECTRUM

GAUSSIAN SPECTRUM



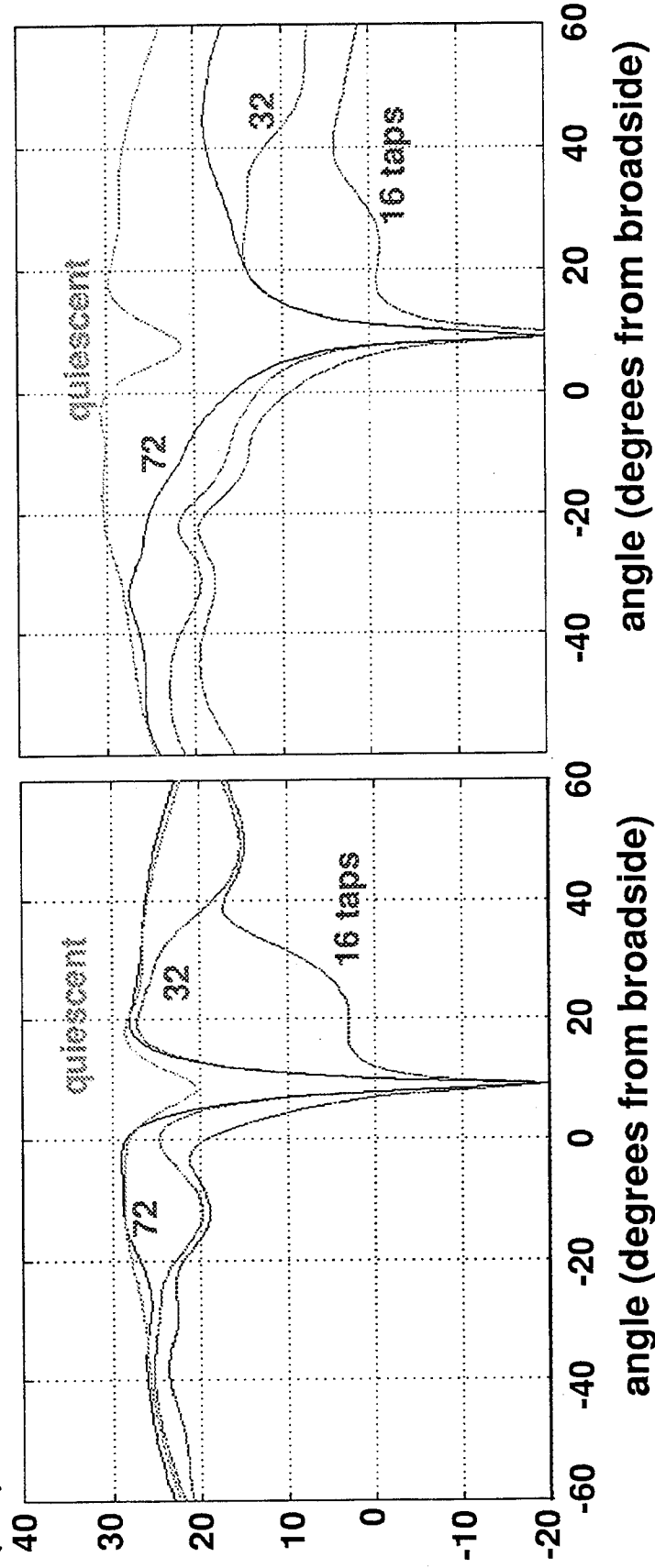
REFERENCE BEAM RESULTS

HUGHES

RIO042 COLLECTED DATA
MOVING JAMMER

SIMULATED
STATIONARY JAMMER

SINR
(dB)



REFERENCE BEAM APPROACH ISSUES

HUGHES

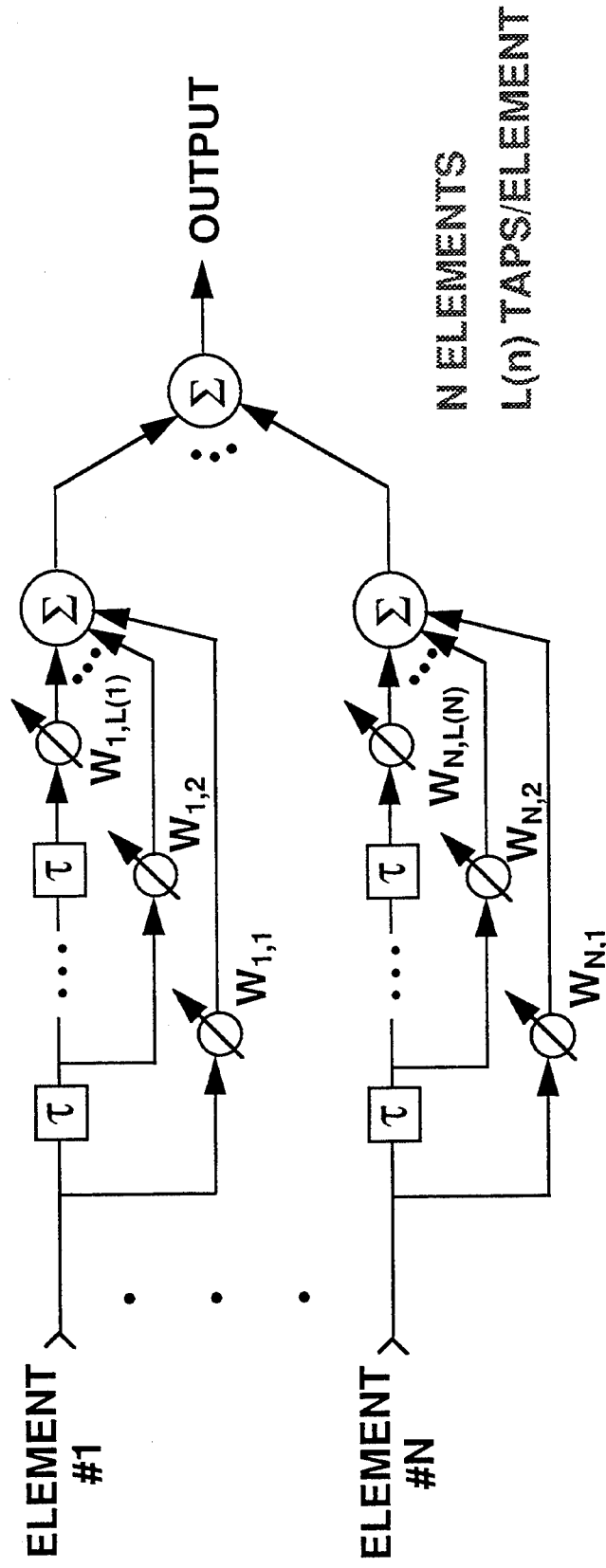
- Advantages of reference beam approach
 - strong sample of jammer (high J/N)
 - fewer adaptive weights
 - minimizes modulation of radar clutter at other angles of arrival

- But
 - relies on strong direct source
 - relies on time delayed version of direct source
 - eclipsing in pulsed radars
 - Doppler dispersion tends to be widest in the specular beam
 - must determine what beam contains direct path
 - requires additional jammer beam for each additional jammer

These issues lead to consideration of other architectures

ELEMENT-SPACE CONFIGURATION

HUGHES

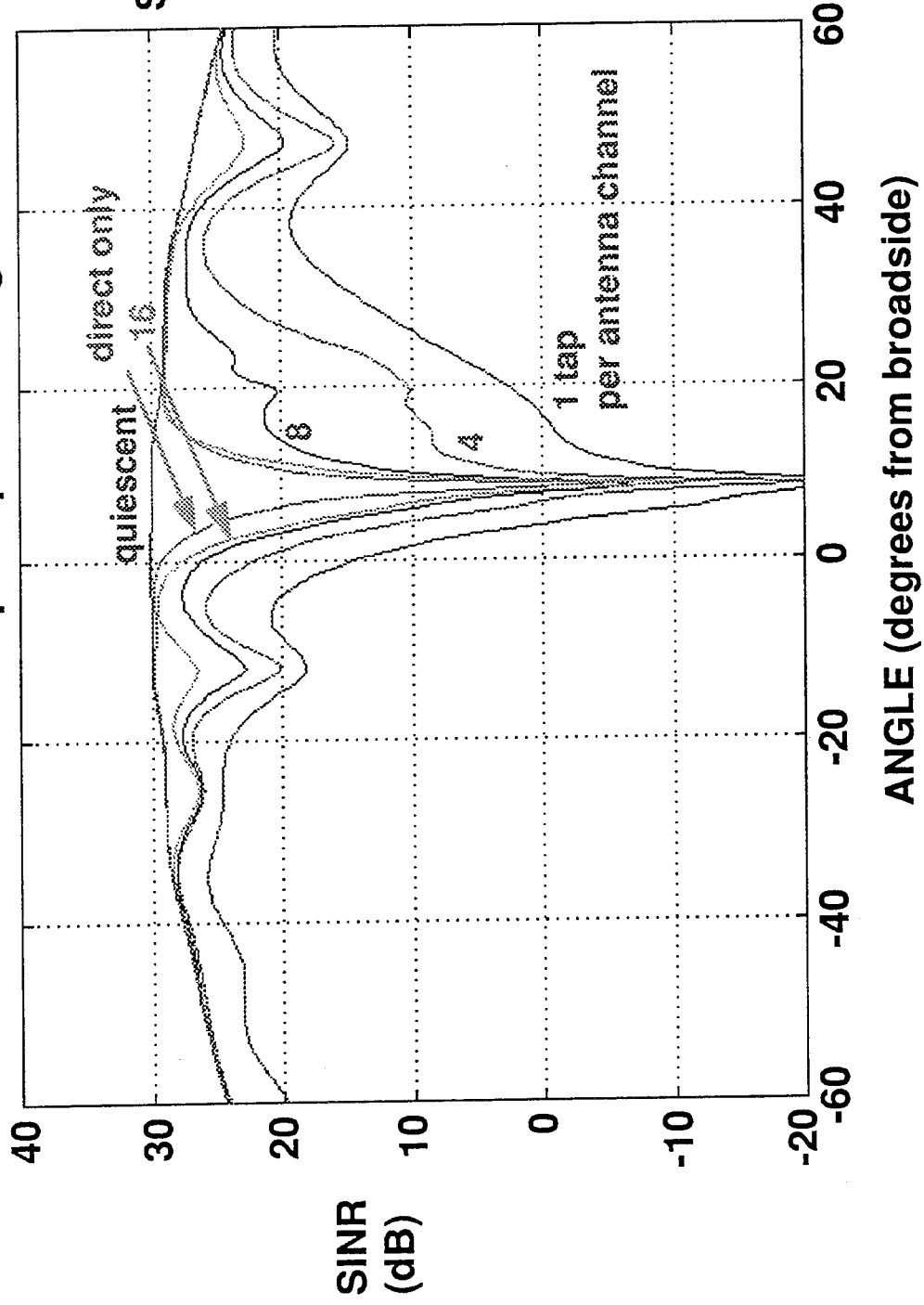


- FROST CONSTRAINT USED TO MAINTAIN FLAT RESPONSE IN TARGET DIRECTION
- NO DOPPLER COMPENSATION SHOWN

EFFECT OF INCREASING TEMPORAL DOF

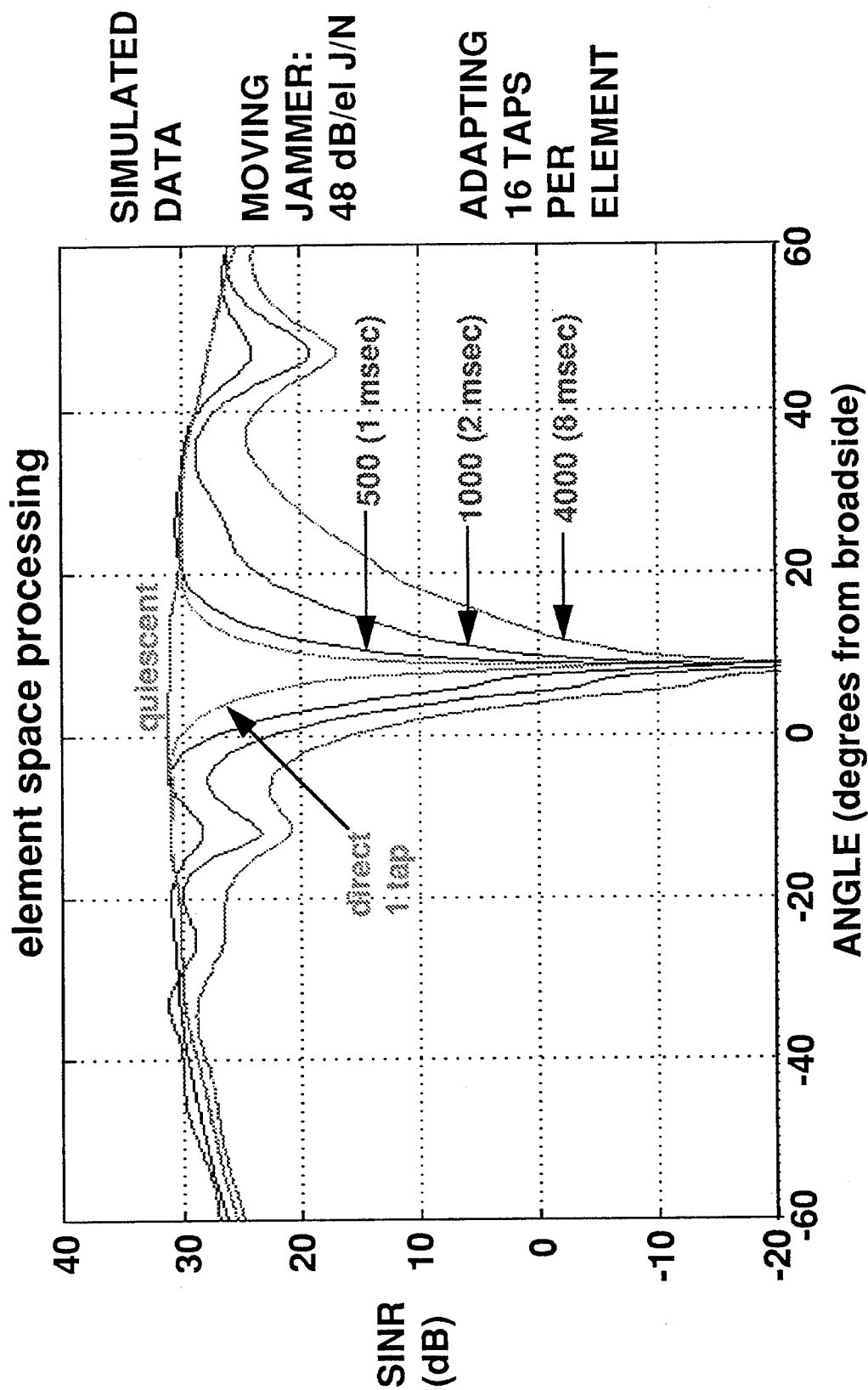
HUGHES

element space processing



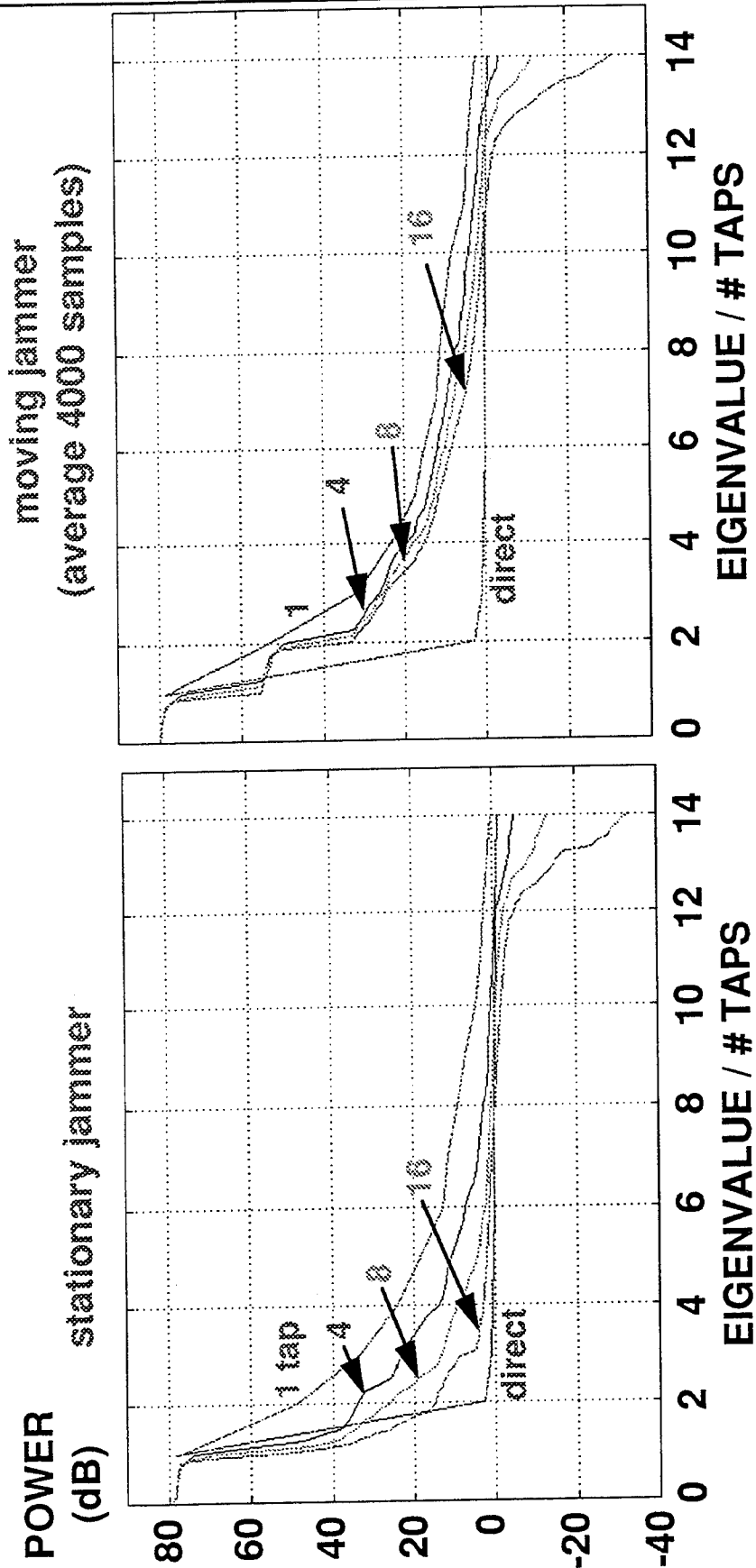
EFFECT OF JAMMER MOTION VS. NUMBER OF SAMPLES AVERAGED

HUGHES



EIGENVALUES FOR SIMULATED DATA

HUGHES



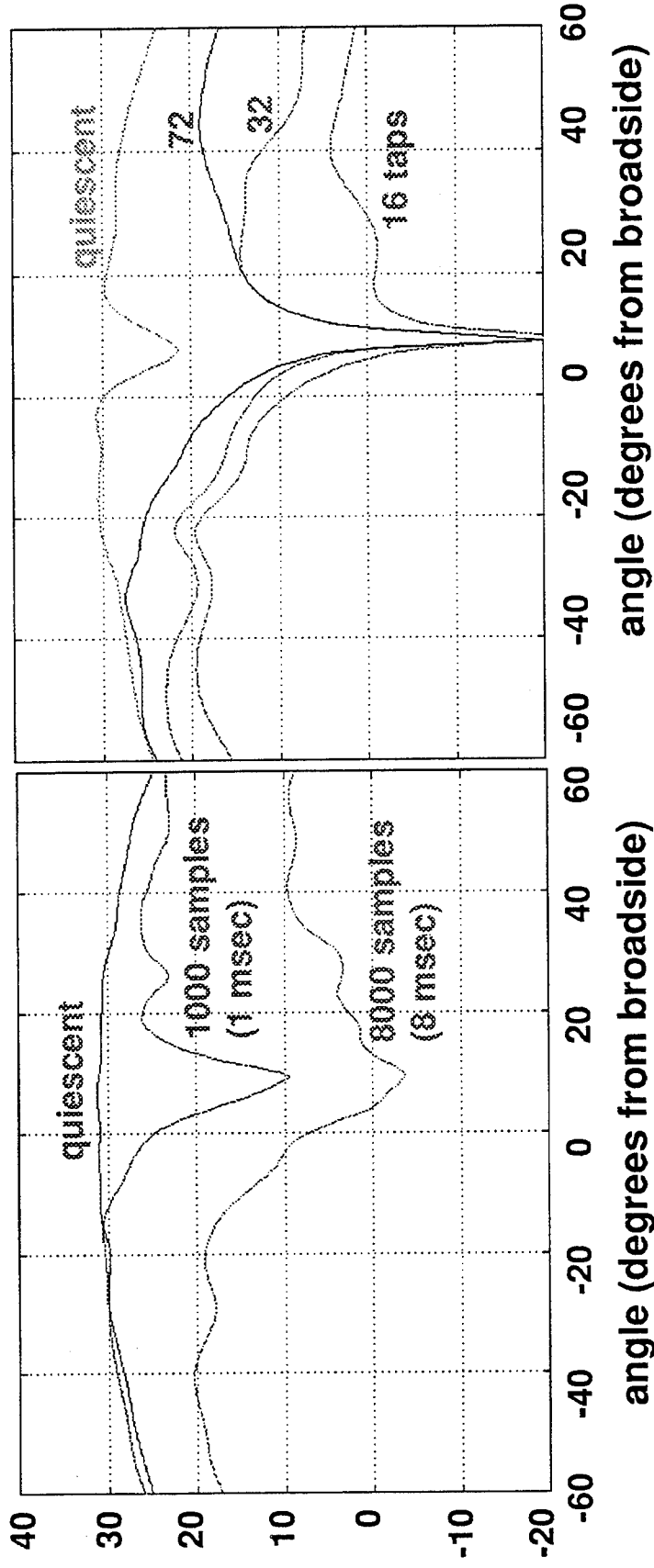
MOUNTAINTOP DATA RESULTS (RIO042)

HUGHES

SINR
(dB)

ELEMENT-SPACE
16-TAPS PER ELEMENT

REFERENCE BEAM *
750 SAMPLES



- * - performance limited by Doppler spread of TSI in reference beam
- performance would improve by using Doppler compensation

OUTLINE

HUGHES

- PROBLEM DESCRIPTION
- OVERVIEW OF PAPERS IN SESSION
- TSI PHENOMENOLOGY
- EFFECT OF TSI ON SYSTEM PERFORMANCE
- CONCEPTS FOR TSI MITIGATION
- PERFORMANCE EXAMPLES, MOUNTAINTOP SCENARIO
 - REFERENCE BEAM TECHNIQUES
 - ELEMENT SPACE TECHNIQUES
- MITIGATION OF COMBINED TSI AND RADAR CLUTTER
- CONCLUSIONS

EFFECT OF TSI MITIGATION ON RADAR PERFORMANCE

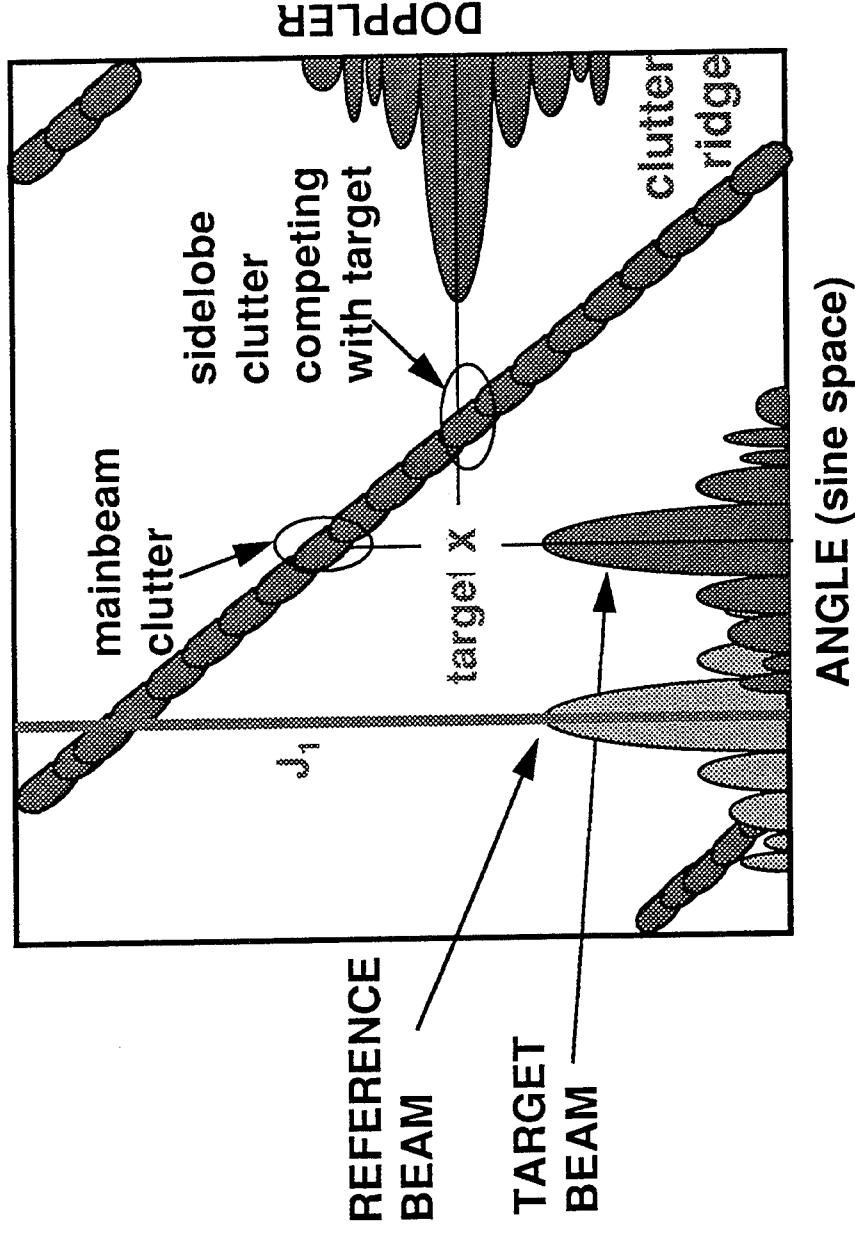
HUGHES

- **PROBLEM:** TSI mitigation requires updating the adaptive weights during a Doppler dwell
 - due to jammer/platform motion
 - modulates the received radar pulses, degrading Doppler filter performance and therefore degrading clutter cancellation
- **PROBLEM:** TSI weights must be estimated in the presence of radar clutter
- **POSSIBLE SOLUTIONS:**
 - combined TSI and radar clutter cancellation
 - clutter cancellation prior to TSI mitigation followed by STAP
 - use of beam stabilization or constraints to minimize modulation

COMBINED TSI AND RADAR CLUTTER

HUGHES

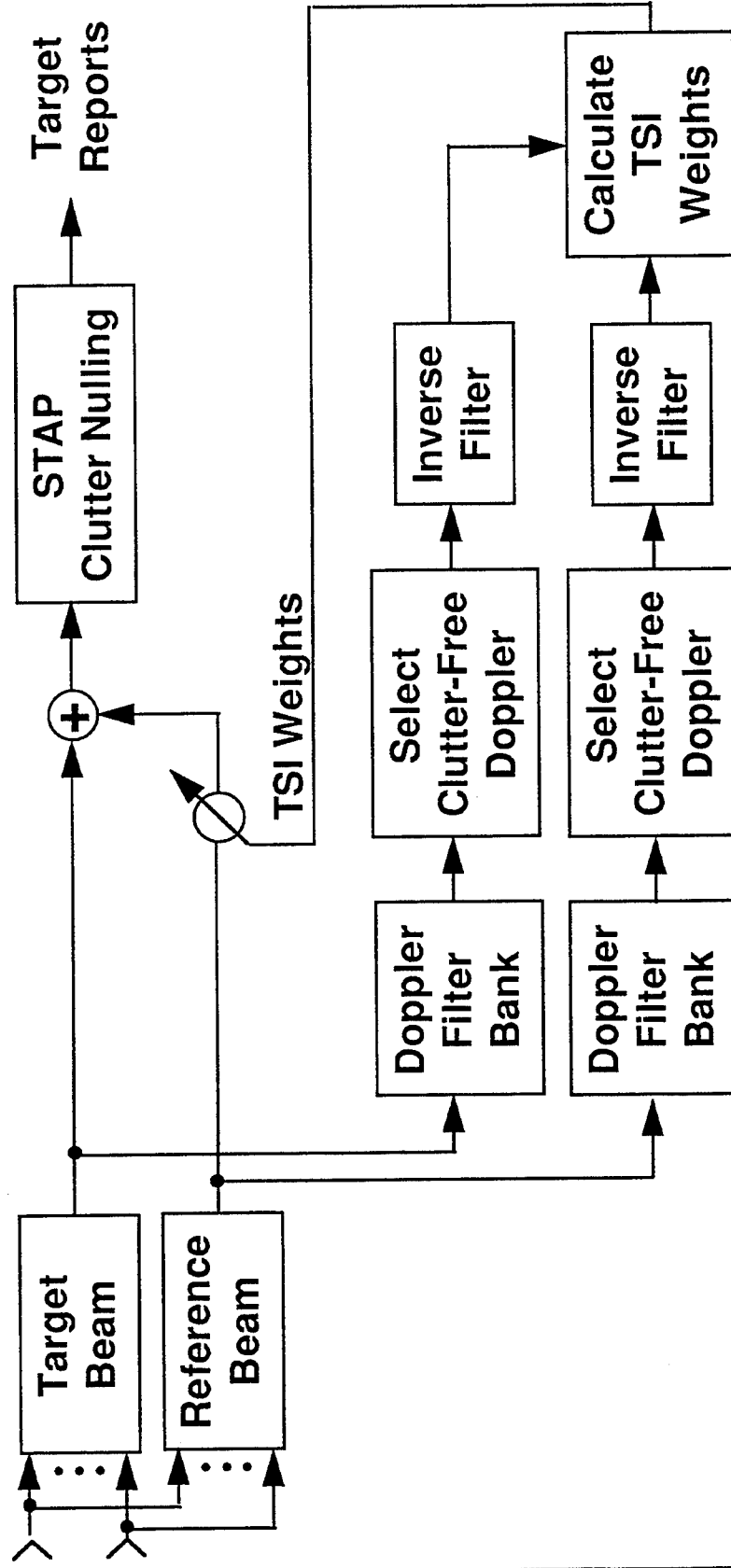
ANGLE/DOPPLER MAP FOR TYPICAL AIRBORNE RADAR



- snapshot of spectrum at selected range cell
- reference beam changes with time as weights update

COMBINED TSI AND RADAR CLUTTER MITIGATION

HUGHES



Two Steps:

1. estimate TSI weights after elimination of radar clutter.
2. compensate for modulation of TSI weights in STAP processor.

- TSI CAN SIGNIFICANTLY DEGRADE PERFORMANCE OF SPATIAL ADAPTIVE PROCESSING TECHNIQUES
 - for strong jamming, potential degraded performance over a large area
 - degradation depends on frequency, beamwidth, terrain, scenarios
 - main beam TSI is greatest problem
- MITIGATION TECHNIQUES TAKE ADVANTAGE OF TEMPORAL CORRELATION PROPERTIES OF TSI (i.e., time delay, Doppler shift)
 - Solutions can require a large number of degrees of freedom
 - methods to simplify processing are needed
 - Reference beam approach has least complexity (# of adaptive weights)
 - useful when strong direct path
 - Element space approach
 - less sensitive to Doppler spread
 - requires fewer time delay taps (less eclipsing)

SUMMARY (continued-2)

HUGHES

- **ACHIEVABLE CANCELLATION PERFORMANCE OF TSI MITIGATION TECHNIQUES IS LIMITED**
 - Limited by product of time delay and Doppler spread of TSI
 - Limited by samples available relative to degrees of freedom
 - Limitation is terrain and scenario dependent
 - Improvement obtained by Doppler compensation (partially offset by need for more degrees of freedom)
- **MODELS OF TSI PHENOMENOLOGY PROVIDE USEFUL DESIGN TOOL**
 - Characterizes TSI correlation properties for different scenarios, terrain
 - Determines number of taps and Doppler compensation needed
- **MITIGATION OF COMBINED TSI AND RADAR CLUTTER**
 - TSI Doppler shift requires frequent update of TSI weights; this degrades STAP performance
 - Areas for future work
 - methods to simplify processing
 - interaction between the nulling processes

CANCELLATION OF TERRAIN SCATTERED JAMMING IN AIRBORNE RADARS

Larry Brennan

Larry Brennan and Associates
9196 Neumann Drive
Elberta, AL 36530
tel: (334) 986-6241
fax: (334) 986-6241
email: lbrennan@gulfel.com

Abstract Multipath jamming, scattered from terrain into a radar main beam, cannot be canceled by angular nulling or angle-Doppler STAP techniques. However, scattered jamming cancellation has been demonstrated using an adaptive filter and consecutive samples (range cells) from an auxiliary beam pointed at the jammer. Alternatively, the necessary auxiliary inputs can be obtained from multiple beams of scattered jamming. In both cases, the adaptive filters approximate the terrain scattering process, providing a signal for subtraction from the main beam. In airborne radars, the scattering process is continually changing, requiring rapid weight updates. Radar clutter must also be canceled in airborne radars, requiring that multiple PRIs of data be combined coherently in some form of Doppler filtering. Clutter-free radar outputs are needed in computing the adaptive weights for scatter cancellation. Methods of satisfying these two requirements (rapid weight updates and long coherent processing intervals) simultaneously are discussed. One option is a two- or three-pulse MTI canceler in the main beam, followed by scatter cancellation. If necessary, the scatter canceler weights can be updated each PRI or several times per PRI. A second option is DFT Doppler processing over many PRIs for clutter removal, followed by scattered jamming cancellation. The clutter-free filter outputs are then used to obtain rotating scatter canceler weights which compensate for the changing bistatic path lengths. The Mountaintop data obtained with an airborne jammer at White Sands Missile Range was used to test these algorithms. Results of these tests are presented and discussed.

CANCELLATION OF TERRAIN SCATTERED JAMMING IN AIRBORNE RADARS

Larry Brennan

ASAP Workshop 13 March 1996

TSJ CANCELLATION IN AIRBORNE RADARS - PROBLEMS

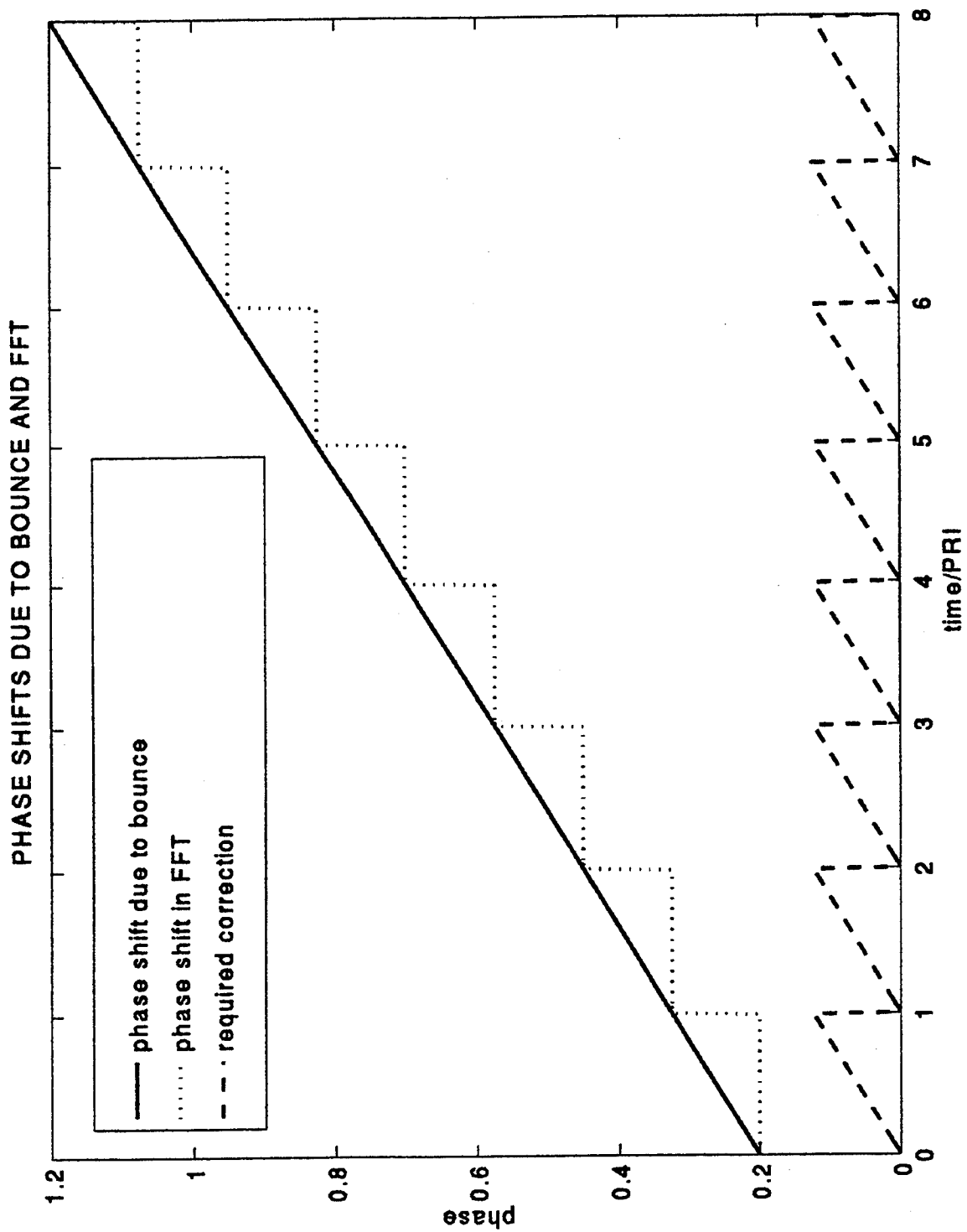
- THE SCATTERING PROCESS IS CHANGING DUE TO MOTION OF THE RADAR AND, USUALLY, MOTION OF THE JAMMER.
- THE TSJ CANCELER WEIGHTS MUST BE UPDATED FREQUENTLY, OR ROTATED, TO FOLLOW THE CHANGING BISTATIC DELAYS.
- RADAR CLUTTER IN THE RECEIVING BEAM(S) PREVENTS DIRECT COMPUTATION OF TSJ CANCELER WEIGHTS.
- WHEN SPACE-TIME ADAPTIVE PROCESSING (STAP) IS REQUIRED FOR CLUTTER CANCELLATION, TSJ IN THE BEAMS PREVENTS DIRECT COMPUTATION OF STAP WEIGHTS.

METHODS OF COMPUTING TSJ CANCELER WEIGHTS

- USE RADAR DEAD TIME - BEFORE AND AFTER CPI OR BEYOND RADAR CLUTTER RANGE DURING EACH PRI - FOR COMPUTATION
- USE 2 OR 3 PULSE MTI TO REMOVE CLUTTER - THEN COMPUTE CANCELER WEIGHTS FOR EACH PRI OR SET OF PRIS.
- PERFORM DOPPLER FILTERING FIRST (E.G., 64 PRI FFT) - THEN USE CLUTTER-FREE FILTERS TO COMPUTE WEIGHTS FOR DELAY TAPS IN MULTIPLE FILTERS IN AUXILIARY CHANNEL(S).
- ADAPT SIMULTANEOUSLY IN 3 DIMENSIONS - ANGLE, DOPPLER, AND DELAY. ANGLE-DOPPLER STAP CANCELS CLUTTER. DELAY TAPS FOR EACH PRI OR FILTER WEIGHTED TO CANCEL TSJ.

TSJ CANCELLATION AFTER DOPPLER PROCESSING

- **DOPPLER FILTER IN THE MAIN BEAM(S) AND JAMMER-TRACKING AUXILIARY BEAM. USE FILTER OUTPUTS IN FURTHER PROCESSING**
- **SELECT A CLUTTER-FREE FILTER IN THE MAIN CHANNEL. CROSS-CORRELATE IT'S OUTPUT WITH ALL FILTERS IN THE AUXILIARY CHANNEL TO FIND DELAY-DOPPLER REGIONS OF TSJ .**
- **COMPUTE ADAPTIVE WEIGHTS FOR DELAYS AND DOPPLER FILTER SPACINGS CONTAINING TSJ. INCLUDE INTRA-PRI PHASE CORRECTION IN COMPUTING AND APPLYING WEIGHTS.**
- **TSJ WEIGHTS COMPUTED FOR ANY CLUTTER-FREE FILTER IN MAIN BEAM CAN BE USED FOR ALL FILTERS. APPLY WEIGHTS AT SAME DELAYS AND MAIN-AUXILIARY FILTER SPACINGS.**



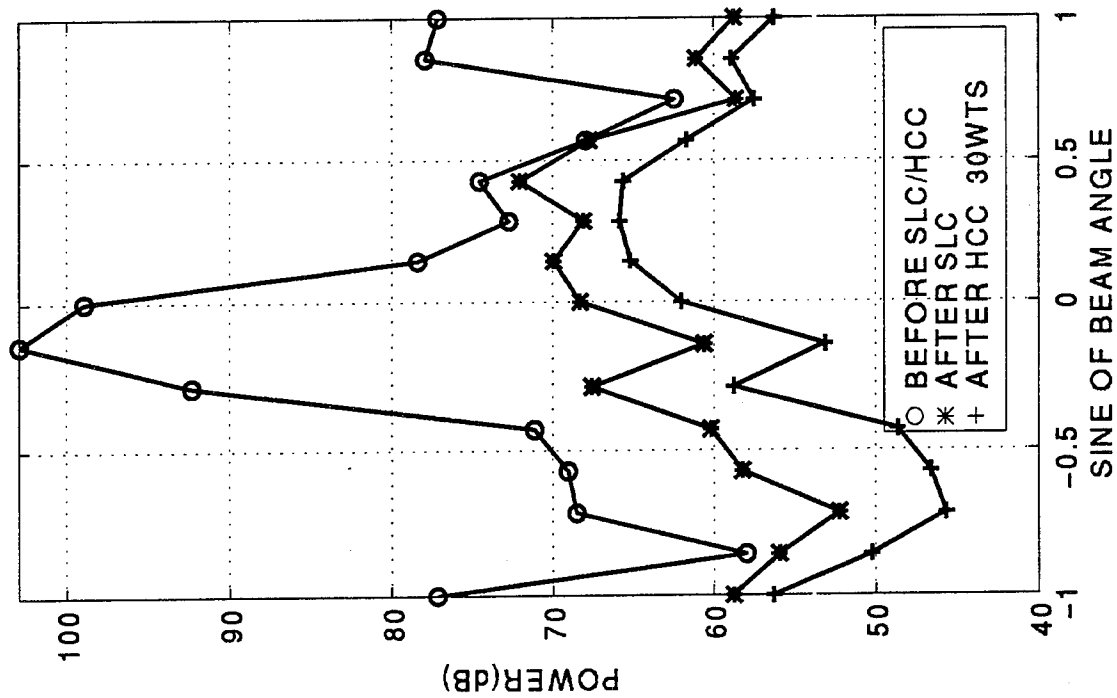
PHASE CORRECTION DURING EACH PRI

- SINCE THE REQUIRED CORRECTION IS THE SAME DURING EACH PRI, IT CAN BE APPLIED AFTER DFT DOPPLER FILTERING.
- THE REQUIRED INTRA-PRI PHASE CORRECTION IS A FUNCTION OF THE SPACING BETWEEN MAIN AND AUXILIARY FILTERS.
- IMPROVEMENT IN TSJ CANCELLATION DUE TO THIS PHASE CORRECTION DEPENDS ON RADAR PARAMETERS (FREQUENCY, PLATFORM VELOCITY, PRF) AND SCATTERING GEOMETRY.
- WITH BISTATIC DOPPLER AMBIGUITIES, SHOULD TEST SEVERAL INTRA-PRI PHASE SLOPES PER FILTER SPACING.

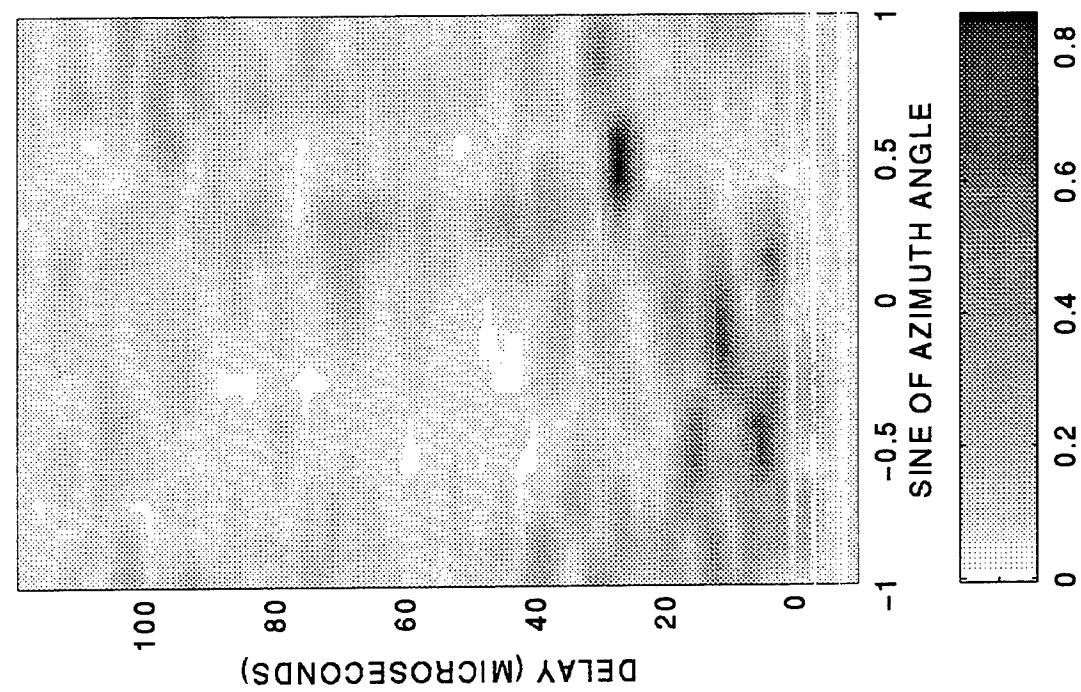
SELECTION OF MOUNTAIN TOP DATA FOR TESTS

- TSJ DATA WERE RECORDED AT WHITE SANDS MISSILE RANGE USING THE LINCOLN LABORATORY RSTER-90 RADAR.
- FILES RECORDED WITH AN AIRBORNE JAMMER WERE TESTED TO FIND AN EXAMPLE WITH DOPPLER SHIFTED TSJ.
- FILE RIO035V1 WAS SELECTED FOR DEMONSTRATING THE CANCELER ALGORITHM. AIRBORNE JAMMER WAS FLYING FAST AT HIGH ALTITUDE OVER MOUNTAINS.
- A MAIN BEAM SCAN ANGLE OF -34 DEG WAS SELECTED. DOPPLER SHIFTED TSJ IS PRESENT AND THE DELAY INTERVAL IS SMALL. THE AUXILIARY BEAM WAS POINTED AT JAMMER (-6 DEG.).

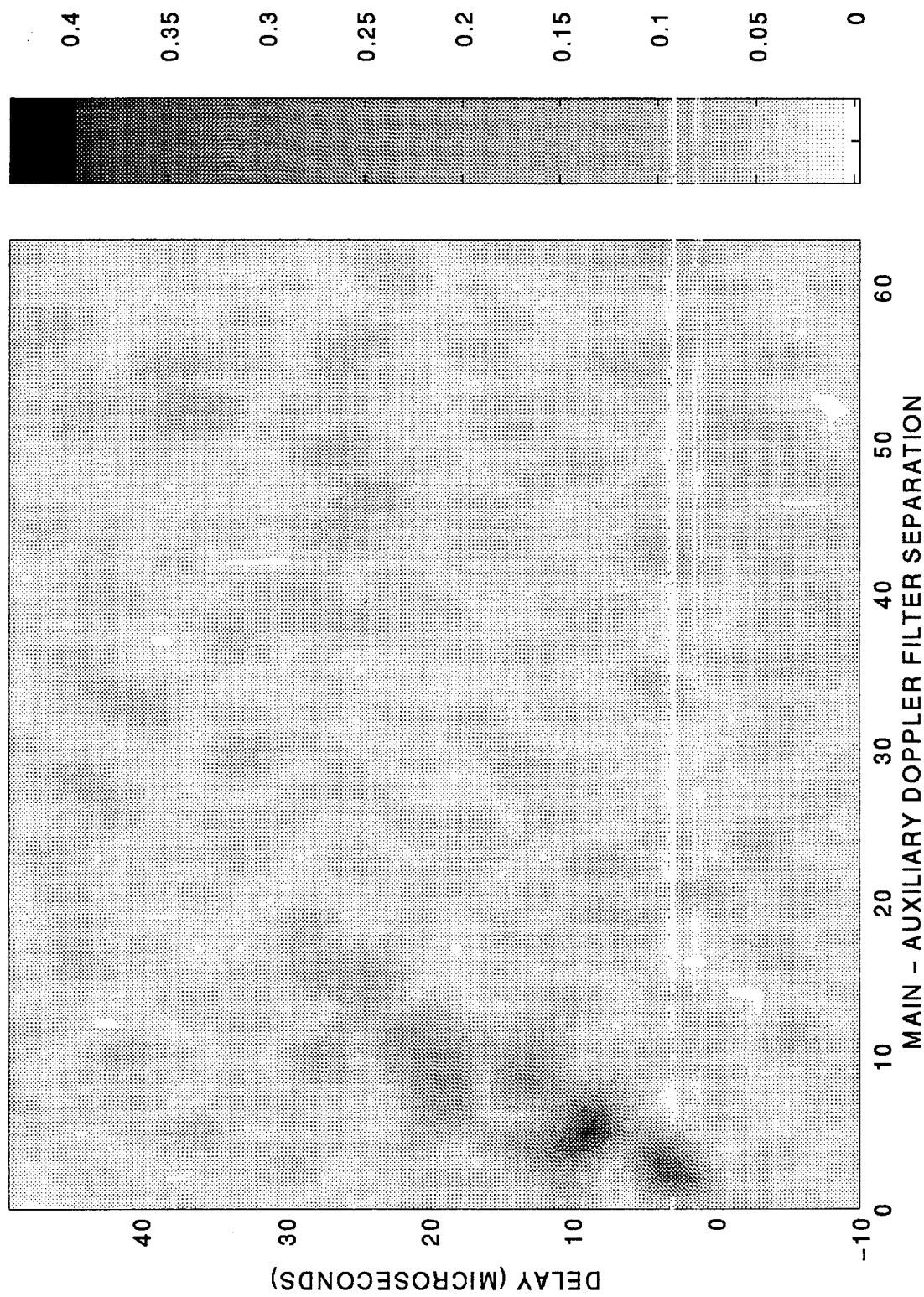
POWER IN BEAMS - RIO035V1

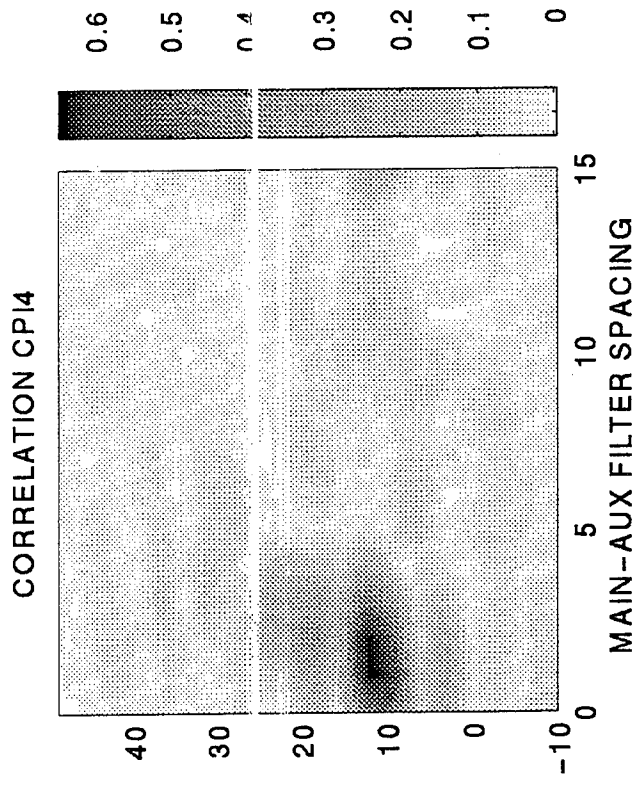
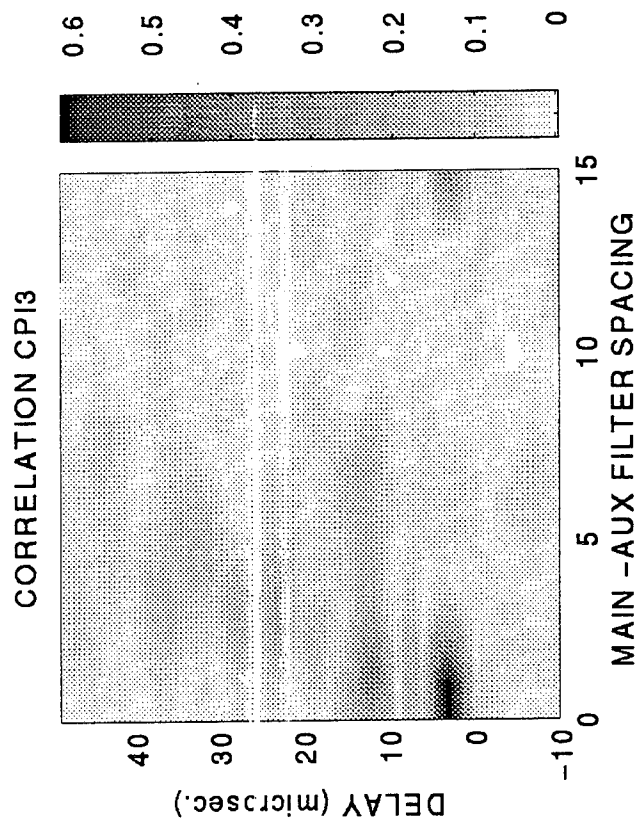
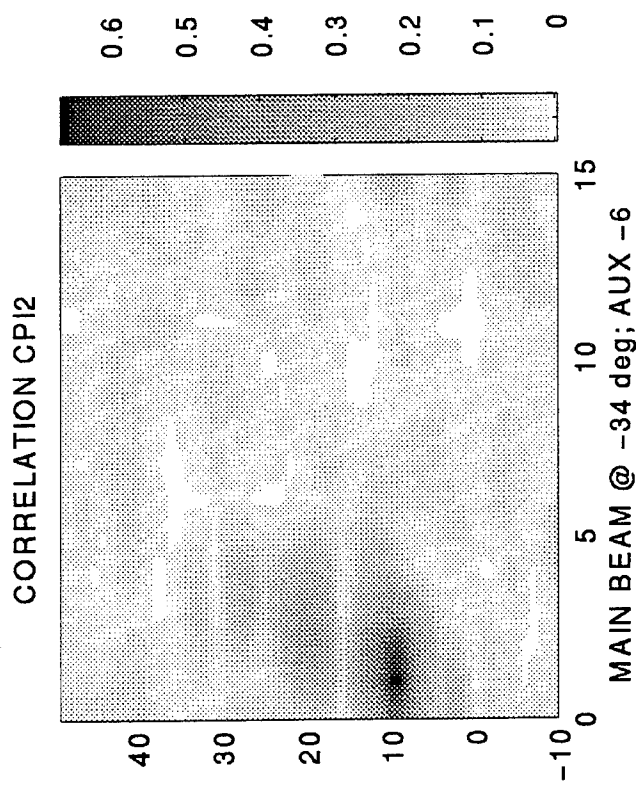
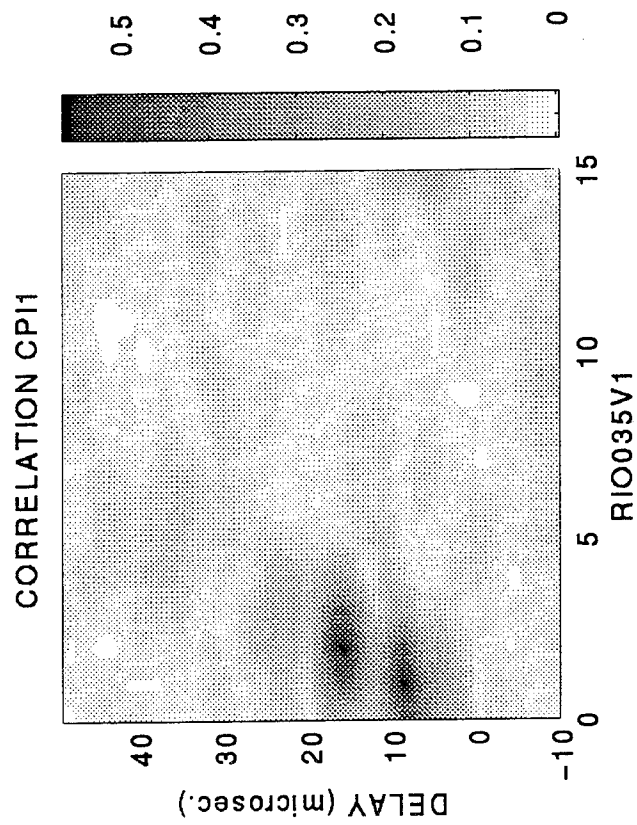


CORRELATION WITH AUX BEAM AT -6 DEG



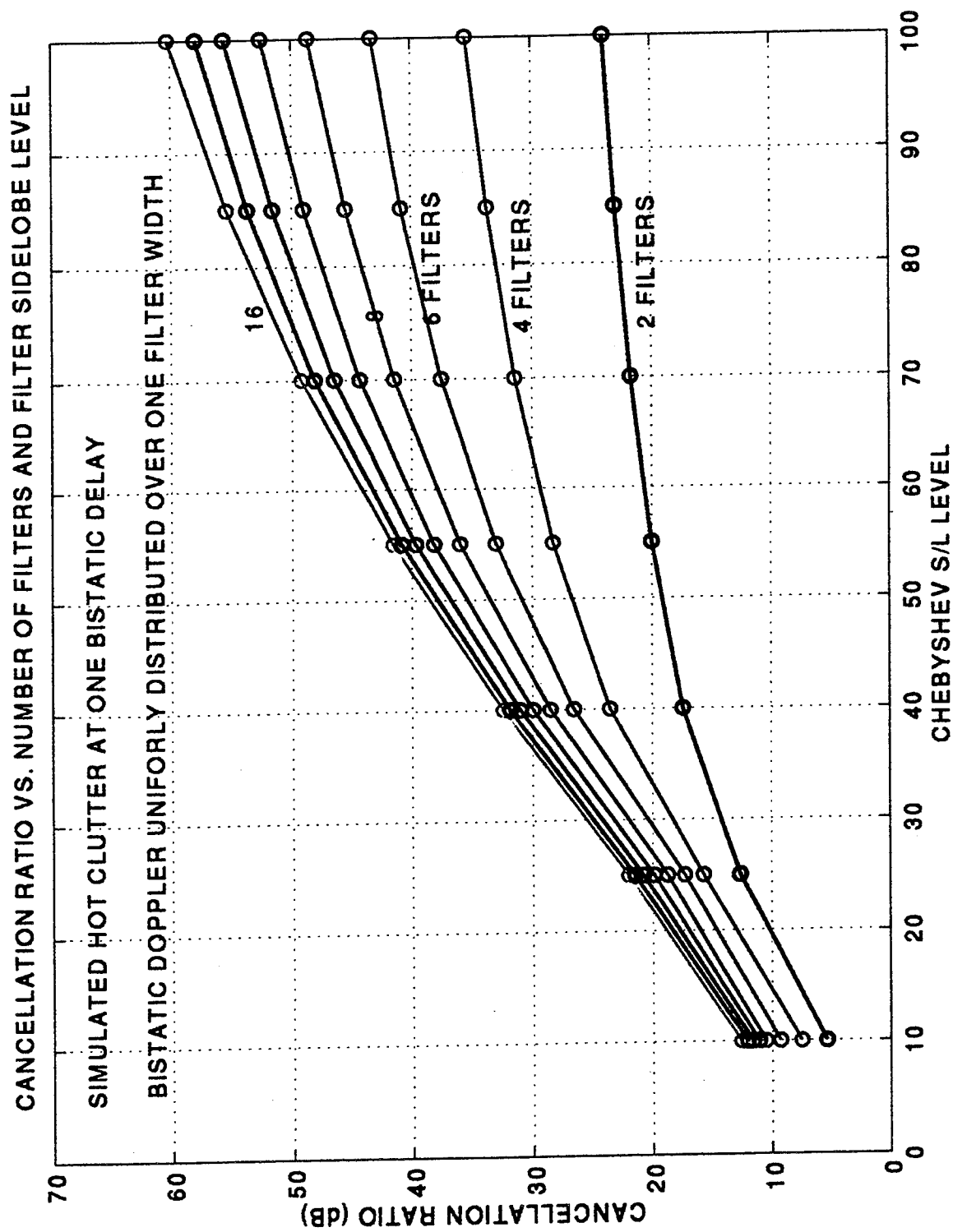
CORRELATION FOR RIO035V1; MAIN BEAM @ -34 DEG; AUX BEAM @ -6 DEG

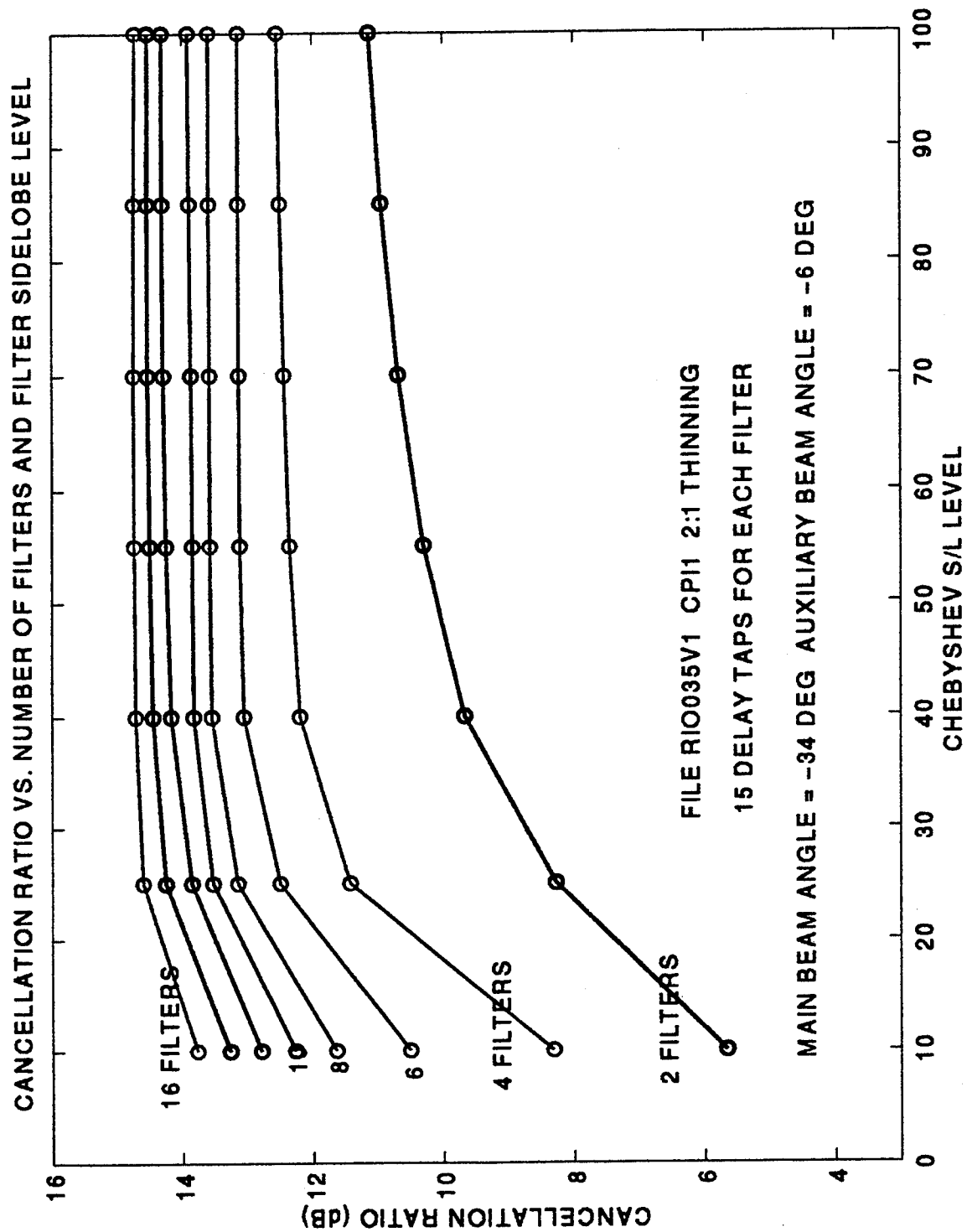


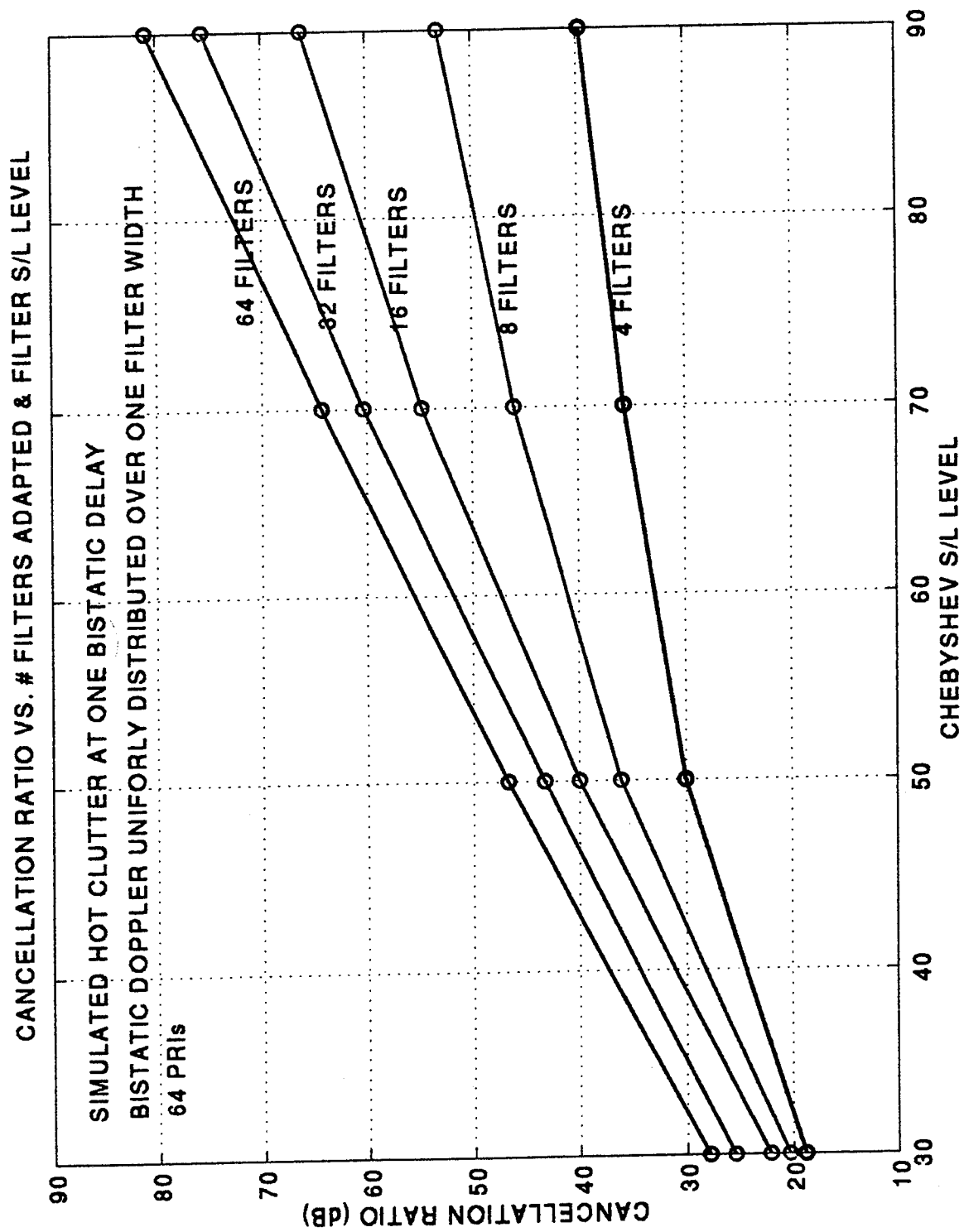


ISSUES IN DESIGN OF TSJ CANCELER

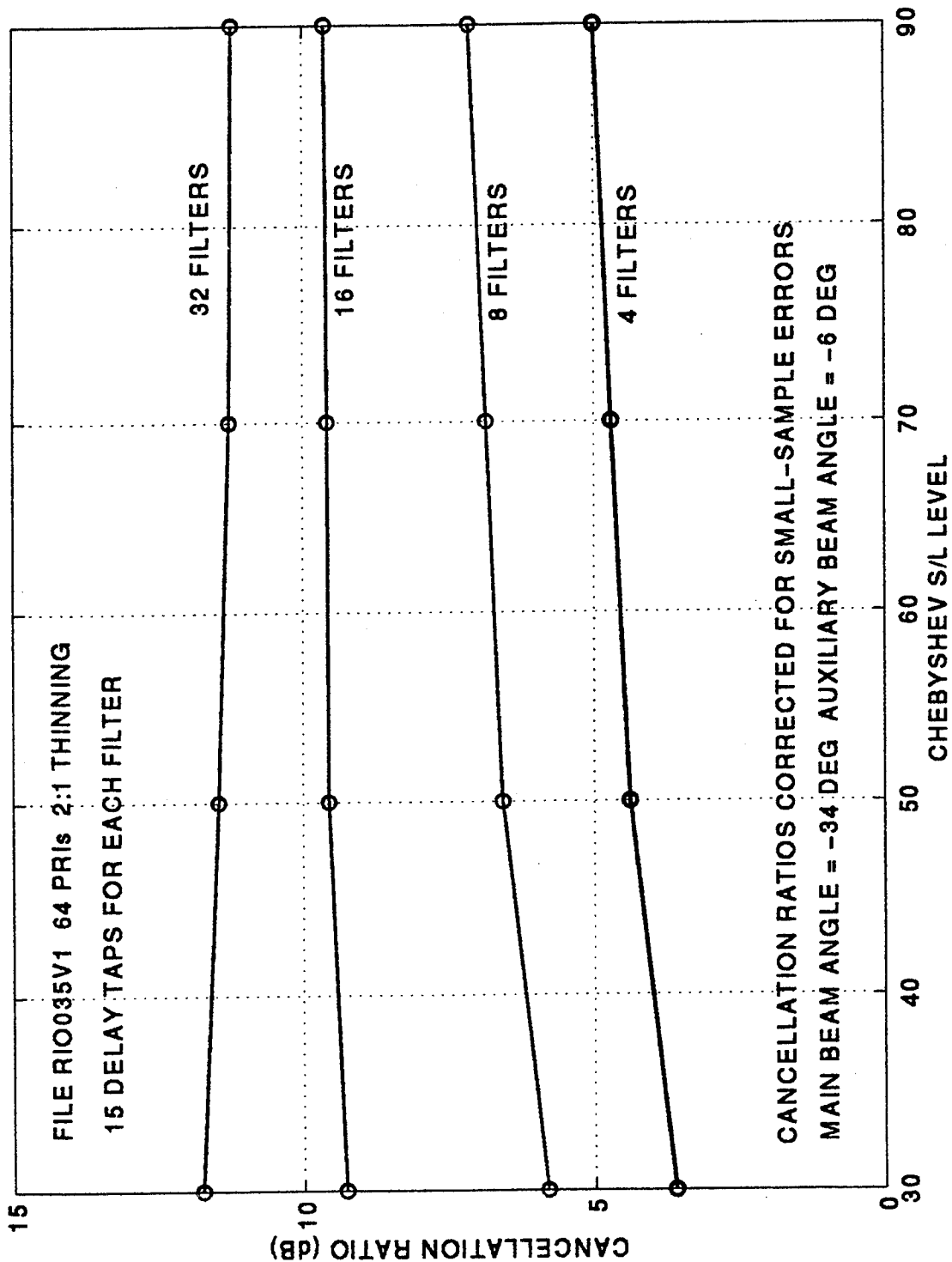
- ➡ ● NUMBER OF FILTERS REQUIRED IN AUXILIARY DATA ARRAY. DETERMINES NUMBER OF WEIGHTS AND COMPLEXITY .
- ➡ ● CHOICE OF DOPPLER FILTER SIDELOBE LEVEL. DOES NOT AFFECT COMPLEXITY OF SIGNAL PROCESSOR.
- WHEN NUMBER OF DOF IS LARGE, A SINGLE FILTER MAY NOT CONTAIN SUFFICIENT SAMPLES FOR COMPUTING WEIGHTS. AVERAGING OVER FILTERS IS A SOLUTION.
- WEIGHTS CAN NOT BE COMPUTED USING FILTERS WITH CLUTTER. THE WEIGHTS OBTAINED FOR ANY MAIN BEAM FILTER CAN BE USED FOR ALL FILTERS WITH SAME MAIN-AUX FILTER SPACINGS.







CANCELLATION RATIO VS. # OF FILTERS ADAPTED AND FILTER S/L LEVEL




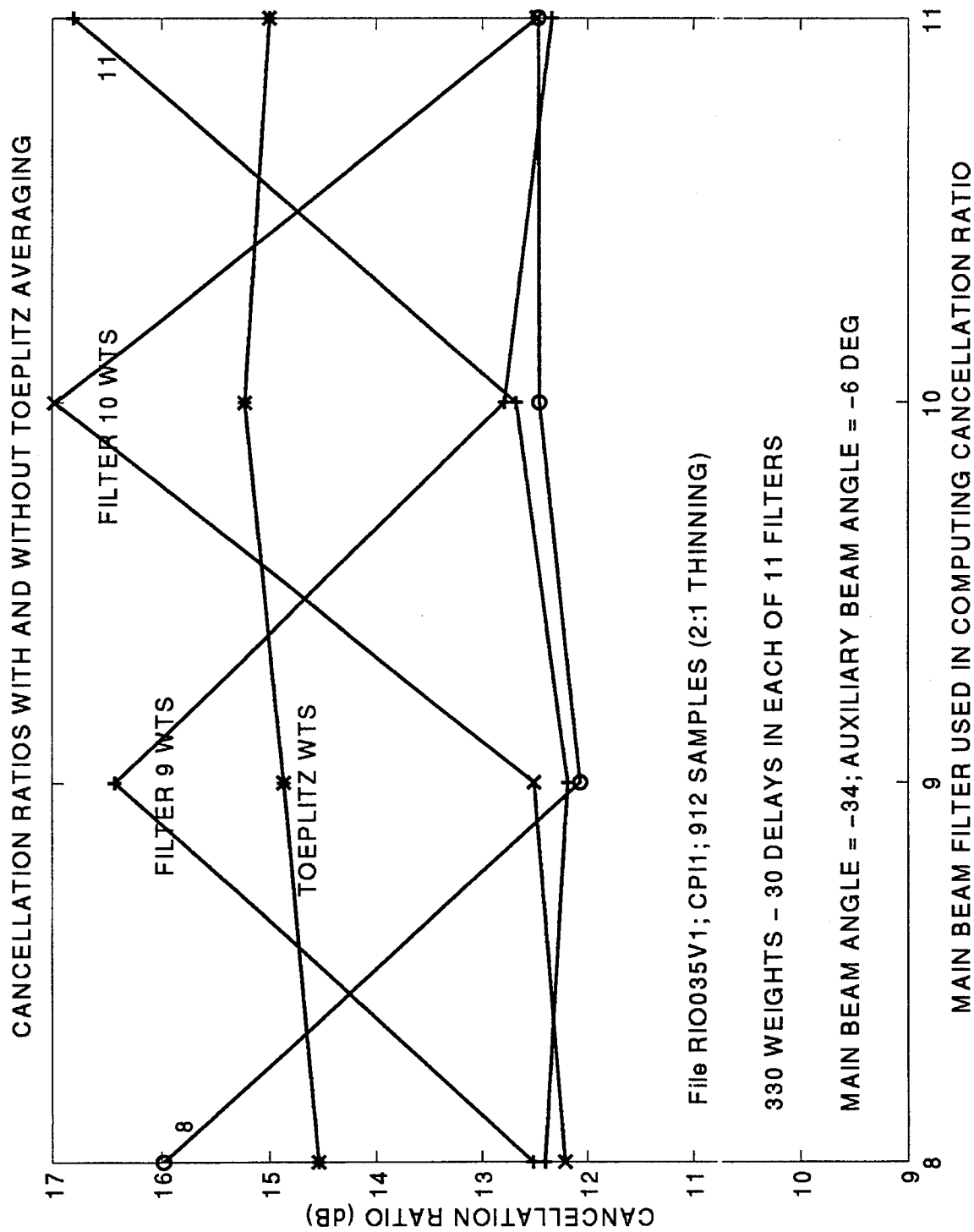
ISSUES IN DESIGN OF TSJ CANCELER

- NUMBER OF FILTERS REQUIRED IN AUXILIARY DATA ARRAY. DETERMINES NUMBER OF WEIGHTS AND COMPLEXITY .

- CHOICE OF DOPPLER FILTER SIDELOBE LEVEL. DOES NOT AFFECT COMPLEXITY OF SIGNAL PROCESSOR.

 ● WHEN NUMBER OF DOF IS LARGE, A SINGLE FILTER MAY NOT CONTAIN SUFFICIENT SAMPLES FOR COMPUTING WEIGHTS. AVERAGING OVER FILTERS IS A SOLUTION.

 ● WEIGHTS CAN NOT BE COMPUTED USING FILTERS WITH CLUTTER. THE WEIGHTS OBTAINED FOR ANY MAIN BEAM FILTER CAN BE USED FOR ALL FILTERS WITH SAME MAIN-AUX FILTER SPACINGS.



SUMMARY

- ADAPTIVE WEIGHTS FOR TSJ CANCELLATION CAN BE COMPUTED USING CLUTTER-FREE DOPPLER FILTER OUTPUTS.
- THE SET OF WEIGHTS COMPUTED FOR ANY CLUTTER-FREE FILTER CAN BE USED FOR TSJ CANCELLATION IN ALL FILTERS.
- THE ADAPTIVE WEIGHTS ARE APPLIED TO MULTIPLE DELAY TAPS IN SEVERAL AUXILIARY CHANNEL FILTERS, OFTEN REQUIRING MANY DEGREES OF FREEDOM. WHEN A LARGE TRAINING SET IS REQUIRED, TOEPLITZ AVERAGING IN DOPPLER CAN BE USED.
- AN INTRA-PRI PHASE CORRECTION IMPROVES CANCELLATION.
- THIS ALGORITHM AND SET OF CONCLUSIONS WERE VALIDATED USING RECORDED TSJ DATA FROM THE MOUNTAIN TOP PROGRAM.

SIGNAL SUBSPACE ISSUES IN TSI MITIGATION

Robert A. Gabel

MIT Lincoln Laboratory
244 Wood Street
Lexington, MA 02173-9108
tel: (617) 981-1035
email: gabel@ll.mit.edu

Abstract Terrain-Scattered Interference (TSI) cancellation architectures have been shown to be effective in mitigating the effects of TSI from both ground-based and airborne jammers. Techniques have been devised for weight training in the presence of monostatic clutter. The approach has been extended to both beam-space and element-space TSI mitigation as preprocessing for subsequent clutter-nulling STAP algorithms. However, the computation cost of TSI mitigation can be high, especially in the presence of the large delay and Doppler dispersions often associated with aircraft-based jammers. This presentation develops approaches to minimizing the cost of TSI mitigation weight training. Algorithm modifications, weight pruning, and trade-offs in the Doppler tracking of weights across a CPI is related to the associated cancellation performance. A portrait of TSI power is displayed as a function of delay, azimuth, Doppler, and time; this is used to motivate the selection of mitigation weights to be implemented. Resulting performance is displayed in terms of the residual jammer power, system SINR, and net array patterns using field data collected under the Mountaintop Program.

SIGNAL SUBSPACE ISSUES IN TSI MITIGATION

**ROBERT A. GABEL
MIT LINCOLN LABORATORY**

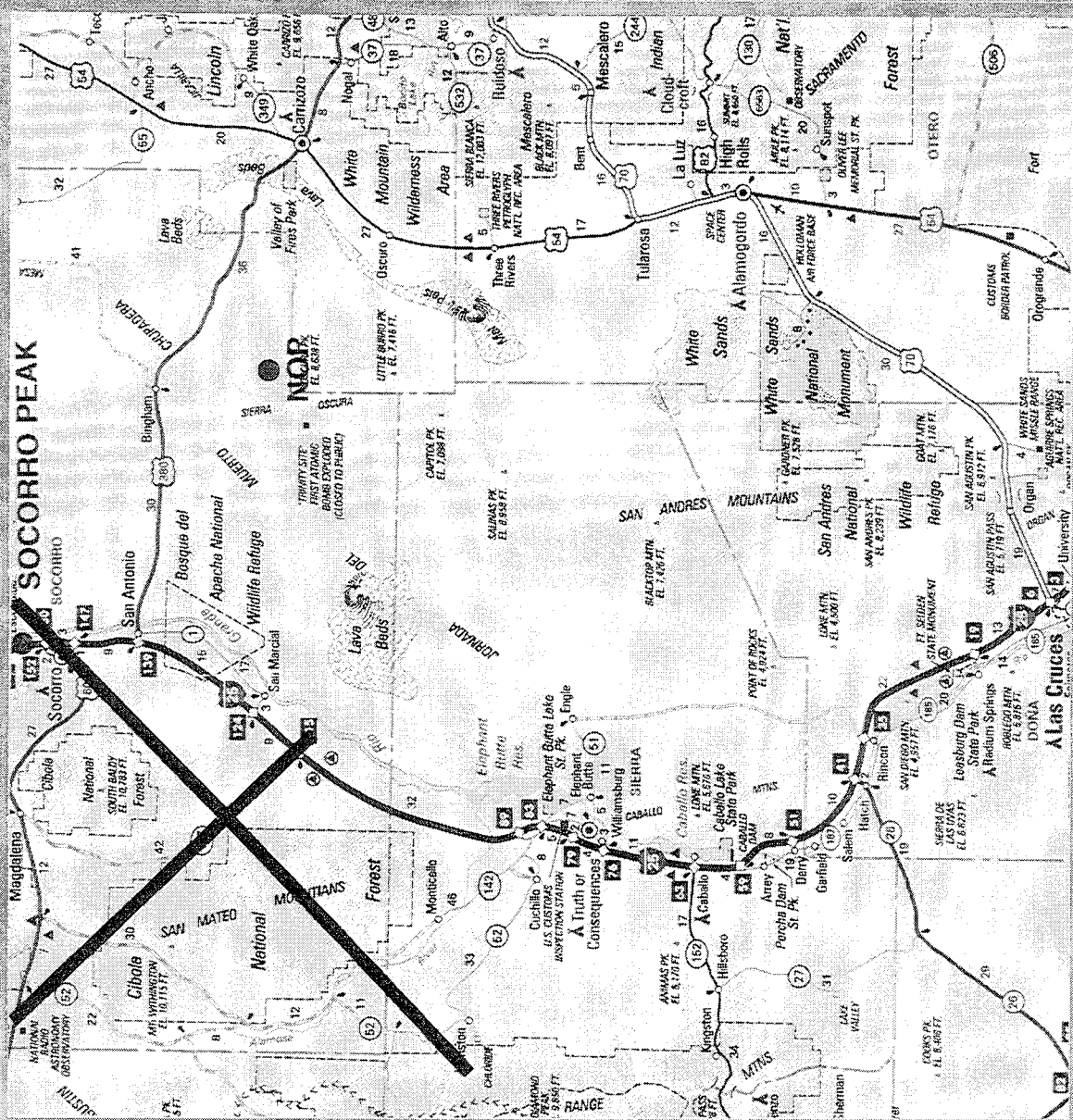
ADAPTIVE SENSOR ARRAY PROCESSING WORKSHOP

13 MARCH 1996

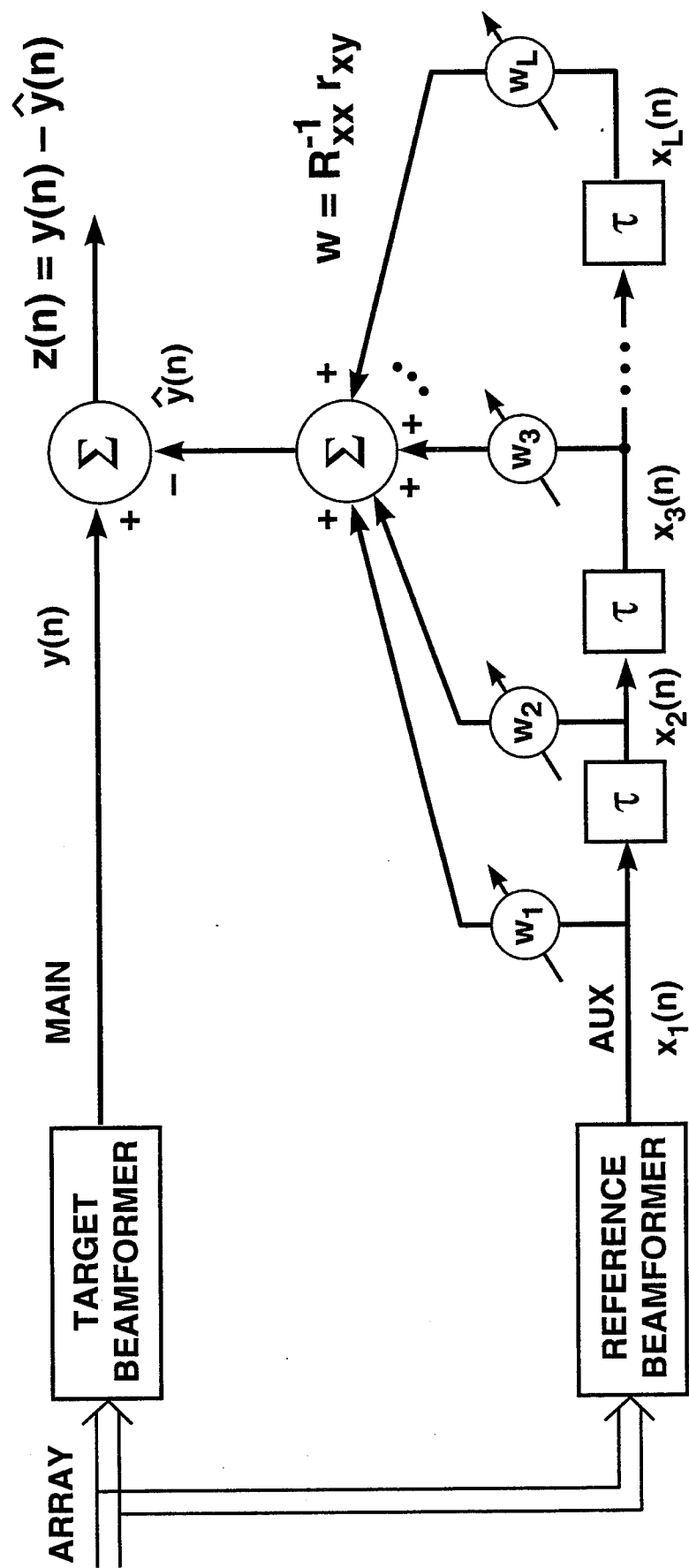
OUTLINE

- **AIRCRAFT JAMMER MITIGATION**
 - **TRAINING IN PRESENCE OF CLUTTER**
 - **DOPPLER-COMPENSATED WEIGHTS**
- **TSI ENERGY PORTRAIT**
 - **DELAY, AZIMUTH, DOPPLER, TIME**
 - **IMPLICATIONS FOR WEIGHT SELECTION**
- **EXTENSION TO MULTIELEMENT ARCHITECTURE**
 - **PREPROCESSOR TO CLUTTER NULLING**
 - **PERFORMANCE ASSESSMENT**
- **SUMMARY**

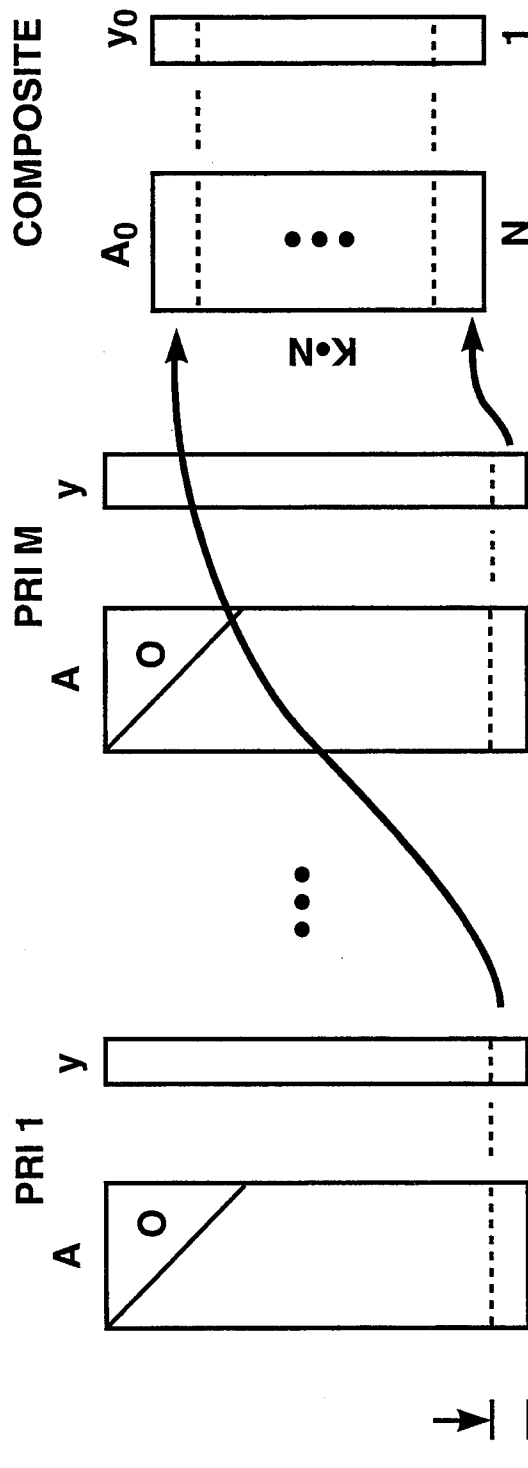
RSTER-90 JAMMER MITIGATION EXPERIMENTS



JAMMER MITIGATION SINGLE-BEAM, SINGLE AUX IMPLEMENTATION



MULTIPLE-PRI TRAINING



$\frac{k}{M} \cdot N \text{ SAMPLES}$

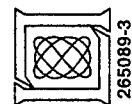
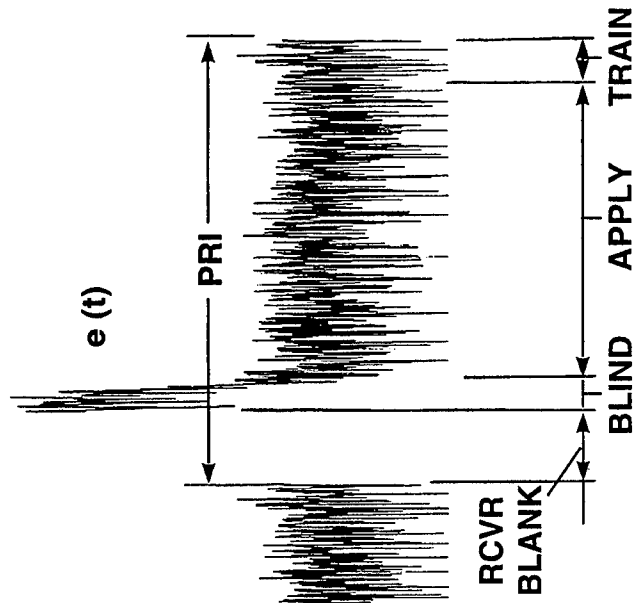
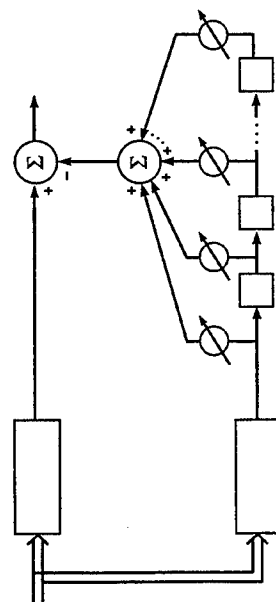
$$R_{xx} = A_0^T A_0$$

$$R_{xy} = A_0^T y_0$$

$$W = R_{xx}^{-1} R_{xy}$$

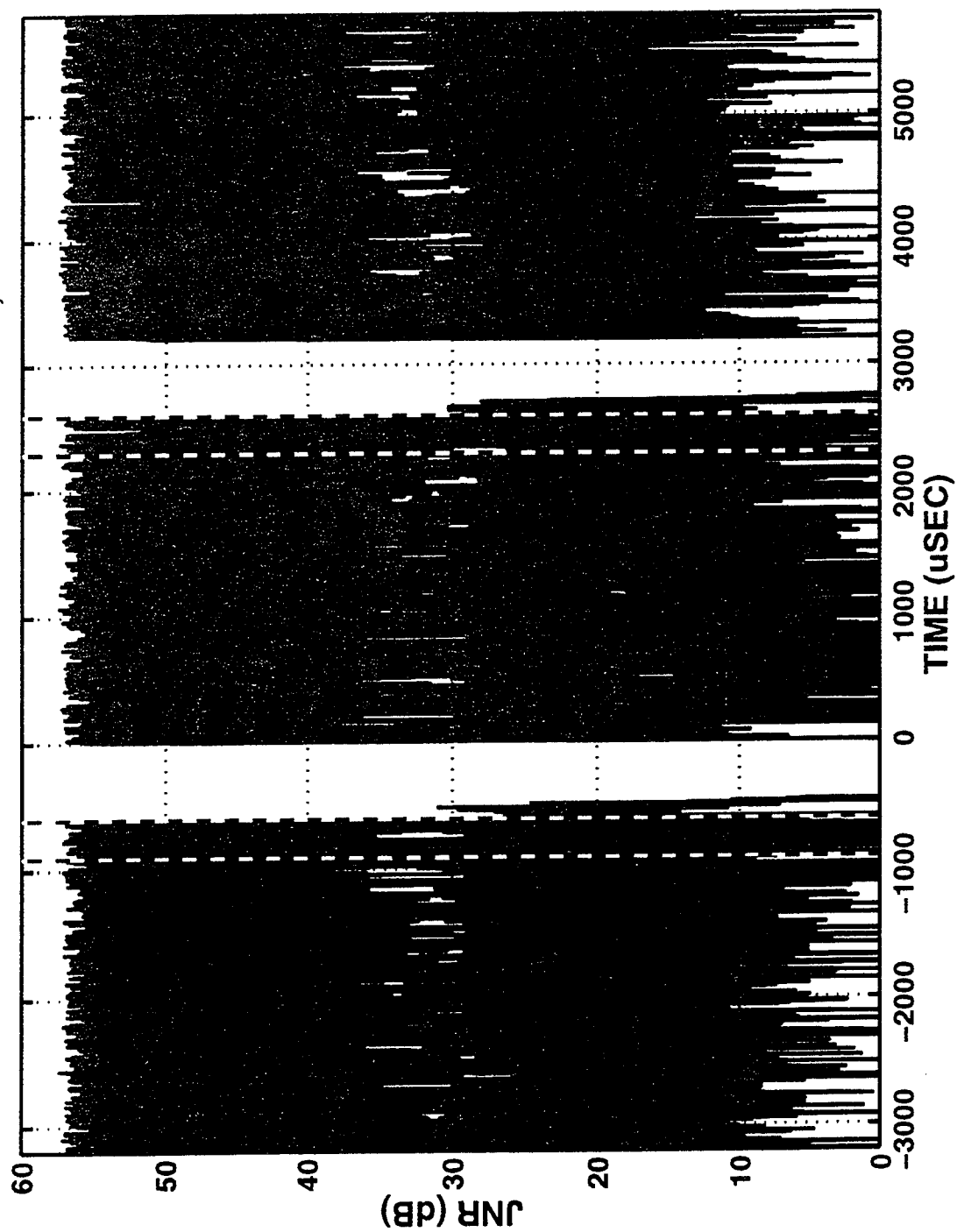
$$\hat{y} = AW$$

$$e = y - \hat{y}$$

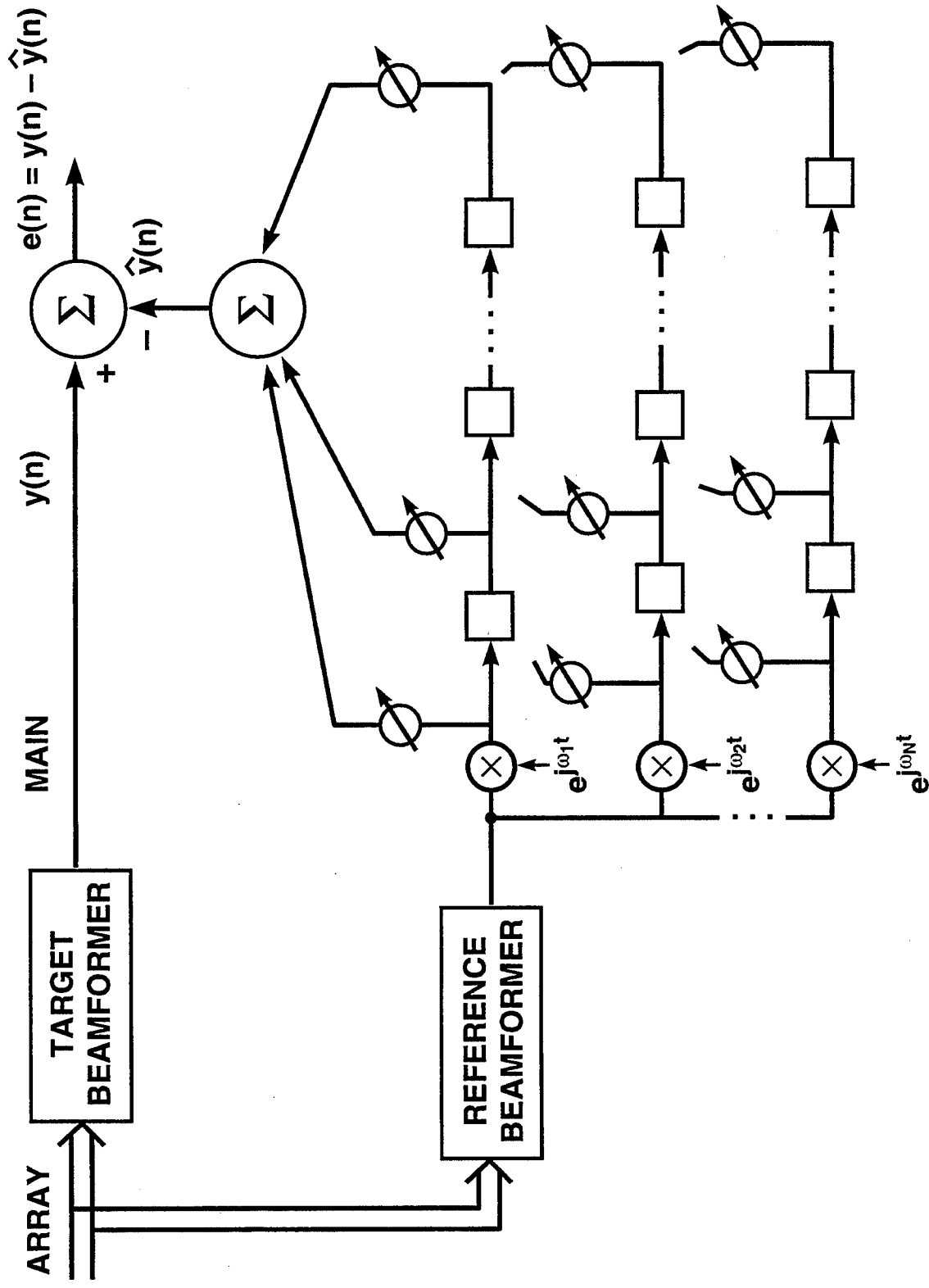


265089-3

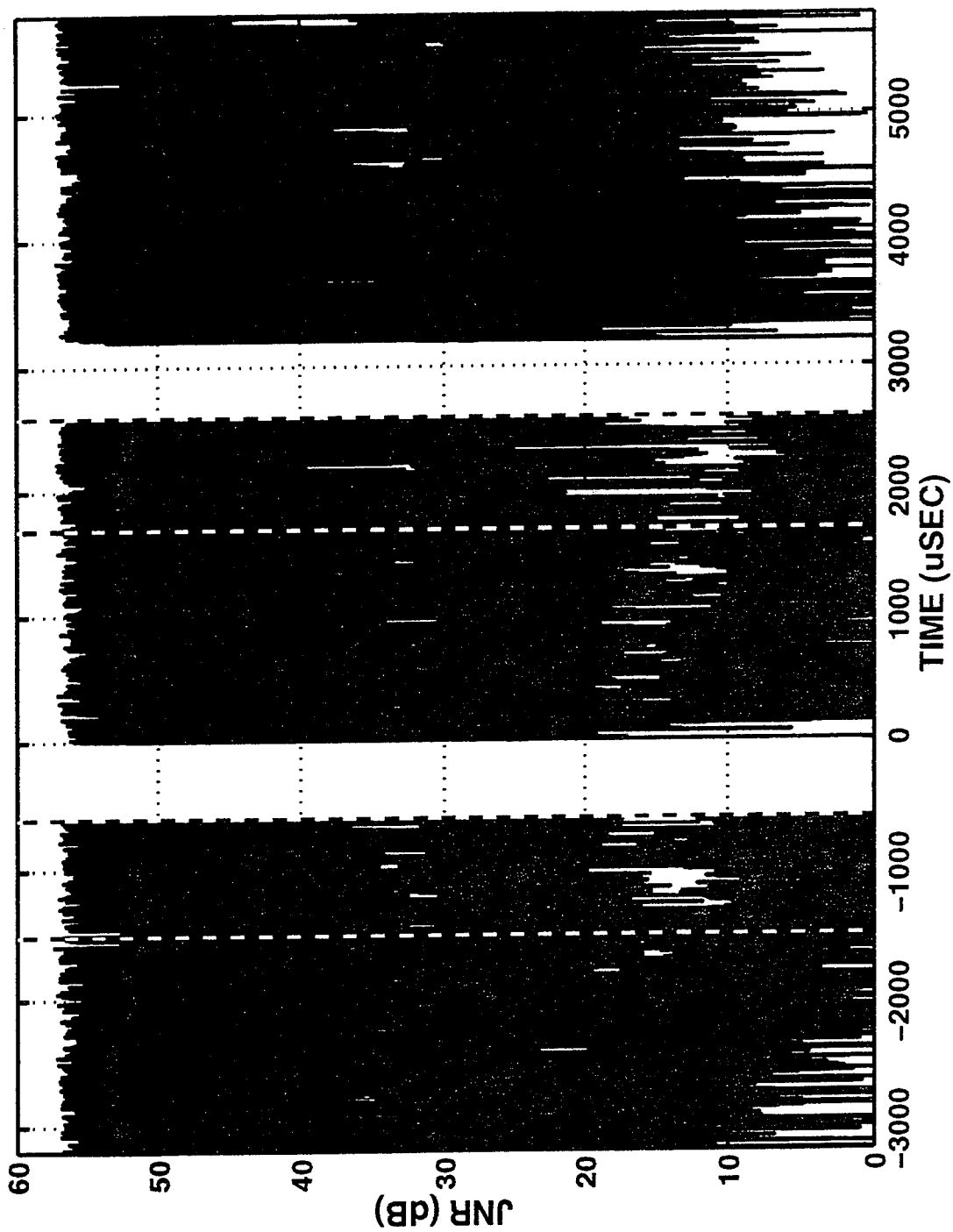
JAMMER PRE- AND POST-MITIGATION, PRI #1-3



JAMMER MULTIPATH CANCELLATION

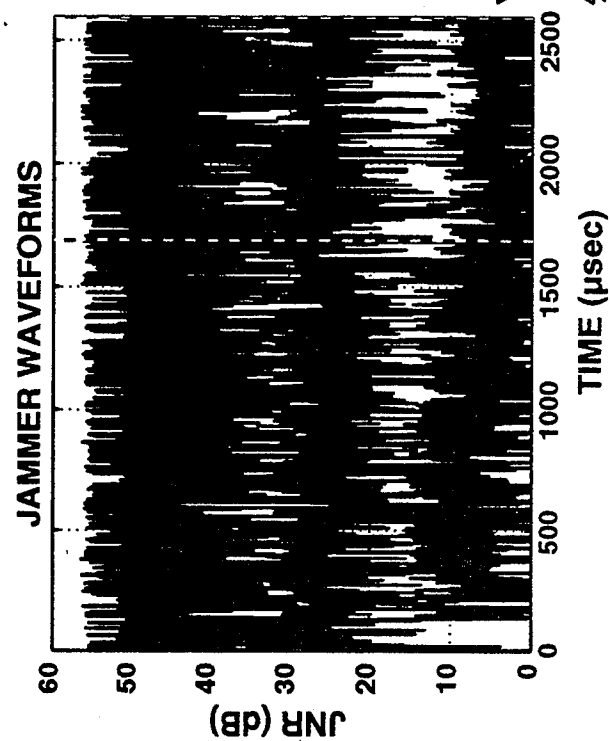
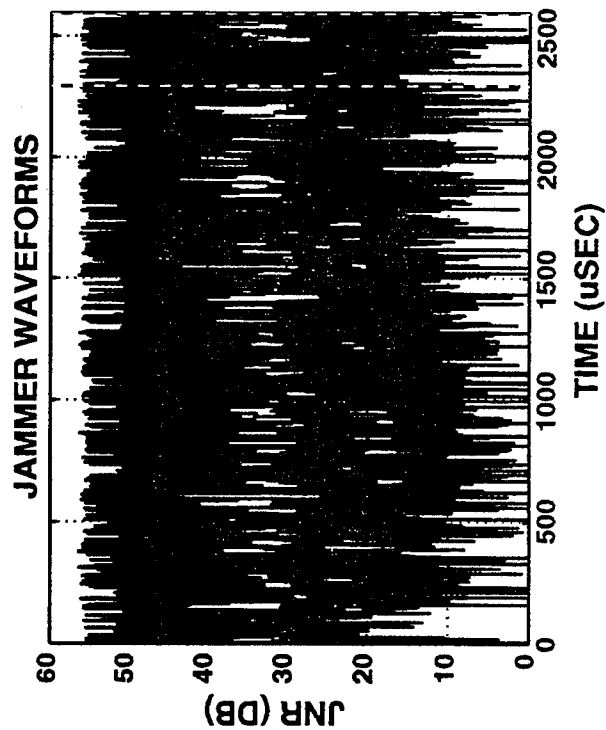
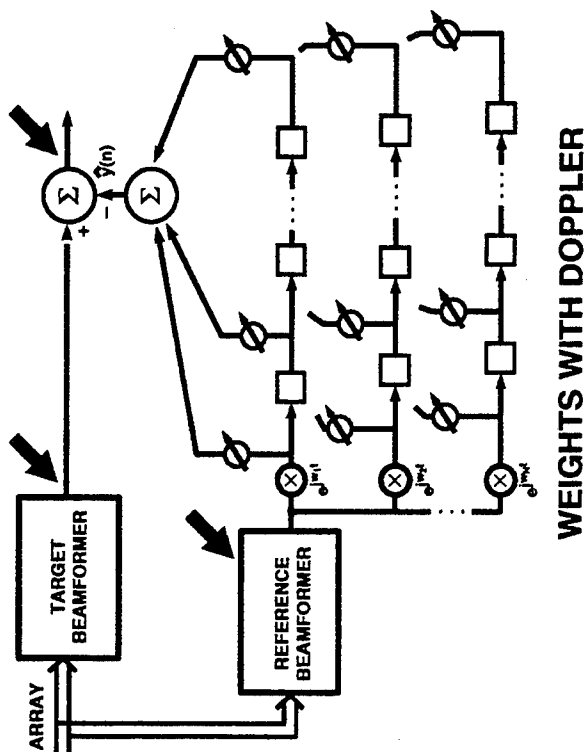
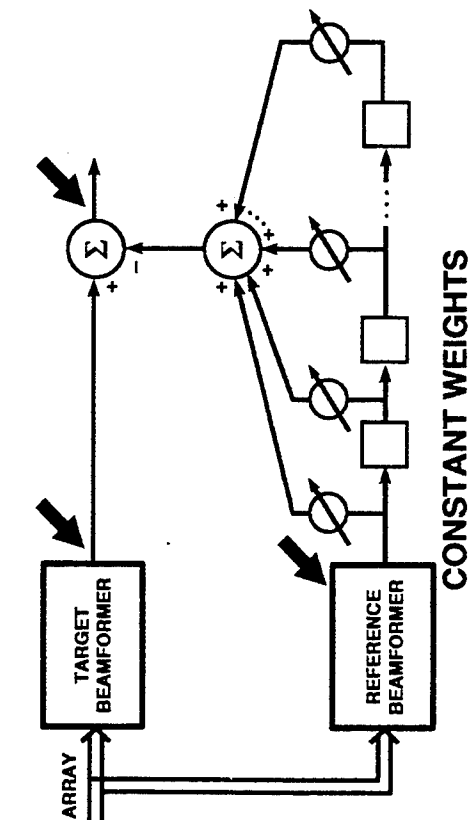


JAMMER PRE- AND POST-MITIGATION, PRI #1-3



JAMMER MULTIPATH CANCELLATION

AIRCRAFT-BASED JAMMER

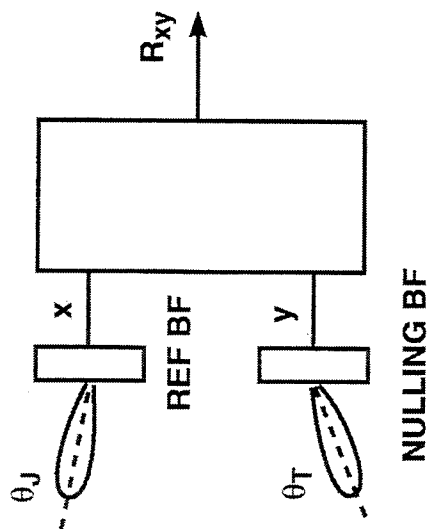


OUTLINE

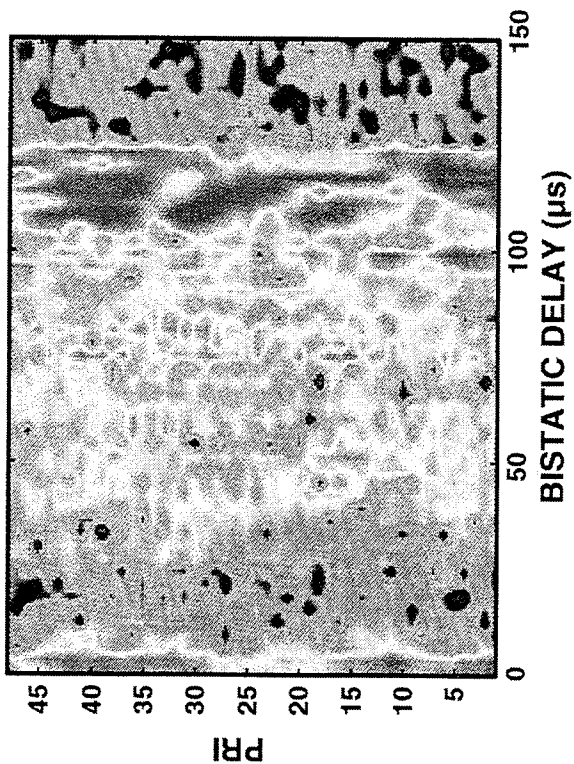
- AIRCRAFT JAMMER MITIGATION
 - TRAINING IN PRESENCE OF CLUTTER
 - DOPPLER-COMPENSATED WEIGHTS
- ➡ ● TSI ENERGY PORTRAIT
 - DELAY, AZIMUTH, DOPPLER, TIME
 - IMPLICATIONS FOR WEIGHT SELECTION
- EXTENSION TO MULTIELEMENT ARCHITECTURE
 - PREPROCESSOR TO CLUTTER NULLING
 - PERFORMANCE ASSESSMENT
- SUMMARY



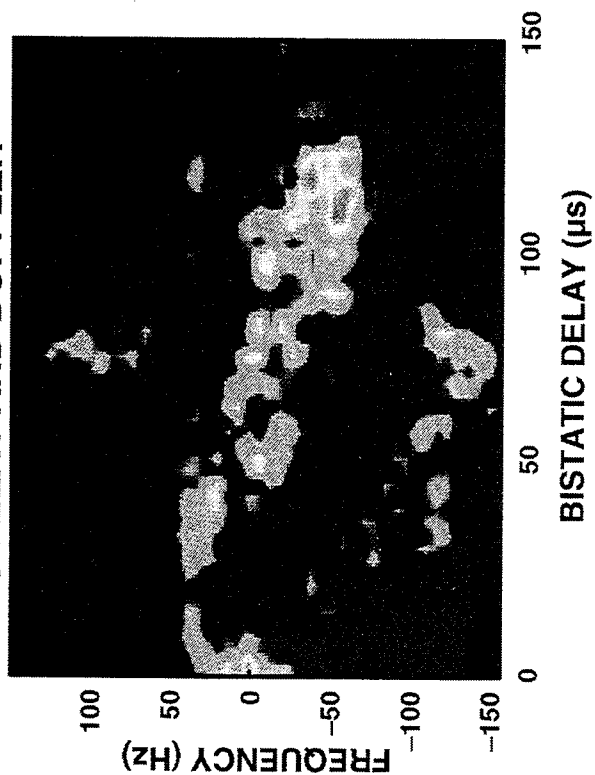
TSI CROSS-COVARIANCE PORTRAITS



CROSS-COVARIANCE MAGNITUDE

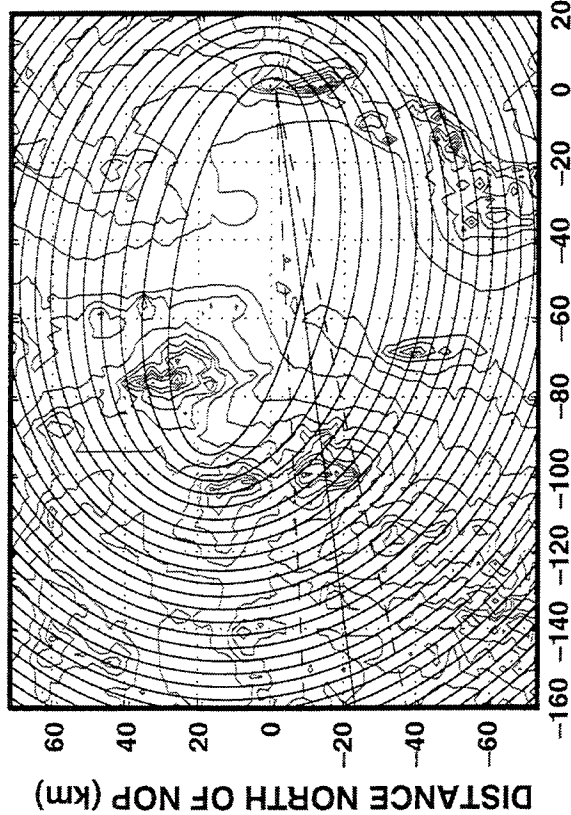


CROSS-COVARIANCE MAGNITUDE
VS DELAY AND DOPPLER

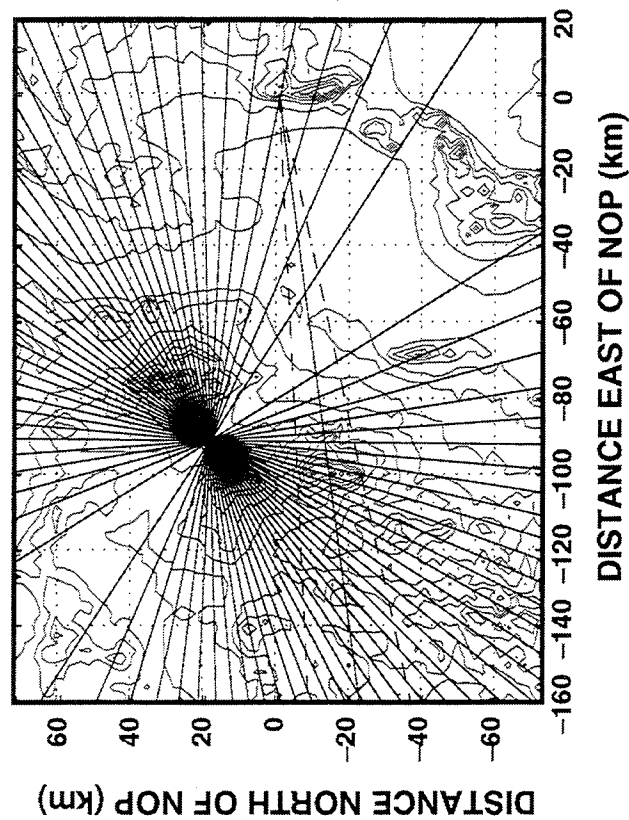


TSI CROSS-COVARIANCE ENERGY DISTRIBUTION

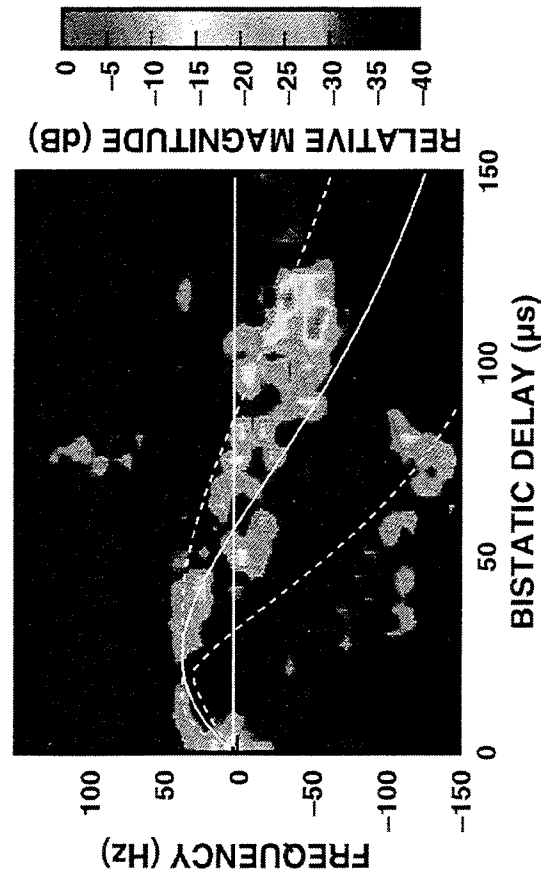
ISO-DELAY CONTOURS



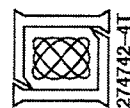
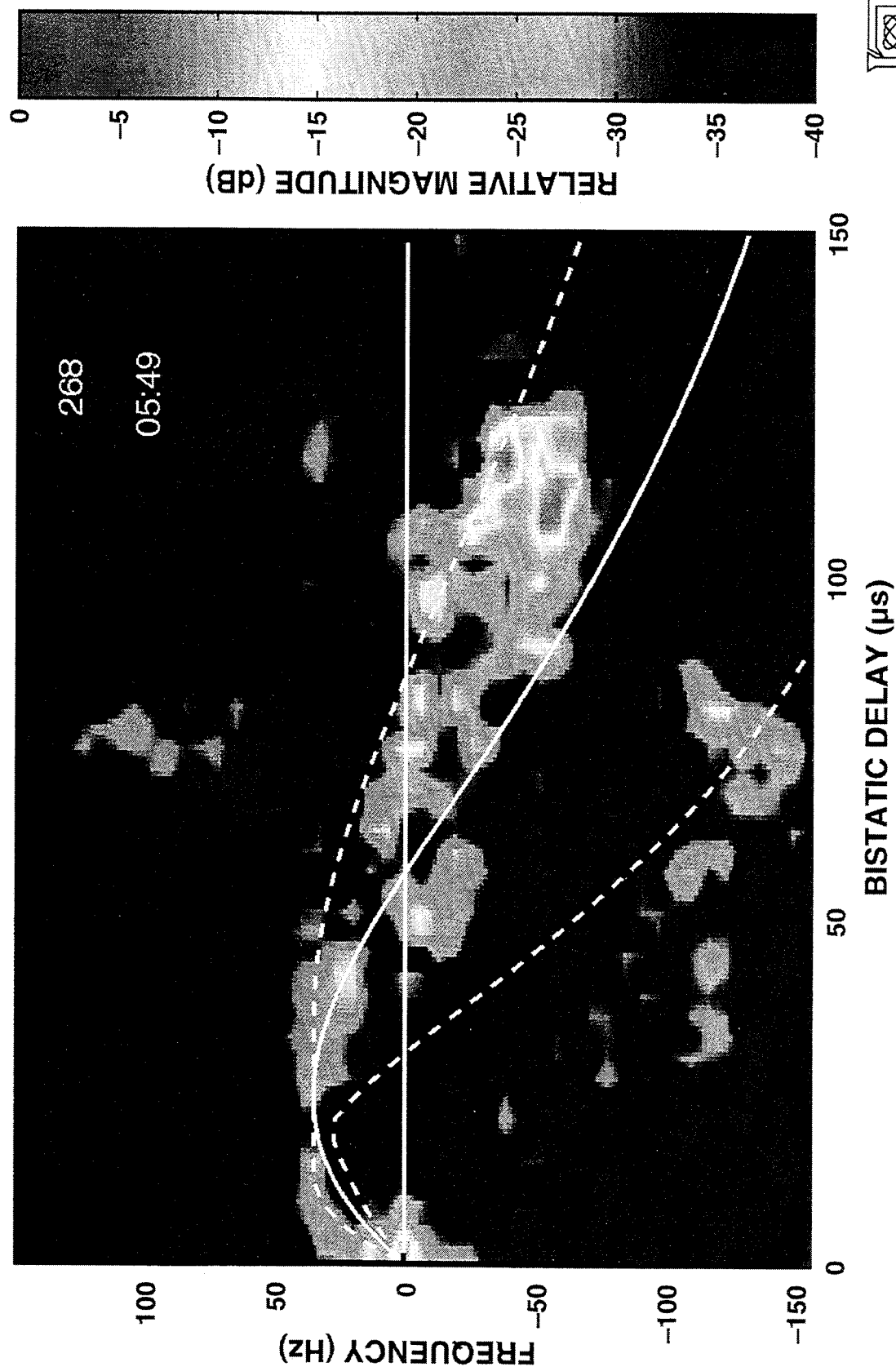
ISO-DOPPLER CONTOURS



CROSS-COVARIANCE vs DELAY AND DOPPLER



CROSS-COVARIANCE MAGNITUDE vs DELAY AND DOPPLER

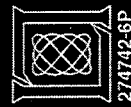


05:49

DOPPLER

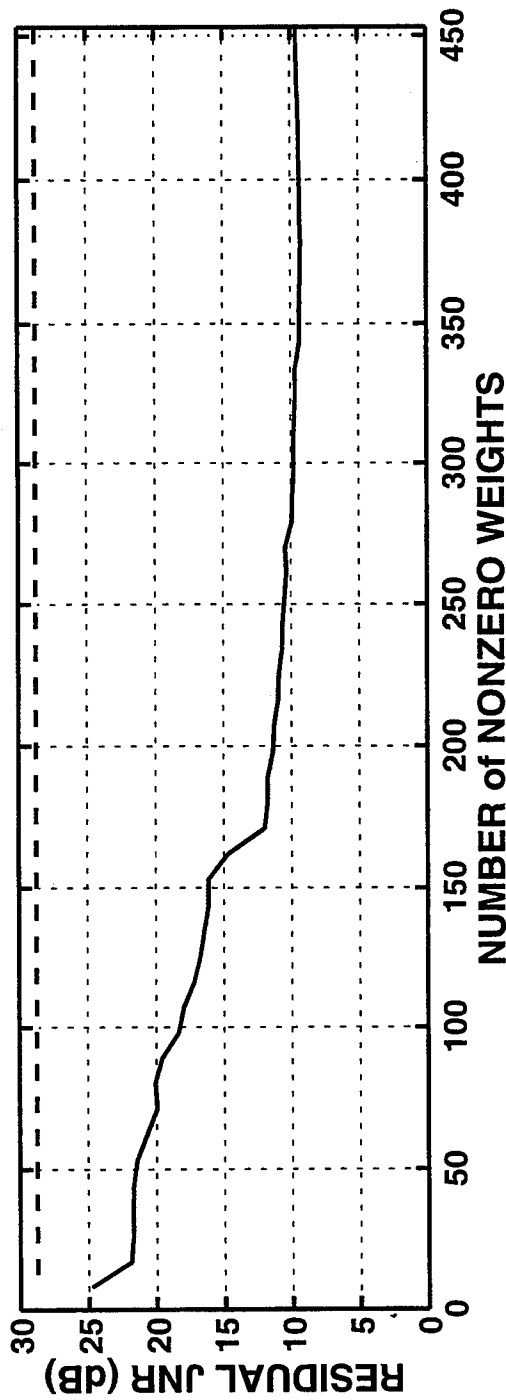
AZIMUTH

DELAY

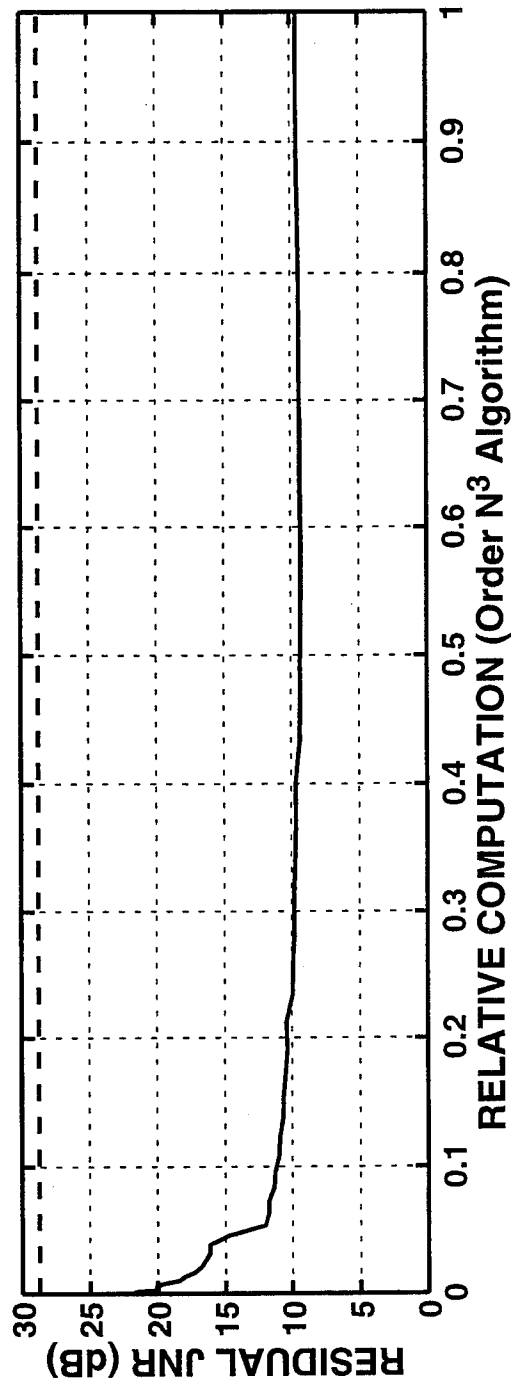


RESIDUAL JNR vs THINNING

RESIDUAL JNR vs NUMBER of WEIGHTS



RESIDUAL JNR vs COMPUTATION COST

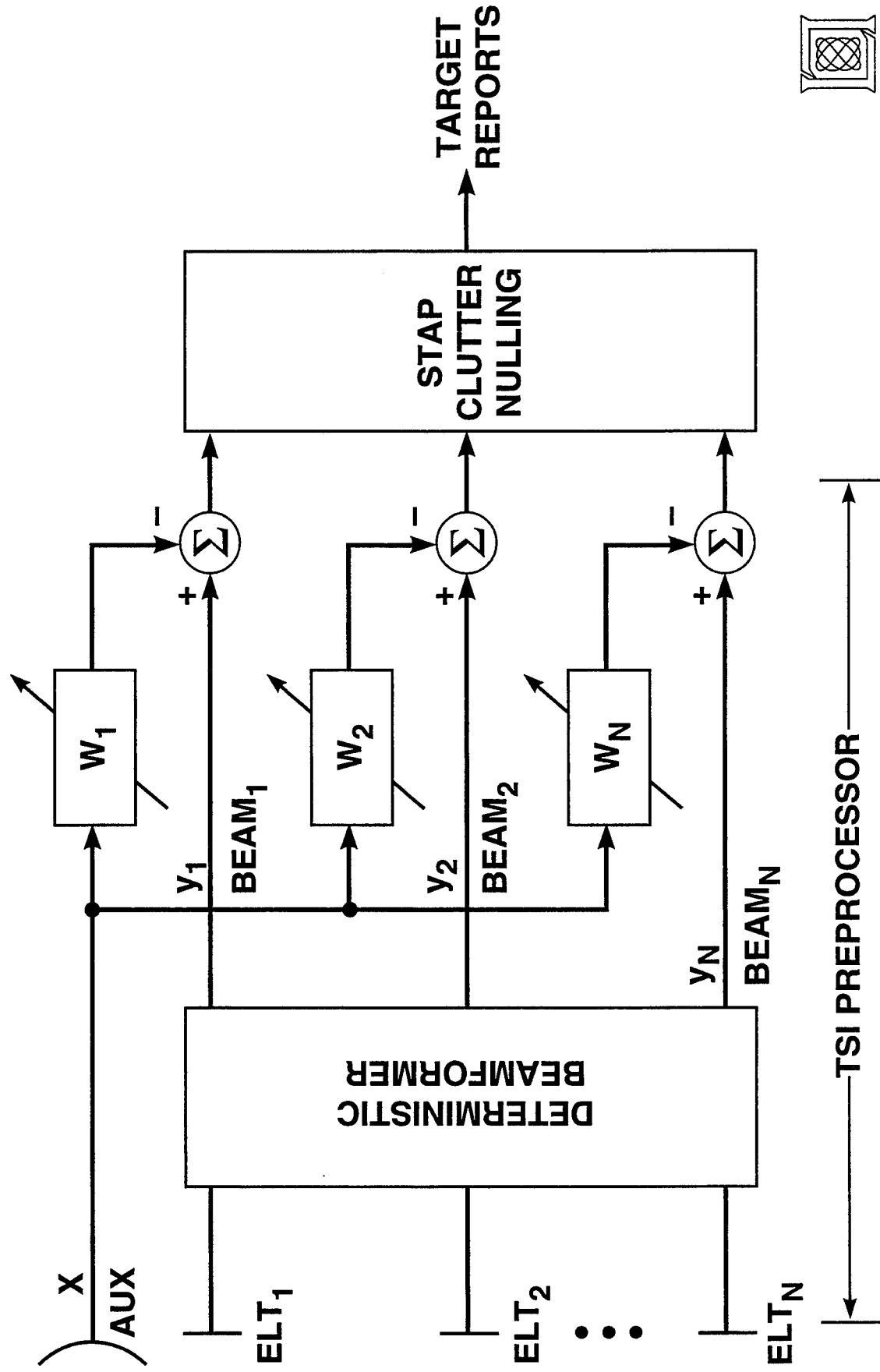


OUTLINE

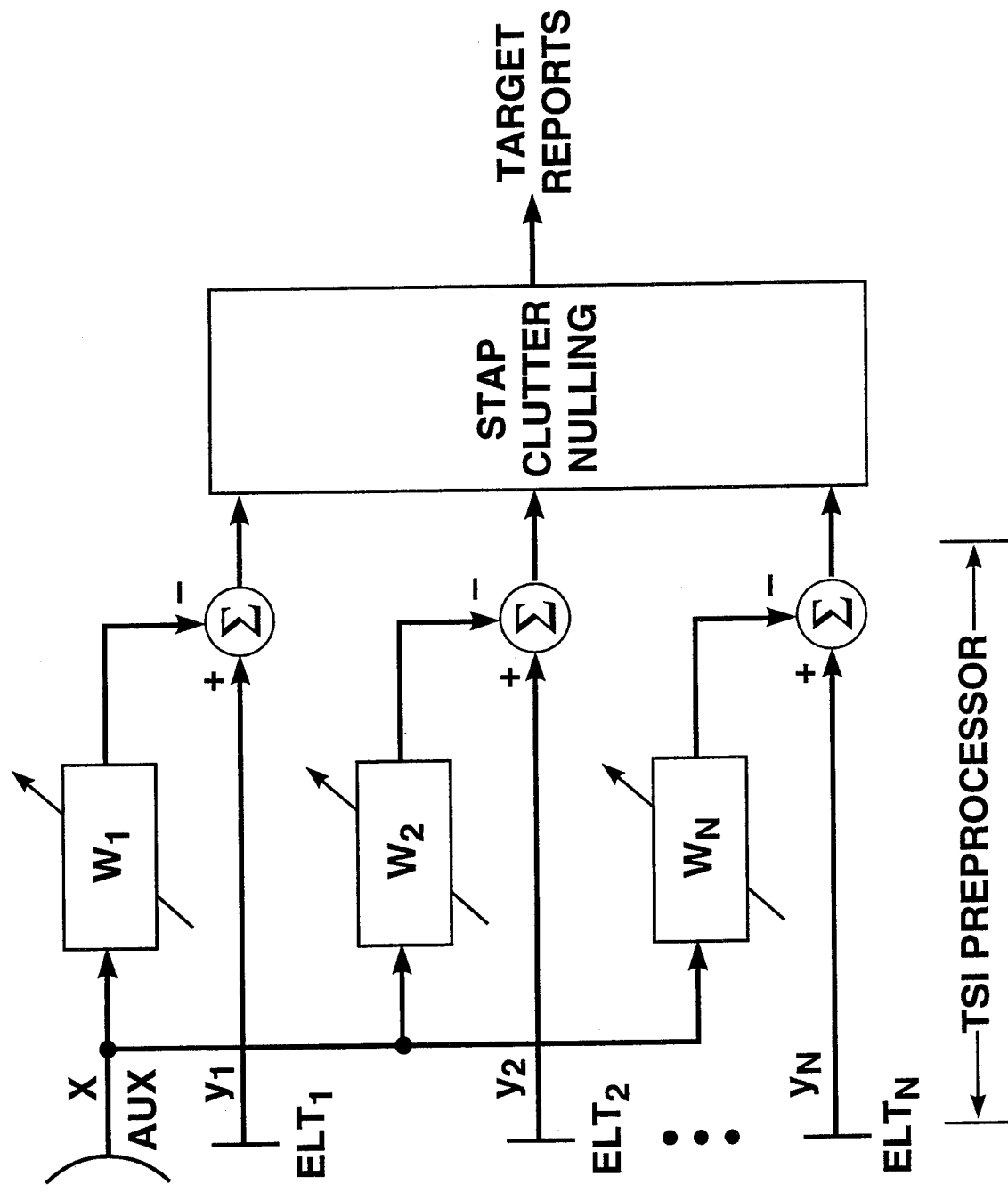
- AIRCRAFT JAMMER MITIGATION
 - TRAINING IN PRESENCE OF CLUTTER
 - DOPPLER-COMPENSATED WEIGHTS
- TSI ENERGY PORTRAIT
 - DELAY, AZIMUTH, DOPPLER, TIME
 - IMPLICATIONS FOR WEIGHT SELECTION
- ➔ ● EXTENSION TO MULTIELEMENT ARCHITECTURE
 - PREPROCESSOR TO CLUTTER NULLING
 - PERFORMANCE ASSESSMENT
- SUMMARY



BEAM-SPACE TSI MITIGATION SINGLE-AUXILIARY IMPLEMENTATION



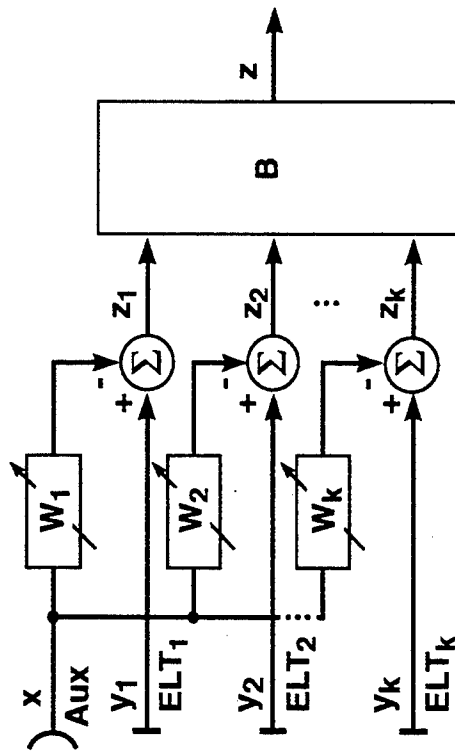
ELEMENT-SPACE TSI MITIGATION SINGLE-AUXILIARY IMPLEMENTATION



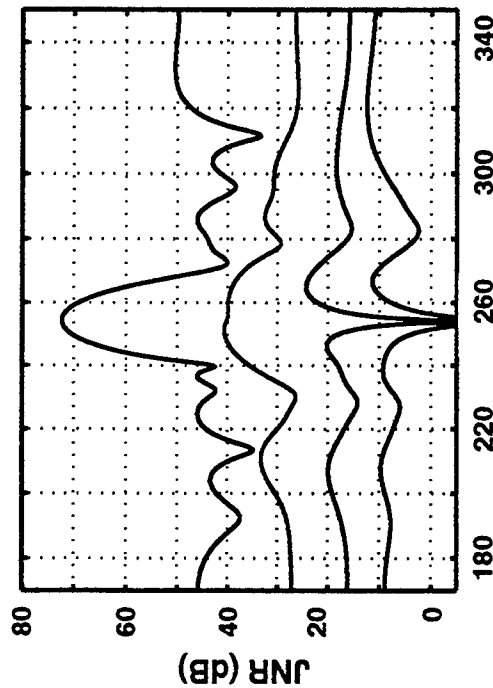
TSI-INDUCED SINR LOSS

SPATIAL PORTRAIT (Typical PRI)

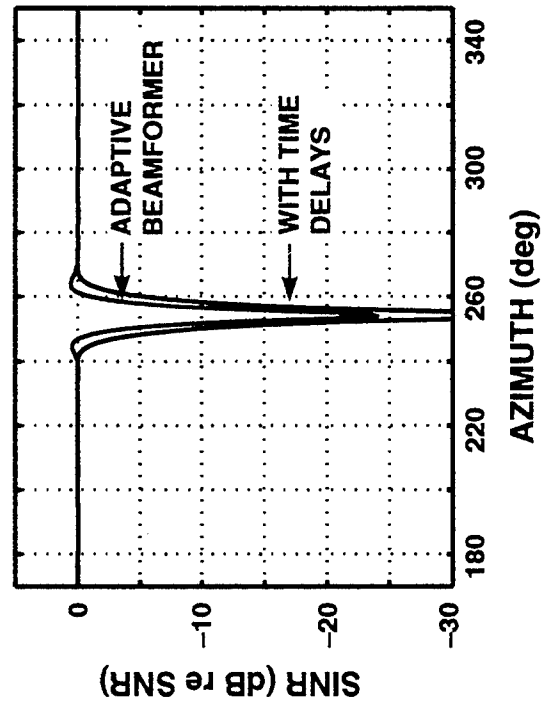
ARCHITECTURE



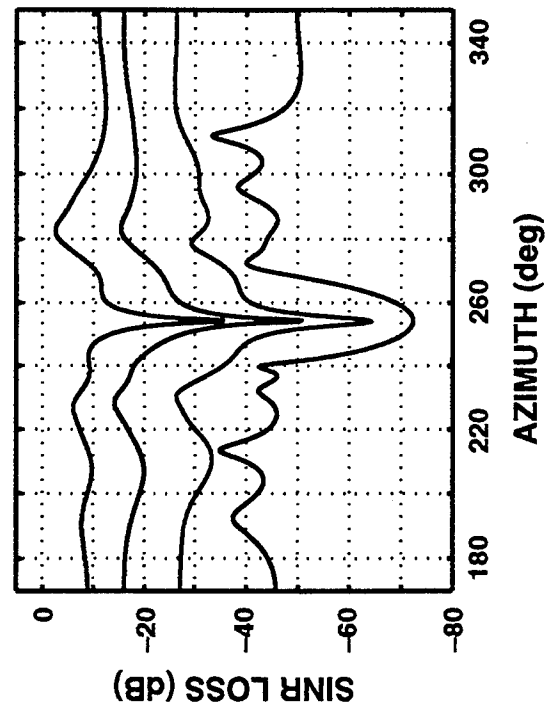
JNR vs AZIMUTH



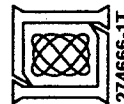
SIGNAL LOSS vs AZIMUTH



SINR LOSS vs AZIMUTH

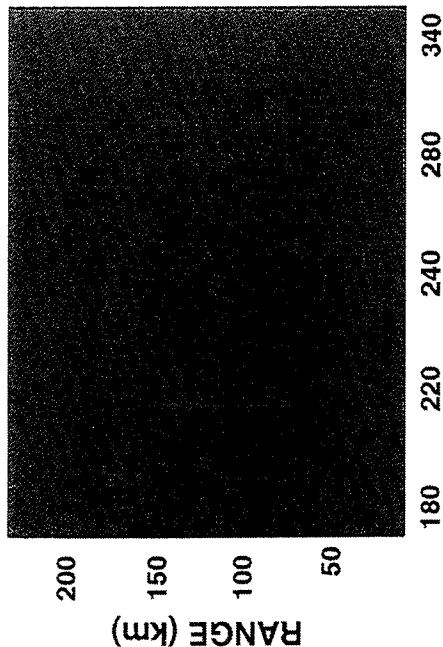


— RAW
— ADAPTIVE BEAMFORMER
— CONSTANT WEIGHTS
— WITH DOPPLER

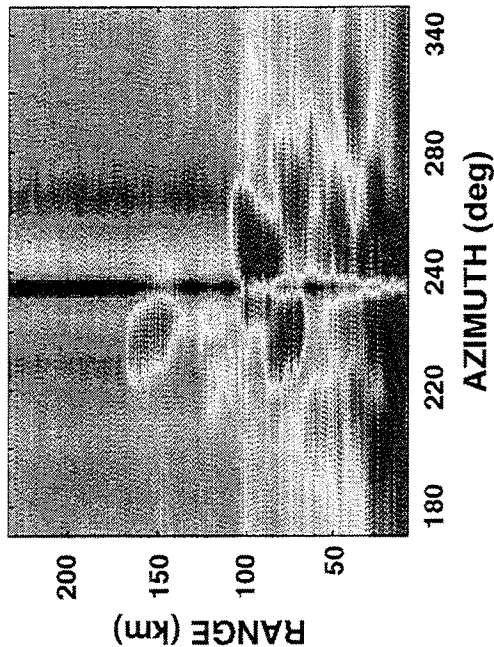


TSI MITIGATION RESIDUAL RANGE-AZIMUTH PORTRAIT (Typical PRI)

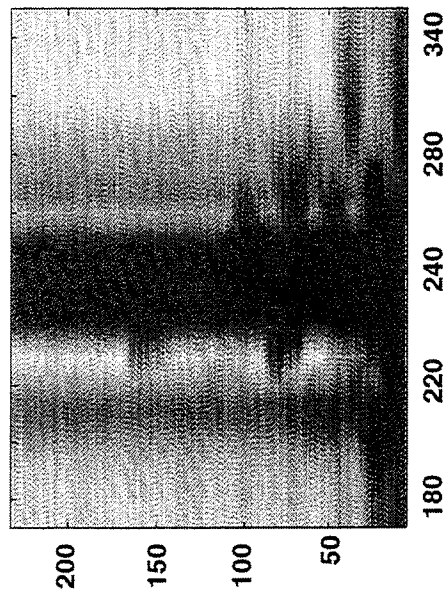
TSI WITH NO MITIGATION



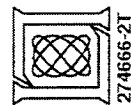
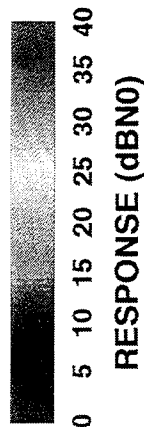
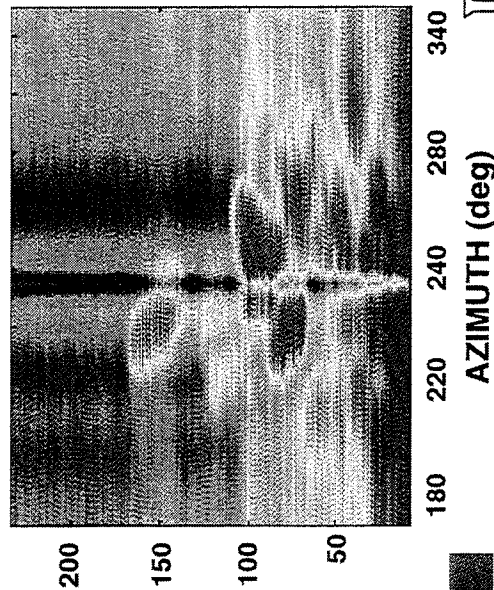
SPATIAL + TEMPORAL MITIGATION
(no Doppler)



SPATIAL-ONLY ADAPTION



SPATIAL + TEMPORAL MITIGATION
(with Doppler)



274666-2T

SUMMARY

- PRESENTED TSI PORTRAIT TO CHARACTERIZE WEIGHT SPACE
 - DELAY, AZIMUTH, DOPPLER, TIME REPRESENTATION
 - IMPLICATIONS FOR WEIGHT SELECTION
- EXAMINED TSI MITIGATION PERFORMANCE vs DOF
 - EXAMPLE: MOUNTAINTOP DATA; RSTER SYSTEM
 - 50% REDUCTION IN REQUIRED SAMPLE SUPPORT
 - 90% REDUCTION IN REQUIRED R_{xx}^{-1} COMPUTATION
- EXTENDED SINGLE-BEAM ARCHITECTURE
 - TRAINING IN PRESENCE OF MONOSTATIC CLUTTER
 - MULTIELEMENT IMPLEMENTATION

SIMULTANEOUS MITIGATION OF MULTIPATH JAMMING AND GROUND CLUTTER

Daniel F. Marshall and Robert A. Gabel

MIT Lincoln Laboratory
244 Wood Street
Lexington, MA 02173-9108
tel: (617) 981-0807
email: dmars@ll.mit.edu

Abstract Studies of the multipath jamming phenomenon have determined that it may potentially degrade the performance of state-of-the-art radar systems. The development of techniques that address this problem is a nascent field, and most work in this area to date has focused on mitigating multipath jamming in isolation. However, airborne surveillance radars will experience multipath jamming and ground clutter interference in combination. Space-Time Adaptive Processing (STAP) has been shown to be effective in nulling both ground clutter interference and clutter in combination with sidelobe jamming. But these algorithms do not effectively accommodate the presence of jamming in the main beam, thus widely scattered multipath jamming may degrade STAP performance over a large area. In the work documented in this paper, a preliminary effort has been made to address the challenge of mitigating the interference environment, where both ground clutter and multipath jamming are present. Our approach has been to combine existing STAP and multipath jamming mitigation techniques. One multipath jamming mitigation architecture produces a beamformed output corresponding to a desired look direction; this processing can be repeated for a number of look directions to form a suitable input to a beam-space STAP architecture. Alternatively, multipath jamming mitigation may be applied to each receive array element individually, providing a front end to any of the several STAP algorithms. The performance of these different approaches is evaluated and compared. Interactions between the jamming and clutter returns and nulling processes are discussed. In particular, the challenges raised by the task of training for jammer mitigation in the presence of clutter are addressed, for both ground-based and airborne jammer sources. The presentation concludes with a discussion of the effectiveness of our mitigation efforts to date, unresolved difficulties, and areas for future work.

**SIMULTANEOUS MITIGATION OF
MULTIPATH JAMMING AND GROUND CLUTTER**

DANIEL F. MARSHALL AND ROBERT A. GABEL

MARCH 13, 1996

**MASSACHUSETTS INSTITUTE OF TECHNOLOGY
LINCOLN LABORATORY
LEXINGTON, MASSACHUSETTS**

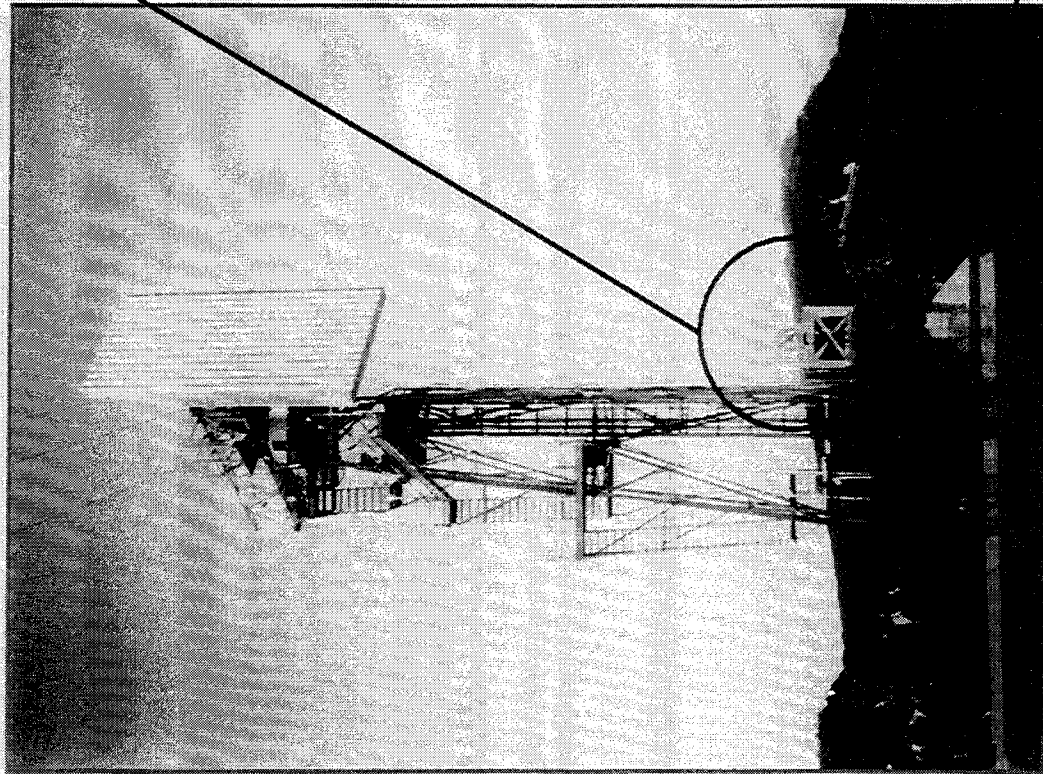
OUTLINE

- **INTRODUCTION**
- **ARCHITECTURES**
- **RESULTS**
- **CONCLUSIONS AND FUTURE WORK**

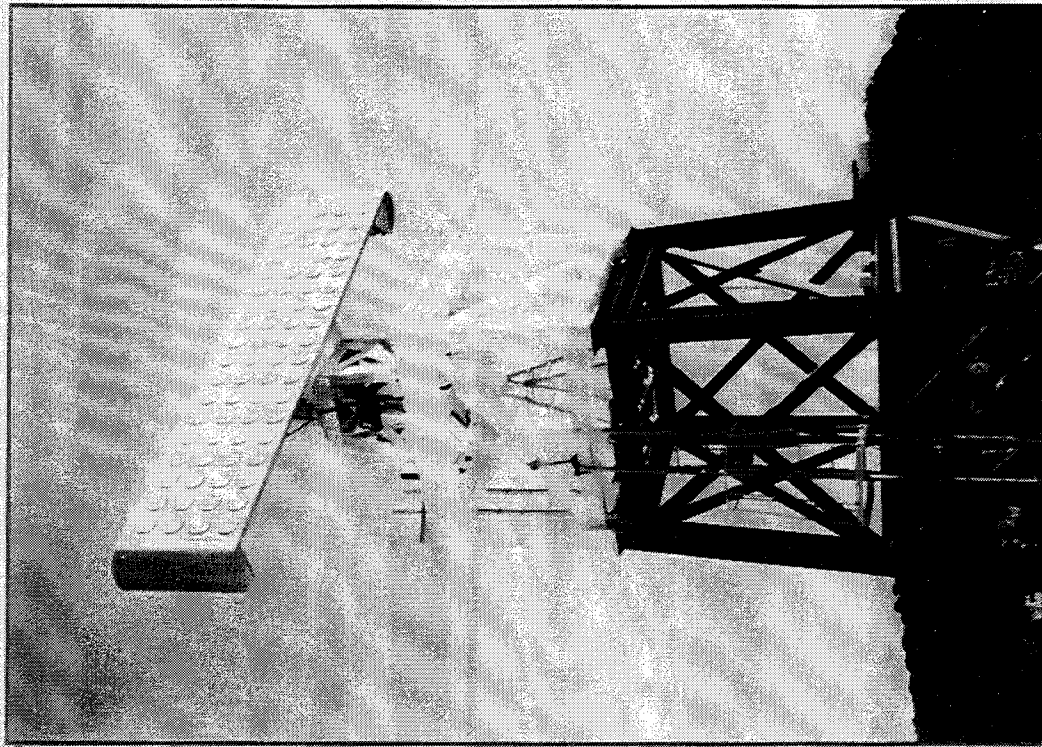
INTRODUCTION

- **THE MULTIPATH JAMMING PROBLEM:**
 - **WORK TO DATE: MITIGATION OF MULTIPATH JAMMING BY ITSELF**
 - **THE REAL-WORLD RADAR PROBLEM: MITIGATION OF BOTH
MULTIPATH JAMMING AND GROUND CLUTTER IN COMBINATION**
 - **THE SUBJECT OF THIS PRESENTATION**
 - **A NASCENT EFFORT**

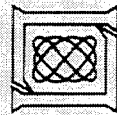
MOUNTAINTOP TEST SITE WHITE SANDS, NEW MEXICO



RSTER-90 ARRAY
14 × 24 ELEMENTS



IDPCA ARRAY
18 × 4 ELEMENTS



241430-1K

OUTLINE

- INTRODUCTION

- ARCHITECTURES

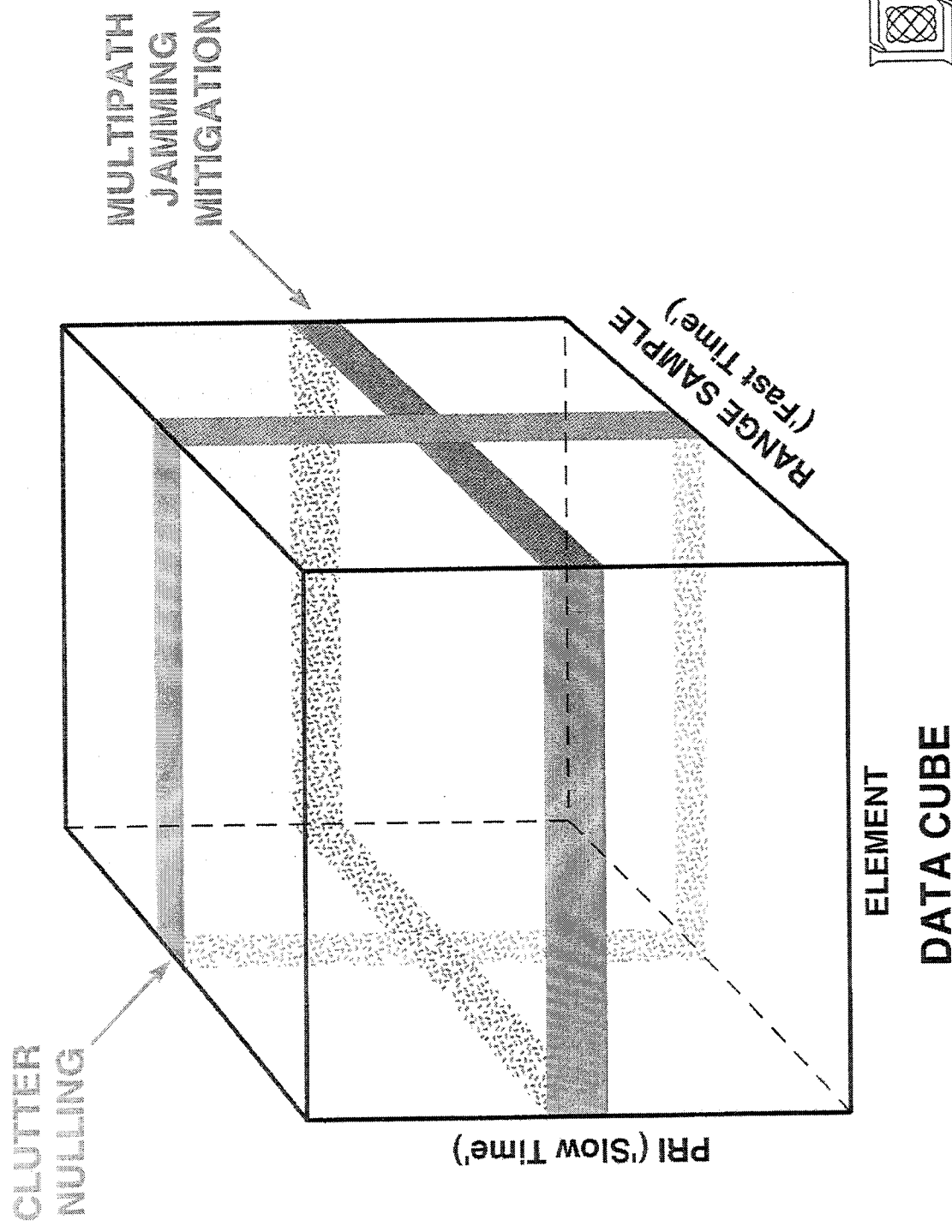


- A CASCADE APPROACH
- REVIEW OF SPACE-TIME ADAPTIVE PROCESSING (STAP)
- REVIEW OF MULTIPATH JAMMING MITIGATION ARCHITECTURES
- SIMULTANEOUS MITIGATION ARCHITECTURES

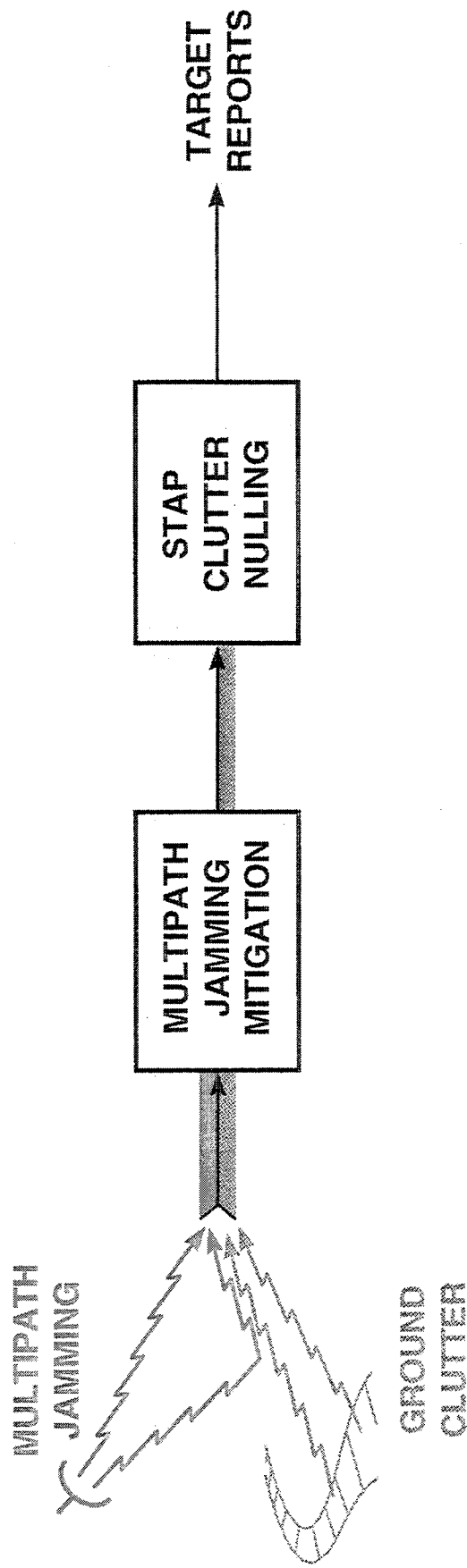
- RESULTS

- CONCLUSIONS AND FUTURE WORK

MULTIPATH JAMMING MITIGATION AND CLUTTER NULLING SPACES

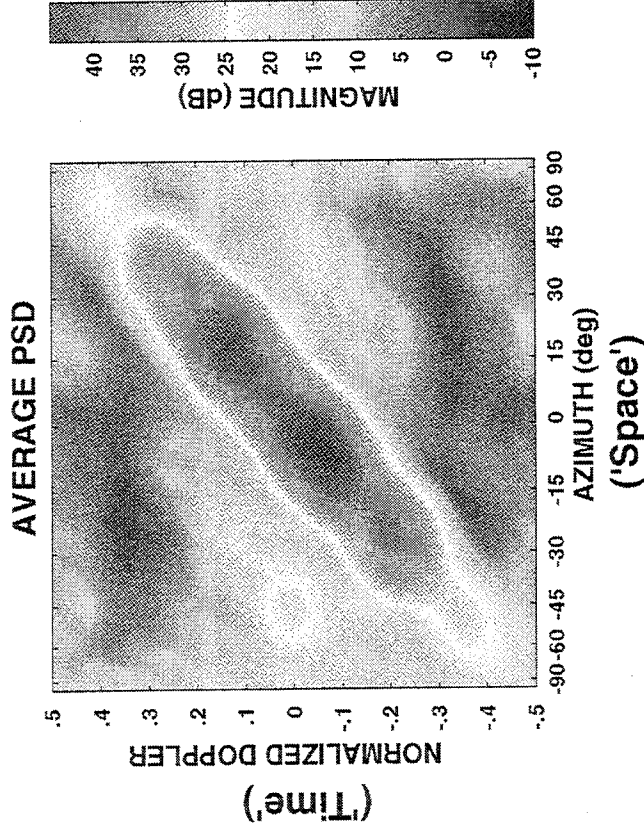


PROPOSED MITIGATION APPROACH

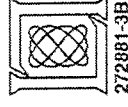


- CASCADE OF EXISTING ARCHITECTURES
- A DECOMPOSITION OF THE FULL 3-D PROBLEM
 - REDUCED COMPUTATION
 - TRAINING ADVANTAGES

SPACE-TIME ADAPTIVE PROCESSING (STAP) FOR GROUND CLUTTER INTERFERENCE MITIGATION



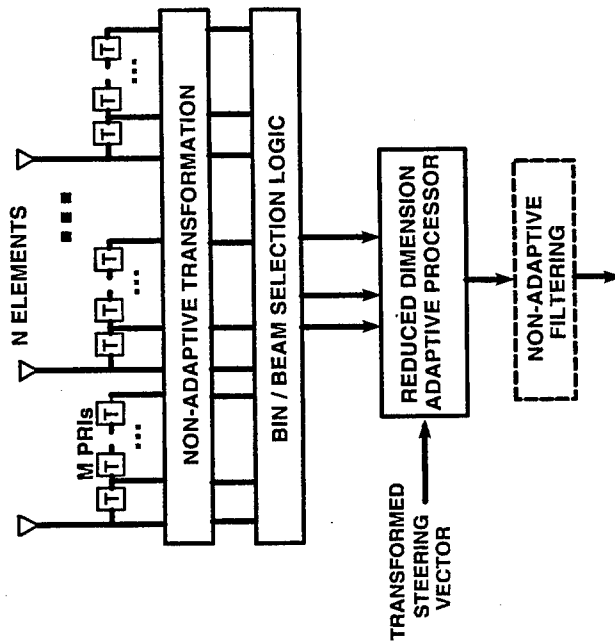
- FROM AN AIRBORNE MOVING RADAR PLATFORM:
 - CLUTTER APPEARS AT ALL ANGLES
 - CLUTTER APPEARS AT SOME OR ALL DOPPLERS
- STAP IS TWO-DIMENSIONAL ADAPTIVE NULLING
 - NULL JUST THE CLUTTER LINE, MAXIMIZE OBSERVABLE SPACE
 - PRACTICAL STAP ARCHITECTURES REDUCE THE SIZE OF THE PROBLEM VIA NONADAPTIVE TRANSFORMATION



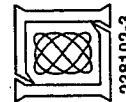
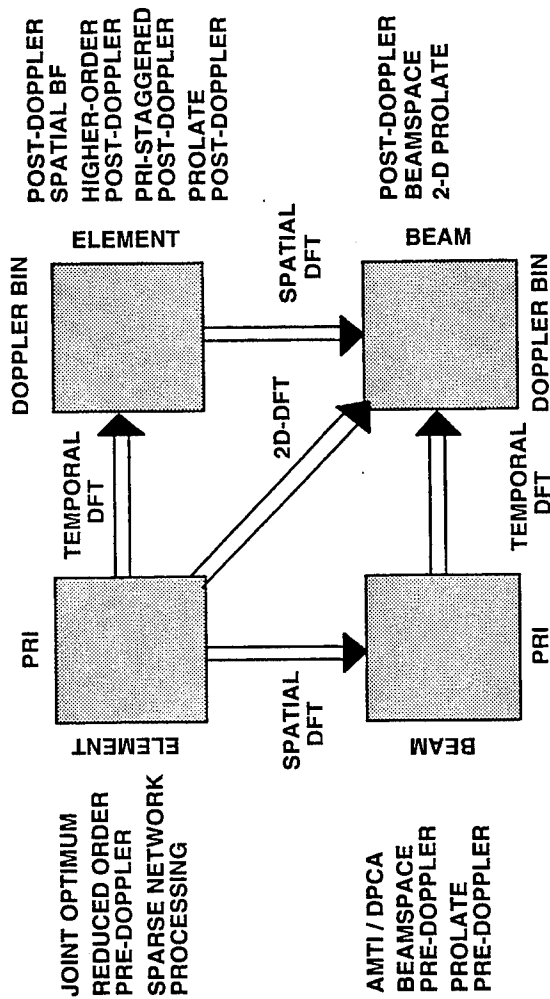
272881-3B

A TAXONOMY OF STAP ARCHITECTURES

GENERAL STRUCTURE



TRANSFORMATION TYPES



238102-3

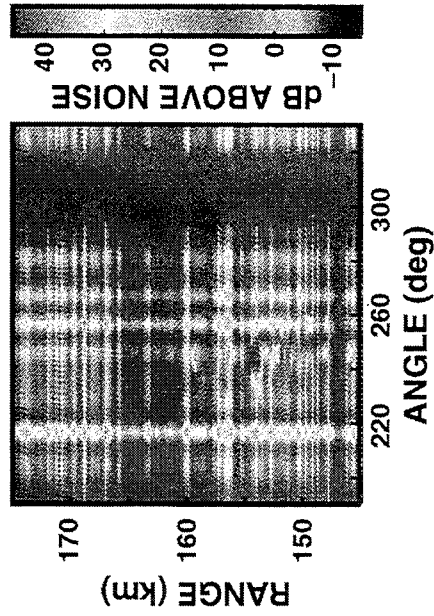
OUTLINE

- INTRODUCTION
- ARCHITECTURES
- RESULTS
 - STATIONARY JAMMER CASE
 - AIRBORNE JAMMER CASE
- CONCLUSIONS AND FUTURE WORK

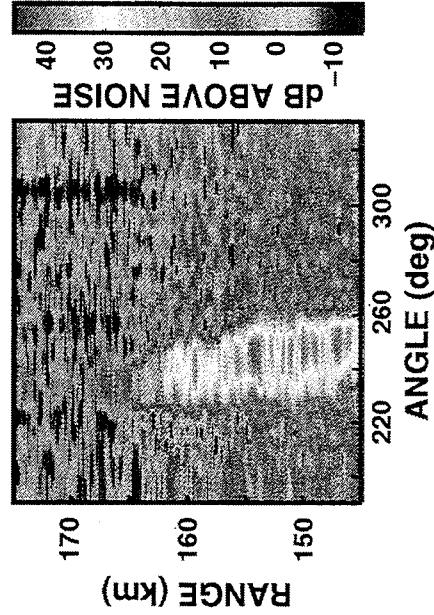


RESULTS: STATIONARY JAMMING POWER OUT vs RANGE AND ANGLE AT -156 Hz

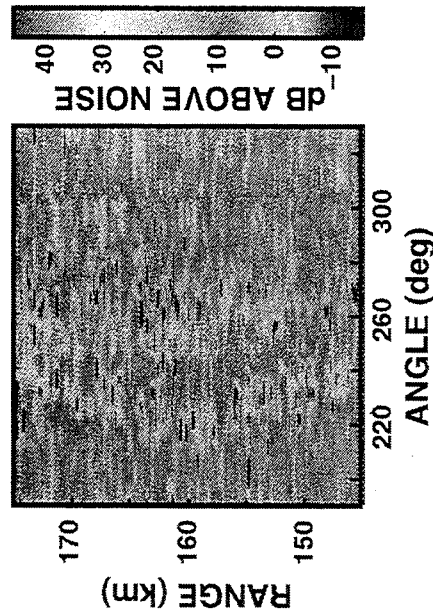
NONADAPTIVE BEAMFORMING



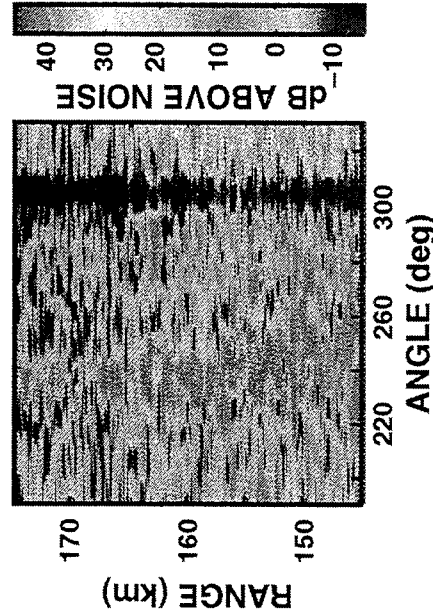
MULTIPATH MITIGATION ONLY
NO DOPPLER-SPACE WEIGHTS



POST-DOPPLER STAP ONLY



MULTIPATH MIT + STAP

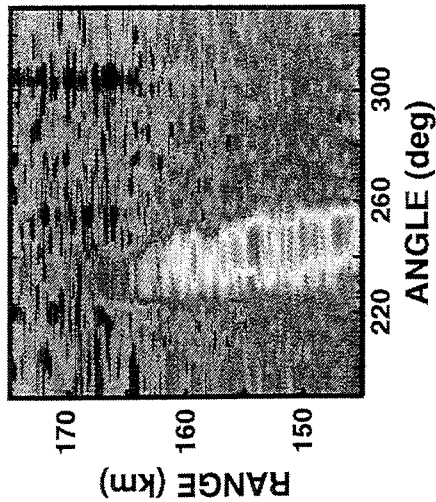


RESULTS: STATIONARY JAMMING

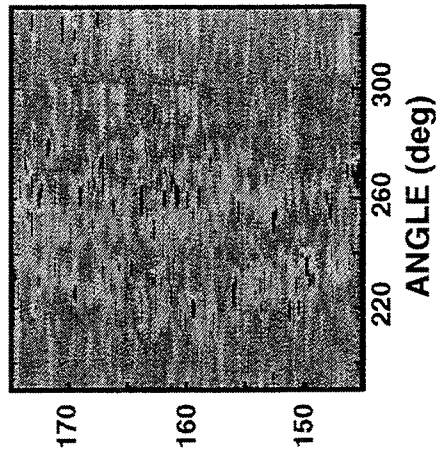
POWER OUT AT -156 Hz, AND WITH TARGET AT 285 deg

MULTIPATH MITIGATION

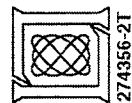
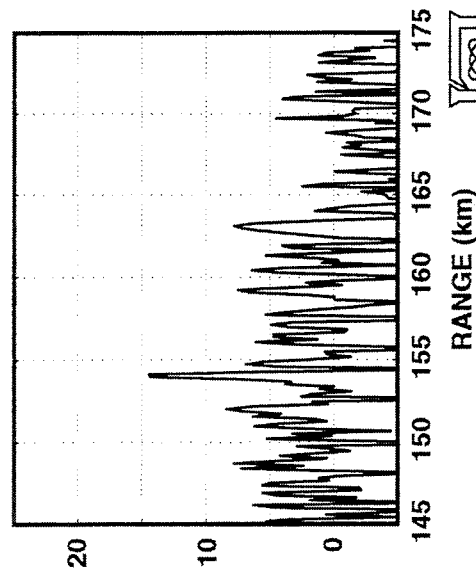
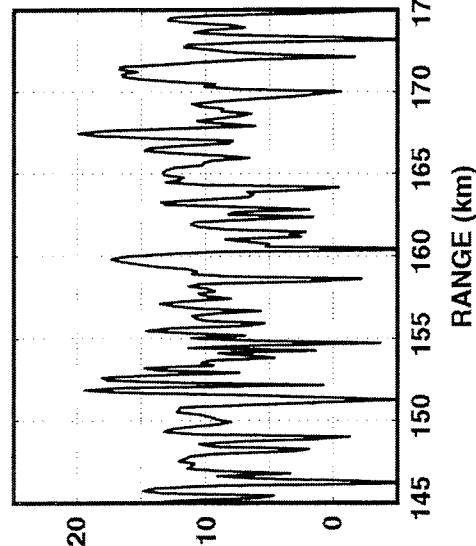
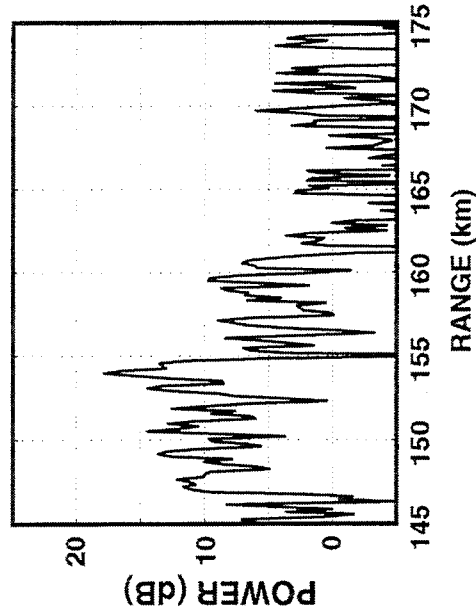
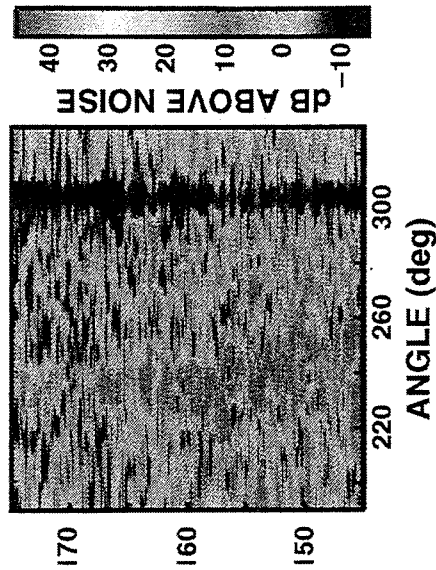
NO DOPPLER SPACE WGTS



POST-DOPPLER STAP



MULTIPATH MIT + STAP



274356-2T

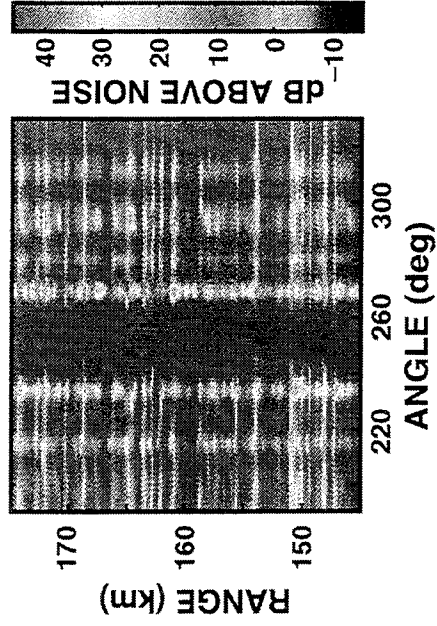
RESULTS: AIRBORNE JAMMING

OUTLINE

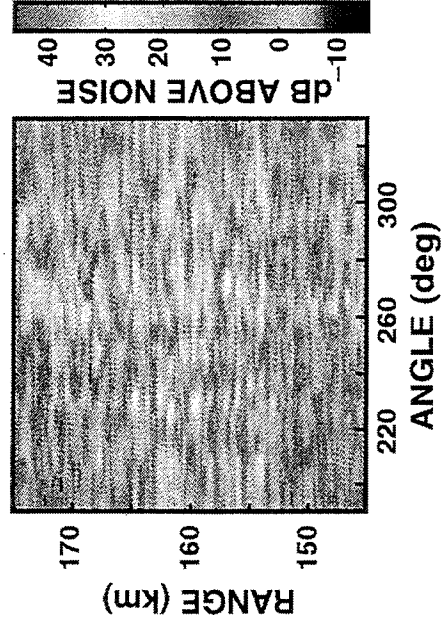
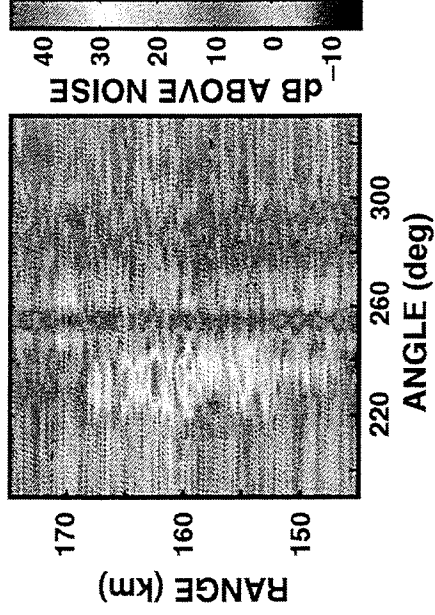
- **INITIAL RESULTS**
 - POWER OUT VS. RANGE AND ANGLE
 - COMPARISON WITH MULTIPATH-ONLY CASE
 - RANGE PLOTS WITH TARGET SIGNAL (~ 0 dBsm)
- **PERFORMANCE COMPARISONS**
 - MULTIPATH MITIGATION: WITHOUT/WITH DOPPLER SPACE WEIGHTS
 - STAP: PRE-DOPPLER/POST-DOPPLER
- **BEST RESULTS**

RESULTS: AIRBORNE JAMMING POWER OUT vs RANGE AND ANGLE AT -78 Hz

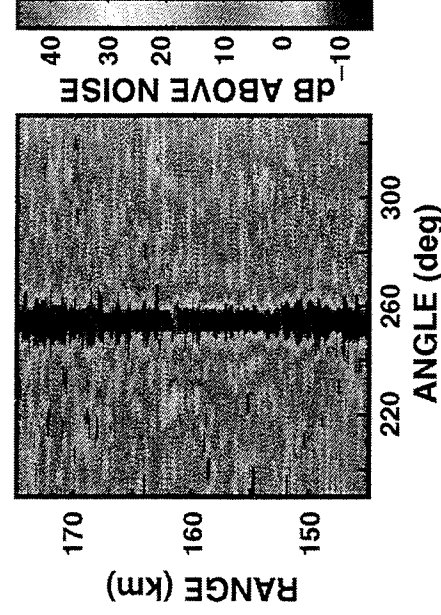
NONADAPTIVE BEAMFORMING



MULTIPATH MITIGATION ONLY
NO DOPPLER SPACE WEIGHTS



POST-DOPPLER STAP ONLY



MULTIPATH MIT + STAP

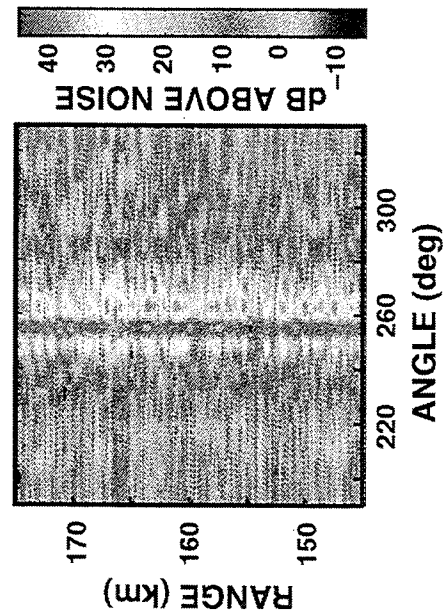


274356-3T

RESULTS: AIRBORNE JAMMING POWER OUT vs RANGE AND ANGLE AT -78 Hz

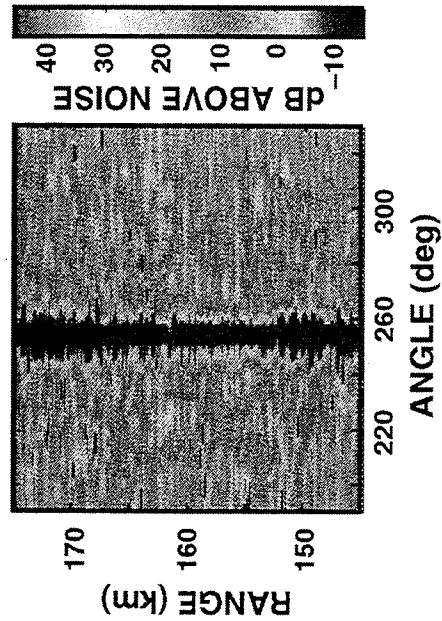
MULTIPATH JAMMING ONLY,
MULTIPATH MITIGATION ONLY

NO DOPPLER-SPACE WEIGHTS



JAMMING AND CLUTTER,
MULTIPATH MIT + POST-DOPPLER STAP

NO DOPPLER-SPACE WEIGHTS

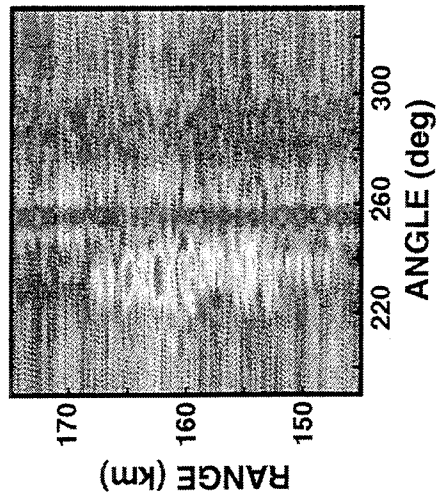


RESULTS: AIRBORNE JAMMING

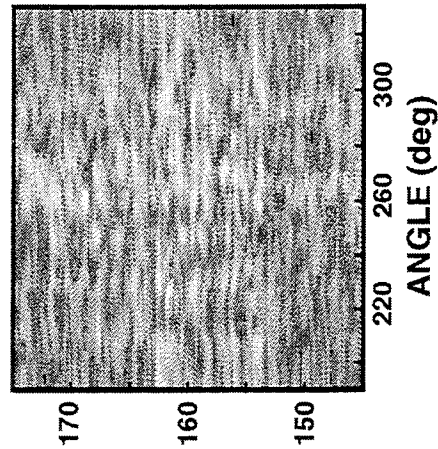
POWER OUT AT -78 HZ, AND WITH TARGET AT 268 deg

MULTIPATH MITIGATION

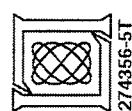
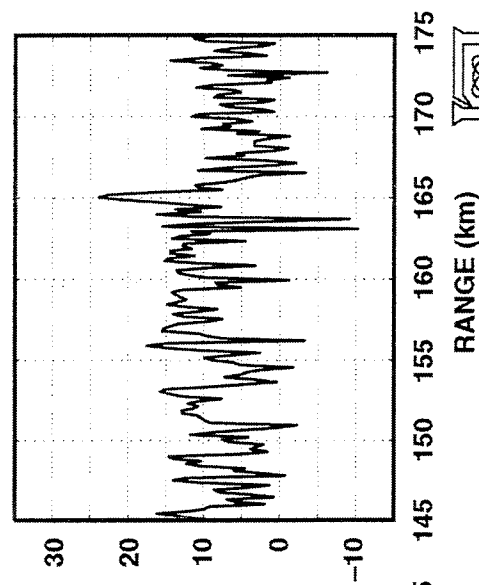
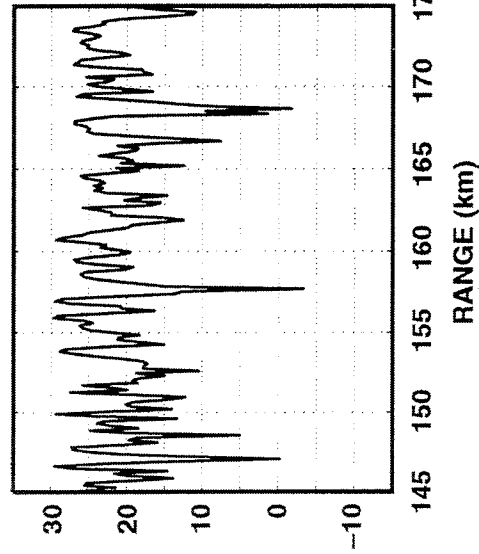
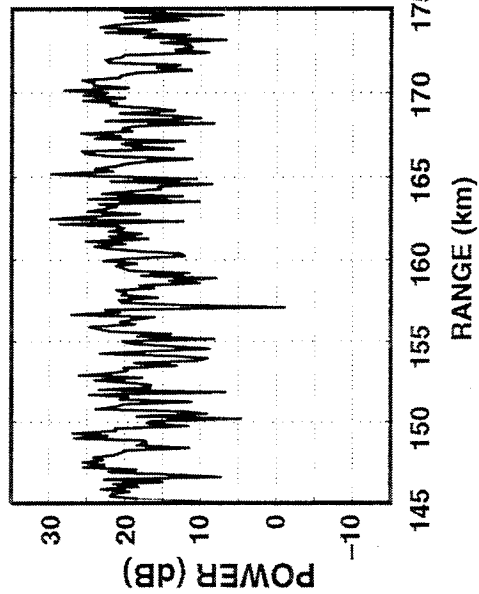
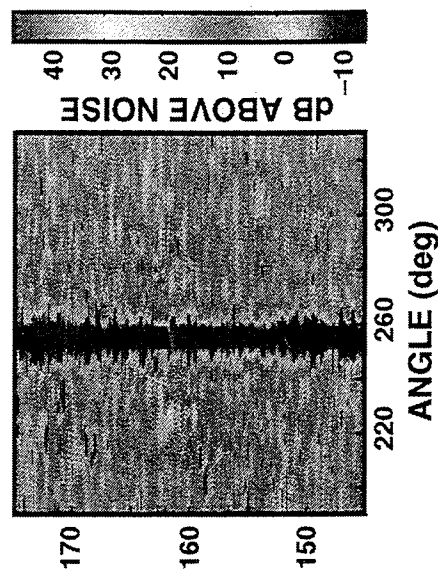
NO DOPP-SPACE WGTS



POST-DOPPLER STAP



MULTIPATH MIT + STAP

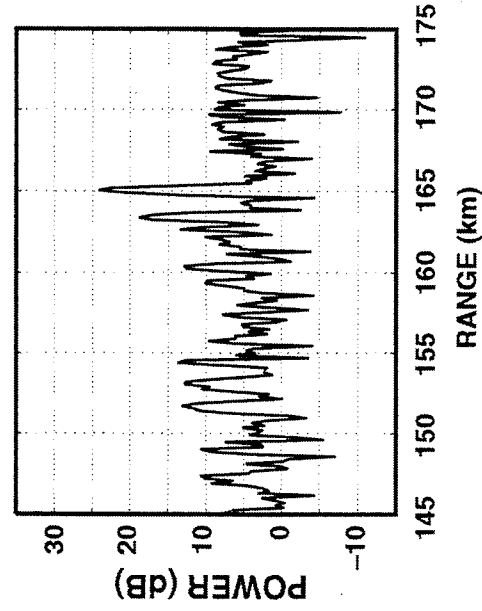
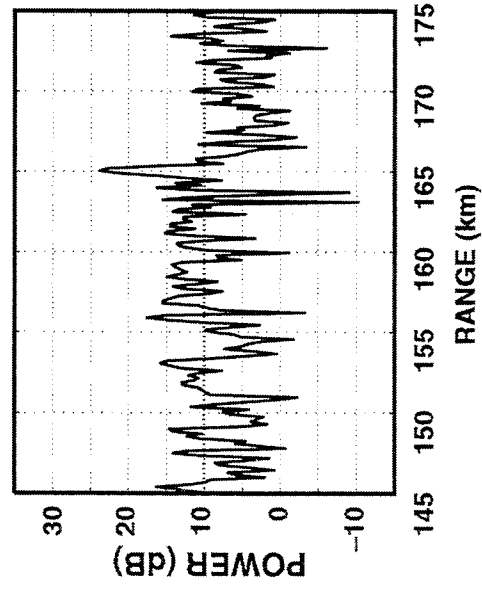
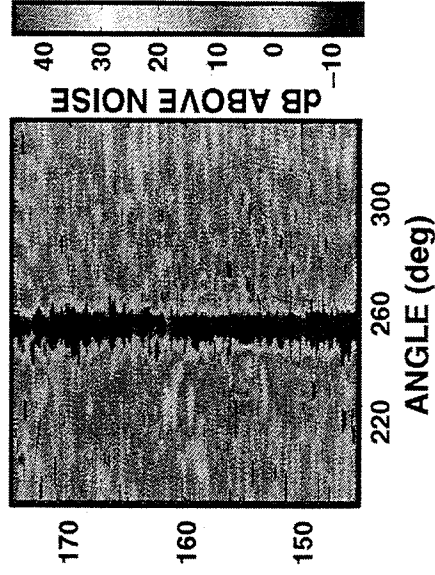
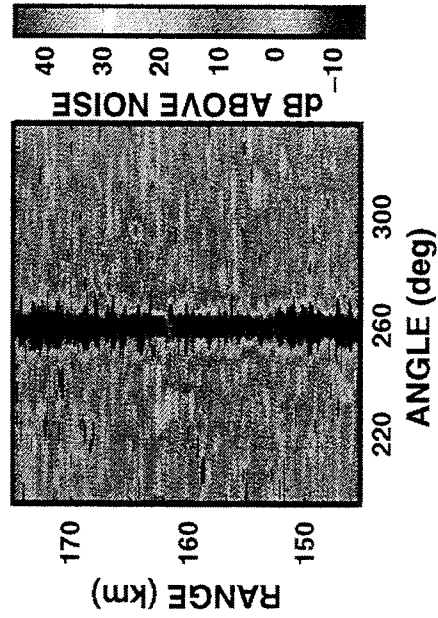


274356-5T

RESULTS: AIRBORNE JAMMING

POWER OUT AT -78 HZ, AND WITH TARGET AT 268 deg

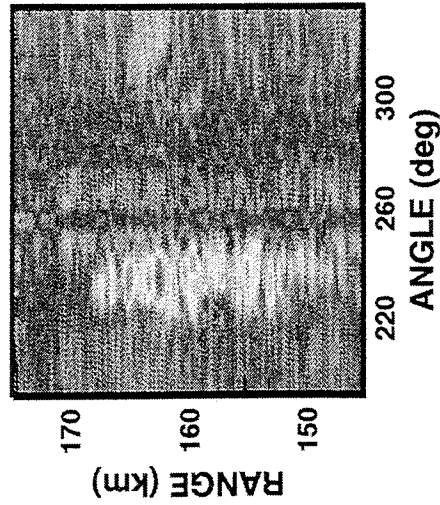
MULTIPATH MITIGATION + POST-DOPPLER STAP
NO DOPPLER-SPACE WEIGHTS WITH DOPPLER-SPACE WEIGHTS



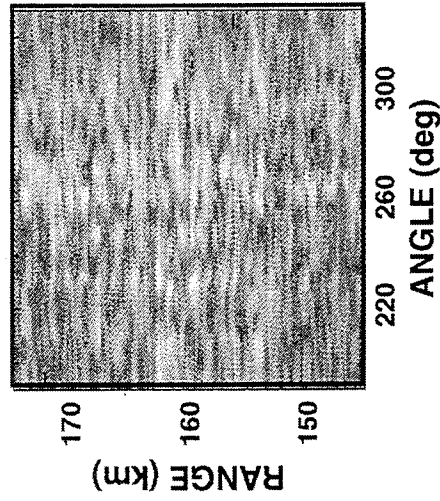
RESULTS: AIRBORNE JAMMING

POWER OUT AT -78 HZ, AND WITH TARGET AT 268 deg

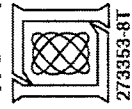
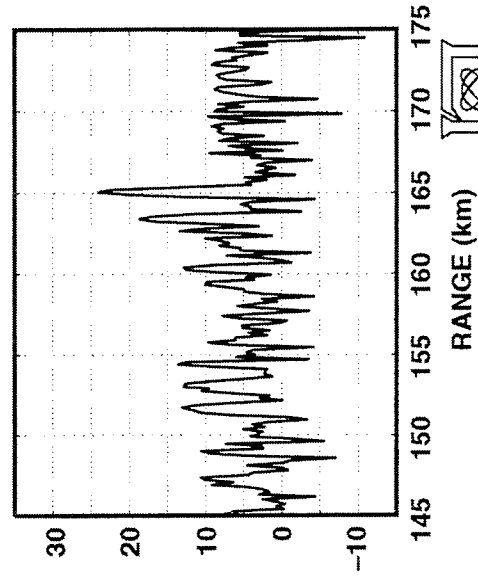
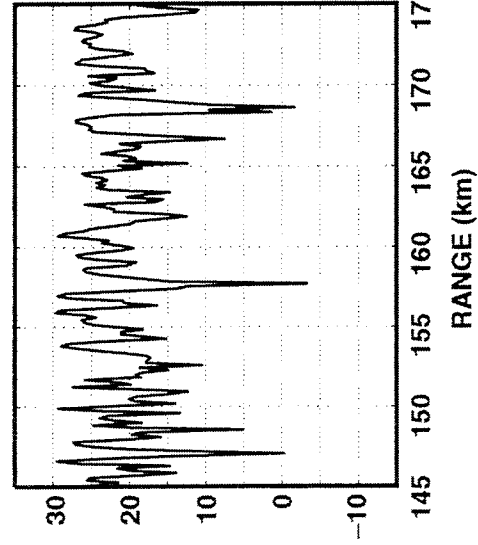
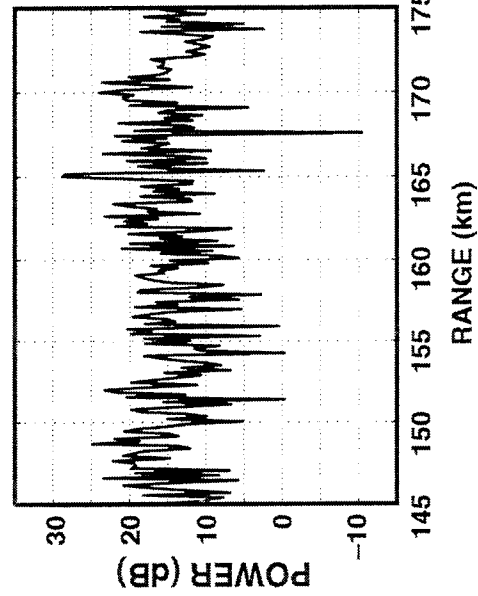
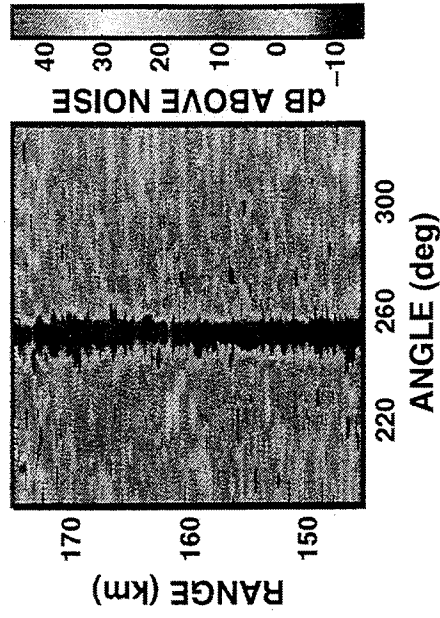
MULTIPATH MITIGATION
WITH DOPP-SPACE WGTS



POST-DOPPLER STAP



MULTIPATH MIT + STAP



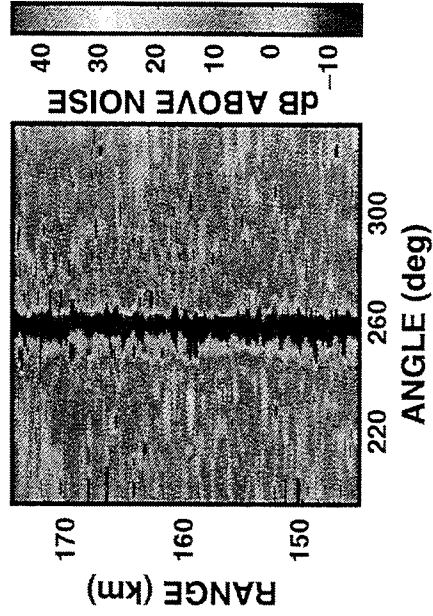
273353-81

RESULTS: AIRBORNE JAMMING

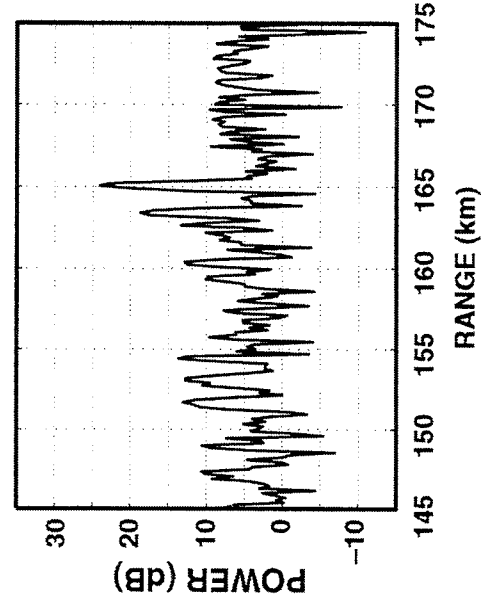
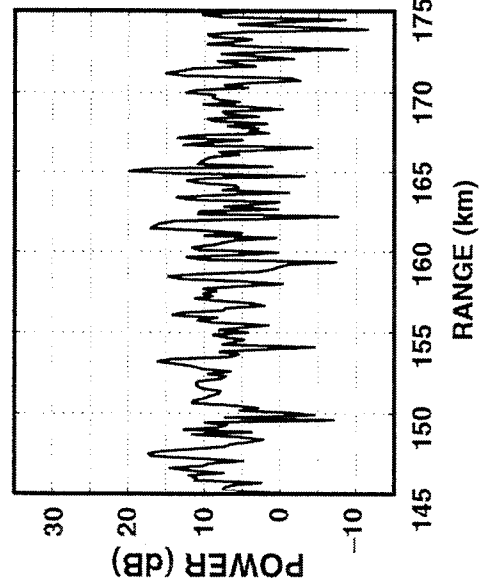
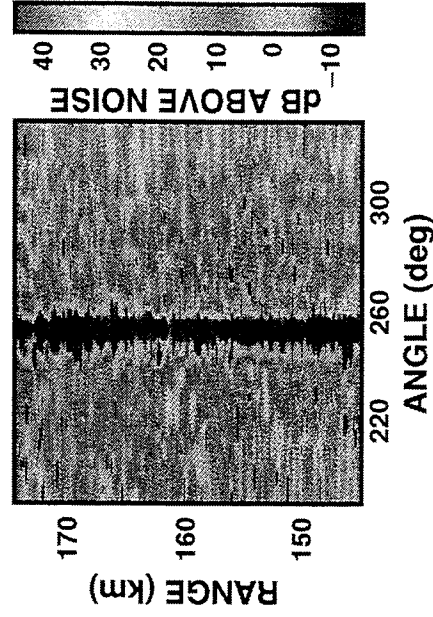
POWER OUT AT -78 Hz, AND WITH TARGET AT 268 deg

MULTIPATH MITIGATION, WITH DOPPLER-SPACE WEIGHTS, + STAP

PRE-DOPPLER STAP



POST-DOPPLER STAP



INTERFERENCE POWER LEVELS IN RECEIVED DATA - PER ELEMENT/PULSE

- **STATIONARY JAMMING CASE:**

- CNR ~ 20 dB
- JNR ~ 56 dB

- **AIRBORNE JAMMING CASE:**

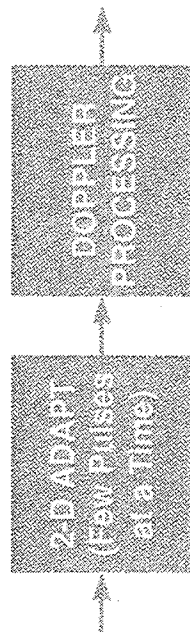
- CNR ~ 22-37 dB
- JNR ~ 60 dB

- **PROCESSING GAINS:**

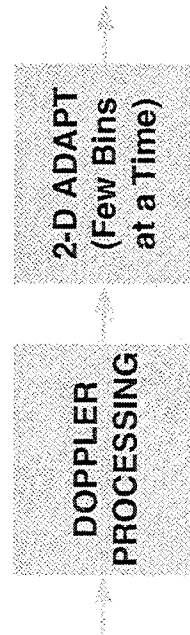
- ARRAY GAIN ADDS 11 dB TO JNR, CNR (14 ELEMENTS)
- COHERENT PROCESSING (DFT) GAIN ADDS 12 dB TO CNR (16 PULSES)

REDUCED DIMENSION STAP ARCHITECTURES

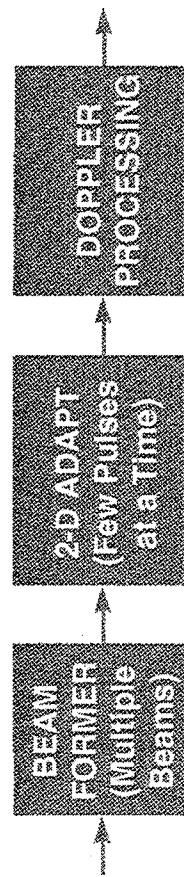
PRE-DOPPLER



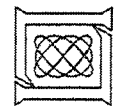
POST-DOPPLER



BEAMSPACE PRE-DOPPLER

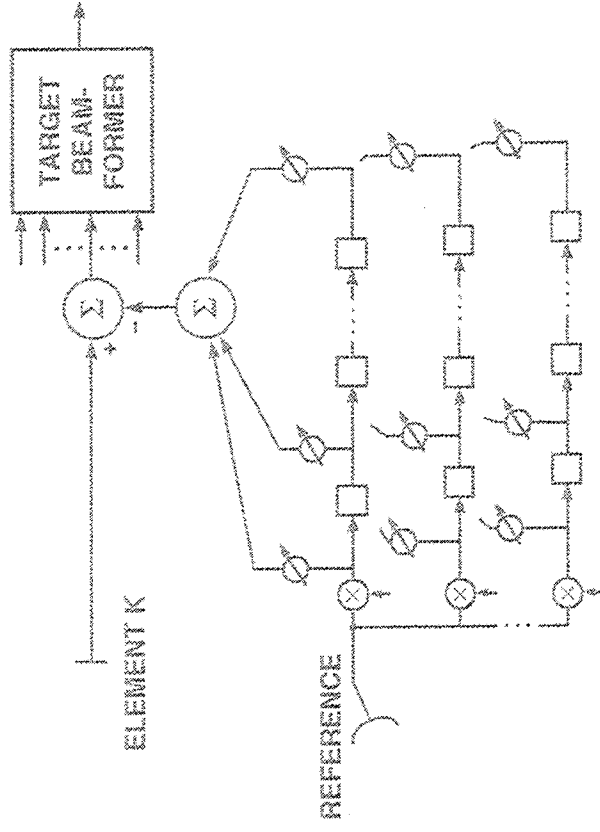


BEAMSPACE POST-DOPPLER



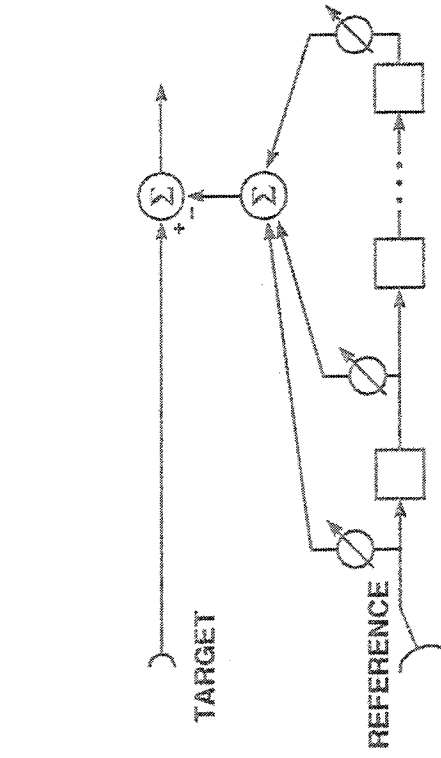
273541-3B

MULTIPATH JAMMING MITIGATION ARCHITECTURES

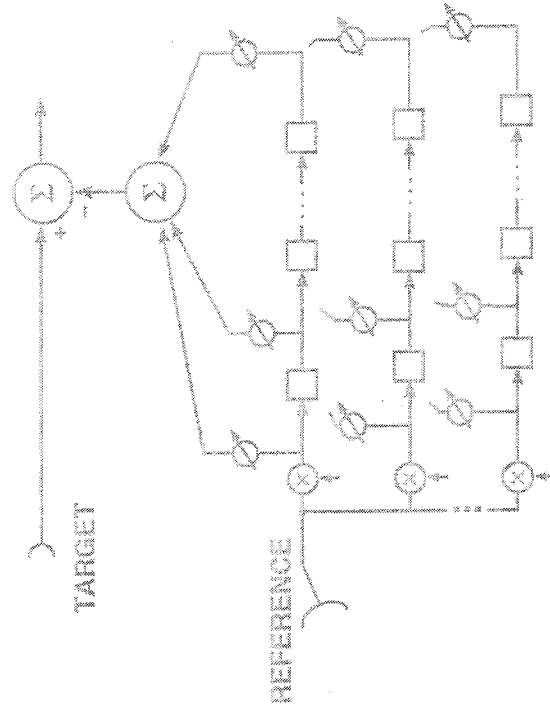


MITIGATE ON EACH ARRAY ELEMENT

WITH DOPPLER-SPACE WEIGHTS



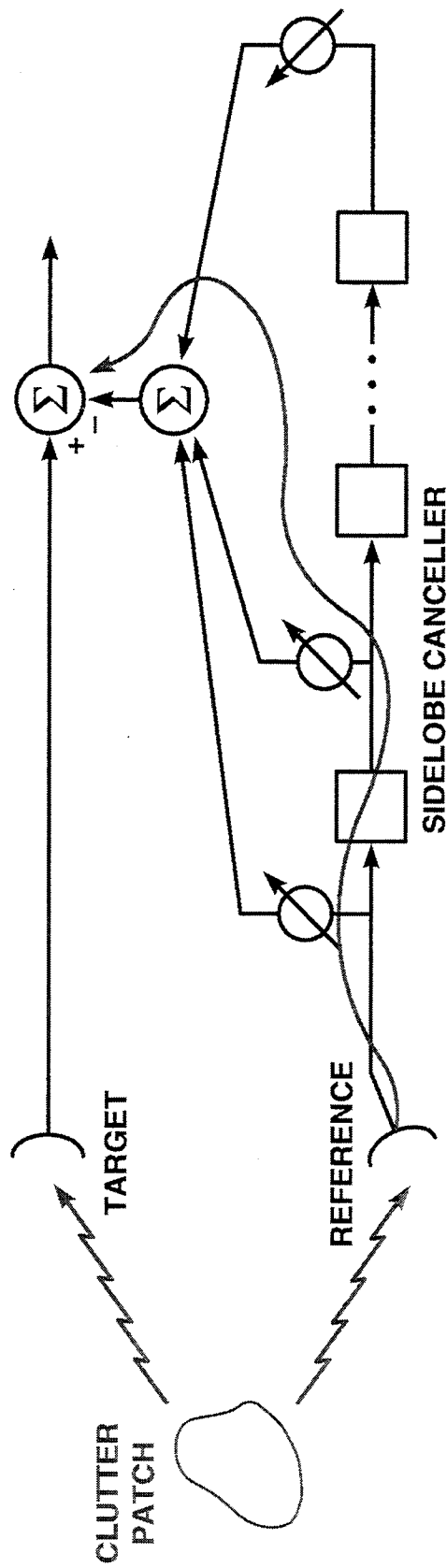
MITIGATE ON PRE-FORMED BEAM



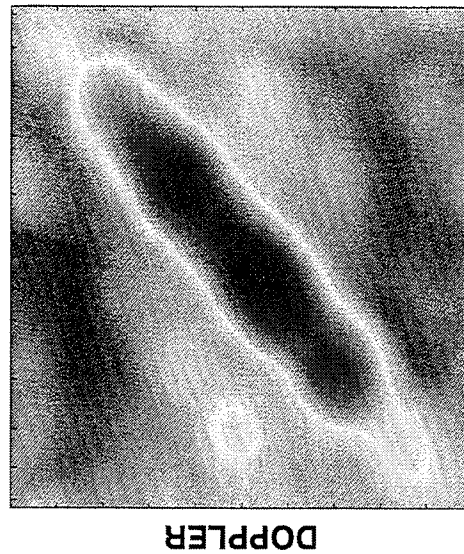
WITH DOPPLER-SPACE WEIGHTS



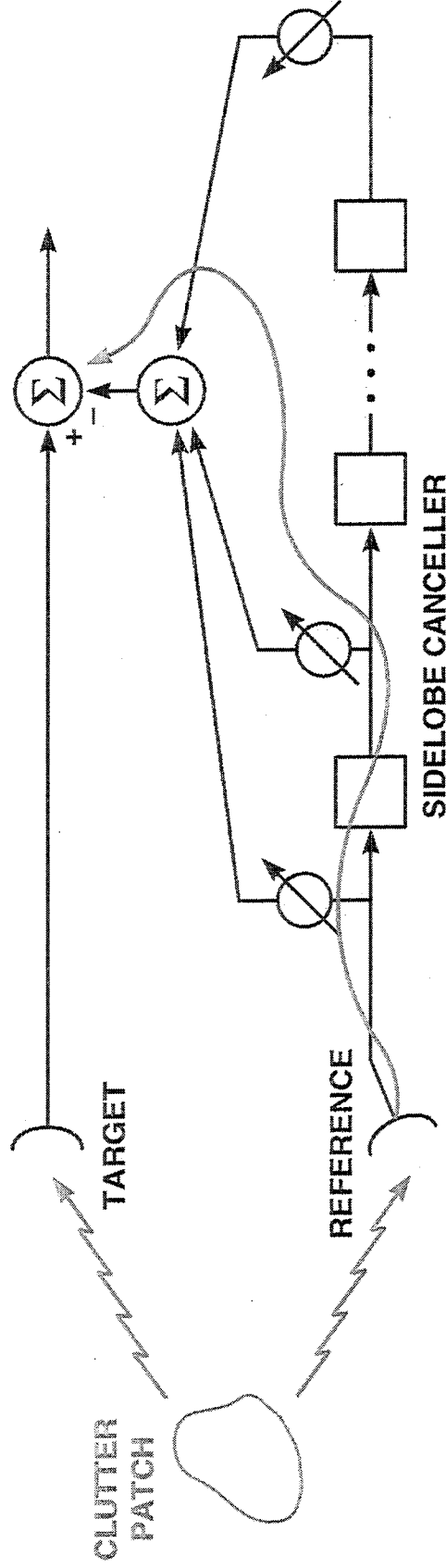
POTENTIAL EFFECT OF MULTIPATH MITIGATION ON CLUTTER



- CLUTTER THROUGH SIDELOBE CANCELLER PATH DIFFERENT ON EVERY PULSE
 - BECAUSE WEIGHTS ARE RECOMPUTED EVERY PULSE (Airborne Jamming Case)
 - MAY SEE SMEARING OF CLUTTER IN DOPPLER
 - WOULD OBSCURE TARGETS NEAR CLUTTER
 - WOULD REQUIRE MORE NULLING DEGREES OF FREEDOM



POTENTIAL EFFECT OF MULTIPATH MITIGATION ON CLUTTER (2)



$$|WEIGHTS| \propto \frac{P_{J, MULTIPATH}}{P_{J, REFERENCE}} = P \text{ (Small if Clean Reference)}$$

$CNR \cdot SLL_{REF} \cdot P < 1 \rightarrow \text{MINIMAL CLUTTER SMEARING}$

MOUNTAINTOP DATA : $CNR \sim 60 \text{ dB}$ (Moderate Clutter)

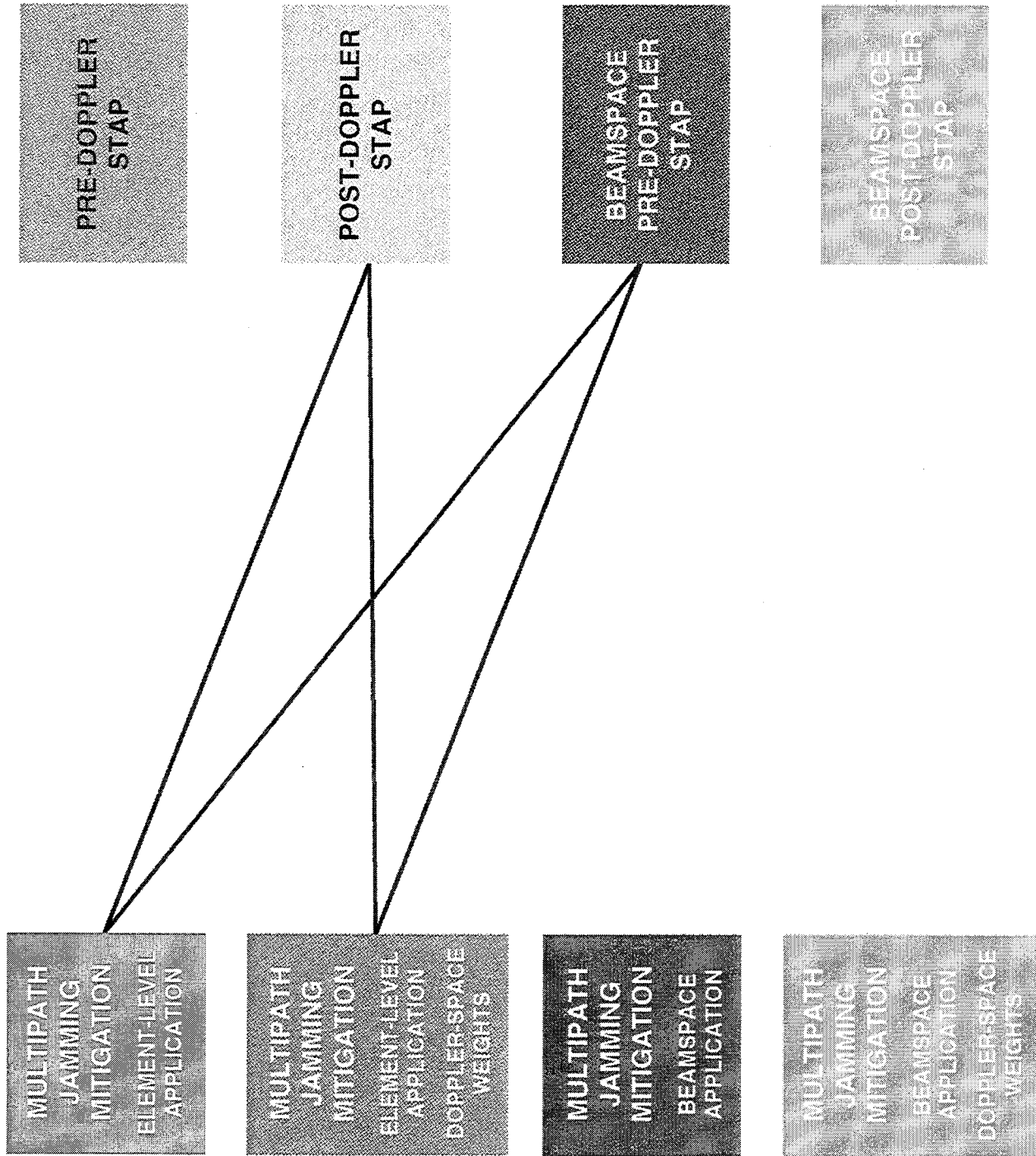
$$SLL_{REF} = -30 \text{ dB}$$

$$P \sim -50 \text{ dB (Clean Reference)}$$

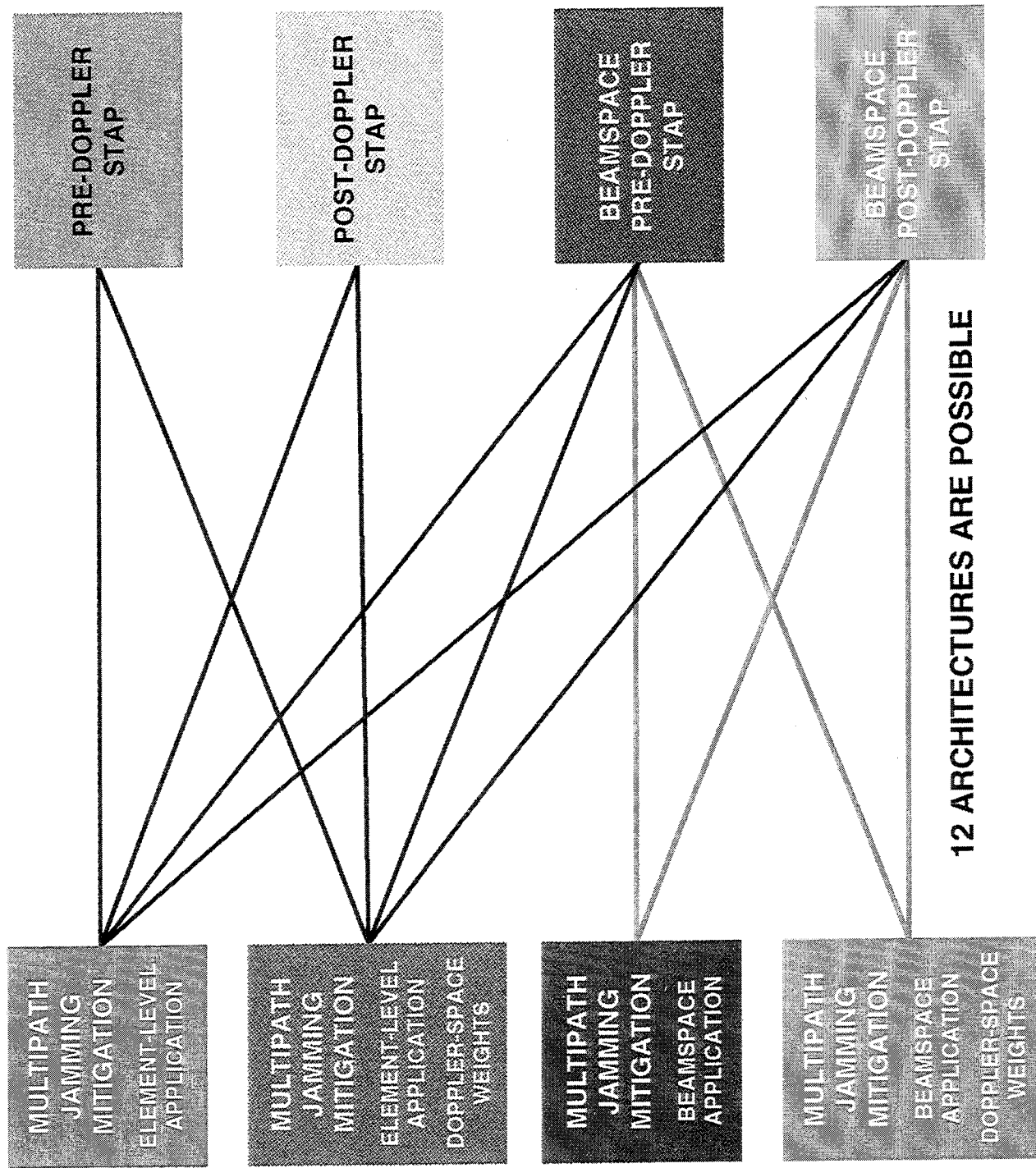
$$\underline{-20 \text{ dB} < 1}$$

$\therefore \text{MINIMAL CLUTTER SMEARING EXPECTED HERE}$

SIMULTANEOUS MITIGATION ARCHITECTURES



SIMULTANEOUS MITIGATION ARCHITECTURES



CONCLUSIONS AND FUTURE WORK

- **INITIAL RESULTS ARE PROMISING**
 - **DEMONSTRATED MITIGATION OF COMBINED MULTIPATH JAMMING AND GROUND CLUTTER**
 - **RESIDUAL INTERFERENCE COMPARABLE TO MULTIPATH-ONLY CASE**
- **CLEAN JAMMING REFERENCE, MODERATE CLUTTER CASE:**
 - **DOPPLER-SPACE WEIGHTS PROVIDE SOME IMPROVEMENT**
 - **DIFFERENT STAP ALGORITHMS PERFORM SIMILARLY**
- **FUTURE WORK**
 - **TRY OTHER CASCADE, MORE GENERAL ARCHITECTURES**
 - **WIDER VARIETY OF DATA SCENARIOS**
 - **STUDY CLUTTER SMEARING PHENOMENOLOGY**
 - **ALTERNATE PERFORMANCE METRICS**

HOT CLUTTER CANCELLATION WITH ORTHOGONAL BEAMSPACE TRANSFORMS

Stephen M. Kogon, Douglas B. Williams, and E. Jeff Holder

Georgia Institute of Technology
777 Atlantic Drive
Digital Signal Processing Laboratory
Atlanta, GA 30332-0250
tel: (404) 854-9832
fax: (404) 894-8363
email: kogon@ee.gatech.edu
email: dbw@eedsp.gatech.edu

Abstract Hot clutter refers to terrain-reflected jammer interference that is incident on the radar array from many azimuth angles and, therefore, distributed throughout the mainbeam. Cancellation methods seek to use interference energy present in other portions of the angular spectrum to remove the mainbeam interference. The conventional adaptive canceller makes use of a single reference beam with sufficient temporal taps to cover the range extent of the hot clutter signal, typically quite large. In this case, all the degrees of freedom have been devoted to temporal adaptivity. However, the hot clutter energy is not limited to the mainbeam and is usually found throughout the angular spectrum. Independent temporally delayed replicas of the interference are present at many different azimuth angles. We propose a hot clutter cancellation method, implemented using a generalized sidelobe canceller structure, that makes use of the entire angular spectrum through an orthogonal beamspace transformation. The temporal window of the resulting canceller is greatly reduced, far below the range extent of the hot clutter, thereby trading off spatial for temporal degrees of freedom. The performance of the full beamspace hot clutter canceller is demonstrated on data collected in the Mountaintop experiment where it is shown to achieve superior performance relative to the single auxiliary beam canceller for the same number of degrees of freedom. Alternatively, cancellation to an acceptable interference level is achieved with a reduction in total degrees of freedom by using all of the spatial information available.

ASAP WORKSHOP 1996

HOT CLUTTER CANCELLATION WITH ORTHOGONAL BEAMSPACE TRANSFORMS

**STEPHEN M. KOGON^{1,2}, DOUGLAS B. WILLIAMS¹,
and E. JEFF HOLDER²**

¹ Digital Signal Processing Laboratory
School of ECE
Georgia Institute of Technology

² Georgia Tech Research Institute
Georgia Institute of Technology

SUPPORT: Air Force Rome Laboratory under the ARPA Mountaintop Program

OUTLINE

- **INTRODUCTION**

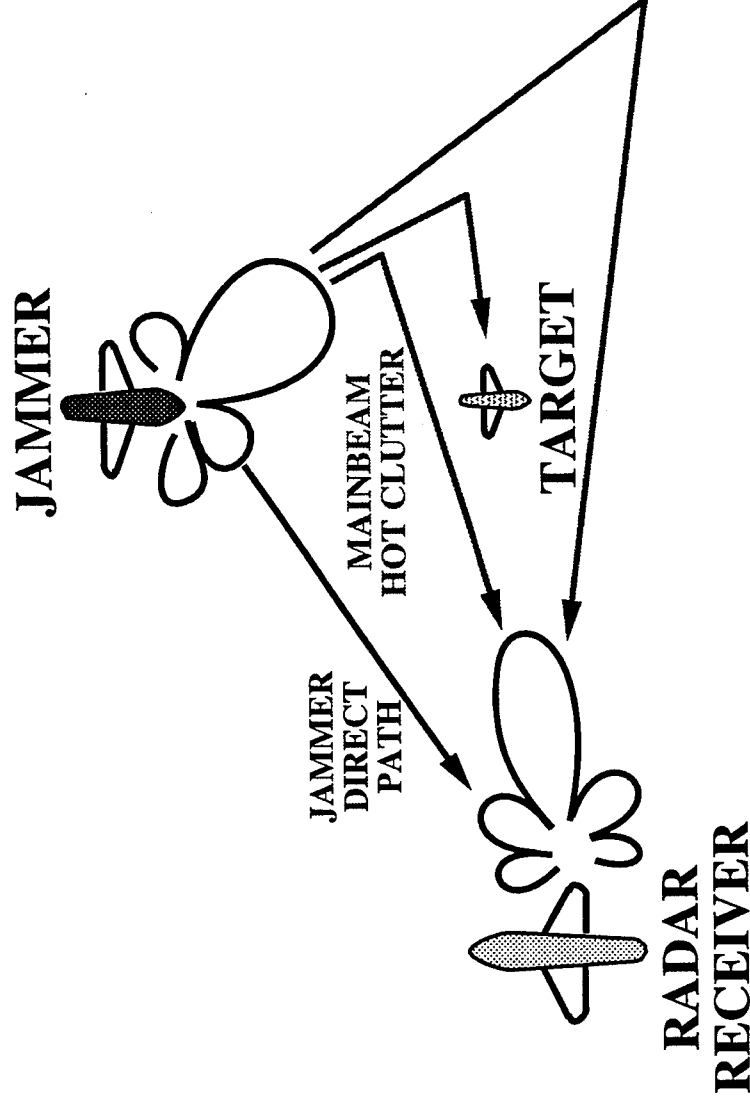
- **HOT CLUTTER DESCRIPTION**
- **SINGLE-BEAM CANCELLER**

- **BEAMSPACE HOT CLUTTER CANCELLER (HCC)**

- **MOUNTAINTOP DATA EXPERIMENTS**

- **GROUND-BASED JAMMER**
- **AIRBORNE JAMMER**
- **TARGET EXTRACTION**

HOT CLUTTER SCENARIO



- MAINBEAM INTERFERENCE (SPATIALLY CORRELATED)
- ALSO KNOWN AS TERRAIN SCATTERED INTERFERENCE (TSI) OR JAMMER MULTIPATH

HOT CLUTTER MITIGATION

HOT CLUTTER CHARACTERISTICS:

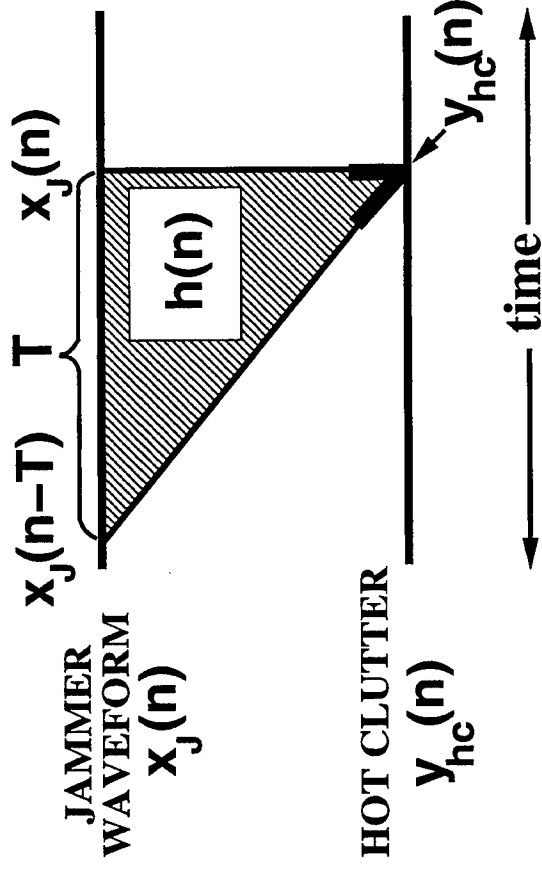
- LARGE RANGE OR TEMPORAL EXTENT
- WIDE ANGULAR AND DOPPLER SPREAD
- HIGHLY DEPENDENT ON:
 - JAMMER INTENSITY AND TRANSMITTER RESPONSE
 - TERRAIN TYPE/CHARACTERISTICS
 - GEOMETRY OF THE SCENARIO, i.e. JAMMER LINE-OF-SIGHT, GRAZING ANGLES

⇒ DATA-ADAPTIVE CANCELLATION

OBJECTIVE:

- FIND COST-EFFECTIVE MITIGATION TECHNIQUES

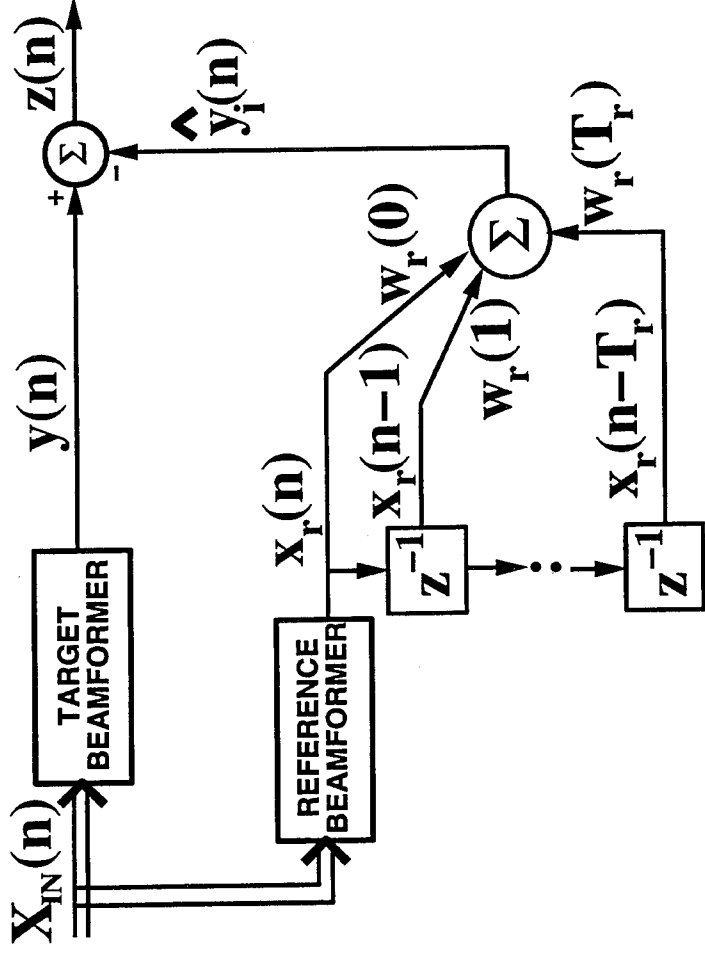
HOT CLUTTER TIMELINE



$$y_{hc}(n) = \sum_{k=0}^T h(k) x_j(n-k) \quad h(n) \text{ is unknown}$$

- EACH HOT CLUTTER SAMPLE IS PRODUCED BY AN INTERVAL ON THE JAMMER WAVEFORM
- EFFECTIVE CANCELLATION ACHIEVED IF:
 - TEMPORAL WINDOW OF CANCELLER EXCEEDS TEMPORAL EXTENT OF HOT CLUTTER
 - SAMPLING FREQUENCY > JAMMER BANDWIDTH

SINGLE-BEAM CANCELLER

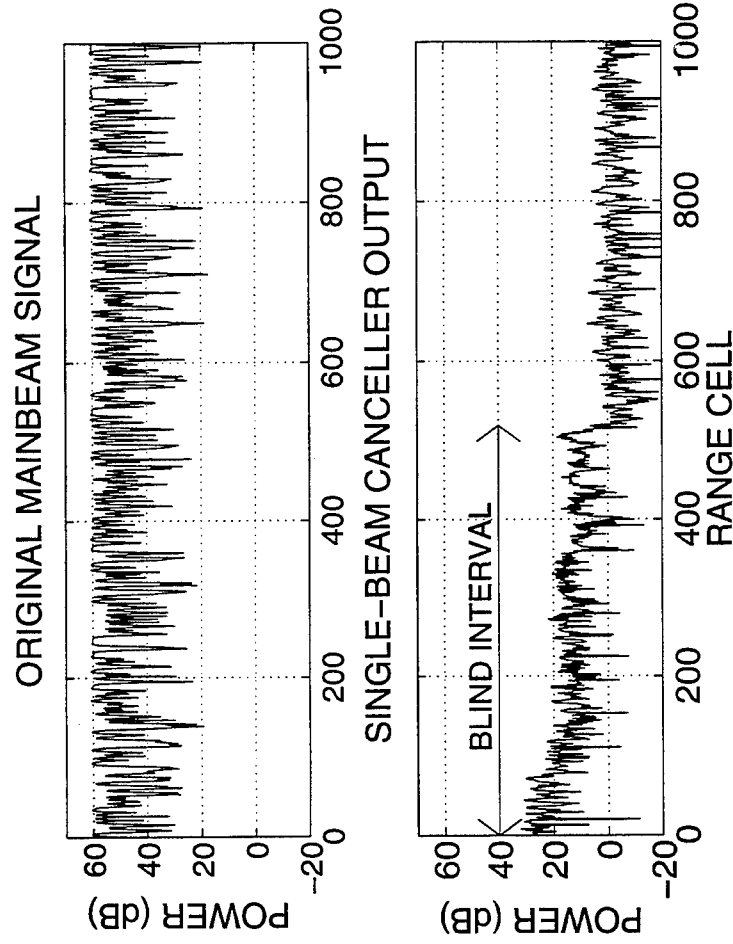


$$\mathbf{w}_r = \mathbf{R}_x^{-1} \mathbf{r}_{xy} \qquad \hat{y}_i(n) = \sum_{k=0}^{T_r} \mathbf{w}_r(k) \mathbf{x}_r(n-k)$$

- REFERENCE BEAMFORMER FOR THE JAMMER DIRECT-PATH SIGNAL
- T_r IS THE TEMPORAL EXTENT OF THE CANCELLER
- EFFECTIVE CANCELLATION IF $T_r > T$ (TYPICALLY VERY LARGE)

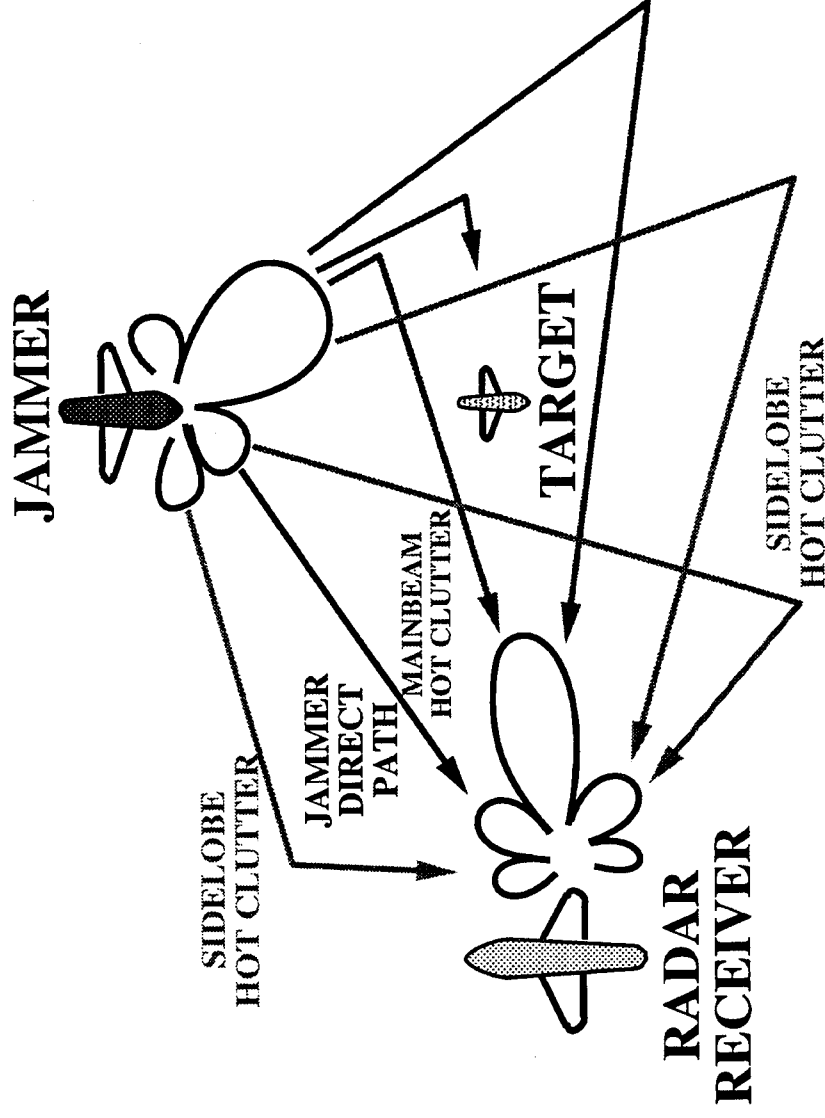
COMMENTS ON SINGLE-BEAM CANCELLER

- DIRECT LINE-OF-SIGHT TO THE JAMMER IS NOT ALWAYS AVAILABLE
- BLIND INTERVAL PROBLEMS DUE TO LARGE TEMPORAL WINDOW



⇒ FULL CANCELLATION CANNOT OCCUR UNTIL THERE IS ENOUGH DATA TO FILL THE TEMPORAL WINDOW

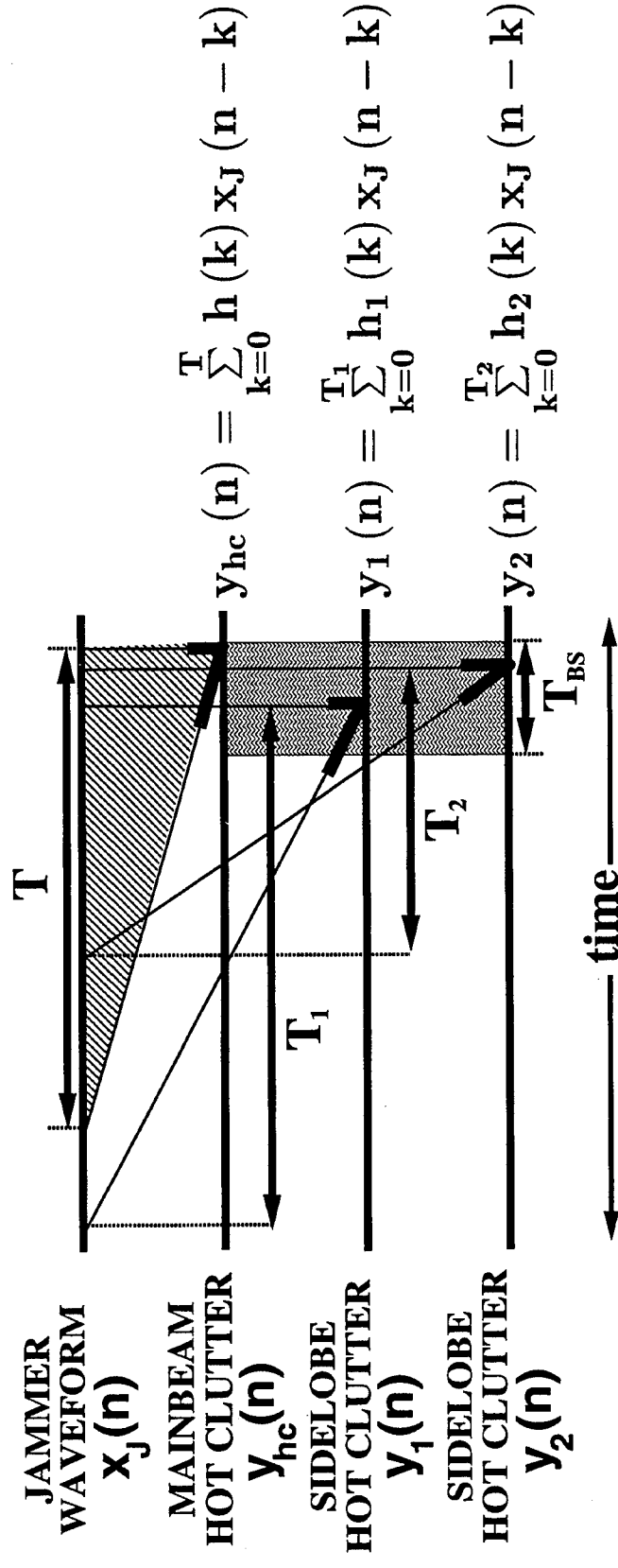
SIDELOBE HOT CLUTTER



- HOT CLUTTER IS ALSO FOUND IN THE SIDELOBES

⇒ EXPLOIT SPATIAL INFORMATION TO IMPROVE CANCELLATION

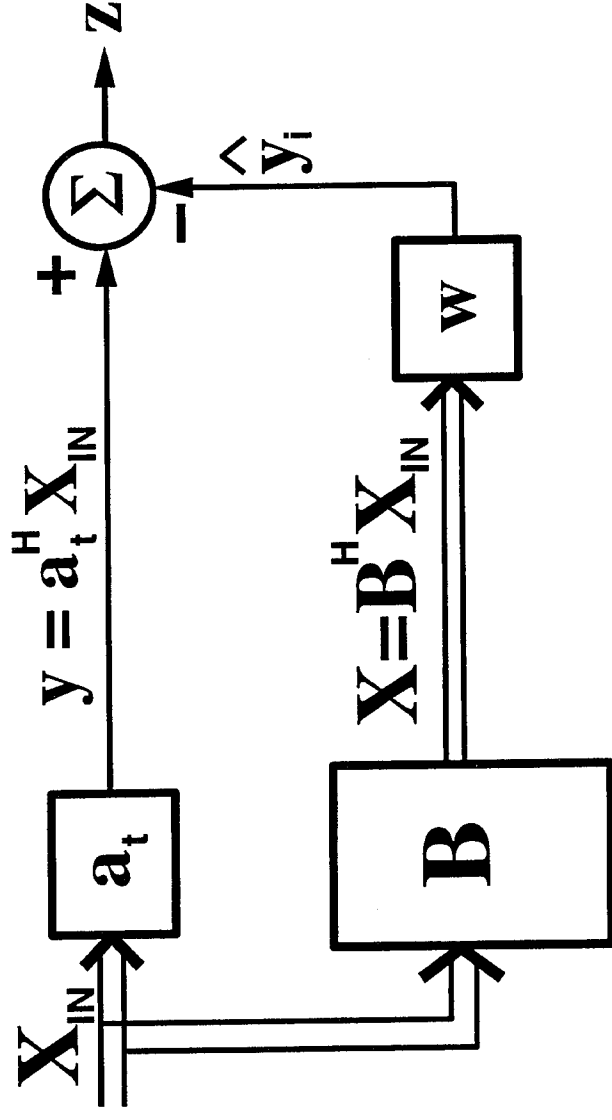
SPATIAL VS. TEMPORAL INFORMATION



- SIDELOBE HOT CLUTTER SIGNALS ARE GENERATED BY SIMILAR INTERVALS ON THE JAMMER WAVEFORM
- SPATIAL DEGREES OF FREEDOM REPRESENT TEMPORAL INFORMATION

⇒ USE SIDELOBE HOT CLUTTER TO REDUCE THE SIZE OF THE TEMPORAL WINDOW FROM T TO T_{BS}

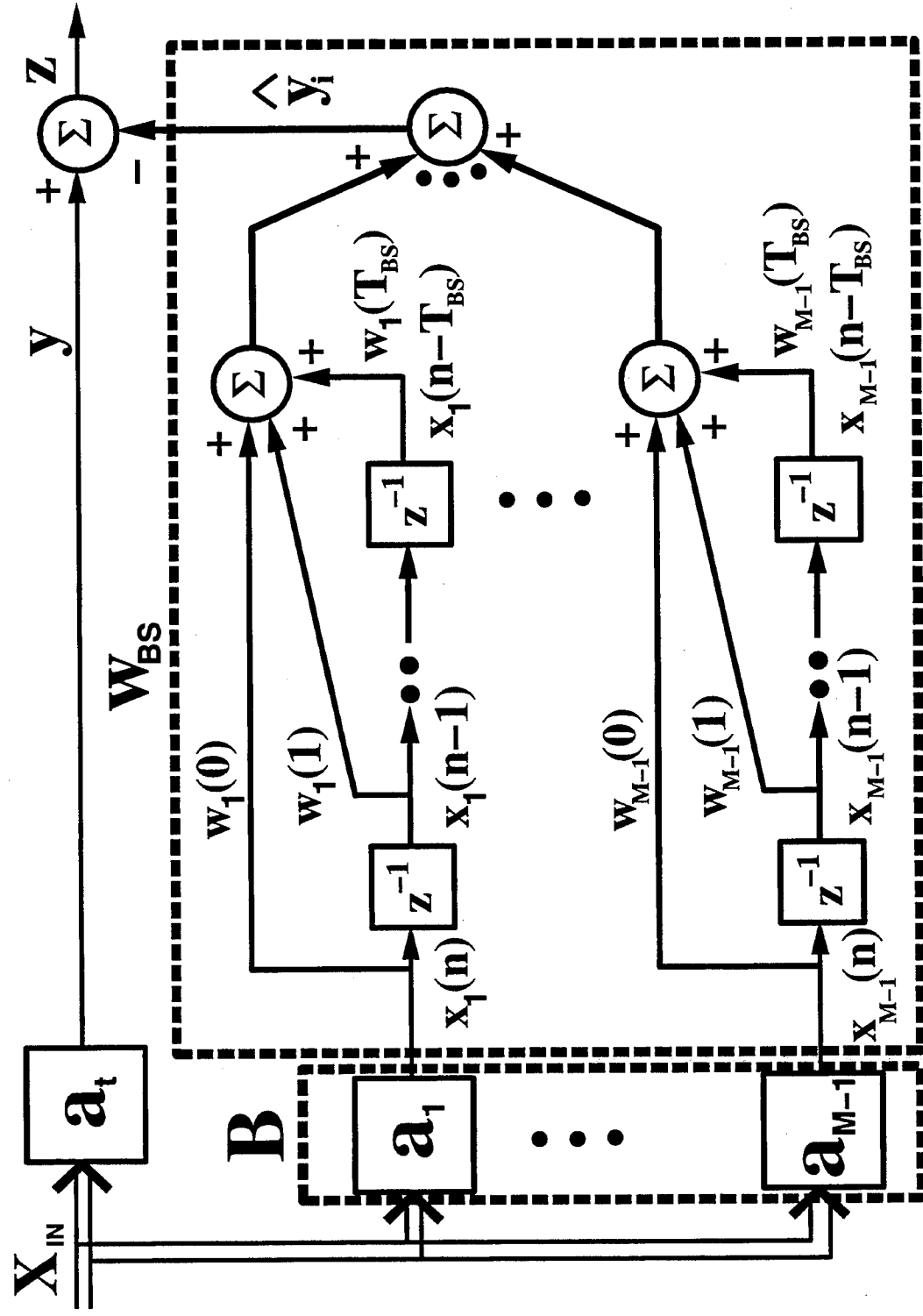
GENERALIZED SIDELOBE CANCELLER



$$w = R_X^{-1} r_{Xy}$$

- a_t IS A PHASE-CENTERED STEERING VECTOR
- BLOCKING MATRIX B IS ORTHOGONAL TO a_t TO PREVENT SIGNAL CANCELLATION (i.e. $B^H \cdot a_t = 0$)

BEAMSPACE HOT CLUTTER CANCELLER



BEAMSPACE HCC (cont.)

- \mathbf{a}_t IS A CONVENTIONAL PHASE-CENTERED STEERING VECTOR AT THE SPATIAL FREQUENCY \mathbf{u}_t OF THE TARGET
- \mathbf{B} IS THE BLOCKING MATRIX WHOSE COLUMNS ARE STEERING VECTORS AT SPATIAL FREQUENCIES REMOVED FROM THE TARGET SPATIAL FREQUENCY BY MULTIPLES OF $\frac{1}{M}$

$$\mathbf{u}_m = \mathbf{u}_t + \frac{1}{M}, \dots, \mathbf{u}_t + \frac{m}{M}, \dots, \mathbf{u}_t + \frac{M-1}{M}$$

$$\mathbf{B} = [\mathbf{a}(\mathbf{u}_1) \cdots \mathbf{a}(\mathbf{u}_m) \cdots \mathbf{a}(\mathbf{u}_{M-1})]$$

- THE BLOCKING MATRIX ENSURES NO TARGET SIGNAL CANCELLATION CAN OCCUR

BEAMSPACE HCC (cont.)

- FORM THE OVERALL DATA VECTOR BY STACKING DELAYED VERSIONS OF THE SIGNALS FROM THE INDIVIDUAL BEAMS

$$\mathbf{X}_m = \begin{bmatrix} x_m(n) \\ x_m(n-1) \\ \vdots \\ x_m(n - T_{bs} + 1) \end{bmatrix}, \mathbf{X} = \begin{bmatrix} \mathbf{X}_1 \\ \mathbf{X}_2 \\ \vdots \\ \mathbf{X}_{M-1} \end{bmatrix}$$

- COMPUTE THE MMSE FILTER (WEIGHTS FOR INDIVIDUAL BEAMS ARE STACKED)

$$\mathbf{w}_{bs} = \mathbf{R}_X^{-1} \mathbf{r}_{Xy}$$

$$\text{WHERE } \mathbf{R}_X = \mathbf{E} \{ \mathbf{X} \mathbf{X}^H \} \text{ AND } \mathbf{r}_{Xy} = \mathbf{E} \{ \mathbf{X} \cdot y^H \}$$

- IMPLEMENTATION FOR FINITE SAMPLE SIZE WITH SAMPLE MATRIX INVERSION (SMI) METHOD

COMMENTS ON BEAMSPACE HCC

- EQUIVALENT TO CONSTRAINED ELEMENT-SPACE PROCESSING SINCE ORTHOGONAL STEERING VECTORS IN THE BLOCKING MATRIX AND THE MAINBEAM MAKE UP A UNITARY TRANSFORM

ADVANTAGES:

- ALLOWS FOR IMPLEMENTATION WITH A FROST CONSTRAINED BEAMFORMER IN A GSC STRUCTURE (i.e. UNCONSTRAINED OPTIMIZATION IN THE LOWER BRANCH)
- HAS A MORE APPEALING INTERPRETATION AS THE PREDICTION OF THE MAINBEAM INTERFERENCE FROM SIDELOBE HOT CLUTTER SIGNALS

CANCELLATION EXPERIMENTS

- COMPARE THE PERFORMANCE OF THE SINGLE-BEAM CANCELLER AND THE BEAMSPACE HCC
- MAINBEAM AT AZIMUTH ANGLE $\phi = 0^\circ$
- VARY THE DEGREES OF FREEDOM (DOF) FOR THE TWO CANCELLERS FROM 65 TO 520
- TEMPORAL WINDOW OF SINGLE-BEAM CANCELLER,

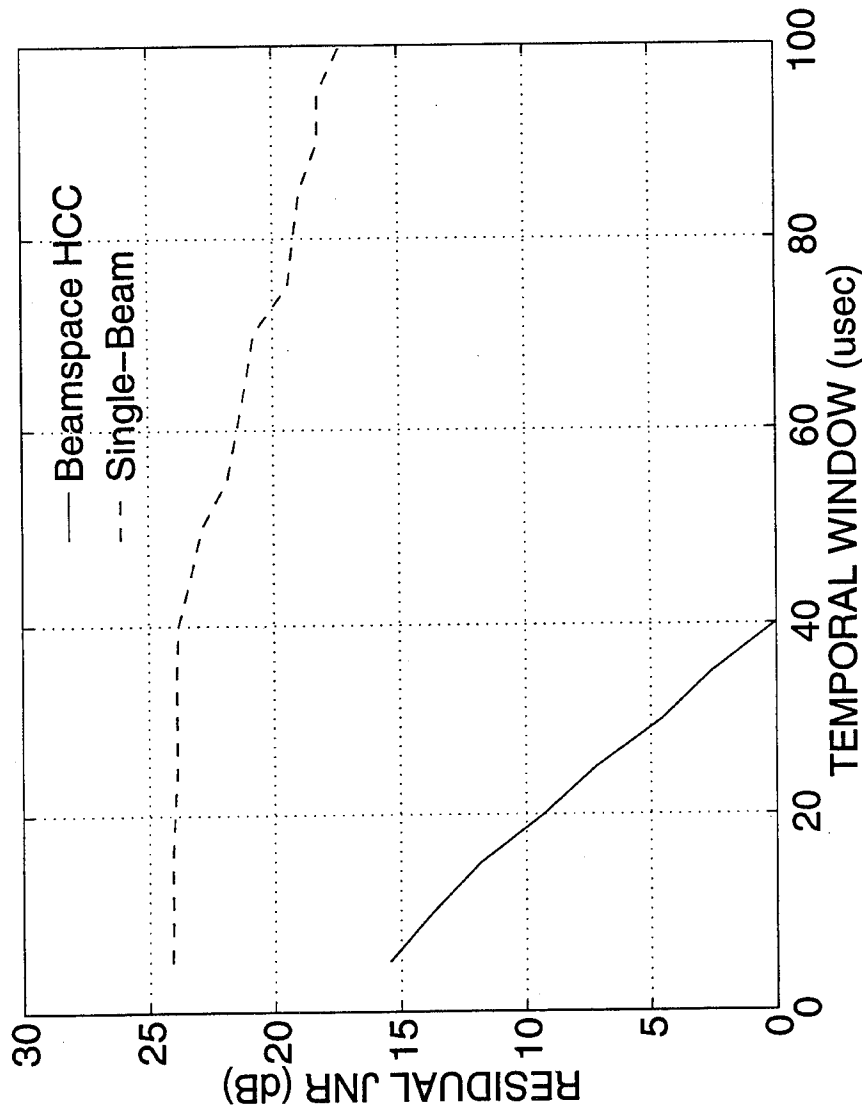
$$T_r = \text{DOF}$$

- TEMPORAL WINDOW OF BEAMSPACE HCC,

$$T_{BS} = \text{DOF}/13$$

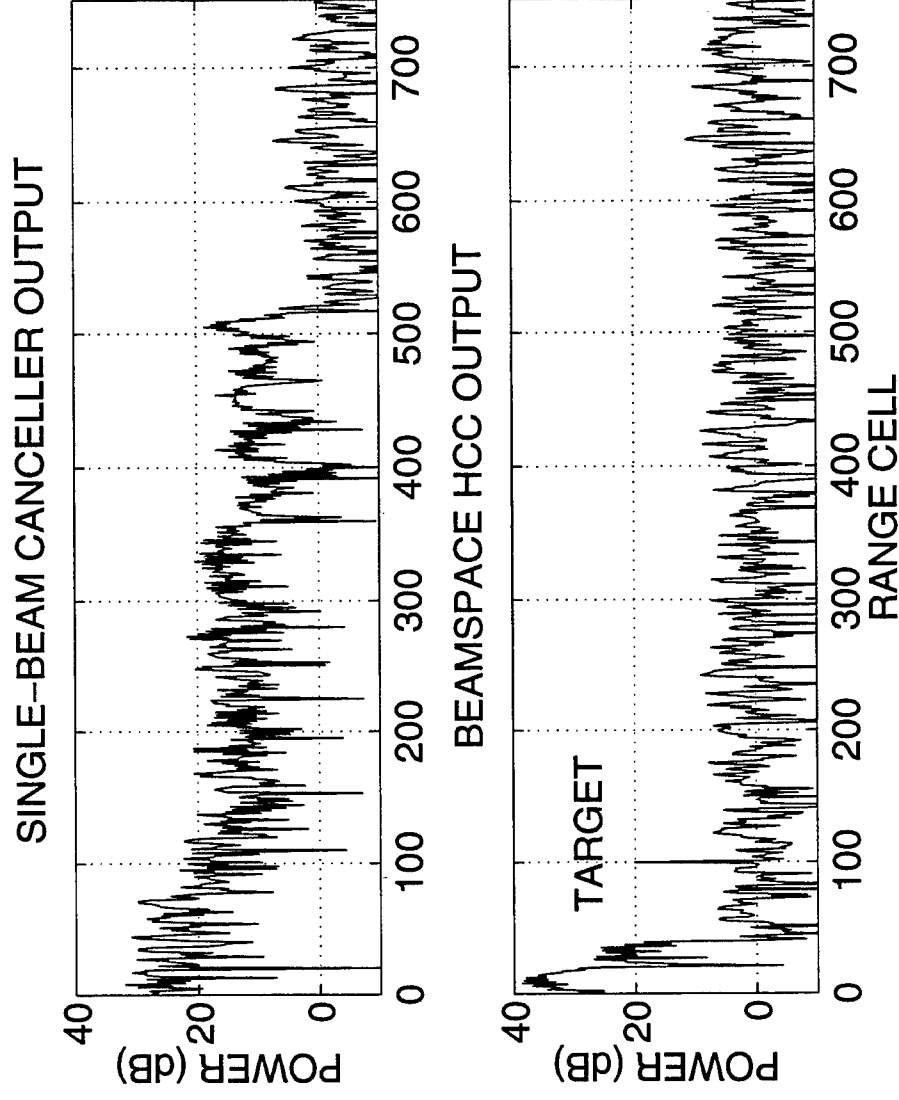
- BOTH METHODS IMPLEMENTED USING SMI TECHNIQUE

CANCELLATION VS. TEMPORAL WINDOW



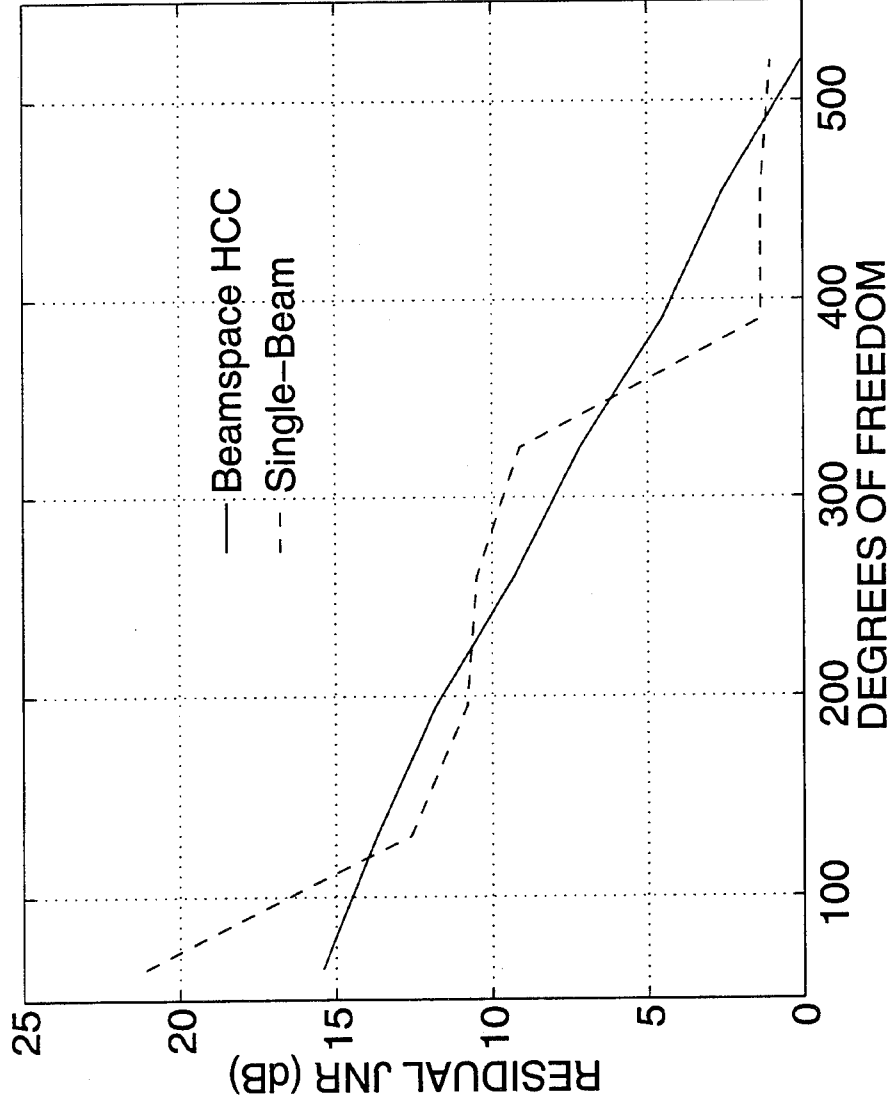
- **GROUND-BASED TSI-PRODUCING JAMMER (FILE = mmitt004v1.mat)**
- **REFERENCE BEAM AT $\phi = 303^\circ$ (BROADSIDE IS $\phi = 270^\circ$)**

BLIND INTERVAL RESULTS



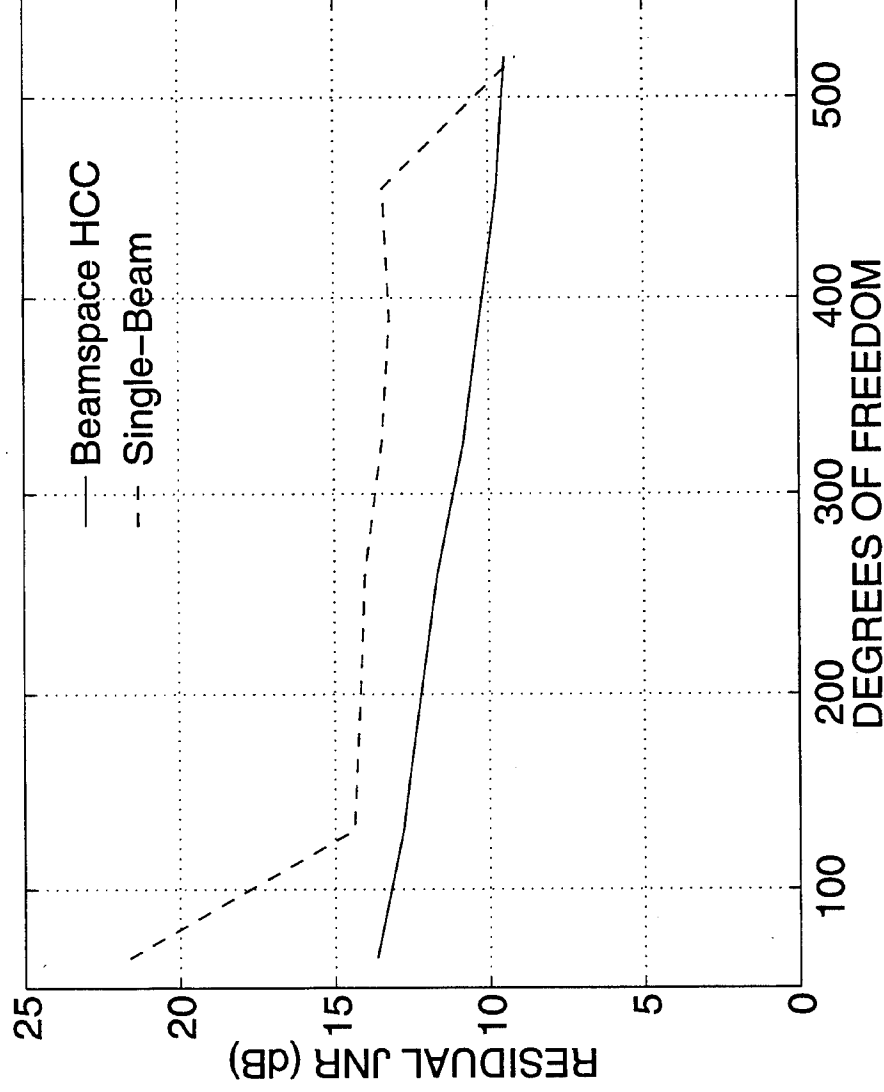
- TARGET INJECTED AT $\phi = 0^\circ$ WITH SNR = 20 dB IN RANGE BIN 100
(FILE = mmitt004v1.mat)
- SAME DEGREES OF FREEDOM FOR BOTH CANCELLERS

GROUND-BASED JAMMER



- GROUND-BASED TSI-PRODUCING JAMMER (FILE = mm1t004v1.mat)
- REFERENCE BEAM AT $\phi = 303^\circ$ (BROADSIDE IS $\phi = 270^\circ$)

GROUND-BASED JAMMER

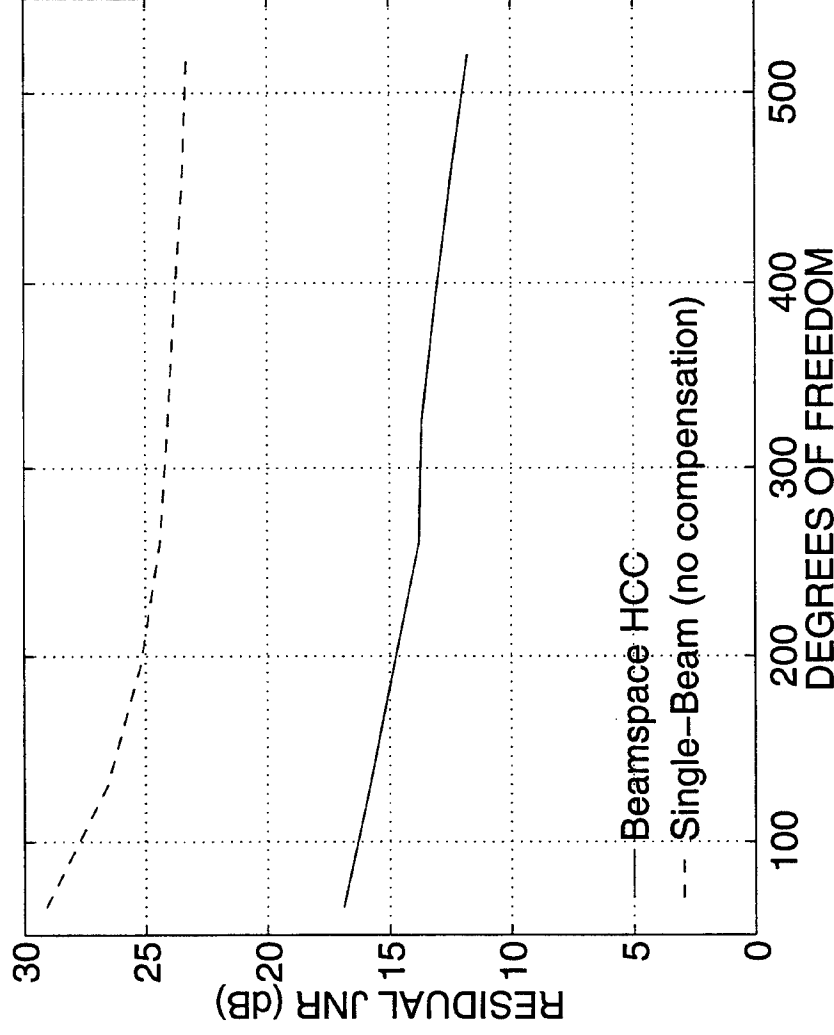


- GROUND-BASED TSI-PRODUCING JAMMER (FILE = mmitt013v1.mat)
- REFERENCE BEAM AT $\phi = 303^\circ$ (BROADSIDE IS $\phi = 230^\circ$)

AIRBORNE TSI JAMMER MITIGATION

- AIRCRAFT MOTION CAUSES DOPPLER SHIFT ON TSI RETURNS.
- DOPPLER COMPENSATION REQUIRED IN ORDER TO ADJUST FOR THE MULTIPATH PHASE SHIFT
- IMPLEMENTED IN SINGLE-BEAM CANCELLER WITH DOPPLER COMPENSATION CHANNELS
 - EACH TSI PATH REQUIRES DOPPLER COMPENSATION RESULTING IN NUMEROUS DOPPLER COMPENSATION CHANNELS
 - DRASTIC INCREASE IN REQUIRED DEGREES OF FREEDOM AND THEREFORE THE COMPUTATIONAL COMPLEXITY REQUIRED FOR CANCELLATION

AIRBORNE TSI JAMMER



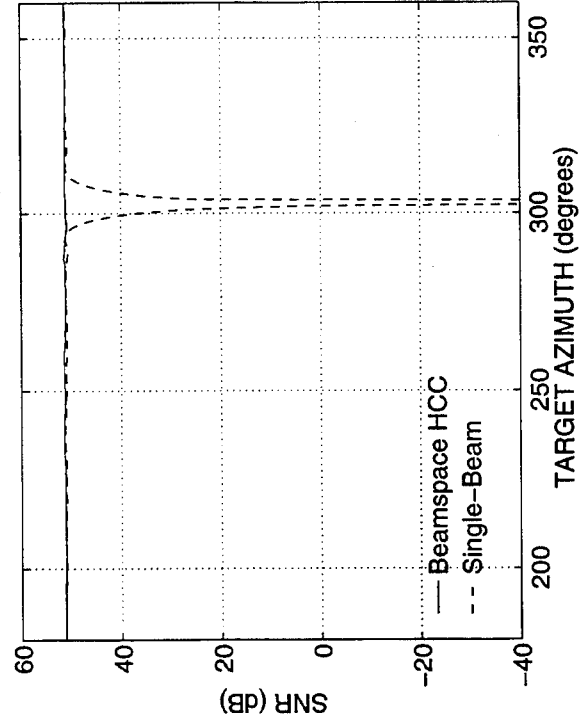
- AIRBORNE TSI-PRODUCING JAMMER (FILE = rio043v1.mat)
- REFERENCE BEAM AT $\phi = 291.9^\circ$ (BROADSIDE IS $\phi = 270^\circ$)
- MULTIPLE BEAMS ALLOW FOR DOPPLER COMPENSATION

TARGET INJECTION EXPERIMENT

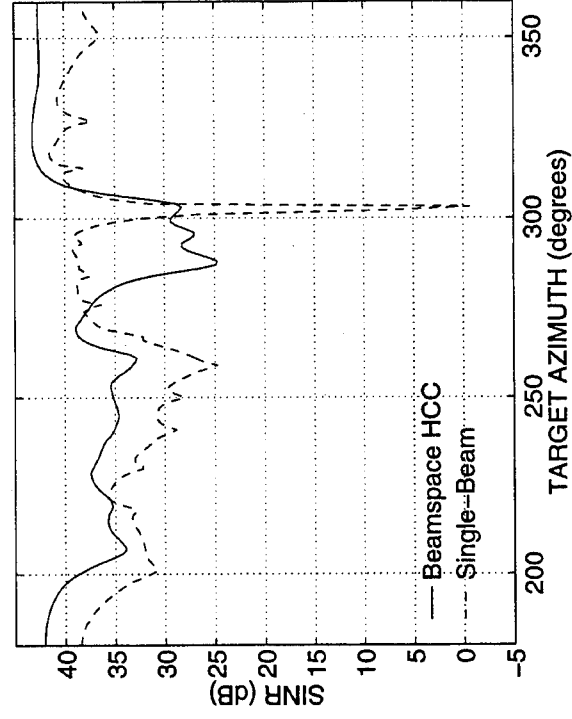
- TSI CANCELLATION SHOULD NOT BE THE ONLY PERFORMANCE CRITERION
 - ⇒ LOOK AT SIGNAL CANCELLATION
- mmitt004v1.mat DATA FILE USED
- TARGET INJECTED WITH SNR = 50 dB IN RANGE CELL 1000
- SWEEP TARGET ACROSS AZIMUTH ($180 < \phi < 360$)
- DEGREES OF FREEDOM = 260
 - 20 TEMPORAL TAPS ON BEAMSPACE HCC
 - 260 TEMPORAL TAPS ON SINGLE-BEAM CANCELLER

TARGET EXTRACTION RESULTS

SNR vs. TARGET AZIMUTH



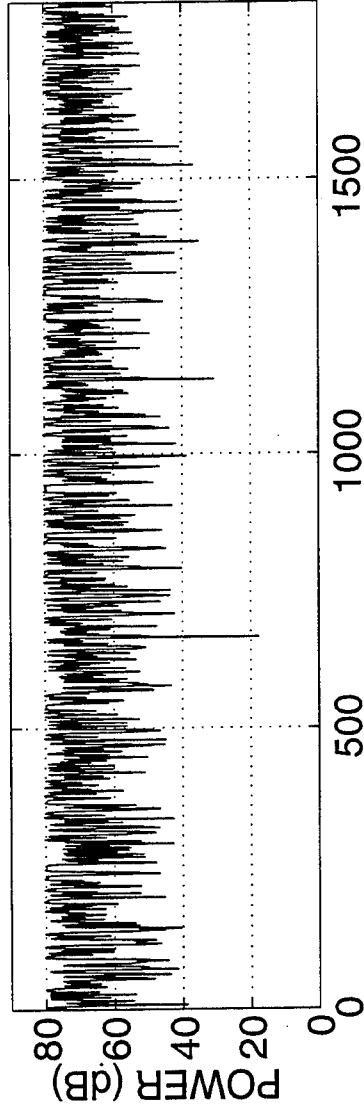
SINR vs. TARGET AZIMUTH



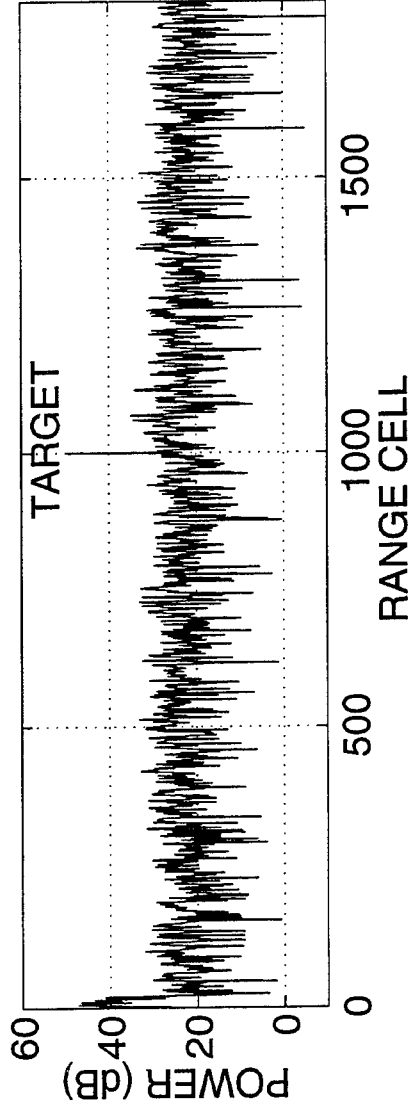
- ASSUME KNOWLEDGE OF TARGET AZIMUTH
- JAMMER LOCATED AT = 303°

MAINBEAM JAMMER RESULT

ORIGINAL MAINBEAM SIGNAL



BEAMSPACE HCC OUTPUT



- TARGET AND JAMMER ARE CO-LOCATED AT 303°
- NO SIGNAL CANCELLATION WITH SUFFICIENT JAMMER SUPPRESSION TO EXTRACT TARGET

CONCLUSIONS

- DEMONSTRATED EFFECTIVE HOT CLUTTER MITIGATION WITH BEAMSPACE HCC
- SIMILAR PERFORMANCE TO THE SINGLE-BEAM CANCELLER FOR A GROUND-BASED JAMMER WITH A DRASTIC REDUCTION IN THE BLIND INTERVAL
- IMPROVES DETECTION PERFORMANCE OF NEAR-FIELD TARGETS
- CANCELLATION OF AIRBORNE JAMMER HOT CLUTTER WITHOUT THE USE OF DOPPLER COMPENSATION CHANNELS
- BEAMSPACE HCC PREVENTS SIGNAL CANCELLATION
- AREAS UNDER INVESTIGATION:
 - WEIGHT-THINNING STRATEGIES FOR DOF REDUCTION
 - BEAMSPACE HCC WITH DOPPLER COMPENSATION

ADAPTIVE HOT CLUTTER MITIGATION USING MULTIPLE LINEAR CONSTRAINTS

Lloyd J. Griffiths

University of Colorado at Boulder
Campus Box 425

College of Engineering and Computer Engineering
Boulder, CO 80309-0425

tel: (303) 492-3511

fax: (303) 492-2758

email: griffith@spot.colorado.edu

Abstract This presentation addresses the application of adaptive array signal processing in airborne radar systems to remove terrain-scattered interference (hot clutter). Hot clutter mitigation in airborne radar systems requires simultaneous adaptation in both space and time. However, unless special care is taken, the time adaptation can adversely affect other radar processing functions such as Doppler extraction. A methodology is described for the design of multiple linear constraints in adaptive radar array processors. The approach presented achieves effective elimination of hot clutter and can be used to either maximize the signal-to-noise ratio of the desired signal or to provide a distortionless time estimate of the signal. Examples are presented using recorded data from the Mountaintop Program to illustrate the effectiveness of the proposed approach and to show comparisons with previous approaches.



ADAPTIVE HOT CLUTTER MITIGATION USING MULTIPLE LINEAR CONSTRAINTS

Lloyd J. Griffiths

University of Colorado

Department of Electrical and Computer Engineering

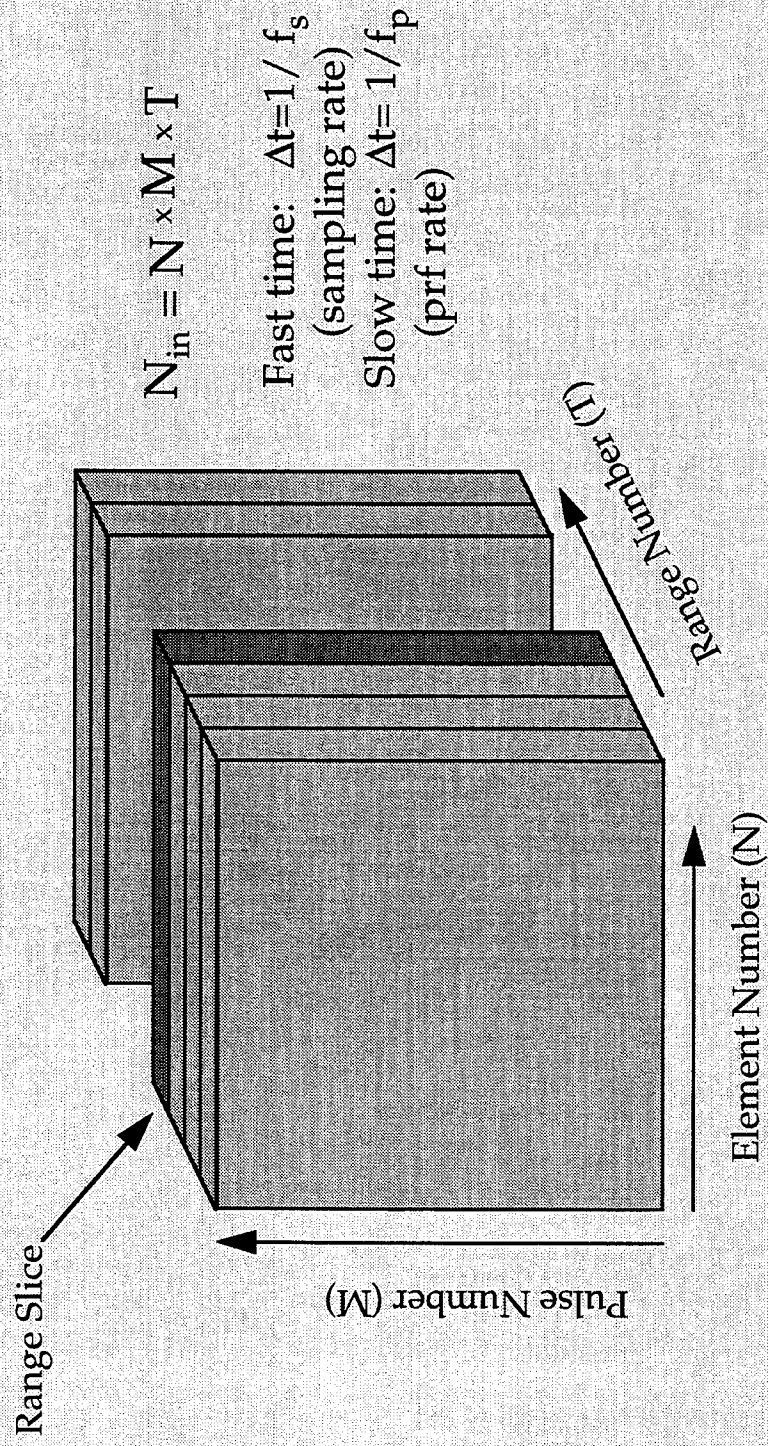
Boulder, CO 80309



SUMMARY

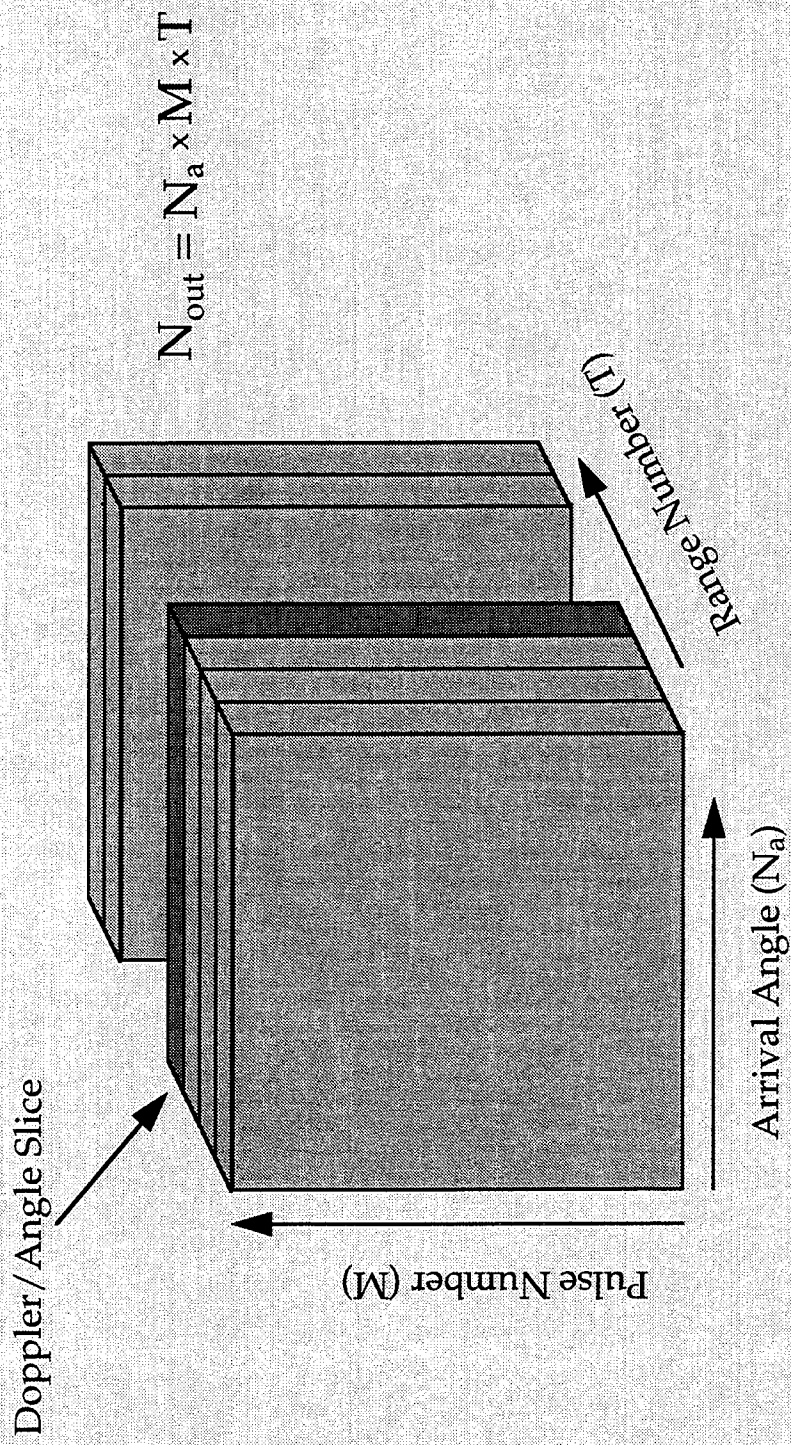
- Data Structures
- STAP Processing Structures
- Maximum Likelihood Processing
- Single-Point Constraint Systems
- Multiple Constraint STAP Structures
- Optimal Detection Structures
- Summary and Conclusions

RADAR INPUT DATA STRUCTURE





RADAR OUTPUT DATA STRUCTURE





STAP PROCESSING

Array snapshot vector (j^{th} pulse): $\mathbf{X}_j(n)$

$$\bar{\mathbf{X}}_j(n) = \begin{bmatrix} X_j(n) \\ X_j(n-1) \\ \vdots \\ X_j(n-L+1) \end{bmatrix} \quad (NL \times 1)$$

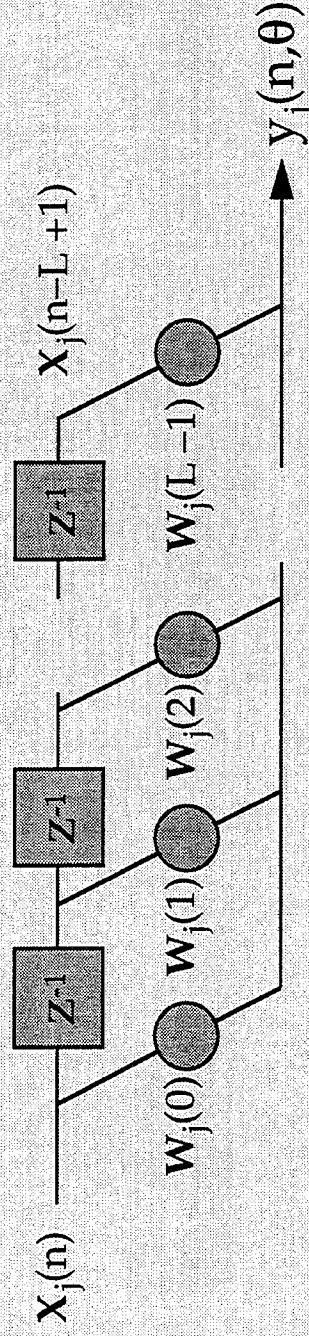
Sample data vector:

$$\bar{\mathbf{W}}_j(\theta) = \begin{bmatrix} W_j(0) \\ W_j(1) \\ \vdots \\ W_j(L-1) \end{bmatrix} \quad (NL \times 1)$$

Weight vector (Steered to θ):

$$\text{Output sample (} n^{\text{th}} \text{ sample):} \quad y_j(n, \theta) = \bar{\mathbf{W}}_j^{\dagger}(\theta) \bar{\mathbf{X}}_j(n)$$

STAP PROCESSING (Cont'd)



Range output for j^{th} pulse at azimuth θ :

$$Y_j(\theta) = \begin{bmatrix} y_j(1, \theta), y_j(2, \theta), \dots, y_j(T, \theta) \end{bmatrix} \quad (1 \times T)$$

$$= \bar{W}_j^+(\theta) \xi_j$$

$$\xi_j = \begin{bmatrix} \bar{X}_{j(1)}, \bar{X}_{j(2)}, \dots, \bar{X}_{j(T)} \end{bmatrix} \quad (NL \times T)$$

352



COVARIANCE STRUCTURE

Data Covariance: $\hat{R}_{\mathbf{xx}} = \frac{1}{T} \boldsymbol{\xi} \boldsymbol{\xi}^+ \quad (\text{NL} \times \text{NL})$

Block Toeplitz: $\hat{R}_{\mathbf{xx}} = \begin{bmatrix} R_0 & R_1 & \cdots & R_{L-1} \\ R_1^+ & R_0 & \cdots & R_{L-1} \\ \vdots & \vdots & \ddots & \vdots \\ R_{L-1}^+ & R_{L-2}^+ & \cdots & R_0 \end{bmatrix} \quad (\text{NL} \times \text{NL})$

$$R_\ell = \frac{1}{(N_2 - N_1)} \sum_{n=N_1}^{N_2} \mathbf{x}_j(n) \mathbf{x}_j^+(n - \ell) \quad (\text{L} \times \text{L})$$



SINGLE LINEAR CONSTRAINT

$$\bar{W}(\theta) = \begin{bmatrix} w(0) \\ w(1) \\ \vdots \\ w(L-1) \end{bmatrix}$$

$$\bar{V}_K(\theta) = \begin{bmatrix} 0 \\ \vdots \\ 0 \\ 0 \\ \vdots \\ 0 \end{bmatrix} = V(\theta)$$

Single-point constraint: $\bar{V}_K^+(\theta) \bar{W}(\theta) = 1 = V^+(\theta) W(K)$

Minimize output power: $\sigma_y^2 = \bar{W}^+(\theta) R_{\bar{X}\bar{X}} \bar{W}(\theta)$

Solution:

$$\bar{W}_{LC-1}(\theta) = \frac{R_{\bar{X}\bar{X}}^{-1} \bar{V}_K(\theta)}{\bar{V}_K^+(\theta) R_{\bar{X}\bar{X}}^{-1} \bar{V}_K(\theta)}$$



SINGLE LINEAR CONSTRAINT & MAX. LIKELIHOOD

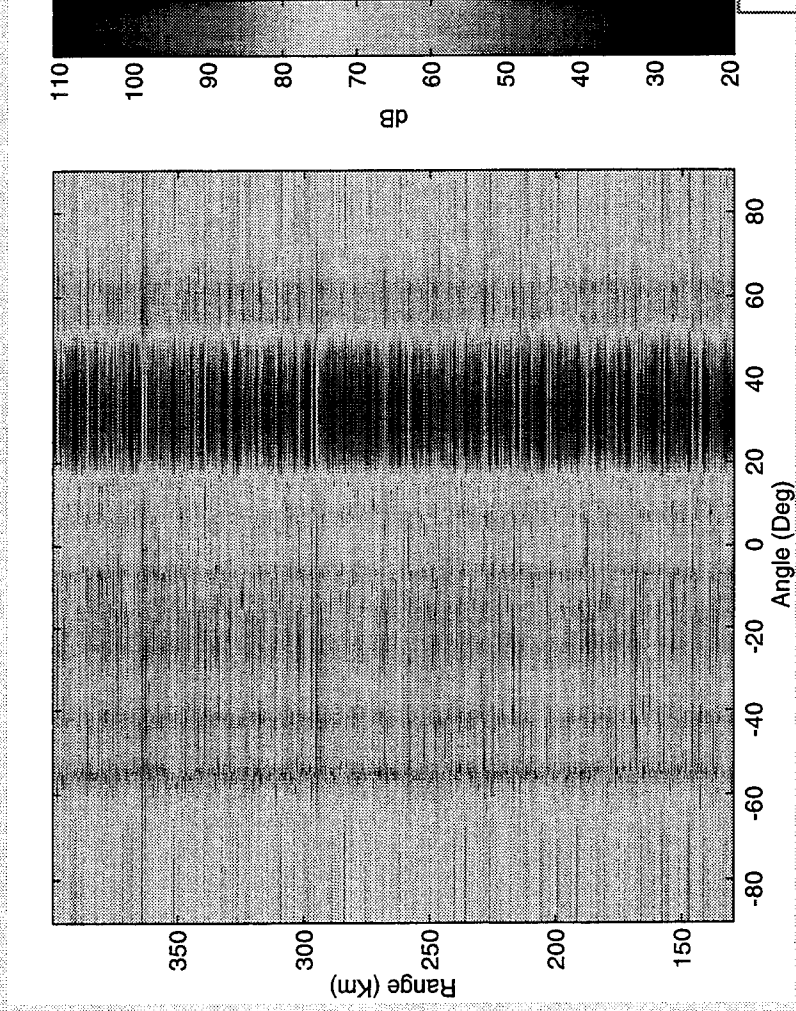
$$\bar{W}_{LC-1}(\theta) = \frac{R_{xx}^{-1} \bar{V}_K(\theta)}{\bar{V}_K^+(\theta) R_{xx}^{-1} \bar{V}_K(\theta)}$$

$$\bar{W}_{ML} = \frac{\hat{R}_{xx}^{-1} \bar{V}_K(\theta)}{\bar{V}_K^+(\theta) \hat{R}_{xx}^{-1} \bar{V}_K(\theta)}$$



MAXIMUM-LIKELIHOOD PROCESSING EXAMPLE

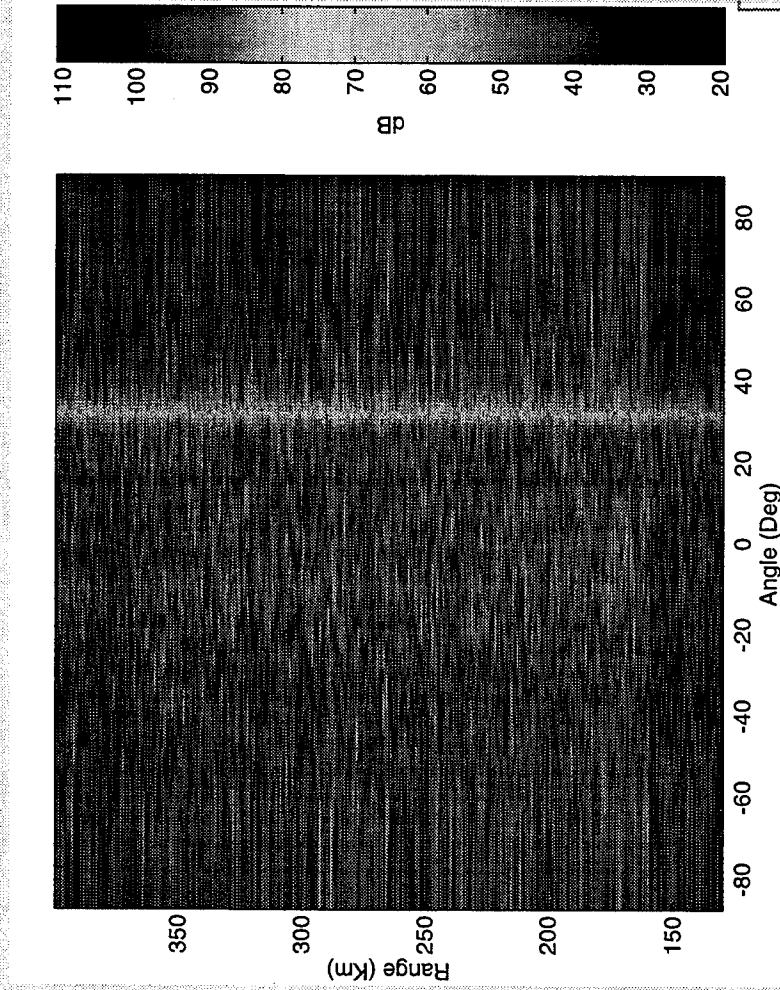
File: MMIT043v1 Conventional steering beamformer
14 weights





MAXIMUM-LIKELIHOOD PROCESSING EXAMPLE

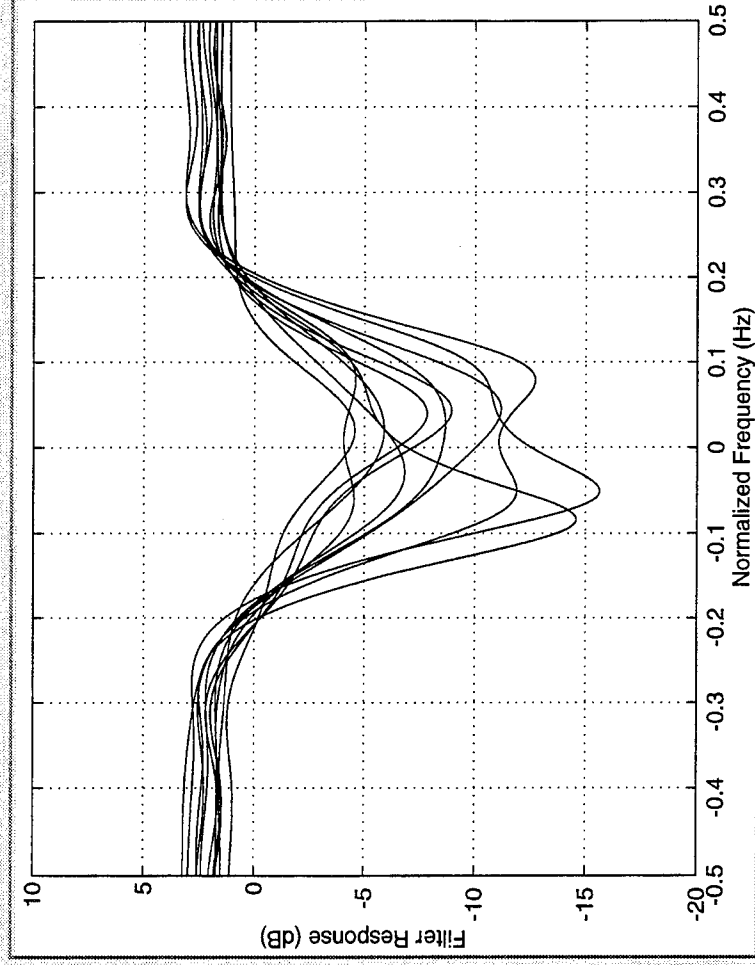
File: MMIT043v1 Maximum-likelihood weights
10 fast-time taps, 140 weights





MAXIMUM-LIKELIHOOD PROCESSING EXAMPLE

File: MMIT043v1 Maximum-likelihood weights
10 fast-time taps, 140 weights



OPTIMAL WEIGHTS FOR HOT CLUTTER

Array snapshot data model for direction θ :

$$\mathbf{X}(n) = \mathbf{s}(n)\mathbf{V}(\theta) + \mathbf{N}(n) \quad (L \times 1)$$

$$\bar{\mathbf{X}}(n) = \begin{bmatrix} \mathbf{X}(n) \\ \mathbf{X}(n-1) \\ \vdots \\ \mathbf{X}(n-L+1) \end{bmatrix} = \mathbf{s}(n) \otimes \mathbf{V}(\theta) + \bar{\mathbf{N}}(n) \quad (NL \times 1)$$

$$\mathbf{s}(n) = \begin{bmatrix} s(n) \\ s(n-1) \\ \vdots \\ s(n-L+1) \end{bmatrix} \quad (L \times 1) \quad \bar{\mathbf{N}}(n) = \begin{bmatrix} \mathbf{N}(n) \\ \mathbf{N}(n-1) \\ \vdots \\ \mathbf{N}(n-L+1) \end{bmatrix} \quad (NL \times 1)$$

DATA MODEL

Space-time snapshot:

$$\bar{\mathbf{X}}(n) = \mathfrak{U}(\theta)\mathbf{s}(n) + \bar{\mathbf{N}}(n)$$

$$\mathfrak{U}(\theta) = \begin{bmatrix} V(\theta) & 0 & 0 & 0 \\ 0 & V(\theta) & 0 & 0 \\ \cdot & \cdot & \cdot & \cdot \\ 0 & 0 & V(\theta) & 0 \\ 0 & 0 & 0 & V(\theta) \end{bmatrix}$$

Exact covariance matrix:

$$\begin{aligned} \mathbf{R}_{\mathbf{XX}} &= \mathbb{E} \left[\bar{\mathbf{X}}(n) \bar{\mathbf{X}}^+(n) \right] \\ &= \mathfrak{U}(\theta) \mathbf{R}_{\mathbf{ss}} \mathfrak{U}^+(\theta) + \mathbf{R}_{\mathbf{NN}} \end{aligned}$$



FIXED ARRAY FREQUENCY RESPONSE IN DIRECTION θ

$$\begin{aligned} y_s &= \overline{W}^+(\theta) \mathcal{A}(\theta) s(n) \\ &= \sum_{\ell=0}^{L-1} \mathbf{w}^+(\ell) V(\theta) s(n-\ell) = \sum_{\ell=0}^{L-1} b_{\ell} s(n-\ell) \end{aligned}$$

Signal from θ is filtered by coefficients determined by data

Use of maximum likelihood (or single linear constraint) forces: $b_K = 1$

Suggests the use of multiple constraints to achieve desired filter response:

$$\text{Constrain: } \mathbf{w}^+(\ell) V(\theta) = b_{\ell}, \quad \ell = 0, 1, \dots, L-1$$

$$\text{Such that } B(\omega) = \sum_{\ell=0}^{L-1} b_{\ell} e^{-j\omega\ell} \quad \text{has desired frequency response}$$

MULTIPLE CONSTRAINT SOLUTION

L linear constraints: $\mathcal{H}^+(\theta) \bar{\mathbf{W}}_{\text{LC}}(\theta) = \begin{bmatrix} b_0 \\ b_1 \\ \vdots \\ b_{L-1} \end{bmatrix} = \mathbf{f}$

Minimize output power: $\sigma_y^2 = \bar{\mathbf{W}}^+(\theta) \mathbf{R}_{\text{xx}} \bar{\mathbf{W}}(\theta)$

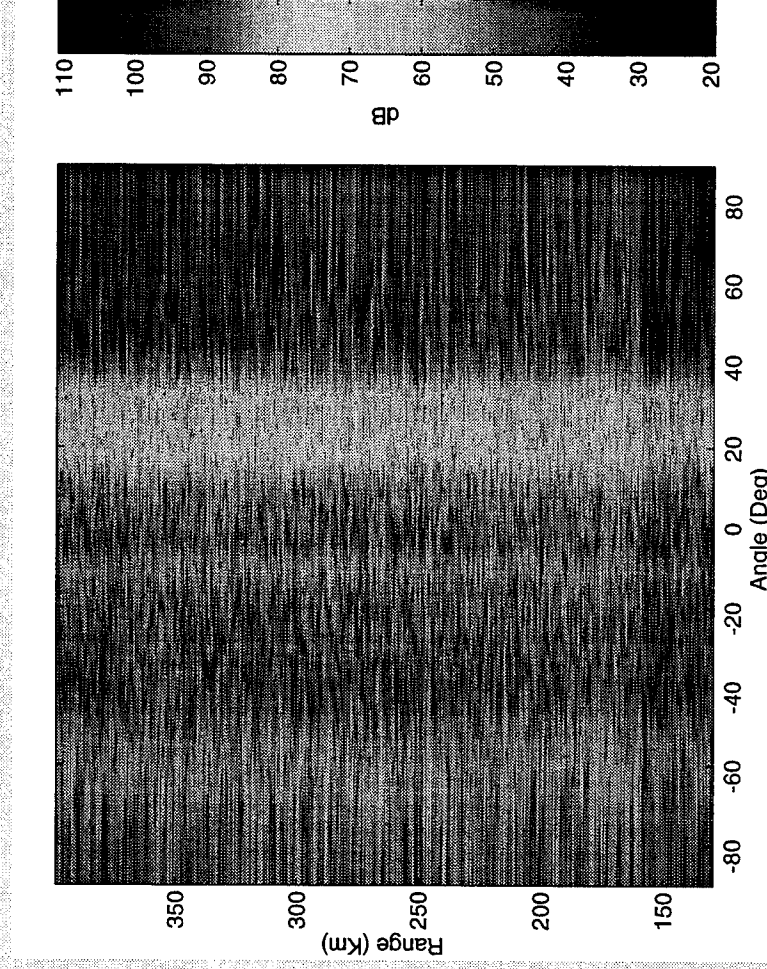
Solution:

$$\bar{\mathbf{W}}_{\text{LC}}(\theta) = \mathbf{R}_{\text{xx}}^{-1} \mathcal{H}(\theta) \left(\mathcal{H}^+(\theta) \mathbf{R}_{\text{xx}}^{-1} \mathcal{H}(\theta) \right)^{-1} \mathbf{f}$$



FIXED ARRAY FREQUENCY RESPONSE EXAMPLE

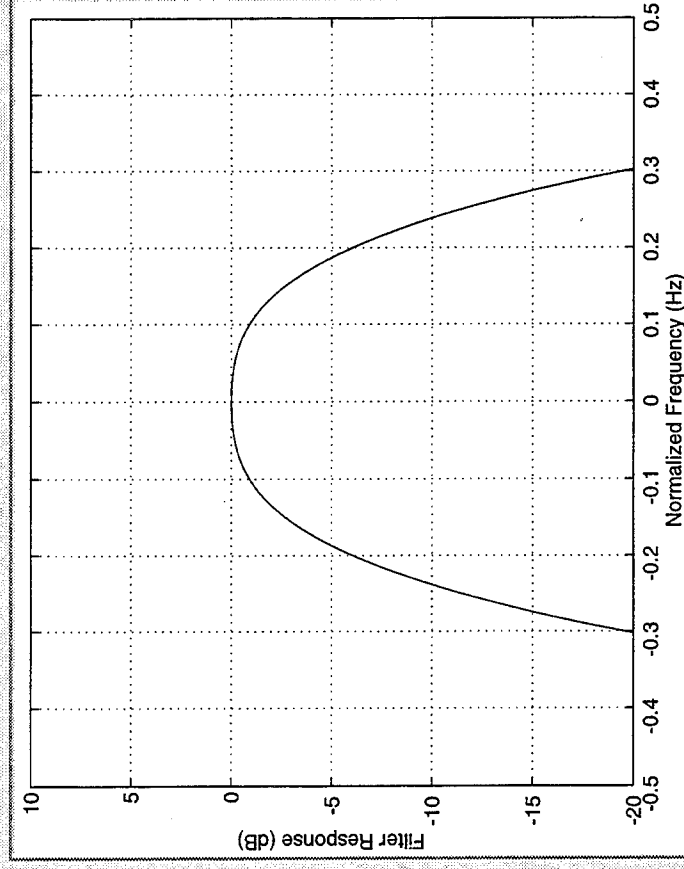
File: MMIT043v1 10-Point Hamming filter, $\omega_{co} = 0.20$
10 fast-time taps, 140 weights





FIXED ARRAY FREQUENCY RESPONSE EXAMPLE

File: MMIT043v1 10-Point Hamming filter, $\omega_{co} = 0.20$
10 fast-time taps, 140 weights





POINT FREQUENCY CONSTRAINTS IN DIRECTION θ

Data model:
$$\bar{X}(n) = \bar{S}(n) + \bar{N}(n)$$

Signal from θ :
$$\bar{S}(n) = \begin{bmatrix} s(n)V(\theta) \\ s(n-1)V(\theta) \\ \vdots \\ s(n-L+1)V(\theta) \end{bmatrix}$$

Sinusoidal signal:
$$s(n) = e^{j\omega n}$$

$$\begin{aligned} \bar{S}(n) &= e^{j\omega n} \begin{bmatrix} V(\theta) \\ e^{j\omega} V(\theta) \\ \vdots \\ e^{j\omega(L-1)} V(\theta) \end{bmatrix} \\ &= e^{j\omega n} \bar{V}(\omega, \theta) \end{aligned}$$

POINT FREQUENCY CONSTRAINTS (Cont'd)

M point constraints to fix frequency response in direction θ :

$$\bar{V}^+(\omega_1, \theta) \bar{W}(\theta) = a_1$$

$$\bar{V}^+(\omega_2, \theta) \bar{W}(\theta) = a_2$$

$$\cdot \quad \cdot$$

$$\bar{V}^+(\omega_M, \theta) \bar{W}(\theta) = a_M$$

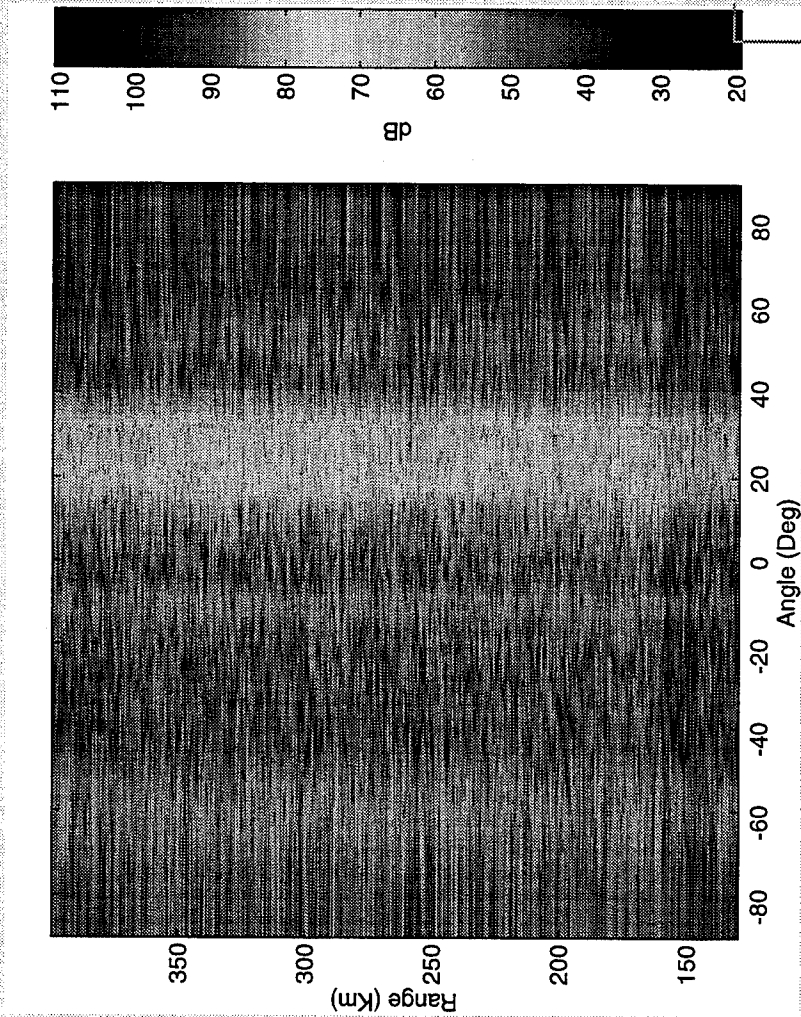
Equivalent expression:
$$C^+ \bar{W}_{LC}(\theta) = \begin{bmatrix} a_1 \\ a_2 \\ \vdots \\ a_M \end{bmatrix} = g$$

$$\bar{W}_{LC}(\theta) = R_{XX}^{-1} C \left(C^+ R_{XX}^{-1} C \right)^{-1} g$$



5-POINT FREQUENCY CONSTRAINT EXAMPLE

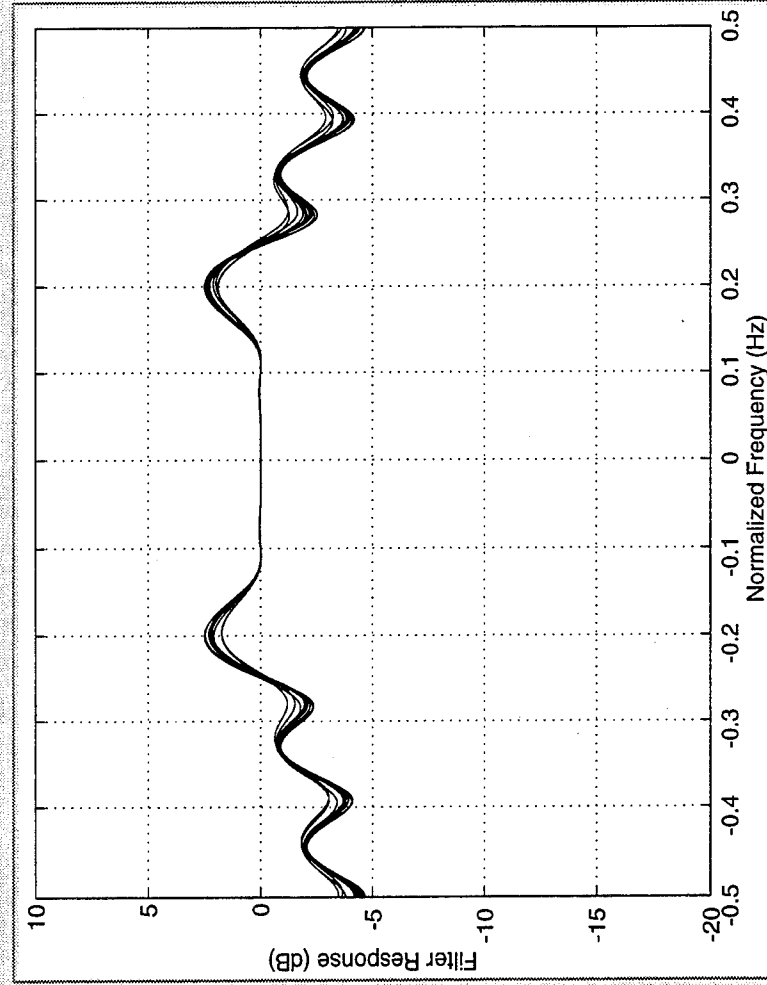
File: MMIT043v1 Constraints at $f = -0.10$, $f = -0.05$, $f = 0$, $f = +0.05$, $f = +0.10$
10 fast-time taps, 140 weights





5-POINT FREQUENCY CONSTRAINT EXAMPLE

File: MMIT043v1 Constraints at $f = -0.10$, $f = -0.05$, $f = 0$, $f = +0.05$, $f = +0.10$
10 fast-time taps, 140 weights





OPTIMUM DETECTION STRUCTURES

Data structure (signal present): $\bar{\mathbf{X}}(n) = \bar{\mathbf{S}}(n) + \bar{\mathbf{N}}(n)$

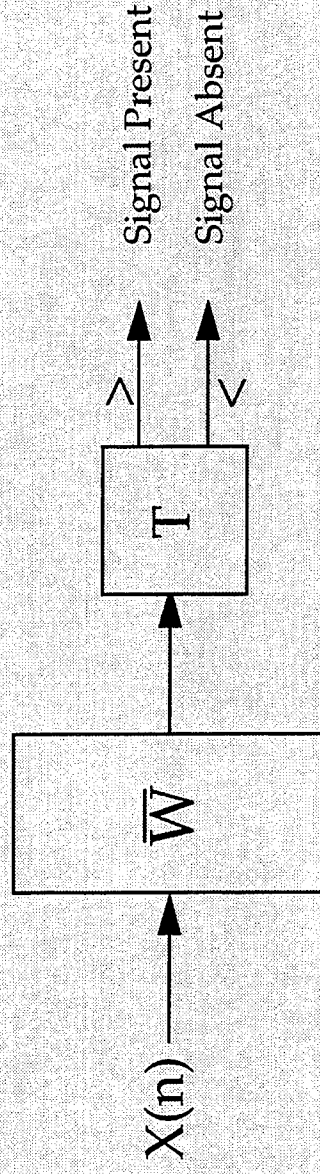
$$= \mathcal{U}(\theta)\mathcal{S} + \bar{\mathbf{N}}(n)$$

Signal assumed known: $\mathcal{S} = \begin{bmatrix} s(0) \\ s(1) \\ \vdots \\ s(L-1) \end{bmatrix}$

Distribution (signal present): Normal $\left(\mathcal{U}(\theta)\mathcal{S}, R_{\mathbf{NN}} \right)$

Distribution (signal absent): Normal $\left(0, R_{\mathbf{NN}} \right)$

OPTIMUM DETECTION STRUCTURES (Cont'd)



Optimum solution: $\bar{W} = R_{NN}^{-1} \mathcal{U}(\theta)$

Covariance structure: $R_{XX} = \mathcal{U}(\theta) \mathcal{U}^{\dagger}(\theta) + R_{NN}$

Alternative solution: $\bar{W} = R_{XX}^{-1} \mathcal{U}(\theta)$ with $T \rightarrow T'$

STEERING VECTOR STRUCTURE: OPTIMUM DETECTION

$$\bar{V}(\theta) = \mathcal{V}(\theta) \tilde{\mathcal{S}} = \begin{bmatrix} s(0) V(\theta) \\ s(1) V(\theta) \\ \vdots \\ s(L-1) V(\theta) \end{bmatrix}$$

Conclusion: Maximum-Likelihood approach optimal for single-point signal.

Interpretation: Coefficients serve as matched filter to known signal.



SUMMARY AND CONCLUSIONS

- Multiple point constraints provide processing flexibility
 - Fixed filtering in direction of arrival (estimation direction)
 - Point constraints to control filtering at prescribed points
- Maximum likelihood approach corresponds to impulse signal
- Optimum detection models suggest matched filtering approach

(Pages 373-399 have been intentionally omitted)

SCALABLE PORTABLE PARALLEL ALGORITHMS FOR STAP

Prashanth B. Bhat, Young W. Lim, and Viktor K. Prasanna

University of Southern California
Department of Electrical Engineering
Los Angeles, CA 90089-2562
tel: (213) 740-4483
fax: (213) 740-4418
email: prasanna@usc.edu

Abstract This presentation summarizes our analytical and experimental results in developing efficient parallel solutions for STAP on general purpose massively parallel systems. In this context, our research consists of designing general algorithmic techniques such as partitioning, mapping, and communication scheduling so as to enable efficient execution on general purpose HPC platforms. To illustrate these techniques, we have designed coarse grained parallel algorithms for various partially adaptive STAP approaches such as HOPD (Higher Order Post Doppler), as well as other Element-Space and Beam-Space approaches, on general purpose massively parallel systems. The algorithms have been implemented using C and MPI (Message Passing Interface standard), thereby ensuring portability across several state-of-the-art HPC platforms. The parallel algorithms have been designed using a realistic model of general purpose distributed memory systems. The model assists us in analyzing performance benefits of algorithmic techniques. For instance, data remapping enables scalable performance in the case of HOPD processing. We have implemented these algorithms on the IBM SP-2 and Cray T3D, and are currently performing implementations on the Intel Paragon. The algorithms have been tested using the ARPA Mountaintop STAP database. The experimental results indicate that the performance scales linearly with system and problem sizes. We have also developed efficient data redistribution schemes to send data which is input from the antenna arrays to the compute nodes. The number of computing nodes is typically much larger than the number of antenna elements. We use our model to design a pipelined communication schedule for this operation. Experimental results indicate improved performance over a straightforward scheduling scheme.

Scalable Portable Parallel Algorithms for STAP

Viktor K. Prasanna
University of Southern California
prasanna@halcyon.usc.edu

Outline:

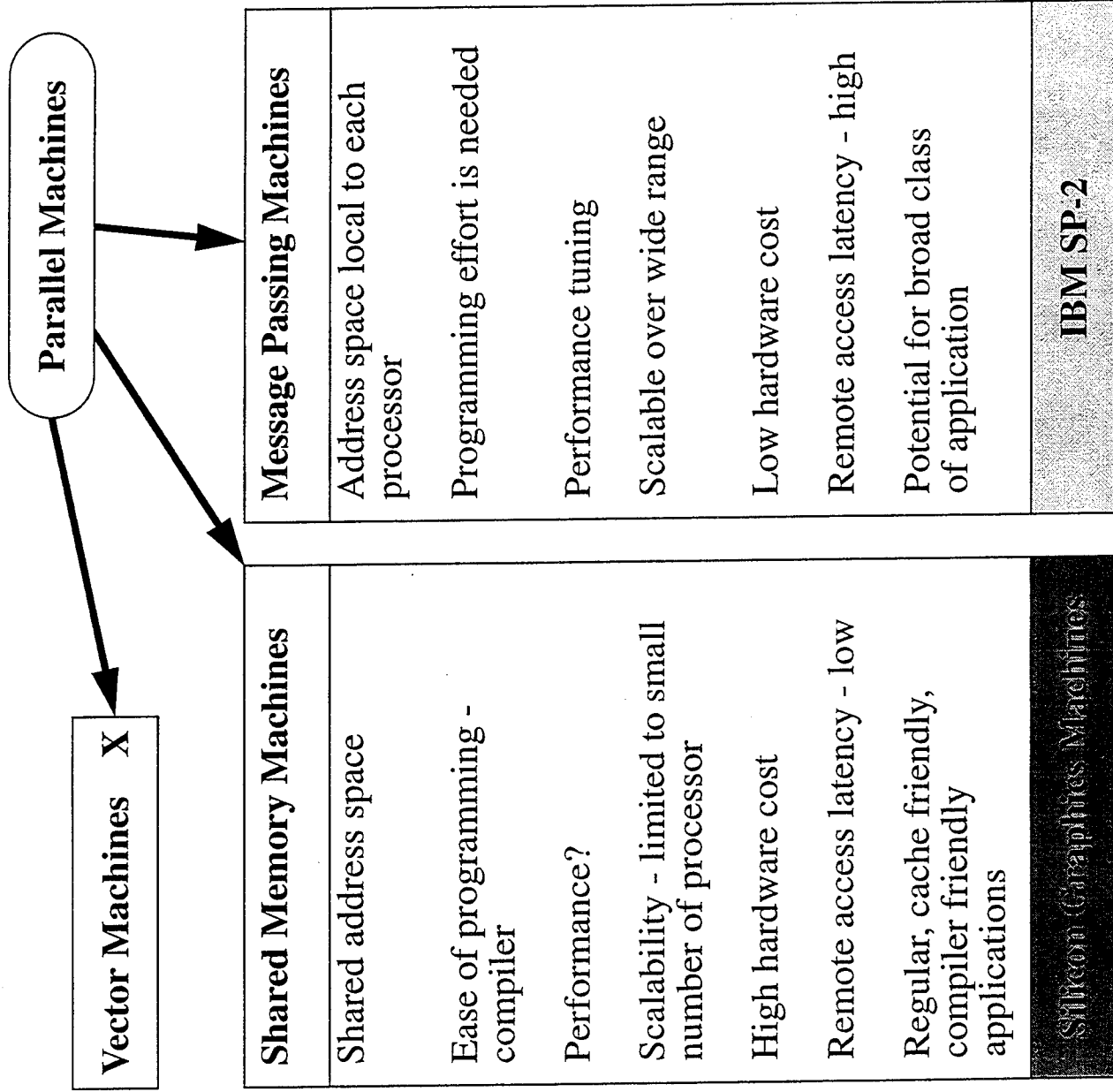
- 1. Goals of this work**
- 2. Choice of parallel machines**
- 3. Scalability and Portability**
- 4. Problems to be studied**
- 5. Our Approach**
- 6. Higher-Order Post-Doppler on SP-2**
- 7. Concluding remarks**

1. Goals of this work

High speed execution of radar signal processing algorithms on state-of-the-art massively parallel machines.

- A. Develop Scalable Parallel Algorithms.
- B. Develop Data Partitioning and Mapping Methods.
- C. Develop Portable Code.
- D. Implement a Complete High-Speed Radar Signal Processing System on a Massively Parallel Machine.

2. Choice of Machines



SP-2

Based on IBM POWER2 Architecture:

Peak Rate of 266 Mflops / Processor
Message Passing

Startup Time: 39 μ sec (using MPL)

Bandwidth: 35 MB/sec/node

Individual Private Address Space

Uniform Latency between Nodes

Multistage Interconnection Network (Omega)

Message Passing Library (MPL)

CRAY T3D

Based on DEC Alpha chip: peak rate of 150 Mflops / processor
Distributed Shared Memory

Local Memory Access Time: 87 ~ 253 nsec

Global Memory Access Time: 1 ~ 2 μ sec (SHMEM)

Global Address Space

Fast Barrier Synchronization

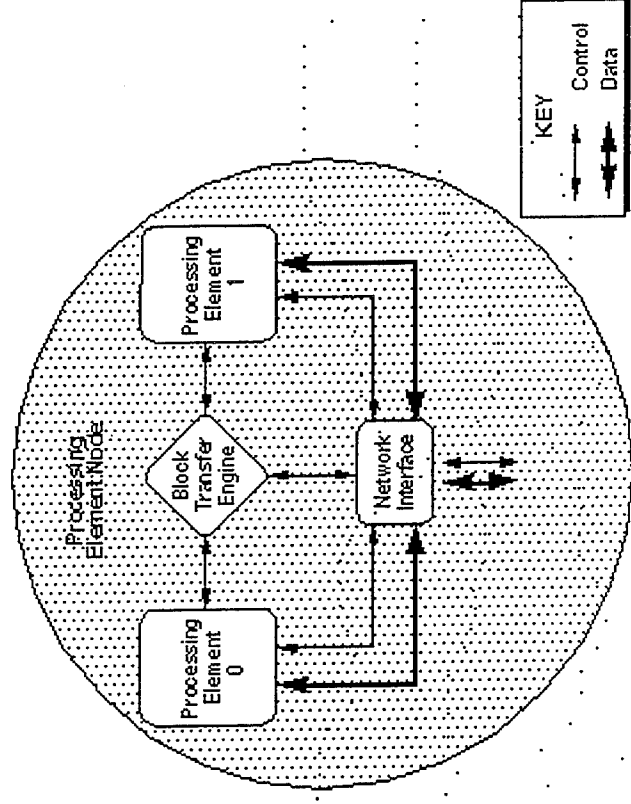
3-D Torus Interconnection Network

Latency Hiding Mechanism

Prefetch Queue

Remote Processor Store

Block Transfer Engine



Computational Characteristics of Message Passing Machines

1. Coarse grain machines

Powerful Processing Nodes.

SP-2: wide nodes → model 590

266 Mflops

2. Large software overhead for message transfer.

SP-2:

≈ 39 μsec overhead/message

local memory access: 100's of nsec

3. High-speed low hardware latency interconnect.

mesh X

hypercube X

SP-2:

switch latency 100's of nsec



3. Scalability

T_s : Serial time

T_p : Parallel time using P processors



Computation Time



Communication Time

$P \uparrow$

Parallel Time \downarrow

How much does T_p reduce?

Scalable:

$$T_p = \frac{T_s}{p}$$

$$1 \leq p \leq \text{upperlimit}$$

large?

Speed-up:

$$\frac{T_s}{T_p}$$

Portability Issues

- Shared Memory Machines
- Message Passing Machines
- New Heterogeneous HPC Platforms for Signal Processing

* Unified Computational Model for algorithm design/analysis

Latency, Start-up time, Bandwidth, Congestion

* MPI (Message Passing Interface)

eg) `MPI_ISEND(buf, count, datatype, dest, tag, comm, request)`

: Asynchronous Nonblocking send command

- Platform independent standard.
- Major step forward in support for library development
 - Many modes for point-to-point communication not supported currently --> opportunities
 - User defined data types

* REAL-TIME MPI Efforts

- Hughes
- Myricom
- NSWC

4. Problems to be studied for high speed implementation

Set of generic problems

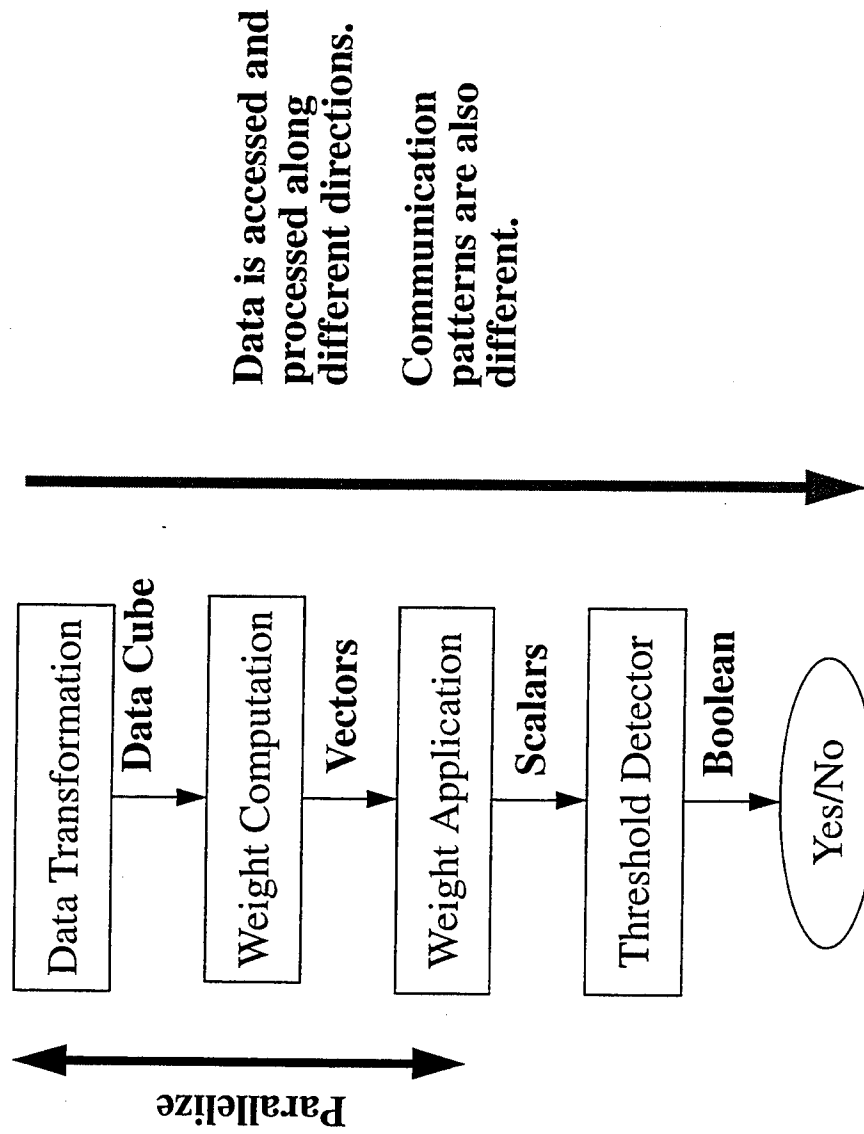
Complexity	Problem	Subproblems
II	1. Doppler Processing	FFT
		Matrix Equation Computation
I	2. Beam Forming	Weight Computation
		Cholesky Factorization
		Matrix Linear Algebra
III	3. CFAR	Sort
		Search

Problem Characteristics

1. Overall system consists of sequence of subproblems
2. Computational requirements and characteristics are different in each subproblem (Bottlenecks exist --> Scheduling)
3. Large amount of data is repeatedly processed in real-time
4. Data is accessed and processed along different directions (Remapping is needed)

Overview from a Computational Perspective

Information Reduction Process



How to distribute data such that

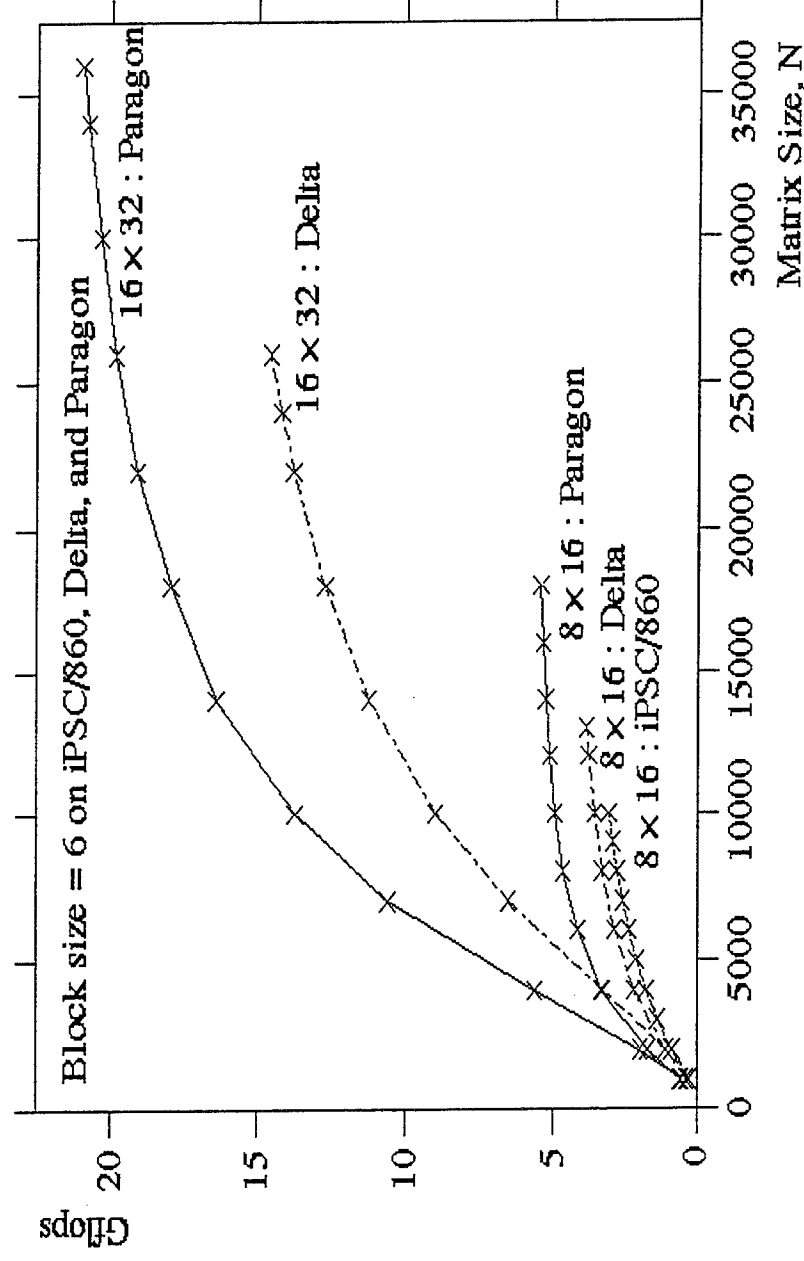
- Load on each PE is well balanced
- Communication time is reduced

Parallel Linear Algebra Library ?

ScaLAPACK

Radar Signal Processing problem size too small -- poor efficiency

Fixed Data Mapping Scheme



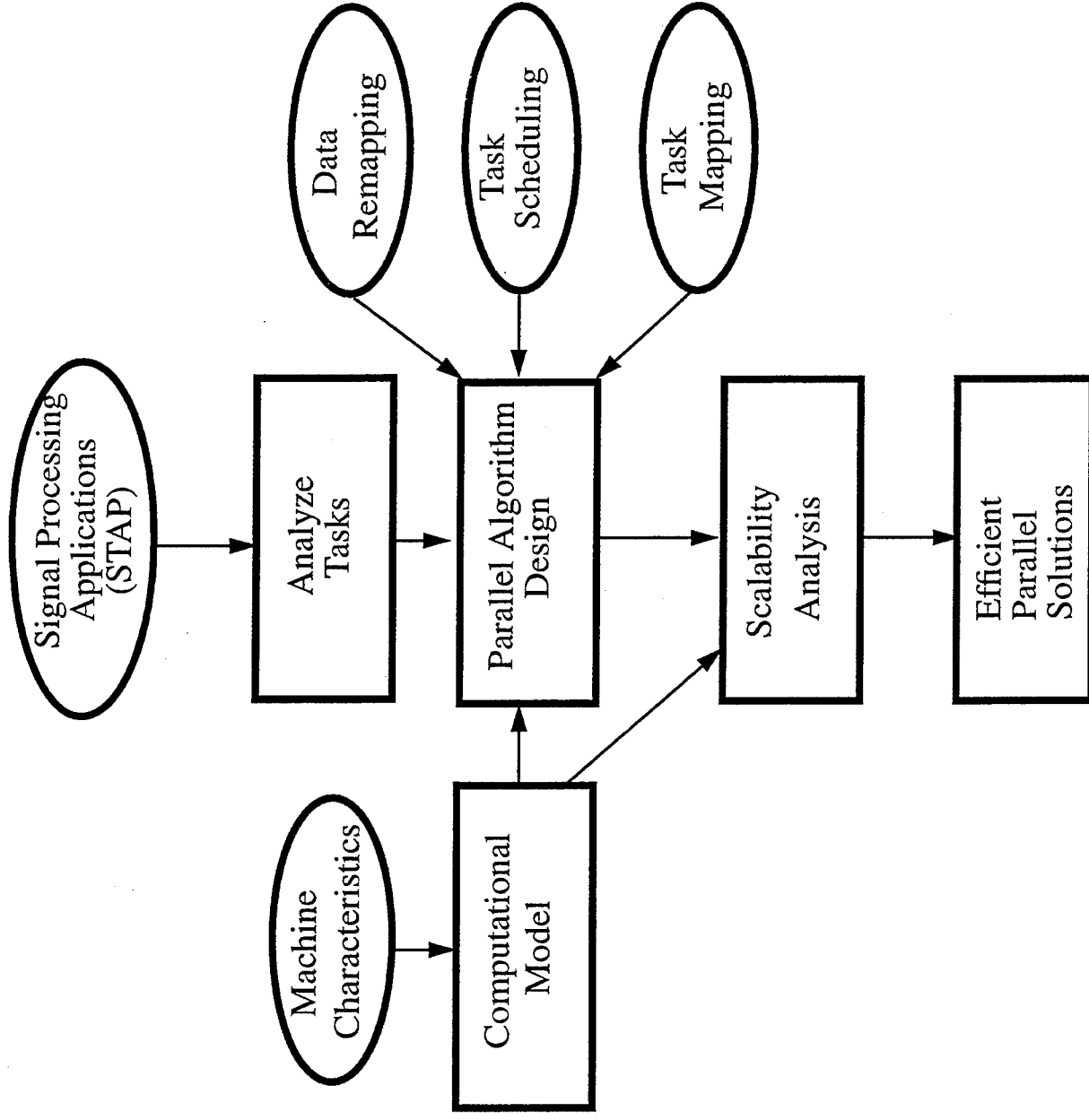
QR factorization on the Intel iPSC/860, Delta, and Paragon
(ORNL Technical Report)

i860: 50Mflops / node --> 16x32 Paragon = 26Gflops

QR Factorization:

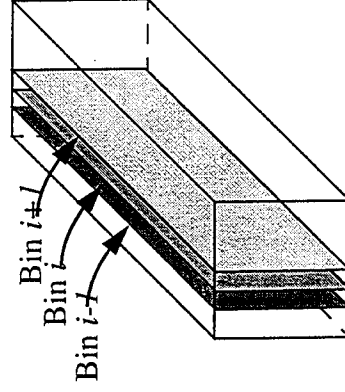
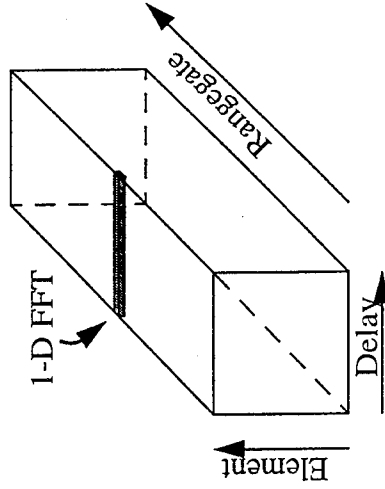
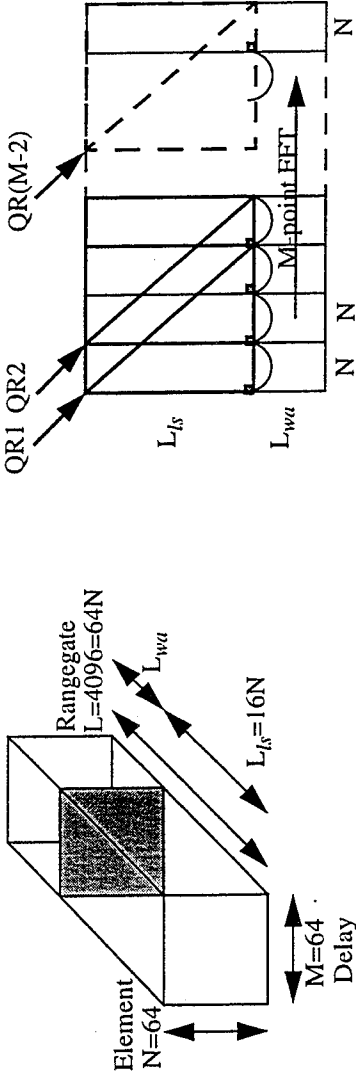
$A = QR$ where R is uppertriangular matrix and $Q^T Q = I$ (orthogonal mat).

5. Approach



6. An Example High Speed Implementation on SP-2

Higher Order Post Doppler STAP [From J. Ward, MIT LL Report]



Computational Requirements

NL M-point FFT Problems

$$(NL) \times 4 \times M \log M$$

$$= 384 \times 2^{20} \text{ Flops} = 380 \text{ MFlops}$$

(M-2) 16N x 3N QR Decomposition Problems

$$(M-2) \{ (3N)^2 \times (16N - 3N/3) \}$$

$$= (M-2) \{ 9N^2 \times 15N \}$$

$$= 2100 \text{ MFlops} \approx 2 \text{ GFlops}$$

Our Parallel Algorithm

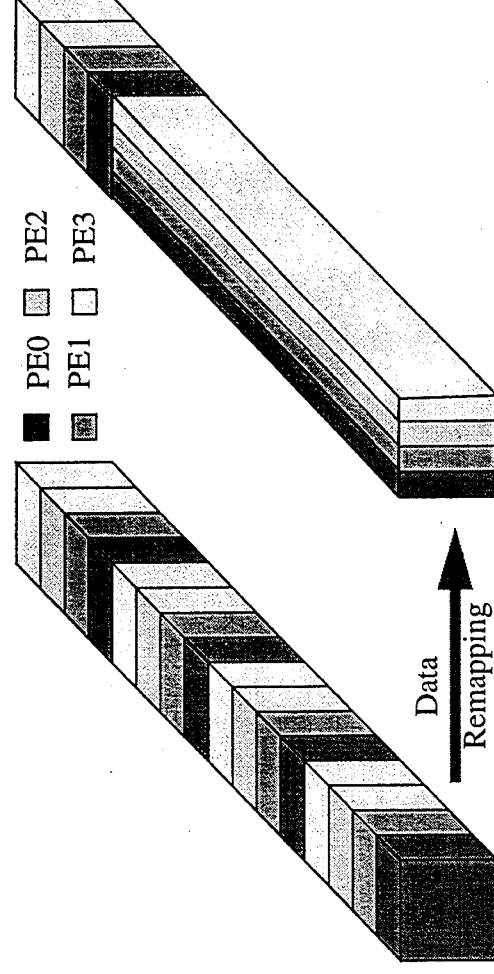
Key Ideas:

1) Data Remapping

QR Decomposition : Computational Bottleneck

Parallel vs. Sequential Approach

Problem Size



2) Scheduling

- Computation and
- Communication to avoid network congestion

Computational Model

T_s : Startup Time

T_d : Transmission Rate

m : Message size in bytes

$$T_s + m \cdot T_d$$

Communication features of various message passing machines

Machine	Ts(μsec)	Td(μsec/byte)	Ts/Td
CM-5	86	0.12	716
SP-2	46	0.035	1314
Paragon	82	0.26	315
iPSC/860	60	0.50	120
iPSC/2	700	0.36	1944

Experimental Results

Computation Time : $O(\frac{9(M-2)N^2(L/4-N) + 9LMN\log M}{p}t_c)$

Communication Time : $O(\frac{LMN}{4p} \cdot T_d)$

Scalable over $p \leq M$

Performance Results

Estimate of remapping and communication times for
M=64, N=64, L_{IS}=1024 on SP-2

p	T _{remap}	T _{comm} (QR) ^a
2	580msec	960msec
4	290msec	1900msec
8	140msec	3600msec
16	70msec	6600msec
32	40msec	12000msec

a. D. P. O'Leary and P. Whitman, "Parallel QR factorization by Householder and modified Gram-Schmidt algorithms, Parallel Computing, 1990. (used by Cornell)

Execution Times on SP-2 for M=N=64, L=4096

p=2	p=4	p=8	p=16	p=32	p=64
45sec	15sec	7.8sec	3.9sec	2.0sec	.96sec

Table 1: Timing Results for FFT& REMAPPING on T3D (msec)^a

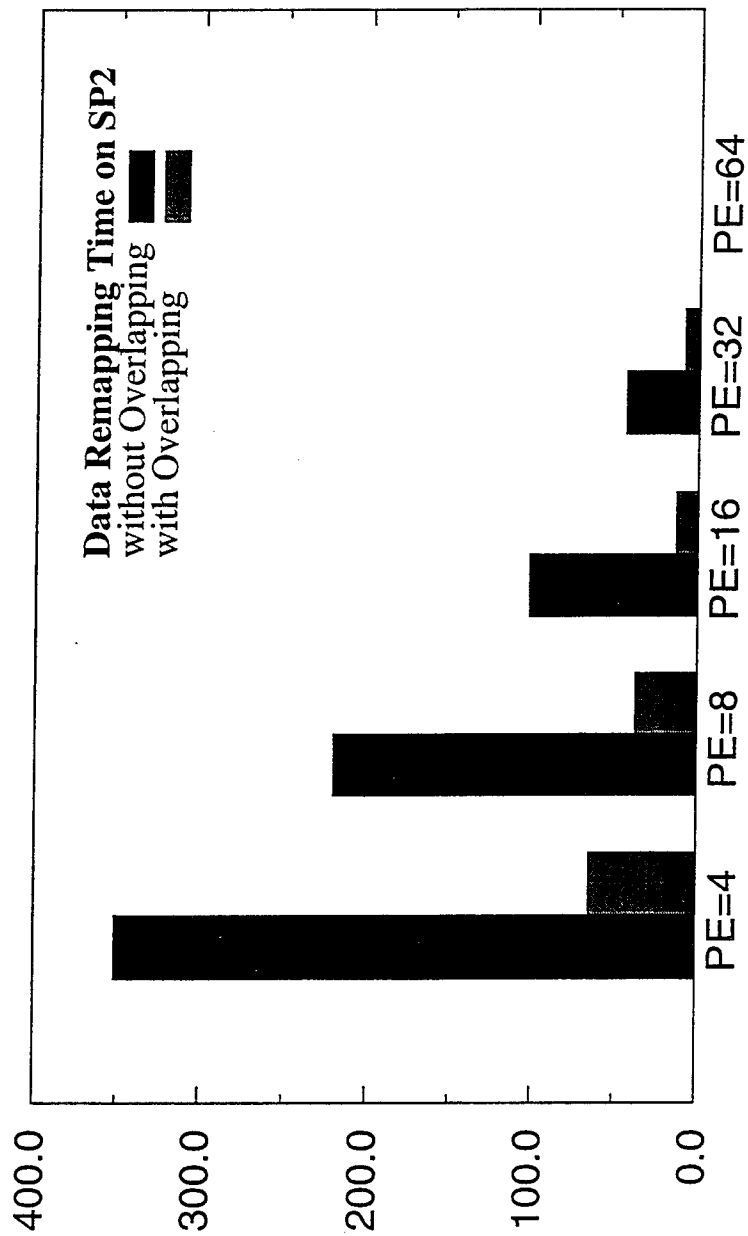
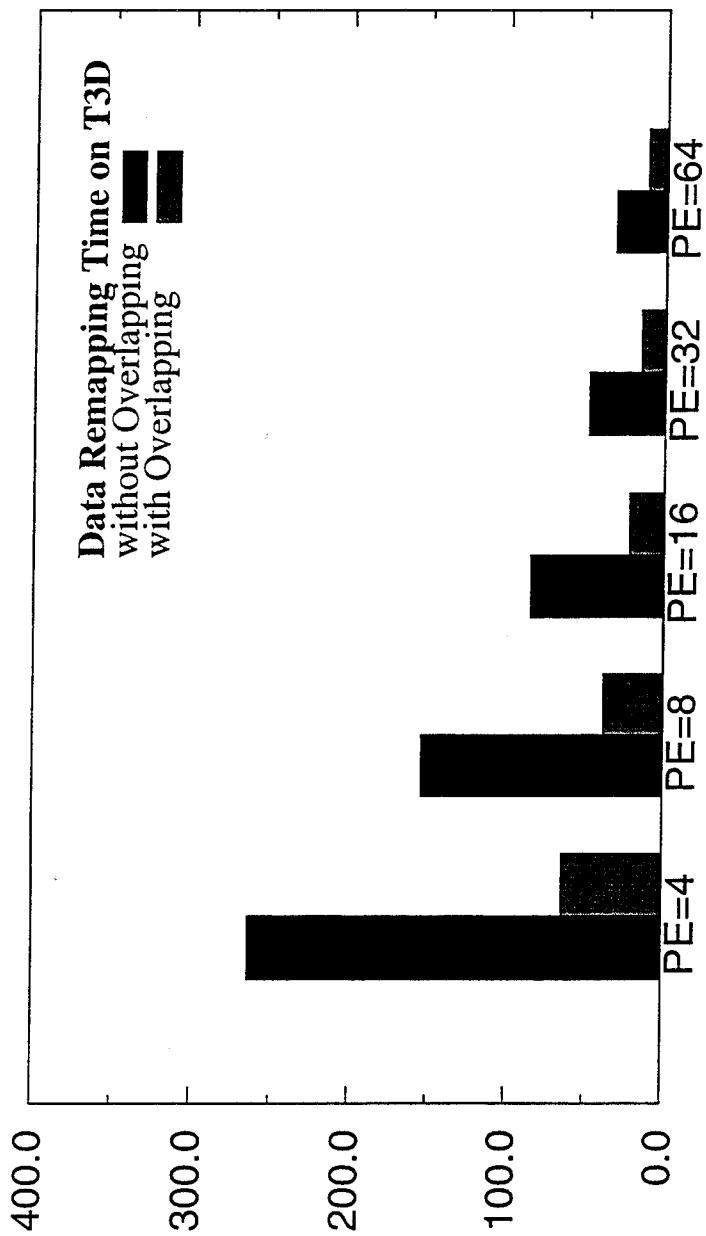
	Number of PEs	PE=4	PE=8	PE=16	PE=32	PE=64
Doppler Proc	Number of 64-point FFT's per PE	65,536	32,768	16,384	8,192	4,096
	Total time for FFTs	12800.0	64200.0	3210.0	1610.0	200.0
	Message size	2MB	512KB	128KB	32KB	8KB
Data Remap	(PE-1) Async Nonblock- ing pt-to-pt communica- tions	63.5	37.6	21.8	15.1	11.8
	(PE-1) Synchronous blocking sen- drecv communications	264.0	154.0	84.5	48.1	32.0

a. No Cray Library was available. Numerical Recipes routine was used.

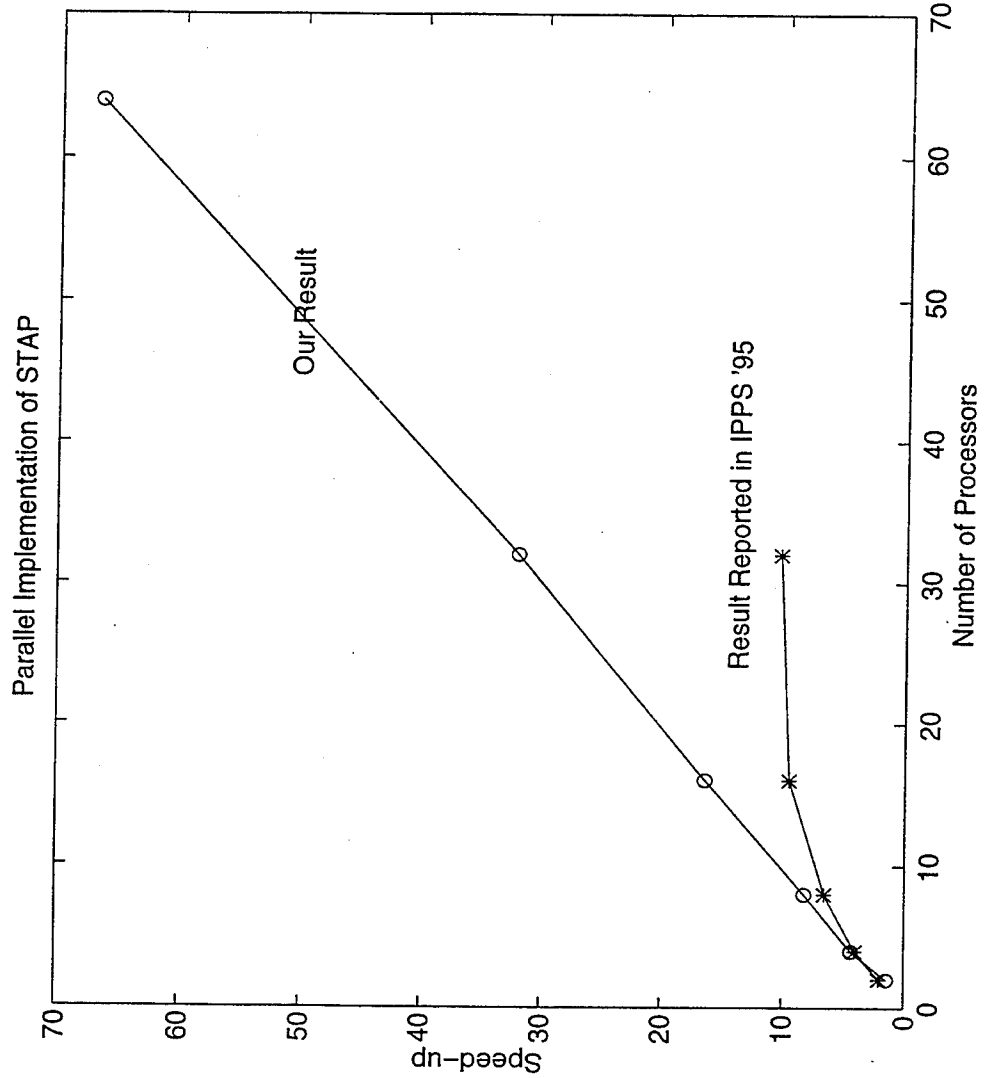
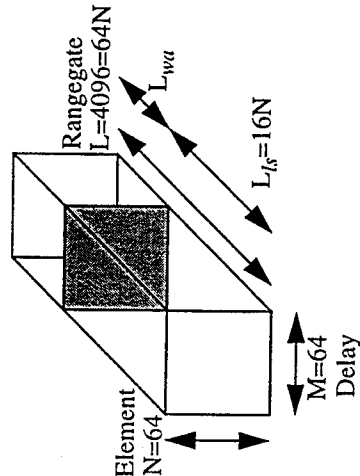
Table 2: Timing Results for FFT& REMAPPING on SP2 (msec)^a

	Number of PEs	PE=4	PE=8	PE=16	PE=32	PE=64
Doppler Proc	Number of 64-point FFT's per PE	65,536	32,768	16,384	8,192	4,096
	Total time for FFTs	1730.0	858.0	428.0	214.0	-
	Message size	2MB	512KB	128KB	32KB	8KB
Data Remap	(PE-1) Async Nonblock- ing pt-to-pt communica- tions	64.7	37.5	13.2	8.57	-
	(PE-1) Synchronous block- ing sendrecv communica- tions	351.0	220.0	101.09	43.99	-

a. IBM ESSL library was used for FFT. MPICH on MHPCC was used. Loadleveler data.



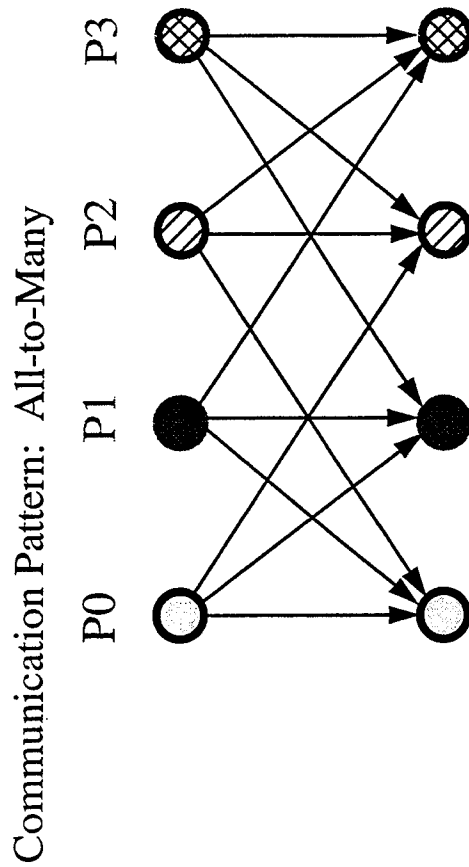
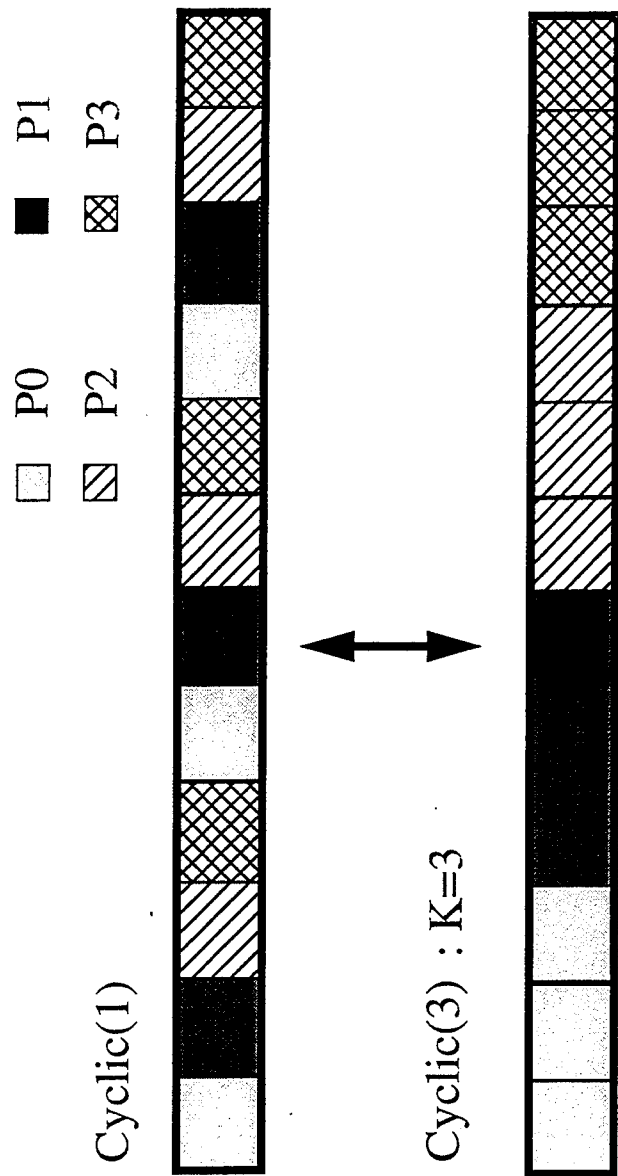
Experimental Results: HOPD STAP on SP-2



7. Concluding Remarks

- Data Remapping
- Overlap computation/communication
- Implementations on SP-2 and T3D for HOPD STAP
- Key Problem - Data Remapping

Block Cyclic Redistribution



- Node Contention Occurs
- Communication Scheduling is Necessary

Previous Efforts

1. “Redistribution of Block Cyclic Data Distributions Using MPI”,
D.W. Walker & S.W. Otto, ORNL
 - Redistribution Takes K or $K-1$ Steps
 - Each Step is Contention Free
 - No Indirect Data Movement
2. “Multi-Phase Redistribution: A Communication Efficient Approach to
Array Redistribution”, S.D. Kaushik, C.-H. Huang, J. Ramanujam, and P.
Sadayappan, OSU
 - Multi-Phase Algorithm
 - Number of Communication Steps = $K_1 + K_2 + K_3$
 $K = K_1, K_2, K_3$
 - More Data Movement - Indirect Data Routing
 - Each Phase uses the Previous Approach
 - Multi-Phase Approach Not Applicable when K is a Prime Number

Our Result

Cyclic(x) to Cyclic(Kx) Redistribution Can be Performed in

$\lceil \log_2 K \rceil$ Steps

for any Value of K

**STAP PROCESSING ON A MULTICOMPUTER:
DISTRIBUTION OF 3-D DATA SETS AND
PROCESSOR ALLOCATION FOR
OPTIMUM INTERPROCESSOR COMMUNICATION**

Mark F. Sklabrin and Thomas H. Einstein

Mercury Computer Systems, Inc.

199 Riverneck Road

Chelmsford, MA 01824-2820

tel: (508) 256-1300, ext. 348

fax: (508) 256-3599

email: einstein@mc.com

Abstract In contrast to conventional two-dimensional radar processing, STAP processing is inherently three-dimensional (i.e., range/pulse/antenna-element). Furthermore, real-time processing requirements for STAP typically range from 20-100 Gflops. Using current processor technology, processing requirements can only be met by using a multiprocessor system composed of several hundred interconnected compute elements (CEs). A major challenge in such an application is the distribution of the 3-D data set over the available CEs in the system. STAP processing generally entails at least three separate processing stages, i.e., one for each dimension of the 3-D data set. At each stage, data is distributed among the CEs for processing in parallel. This requires that entire vectors of data, along the dimension being processed at a given stage, be resident in the local memory of each CE. Each CE will process one or more vectors along the given processing dimension. The requisite redistribution of data between stages is called a distributed "corner-turn" and is affected by interprocessor communication. This paper describes a paradigm for distributing the 3-D STAP data set among the CEs in the multicomputer so as to maximize the efficiency of the interprocessor communications performed between stages. Specifically, the data is distributed so that the number of other CEs with which each CE has to communicate during any distributed "corner-turn" between stages is minimized. A further feature of the subject data distribution scheme is that the limiting number of CEs over which the 3-D STAP data may be distributed is increased to equal the product of the two smallest dimensions of the data set. This is especially important in STAP applications because of the large number of CEs required to satisfy the specified processing load.

STAP Processing on Multiprocessor Systems:

Distribution of 3-D Data Sets and Processor Allocation for Efficient Interprocessor Communication

Mark Skalabrin (marks@mc.com)

Tom Einstein (einstein@mc.com)

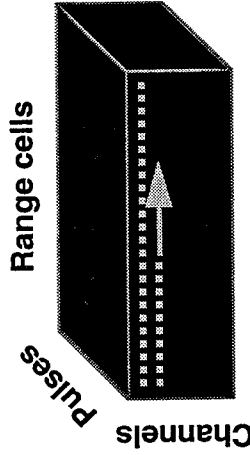
ASAP Workshop

2/96

Computer Systems, Inc.
MERCURY

Elements of STAP Processing

➤ The STAP Data Set



➤ STAP Processing Dimensions

At each processing stage, data access is either vector oriented along a cube dimension, or plane oriented along a pair of cube dimensions.

Processing Stage

Processing Dimension(s)

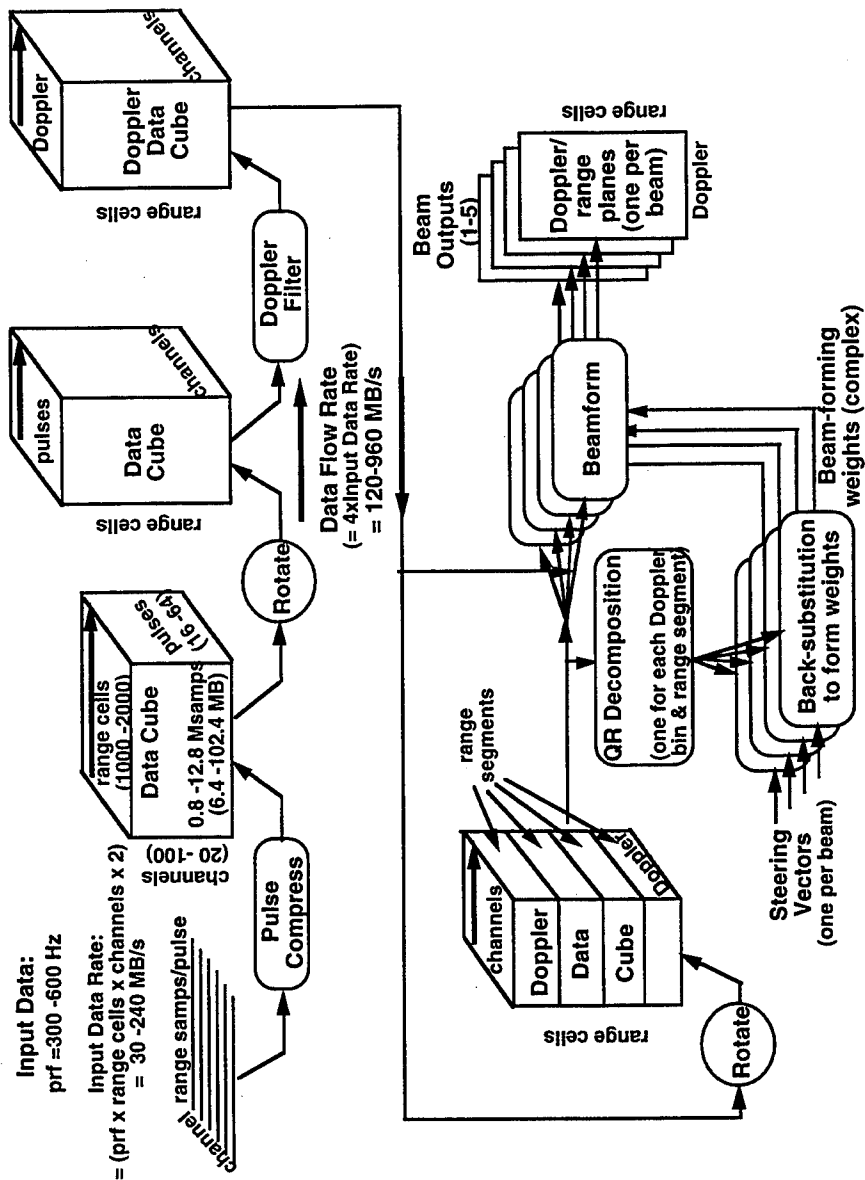
Pulse Compression	----- Range
Doppler Filtering	----- Pulse
Beam Weight Computation	---- Range/Channel
(QR Decomposition)	
Beam Formation	----- Channel

ASAP Workshop

2/96

Computer Systems, Inc.
MERCURY

Example STAP Processing Flow



Stressing Requirements: Throughput, Latency, IPC

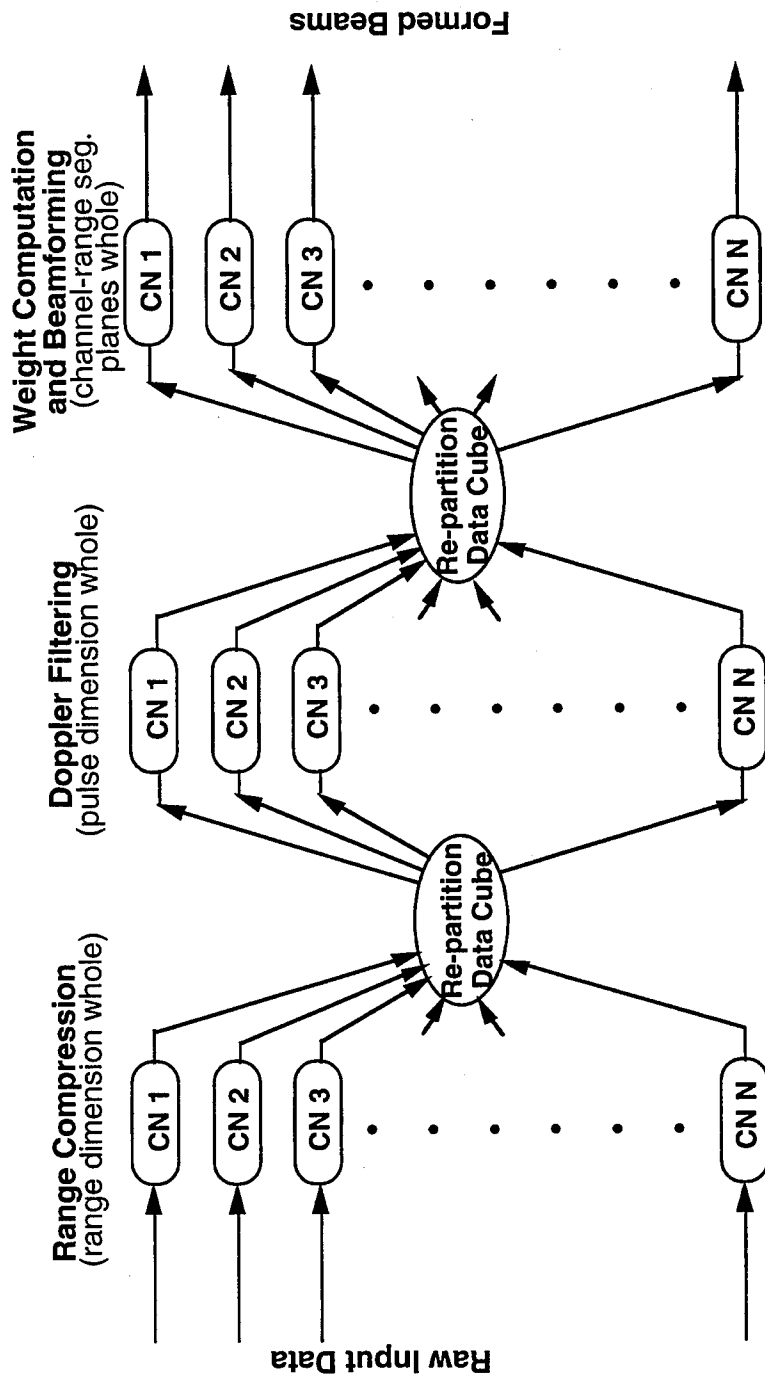
Computer Systems, Inc.
MERCURY

ASAP Workshop

STAP Processing Distribution challenges

- To reduce latency, the processing at each stage must be partitioned over multiple processors.
 - ★ SPMD distribution is required.
 - ★ 100s of processors can be required.
- Data set must be partitioned so that the computational load is evenly distributed at each processing stage.
- Data set must be re-partitioned between stages since each stage processes data along a different dimension of the data cube.

STAP Processing Distribution Example



ASAP Workshop

2/96

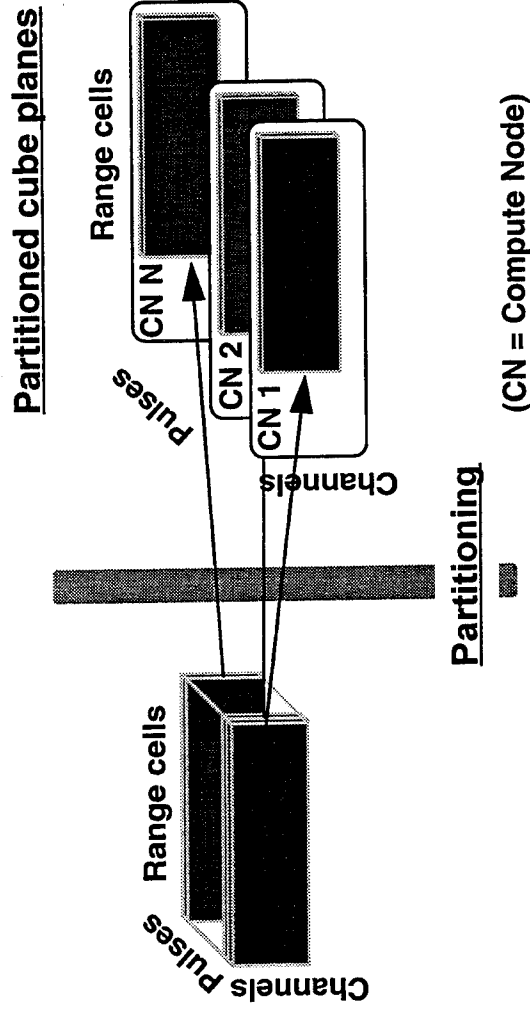
CN = Compute Node

Computer Systems, Inc.
MERCURY

A Comparison of Two Methods of Data Set Partitioning

Method 1: Partitioning by date planes

- Each processor gets one or more data planes (XY, XZ, or YZ) of the cube.
- Processing is performed on at least one of the two “whole” dimensions of the distributed planes.



ASAP Workshop

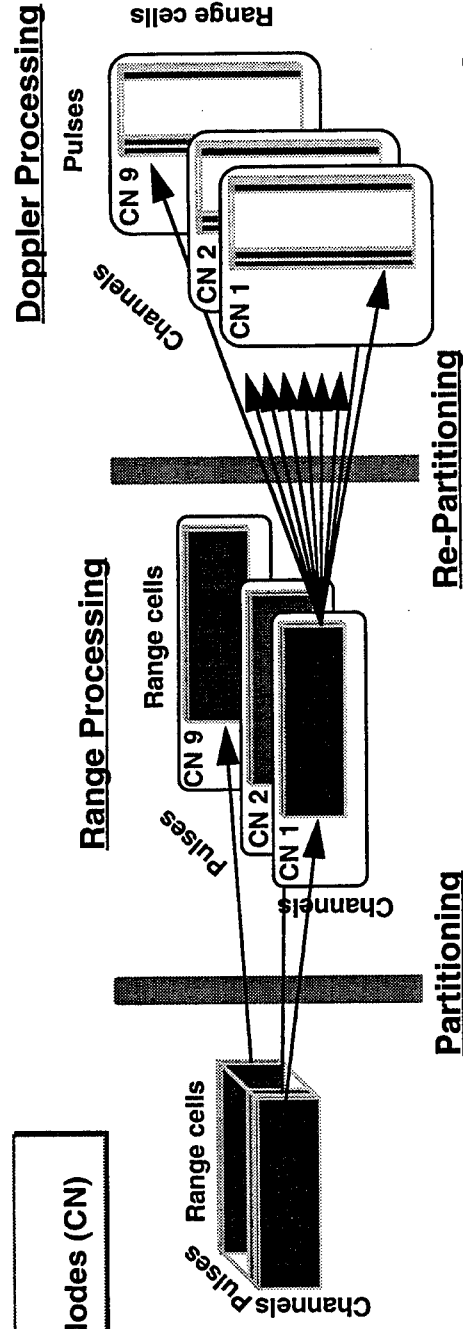
Computer Systems, Inc.
MERCURY

A Comparison of Two Methods of Data Set Partitioning

Method 1: Partitioning by data planes is NOT efficient

- ☹ The number of processors over which data may be partitioned is limited to the number of possible planes.
 - ★ Maximum number of processors = Smallest dimension of the cube
- ☹ Data re-partitioning between stages requires interprocessor communication between all N processors.
 - ★ Requires approximately N^2 interprocessor transfers

Example:
9 Compute Nodes (CN)



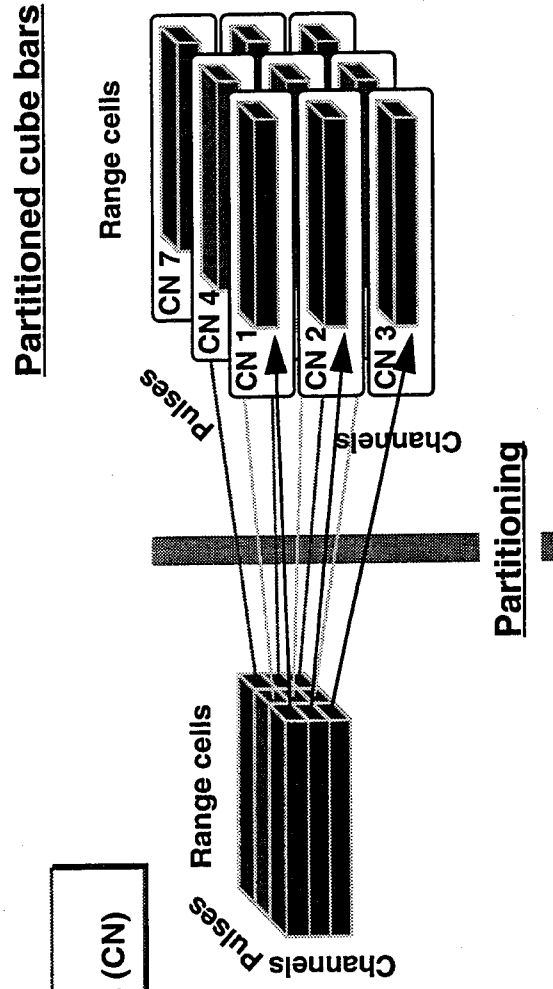
Computer Systems, Inc.
MERCURY

ASAP Workshop

A Comparison of Two Methods of Data Set Partitioning

Method 2: Partitioning by sub-cube "bars"

- Each processor gets a sub-cube bar with the processing dimension whole.
- Two of the three dimensions of the cube are potentially segmented.

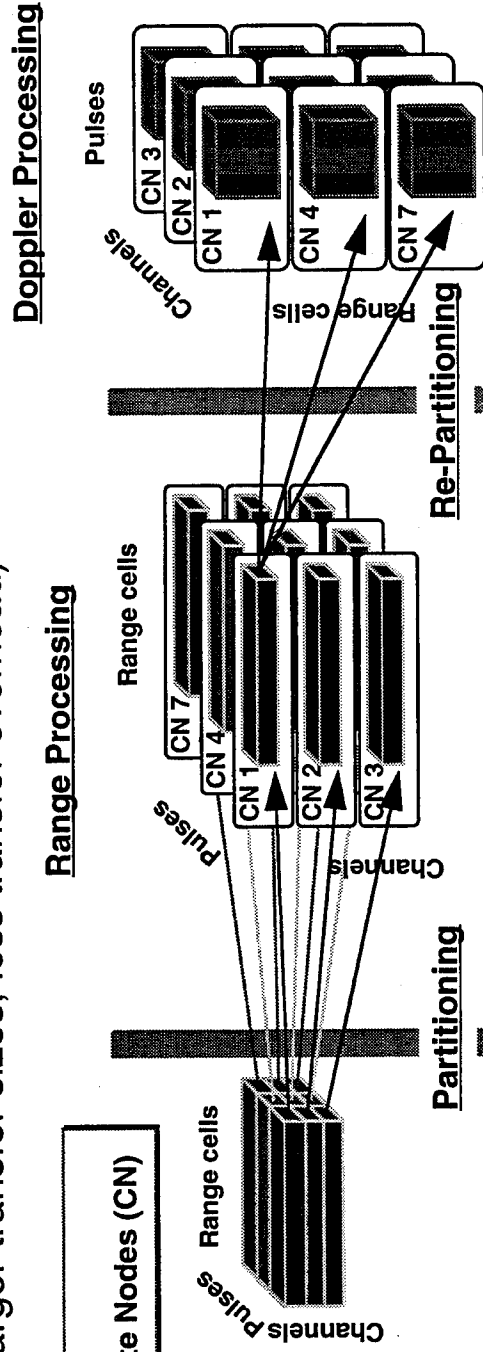


A Comparison of Two Methods of Data Set Partitioning

Method 2: Partitioning by sub-cube "bars" is better

- ☺ The number of processors over which data may be partitioned is extended to the number of possible bars.
- ★ Limited to the product of the two smallest dimensions
- ☺ Data re-partitioning between stages requires interprocessor communication only between processors in the same row or column of bars.
- ★ Requires approximately \sqrt{N} sets of N interprocessor transfers (larger transfer sizes, less transfer overhead)

Example:
9 Compute Nodes (CN)



Computer Systems, Inc.
MERCURY

ASAP Workshop

A methodology for effective STAP processing distribution

Step 1: Partition the data cube over a two dimensional "process set"

Step 2: Process on "whole" dimension.

Step 3: Re-partition data cube to make next processing dimension whole.

Step 4: Rotate data cube to make processing dimension sequential in memory.

Step 5: Repeat steps 1-4 for each processed dimension.

ASAP Workshop

2/96

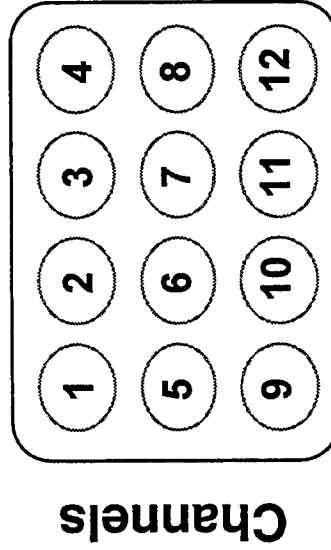
Computer Systems, Inc.
MERCURY

Data Set Partitioning

The PAS Process sets

- A process set is a logical grouping of processes that can share data and synchronize with each other and other process sets.
- Data set partitioning is achieved by dividing dimensions of the data set by dimensions of the process set.

Range cells



Example: Two-dimensional process set

A 3x4 process set (12 total processes).

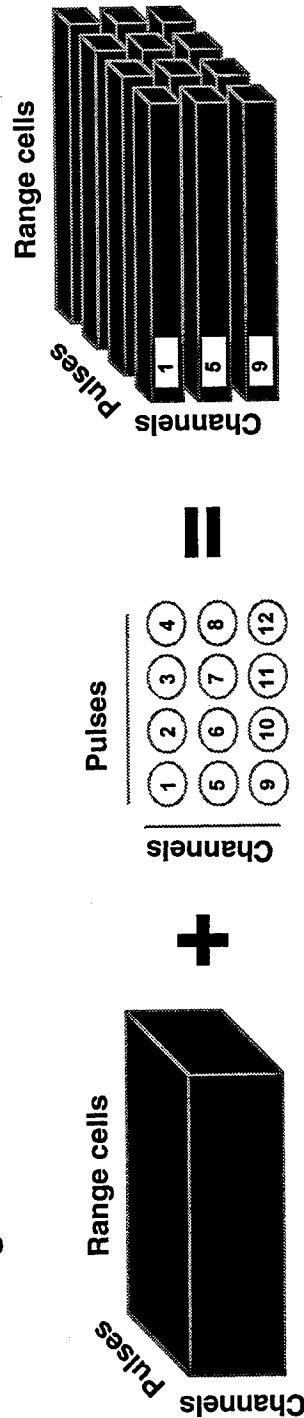
Each process receives 1/3 of the channels and 1/4 of the range cells.

The pulse dimension is un-segmented (whole) on each process.

Data Set Partitioning Examples

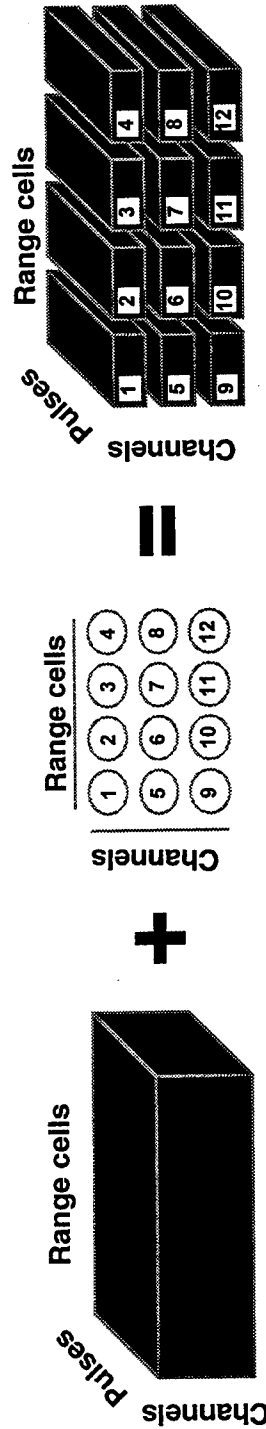
Example 1: Channel and Pulse Dimension Segmented

- Data set with channel and pulses dimensions applied to a 3x4 member process set. The range cell dimension is whole in the resulting partitioned data set.



Example 2: Channels and Range Cell Dimensions Segmented

- Data set with pulse and range cell dimensions applied to a 3x4 member process set. The pulse dimension is whole in the resulting partitioned data set.



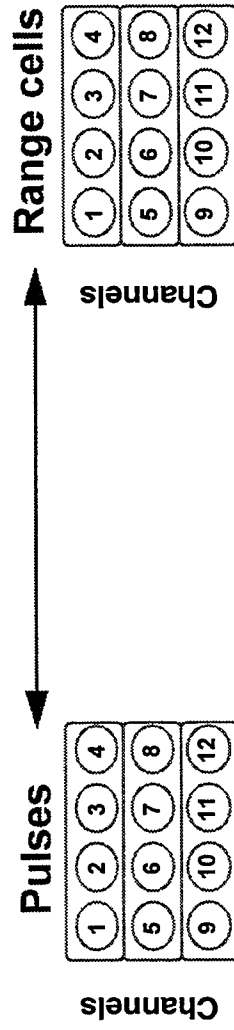
ASAP Workshop

2/96

Computer Systems, Inc.
MERCURY

Data Set Re-partitioning

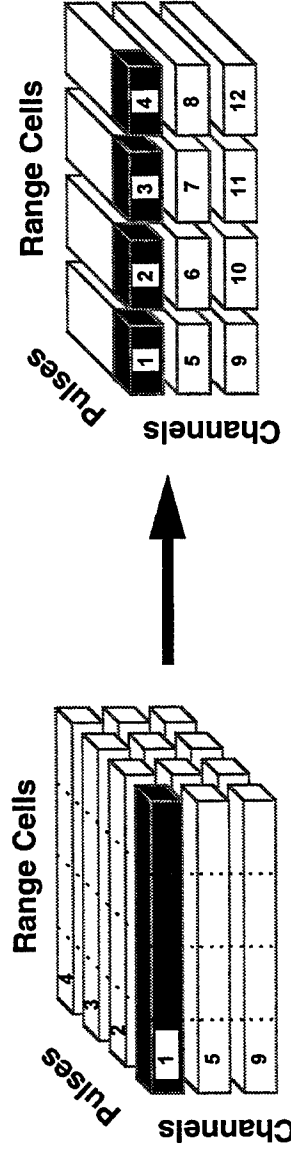
- Once processing on a dimension is complete, the cube must be re-partitioned to change which dimension is whole.
- Re-partitioning involves exchanging the current whole dimension with the next whole dimension to be processed.



Range Dimension is Whole

Pulse Dimension is Whole

- Data exchange is required only between processors in the same row (or column) of the two dimensional process set (i.e. process 1 transfers data only to process 2, 3, and 4).

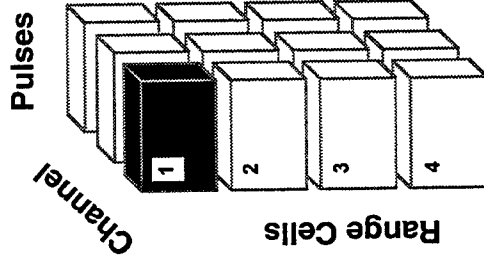


ASAP Workshop

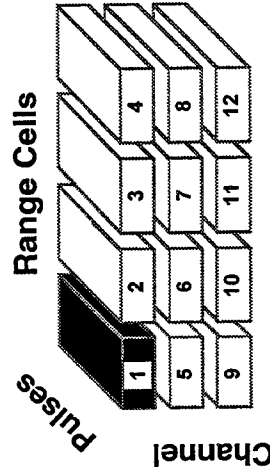
Computer Systems, Inc.
MERCURY

Data Set Rotation

- Rotation of the re-partitioned data set is required to make the “whole” dimension sequential in memory.
- Rotation does not change the dimensions assigned to the process set (partitioning is unchanged).
- Rotation is local to each processor and requires no inter-processor communication.



Rotate XYZ to ZXY



Example STAP Processing Flow

Range and Doppler Processing

Range Processing:
 cfft(range, FORWARD)
 cvmul(range, filter, range)
 cfft(range, INVERSE)

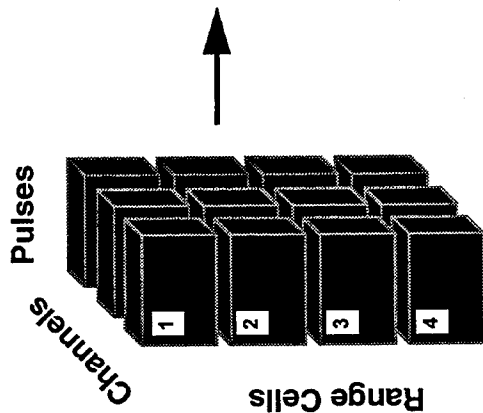
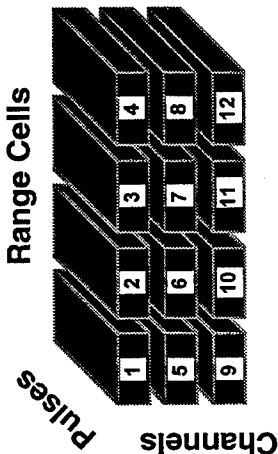
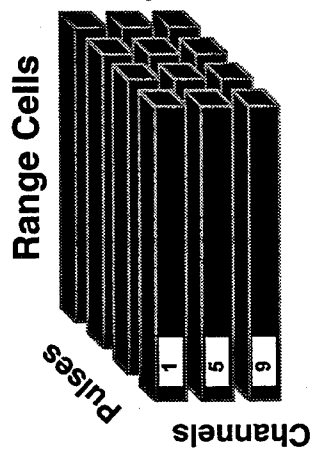
Re-Partitioning:
 To: Pulse Dimension Whole

Range Cells			
1	2	3	4
5	6	7	8
9	10	11	12

Channels

Rotation:
 XYZ to ZXY

Doppler Processing:
 cfft(pulse, FORWARD)



Example STAP Processing Flow

QRD, Back-substitution, and Beamforming

Re-Partitioning*:

To: Channel Dimension Whole

Range Cells

Doppler	1	2	3	4
1	1	2	3	4
2	5	6	7	8
3	9	10	11	12

Rotation:

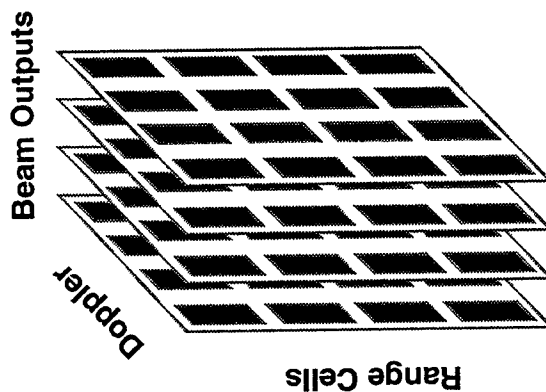
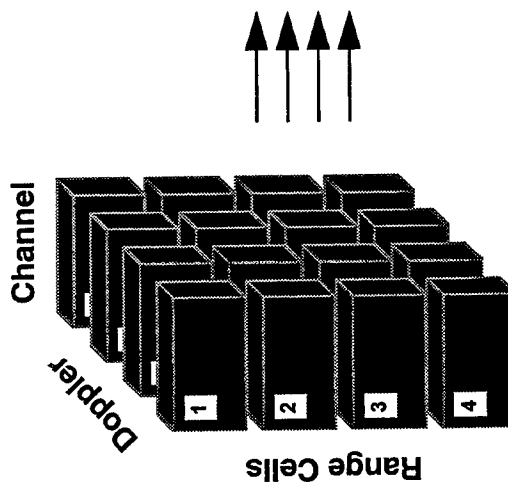
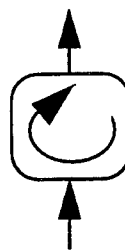
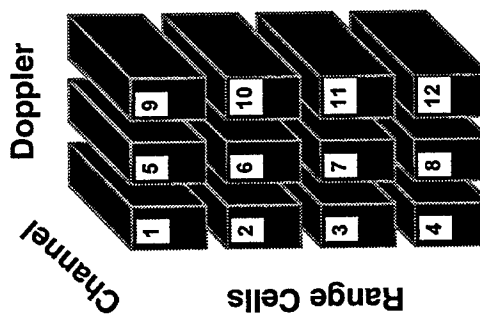
XYZ to ZYX

QR Decomposition* &

Back-substitution:

Output beamforming weights.

Beamforming:



*If the number of required processors exceeds [range segments * doppler cells] multiple processors are used in a pipeline to execute the QR Decomposition.

ASAP Workshop

Computer Systems, Inc.
MERCURY

Summary

- Significant gains in scalability and performance can be gained by distributing STAP data sets as sub-cube bars.
 - ★ Maximum number of processors over which the data set can be distributed is equal to the product of the two smallest dimensions of the data cube.
 - ★ Interprocessor communication between processing stages is isolated to disjoint clusters of processors.
 - ★ The efficiency of interprocessor communication is increased by reducing the number of required transfers and increasing the transfer size.
- Mercury has developed an effective methodology for partitioning the 3D data set for STAP processing.
 - ★ Sequenced partitioning, rotation, and processing steps provide a structured and efficient programming methodology.

STAP DETECTION WITH SUB-GAUSSIAN DISTRIBUTIONS AND FRACTIONAL LOWER-ORDER STATISTICS FOR AIRBORNE RADAR

George A. Tsihrintzis and Chrysostomos L. Nikias

University of Virginia
Department of Electrical Engineering
Thornton Hall

Charlottesville, VA 22903-2442
tel: (804) 924-6146
fax: (804) 924-8818
email: gat6v@va.edu

University of Southern California
Department of Electrical Engineering
Los Angeles, CA 90089-2564
email: nikias@siipi.usc.edu

Abstract We address the problem of coherent detection of a signal embedded in heavy-tailed noise modeled as a sub-Gaussian, alpha-stable process. We assume that the signal is a complex-valued vector of length L , known only within a multiplicative constant. The dependence structure of the noise, i.e., the underlying matrix of the sub-Gaussian process, is not known. The intent is to implement a generalized likelihood ratio detector which employs robust estimates of the unknown noise underlying matrix and the unknown signal strength. The performance of the proposed adaptive detector is compared to that of an adaptive matched filter that uses Gaussian estimates of the noise underlying matrix and the signal strength and is found to be clearly superior. The proposed new algorithms are theoretically analyzed and illustrated in a Monte-Carlo simulation.

SUB-GAUSSIAN RANDOM PROCESSES: DEFINITIONS, KEY RESULTS, AND
APPLICATIONS

George A. Tsihrintzis

Communication Systems Lab
Department of Electrical Engineering
University of Virginia
Charlottesville, VA 22903 - 2442

and

Chrysostomos L. Nikias

Signal and Image Processing Institute
Department of Electrical Engineering - Systems
University of Southern California
Los Angeles, CA 90089 - 2564

March 1996

OVERVIEW

- Symmetric Alpha-Stable (S α S) Random Variables and Processes
- Sub-Gaussian Random Processes
- Estimation of the Underlying Matrix of a Sub-Gaussian Process
- Signal Detection in Sub-Gaussian Noise
- Conclusions and Future Research

$S_{\alpha S}$ DISTRIBUTIONS

HISTORICAL OUTLINE

- Holtzmark, 1919
- Lévy, 1925
- Feller, 1966
- Mandelbrot, 60's
- Stuck and Kleiner, 1974
- Stuck, 1978
- Cambanis, Taqu, Koutrouvelis, Dumouchel, . . . , 70's and 80's
- Zolotarev, 1983 (Russian ed.) and 1986 (English ed.)
- Shao and Nikias, 1993 and Nikias and Shao, 1995
- Signal Processing Applications by Tsihrintzis, Tsakalides, and Ma in Nikias's research group

SaS DISTRIBUTIONS

DEFINITIONS

S α S pdfs are completely characterized by the following three parameters:

- *Characteristic Exponent* (α , $0 < \alpha \leq 2$): Heaviness of tails of pdf
- *Dispersion* (γ , $\gamma > 0$): Scale parameter determining spread of pdf
- *Location Parameter* (δ , $-\infty < \delta < \infty$): Point of symmetry of pdf

PLOTS OF SYMMETRIC, ALPHA-STABLE PDFs

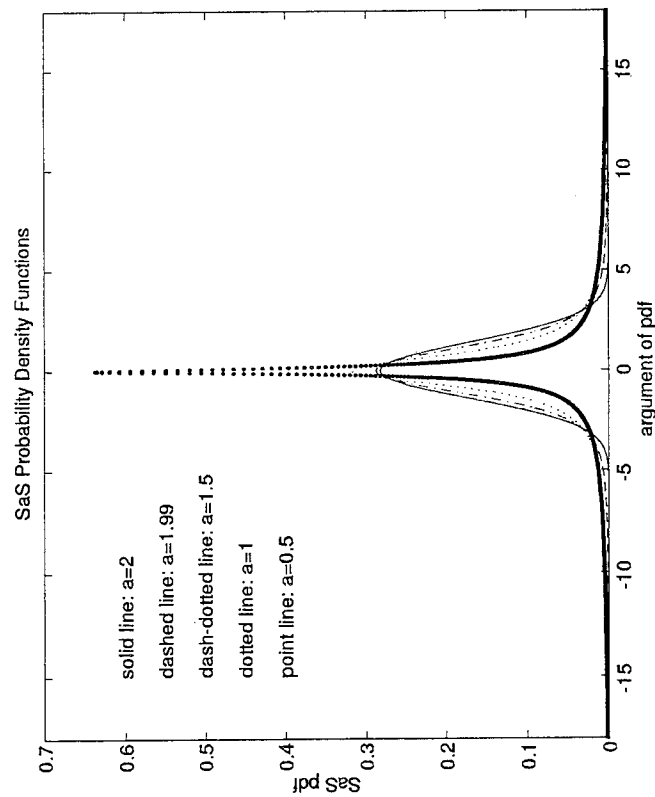


Figure 1:

PROPERTIES (1)

Motivation for the use of S α S random processes as statistical models for signals and noise:

- Naturally arise as limiting processes via the Generalized Central Limit Theorem
- Contain Gaussian and Cauchy random processes as subclasses
- Share many of the properties of Gaussian random processes, such as the stability property

PROPERTIES (2)

- With the exception of the Gaussian and the Cauchy pdf, no closed-form expressions are known for the remaining S α S pdfs
- Unlike Gaussian processes, have finite p^{th} order moments only for $p < \alpha$
- Classical Gaussian signal processing (signal detection, estimation, and reconstruction) results are inapplicable or even unavailable for non-Gaussian, S α S signal processing
- Stands a challenge to the signal processing community to address these signal processing problems within a S α S framework

SUB-GAUSSIAN RANDOM PROCESSES

DEFINITION

A sub-Gaussian random vector \underline{X} has characteristic function

$$\phi(\underline{t}) = \exp\left[-\frac{1}{2}(\underline{t}^T \underline{\underline{R}} \underline{t})^{\frac{\alpha}{2}}\right],$$

where the *underlying* matrix $\underline{\underline{R}}$ is positive-definite

FACTS

Theorem 1: A sub-Gaussian random vector \underline{X} has a multivariate SoS distribution

Theorem 2: A sub-Gaussian random vector \underline{X} with underlying matrix $\underline{\underline{R}}$ can be expressed as

$$\underline{X} = \eta^{\frac{1}{2}} \underline{Y},$$

where \underline{Y} is a Gaussian random vector of mean zero and covariance matrix $\underline{\underline{R}}$ and η is a positive stable random variable of characteristic exponent $\frac{\alpha}{2}$

SIMULATION OF SUB-GAUSSIAN NOISE VECTORS

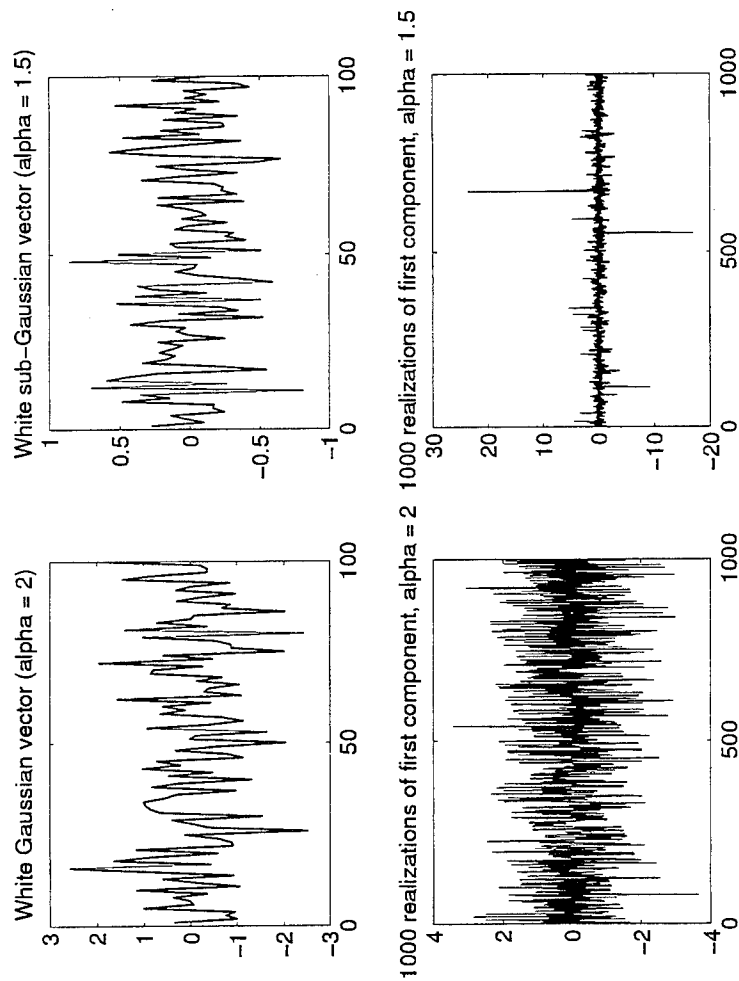


Figure 2:

ESTIMATION OF THE UNDERLYING MATRIX
OF A SUB-GAUSSIAN PROCESS

COVARIATION BETWEEN S α S RANDOM VARIABLES

Let x_1 and x_2 be two S α S random variables. Their covariation is defined as

$$[x_1, x_2]_\alpha = \frac{\mathcal{E}\{x_1 x_2^{<p-1>}\}}{\mathcal{E}\{|x_2|^p\}} \gamma_2,$$

where the notation

$$(\cdot)^{<a>} \equiv |\cdot|^{a-1}(\cdot)$$

is used

ESTIMATION OF THE UNDERLYING MATRIX OF A SUB-GAUSSIAN PROCESS

FACT

Theorem 3: Let \underline{X} be a sub-Gaussian random vector with underlying matrix \underline{R} and define its covariation matrix \underline{C} with elements $C_{ij} = [X_i, X_j]_\alpha$. Then:

$$C_{ij} = 2^{-\frac{\alpha}{2}} R_{ij} R_{jj}^{\frac{\alpha-2}{2}}$$

or, equivalently,

$$\begin{aligned} R_{jj} &= 2 C_{jj}^{\frac{2}{\alpha}} \\ R_{ij} &= 2^{\frac{\alpha}{2}} C_{ij} R_{jj}^{\frac{\alpha-2}{2}} \end{aligned}$$

UNDERLYING MATRIX ESTIMATORS (1)

Consider the estimation of the underlying matrix $\underline{\underline{R}}_{64 \times 64} = \text{diag}(1, 1, \dots, 1)$ from $K = 500$ independent realizations using the estimators

$$\hat{\underline{\underline{R}}} = \frac{1}{K} \sum_{k=1}^K \underline{\underline{X}}_k^T \underline{\underline{X}}_k$$

$\hat{\underline{\underline{R}}} =$ as obtained from covariation matrix estimates

The mean over 100 Monte-Carlo runs of the 32nd row in the estimated matrix is shown next for $\alpha = 2$ and $\alpha = 1.5$

ESTIMATION OF THE UNDERLYING MATRIX OF A SUB-GAUSSIAN PROCESS

UNDERLYING MATRIX ESTIMATORS (2)

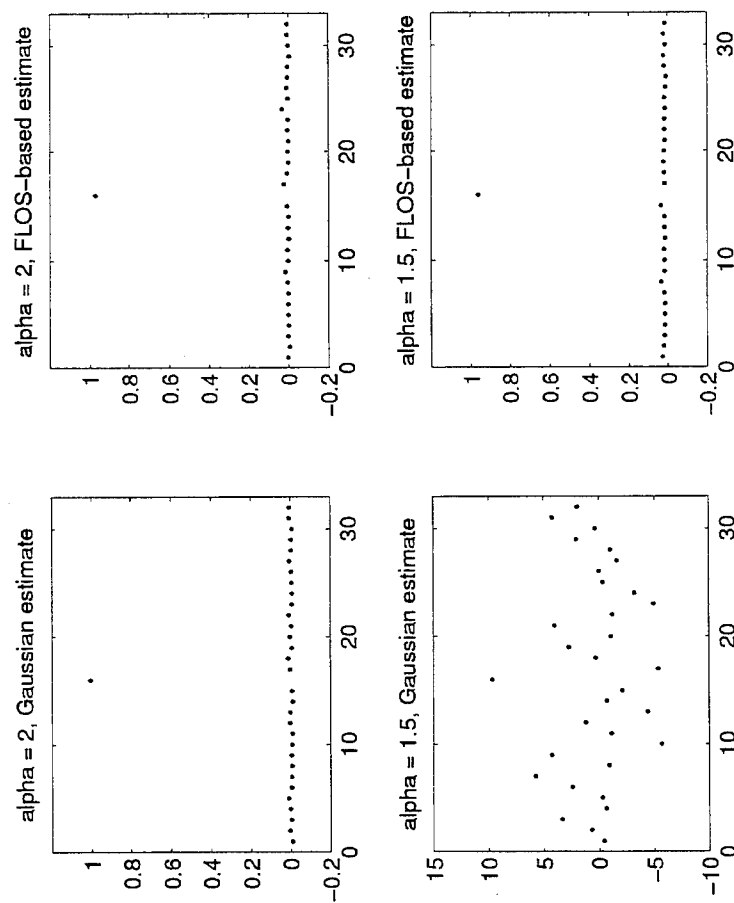


Figure 3:

ESTIMATION OF THE UNDERLYING MATRIX OF A SUB-GAUSSIAN PROCESS

SIGNAL DETECTION IN SUB-GAUSSIAN NOISE

PROBLEM FORMULATION

- Hypothesis testing problem:

$$H_0 : \underline{X}^k = \underline{N}^k$$

$$k = 1, 2, 3, \dots, K$$

$$H_1 : \underline{X}^k = A\underline{S} + \underline{N}^k,$$

where \underline{S} is a known signal vector, A is an unknown signal amplitude, and \underline{N}^k are independent, identically distributed sub-Gaussian random vectors of characteristic exponent α and unknown underlying matrix \underline{R} .

- Approach: Generalized likelihood ratio
- Difficulty: Lack of closed-form expression for general sub-Gaussian pdf
- Solution: Use multidimensional Cauchy pdf

GENERALIZED LIKELIHOOD RATIO TESTS

- Gaussian:

$$t_G = (2/K) \sum_{k=1}^K (\hat{A}\underline{S})^T \hat{\underline{\underline{R}}}^{-1} \underline{X}^k - |\hat{A}|^2 \underline{S}^T \hat{\underline{\underline{R}}}^{-1} \underline{S}$$

- Cauchy:

$$t_C = - \sum_{k=1}^K \log \left[\frac{1 + (\underline{X}^k - \hat{A}\underline{S})^T \hat{\underline{\underline{R}}}^{-1} (\underline{X}^k - \hat{A}\underline{S})}{1 + \underline{X}^{kT} \hat{\underline{\underline{R}}}^{-1} \underline{X}^k} \right],$$

where \hat{A} = sample-median $(\underline{S}^T \underline{X}^1, \underline{S}^T \underline{X}^2, \dots, \underline{S}^T \underline{X}^K)$, $\hat{A} = (1/K) \sum_{k=1}^K \underline{S}^T \underline{X}^k$, and $\hat{\underline{\underline{R}}}$ and $\hat{\underline{\underline{R}}}^{-1}$ are obtained as stated before.

PERFORMANCE EVALUATION (1)

Simulation parameters:

- White sub-Gaussian noise, i.e., $\underline{\underline{R}} = \text{diag} = (1, 1, \dots, 1)$
- Length of observation vector $\underline{X} = 8$
- Number of independent observations $K = 10$
- Fractional, lower-order moment in underlying matrix estimator $p = 0.6$
- Number of Monte-Carlo runs 10,000

PERFORMANCE EVALUATION (2)

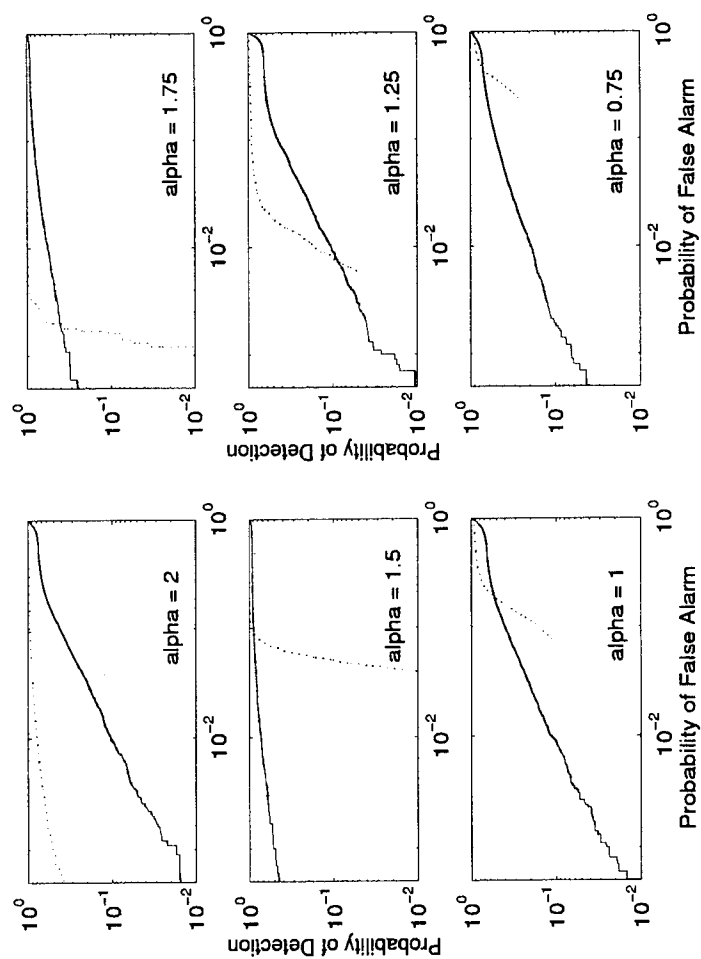


Figure 4: Gaussian (dashed line) versus Cauchy (solid line) detector

PERFORMANCE EVALUATION (3)

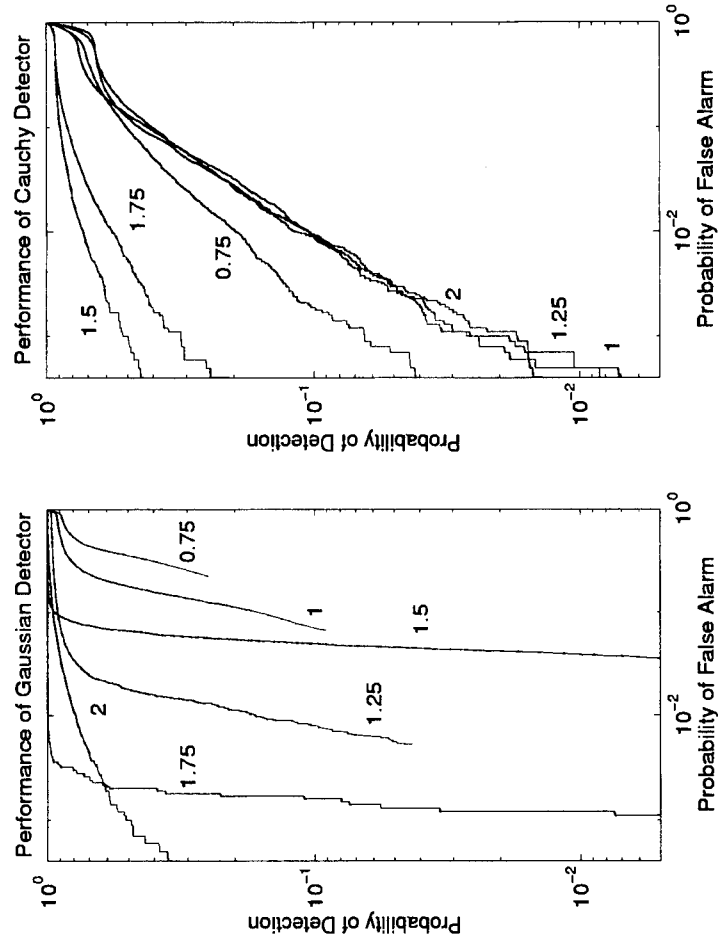


Figure 5: Gaussian (left column) versus Cauchy (right column) detector performance

CONCLUSIONS AND FUTURE WORK

CONCLUSIONS AND FUTURE WORK

- S α S processes
 - form a class of statistical models with interesting properties
 - are useful in modeling impulsive phenomena and time series containing outliers
 - provide a paradigm for signal processing with fractional, lower-order statistics
- Sub-Gaussian processes form a special subclass of S α S processes which combine capabilities to model impulsiveness and dependence structure
- A generalized likelihood ratio signal detector designed using the multivariate Cauchy distribution will be robust in the class of sub-Gaussian noises
- Applications of the above findings in radar, as well as extensions to other signal detection problems are currently under examination
- Extension to the detection of fading targets and study of the performance of several receiver diversity systems in alpha-stable impulsive interference

CONCLUSIONS AND FUTURE WORK

ADAPTIVE ARRAY PROCESSING IN NON-GAUSSIAN ENVIRONMENTS

Christ D. Richmond

Massachusetts Institute of Technology
305 Memorial Drive, Room 512B
Cambridge, MA 02139
tel: (617) 225-9832 or (617) 981-0346
email: richmond@boreas.mit.edu

Abstract Recently, non-Gaussian signal and array processing has received increased attention. The power resolution of available technologies based on sophisticated statistical processing techniques brings into question the classic assumption of data normality. Hence, there exists a need for statistical performance analyses which address in a relatively general sense a plurality of possible non-Gaussian distributions, especially in adaptive array scenarios which often involve estimation of the data covariance via the sample covariance matrix (SCM). The theory of complex multivariate elliptically contoured (MEC) distributions provides one such vehicle to perform such analyses. In this presentation we replace the classic assumption of data normality with one of MEC distributed data and reexamine many of the important Gaussian-based results of adaptive array detection and signal estimation. In particular, Kelly's Generalized Likelihood Ratio Test is shown to be optimal over a broad class of MECs. The PFA and CFAR loss are shown invariant over this entire MEC class, and PD is data distribution dependent. Exact statistical analyses of the SCM based LCMV and GSC beamformers, which include pdfs for their SCM-based weightings, beam responses, and beamformer outputs are given. All results suggest significant robustness implications to adaptive array processing in non-Gaussian environments.

Adaptive Array Processing in Non-Gaussian Environments

by Christ D. Richmond

Department of Electrical Engineering and Computer Science
Massachusetts Institute of Technology

ASAP Workshop MIT Lincoln Laboratory March 14, 1996

Outline 1

I. Problem Statement/Notation

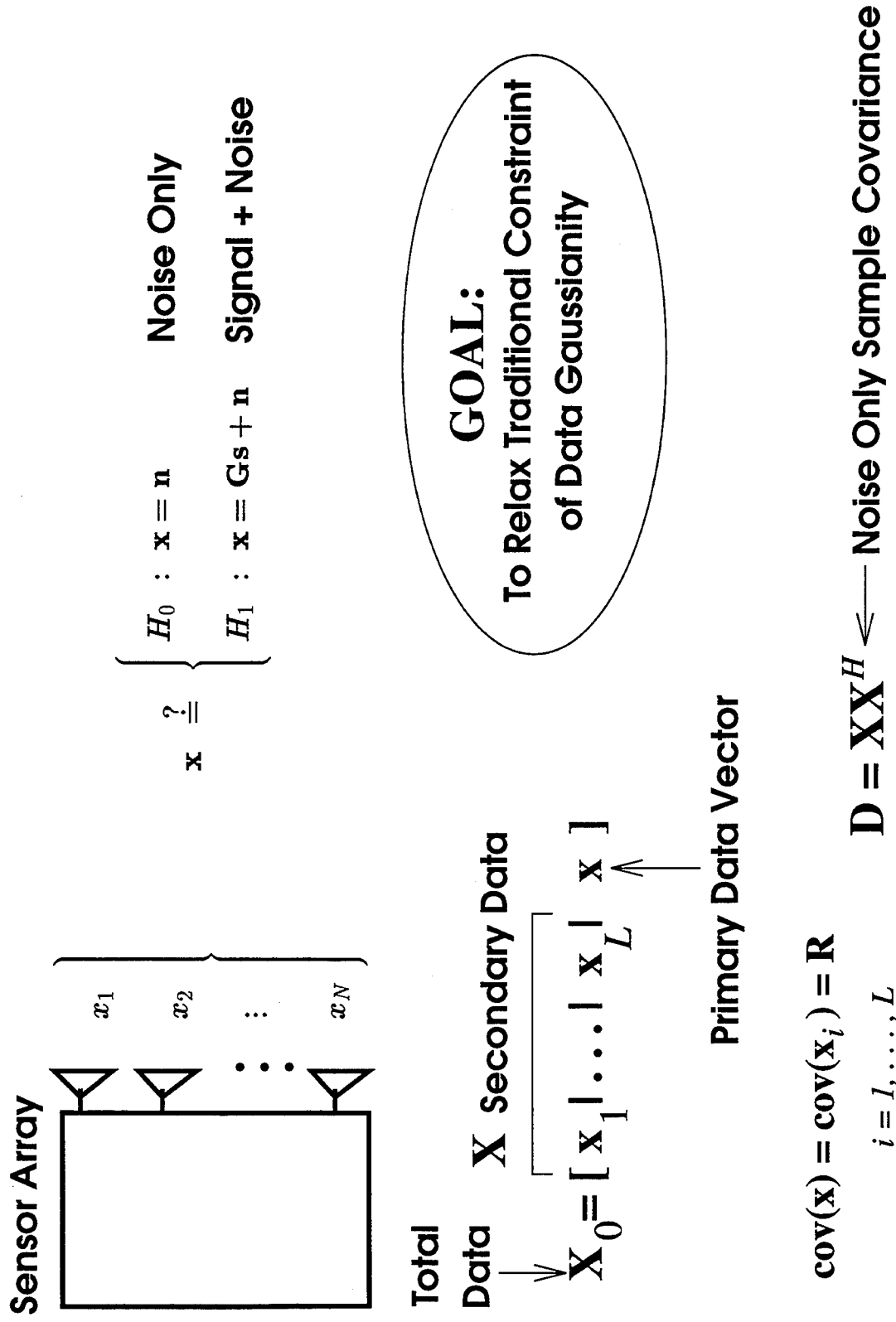
A. Adaptive Array Detection/Estimation

(1) Unknown Data Covariance/Signal

(2) Training Set Available

B. Previous Work/New Contributions

Adaptive Array Detection (AAD) / Estimation



Gaussian Based Array Processing

Capon, Goodman (1970)	-----	Spectral Estimation
Reed, Mallett, Brennan (1974)	-----	Adaptive Detection
<i>Khatri, Rao (1985,1987)</i>	-----	Adaptive Detection
Kelly (1985)	-----	Adaptive Detection
Kelly, Forsythe (1989)	-----	Adaptive Detection/Estimation
Steinhardt (1991)	-----	Adaptive Estimation
Robey, Fuhmann, Kelly, Nitzberg (1992)	-----	Adaptive Detection

New Results

- Show that over a Broad Class of Multivariate Elliptically Contoured (MEC) distributions both the GLRT and AMF Detectors :
 - Remain "Optimal " Detectors
 - Have invariant PDFs in absence of target (Under H_0)
- Gaussian Based ML estimates remain ML under many MECs
 - PDFs for Adaptive Beamformers/Power Spectral Estimator

Outline 2

II. Gaussian Based Detectors

A. GLRT

B. AMF

Gaussian Based GLRT & AMF

- Kelly said let data matrix \mathbf{X}_0 have complex normal densities

$$g_{H_i} = |\mathbf{R}|^{-(L+1)} \pi^{-N(L+1)} \exp[-\text{tr} \mathbf{R}^{-1} (\mathbf{X}_0 - \mathbf{M}_i) (\mathbf{X}_0 - \mathbf{M}_i)^H], \quad i = 0, 1$$

$$H_0 : \mathbf{M}_0 = \mathbf{0}_{N \times (L+1)} \quad H_1 : \mathbf{M}_1 = [\mathbf{0}_{N \times L} | \mathbf{G} \mathbf{s}]$$

GLRT

Use ML estimates
of Unknowns

$$\left[\frac{\max_{\mathbf{s}, \mathbf{R}} g_{H_1}(\cdot)}{\max_{\mathbf{R}} g_{H_0}(\cdot)} \right]^{\frac{1}{(L+1)}} =$$

$$t_{GLRT}(\mathbf{X}_0) = \frac{1 + \mathbf{x}^H \mathbf{D}^{-1} \mathbf{x}}{1 + \mathbf{x}^H \mathfrak{P}(\mathbf{G} | \mathbf{D}^{-1}) \mathbf{x}}$$

- AMF says define ML signal estimate, then normalize by noise power to achieve CFAR (Robey, et. al.)

$$t_{AMF}(\mathbf{X}_0) = \mathbf{x}^H \mathbf{D}^{-1} \mathbf{G} (\mathbf{G}^H \mathbf{D}^{-1} \mathbf{G})^{-1} \mathbf{G}^H \mathbf{D}^{-1} \mathbf{x} = \frac{|\mathbf{g}^H \mathbf{D}^{-1} \mathbf{x}|^2}{\mathbf{g}^H \mathbf{D}^{-1} \mathbf{g}}$$



when $\mathbf{G} = \mathbf{g}$

Outline 3

III. MEC Based Detectors

A. Problem Reformulation

B. Derivation of Solutions

C. PFA and PD

MEC Based Detector: AAD Problem Reformulation

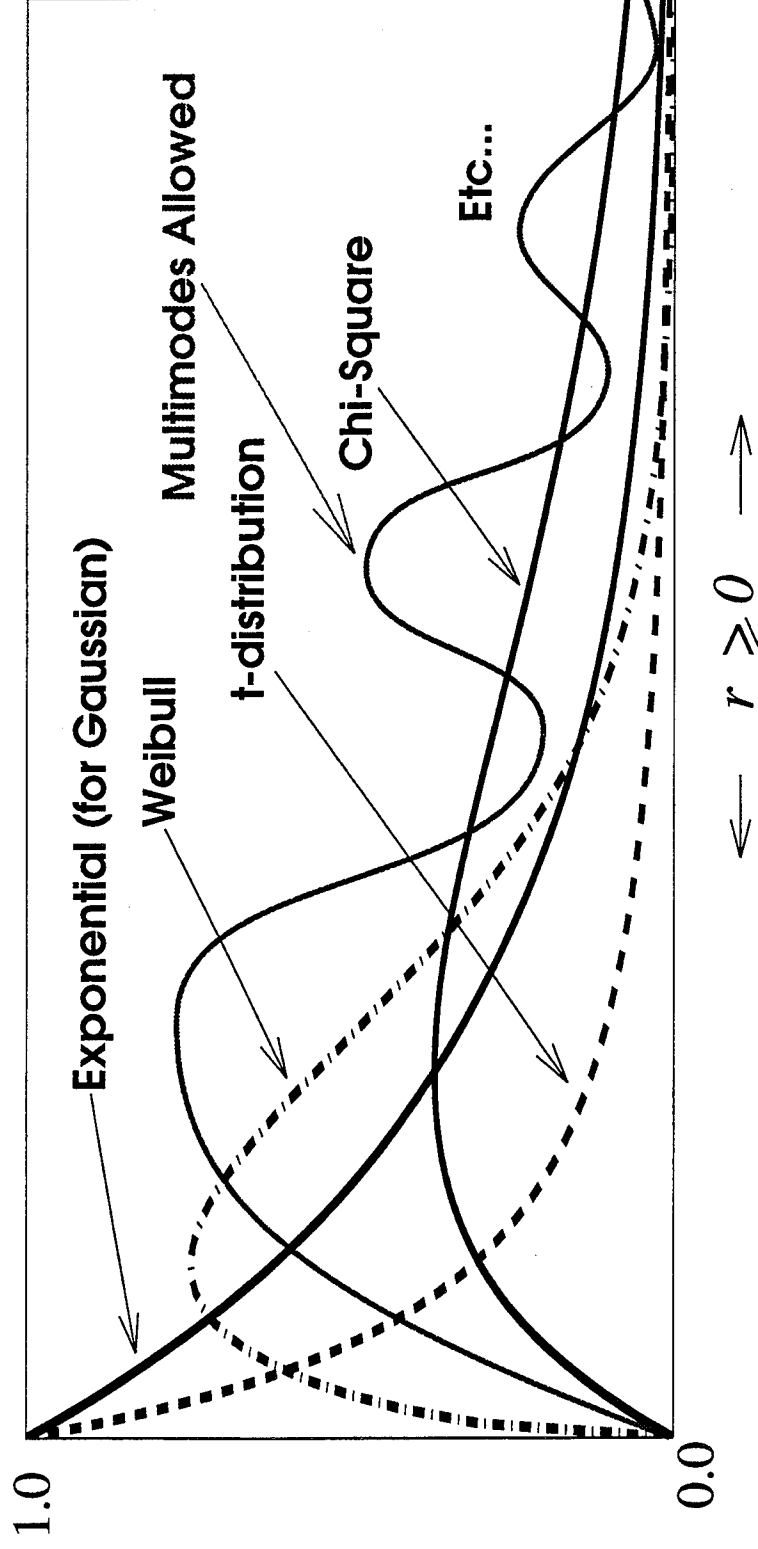
Let data matrix \mathbf{X}_0 have MEC densities given by

$$g_{H_i} = |\mathbf{R}|^{-(L+1)} g[\text{tr} \mathbf{R}^{-1}(\mathbf{X}_0 - \mathbf{M}_i)(\mathbf{X}_0 - \mathbf{M}_i)^H], \quad i = 0, 1$$

$$H_0 : \mathbf{M}_0 = \mathbf{0}_{N \times (L+1)}$$

$$H_1 : \mathbf{M}_1 = [\mathbf{0}_{N \times L} | \mathbf{G} \mathbf{s}]$$

- $g(r)$ is a scalar function on $r \geq 0$:



Derivation of MEC GLRT Detector: Maximizing over \mathbf{R}

GLRT

$$\frac{\left[\frac{\max_{\mathbf{s}, \mathbf{R}} g_{H_1}(\cdot)}{\max_{\mathbf{R}} g_{H_0}(\cdot)} \right]^{\frac{1}{(L+1)}}}{\left[\frac{\max_{\mathbf{s}, \mathbf{R}} g_{H_1}(\cdot)}{\max_{\mathbf{R}} g_{H_0}(\cdot)} \right]^{\frac{1}{(L+1)}}} = ?$$

Use ML estimates
of Unknowns

Consider maximizing likelihood functions over data covariance \mathbf{R}

Let $\mathbf{D}_0 = (\mathbf{X}_0 - \mathbf{M})(\mathbf{X}_0 - \mathbf{M})^H$ and $\mathbf{A} = \mathbf{R}^{-1/2} \mathbf{D}_0 \mathbf{R}^{-1/2}$

$$\begin{aligned} \max_{\mathbf{R}} \mathcal{L}(\mathbf{s}, \mathbf{R}) &= \max_{\mathbf{R}} |\mathbf{R}|^{-(L+1)} g[\text{tr} \mathbf{R}^{-1} (\mathbf{X}_0 - \mathbf{M})(\mathbf{X}_0 - \mathbf{M})^H] \\ &= \max_{\mathbf{A}} |\mathbf{D}_0|^{-(L+1)} |\mathbf{A}|^{(L+1)} g[\text{tr} \mathbf{A}] = |\mathbf{D}_0|^{-(L+1)} \left[\prod_{i=1}^N \lambda_i^{\frac{1}{N}}(\mathbf{A}) \right]^{N(L+1)} \\ &\leq |\mathbf{D}_0|^{-(L+1)} \left[\frac{1}{N} \sum_{i=1}^N \lambda_i(\mathbf{A}) \right]^{N(L+1)} g \left[\sum_{i=1}^N \lambda_i(\mathbf{A}) \right] \end{aligned}$$

Equality is obtained if and only if

$$\lambda_i(\mathbf{A}) = \lambda_0 \quad \text{for all } i \implies \mathbf{A} = \lambda_0 \mathbf{I} \implies \mathbf{R} = \mathbf{D}_0 / \lambda_0$$

$$\max_{\mathbf{R}} \mathcal{L}(\mathbf{s}, \mathbf{R}) = |\mathbf{D}_0|^{-(L+1)} \max_{\lambda_0} \lambda_0^{N(L+1)} g(N\lambda_0) = |\mathbf{D}_0|^{-(L+1)} \cdot h_{MAX} \implies$$

$$\lambda_0 = \tau_{MAX} \implies \hat{\mathbf{R}}_{ML} = \mathbf{D}_0 / \tau_{MAX} \implies \begin{array}{l} \text{Sample Covariance Remains} \\ \text{ML Estimate of Data Covariance} \end{array}$$

Derivation of MEC GLRT Detector: Maximizing over \mathbf{s}

Recall likelihood function $\max_{\mathbf{R}} \mathcal{L}(\mathbf{s}, \mathbf{R}) = |\mathbf{D}_0|^{-(L+1)} \cdot h_{MAX}$

- Maximizing $g_{H_0}(\cdot)$ over all unknowns done, but must maximize $g_{H_1}(\cdot)$ over unknown signal \mathbf{s}

To maximize likelihood we minimize determinant :

$$|\mathbf{D}_0| = |\mathbf{D}| \cdot [1 + (\mathbf{x} - \mathbf{G}\mathbf{s})^H \mathbf{D}^{-1} (\mathbf{x} - \mathbf{G}\mathbf{s})]$$

Thus, let $\widehat{\mathbf{W}}_{ML} = \mathbf{D}^{-1} \mathbf{G} (\mathbf{G}^H \mathbf{D}^{-1} \mathbf{G})^{-1}$ and $\mathfrak{P}(\mathbf{V}|\mathbf{H}) = \mathbf{H} - \mathbf{H}\mathbf{V}(\mathbf{V}^H \mathbf{H}\mathbf{V})^{-1} \mathbf{V}^H \mathbf{H}$

Completing the square we obtain

$$(\mathbf{x} - \mathbf{G}\mathbf{s})^H \mathbf{D}^{-1} (\mathbf{x} - \mathbf{G}\mathbf{s}) = (\mathbf{s} - \widehat{\mathbf{W}}_{ML}^H \mathbf{x})^H (\mathbf{G}^H \mathbf{D}^{-1} \mathbf{G}) (\mathbf{s} - \widehat{\mathbf{W}}_{ML}^H \mathbf{x}) + \mathbf{x}^H \mathfrak{P}(\mathbf{G}|\mathbf{D}^{-1}) \mathbf{x}$$

Hence $\arg \max_{\mathbf{s}} \mathcal{L}[\mathbf{s}, \mathbf{D}_0 / r_{MAX}] = (\mathbf{G}^H \mathbf{D}^{-1} \mathbf{G})^{-1} \mathbf{G}^H \mathbf{D}^{-1} \mathbf{x} = \hat{\mathbf{s}}_{ML}$ 

Sample Covariance Based LCMV
Beamformer Remains ML Signal Estimate

- Thus, usual Gaussian based AMF detector obtained under other MECs

MEC Based Decision Statistic

Thus, the maximized likelihoods are

$$\max_{\mathbf{R}} g_{H_0}(\cdot) = [|\mathbf{D}| \cdot (1 + \mathbf{x}^H \mathbf{D}^{-1} \mathbf{x})]^{-(L+1)} \quad \max_{\mathbf{s}, \mathbf{R}} g_{H_1}(\cdot) = \{|\mathbf{D}| \cdot [1 + \mathbf{x}^H \mathbf{p}(\mathbf{G}|\mathbf{D}^{-1})\mathbf{x}]\}^{-(L+1)}$$

The Resulting MEC
Based Decision
Statistic is given by :

$$\left[\frac{\max_{\mathbf{s}, \mathbf{R}} g_{H_1}(\cdot)}{\max_{\mathbf{R}} g_{H_0}(\cdot)} \right]^{\frac{1}{(L+1)}} = \frac{1 + \mathbf{x}^H \mathbf{D}^{-1} \mathbf{x}}{1 + \mathbf{x}^H \mathbf{p}(\mathbf{G}|\mathbf{D}^{-1})\mathbf{x}} \underset{H_0}{\overset{H_1}{> <}} \eta$$

Recapitulation / Remarks

- Showed that Under Broad Class of MECs:
 - GLRT and AMF detectors remains the same
 - ML Signal parameter estimate remains the same
 - Adaptive Beamforming
 - Adaptive Power Spectral Estimation

Performance: PDF of MEC Based Detectors

PFA :

Under hypothesis H_0 both the GLRT and AMF statistic are scale invariant such that $t(c\mathbf{X}_0) = t(\mathbf{X}_0)$ at least for $c > 0$. The pdfs of statistics with this property are completely invariant over all MECs.

PD :

To simplify let $\mathbf{G} = \mathbf{g}$. Define the integral operation

$$g_{K:M}(r) \triangleq \frac{\pi^{K-M}}{(K-M-1)!} \int_0^\infty a^{K-M} g(r+a) da$$

Then the MEC based GLRT statistic has pdf such that

$t_{GLRT}(\mathbf{X}_0) \stackrel{d}{=} 1 + \frac{|\tilde{\mathbf{u}}|^2}{\alpha}$ where the joint pdf for $\tilde{\mathbf{u}}$ and α is given by

$$\frac{\pi^{(L-N+1)}}{(L-N)!} \rho_{RMB} \alpha^{L-N} g_{N(L+1):L-N+2} \left(\left| \tilde{\mathbf{u}} - S \sqrt{\mathbf{g}^H \mathbf{R}^{-1} \mathbf{g}} \right|^2 \rho_{RMB} + \alpha \right)$$

Outline 4

IV. Adaptive Beamforming: PDFs of SCB

A. Weightings

B. Beam Responses

C. Beamformer Outputs

Adaptive Beamforming

Signal Estimate and Beamformer Output are Respectively of Forms

$$\hat{\mathbf{s}} = \mathbf{W}^H \mathbf{x} \quad \text{and} \quad \hat{y} = \mathbf{w}^H \mathbf{x}$$

Beamforming Structures Considered Include Sample Covariance Based:

- Maximum Likelihood (ML) Signal Estimator
- Linearly Constrained Minimum Variance (LCMV) Beamformer
- Generalized Sidelobe Canceller (GSC) Implementation of LCMV

Beamformer Weightings

R Known:

Clairvoyant Weightings

$$\begin{aligned} \text{ML: } \mathbf{W}_{ML} &= \mathbf{R}^{-1} \mathbf{G} (\mathbf{G}^H \mathbf{R}^{-1} \mathbf{G})^{-1} \\ \text{LCMV: } \mathbf{w}_{LCMV} &= \mathbf{W}_{ML} \mathbf{f} \quad (\text{also MVDR}) \\ \text{GSC: } \mathbf{w}_{gsc} &= \mathbf{W}_{GSC} \mathbf{f} \\ \mathbf{W}_{GSC} &= [\mathbf{I}_N - \mathbf{G}_\perp \boldsymbol{\Omega}_{GSC}] \mathbf{G} (\mathbf{G}^H \mathbf{G})^{-1} \\ \boldsymbol{\Omega}_{GSC} &= (\mathbf{G}_\perp^H \mathbf{R} \mathbf{G}_\perp)^{-1} \mathbf{G}_\perp^H \mathbf{R} \end{aligned}$$

R Unknown:

SCB Weightings

$$\begin{aligned} \hat{\mathbf{W}}_{ML} &= \mathbf{D}^{-1} \mathbf{G} (\mathbf{G}^H \mathbf{D}^{-1} \mathbf{G})^{-1} \\ \hat{\mathbf{w}}_{LCMV} &= \hat{\mathbf{W}}_{ML} \mathbf{f} \quad (\text{also MVDR}) \\ \hat{\mathbf{w}}_{gsc} &= \hat{\mathbf{W}}_{GSC} \mathbf{f} \\ \hat{\mathbf{W}}_{GSC} &= [\mathbf{I}_N - \mathbf{G}_\perp \hat{\boldsymbol{\Omega}}_{GSC}] \mathbf{G} (\mathbf{G}^H \mathbf{G})^{-1} \\ \hat{\boldsymbol{\Omega}}_{GSC} &= (\mathbf{G}_\perp^H \mathbf{D} \mathbf{G}_\perp)^{-1} \mathbf{G}_\perp^H \mathbf{D} \end{aligned}$$

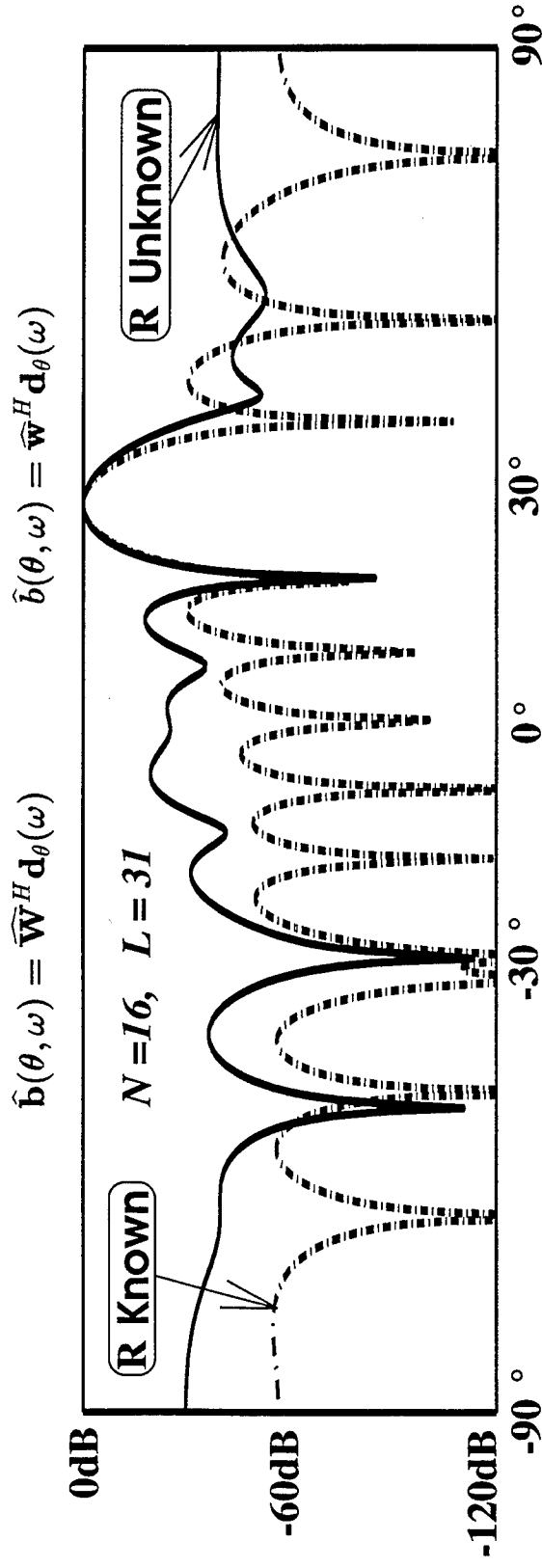
Beamformer PDFs

Beamformer Weightings: Unified Stochastic Representation Over MECs

$$\left. \begin{array}{l} \widehat{\mathbf{W}} \stackrel{d}{=} \mathbf{W} - \mathbf{A}\mathcal{T}\mathbf{B} \\ \widehat{\mathbf{w}} \stackrel{d}{=} \mathbf{w} - \mathbf{C}\mathcal{T}\mathbf{d} \end{array} \right\} \mathcal{T} \text{ is Standardized complex Multivariate t-distr.}$$

A, B, C, d are Deterministic matrices

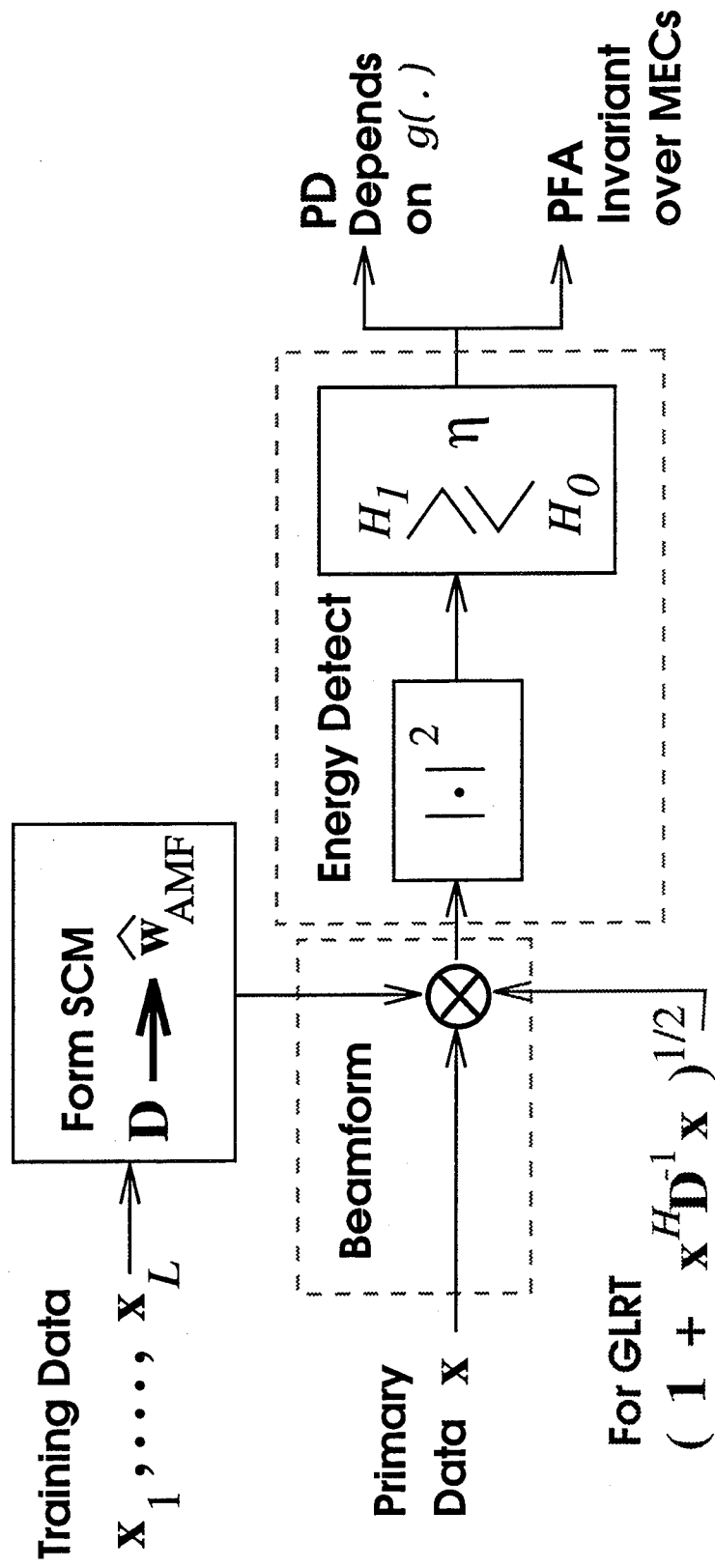
Beam Responses:



$$\widehat{\mathbf{b}}(\theta, \omega) = \widehat{\mathbf{W}}^H \mathbf{d}_\theta(\omega) \quad \text{and} \quad \widehat{\mathbf{b}}(\theta, \omega) = \widehat{\mathbf{w}}^H \mathbf{d}_\theta(\omega) \text{ are Generalized complex t-distr.}$$

Beamformer Outputs: Depends on $g(\cdot)$.

MEC Based Detectors



Outline 5

V. Miscellaneous Results

A. MEC Based Spectral Estimation

B. Structured Covariance Estimation

Spectral Estimation w/ MEC Data

Recall Capon's Sample Covariance Based Power Spectral Estimator

$$P_{Capon}(\theta, \omega) = \frac{1/r_{MAX}}{\mathbf{d}_{\theta}^H(\omega) \mathbf{D}^{-1} \mathbf{d}_{\theta}(\omega)} \stackrel{d}{=} Z_g \times \frac{1/r_{MAX}}{\mathbf{d}_{\theta}^H(\omega) \mathbf{R}^{-1} \mathbf{d}_{\theta}(\omega)}$$

$$Z_g \stackrel{d}{=} \left\{ \begin{array}{ll} \chi_{L-N+1}^2 & \text{Complex Gaussian Data (Capon, Goodman 1970)} \\ ? & \text{Arbitrary Complex MEC Data, Depends on } g(.). \end{array} \right.$$

MEC Structured Covariance Estimation

Following Burg et al, let objective function be the complex MEC pdf

$$p(\mathbf{D}, \mathbf{R}) = |\mathbf{R}|^{-L} g[\text{tr}(\mathbf{R}^{-1} \mathbf{D})]$$

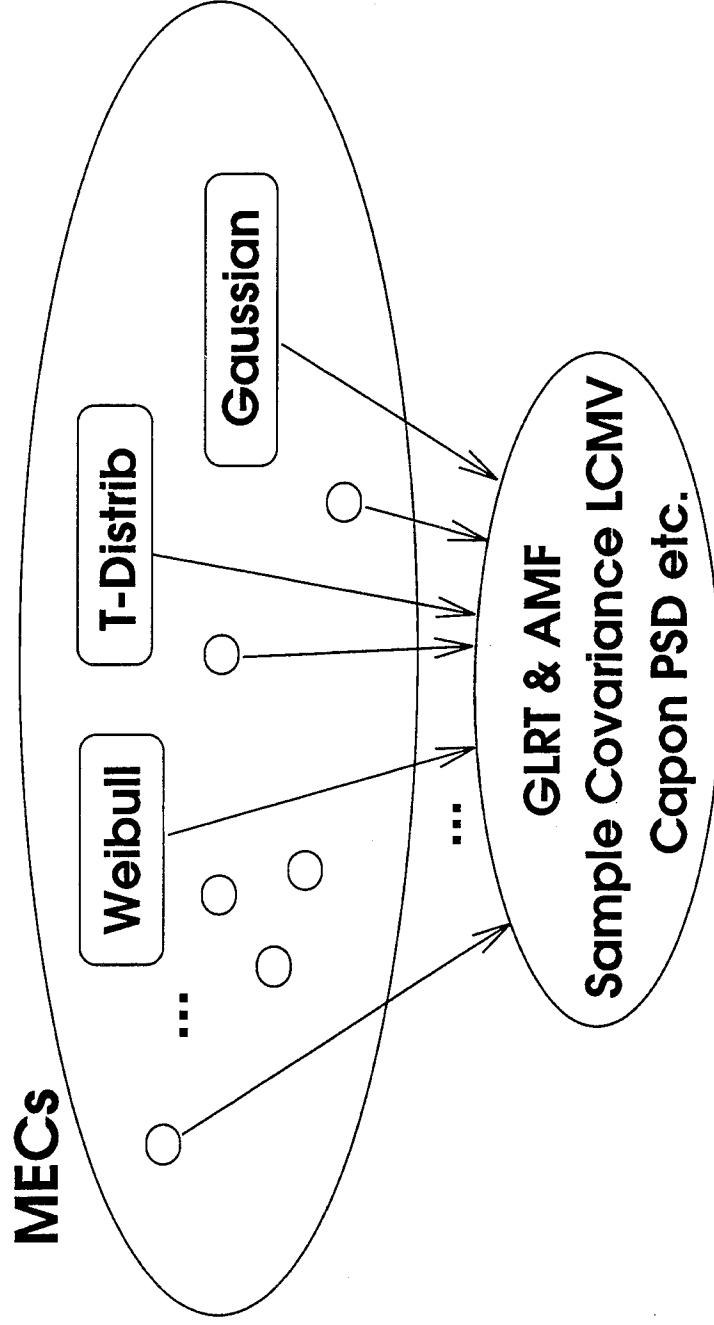
Can Show that Generalized Trace Condition Becomes

$$\text{tr} \left[\left(\mathbf{R}^{-1} + \mathbf{R}^{-1} (\mathbf{D}/L) \mathbf{R}^{-1} \times \frac{d}{dr} \log g(r) \right) \delta \mathbf{R} \right]_{r=\text{tr}(\mathbf{R}^{-1} \mathbf{D})} = \langle \nabla_{\mathbf{R}} p, \delta \mathbf{R} \rangle = 0$$

and Generalized Gradient is given by

$$\nabla_{\mathbf{R}} p \propto \mathbf{R}^{-1} + \mathbf{R}^{-1} (\mathbf{D}/L) \mathbf{R}^{-1} \times \left(\frac{d}{dr} \log g(r) \right)_{r=\text{tr}(\mathbf{R}^{-1} \mathbf{D})}$$

Concluding Remarks



- All results have significant robustness implications to adaptive array processing in non-Gaussian environments

**A GENERALIZATION OF THE ADAPTIVE MATCHED FILTER
RECEIVER FOR ARRAY DETECTION IN A CLASS OF
NON-GAUSSIAN INTERFERENCE**

Ram Raghavan and Nick Pulsone

Northeastern University
Department of Electrical and Computer Engineering
409 Dana Research Center
Boston, MA 02115
tel: (617) 373-5114
fax: (617) 373-8970
email: raghavan@cdsp.neu.edu

Abstract The adaptive matched filter (AMF) receiver proposed by Robey et al. ("A CFAR Adaptive Matched Filter Detector," IEEE Trans. on Aerospace and Electronic Systems, vol. AES-28, no.1, pp. 208-216, Jan. 1992) for array detection in Gaussian interference is generalized to handle a class of non-Gaussian interference models. In this work, interference is modeled as complex, zero-mean spherically invariant random vectors whose covariance matrix is unknown to the receiver. We first address the problem of obtaining a maximum likelihood (ML) estimate of the interference covariance matrix from a given finite set of secondary interference vectors. The ML covariance estimate is shown to be expressible in the form of a weighted sample covariance of the secondary interference vectors. The positive weights used in the estimator are shown to be generated recursively using the Expectation-Maximization (EM) algorithm. Conditions necessary to ensure uniqueness of the covariance matrix estimate are discussed. We then describe the structure of the resulting AMF receiver and show that a desirable implication of the above uniqueness property is that the false alarm performance of the AMF detector is independent of the actual (but unknown) covariance matrix of the interference, i.e., the detector is CFAR. Furthermore, the structure of the receiver is seen to suggest a broad class of algorithms for array detection problems. We conclude the presentation with some results of the detection performance of the proposed approach.

**A GENERALIZATION OF THE AMF RECEIVER FOR
ARRAY DETECTION IN A CLASS OF NON-GAUSSIAN
INTERFERENCE***

Ram Raghavan
Nick Pulsoni
Northeastern University
Boston, MA

ASAP 1996, MARCH 14.

* work sponsored by ARPA / Rome Laboratory under grant F30602-95-1-0009

OUTLINE

- Background and Problem Formulation.
- Non-Gaussian Statistical Model.
- Interference Covariance Matrix Estimation.
- A Generalization of the AMF Receiver.
- Uniqueness and CFAR Property of Test.
- Results and Summary.

HYPOTHESIS TEST

C^N Partitioned into subspaces V_s and V_I :

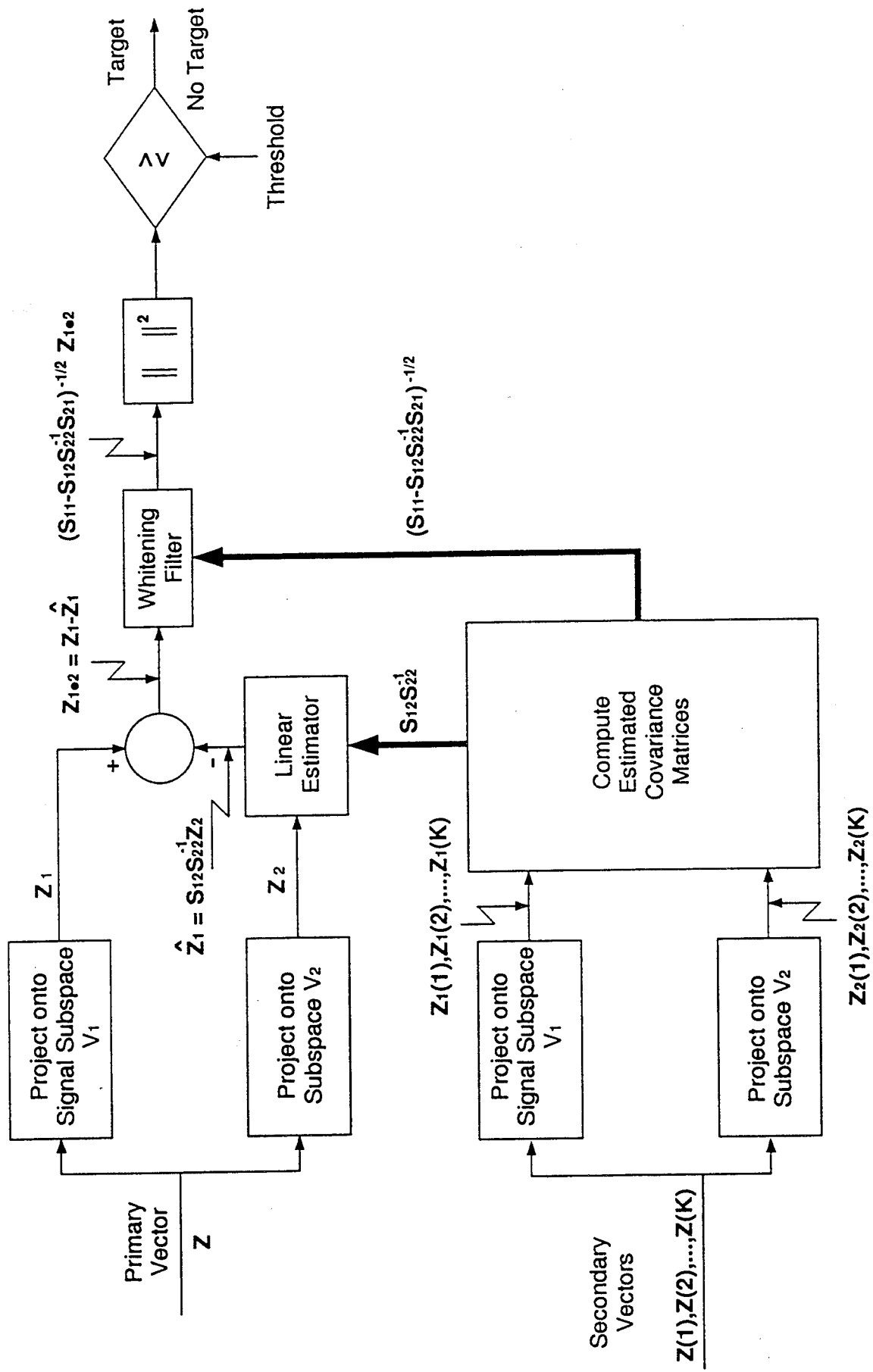
$$V_s + V_I = C^N \text{ and } V_s \cap V_I = 0^N$$

$Z \in C^N$ denotes vector under test

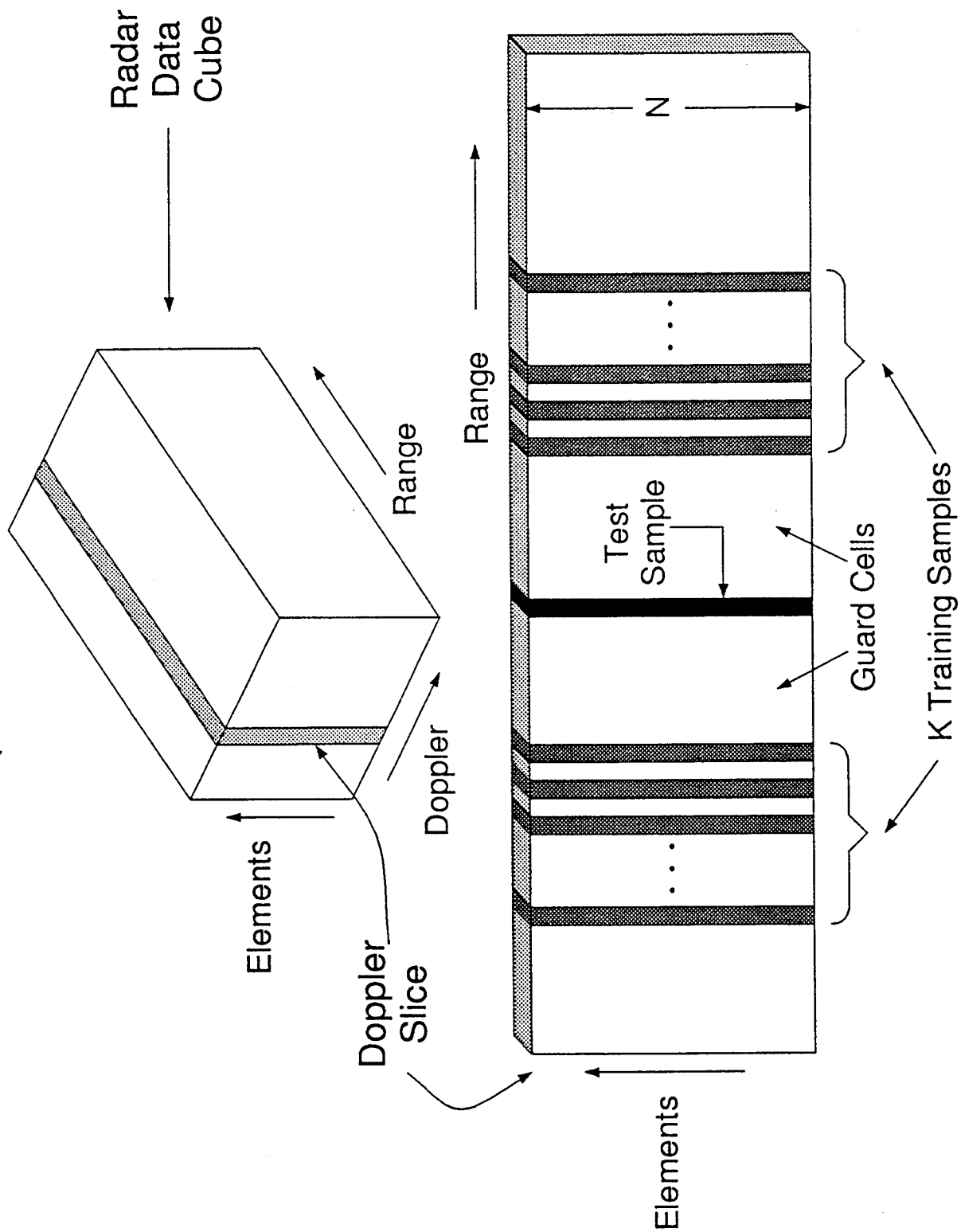
$$Z = z_I \quad (H_0) \quad \text{vs.} \quad Z = \alpha s + z_I \quad (s \in V_s) \quad (H_1)$$

$E[z_I z_I']$ and α are unknown

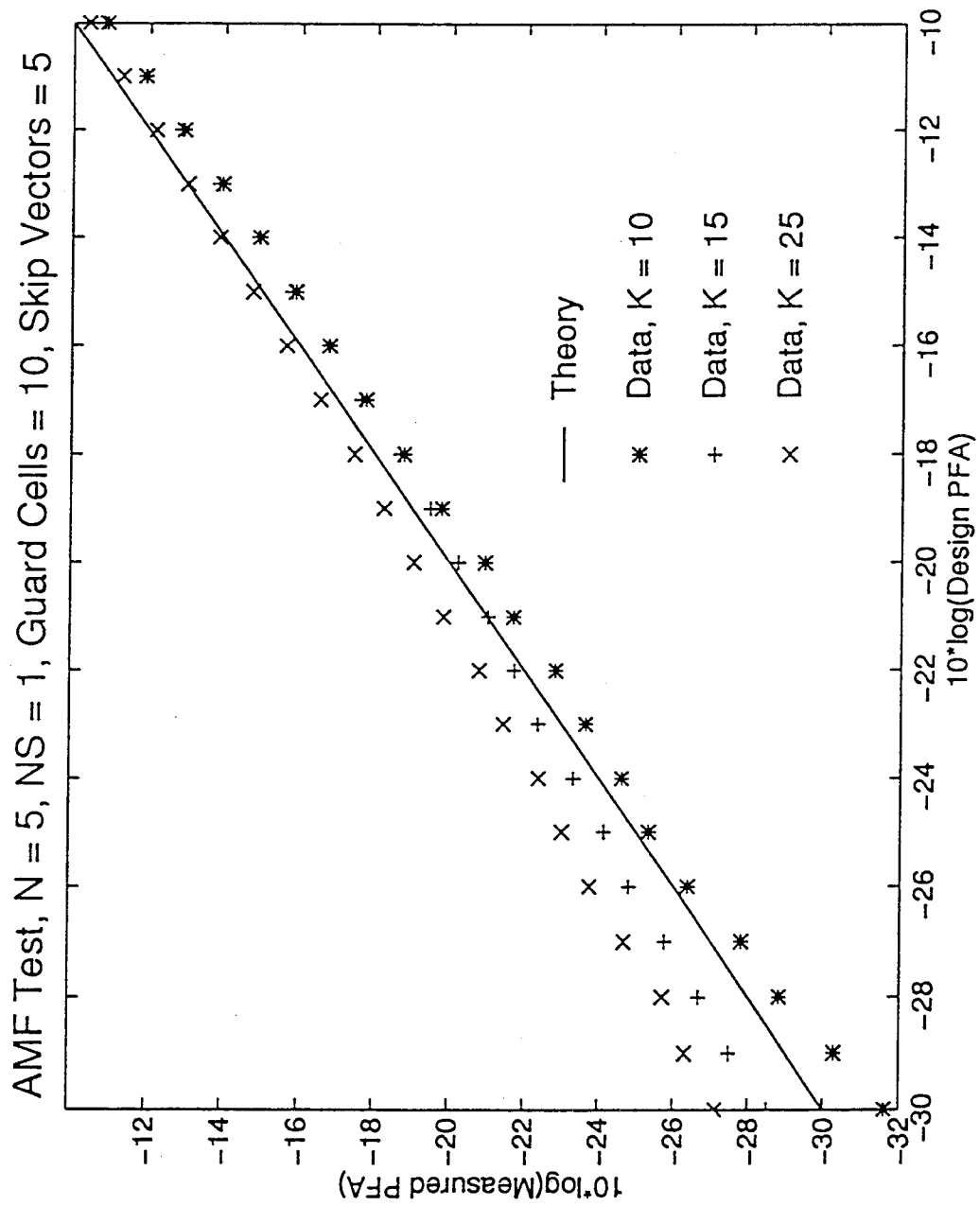
Block Diagram of the AMF Receiver



Monostatic Clutter Mitigation (Airborne Platform)



Data File: idpca65v1.mat



STATISTICAL MODEL

Complex Secondary N-Vectors : $\{ Z_1, Z_2, \dots, Z_K \}$ modeled by the class of Elliptically Symmetric Distributions.

$$f(z_1, z_2, \dots, z_K | \Lambda = R) = \prod_{i=1}^K \frac{h(z_i' R^{-1} z_i)}{|R|}$$

STATISTICAL MODEL (cont.)

Elliptically Symmetric Distributions Specialized to Gaussian Mixture Models

$$f(\mathbf{z}_i | \mathbf{Y}_i = \mathbf{y}_i; \Lambda) = \frac{\exp(-\mathbf{z}_i' \Lambda^{-1} \mathbf{z}_i / \mathbf{y}_i^2)}{(\pi^N |\Lambda| \mathbf{y}_i^{2N})}$$

$$f(\mathbf{z}_i | \Lambda) = \int_0^\infty f(\mathbf{z}_i | \mathbf{Y}_i = \mathbf{y}_i; \Lambda) f(\mathbf{y}_i) d\mathbf{y}_i$$

$$= \frac{h_{2N}(\mathbf{z}_i' \Lambda^{-1} \mathbf{z}_i)}{|\Lambda|}$$

COVARIANCE MATRIX ESTIMATION

Secondary Vectors: $\{Z_1, Z_2, \dots, Z_K\}$

Model: $Z_i = X_i \times Y_i \quad ; i=1, 2, \dots, K$

$X_i \rightarrow$ N-by-1 complex Gaussian vector

Covariance Matrix = Λ

$Y_i \rightarrow$ Scalar random variable with PDF $f(y)$

$K \rightarrow$ Number of Secondary vectors

ML ESTIMATE OF COVARIANCE MATRIX (cont.)

$$R \rightarrow R + \partial R \Rightarrow \partial f(z_1, z_2, \dots, z_K | \Lambda = R) = 0$$

$$\text{ML estimate satisfies: } R = \frac{1}{K} \sum_{i=1}^K g_{2N} (z_i' R^{-1} z_i) z_i z_i'$$

$$g_{2N}(q) = -\frac{1}{h_{2N}(q)} \times \frac{\partial h_{2N}(q)}{\partial q}$$

$$\text{EM Recursion: } R_n = \frac{1}{K} \sum_{i=1}^K g_{2N} (z_i' R_{n-1}^{-1} z_i) z_i z_i' ; n = 1, 2, \dots$$

SOME PROPERTIES OF ML COVARIANCE ESTIMATE

Convergence to a solution assured by the EM algorithm

A sufficient condition to establish uniqueness of solution is that $q \times g_{2N}(q)$ be a strictly monotone function

Given a unique solution, transformation of secondary vectors by any non-singular matrix A :

$$Z_i \rightarrow A \cdot Z_i \Rightarrow R \rightarrow A \cdot R \cdot A'$$

AMF DETECTOR FOR GAUSSIAN MIXTURE MODEL

\hat{R} : estimate of interference covariance matrix

s : steering vector ; z : test vector

$T(\cdot)$: adaptive threshold

$$\begin{array}{cc} H_1 & > \\ \frac{|s' \hat{R}^{-1} z|^2}{s' \hat{R}^{-1} s} & T(z' \hat{R}^{-1} z) \\ H_0 & < \end{array}$$

CFAR PROPERTY

Uniqueness of ML solution implies that $\frac{|s'\hat{R}^{-1}z|^2}{s'\hat{R}^{-1}s}$ and $T(z'\hat{R}^{-1}z)$ are independent (under hypothesis H_0) of the true covariance matrix Λ of the interference.

Therefore the Probability of false alarm of the generalized AMF test is independent of Λ .

SAMPLE RESULTS

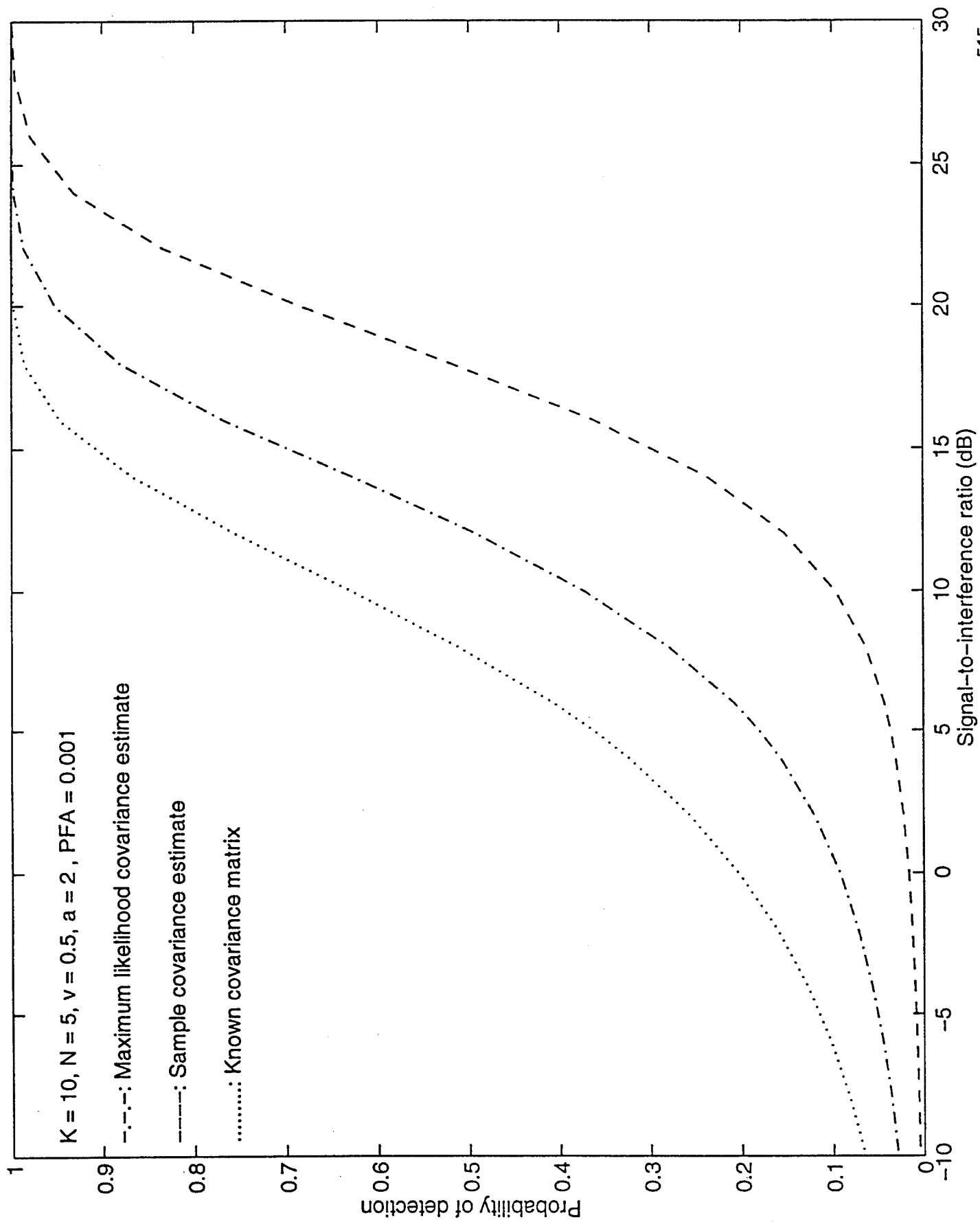
Parameters used:

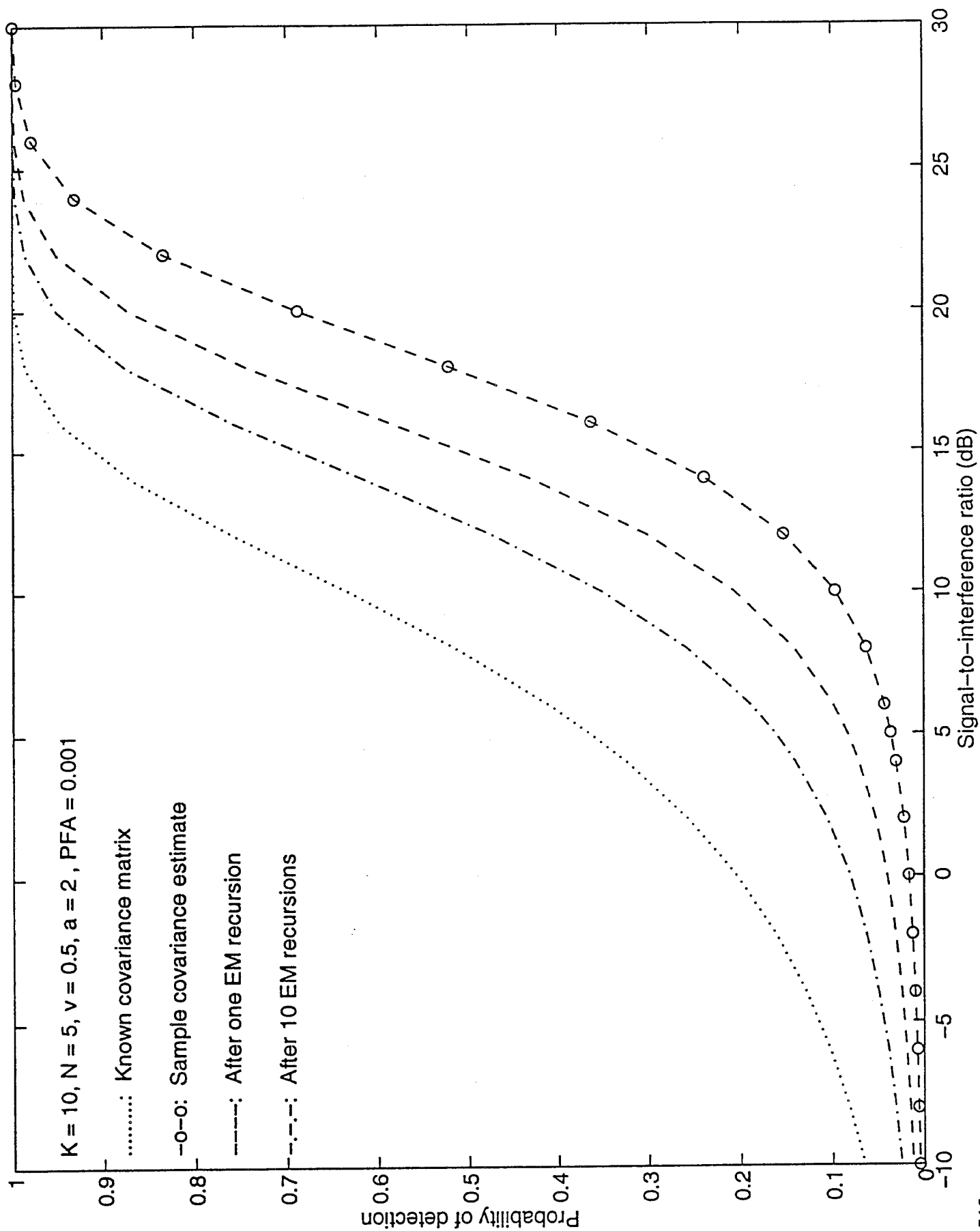
Define $W = Y^2$,

$$f_W(w) = \frac{w^{v-1} e^{-w/a}}{\Gamma(v) a^v} u(w)$$

$v=0.5$ and $a=2$ ($\Rightarrow E[W]=1$)

$N=5$; $K=10$; $PFA = 0.001$





SUMMARY

- Considered a generalization of AMF receiver to a class of non-Gaussian interference models.
- Non-Gaussian statistical model considered was the class of elliptically symmetric densities specialized to Gaussian mixture models.
- For the ML covariance estimation problem showed convergence and uniqueness of solution.
- Structure of resulting AMF receiver shown to be very similar to the AMF receiver for Gaussian interference.
- CFAR property of test established subject to uniqueness of ML solution .

DETECTION PERFORMANCE WITH COMBINED ADAPTIVE FILTERS

Steven T. Smith

MIT Lincoln Laboratory
244 Wood Street
Lexington, MA 02173-9108
tel: (617) 981-3106
email: stsmith@ll.mit.edu

Abstract Adaptive filtering is used by radar systems to detect targets in the presence of jamming and clutter interference whose precise signal characteristics are unknown a priori. The adaptive radar's detection performance depends upon the number of samples used to estimate the interference, as well as factors associated with nonadaptive detectors such as the target's signal strength, steering vector mismatch, and the methods of combining multiple pulses or coherent pulse intervals, clustering, and tracking. The radar's ultimate detection performance can be predicted by making assumptions about the statistics of the filter output. Whereas the Gaussian assumption is preponderant for nonadaptive radars, this assumption certainly does not hold for adaptive radars whose use of data to construct adaptive filters significantly alters the signal's statistics. The complicated statistics of adaptive filter outputs frustrates a closed-form analysis of their combination using all but the simplest integration methods. Therefore, approximation methods are appropriate for this problem. This presentation addresses the problem of determining detection performance when the outputs of several adaptive filters are combined. New results showing the moments of the adaptive matched filter (AMF) and generalized likelihood ratio test (GLRT) are given, which contain the effects of finite sample support, steering vector mismatch, and fluctuating and nonfluctuating targets. These results are used to analyze the detection performance of certain space-time adaptive processing (STAP) algorithms utilizing a variety of post-STAP detection schemes. For example, the performance of post-STAP binary integration (m-out-of-n detector) is compared to the performance of post-STAP square-law integration. All methods are compared to the performance achieved using a nonadaptive matched filter.

DETECTION PERFORMANCE WITH COMBINED ADAPTIVE FILTERS

**STEVEN T. SMITH
LINCOLN LABORATORY
MASSACHUSETTS INSTITUTE OF TECHNOLOGY**

1996 ASAP WORKSHOP

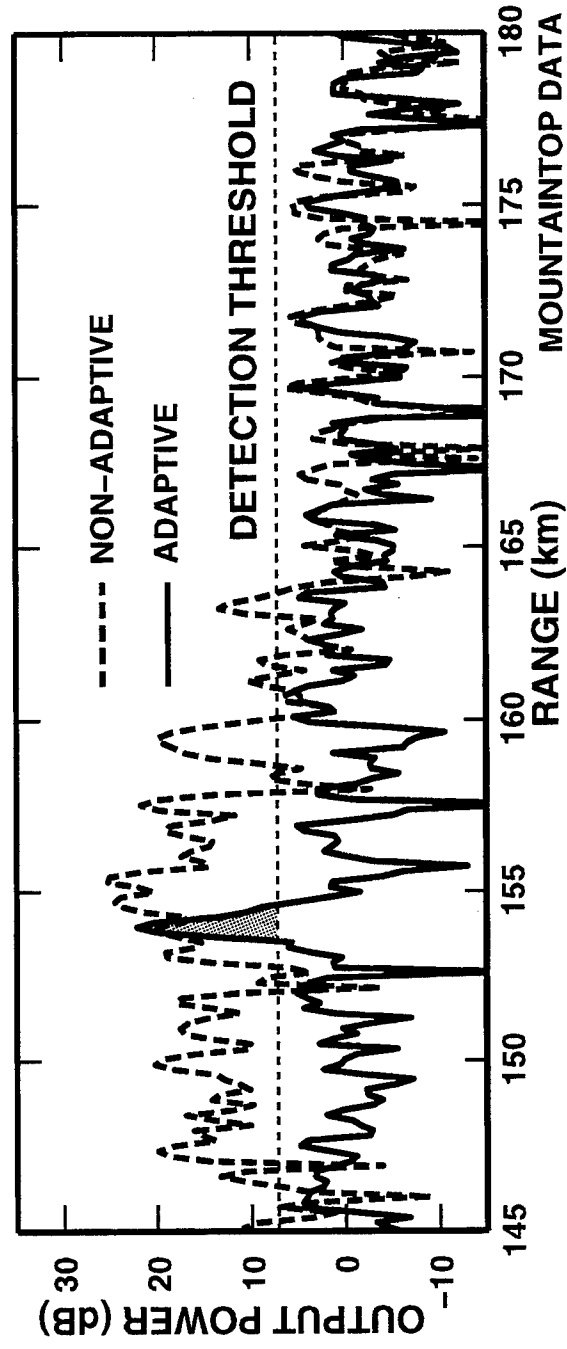
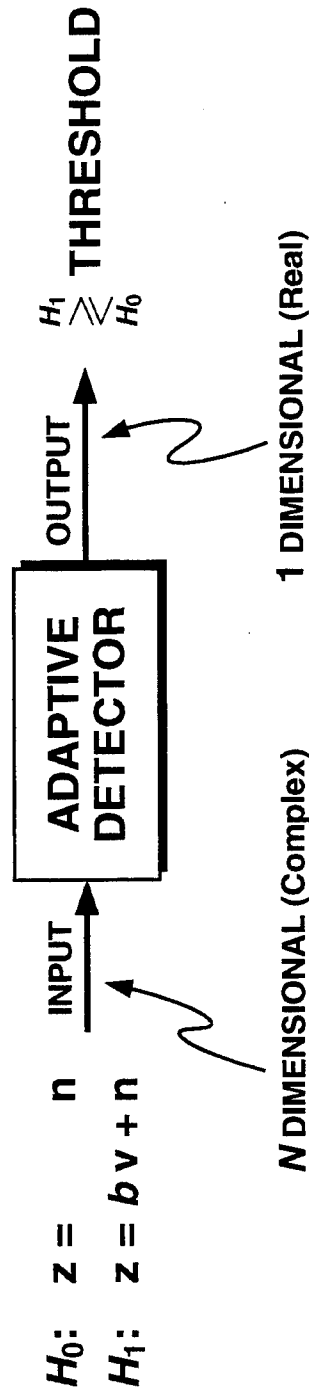
This work was sponsored by DARPA under Air Force contract F19628-95-C-0002. Opinions, interpretations, conclusions, and recommendations are those of the author and are not necessarily endorsed by the United States Air Force.

OUTLINE

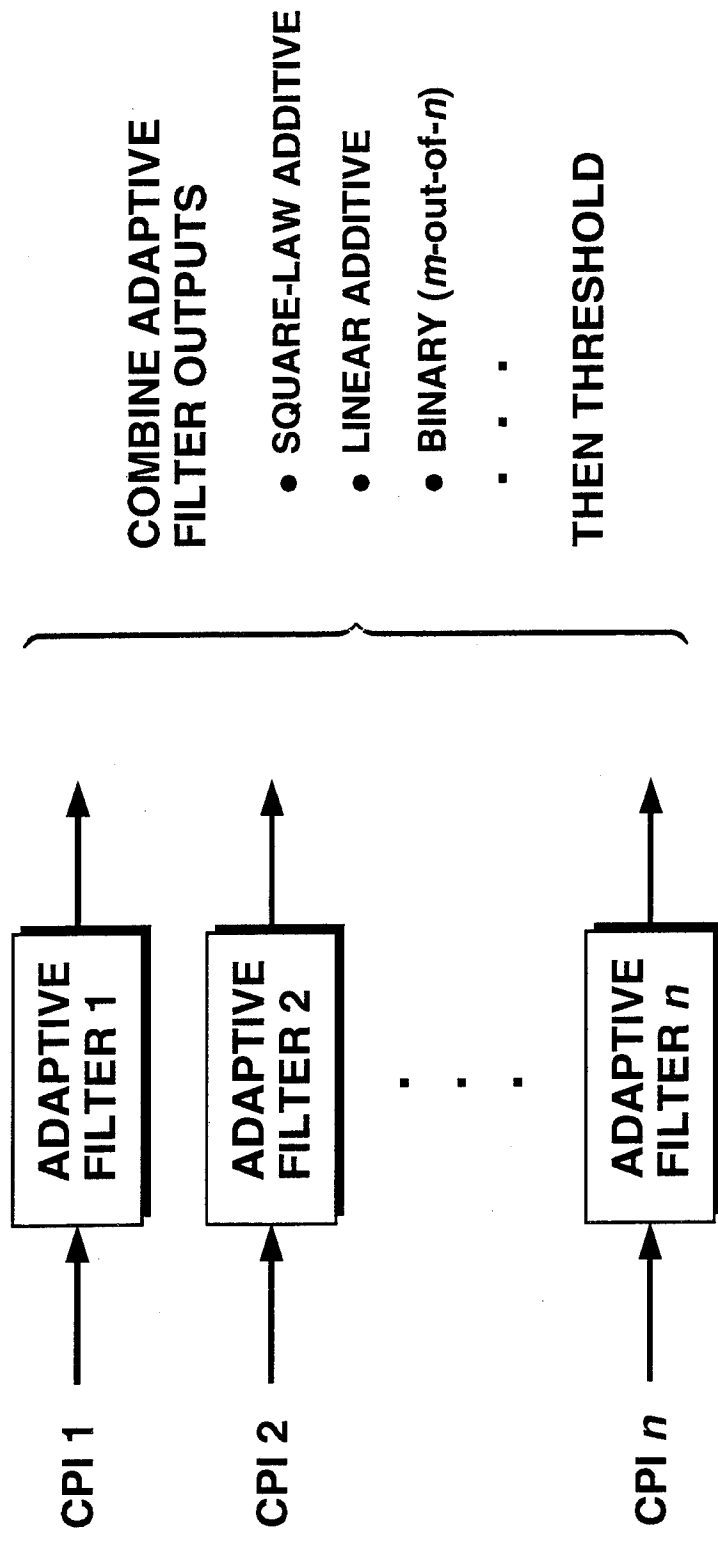
- **RADAR ADAPTIVE DETECTION PROBLEM**
- **STATISTICS OF ADAPTIVE DETECTORS**
- **COMBINING ADAPTIVE FILTER OUTPUTS**
- **CONCLUSIONS AND FUTURE WORK**

ADAPTIVE DETECTION PROBLEM

NOISE-ONLY VS. SIGNAL-PLUS-NOISE



RADAR ADAPTIVE DETECTION PROBLEM



- POST-STAP PROCESSING MAY INCLUDE
 - NONCOHERENT COMBINATION
 - CFAR THRESHOLDING
 - CLUSTERING
 - TRACKING

RADAR DETECTION PERFORMANCE

DEPENDENCIES AND ASSUMPTIONS

- **INPUT SIGNAL STATISTICS**
 - DETERMINISTIC PLUS INTERFERENCE-PLUS-NOISE
 - RAYLEIGH DISTRIBUTED AMPLITUDE
- **INTERFERENCE-PLUS-NOISE STATISTICS**
 - MULTIVARIATE GAUSSIAN
- **ADAPTIVE FILTER**
 - MATCHED FILTER
 - ADAPTIVE MATCHED FILTER (RMB, Robey et al.)
 - GENERALIZED LIKELIHOOD RATIO TEST (Kelly, Khatri)
- **COMBINATION OF MULTIPLE CPIS**
 - SQUARE-LAW / BINARY

RADAR DETECTION PERFORMANCE

**GOAL: ANALYZE DETECTION PERFORMANCE AFTER
COMBINING MULTIPLE POST-STAP CPIs**

REQUIRE: STATISTICS OF ADAPTIVE FILTER OUTPUTS

- **POSSIBLE APPEALING OUTCOMES:**
 - **ADAPTIVE STATISTICS ARE EASY** (No)
 - **EFFICIENT APPROXIMATIONS EXIST** (Yes)
 - **MODIFIED MATCHED FILTER RESULTS APPLY** (Sometimes)

CONTRIBUTIONS

- CLOSED FORM STATISTICS
 - COMPACT FORM

- NEW SERIES APPROXIMATION
 - MOMENT BASED

- EMPIRICAL APPROXIMATION
 - MATCHED FILTER PLUS LOSS

COMPLEXITY

ACCURACY

OUTLINE

- **RADAR ADAPTIVE DETECTION PROBLEM**
- **STATISTICS OF ADAPTIVE DETECTORS**
 - **REVIEW ADAPTIVE DETECTOR THEORY**
 - **CLOSED FORM AMF STATISTICS**
 - **ENGINEERING APPROXIMATIONS**
 - **POST-STAP DETECTION EXAMPLES**
- **COMBINING ADAPTIVE FILTER OUTPUTS**
- **CONCLUSIONS AND FUTURE WORK**

ADAPTIVE DETECTORS

- MATCHED FILTER (MF)

$$A = \frac{|v^H R^{-1} z|^2}{v^H R^{-1} v} \gtrless_{H_0}^{H_1} \text{THRESHOLD}$$

$$R = E[nn^H]$$

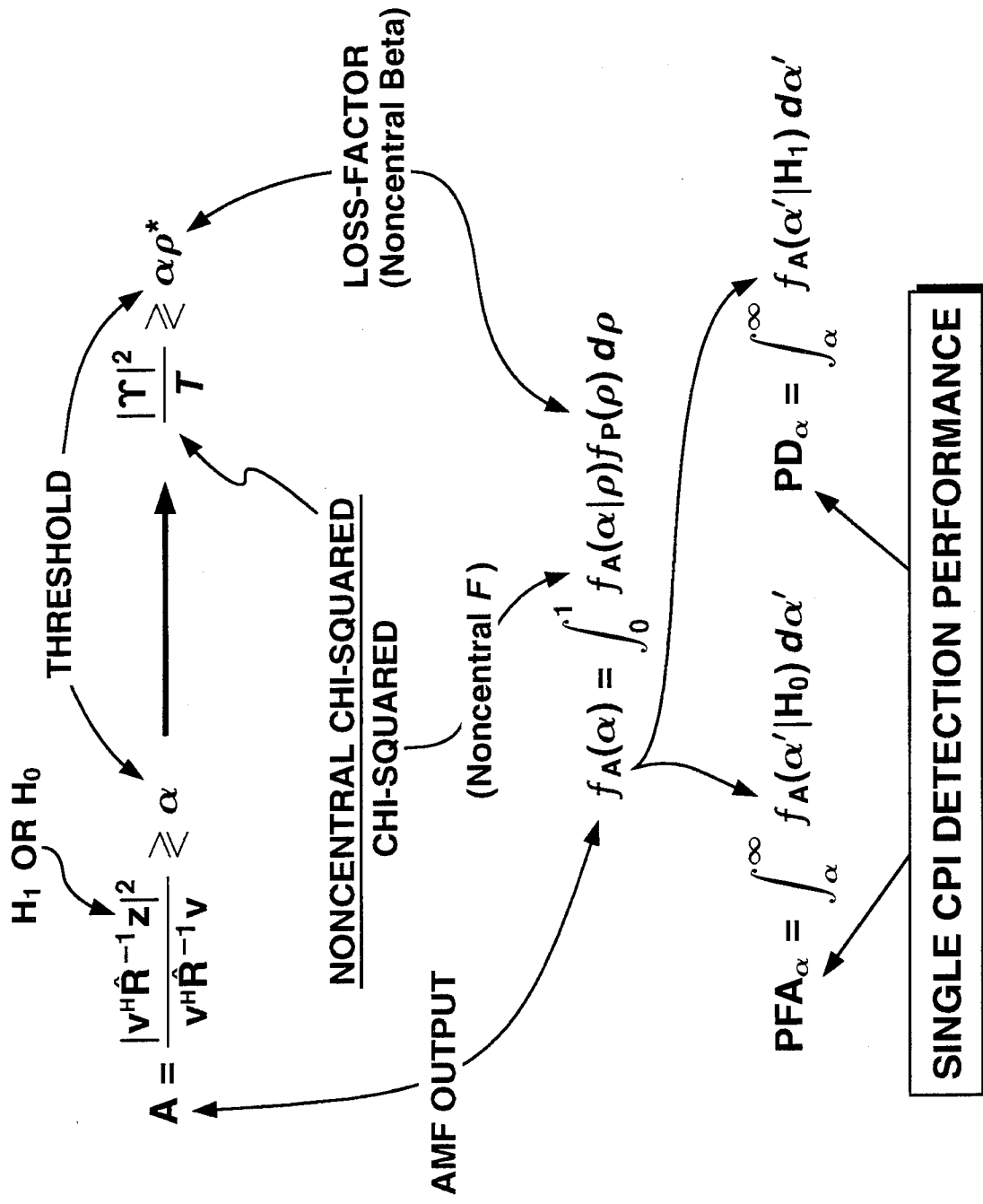
- ADAPTIVE MATCHED FILTER (AMF)

$$A = \frac{|v^H \hat{R}^{-1} z|^2}{v^H \hat{R}^{-1} v} \gtrless_{H_0}^{H_1} \text{THRESHOLD}$$

$$\hat{R} = \frac{1}{K} \sum_{k=1}^K n_k n_k^H$$

- GENERALIZED LIKELIHOOD RATIO TEST (GLRT)

AMF DETECTOR STATISTICS



*BASED UPON RMB, KELLY, ROBNEY, BOROSON

AMF PROBABILITY DISTRIBUTION

$$\text{AMF: } f_A(\alpha|\rho) = \frac{L\rho}{(1+\alpha\rho)^{L+1}} e^{-a\rho} {}_1F_1\left(\begin{matrix} L+1; \\ 1; \end{matrix} \frac{a\rho^2\alpha}{1+\alpha\rho}\right)$$

$$\text{LOSS-FACTOR: } f_P(\rho) = \frac{K!}{L!(N-2)!} \rho^L (1-\rho)^{N-2} e^{-c} {}_1F_1\left(\begin{matrix} K+1; \\ N-1; \end{matrix} (1-\rho)c\right)$$

WHERE

a = SINR IN STEERING VECTOR DIRECTION

c = SINR IN STEERING VECTOR DIRECTION'S ORTHOGONAL COMPLEMENT

$$t = a + c$$

N = DIMENSIONALITY

K = SAMPLE SUPPORT, $L = K - N + 1$

${}_1F_1$ = CONFLUENT HYPERGEOMETRIC FUNCTION

Φ_1 = CONFLUENT HYPERGEOMETRIC FUNCTION OF TWO VARIABLES

- COMPLICATED UNCONDITIONAL PDF OF AMF

- USE MOMENTS INSTEAD: $\nu_k = E[\alpha^k]$

AMF PROBABILITY DISTRIBUTION

$$f_A(\alpha) = \frac{L(L+1)}{K(K+1)} \sum_{k=0}^{\infty} \frac{(L+1)_k (a\alpha)^k}{(1)_k k!} \sum_{\ell=0}^L (-L-1)_{\ell}^{\ell} \frac{(-c)^{\ell}}{\ell!} \\ \times \frac{(L+2)_{2k}}{(K+2)_{2k+\ell}} \Phi_1 \left(\begin{matrix} L+2+2k, L+1+k; \\ K+2+2k+\ell; \end{matrix} -\alpha/K, -t \right)$$

WHERE

a = SINR IN STEERING VECTOR DIRECTION

c = SINR IN STEERING VECTOR DIRECTION'S ORTHOGONAL COMPLEMENT

$t = a + c$

N = DIMENSIONALITY

K = SAMPLE SUPPORT, $L = K - N + 1$

${}_1F_1$ = CONFLUENT HYPERGEOMETRIC FUNCTION

Φ_1 = CONFLUENT HYPERGEOMETRIC FUNCTION OF TWO VARIABLES

• COMPLICATED UNCONDITIONAL PDF OF AMF

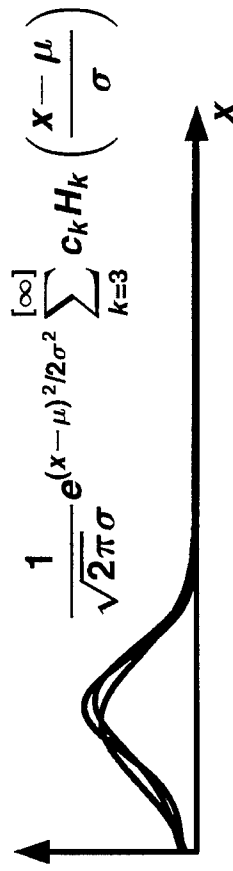
• USE MOMENTS INSTEAD: $\nu_k = E[\alpha^k]$



PDF APPROXIMATIONS

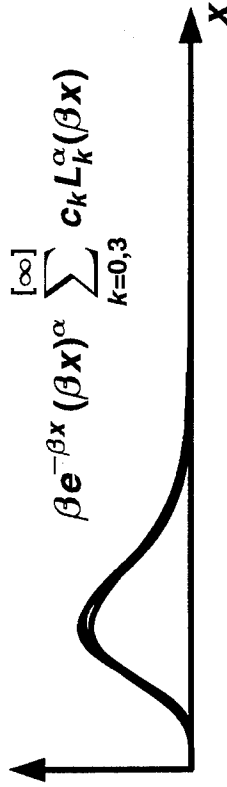
DETERMINE APPROXIMATION PARAMETERS USING MOMENTS

• GRAM-CHARLIER SERIES



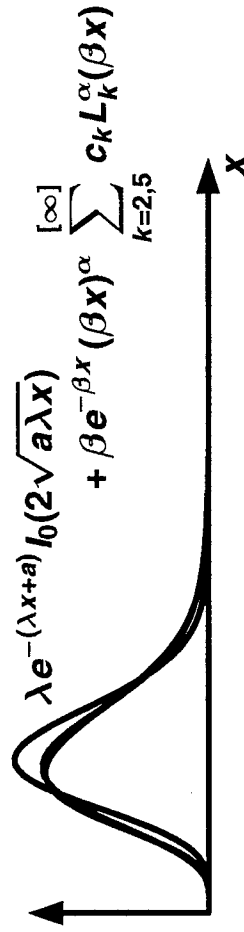
DETERMINE: μ, σ, c_k
USING: ν_1, ν_2, \dots

• LAGUERRE SERIES



DETERMINE: α, β, c_k
USING: ν_1, ν_2, \dots

• MODIFIED LAGUERRE SERIES



DETERMINE: $\lambda, \alpha, \beta, c_k$
USING: ν_1, ν_2, \dots



AMF MOMENTS

• NONFLUCTUATING TARGET

$$E \alpha^n = K^n n! \frac{(L)_{-n}(L+1)_{-n}}{(K+1)_{-n}} \sum_{k=0}^n \frac{(-n)_k(L+1-n)_k(-a)^k}{(1)_k(K+1-n)_k} \frac{k!}{k!} {}_1F_1 \left(\begin{matrix} -n+k; \\ K+1-n+k \end{matrix} \right)$$

- FINITE SUM
- POLYNOMIALS IN a AND c
- MEAN = $\frac{K(K+La+c)}{L(L-1)}$

• CPI-to-CPI FLUCTUATING TARGET

$$E \alpha^n = K^n n! \frac{(L)_{-n}(L+1)_{-n}}{(K+1)_{-n}} \sum_{k=0}^n \frac{(-n)_k(L+1-n)_k(-a\sigma)^k}{(K+1-n)_k} \frac{k!}{k!} \times {}_2F_1 \left(\begin{matrix} -n+k, k+1 \\ K+1-n+k; \end{matrix} -c\sigma \right)$$

AMF PROBABILITY OF FALSE ALARM

- PROBABILITY DENSITY (Noise Only)

$$f_A(\alpha|H_0) = \frac{L(L+1)}{K(K+1)} {}_2F_1 \left(\begin{matrix} L+1, L+2 \\ K+2; -\alpha/K \end{matrix} \right)$$

- AMF HAS HIGH TAILS

$$AMF \sim O \left(\frac{1}{\alpha^{L+1}} \right) \text{ as } \alpha \rightarrow \infty$$

$$MF = \exp(-\alpha)$$

- EXAMPLE OF “CFAR LOSS”

- AMF APPROACHES MF AS SAMPLE SUPPORT K INCREASES

- PROBABILITY OF FALSE ALARM

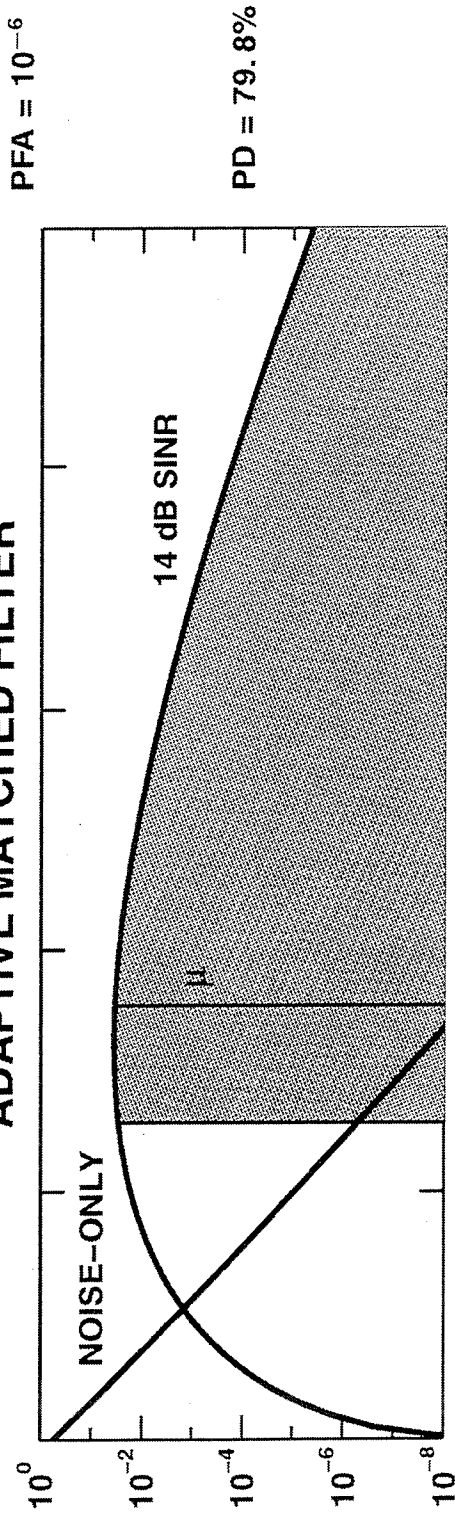
$$PFA_\alpha = {}_2F_1(L, L+1; K+1; -\alpha/K)$$



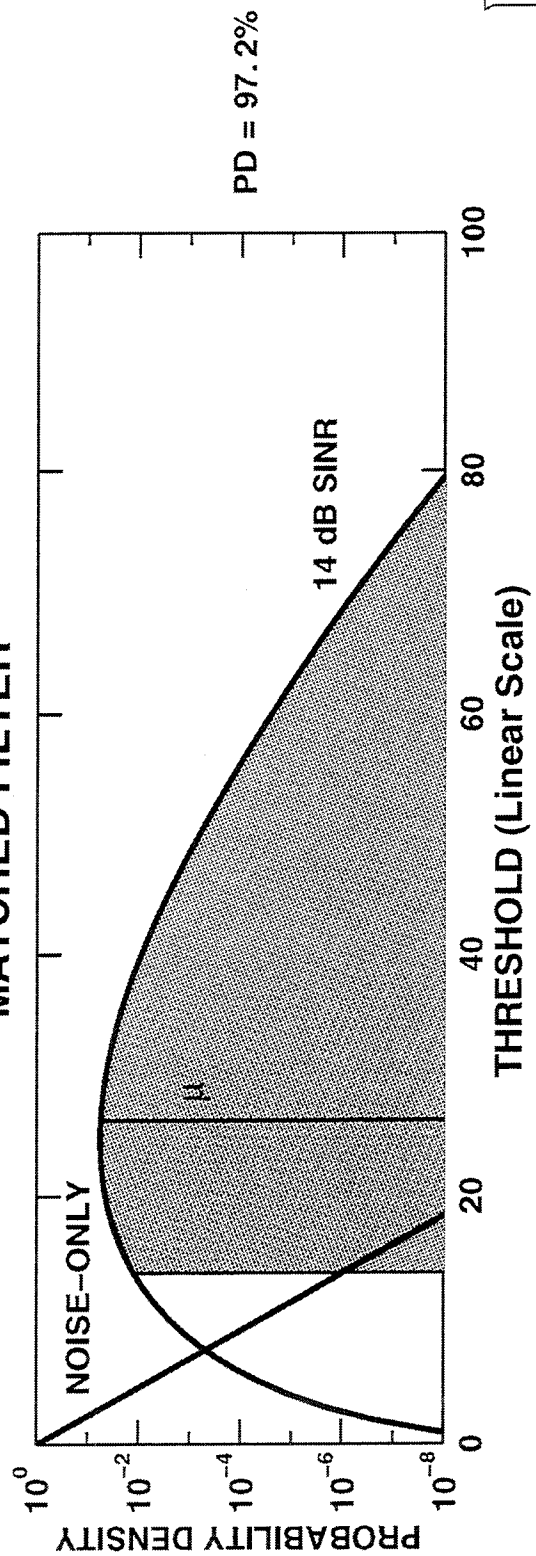
EFFECT OF ADAPTATION ON PDF

DIMENSIONALITY = $3 \cdot 18$, SAMPLE SUPPORT = $4N$

ADAPTIVE MATCHED FILTER



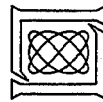
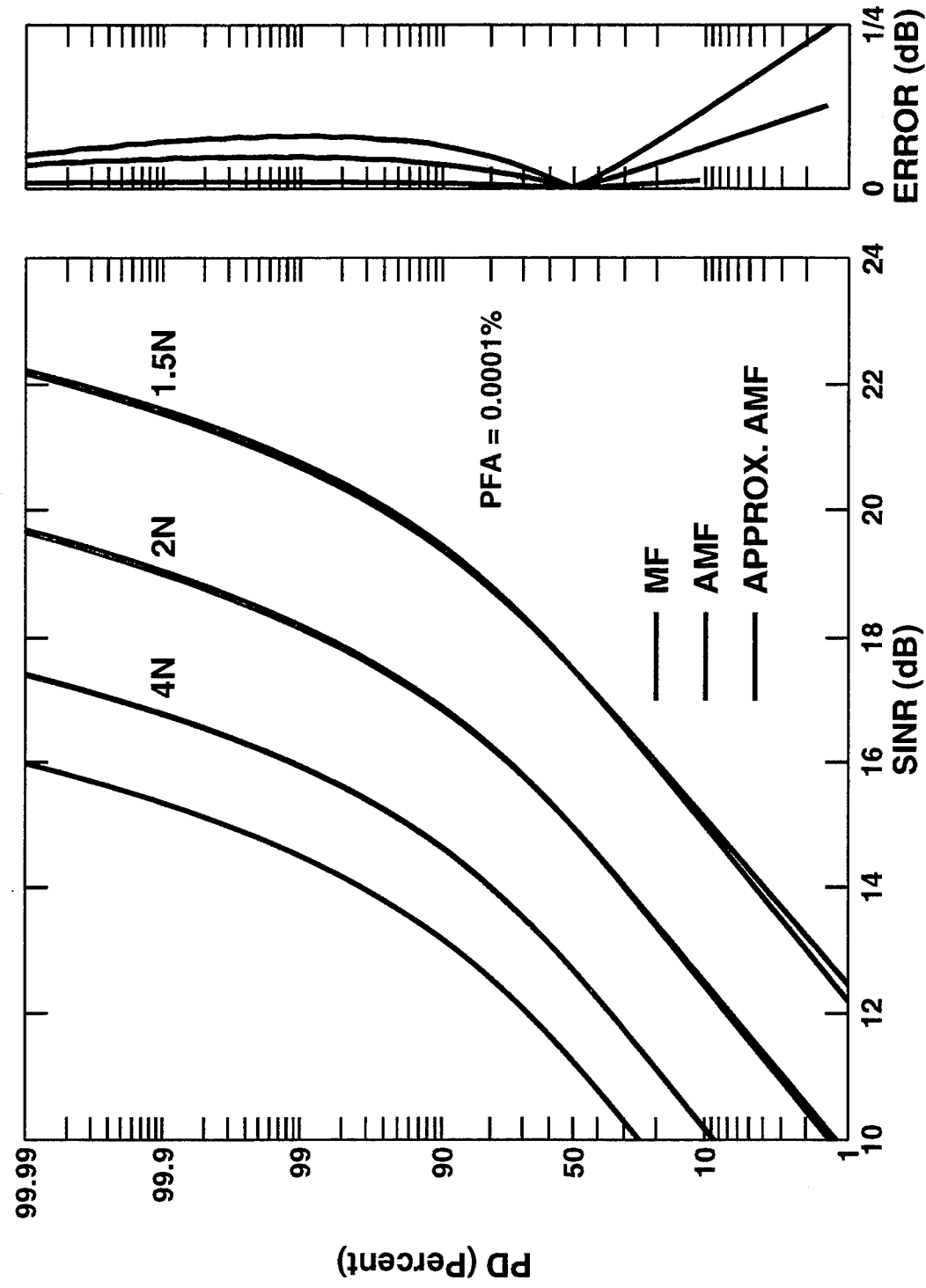
MATCHED FILTER



RESULT HOLDS FOR ANY POST-DOPPLER ALGORITHM

PROBABILITY OF DETECTION

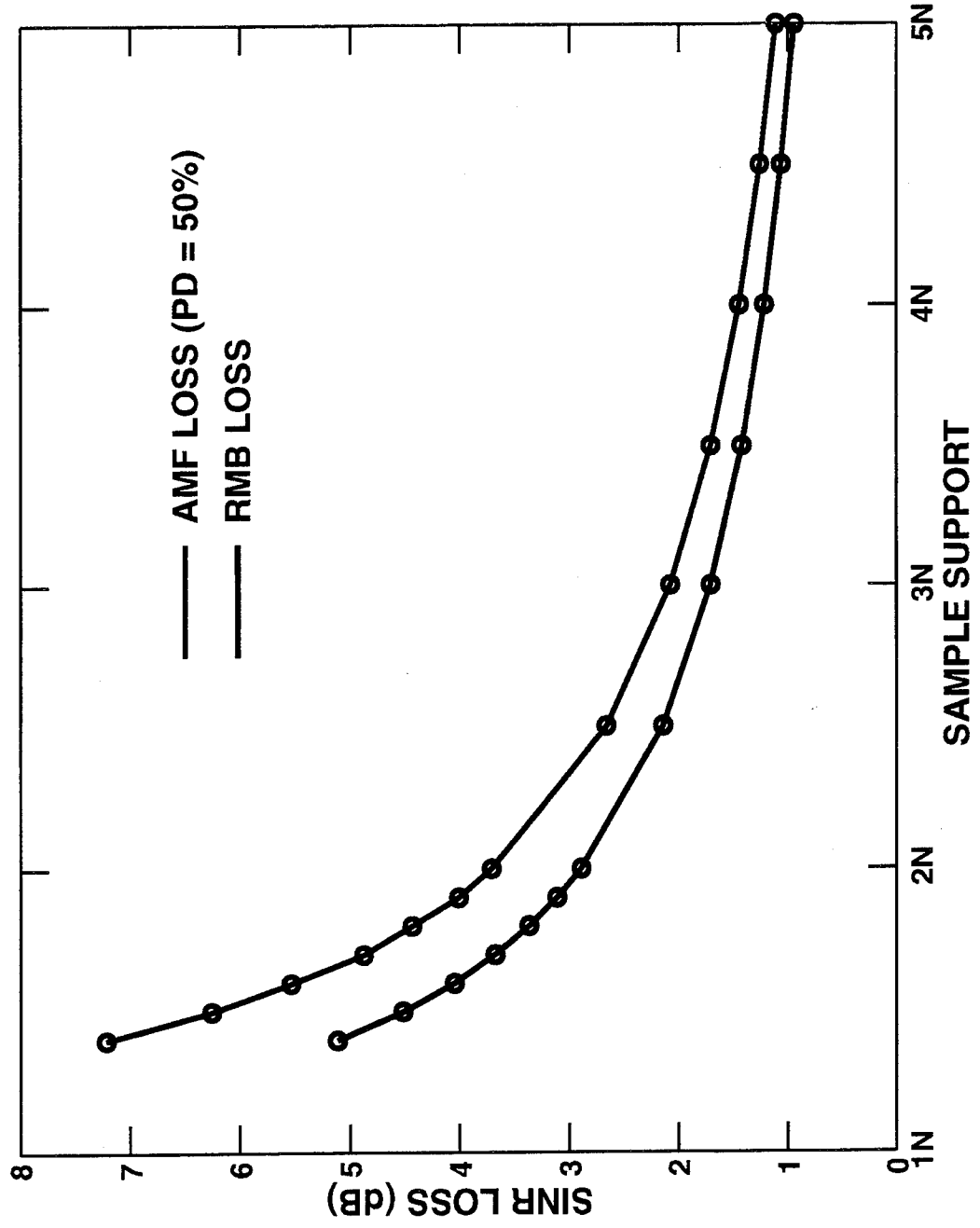
DIMENSIONALITY = $3 \cdot 18$



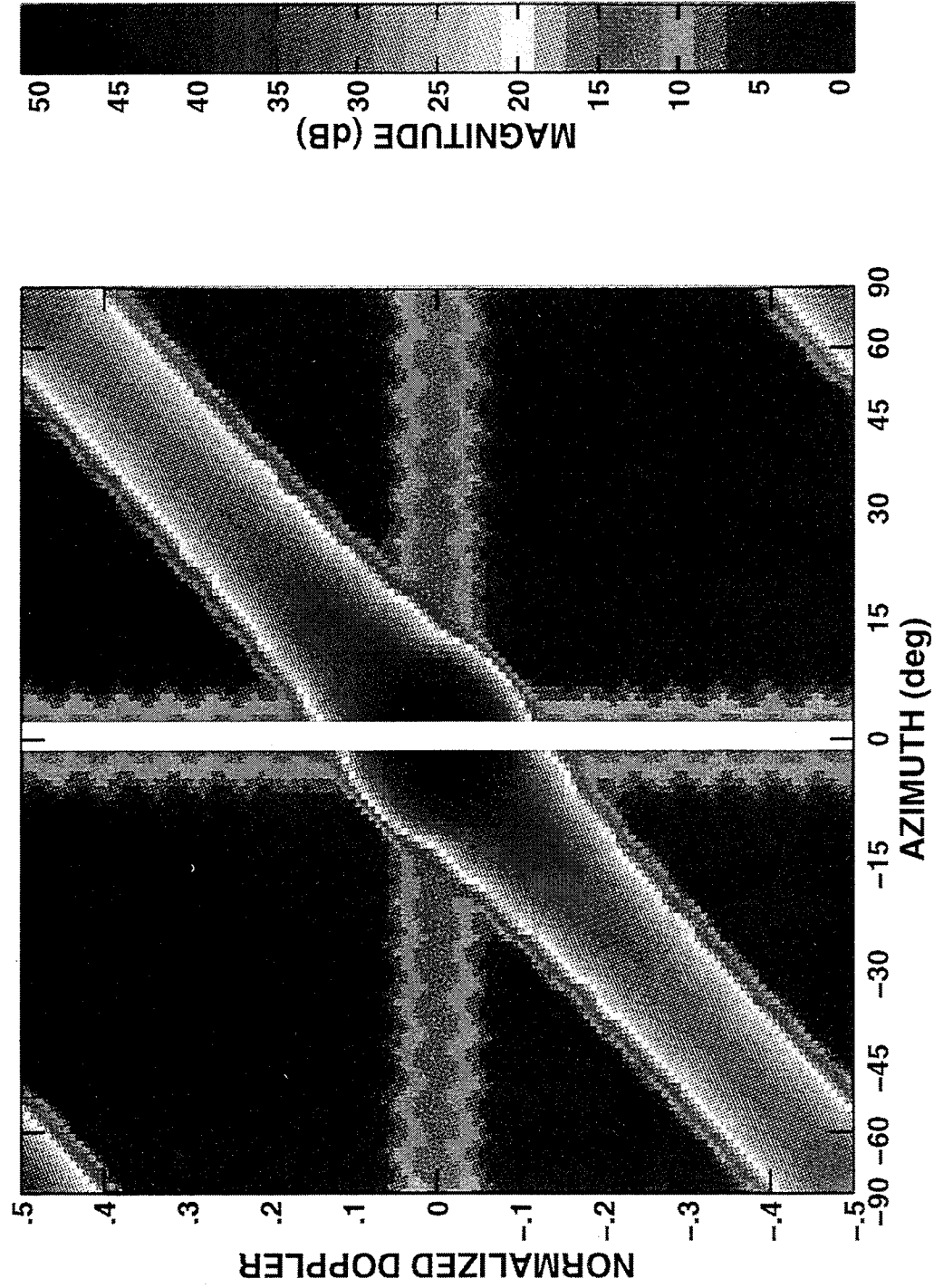
031496-15

SINR LOSS VS. SAMPLE SUPPORT

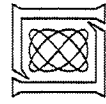
DIMENSIONALITY = $3 \cdot 18$



CLUTTER POWER SPECTRAL DENSITY



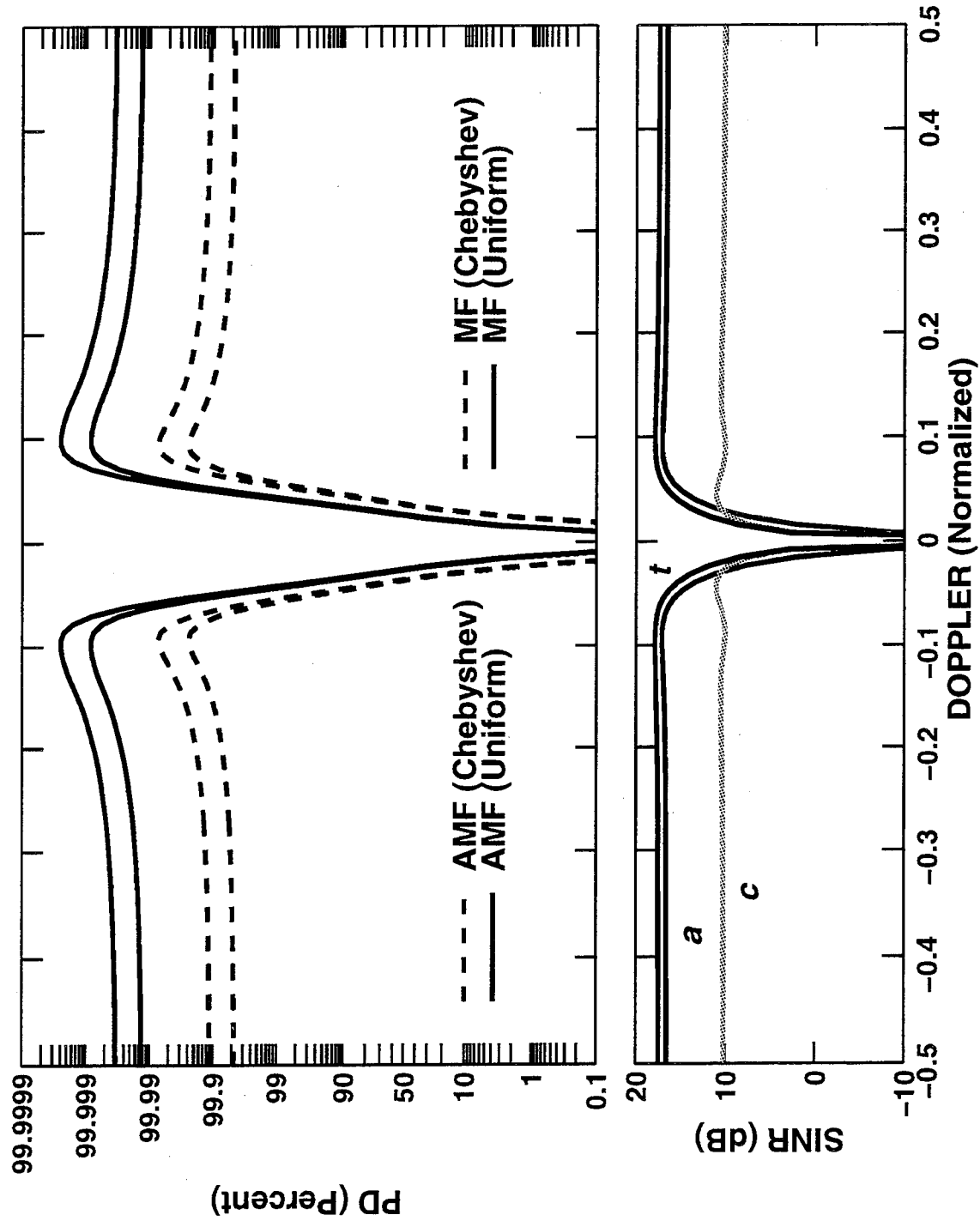
ARRAY NORMAL BROADSIDE, 18 ELEMENT ARRAY, 18 PULSE CPI
 33 dB CNR FRONT + BACK LOBE, 40 dB SPATIAL AND DOPPLER CHEBYSHEV TAPERS



031496-17

PROBABILITY OF DETECTION VS. DOPPLER

DIMENSIONALITY = $3 \cdot 18$, SAMPLE SUPPORT = $4N$



OUTLINE

- **RADAR ADAPTIVE DETECTION PROBLEM**
- **STATISTICS OF ADAPTIVE DETECTORS**
- **COMBINING ADAPTIVE FILTER OUTPUTS**
- **CONCLUSIONS AND FUTURE WORK**



ADAPTIVE FILTER COMBINATION

- PRE-DOPPLER VS. POST-DOPPLER

PRE-DOPPLER:



POST-DOPPLER:



- PRE-DOPPLER COHERENTLY COMBINES MULTIPLE
DEPENDENT ADAPTIVE FILTER OUTPUTS

DEMANDS MONTE CARLO ANALYSIS

- SQUARE-LAW INTEGRATION

E.G., OUTPUT = CPI 1 + CPI 2 + CPI 3

- OPTIMAL FOR SIMPLISTIC ENVIRONMENTS, SMALL SINR,
LARGE SAMPLE SUPPORT

- BINARY (*m*-out-of-*n*) COMBINATION

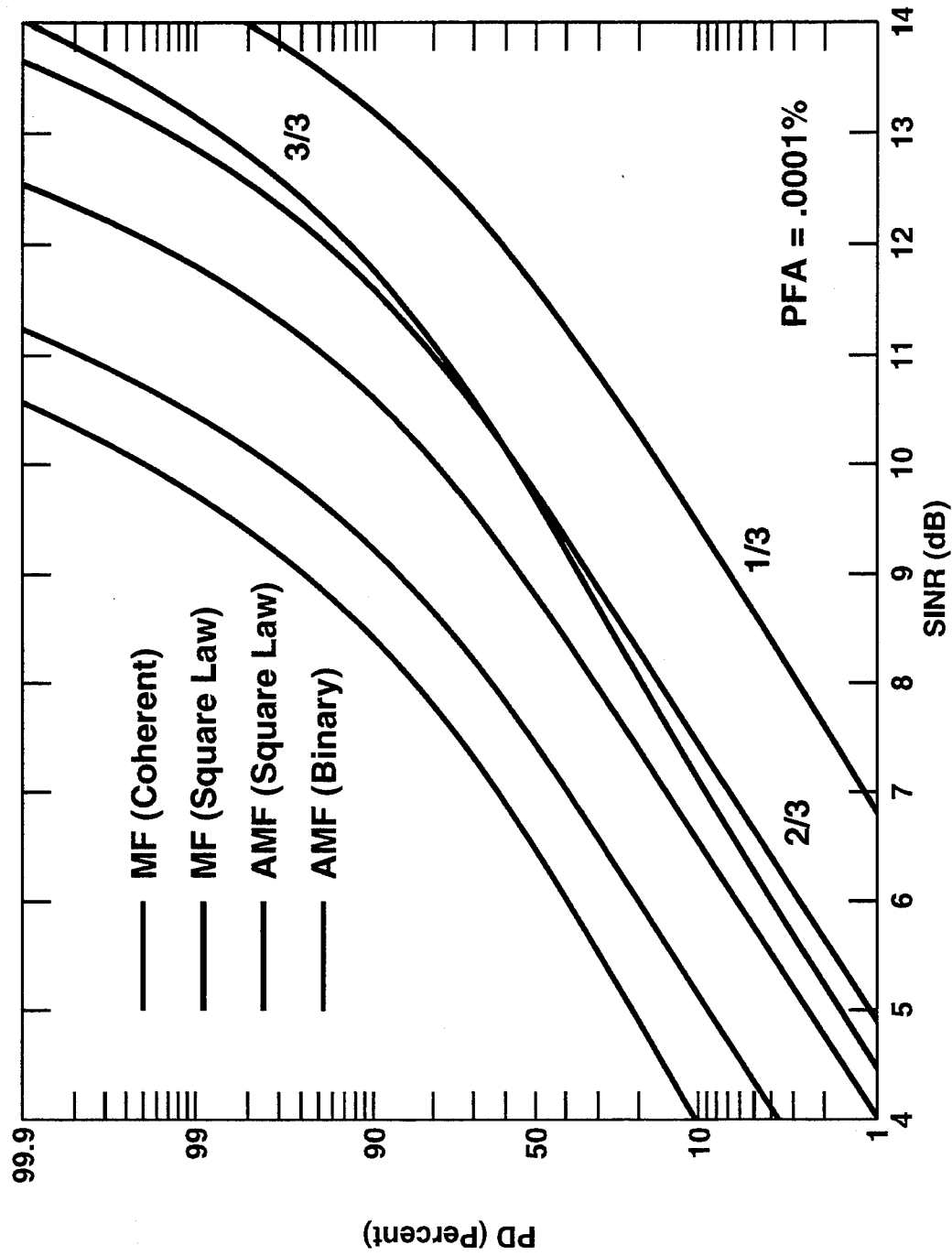
E.G.,



- ROBUST AGAINST IMPULSIVE INTERFERENCE

SQUARE-LAW VS. BINARY COMBINATION

3 CPIs, DIMENSIONALITY = $3 \cdot 18$, SAMPLE SUPPORT = $4N$



CONCLUSIONS

- **ANALYZED DETECTION PERFORMANCE WITH SINGLE/COMBINED POST-STAP CPIs**
- **DEVELOPED NEW CLOSED-FORM AMF STATISTICS AND APPROXIMATIONS**
- **USE MATCHED FILTER (Plus SINR Loss) FOR QUICK ANALYSIS OF STAP DETECTION PERFORMANCE**
 - PD vs. SINR, MINIMUM DETECTABLE VELOCITY
 - *NOT* CFAR THRESHOLD
- **BINARY DETECTOR APPROPRIATE FOR POST-STAP DETECTION**
 - **SMALL LOSS (About 1 dB) COMPARED TO OPTIMUM NONFLUCTUATING TARGET**

FUTURE WORK

- **FLUCTUATING TARGET MODELS**
- **GENERALITY OF APPROXIMATIONS**
 - **ADAPTIVE $\hat{=}$ CLASSICAL + LOSS?**
- **PRE-DOPPLER PERFORMANCE**
- **NON-IDEAL CONDITIONS**
 - **DEPENDENT / NON-IDENTICALLY DISTRIBUTED SNAPSHOTS**
 - **NONHOMOGENEOUS CPIs**
 - **CELL-AVERAGING CFAR**

HYPERGEOMETRIC FUNCTIONS

- GEOMETRIC SERIES

$$\frac{1}{1-z} = 1 + z + z^2 + \dots$$

- POCHAMMER'S SYMBOL

$$(a)_n = a(a+1) \dots (a+n-1) = \frac{\Gamma(a+n)}{\Gamma(a)} \quad (a)_0 = 1$$

$$(a)_{-n} = (-1)^n (-a+1)_{-1}^{-1}$$

- HYPERGEOMETRIC SERIES (Gauss)

$${}_2F_1(a, b; c; z) = \sum_{k=0}^{\infty} \frac{(a)_k (b)_k}{(c)_k} \frac{z^k}{k!} = 1 + \frac{ab}{c} z + \frac{a(a+1)b(b+1)}{c(c+1)} \frac{z^2}{2!} + \dots \quad |z| < 1$$

- CONFLUENT HYPERGEOMETRIC SERIES (Kummer)

$${}_1F_1(a; c; z) = \sum_{k=0}^{\infty} \frac{(a)_k}{(c)_k} \frac{z^k}{k!} = 1 + \frac{a}{c} z + \frac{a(a+1)}{c(c+1)} \frac{z^2}{2!} + \dots$$

**EXPLICIT ZIV-ZAKAI LOWER BOUND FOR
BEARING ESTIMATION USING PLANAR ARRAYS**

Kristine L. Bell, Yariv Ephraim, and Harry L. Van Trees

George Mason University
C3I Center, MS 4B5
341 Science and Technology Building II
Fairfax, VA 22030-4444
tel: (703) 993-1707
fax: (703) 993-1706
email: kbell@gmu.edu

Abstract Estimating the two-dimensional direction-of-arrival, or bearing, of a narrowband planewave signal using a planar array of sensors has applications in many fields. It is a highly nonlinear problem for which calculation of the exact estimation performance is intractable, and lower bounds on the mean square estimation error are used for evaluating performance. In this work, the theory of the Ziv-Zakai lower bound is extended to handle vector parameters with arbitrary continuous prior probability density functions, and applied to the bearing estimation problem. The resulting bound has a simple closed form expression which is a function of the signal wavelength, the signal-to-noise ratio (SNR), the number of data snapshots, the number of sensors in the array, and the array configuration. Analysis of the bound suggests that there are several regions of operation, and expressions for the thresholds separating the regions are provided. In the asymptotic region where the number of snapshots and/or SNR are large, the bound approaches the inverse Fisher information. In the a priori performance region where the number of snapshots or SNR is small, the bound approaches the a priori covariance. In the transition region, the bound varies smoothly between the two extremes. Results from simulation of the maximum likelihood estimator (MLE) demonstrate that the bound closely predicts the performance of the MLE in all regions.

EXPLICIT ZIV-ZAKAI LOWER BOUND FOR BEARING ESTIMATION USING PLANAR ARRAYS

Kristine L. Bell

Yariv Ephraim

Harry L. Van Trees

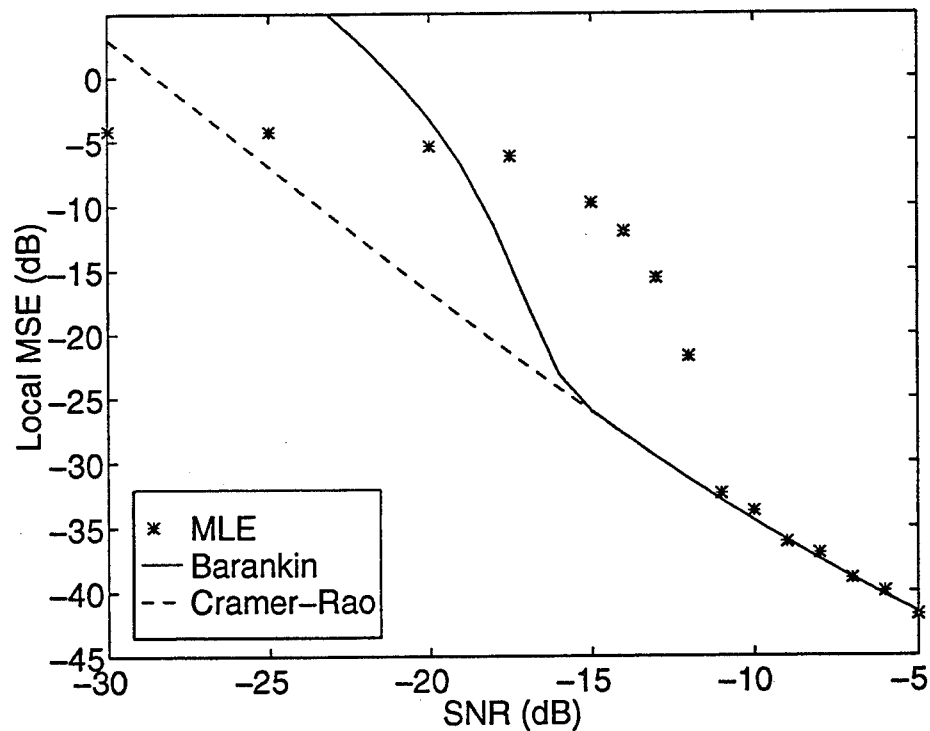
Center of Excellence in C³I
George Mason University

OUTLINE

- Discussion of bounds
- Extended Ziv-Zakai bound
- Application to bearing estimation
- Summary

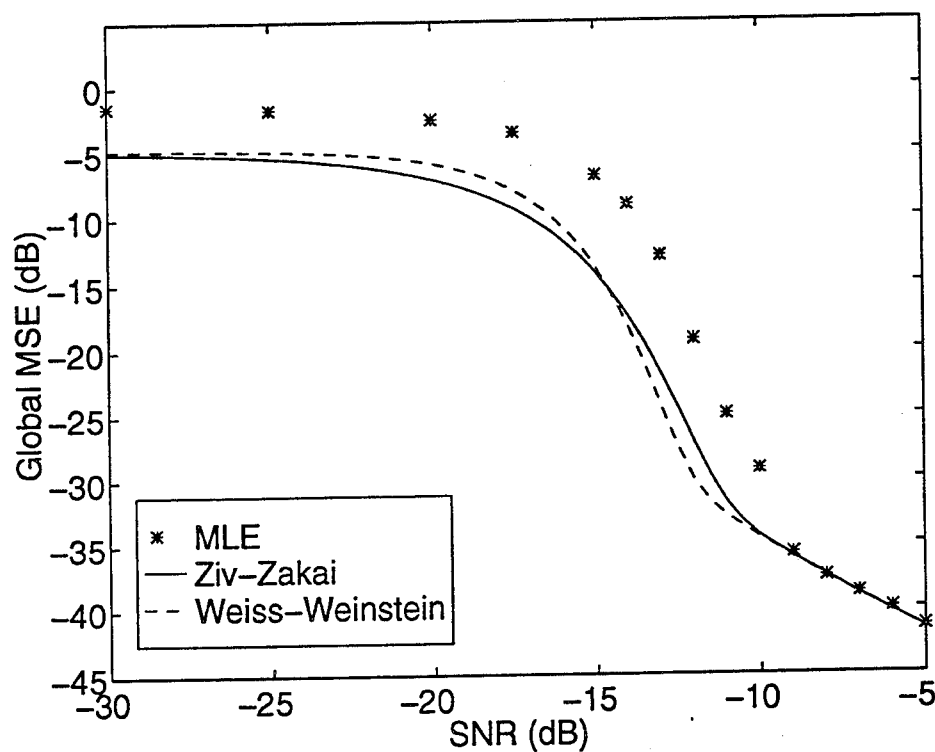
LOCAL BOUNDS

- Cramér-Rao, Barankin, others
- Properties
 - Parameters assumed non-random
 - Provide bound at each parameter value
- Drawbacks
 - Place constraints on estimator (e.g. unbiased)
 - Do not incorporate prior knowledge



BAYESIAN BOUNDS

- Bayesian Cramér-Rao, Ziv-Zakai, Weiss-Weinstein
- Properties
 - Parameters are random variables
 - Provide global bound averaged over prior pdf
 - No bias assumptions
- Drawbacks
 - Bayesian framework not always applicable
 - Global bound may be strongly influenced by values which contribute large errors



ZIV-ZAKAI BOUND

- Relates MSE to the minimum probability of error in a binary hypothesis testing problem
- Derived for scalar, uniformly distributed random variable
- Extension
 - Arbitrarily distributed, continuous vector random variable
 - Key to extension is straightforward proof of existing bound

BINARY DETECTION PROBLEM

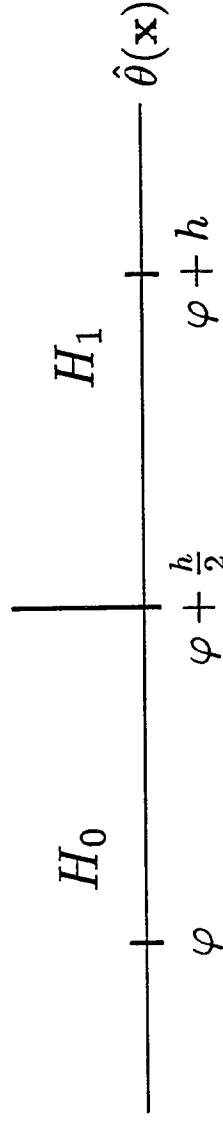
- Definition

$$H_0 : \theta = \varphi; \quad \Pr(H_0) = \frac{1}{2}; \quad \mathbf{x} \sim p(\mathbf{x}|\theta = \varphi)$$

$$H_1 : \theta = \varphi + h; \quad \Pr(H_1) = \frac{1}{2}; \quad \mathbf{x} \sim p(\mathbf{x}|\theta = \varphi + h),$$

- Optimal decision rule is likelihood ratio test

- Suboptimal decision rule



- Probability of error

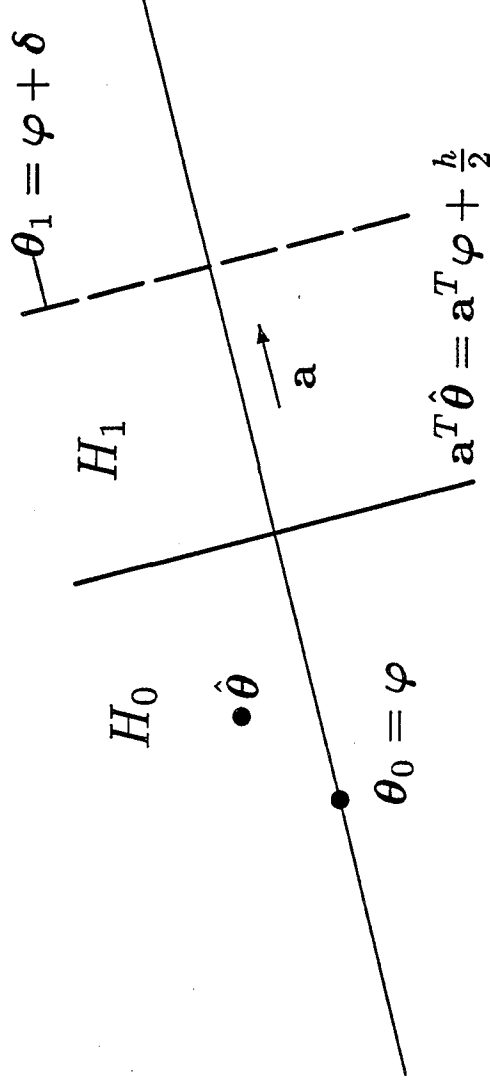
$$P_{\hat{\theta}} = \frac{1}{2} \Pr\left(\hat{\theta} > \varphi + \frac{h}{2} \middle| \theta = \varphi\right) + \frac{1}{2} \Pr\left(\hat{\theta} \leq \varphi + \frac{h}{2} \middle| \theta = \varphi + h\right)$$

EXTENDED ZIV-ZAKAI BOUND - SCALAR

$$\begin{aligned}
 \overline{\epsilon^2} &= \frac{1}{2} \int_0^\infty \Pr \left(|\epsilon| \geq \frac{h}{2} \right) h \, dh \\
 &= \frac{1}{2} \int_0^\infty \left\{ \int_{-\infty}^\infty p(\varphi) \Pr \left(\epsilon > \frac{h}{2} \middle| \theta = \varphi \right) \right. \\
 &\quad \left. + p(\varphi + h) \Pr \left(\epsilon \leq -\frac{h}{2} \middle| \theta = \varphi + h \right) d\varphi \right\} h \, dh \\
 &\geq \int_0^\infty \left\{ \int_{-\infty}^\infty \min(p(\varphi), p(\varphi + h)) \cdot \left[\frac{1}{2} \Pr \left(\hat{\theta} > \varphi + \frac{h}{2} \middle| \theta = \varphi \right) \right. \right. \\
 &\quad \left. \left. + \frac{1}{2} \Pr \left(\hat{\theta} \leq \varphi + \frac{h}{2} \middle| \theta = \varphi + h \right) \right] d\varphi \right\} h \, dh \\
 &= \int_0^\infty \left\{ \int_{-\infty}^\infty \min(p(\varphi), p(\varphi + h)) P_{\hat{\theta}}(\varphi, \varphi + h) d\varphi \right\} h \, dh \\
 &\geq \int_0^\infty \left\{ \int_{-\infty}^\infty \min(p(\varphi), p(\varphi + h)) P_e(\varphi, \varphi + h) d\varphi \right\} h \, dh
 \end{aligned}$$

EXTENDED ZIV-ZAKAI BOUND - VECTOR

- Suboptimal decision rule in binary detection problem

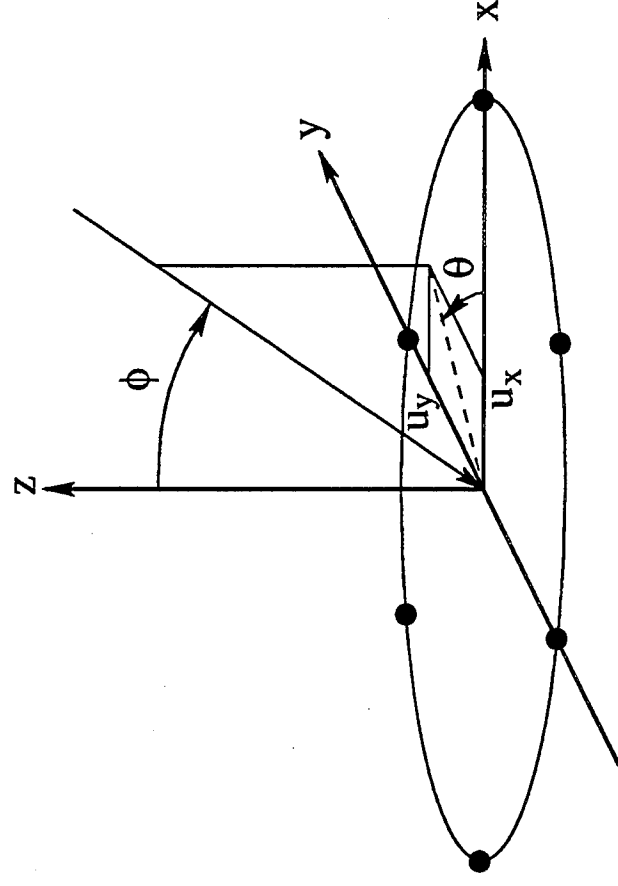


- Vector bound

$$\mathbf{a}^T \mathbf{R}_e \mathbf{a} \geq \int_0^\infty \left\{ \max_{\delta : \mathbf{a}^T \delta = h} \min (p(\varphi), p(\varphi + \delta)) P_e(\varphi, \varphi + \delta) d\varphi \right\} h dh$$

APPLICATION TO BEARING ESTIMATION

- Planar array
- Bound MSE in estimating two-dimensional bearing
- Closed form expression for EZZB
- Threshold expressions
- Comparison with WWB
- Comparison with MLE simulations



2-D BEARING ESTIMATION PROBLEM

- Planar array of M sensors

$$\mathbf{D} = \begin{bmatrix} \mathbf{d}_1 & \cdots & \mathbf{d}_M \end{bmatrix}$$

- DOA of planewave

$$\mathbf{u} = \begin{bmatrix} u_x \\ u_y \end{bmatrix} = \begin{bmatrix} \cos \theta \sin \phi \\ \sin \theta \sin \phi \end{bmatrix}$$

- $p(\mathbf{u})$ defined on unit disk, circular contours, covariance \mathbf{R}_u
- Received signal vector snapshots ($n = 1, \dots, N$)

$$\mathbf{x}(t_n) = \mathbf{E}(\mathbf{u})s(t_n) + \mathbf{n}(t_n)$$

$$\mathbf{E}(\mathbf{u}) = \begin{bmatrix} e^{-j\omega_0\tau_1} & \cdots & e^{-j\omega_0\tau_M} \end{bmatrix}^T$$

$$\tau_i = \frac{\mathbf{u}^T \mathbf{d}_i}{c}$$

EVALUATION OF EZZB

- Bound simplifies when $P_e(\varphi, \varphi + \delta) = P_e(\delta)$

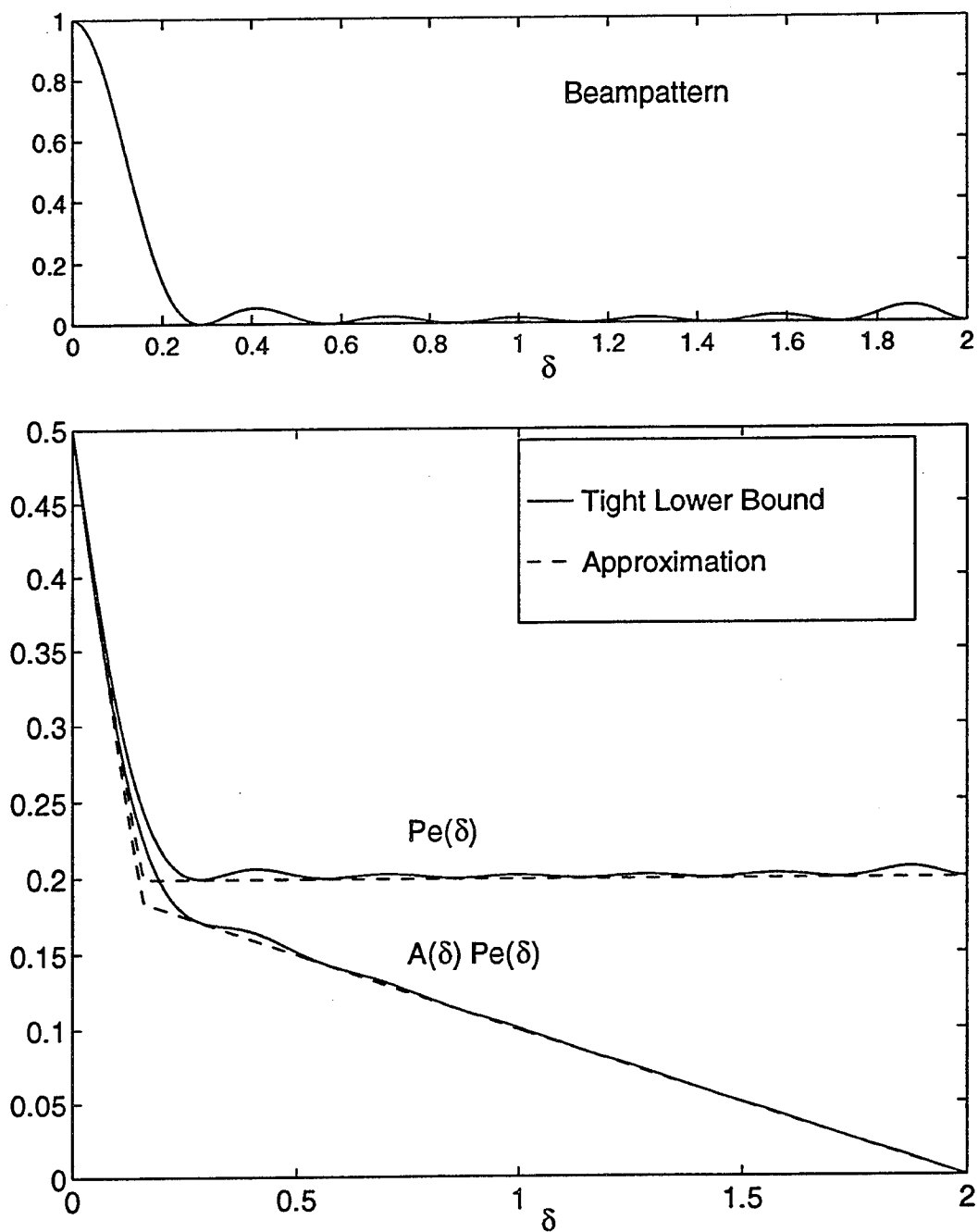
$$\mathbf{a}^T \mathbf{R} \mathbf{e} \mathbf{a} \geq \int_0^\infty \left\{ \max_{\delta : \mathbf{a}^T \delta = h} A(\delta) P_e(\delta) \right\} h \, dh$$

where

$$A(\delta) = \int \min(p(\varphi), p(\varphi + \delta)) \, d\varphi$$

- Evaluation
 - Simplifying approximations to $P_e(\delta)$ and $A(\delta)$
 - Maximization becomes problem of minimizing quadratic form $\delta^T \mathbf{W} \delta$ subject to linear constraint $\mathbf{a}^T \delta = h$
 - Final integral has closed form solution

SIMPLIFYING APPROXIMATIONS



EXPLICIT EZZB FOR PLANAR ARRAY

$$\mathbf{a}^T \mathbf{R}_{\epsilon} \mathbf{a} \geq \mathbf{a}^T \left\{ \mathbf{R}_{\mathbf{u}} \cdot 2\Phi \left(\sqrt{\frac{N\gamma}{2}} \right) + \mathbf{J}^{-1} \cdot \Gamma_{\frac{3}{2}} \left(\frac{N\gamma}{4} \right) \right\} \mathbf{a}$$

- As $N\gamma \rightarrow 0$, EZZB $\rightarrow \mathbf{R}_{\mathbf{u}}$
- As $N\gamma \rightarrow \infty$, EZZB $\rightarrow \mathbf{J}^{-1}$

$$\begin{aligned} \gamma &= \left(\frac{M\sigma_s^2}{\sigma_n^2} \right)^2 / \left(1 + \frac{M\sigma_s^2}{\sigma_n^2} \right) & \Phi(z) &= \int_z^\infty \frac{1}{\sqrt{2\pi}} e^{-\frac{v^2}{2}} dv \\ \mathbf{J} &= -N\gamma \mathbf{G}''(\mathbf{0}) & \Gamma_{\frac{3}{2}}(z) &= \frac{2}{\sqrt{\pi}} \int_0^z e^{-v} v^{\frac{1}{2}} dv \\ \mathbf{G}''(\mathbf{0}) &= -\frac{2}{M} \left(\frac{2\pi}{\lambda_0} \right)^2 \mathbf{D} \left(\mathbf{I} - \frac{1}{M} \mathbf{1}\mathbf{1}^T \right) \mathbf{D}^T \end{aligned}$$

THRESHOLDS

- A priori performance region
 - λ_p denotes value of $N\gamma$ where bound is within ≈ 3 dB of prior covariance

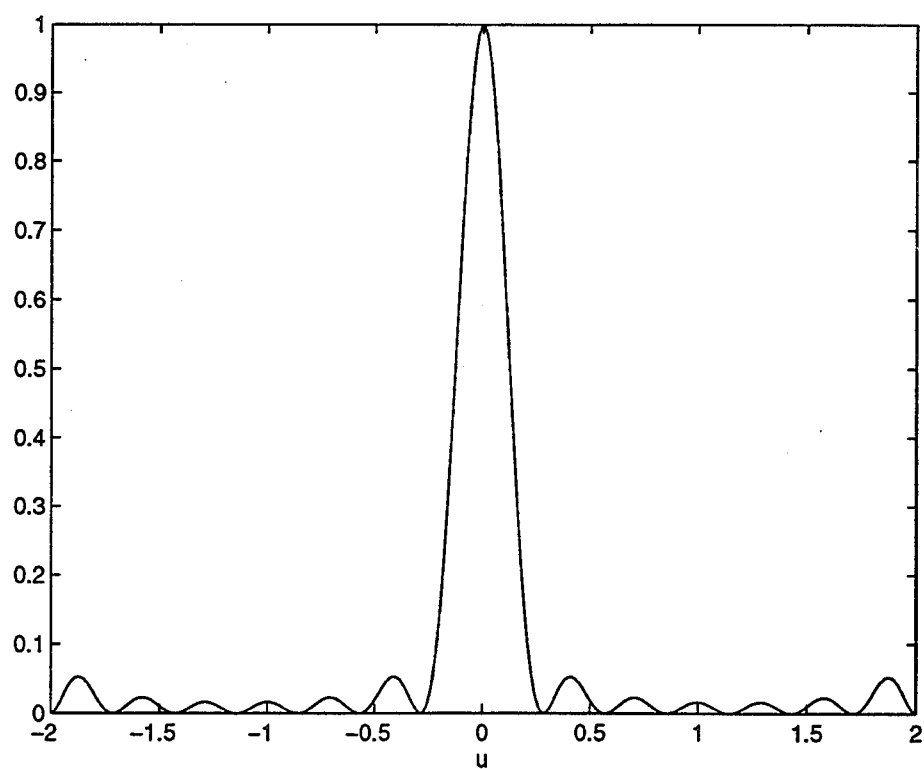
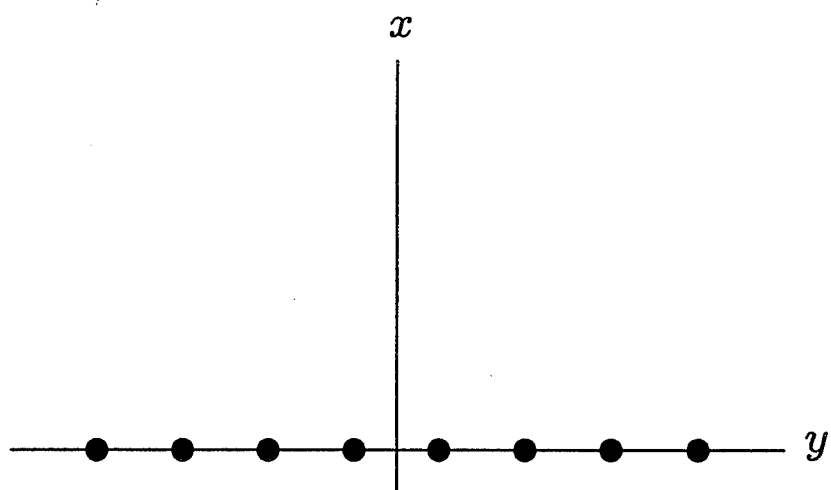
$$\lambda_p = 2 \left\{ \Phi^{-1} \left(\frac{1}{4} \right) \right\}^2 \approx 1.$$

- Asymptotic region
 - $\lambda_a(\mathbf{a})$ denotes value of $N\gamma$ where bound exceeds \mathbf{J}^{-1} by small amount (10 per cent)

$$\left(\frac{\lambda_a(\mathbf{a})}{2} \right) \Phi \left(\sqrt{\frac{\lambda_a(\mathbf{a})}{2}} \right) = -\frac{0.1}{4} \frac{\mathbf{a}^T \mathbf{G}''(0)^{-1} \mathbf{a}}{\mathbf{a}^T \mathbf{R}_u \mathbf{a}}$$

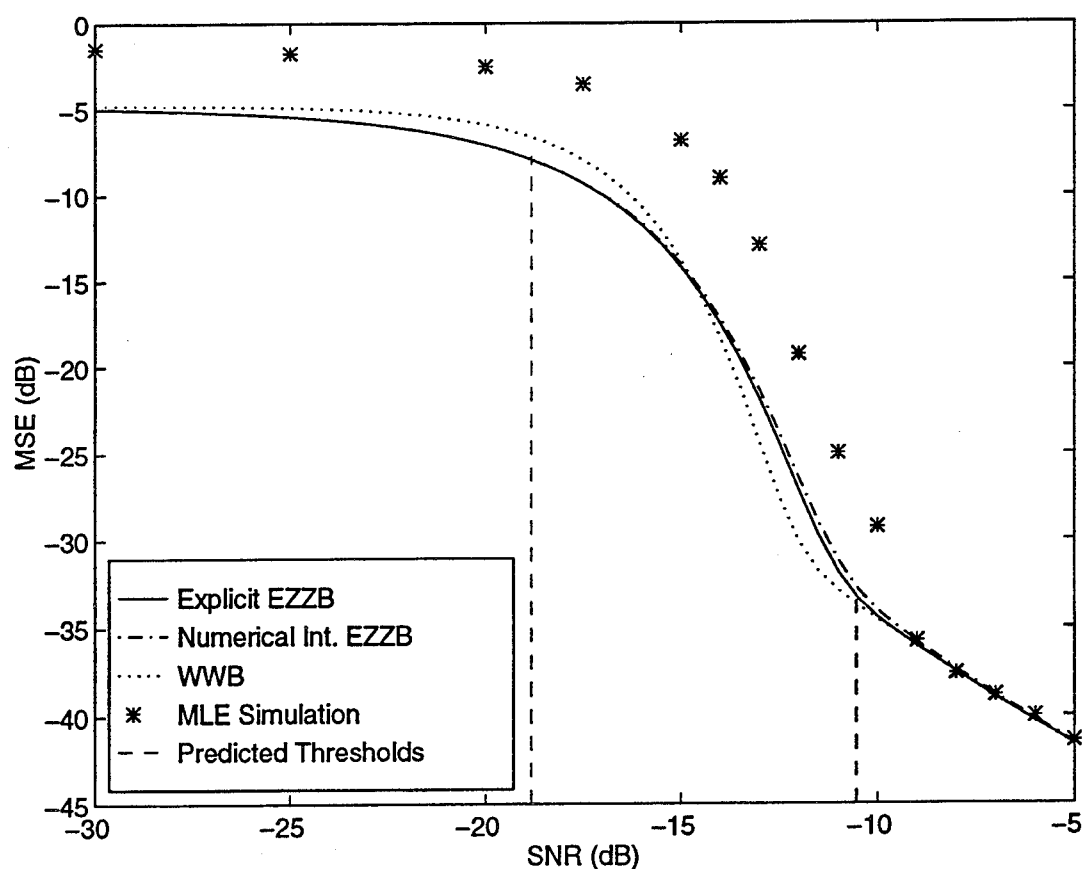
UNIFORM LINEAR ARRAY

$$(M = 8, d = \frac{7}{16}\lambda_0)$$



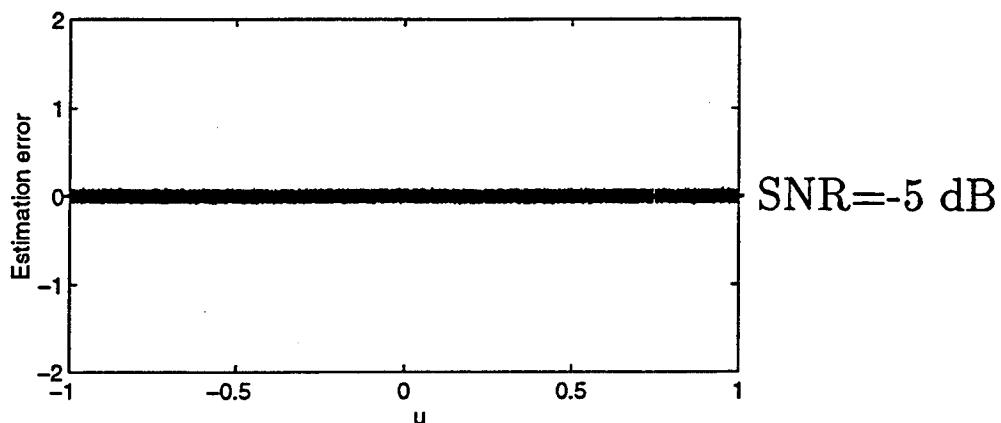
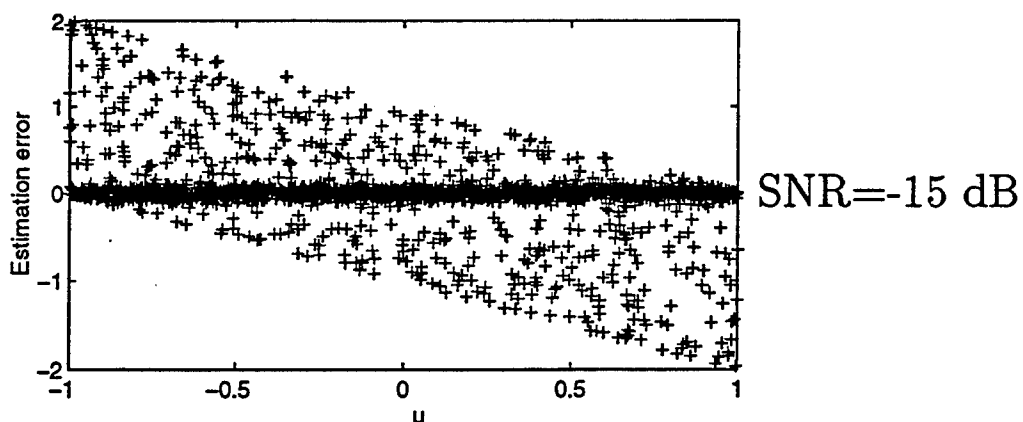
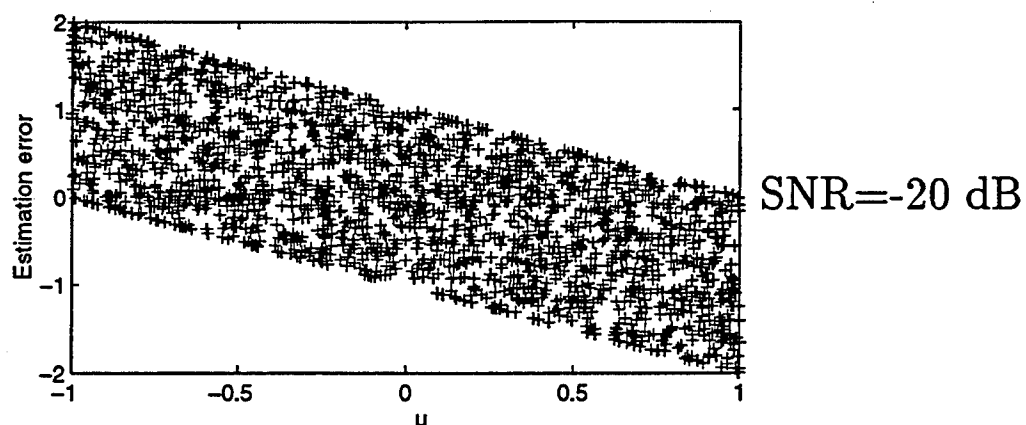
COMPARISON OF BOUNDS FOR LINEAR ARRAY

$$(M = 8, d = \frac{7}{16}\lambda_0, N = 100)$$



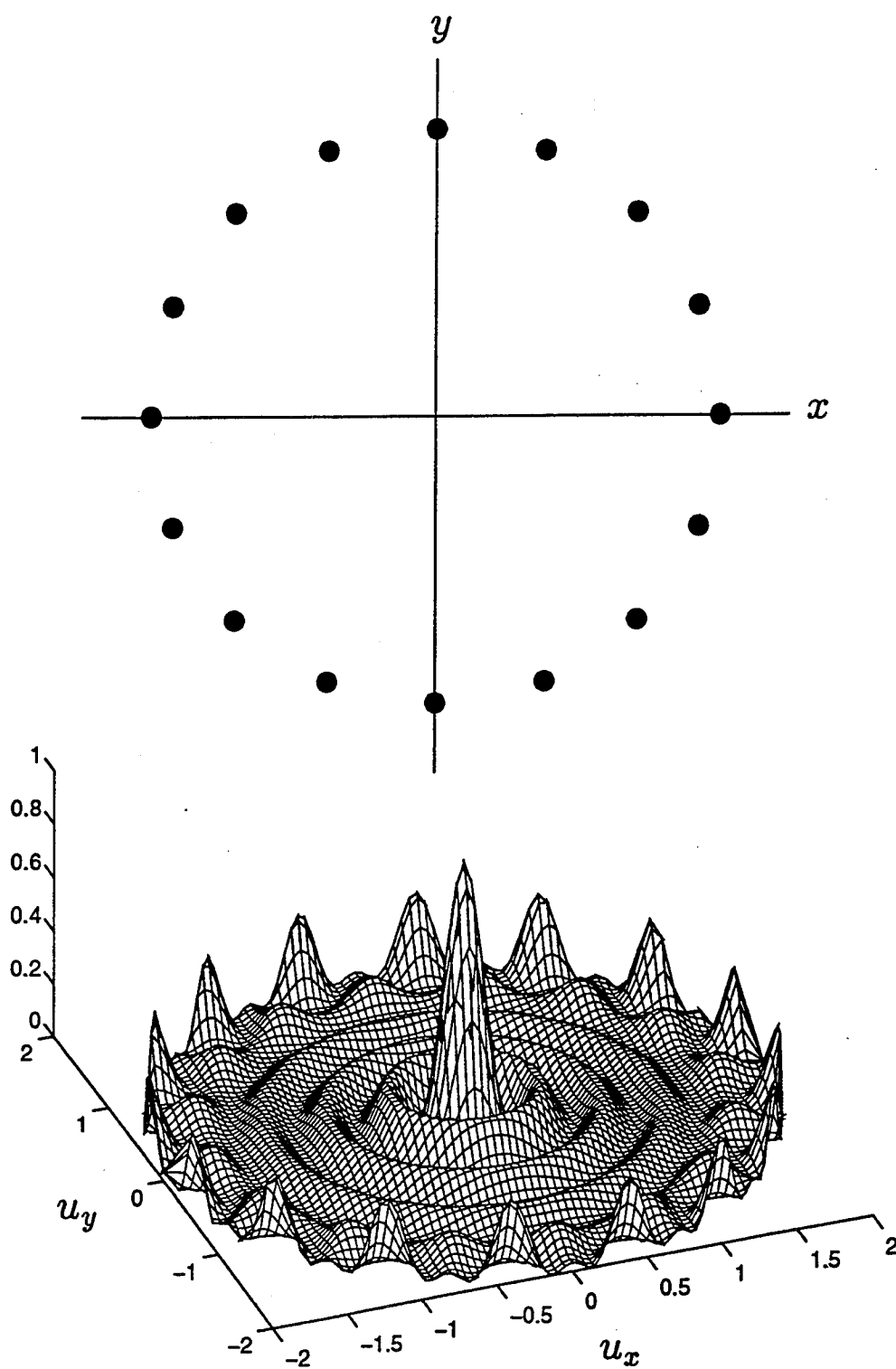
UNIFORM LINEAR ARRAY MLE SIMULATION

$(M = 8, d = \frac{7}{16}\lambda_0, N = 100, L = 2000)$



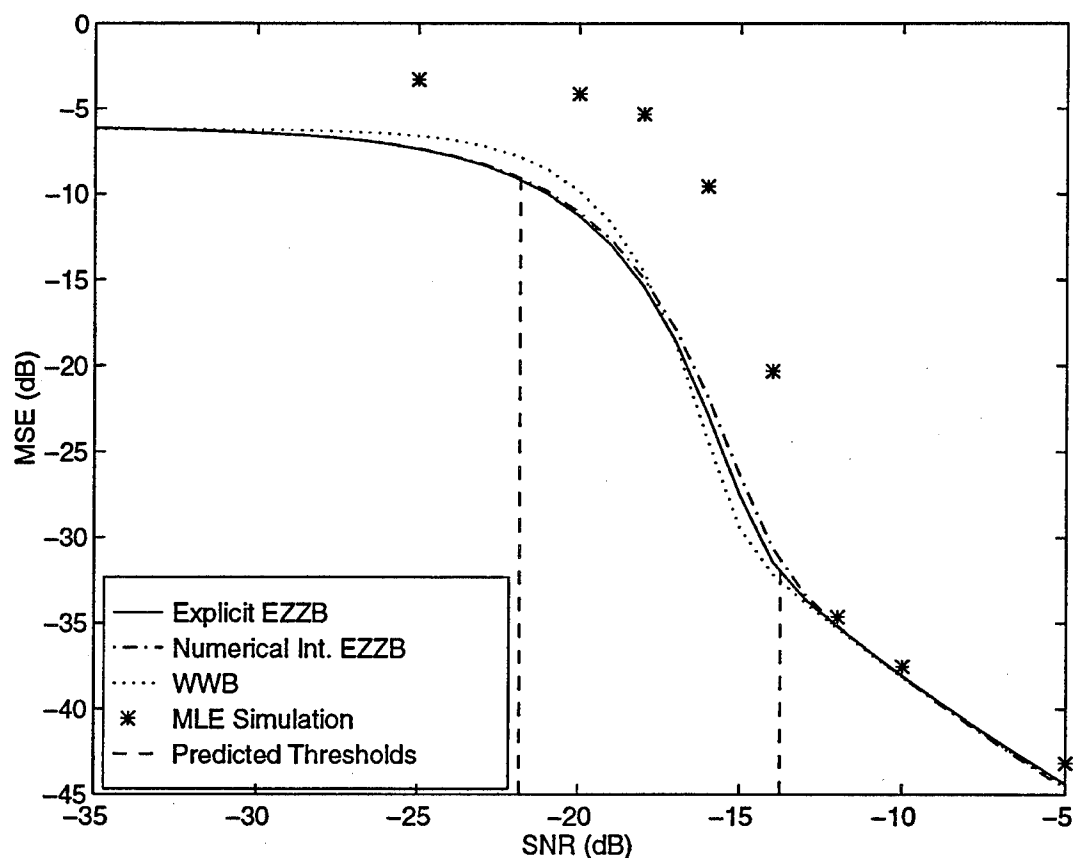
CIRCULAR ARRAY

$$(M = 16, d = \frac{\lambda_0}{2})$$



COMPARISON OF BOUNDS FOR CIRCULAR ARRAY

$$(M = 8, d = \frac{\lambda_0}{2}, N = 100)$$



SUMMARY

- Extended Ziv-Zakai bound for vectors of parameters with arbitrary continuous prior distributions
- Applied EZZB to two-dimensional bearing estimation problem for arrays with different geometries
 - Simple expressions for bound and thresholds
- Explicit EZZB close to numerically evaluated EZZB and WWB
- Predicted thresholds accurate
- MLE simulation performance close to bound

ANGLE AND DOPPLER ESTIMATION WITH SPACE-TIME ADAPTIVE PROCESSING RADAR

James Ward

MIT Lincoln Laboratory
244 Wood Street
Lexington, MA 02173-9108
tel: (617) 981-0617
email: jward@ll.mit.edu

Abstract The benefits of space-time adaptive processing (STAP) for improved interference suppression and target detection are well established. This presentation considers target parameter (angle and velocity) estimation with an airborne radar employing STAP. Cramer-Rao bounds for target angle and Doppler estimation accuracy are derived for an arbitrary interference scenario. These bounds show that in clutter, angle accuracy depends on Doppler and vice-versa. The bounds also provide the portions of the Doppler space and coverage sector over which a specified level of accuracy can be achieved. The maximum likelihood (ML) estimator is examined. A computationally efficient approximation to the ML estimator is developed and applied to several STAP architectures. Simulation results are presented and compared with the Cramer-Rao bound. It is shown that for targets close to the clutter ridge, the new estimators provide significantly better accuracy than conventional angle and velocity estimators that only utilize one-dimensional information after initial STAP detection.

ANGLE AND DOPPLER ESTIMATION WITH STAP RADAR

JAMES WARD

***4TH ANNUAL
ADAPTIVE SENSOR ARRAY PROCESSING WORKSHOP***

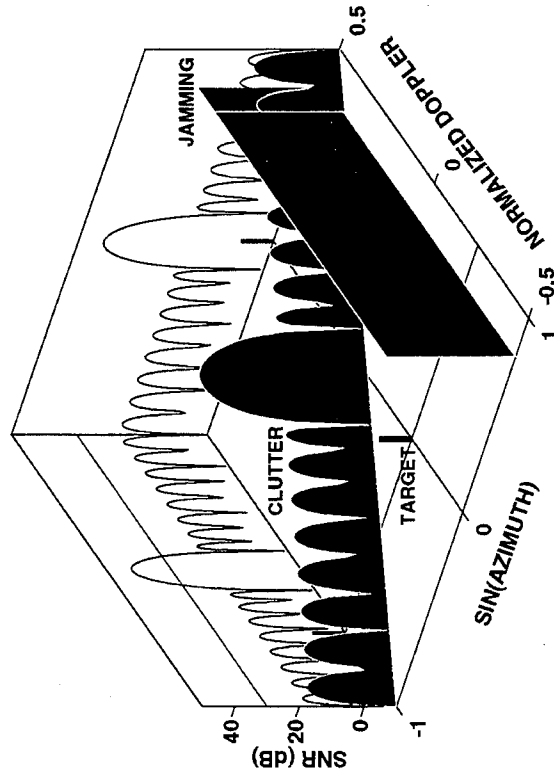
14 MARCH 1996

OUTLINE

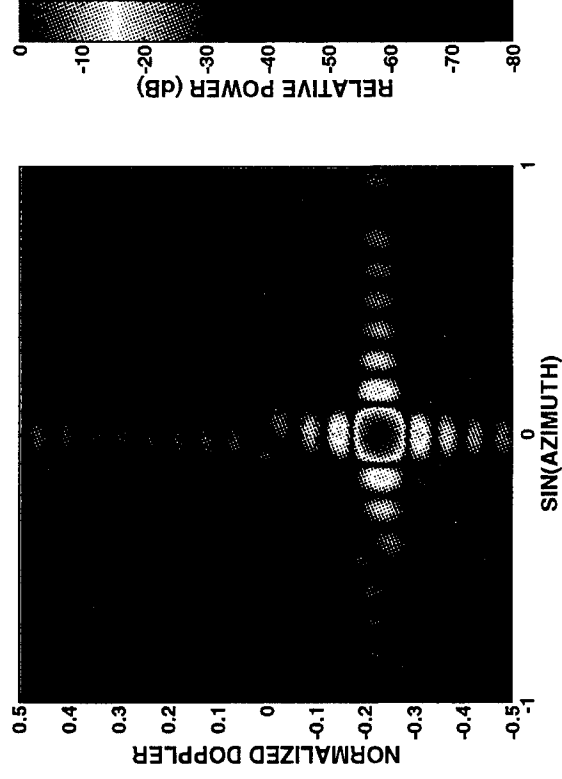
- **INTRODUCTION**
- **CRAMÉR-RAO BOUND ANALYSIS**
- **STAP ESTIMATION ALGORITHMS**
- **SUMMARY AND CONCLUSIONS**

SPACE-TIME ADAPTIVE PROCESSING (STAP)

INTERFERENCE POWER SPECTRUM



STAP RESPONSE



- MOST ANALYSES HAVE EMPHASIZED STAP NULLING AND DETECTION PERFORMANCE
- TARGET ACCURACY IS ALSO A PRIMARY CONCERN
- TARGET PARAMETER ESTIMATION MUST BE REEXAMINED FOR STAP RADAR

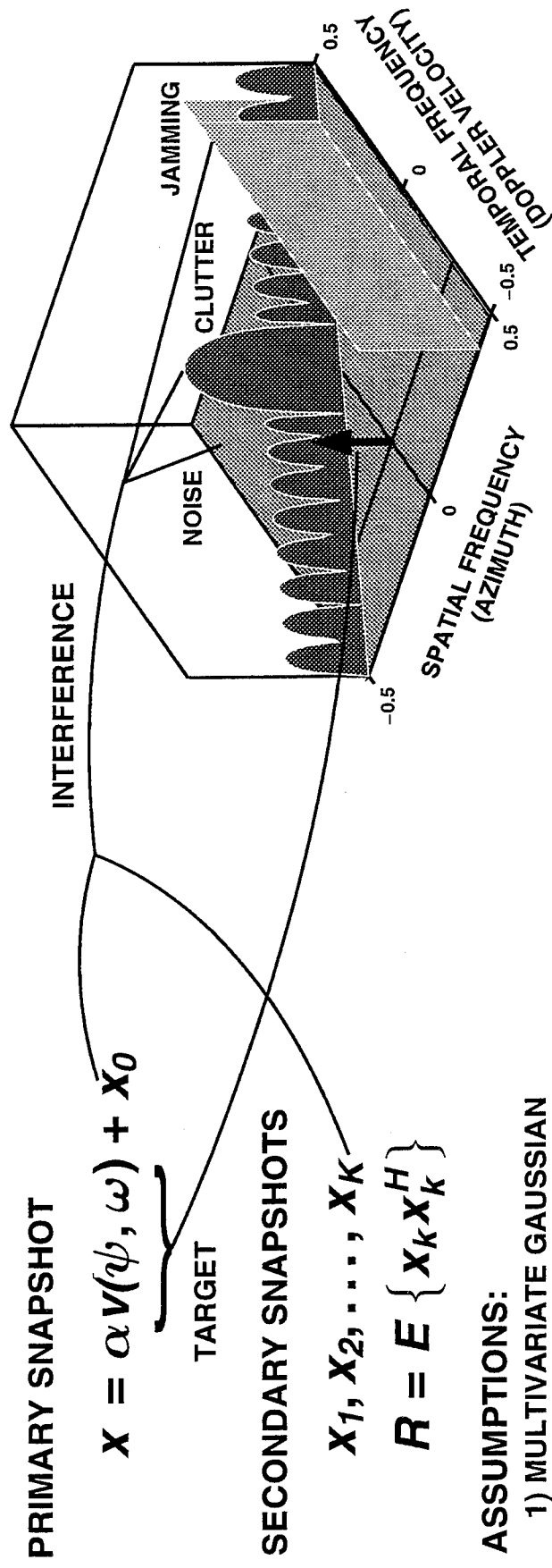
QUESTIONS

- WHAT'S THE BEST ANGLE AND DOPPLER ACCURACY POSSIBLE IN A STAP RADAR?
 - CRAMÉR-RAO BOUND ANALYSIS
- HOW SHOULD ONE ESTIMATE ANGLE AND VELOCITY IN A STAP RADAR?
 - DO "CONVENTIONAL" 1-D ESTIMATORS PERFORM WELL?
 - IS THERE ROOM FOR IMPROVEMENT (CLOSE TO CLUTTER RIDGE)?
 - DO TRUE STAP ESTIMATORS PERFORM BETTER?
 - IF SO, AT WHAT COST IN COMPUTATIONAL COMPLEXITY?

OUTLINE

- **INTRODUCTION**
- **CRAMÉR-RAO BOUND ANALYSIS**
- **STAP ESTIMATION ALGORITHMS**
- **SUMMARY AND CONCLUSIONS**

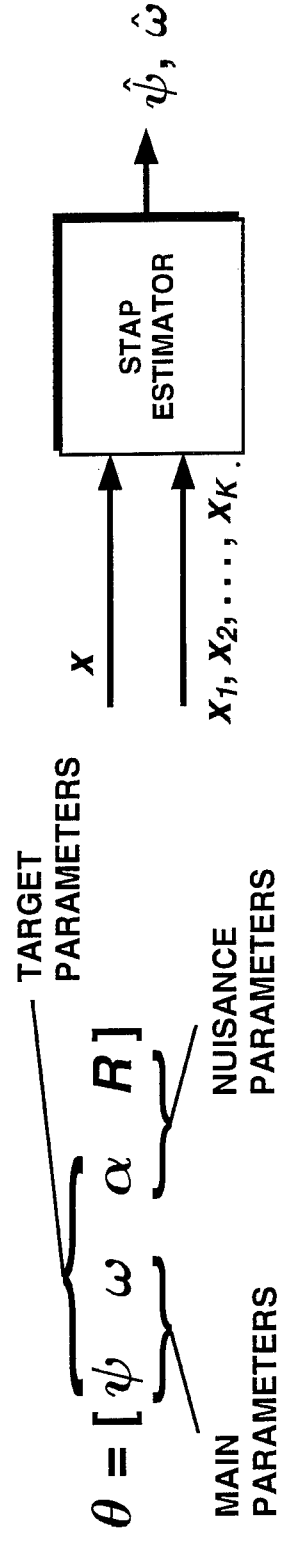
DATA MODEL AND ASSUMPTIONS



ASSUMPTIONS:

- 1) MULTIVARIATE GAUSSIAN
- 2) TARGET ONLY IN PRIMARY SNAPSHOT
- 3) COMMON INTERFERENCE COVARIANCE MATRIX

A MULTIPLE PARAMETER ESTIMATION PROBLEM:

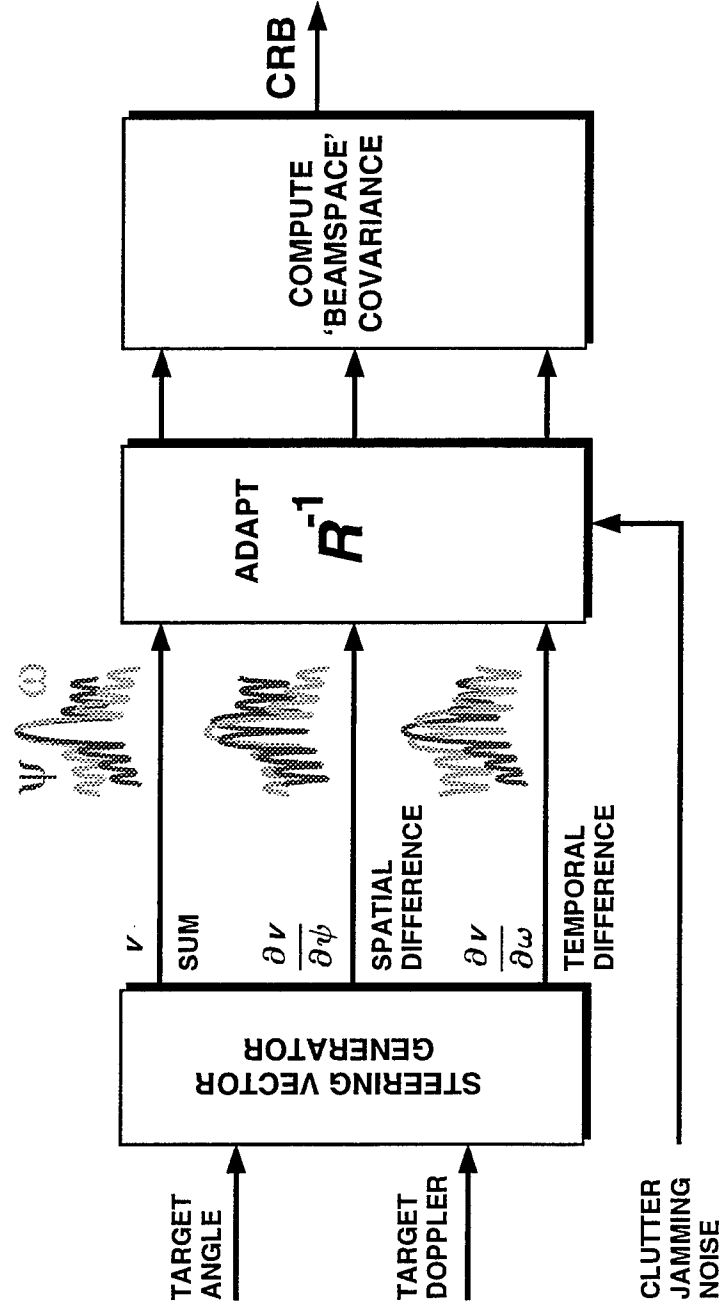


THE STAP CRAMÉR-RAO BOUND (CRB)

CRB DEFINITION:

$$C = E \{ (\hat{\theta} - \theta)(\hat{\theta} - \theta)^T \} \geq \left[-E \left\{ \frac{\partial^2 \log p(x|\theta)}{\partial \theta_i \partial \theta_j} \right\} \right]^{-1}$$

STAP CRB COMPUTATION:



STAP CRB RESULTS (1)

- ERROR COVARIANCE MATRIX (TARGET PARAMETERS ONLY):

$$C_{CRB} = \frac{1}{2} \begin{bmatrix} \mu^2 \delta_s & \mu^2 \beta_d & \mu \beta_s & \mu^2 \gamma_s \\ \mu^2 \beta_d & \mu^2 \delta_t & \mu \beta_t & \mu^2 \gamma_t \\ \mu \beta_s & \mu \beta_t & \xi & 0 \\ \mu^2 \gamma_s & \mu^2 \gamma_t & 0 & \mu^2 \xi \end{bmatrix}^{-1}$$

- VARIANCES OF PRIMARY TARGET PARAMETERS:

$\sigma_\psi^2 \geq \frac{\delta_t \sin^2 \zeta_t}{2\mu^2(\delta_s \delta_t \sin^2 \zeta_s \sin^2 \zeta_t - \epsilon^2)}$	SPATIAL FREQUENCY
$\sigma_\omega^2 \geq \frac{\delta_s \sin^2 \zeta_s}{2\mu^2(\delta_s \delta_t \sin^2 \zeta_s \sin^2 \zeta_t - \epsilon^2)}$	TEMPORAL FREQUENCY

- THE CRB FOR THE TARGET PARAMETERS IS THE SAME FOR KNOWN AND UNKNOWN COVARIANCE DATA MODELS

STAP CRB RESULTS (2)

- REDUCES TO FAMILIAR FORM IN WHITE NOISE ONLY:

$$\sigma_{\psi 0}^2 \geq \frac{6}{MN(ESNR)(N^2 - 1)},$$

$$\sigma_{\omega 0}^2 \geq \frac{6}{MN(ESNR)(M^2 - 1)},$$

$ESNR =$ TARGET SNR PER ELEMENT PER PULSE

$N =$ NUMBER OF ELEMENTS

$M =$ NUMBER OF PULSES

- VARIANCES IN PREFERRED COORDINATES:

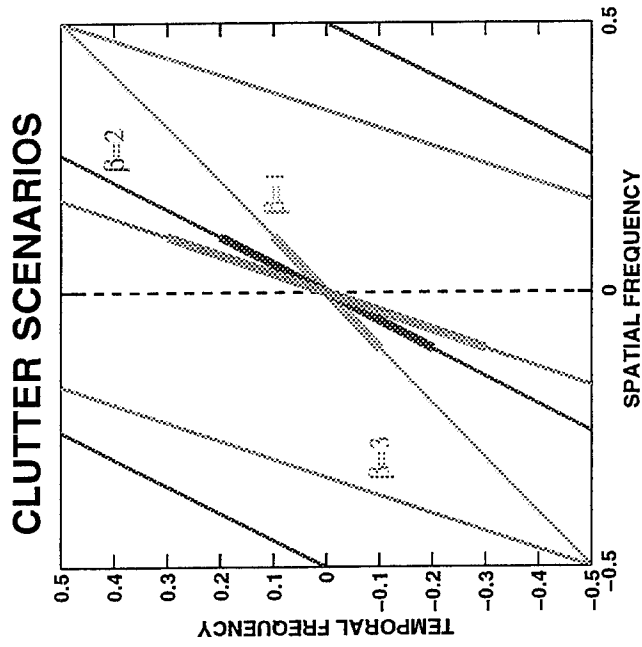
$$\sigma_{\phi}^2 \geq \frac{\delta_t \sin^2 \zeta_t}{\left(\frac{2\pi d}{\lambda}\right)^2 2\mu^2 (\delta_s \delta_t \sin^2 \zeta_s \sin^2 \zeta_t - \epsilon^2) \cos^2 \phi}$$

AZIMUTH

$$\sigma_v^2 \geq \frac{\delta_s \sin^2 \zeta_s}{\left(\frac{4\pi}{\lambda f_r}\right)^2 2\mu^2 (\delta_s \delta_t \sin^2 \zeta_s \sin^2 \zeta_t - \epsilon^2)}$$

RADIAL VELOCITY

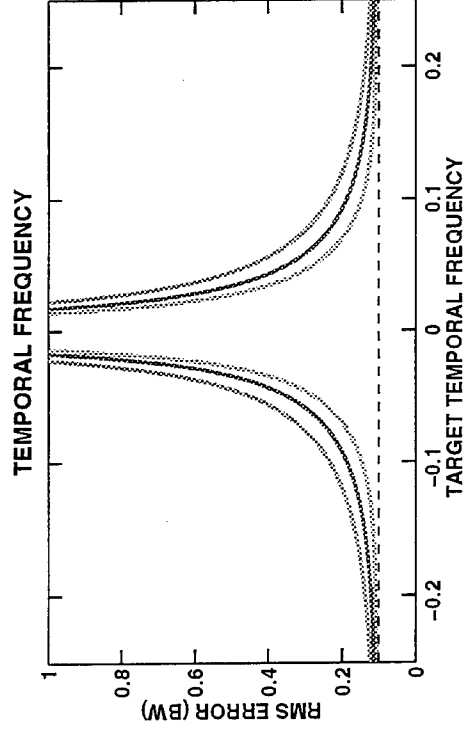
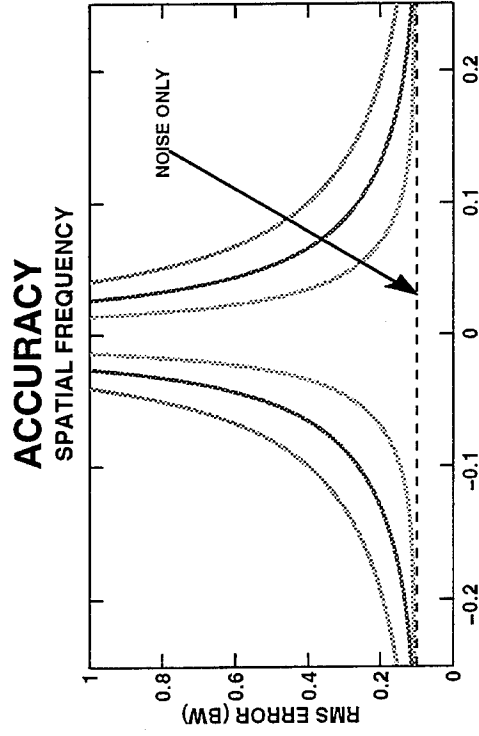
CLUTTER IMPACT ON STAP ACCURACY



- ESTIMATION PERFORMANCE DEGRADES AS PLATFORM VELOCITY INCREASES

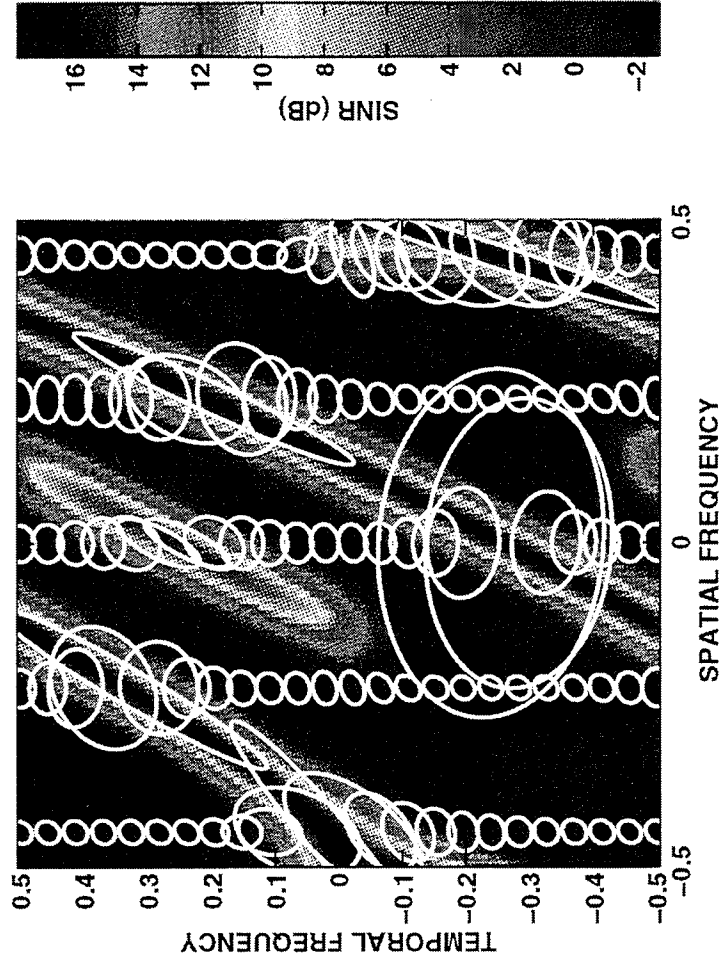
$$\beta = \frac{2v}{d(PRF)}$$

- ANGLE ACCURACY DEGRADED MORE THAN DOPPLER ACCURACY



10 ELEMENT ARRAY, 10 PULSES/CPI
CNR = 40 dB, SNR = -8 dB

STAP ERROR ELLIPSES



8 ELEMENT ARRAY, 8 PULSES/CPI
 ROTATING ARRAY, SCAN ANGLE = 15° , SNR = 0 dB
 CNR = 50 dB, $\beta = 2$

95% CONFIDENCE (2σ) ELLIPSES
 SIZE AND ORIENTATION OF ERROR ELLIPSE CHANGES AS TARGET
 GETS CLOSE TO CLUTTER RIDGE

OUTLINE

- **INTRODUCTION**
- **CRAMÉR-RAO BOUND ANALYSIS**
- **STAP ESTIMATION ALGORITHMS**
- **SUMMARY AND CONCLUSIONS**

MAXIMUM LIKELIHOOD (ML) ESTIMATION OF TARGET ANGLE AND DOPPLER

MAXIMIZE THE LOG-LIKELIHOOD OVER UNKNOWN PARAMETERS:

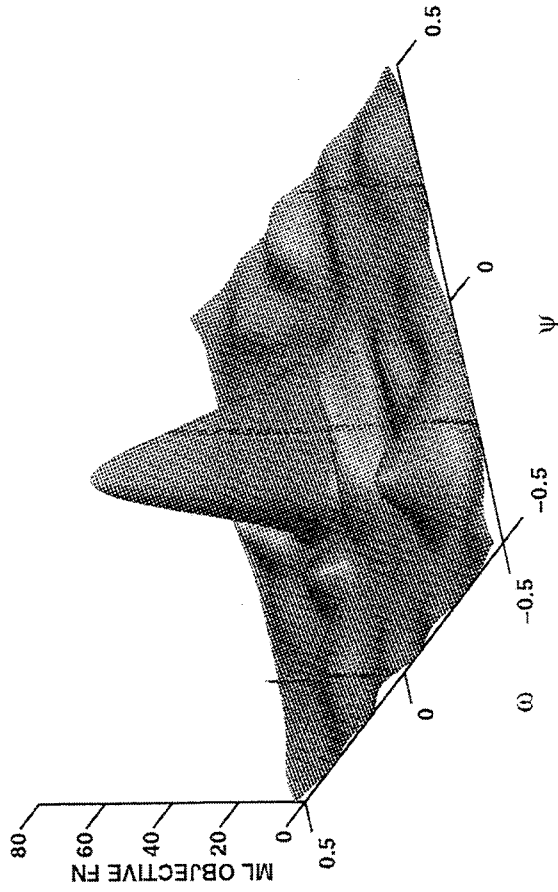
$$\begin{bmatrix} \hat{\psi} \\ \hat{\omega} \end{bmatrix} = \underset{[\psi \ \omega]^T}{\operatorname{argmax}} \frac{|v^H(\psi, \omega) \hat{R}^{-1} x_0|^2}{v^H(\psi, \omega) \hat{R}^{-1} v(\psi, \omega)}$$

- SEVERAL INTERPRETATIONS:
 - FORM GRID OF ADAPTIVE FILTERS, CHOOSE ANGLE, DOPPLER OF FILTER WITH MAX 'SINR'
 - MAXIMIZE OVER A GRID OF ADAPTIVE MATCHED FILTER (AMF) DETECTOR OUTPUTS
 - MAXIMIZE THE PROJECTION OF WHITENED STEERING VECTOR ONTO WHITENED TARGET SNAPSHOT
- FORM OF ML ESTIMATOR IS THE SAME FOR BOTH KNOWN AND UNKNOWN COVARIANCE DATA MODELS
- ASYMPTOTICALLY UNBIASED AS SNR GETS LARGE

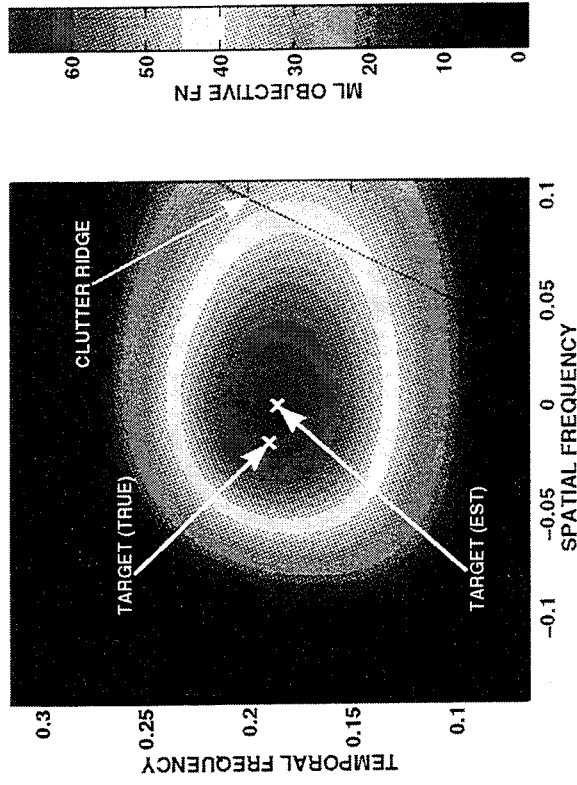
THE STAP ML OBJECTIVE FUNCTION

PEAK PROVIDES ESTIMATED TARGET PARAMETERS

FULL VIEW



CLOSE UP AT PEAK

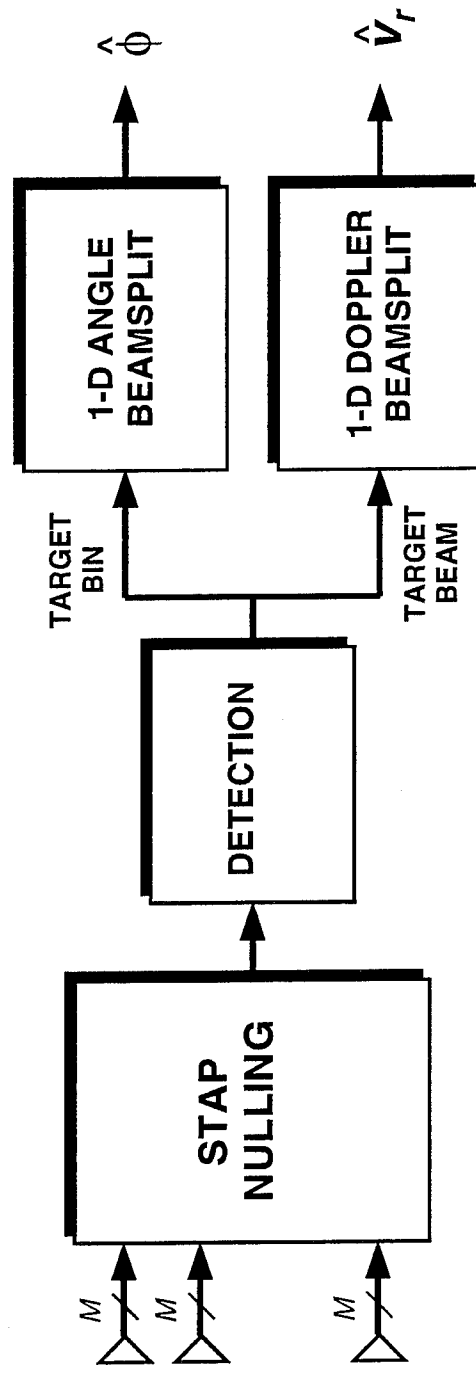


8 ELEMENT ARRAY, 8 PULSE CPI, 320 SAMPLES
 TARGET AT $\psi_t = -0.01, \omega_t = 0.19$, SINR = 13 dB
 CNR = 40 dB, $\beta = 2$

OPTIMIZATION APPROACHES

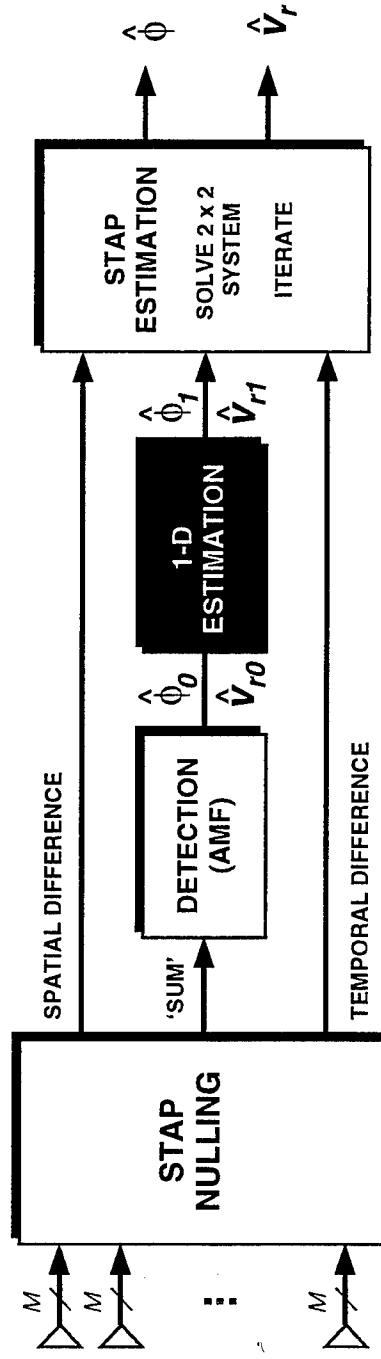
- **GLOBAL SEARCH**
 - **COMPUTATIONALLY CUMBERSOME DENSE 2-D GRID SEARCH**
- **'CONVENTIONAL'**
 - **SEPARATE 1-D OPTIMIZATIONS AFTER STAP NULLING**
- **NEWTON'S METHOD**
 - **REQUIRES FIRST AND SECOND DERIVATIVE FILTERS**
- **QUASI-NEWTON METHOD**
 - **APPROXIMATE HESSIAN WITH 'SUM', 'SPATIAL DIFFERENCE', AND 'TEMPORAL DIFFERENCE' FILTERS**

'CONVENTIONAL' 1-D STAP ESTIMATOR



- SIMILAR TO ESTIMATORS IN CONVENTIONAL (NON-STAP) RADARS

QUASI-NEWTON STAP ML ESTIMATOR



- HESSIAN APPROXIMATED FROM THREE SPACE-TIME FILTERS
 - TARGET COMPONENT FROM INITIAL CONDITION
 - INTERFERENCE COMPONENT FROM SAMPLE COVARIANCE MATRIX
- CONVERGENCE DEPENDENT ON INITIAL CONDITION
 - COARSE DETECTION GRID INSUFFICIENT
- SOLVE 2×2 LINEAR SYSTEM FOR EACH ITERATION

QUASI-NEWTON STAP ESTIMATOR – THE MATH

- QUASI-NEWTON ITERATION

$$\begin{bmatrix} \hat{\psi}_{k+1} \\ \hat{\omega}_{k+1} \end{bmatrix} = \begin{bmatrix} \hat{\psi}_k \\ \hat{\omega}_k \end{bmatrix} - H_k^{-1} g_k$$

- GRADIENT VECTOR (EXACT)

$$g_\psi = \frac{2}{\xi^2} \text{Re}(\xi y_o y_s^* - |y_o|^2 \eta_s) \quad , \quad g_\omega = \frac{2}{\xi^2} \text{Re}(\xi y_o y_t^* - |y_o|^2 \eta_t)$$

- HESSIAN MATRIX (APPROXIMATED)

$$H_{\psi\psi} = -\frac{2|y_o|^2}{\xi^3} (\xi \delta_s - |\eta_s|^2) \quad , \quad H_{\omega\omega} = -\frac{2|y_o|^2}{\xi^3} (\xi \delta_t - |\eta_t|^2)$$

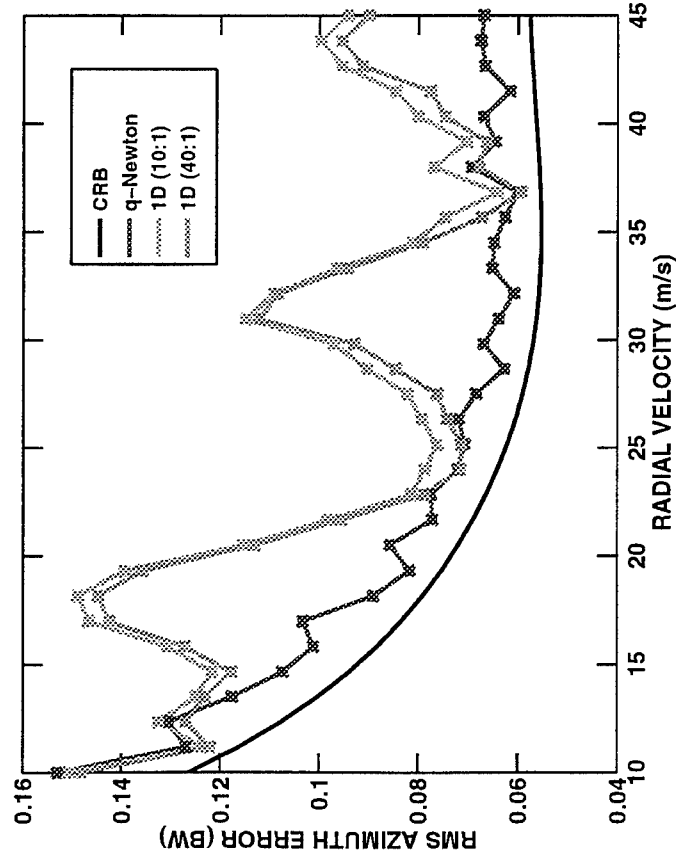
$$H_{\psi\omega} = -\frac{2|y_o|^2}{\xi^3} \text{Re}(\xi \eta_{st} - \eta_s^* \eta_t)$$

- SAMPLE ESTIMATES OF THE SAME TERMS THAT WERE USED IN THE CRAMÉR-RAO BOUND!

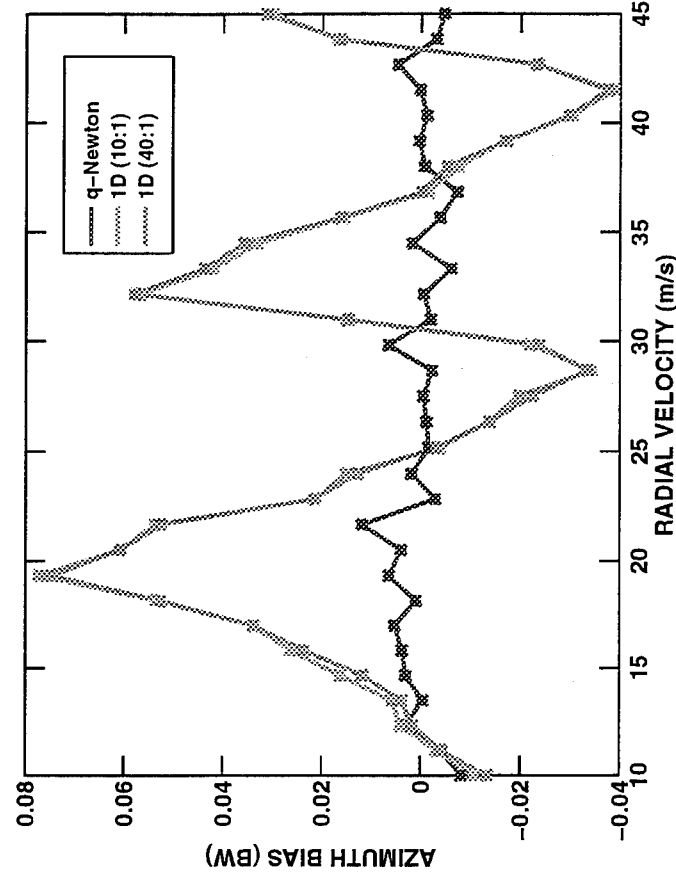
PERFORMANCE VERSUS TARGET DOPPLER

AZIMUTH ERROR

RMS ERROR



BIAS

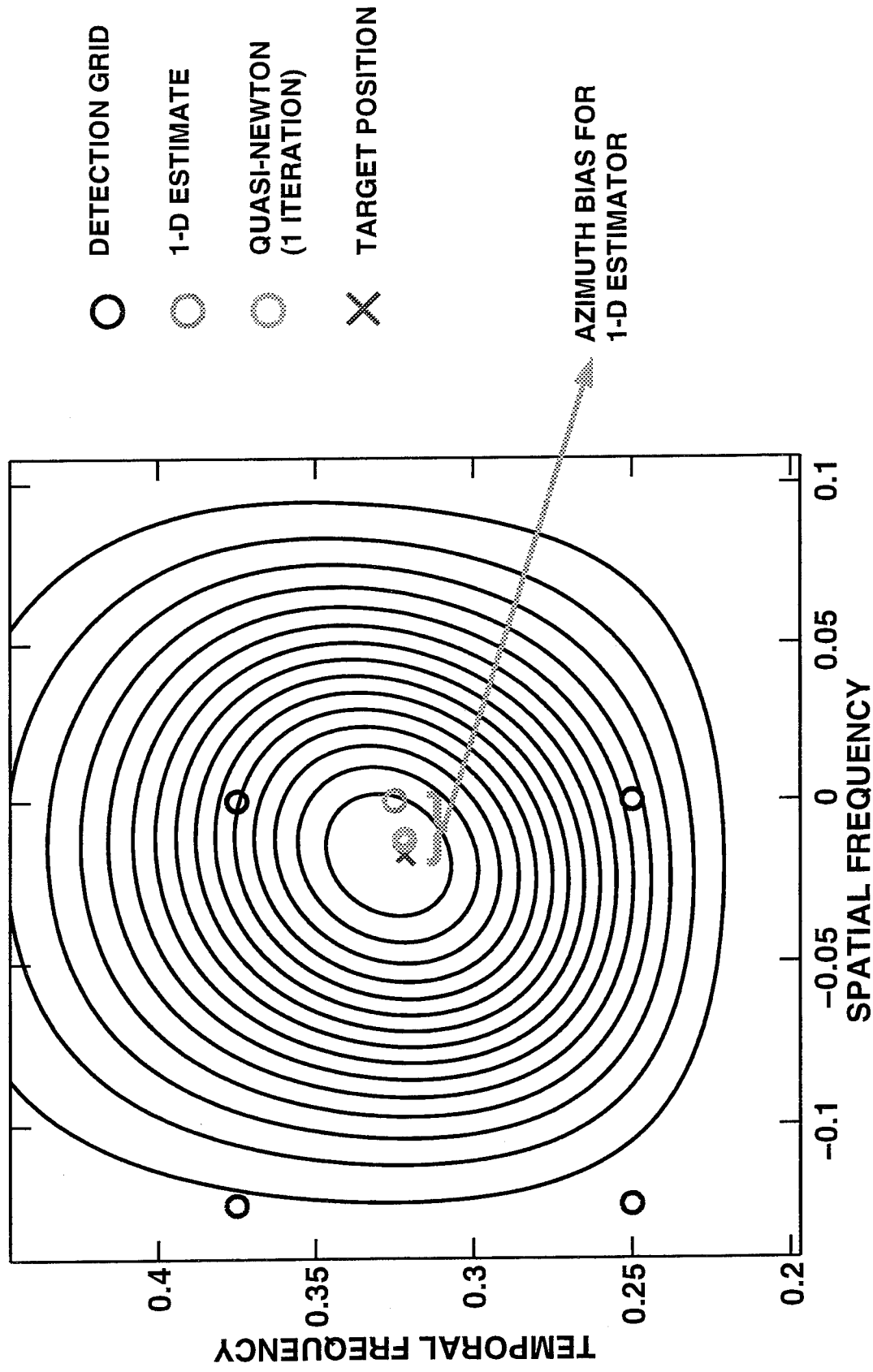


8 ELEMENT ARRAY, 8 PULSE CPI, 320 SAMPLES, 400 TRIALS

TARGET: AT $\psi_t = -0.017$, $SNR = 0$ dB

CLUTTER: $CNR = 40$ dB, $\beta = 2$

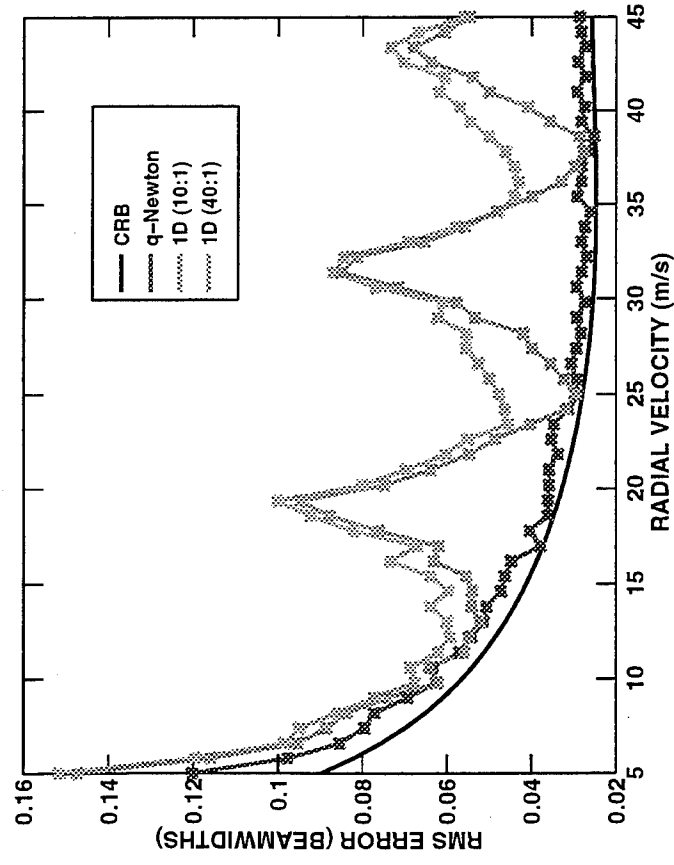
BIAS IN CONVENTIONAL 1-D ESTIMATOR



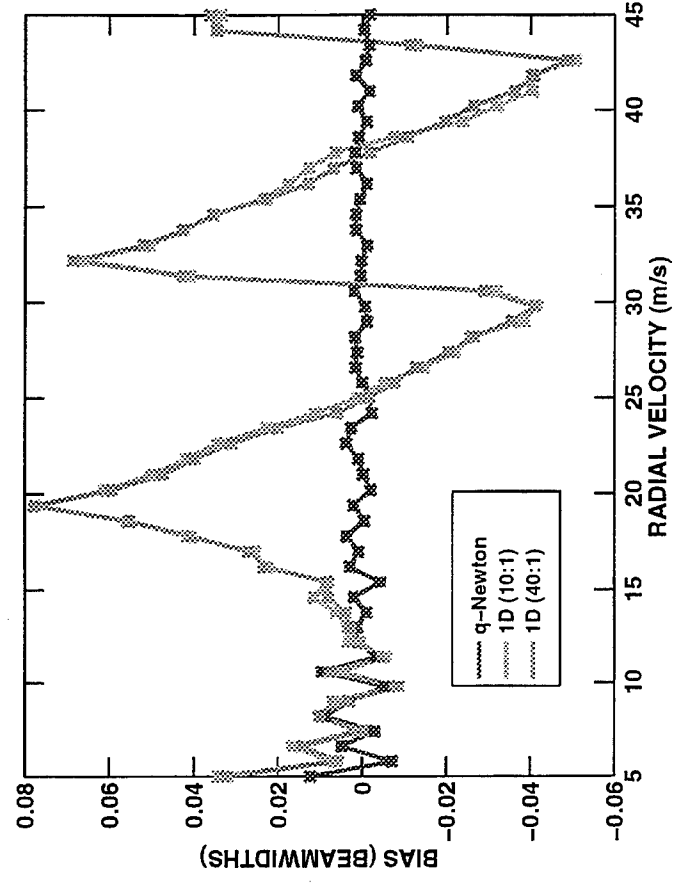
PERFORMANCE VERSUS TARGET DOPPLER

AZIMUTH ERROR

RMS ERROR



BIAS



8 ELEMENT ARRAY, 8 PULSE CPI, 320 SAMPLES, 400 TRIALS

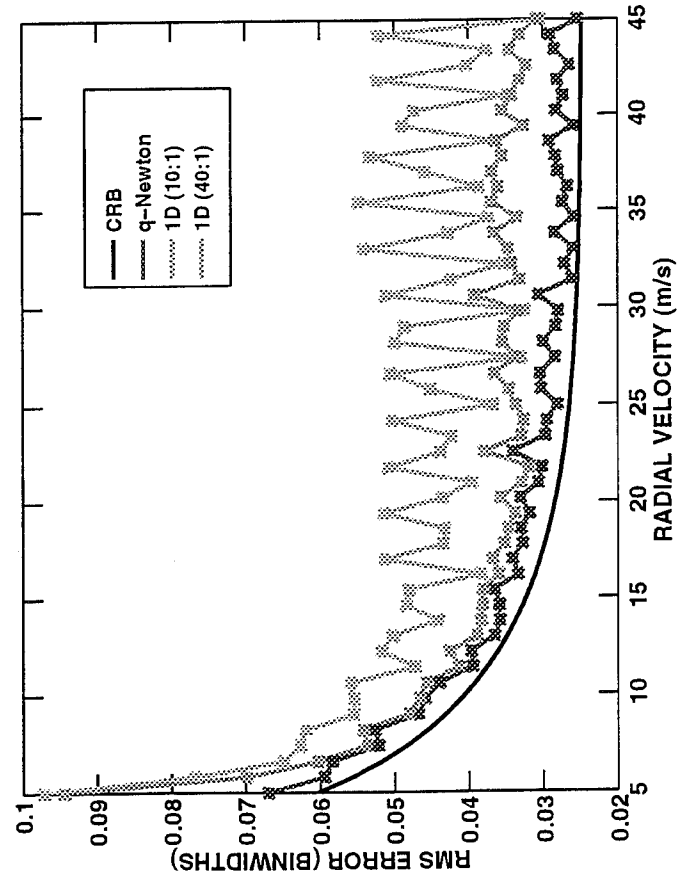
TARGET: AT $\psi_t = -0.017$, SNR = 6.9 dB

CLUTTER: CNR = 40 dB, $\beta = 2$

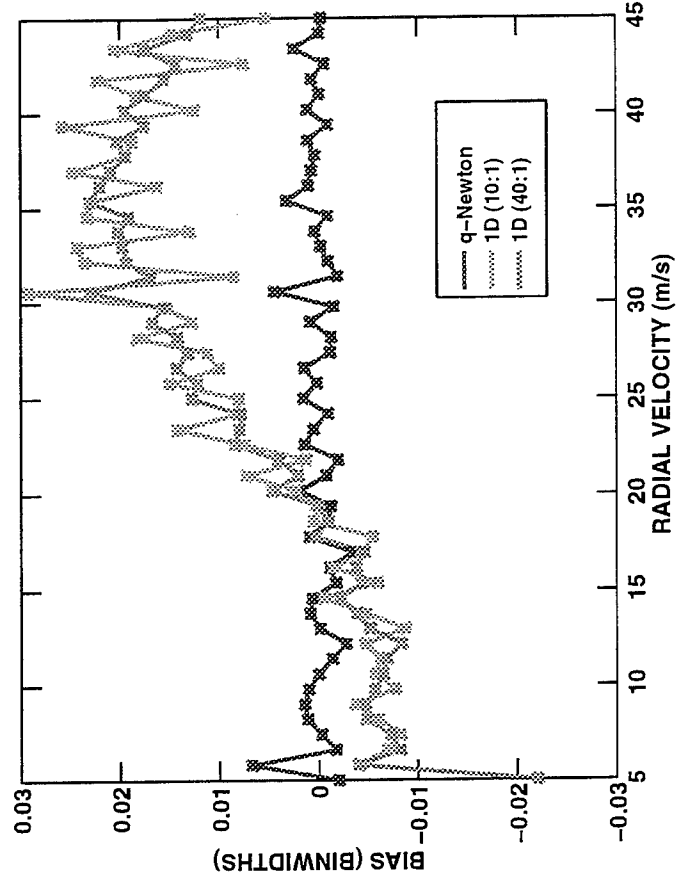
PERFORMANCE VERSUS TARGET DOPPLER

DOPPLER VELOCITY ERROR

RMS ERROR



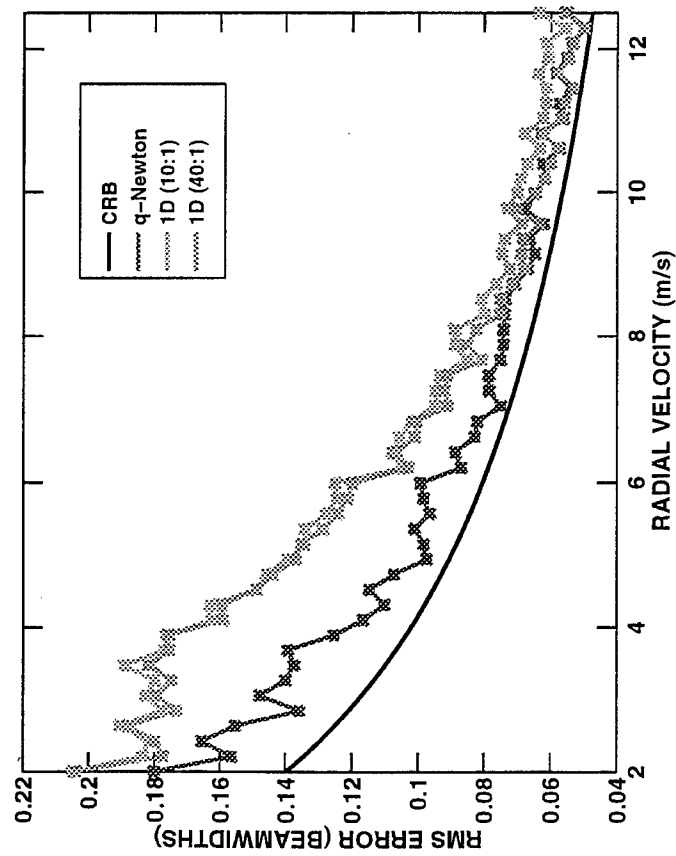
BIAS



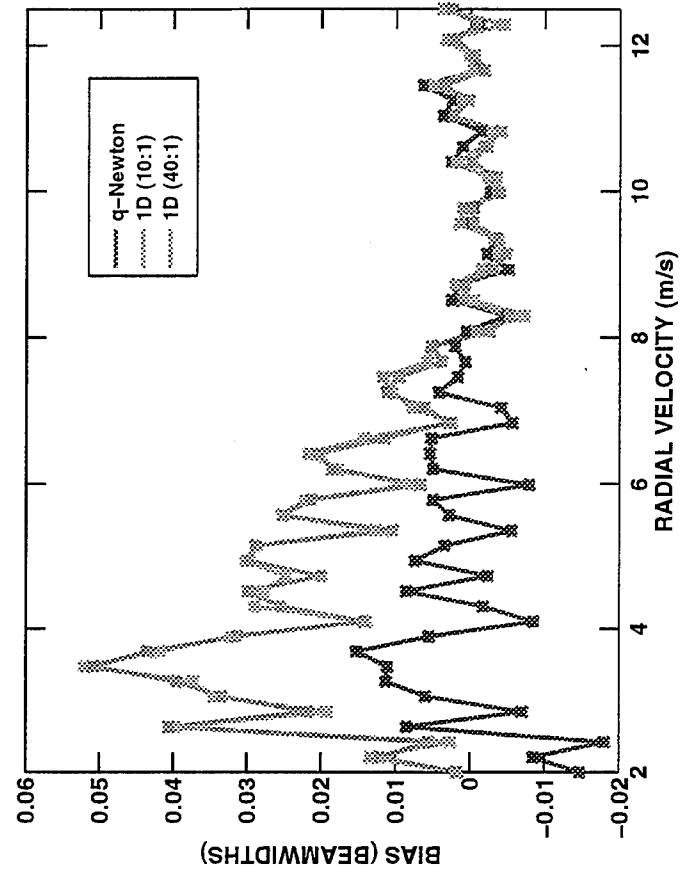
CLOSE TO THE CLUTTER RIDGE

AZIMUTH ERROR

RMS ERROR



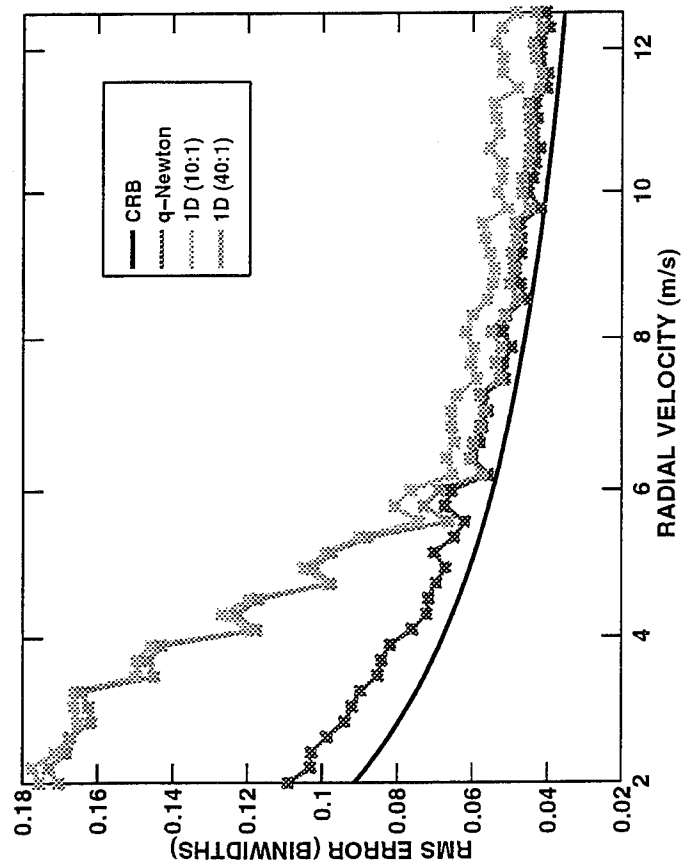
BIAS



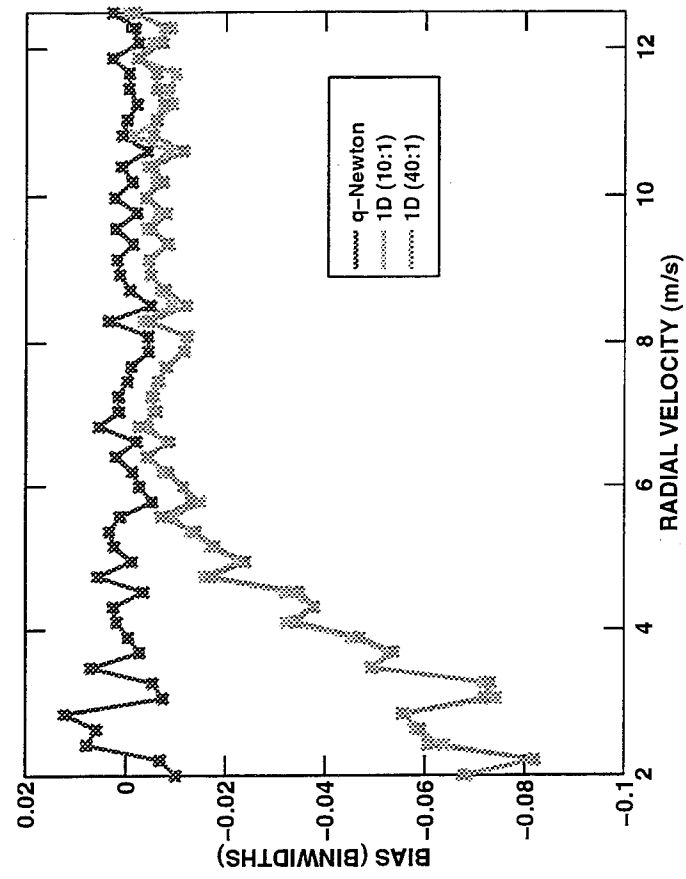
CLOSE TO THE CLUTTER RIDGE

DOPPLER VELOCITY ERROR

RMS ERROR



BIAS



SUMMARY AND CONCLUSIONS

- **DERIVED CRAMÉR-RAO BOUND FOR ANGLE AND DOPPLER ACCURACY WITH STAP RADAR**
- **DEVELOPED A QUASI-NEWTON ALGORITHM FOR STAP MAXIMUM LIKELIHOOD ANGLE-DOPPLER ESTIMATION**
 - **REQUIRES ADAPTIVE SPACE-TIME SUM AND DIFFERENCE FILTERS**
 - **REQUIRES THE SOLUTION OF A 2×2 LINEAR SYSTEM FOR EACH ITERATION**
 - **GOOD INITIAL CONDITION REQUIRED**
- **EVALUATED NEW AND CONVENTIONAL ESTIMATORS WITH MONTE CARLO SIMULATION**
 - **CONVENTIONAL 1-D ESTIMATOR EXHIBITS LOCATION-DEPENDENT BIAS AND POOR PERFORMANCE NEAR CLUTTER RIDGE**
 - **NEW ESTIMATOR IS UNBIASED AND PROVIDES IMPROVED ACCURACY CLOSE TO CLUTTER RIDGE**

RADOME EFFECTS ON TWO-DIMENSIONAL ANGLE ESTIMATION

Ralph T. Compton, Jr.

Compton Research, Inc.
477 Poe Avenue
Worthington, OH 43085-3036
tel: (614) 885-0907
fax: (614) 885-0907

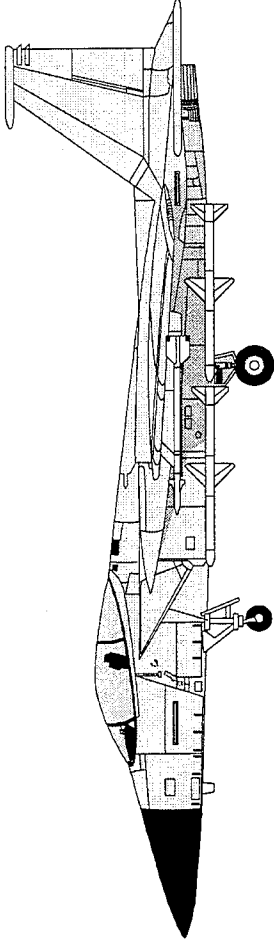
email: compton@ee.eng.ohio-state.edu

Abstract This presentation describes the effects of a radome on the performance of a two-dimensional adaptive maximum likelihood angle estimation technique. The problem of interest is to estimate the azimuth and elevation angles of a target using a four-quadrant circular antenna behind a radome similar to that of an Advanced Tactical Fighter (ATF). It is assumed that mainbeam jamming may be present along with the target signal. The presentation describes the use of adaptive maximum likelihood angle estimation to solve this problem and shows how the radome and the jamming affect the means and variances of the estimates.

**RADOME EFFECTS
ON
TWO-DIMENSIONAL ANGLE ESTIMATION***

**TED COMPTON
COMPTON RESEARCH, INC.**

*THIS WORK FUNDED BY WL/AARM-3, WRIGHT-PATTERSON AFB, OH



PURPOSE

- EVALUATE ANGLE ESTIMATION TECHNIQUES THAT CAN OPERATE IN THE PRESENCE OF MAIN BEAM JAMMING
- DETERMINE THE EFFECTS OF A RADOME ON 2-D ANGLE ESTIMATION
- THIS TALK WILL FOCUS ON THE ADAPTIVE MAXIMUM LIKELIHOOD METHOD

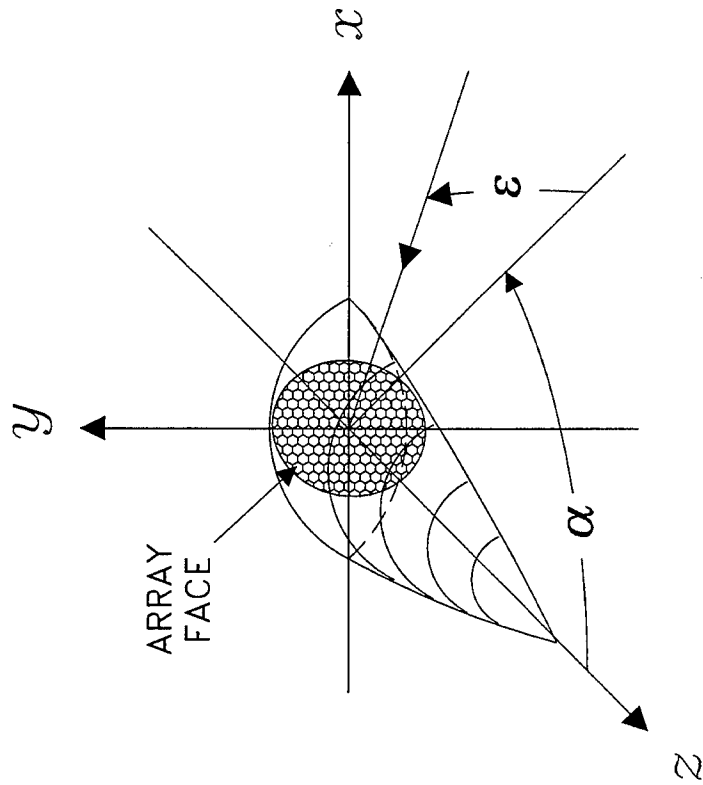
OUTLINE

- DESCRIBE ANTENNA AND RADOME
- DESCRIBE METHOD OF CALCULATING RECEIVED SIGNALS BEHIND THE RADOME
- REVIEW ADAPTIVE MAXIMUM LIKELIHOOD ANGLE ESTIMATION
- SHOW TYPICAL ML-SURFACES THAT MUST BE SEARCHED TO OBTAIN THE ANGLE ESTIMATES
- SHOW TYPICAL RADOME INDUCED ERRORS IN THE ESTIMATED ANGLES

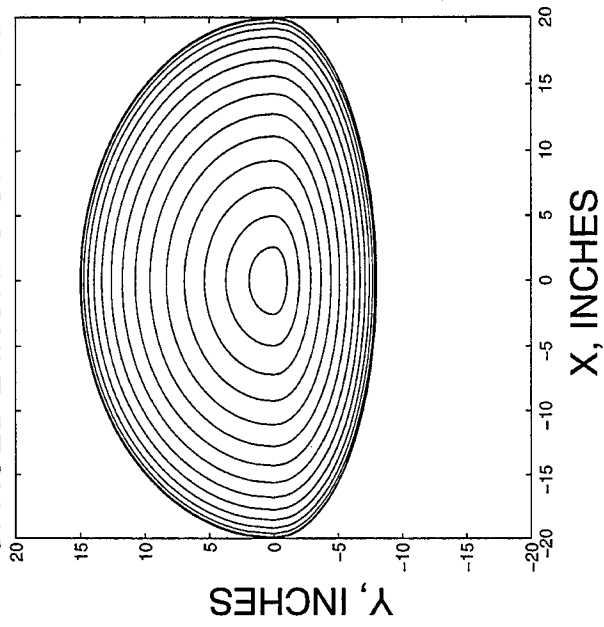
RADOME

CRI

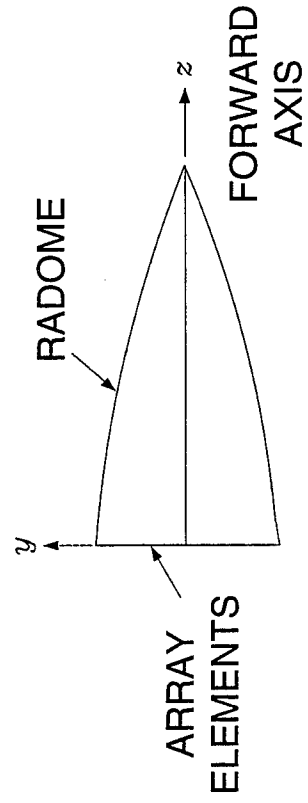
CIRCULAR ANTENNA BEHIND RADOME



RADOME CONTOURS SPACED 2 INCHES ON Z-AXIS

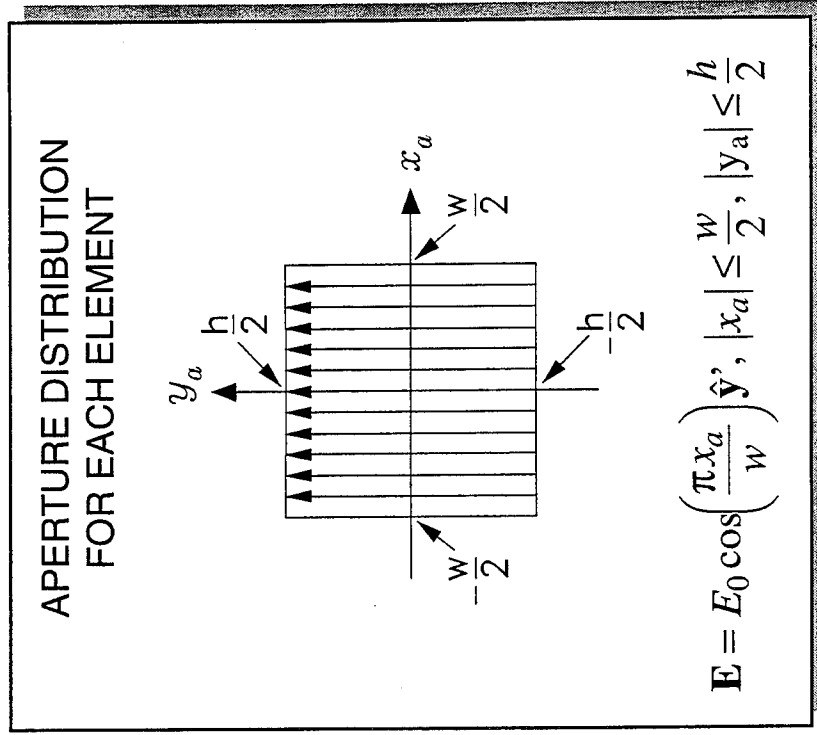
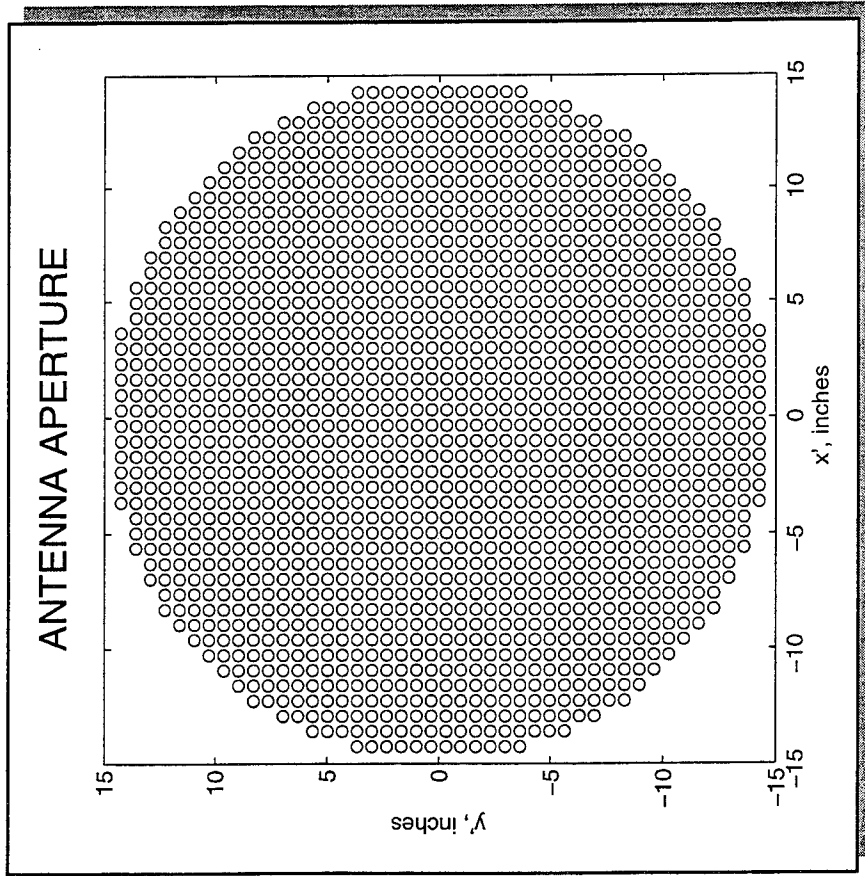


SIDE VIEW



CIRCULAR ANTENNA APERTURE

CRI



1568 ELEMENTS

ELEMENT SPACING = 0.663 INCHES = 0.505 λ

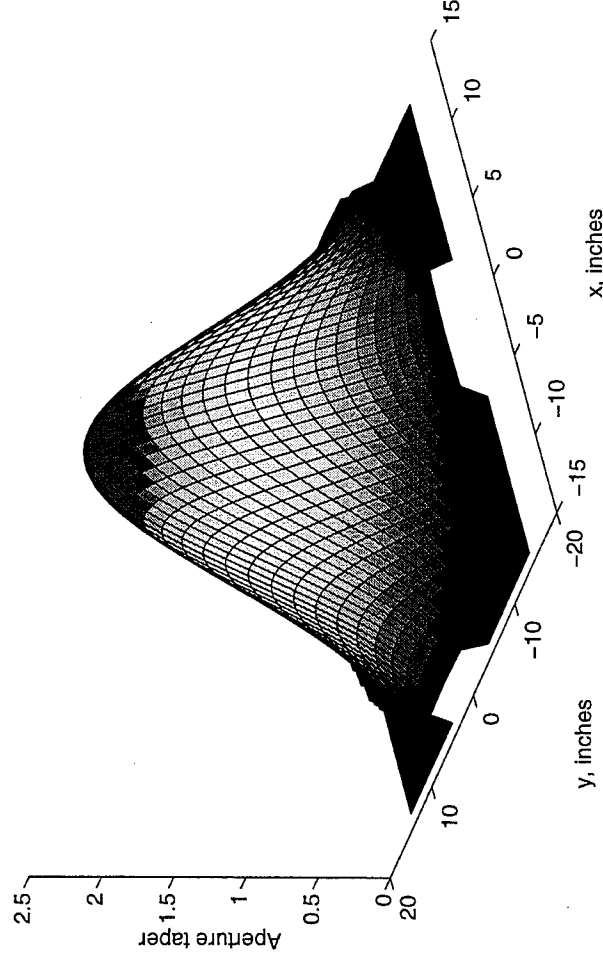
ARRAY DIAMETER = 28.5 INCHES = 21.72 λ

RESULTS CALCULATED AT 9 GHz

ANTENNA QUADRANT SIGNALS

CRI

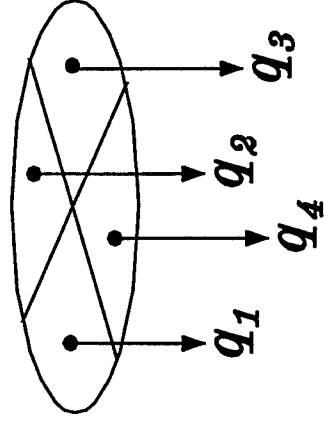
APERTURE SIDELobe TAPER a_k



MAIN BEAM STEERING

MAIN BEAM CAN BE STEERED TO ARBITRARY AZIMUTH AND ELEVATION ANGLES α_0 AND ϵ_0 BY CONTROLLING PHASE SHIFT ϕ_k ON ELEMENT k

QUADRANT SIGNALS



$$q_k = \sum_{n \in Q_k} w_n v_n, \quad 1 \leq k \leq 4$$

$$w_k = a_k e^{j\phi_k}$$

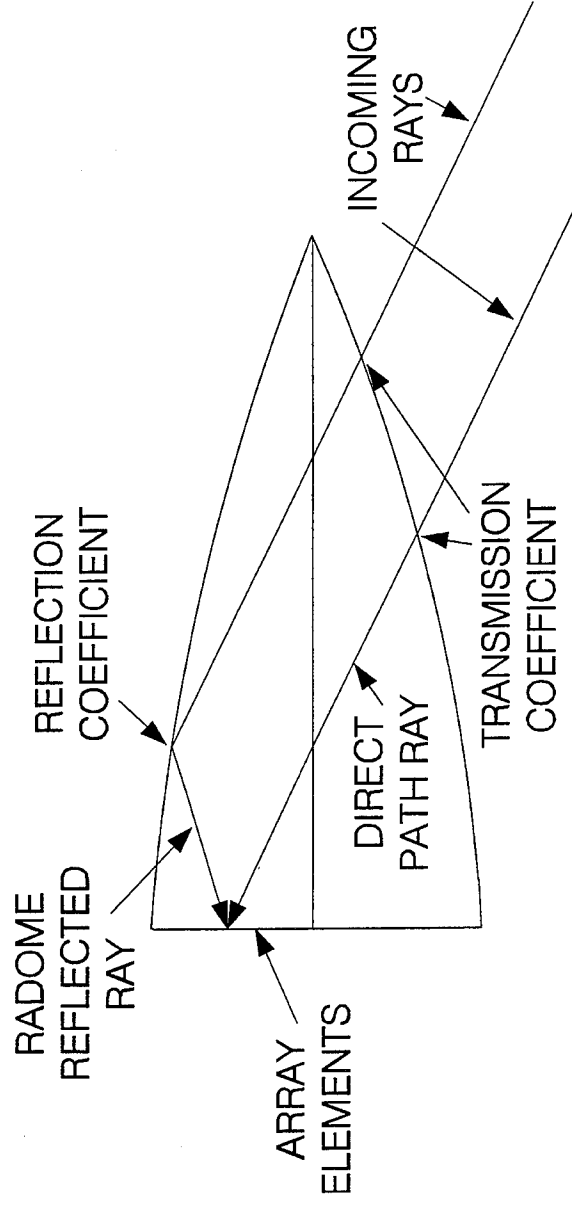
$$\mathbf{X} = \begin{bmatrix} q_1 \\ q_2 \\ q_3 \\ q_4 \end{bmatrix} = \text{SIGNAL VECTOR}$$

CALCULATION OF RECEIVED SIGNALS BEHIND RADOME

CRI

SIGNAL RECEIVED AT EACH ANTENNA ELEMENT CONSISTS OF:

- DIRECT PATH CONTRIBUTION
- RADOME REFLECTED CONTRIBUTION (PHYSICAL OPTICS)



ADAPTIVE MAXIMUM LIKELIHOOD ANGLE ESTIMATION*

CRI

WE ASSUME THE SIGNALS RECEIVED ON EACH ANTENNA QUADRANT CONTAIN A DESIRED SIGNAL, A JAMMING SIGNAL, AND THERMAL NOISE.

$$\text{SIGNAL VECTOR } \mathbf{X} = \mathbf{X}_d(A_d, \psi_d, \alpha_d, \epsilon_d) + \mathbf{X}_j + \mathbf{X}_n$$

WHERE THE DESIRED SIGNAL HAS UNKNOWN PARAMETERS

$$\begin{aligned} A_d &= \text{AMPLITUDE} \\ \psi_d &= \text{CARRIER PHASE} \\ \alpha_d &= \text{AZIMUTH ANGLE} \\ \epsilon_d &= \text{ELEVATION ANGLE} \end{aligned}$$

IN ADAPTIVE ML ANGLE ESTIMATION, THE JAMMING IS CONSIDERED PART OF THE BACKGROUND NOISE AND IS INCLUDED IN THE COVARIANCE MATRIX. THE PDF OF THE RECEIVED SIGNAL VECTOR IS

$$p(\mathbf{X}|A_d, \psi_d, \alpha_d, \epsilon_d) = \pi^{-4} |\mathbf{M}_x|^{-1} e^{-(\mathbf{X}-\mathbf{X}_d)^H \mathbf{M}_x^{-1} (\mathbf{X}-\mathbf{X}_d)}$$

WITH COVARIANCE MATRIX

$$\mathbf{M}_x = E[(\mathbf{X}_j + \mathbf{X}_n)(\mathbf{X}_j + \mathbf{X}_n)^H]$$

*R. C. Davis, L. E. Brennan and I. S. Reed, "Angle Estimation with Adaptive Arrays in External Noise Fields," *IEEE Trans. on Aerospace and Electronic Systems*, vol. AES-12, no. 2 (March 1976), pp. 179-186.

ADAPTIVE MAXIMUM LIKELIHOOD ANGLE ESTIMATION

CRI

LET \mathbf{X}_s = MEASURED SAMPLE OF SIGNAL VECTOR \mathbf{x}

THE DESIRED SIGNAL PARAMETERS ARE ESTIMATED BY FINDING THE PEAK OF

$$p(\mathbf{X}_s | A, \psi, \alpha, \epsilon) = \pi^{-4} |\mathbf{M}_x|^{-1} e^{[\mathbf{X}_s - b\mathbf{V}(\alpha, \epsilon)]^H \mathbf{M}_x^{-1} [\mathbf{X}_s - b\mathbf{V}(\alpha, \epsilon)]}$$

WHERE

$$b = A_d e^{j\psi_d}, \quad \mathbf{V}(\alpha, \epsilon) = \begin{bmatrix} q_1(\alpha, \epsilon) \\ q_2(\alpha, \epsilon) \\ q_3(\alpha, \epsilon) \\ q_4(\alpha, \epsilon) \end{bmatrix}$$

AND

$q_k(\alpha, \epsilon)$ = VOLTAGE RECEIVED ON QUADRANT k DUE TO SIGNAL FROM α, ϵ

THE UNKNOWN PARAMETERS A_d AND ψ_d CAN BE ELIMINATED. THE ANGLE ESTIMATES ARE THEN THE VALUES OF α, ϵ THAT MAXIMIZE

$$Q(\alpha, \epsilon) = \frac{|\mathbf{X}_s \mathbf{M}_x^{-1} \mathbf{V}(\alpha, \epsilon)|^2}{\mathbf{V}^H(\alpha, \epsilon) \mathbf{M}_x^{-1} \mathbf{V}(\alpha, \epsilon)}$$

CALCULATION OF $Q(\alpha, \varepsilon)$

CR1

TO USE THE AMLE TECHNIQUE, WE COLLECT K INDEPENDENT SAMPLES OF THE SIGNAL VECTOR WHEN THE TARGET SIGNAL IS NOT PRESENT,

$$\mathbf{X}_k = \mathbf{X}_j(k) + \mathbf{X}_n(k), \quad 1 \leq k \leq K$$

AND FORM THE SAMPLE COVARIANCE MATRIX

$$\hat{\mathbf{M}} = \frac{1}{K} \sum_{k=1}^K \mathbf{X}_k \mathbf{X}_k^H$$

THEN WE COLLECT ONE SAMPLE WHEN THE TARGET SIGNAL IS PRESENT,

$$\mathbf{X}_s = \mathbf{X}_d + \mathbf{X}_j + \mathbf{X}_n$$

Q IS CALCULATED FROM THESE QUANTITIES,

$$Q(\alpha, \varepsilon) = \frac{|\mathbf{X}_s \hat{\mathbf{M}}_x^{-1} \mathbf{V}(\alpha, \varepsilon)|^2}{\mathbf{V}^H(\alpha, \varepsilon) \hat{\mathbf{M}}_x^{-1} \mathbf{V}(\alpha, \varepsilon)}$$

AN IMPORTANT ISSUE:

HOW TO CALCULATE THE STEERING VECTOR

CRI

- TO FIND THE PEAK OF Q ,

$$Q(\alpha, \varepsilon) = \frac{|\mathbf{X}_s \hat{\mathbf{M}}_x^{-1} \mathbf{V}(\alpha, \varepsilon)|^2}{\mathbf{V}^H(\alpha, \varepsilon) \hat{\mathbf{M}}_x^{-1} \mathbf{V}(\alpha, \varepsilon)}$$

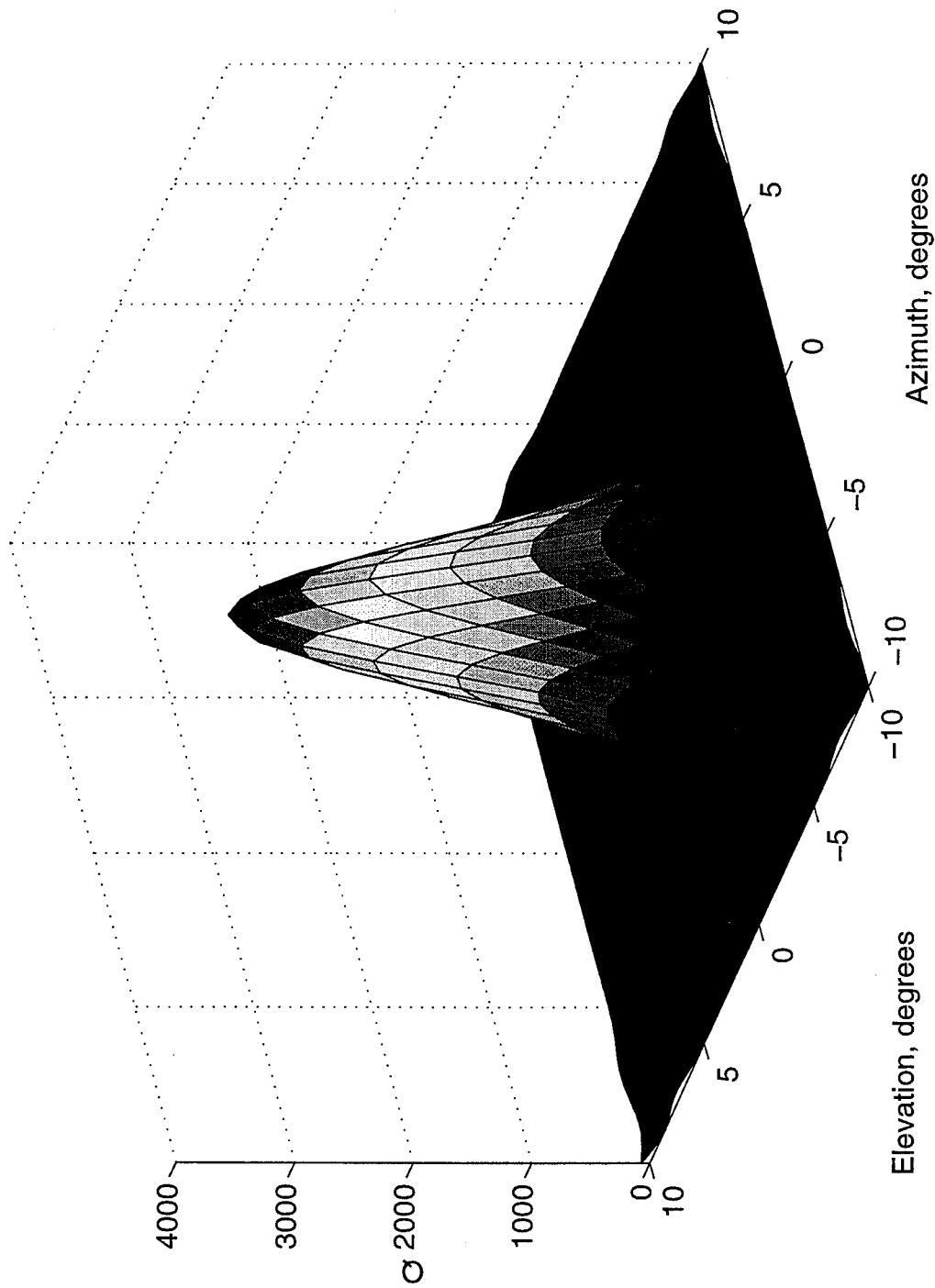
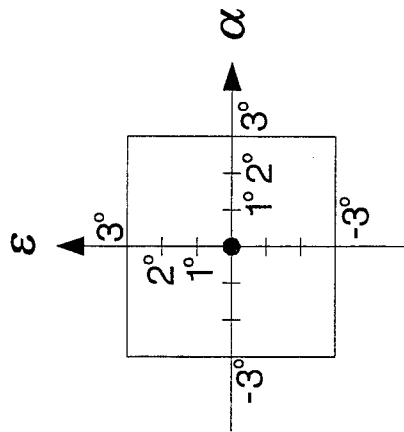
THE STEERING VECTOR $\mathbf{V}(\alpha, \varepsilon)$ MUST BE CALCULATED FOR MANY DIFFERENT α, ε .

- IDEALLY THE STEERING VECTOR SHOULD BE CALCULATED BEHIND THE RADOME. HOWEVER, THAT REQUIRES THE USE OF A LONG-RUNNING RADOME CODE.
- INSTEAD, IT IS SIMPLER TO CALCULATE THE STEERING VECTOR WITHOUT THE RADOME.
- IN THIS WORK WE INVESTIGATE THE ESTIMATE BIAS CAUSED BY USING A FREE-SPACE STEERING VECTOR.

Q-SURFACE

SNR=30 dB, $\alpha_0=\varepsilon_0=0^\circ$, $\alpha_d=\varepsilon_d=0^\circ$, NO JAMMING, NO RADOME

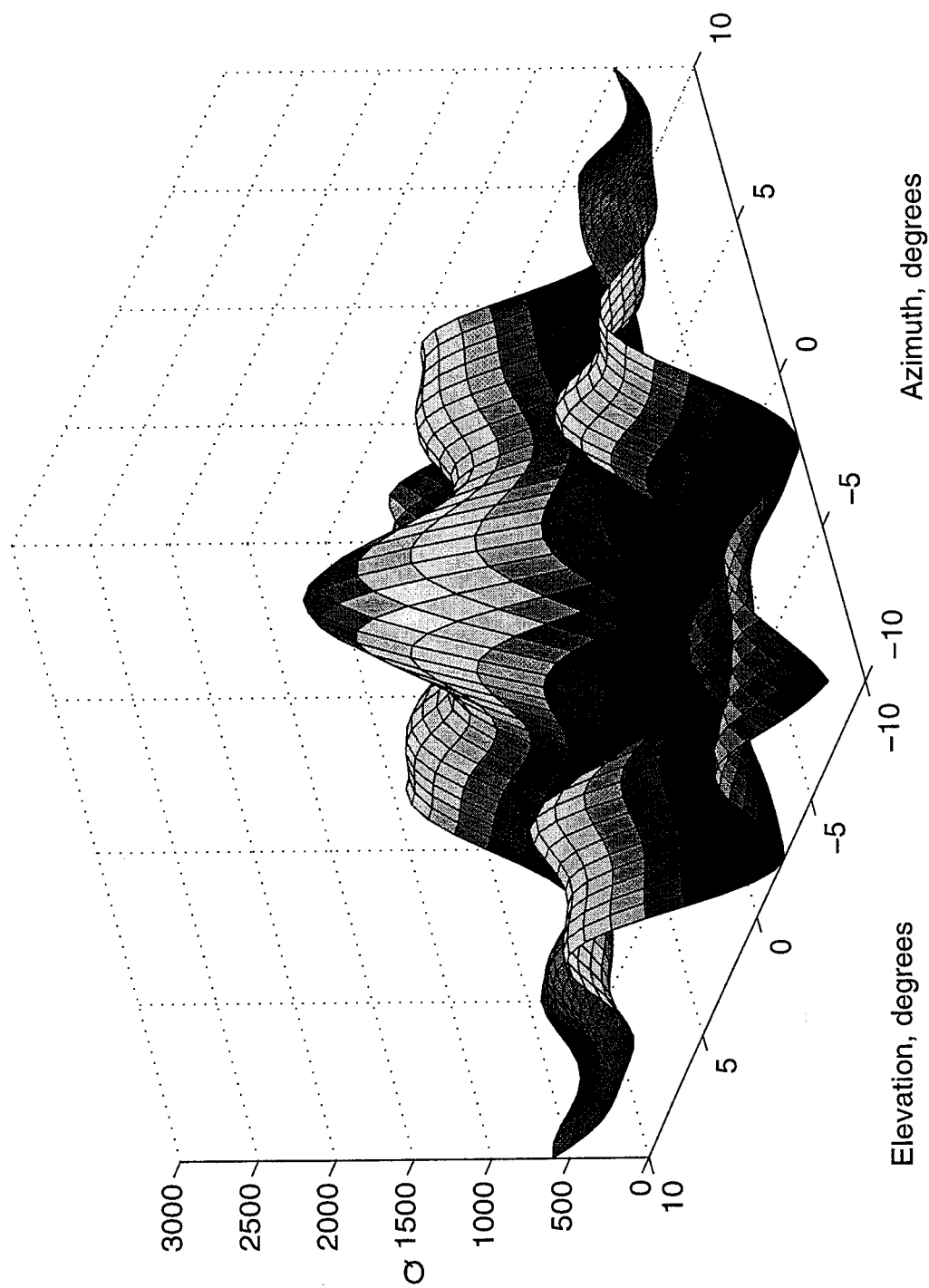
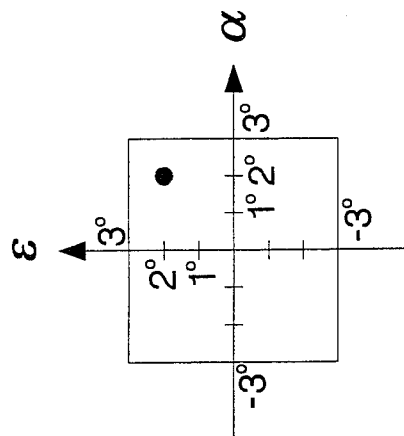
CRI



Q-SURFACE

SNR=30 dB, $\alpha_0=\varepsilon_0=0^\circ$, $\alpha_d=\varepsilon_d=2^\circ$, NO JAMMING, NO RADOME

CRI

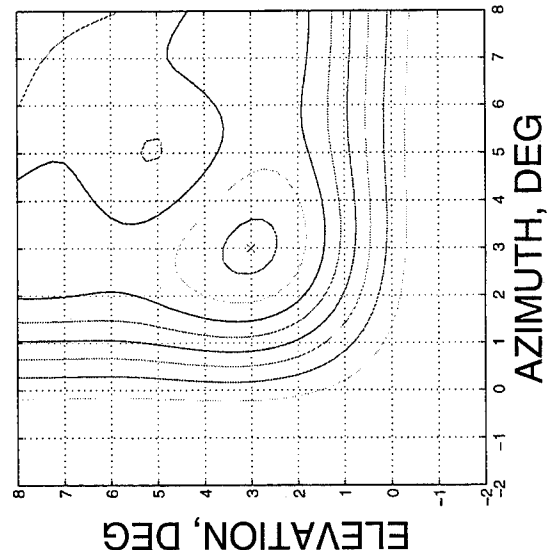
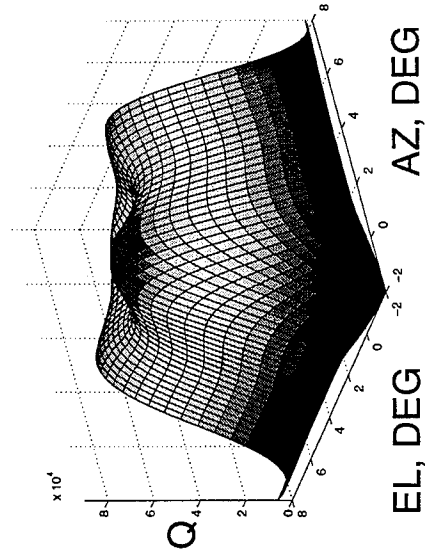


Q-SURFACES

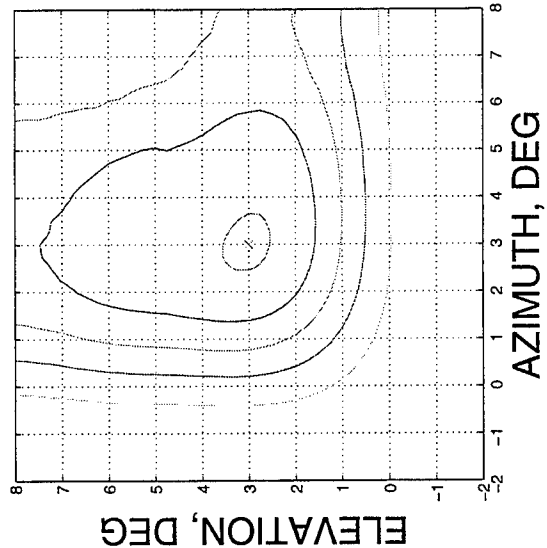
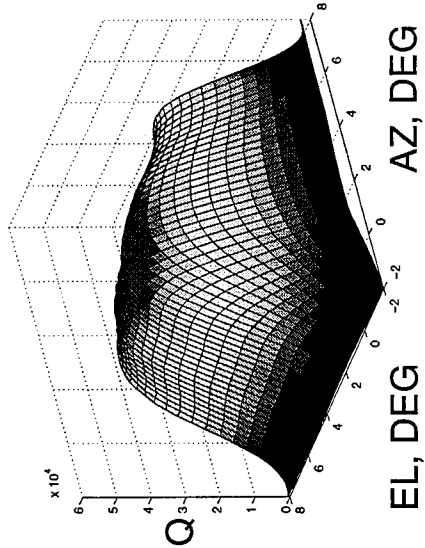
SNR=30 dB, $\alpha_0=\epsilon_0=0^\circ$, $\alpha_d=\epsilon_d=3^\circ$, NO JAMMING

CRI

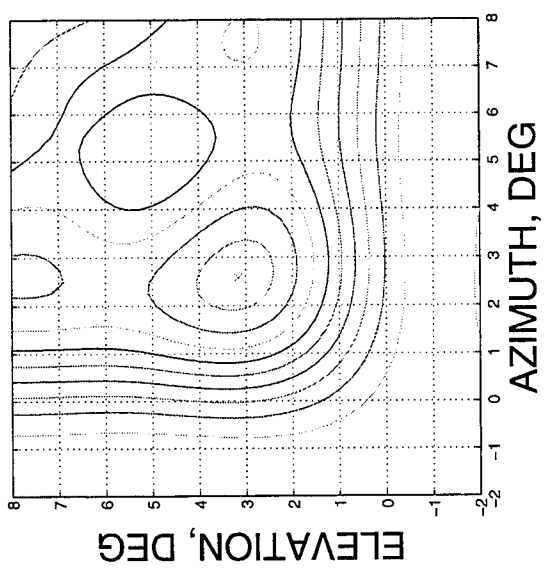
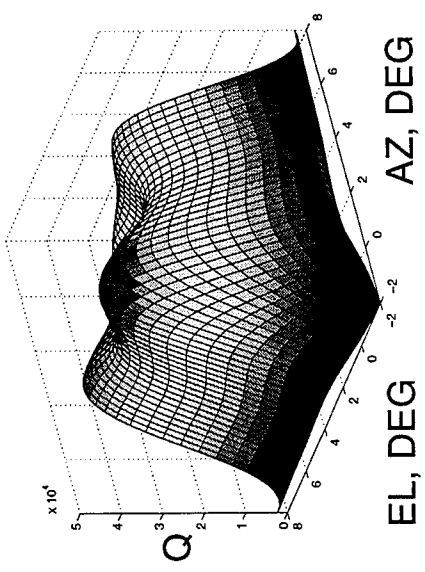
NO RADOME



RADOME PRESENT
RADOME IN STEERING VECTOR



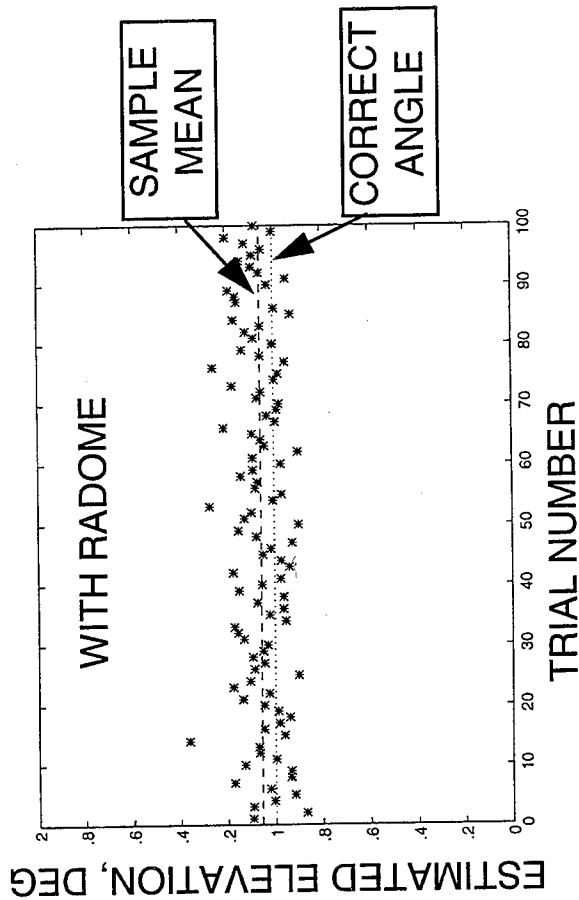
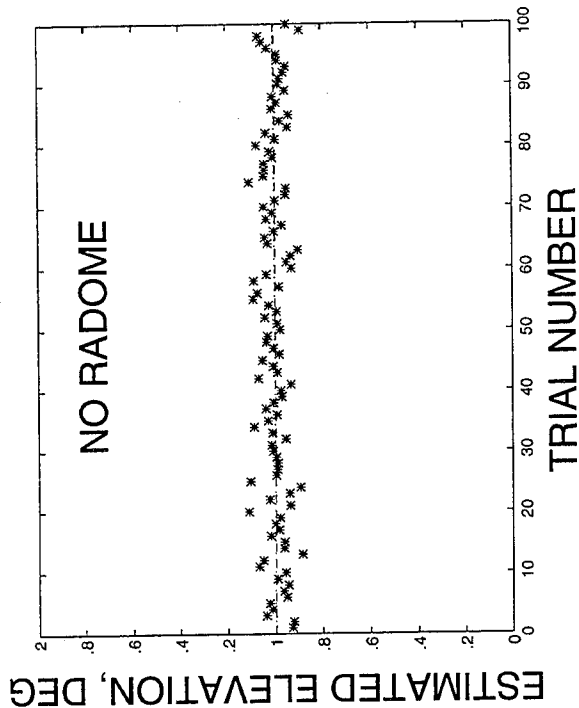
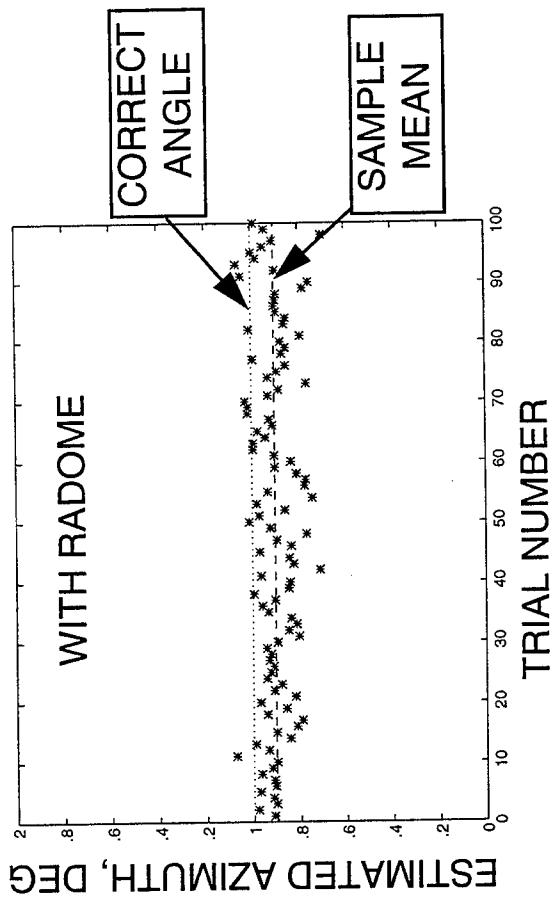
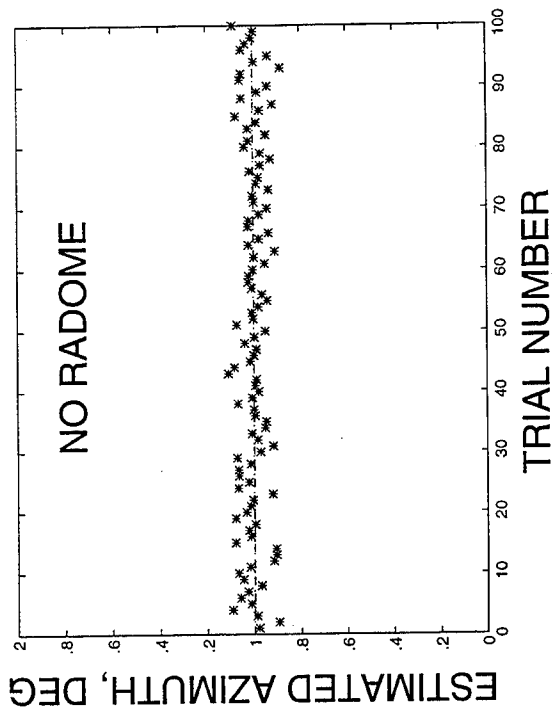
RADOME PRESENT
NO RADOME IN STEERING VECTOR



MONTE CARLO TRIALS

(SNR=30 dB, $\alpha_0=\varepsilon_0=0^\circ$, $\alpha_d=\varepsilon_d=1^\circ$, NO JAMMING)

CRI

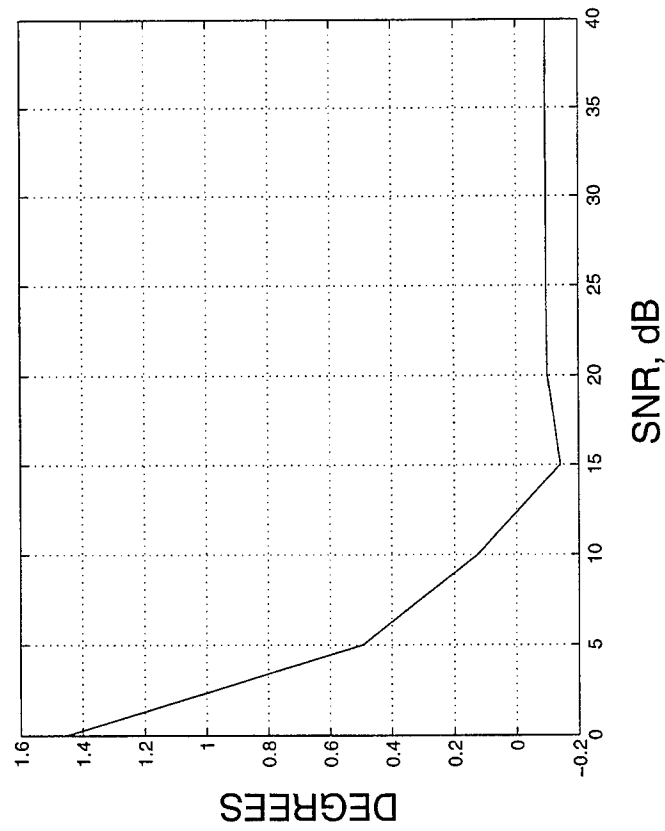


AZIMUTH BIAS AND STANDARD DEVIATION VS. SNR

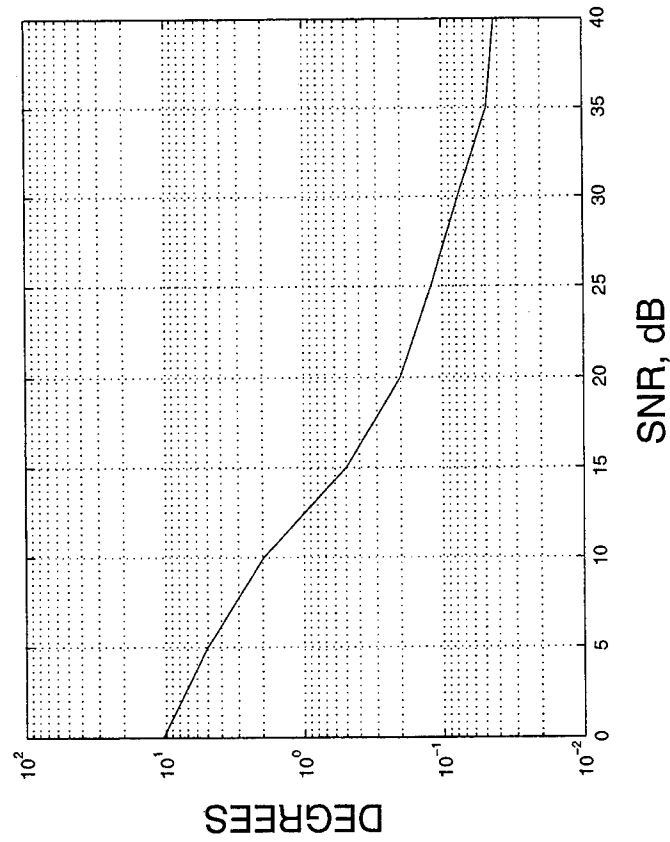
CRI

(WITH RADOME, $\alpha_0 = \varepsilon_0 = 0^\circ$, $\alpha_d = \varepsilon_d = 1^\circ$, NO JAMMING)

AZIMUTH BIAS



AZIMUTH STANDARD DEVIATION

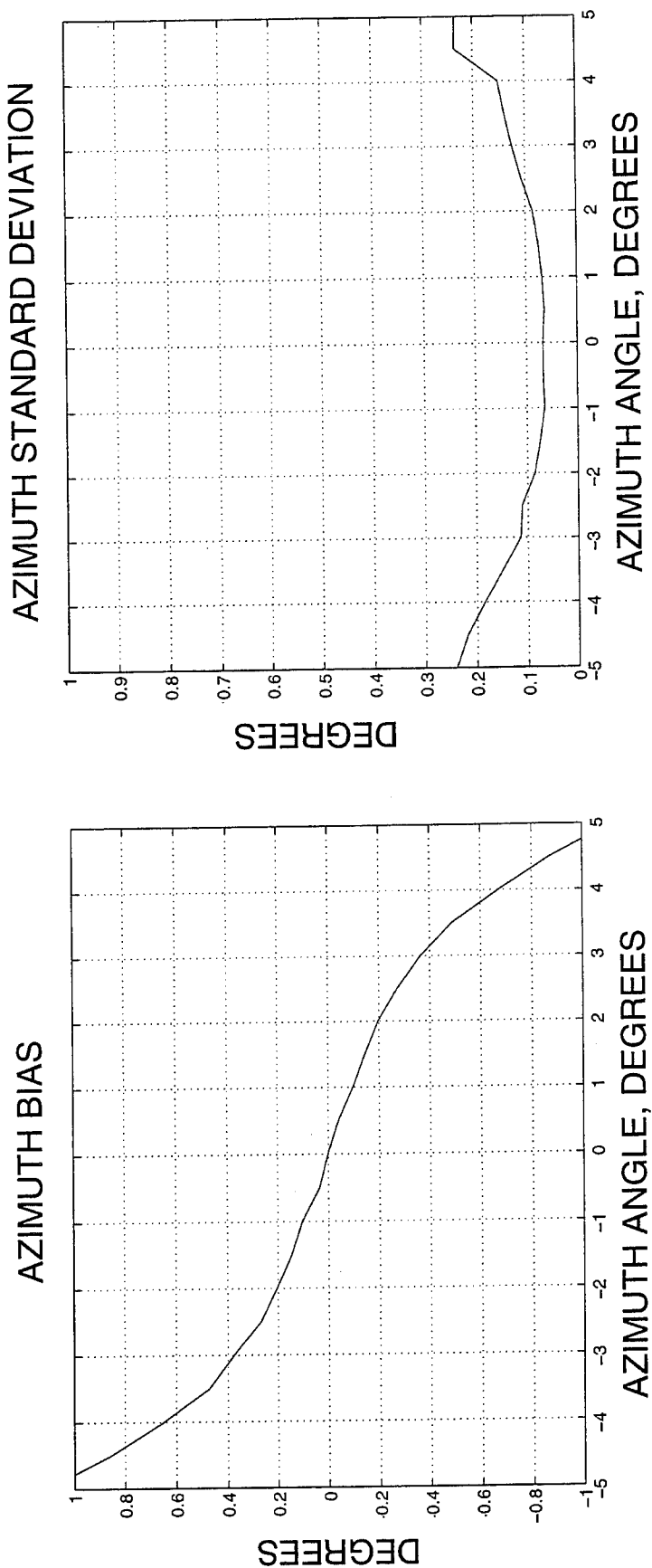


CURVES ARE COMPUTED FROM 100 MONTE CARLO TRIALS WITH 8 SNAPSHOTS IN THE SAMPLE COVARIANCE MATRIX.

AZIMUTH BIAS AND STANDARD DEVIATION VS. AZIMUTH ANGLE

(WITH RADOME, SNR=30 dB, $\alpha_0=\varepsilon_0=0^\circ$, $\varepsilon_d=0^\circ$, NO JAMMING)

CRI

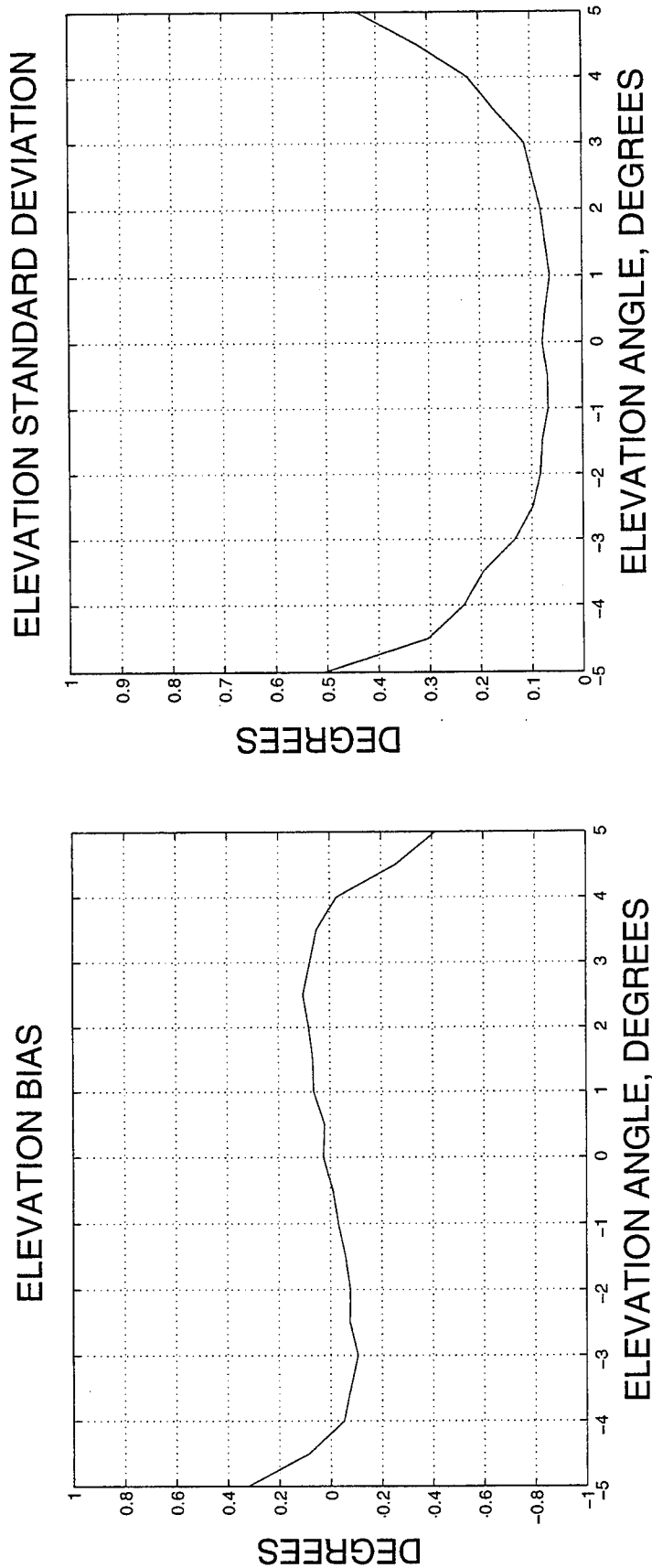


CURVES ARE COMPUTED FROM 100 MONTE CARLO TRIALS
WITH 8 SNAPSHOTS IN THE SAMPLE COVARIANCE MATRIX.

ELEVATION BIAS AND STANDARD DEVIATION VS. ELEVATION ANGLE

(WITH RADOME, SNR=30 dB, $\alpha_0=\varepsilon_0=0^\circ$, $\alpha_d=0^\circ$, NO JAMMING)

CRI



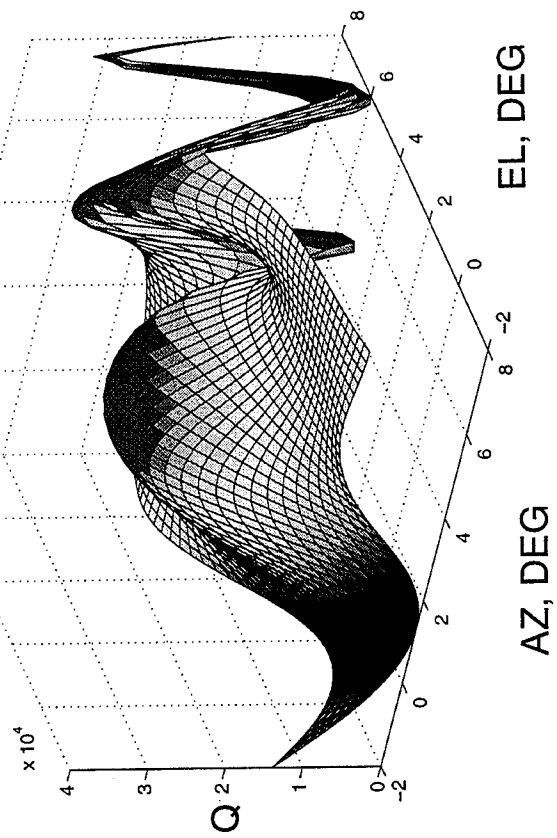
CURVES ARE COMPUTED FROM 100 MONTE CARLO TRIALS
WITH 8 SNAPSHOTS IN THE SAMPLE COVARIANCE MATRIX.

Q-SURFACE WITH JAMMING

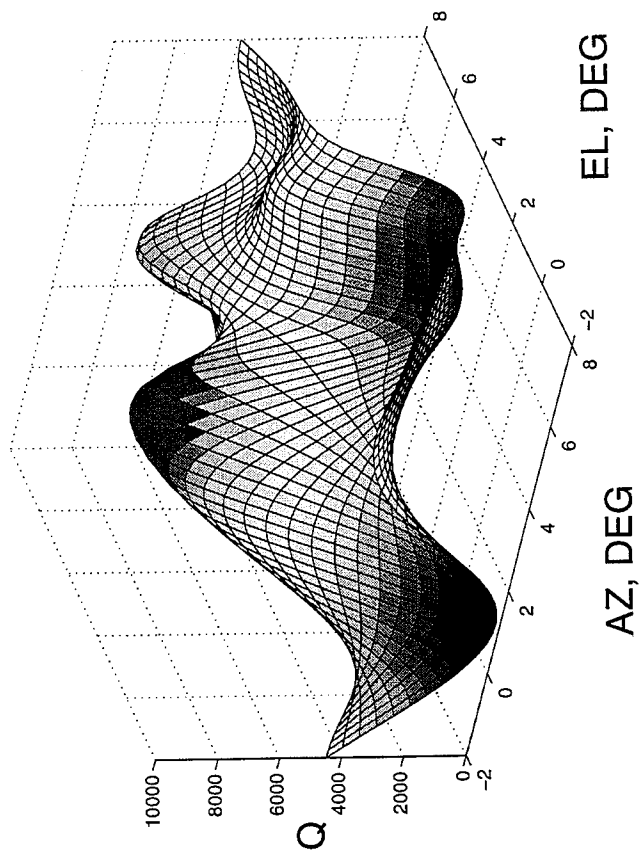
SNR=30 dB, $\alpha_0=\epsilon_0=0^\circ$, $\alpha_d=\epsilon_d=3^\circ$, JNR=40 dB, $\alpha_j=\epsilon_j=5^\circ$

CRI

NO RADOME



RADOME PRESENT
FREE-SPACE STEERING VECTOR

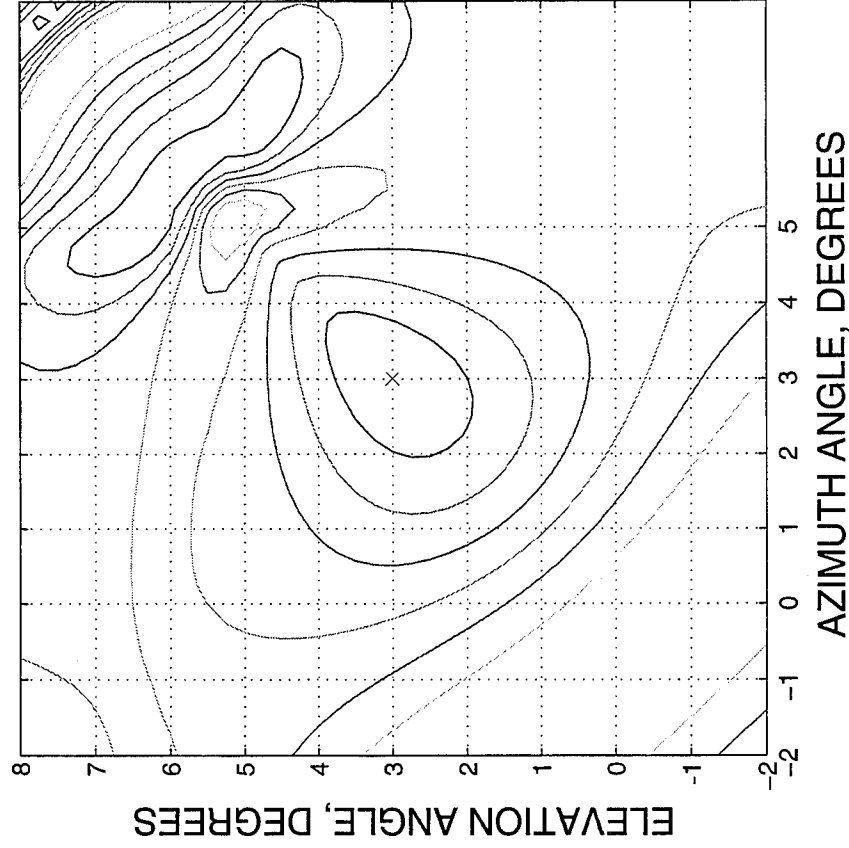


Q-SURFACE WITH JAMMING

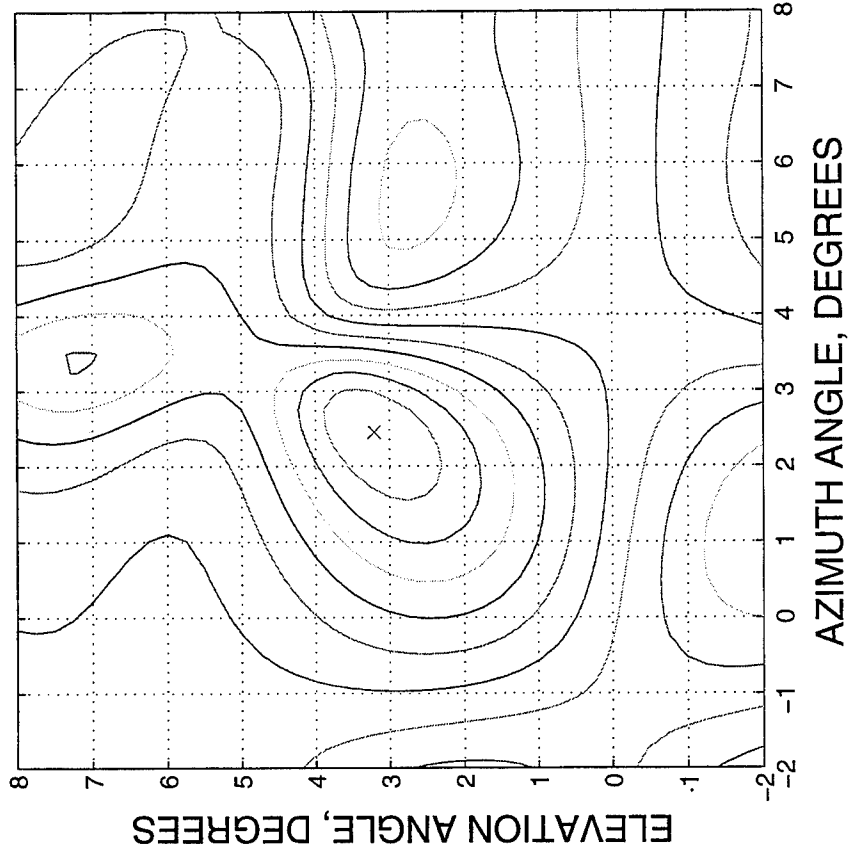
SNR=30 dB, $\alpha_0=\epsilon_0=0^\circ$, $\alpha_d=\epsilon_d=3^\circ$, JNR=40 dB, $\alpha_j=\epsilon_j=5^\circ$

CRI

NO RADOME



RADOME PRESENT
FREE-SPACE STEERING VECTOR



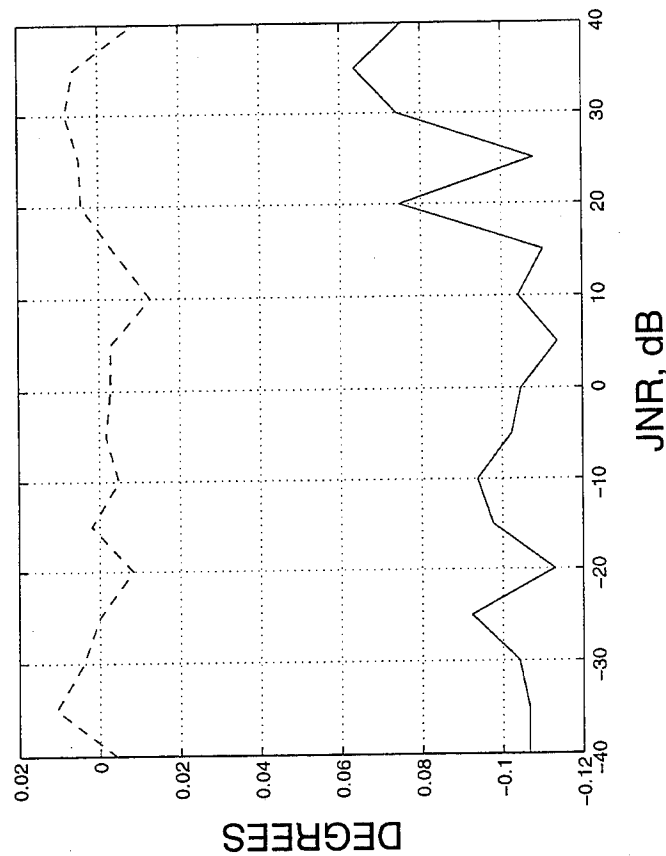
AZIMUTH BIAS AND STANDARD DEVIATION VS. JNR

CRI

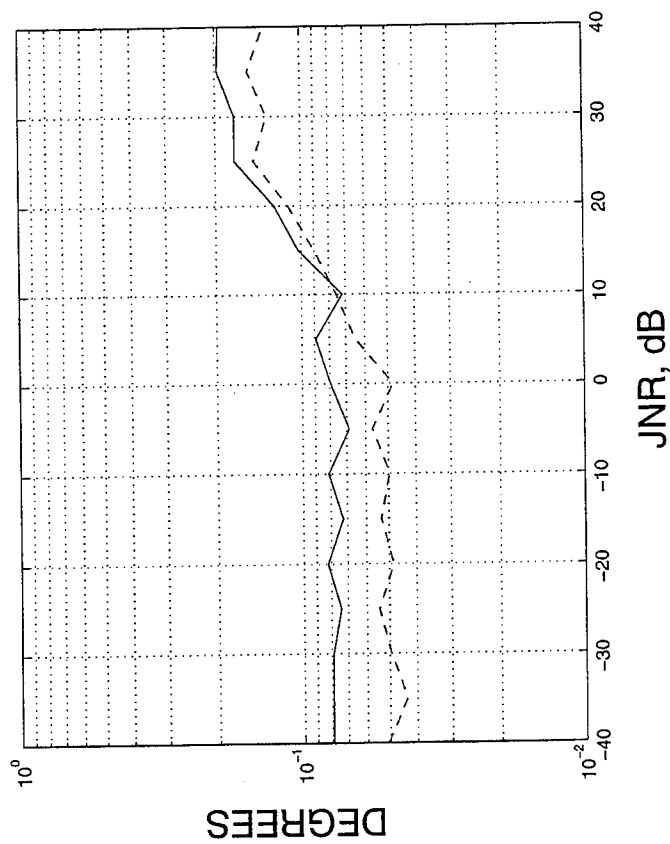
(WITH RADOME, SNR=30 dB, $\alpha_0=\epsilon_0=0^\circ$, $\alpha_d=\epsilon_d=1^\circ$, WITH JAMMING, $\alpha_j=\epsilon_j=2^\circ$)



AZIMUTH BIAS



AZIMUTH STANDARD DEVIATION



CURVES ARE COMPUTED FROM 100 MONTE CARLO TRIALS
 WITH 8 SNAPSHOTS IN THE SAMPLE COVARIANCE MATRIX.

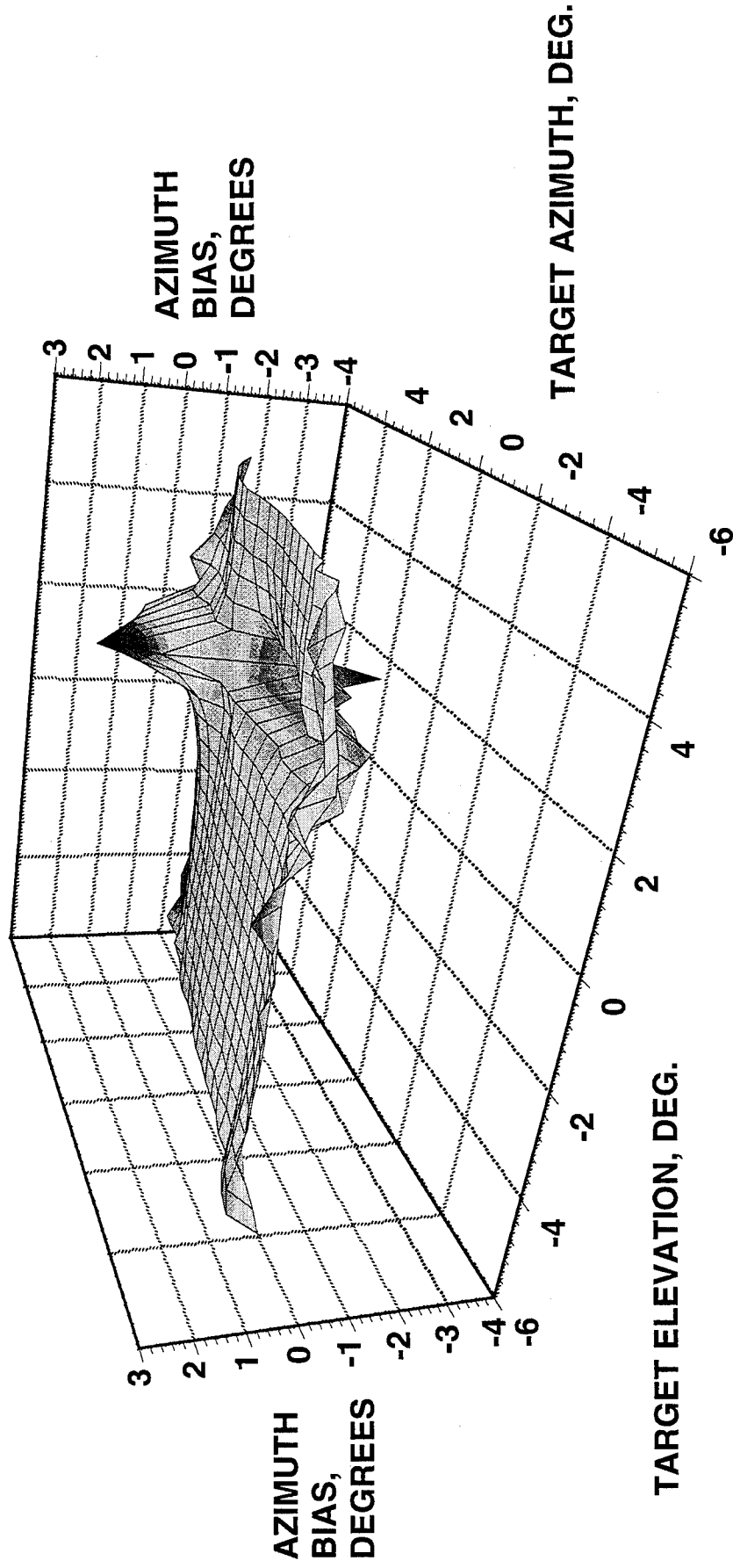
AZIMUTH BIAS NEAR THE JAMMER ANGLE

CRI

(WITH RADOME, SNR=30 dB, $\alpha_0=\epsilon_0=0^\circ$, JNR=40 dB, $\alpha_j=\epsilon_j=2^\circ$)

MAIN LIMITATION OF THIS APERTURE CONFIGURATION

- AZIMUTH ESTIMATE UNRELIABLE WHEN TARGET AND JAMMER HAVE THE SAME ELEVATION ANGLE
- ELEVATION ESTIMATE UNRELIABLE WHEN TARGET AND JAMMER HAVE THE SAME AZIMUTH ANGLE



CONCLUSIONS

CRI

- ADAPTIVE ML ANGLE ESTIMATION CAN BE USED IN THE PRESENCE OF MAIN BEAM JAMMING.
- HOWEVER, WHEN THE APERTURE IS DIVIDED INTO QUADRANTS,
 - THE AZIMUTH ESTIMATE IS BAD WHEN THE TARGET AND JAMMER HAVE THE SAME ELEVATION ANGLE
 - THE ELEVATION ESTIMATE IS BAD WHEN THE TARGET AND JAMMER HAVE THE SAME AZIMUTH ANGLE
- FOR THIS RADOME, USING A FREE-SPACE STEERING VECTOR IN THE ESTIMATOR CAUSES AZIMUTH AND ELEVATION BIASES UP TO ABOUT $\pm 0.2^\circ$.

3-D JAMMER LOCALIZATION

Scott D. Coutts

MIT Lincoln Laboratory
244 Wood Street
Lexington, MA 02173-9108
tel: (617) 981-5789
email: scoutts@ll.mit.edu

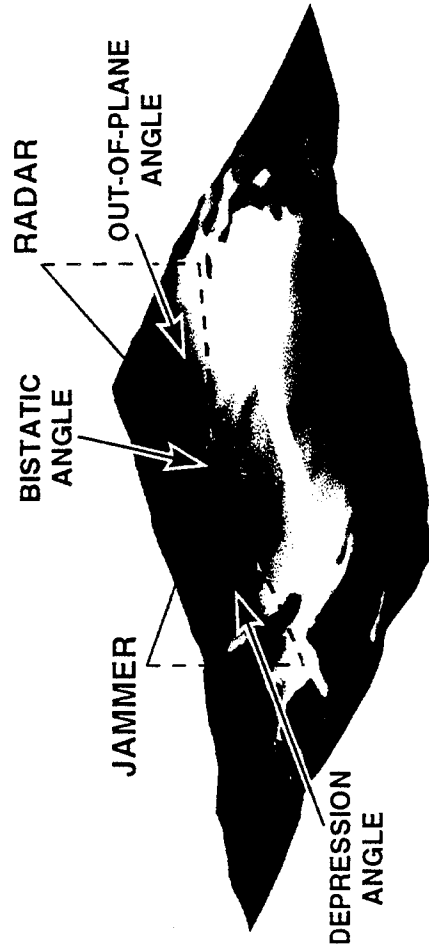
Abstract Passive jammer localization is an important ECCM technique concerned with the estimation of jammer location parameters such as azimuth, range, heading, velocity, etc. Commonly used localization techniques employ correlators to estimate Time-Difference-of-Arrival (TDOA) for delayed (and possibly Doppler shifted) replicas of the jamming waveform received by multiple sensors or by a single sensor in conjunction with specular multipath. The desired location parameters are obtained by solving a set of nonlinear equations based on the TDOA estimates and knowledge of the sensor positions. This paper contains a discussion of passive localization techniques and the development of a new technique which exploits out-of-plane jammer multipath signals. A simple statistical model is presented and used to derive the maximum likelihood estimator and the Cramer-Rao lower bounds. Monte-Carlo simulations confirming the estimates and bound calculations are also presented. Several possible jamming waveforms are considered including barrage and narrow-band noise, as well as more sophisticated, self-correlated waveforms. Finally, these techniques are used with Mountaintop field data to estimate the range, heading, and velocity of airborne jammers flying over White Sands Missile Test Range.

3-D JAMMER LOCALIZATION

SCOTT D. COUTTS
MIT LINCOLN LABORATORY

14 MARCH 1996

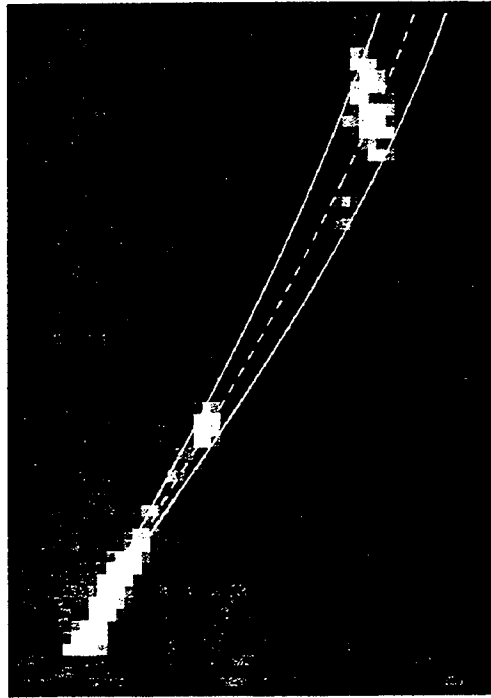
LOCALIZATION USING OUT-OF-PLANE SCATTER



ASAP

ADAPTIVE SENSOR ARRAY PROCESSING

Workshop
15-17 March 1994

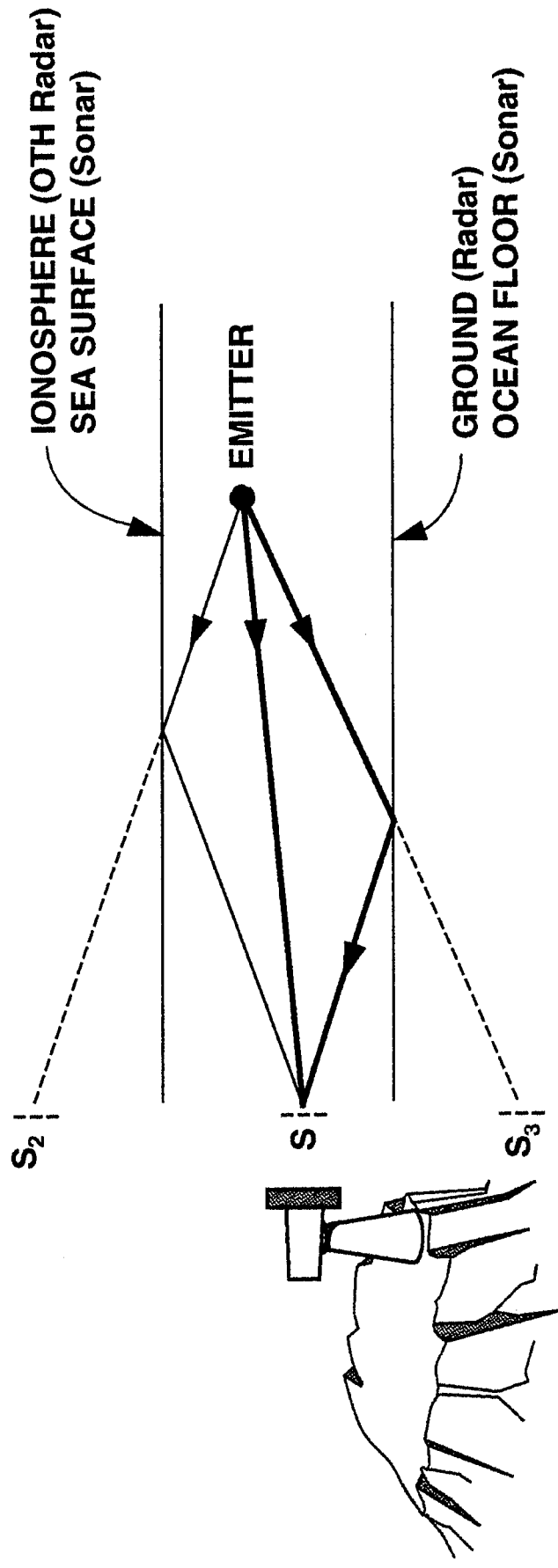


MIT LINCOLN LABORATORY
244 WOOD STREET
LEXINGTON, MA 02173-9108

OUTLINE

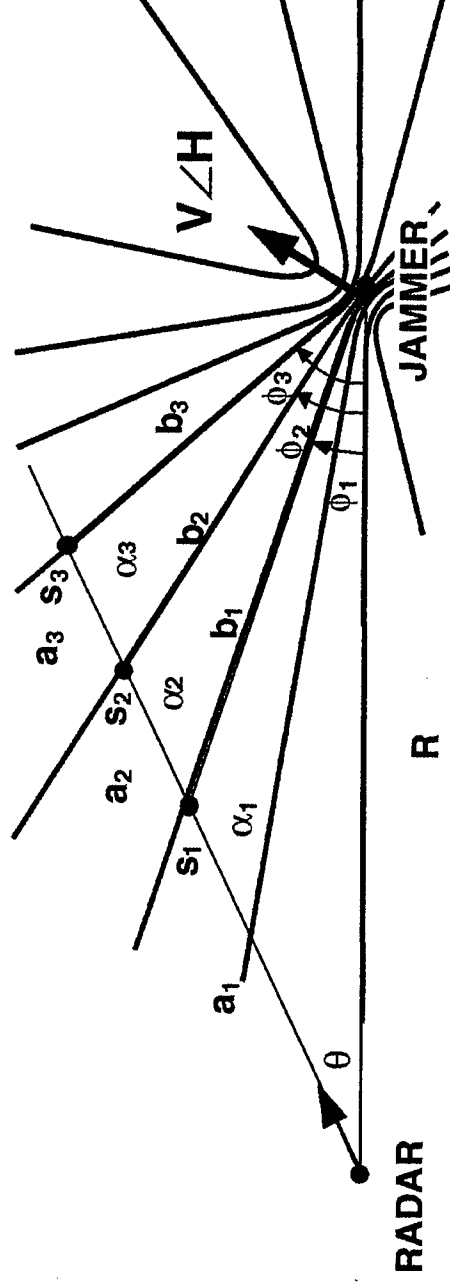
- **INTRODUCTION**
- **PROBLEM FORMULATION FOR MOVING JAMMERS**
- **JAMMER LOCALIZATION USING MOUNTAINTOP FIELD DATA**

LOCALIZATION USING IN-PLANE MULTIPATH



- SINGLE SENSOR TECHNIQUES OFTEN USE IN-PLANE MULTIPATH
- VIRTUAL SENSORS CREATED BY SENSOR IMAGES
- TIME DIFFERENCE OF ARRIVAL (TDOA) ESTIMATES OBTAINED BY AUTOCORRELATION
 - TDOA ESTIMATES AND SENSOR POSITION ESTIMATES USED TO LOCALIZE EMITTER
- TDOA ESTIMATES REQUIRE HIGH INSTANTANEOUS BANDWIDTH (Several MHz for Typical Mountaintop Geometries)

LOCALIZATION USING OUT-OF-PLANE SCATTER



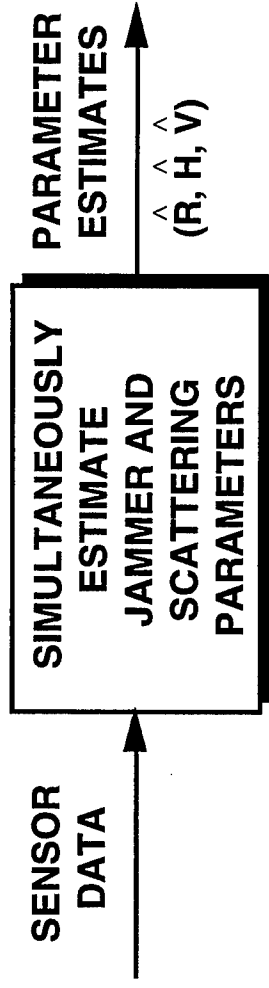
- EACH SCATTERING POINT DEFINES A TRIANGLE
- SCATTERER AZIMUTH θ AND DELAY $D_i = a_i + b_i - R$ KNOWN (Measured)
- USING THE LAW OF COSINES $R = (a_i D_i - D_i^2 / 2) / (D_i - a_i + a_i \cos \theta)$
 - ONE EQUATION WITH TWO UNKNOWNS (R, a_i)
 - FOR N SCATTERERS WE HAVE N EQUATIONS WITH $N+1$ UNKNOWN
- JAMMER DOPPLER PROVIDES KEY FOR PASSIVE LOCALIZATION

$$\phi_i \approx -H + \cos^{-1} \left(\cos H - \frac{f_i \lambda}{V} \right) \text{ and } R = D_i / \left(\frac{\sin \phi_i}{\sin \alpha_i} + \frac{\sin \theta}{\sin \alpha_i} - 1 \right)$$

OUTLINE

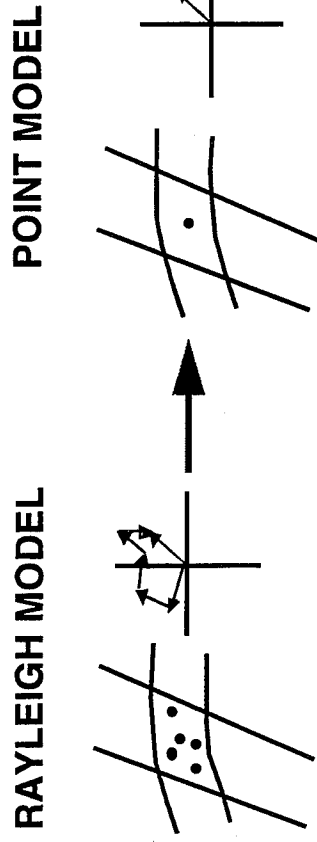
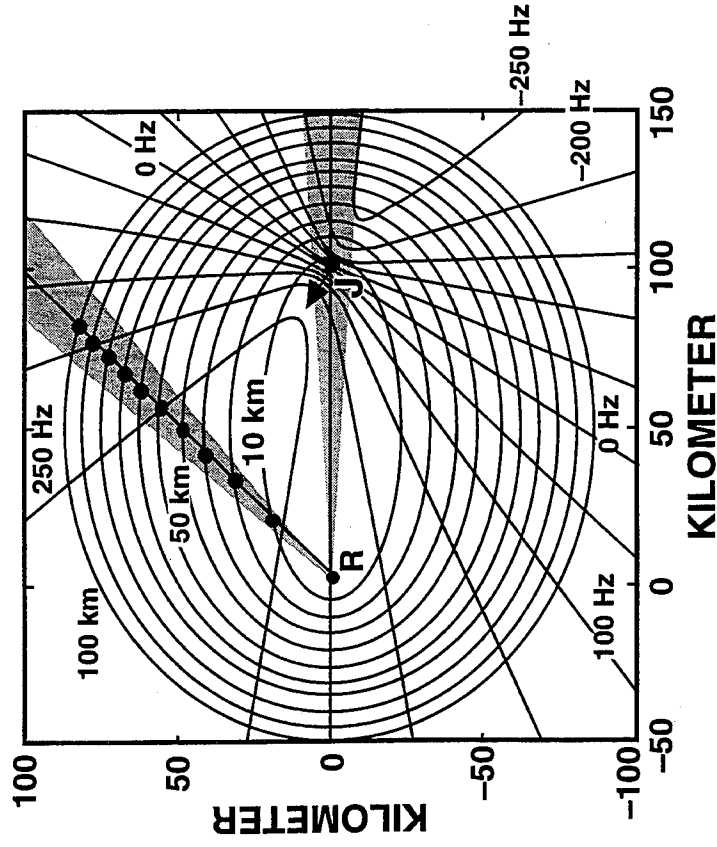
- **INTRODUCTION**
- **PROBLEM FORMULATION FOR MOVING JAMMERS**
 - **PARAMETER ESTIMATION MODEL**
 - **STATISTICAL FORMULATION FOR HOMOGENEOUS CLUTTER**
 - **MAXIMUM LIKELIHOOD ESTIMATOR**
 - **CRAMER-RAO LOWER BOUNDS**
 - **MONTE-CARLO SIMULATIONS**
- **JAMMER LOCALIZATION USING MOUNTAINTOP FIELD DATA**

PARAMETER ESTIMATION MODEL



- DESIRED PARAMETERS ARE JAMMER RANGE, HEADING, AND VELOCITY (R, H, V)
 - SCATTERING PARAMETERS ARE NUISANCE PARAMETERS
- HOMOGENEOUS CLUTTER ASSUMPTION SIMPLIFIES MODEL DEVELOPMENT
 - TREAT CLUTTER PATCH AZIMUTH AND RELATIVE TIME DELAY AS INDEPENDENT VARIABLES
 - NEED TO ESTIMATE DOPPLER
 - AN INHOMOGENEOUS MODEL REQUIRES ADDITIONAL STEPS
 - NEED TO ESTIMATE AZIMUTH, TIME DELAY, AND DOPPLER

MODEL FOR HOMOGENEOUS CLUTTER



• ASSUMPTIONS

- NARROW BEAMS AND CLOSELY SPACED DELAY CELLS
- SCATTER ORIGINATES FROM CENTER OF DELAY-AZIMUTH CELL
- PERFECT REPLICA OF JAMMER WAVEFORM OBTAINED BY REFERENCE BEAM
- JAMMER-TO-NOISE RATIO GREATER THAN 65 dB
- JAMMER AZIMUTH KNOWN OR ESTIMATED INDEPENDENTLY

STATISTICAL MODEL

- DESIRED SIGNAL COMPONENT CONSISTS OF DELAYED AND DOPPLER SHIFTED REPLICAS OF THE JAMMER WAVEFORM $s(n)$

$$m(n) = \sum_{p=1}^P a_p s(n - D_p) e^{jn\omega_p}$$

- OBSERVED SIGNAL $z(n)$ CONSISTS OF DESIRED SIGNAL PLUS NOISE

$$z(n) = m(n) + g(n)$$

- OBSERVATIONS OBEY MULTIVARIATE GAUSSIAN PDF

$$f_z(z) = \left(\frac{1}{\pi^N |R|} \right) e^{-(z-m)^H R^{-1} (z-m)}$$

- LIKELIHOOD FUNCTION FOR SIMPLIFIED NOISE ASSUMPTION

$$f_z(z|\alpha) = \left(\frac{1}{\pi^N \sigma^2} \right) e^{-|z-m(\alpha)|^2 / \sigma^2}$$

MAXIMUM LIKELIHOOD ESTIMATOR

- MINIMIZE EXPONENT OF LIKELIHOOD FUNCTION
- TIME-VARYING LEAST-SQUARES FILTER

$$m(n) = \sum_{p=1}^P a_p^* s(n - D_p) e^{j\omega_p(n - D_p)}$$

$$R_{ss}(p, k) = \sum_{n=P}^N s(n - D_k) e^{j\omega_k(n - D_k)} s^*(n - D_p) e^{-j\omega_p(n - D_p)},$$

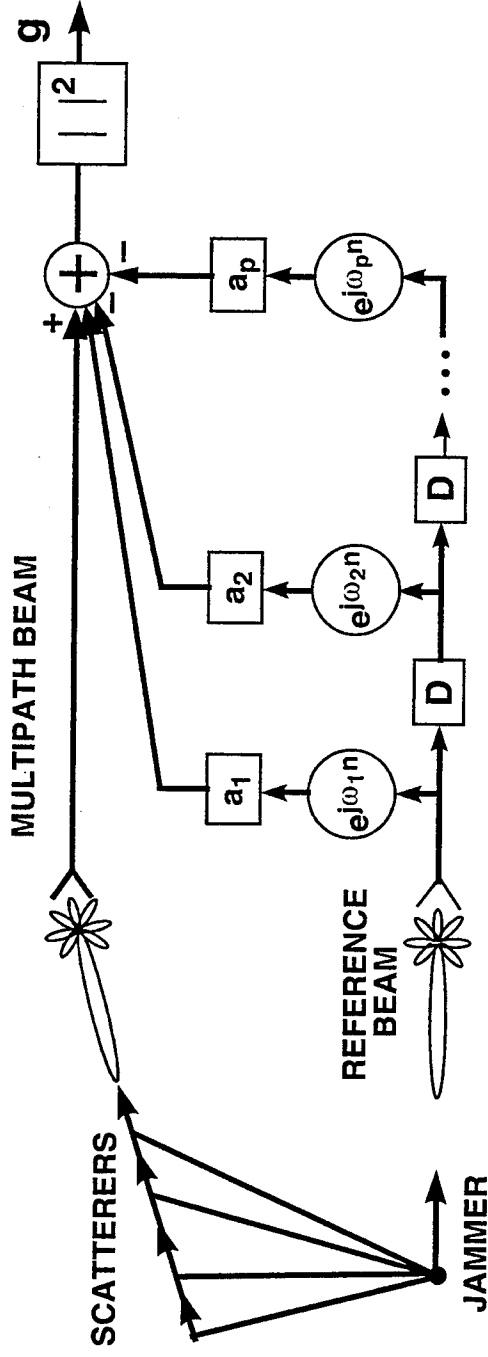
$$1 \leq p, k \leq P$$

$$r_{sz}(p, k) = \sum_{n=P}^N s(n - D_k) e^{j\omega_k(n - D_k)} z^*(n), \quad 1 \leq p, k \leq P$$

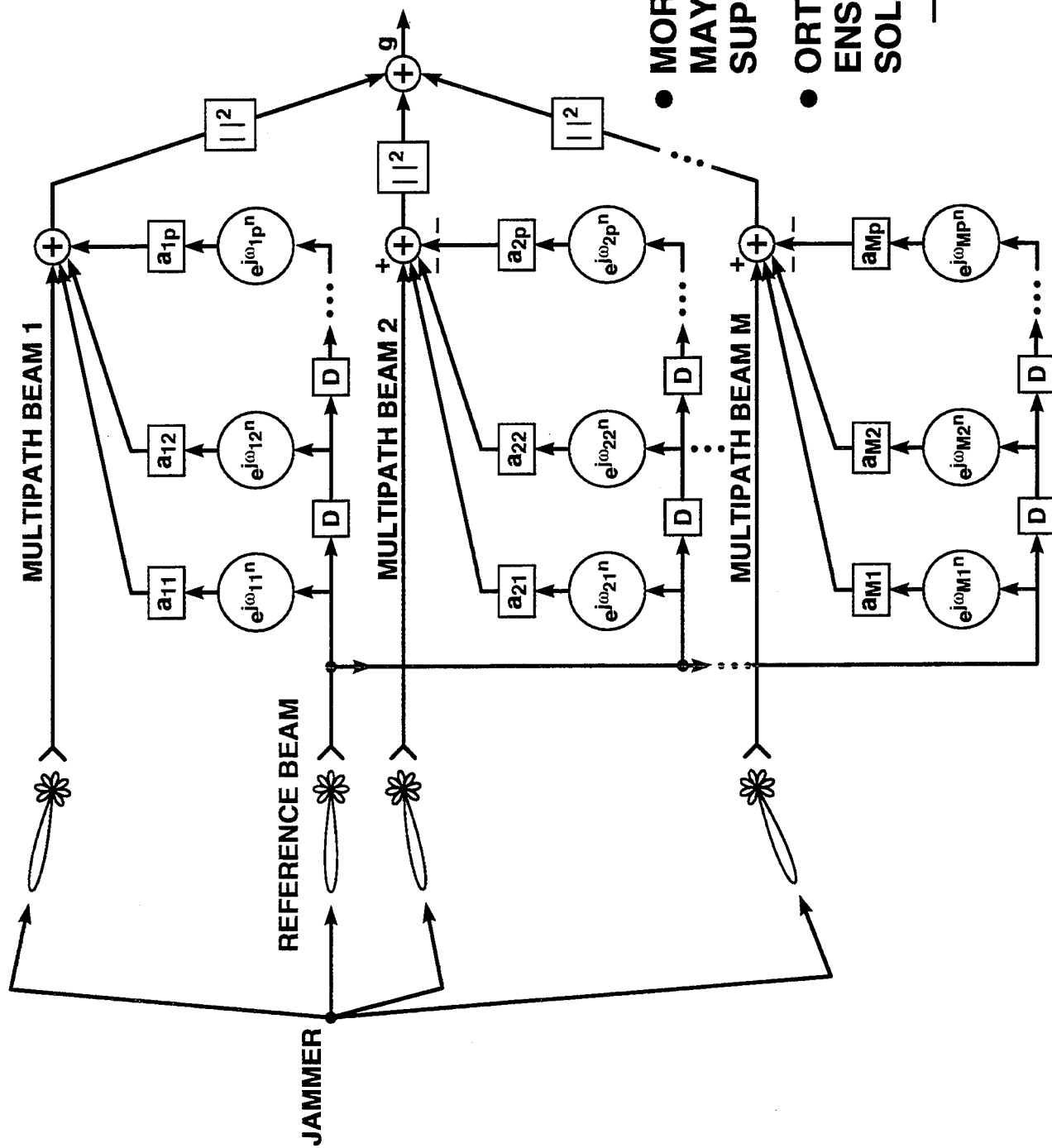
$$\hat{a} = R_{ss}^{-1} r_{sz}$$

MAXIMUM LIKELIHOOD ESTIMATOR (Cont.)

- PERFORM 3-D SEARCH OVER DENSE PARAMETER GRID
 - PARAMETERS ARE $\{R, H, V\}$ (Range, Heading and Velocity)
 - COMPUTE DOPPLER MODULATORS FOR EACH PARAMETER SET
 - COMPUTE OPTIMUM LS WEIGHTS FOR EACH SET OF MODULATORS
- PARAMETER SET WITH MINIMUM TOTAL ERROR IS MLE



MLE FOR MULTIPLE MULTIPATH BEAMS



- MORE THAN ONE BEAM MAY BE REQUIRED TO SUPPRESS AMBIGUITIES
 - ORTHOGONAL BEAMS ENSURE INDEPENDENT SOLUTIONS
- M P SIZED PROBLEMS

CRAMER-RAO LOWER BOUNDS

$$\sigma_{\alpha_k}^2 = (\mathbf{F}^{-1})_{kk}$$

$$\mathbf{F}_{ij} = -\mathbf{E} \left\{ \frac{\partial}{\partial \alpha_i \partial \alpha_j} \ln f(\mathbf{z}|\alpha) \right\}$$

$$\ln(f_z(\mathbf{z}|\alpha)) = \ln \left(\frac{1}{\pi^N \sigma^{2N}} \right) - (\mathbf{z} - \mathbf{m})^H (\mathbf{z} - \mathbf{m}) / \sigma^2$$

$$\mathbf{m}(\mathbf{n}) = \sum_{p=1}^P a_p s(\mathbf{n} - \mathbf{D}_p) e^{jn\omega_p}$$

$$\omega(R, H, V) = \frac{V}{\lambda} \left[\cos \left(H - \cos H + \frac{(D_p^2 + 2RD_p \sin \theta)}{D_p^2 + 2R^2 + 2RD_p - 2(R^2 + RD_p \cos \theta)} \right) \right]$$

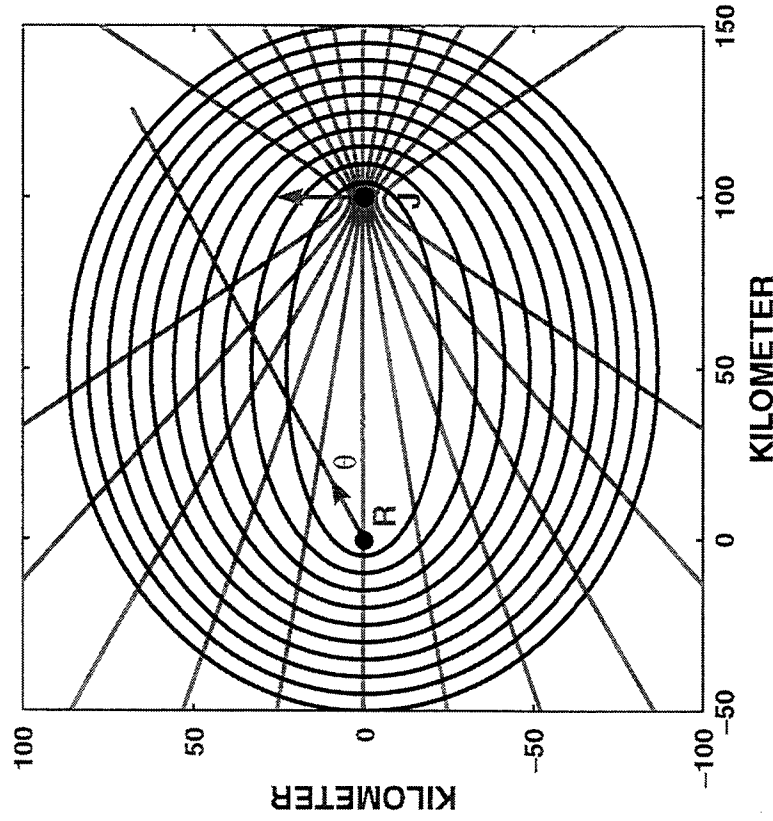
($\omega(R, H, V)$ Derived from a 2-D Approximation Ignoring Altitude)

FISHER INFORMATION MATRIX

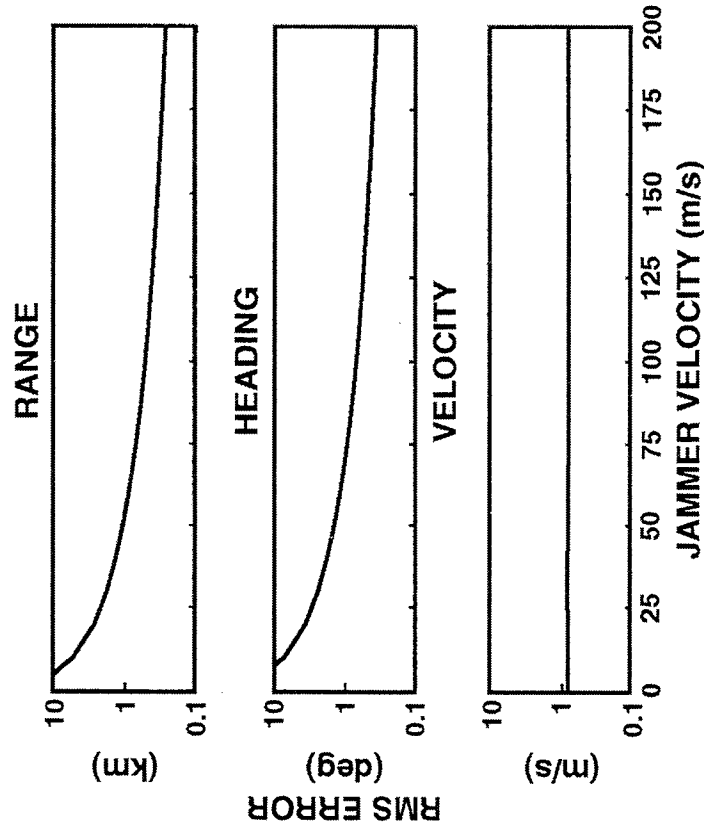
$$F = \begin{bmatrix} \begin{matrix} \text{JAMMER} \\ \text{TERMS} \\ \text{COUPLED} \end{matrix} & \begin{matrix} \text{JAMMER AND} \\ \text{PHASE TERMS} \\ \text{COUPLED} \end{matrix} & 0 & 0 & 0 & 0 & 0 & 0 & 0 & 0 & 0 & 0 & 0 & 0 & 0 & 0 \\ \begin{matrix} \text{JAMMER AND} \\ \text{PHASE TERMS} \\ \text{COUPLED} \end{matrix} & \begin{matrix} \text{JAMMER} \\ \text{AND} \\ \text{PHASE} \\ \text{TERMS} \\ \text{COUPLED} \end{matrix} & 0 & 0 & 0 & 0 & 0 & 0 & 0 & 0 & 0 & 0 & 0 & 0 & 0 & 0 \\ 0 & 0 & \text{PHASE TERMS} & 0 & 0 & 0 & 0 & 0 & 0 & 0 & 0 & 0 & 0 & 0 & 0 & 0 \\ 0 & 0 & 0 & \text{AMPLITUDE TERMS} & 0 & 0 & 0 & 0 & 0 & 0 & 0 & 0 & 0 & 0 & 0 & 0 \\ 0 & 0 & 0 & 0 & 0 & 0 & 0 & 0 & 0 & 0 & 0 & 0 & 0 & 0 & 0 & 0 \\ 0 & 0 & 0 & 0 & 0 & 0 & 0 & 0 & 0 & 0 & 0 & 0 & 0 & 0 & 0 & 0 \\ 0 & 0 & 0 & 0 & 0 & 0 & 0 & 0 & 0 & 0 & 0 & 0 & 0 & 0 & 0 & 0 \\ 0 & 0 & 0 & 0 & 0 & 0 & 0 & 0 & 0 & 0 & 0 & 0 & 0 & 0 & 0 & 0 \\ 0 & 0 & 0 & 0 & 0 & 0 & 0 & 0 & 0 & 0 & 0 & 0 & 0 & 0 & 0 & 0 \\ 0 & 0 & 0 & 0 & 0 & 0 & 0 & 0 & 0 & 0 & 0 & 0 & 0 & 0 & 0 & 0 \\ 0 & 0 & 0 & 0 & 0 & 0 & 0 & 0 & 0 & 0 & 0 & 0 & 0 & 0 & 0 & 0 \\ 0 & 0 & 0 & 0 & 0 & 0 & 0 & 0 & 0 & 0 & 0 & 0 & 0 & 0 & 0 & 0 \\ 0 & 0 & 0 & 0 & 0 & 0 & 0 & 0 & 0 & 0 & 0 & 0 & 0 & 0 & 0 & 0 \\ 0 & 0 & 0 & 0 & 0 & 0 & 0 & 0 & 0 & 0 & 0 & 0 & 0 & 0 & 0 & 0 \end{bmatrix}$$

LOWER BOUNDS vs JAMMER VELOCITY

GEOMETRY



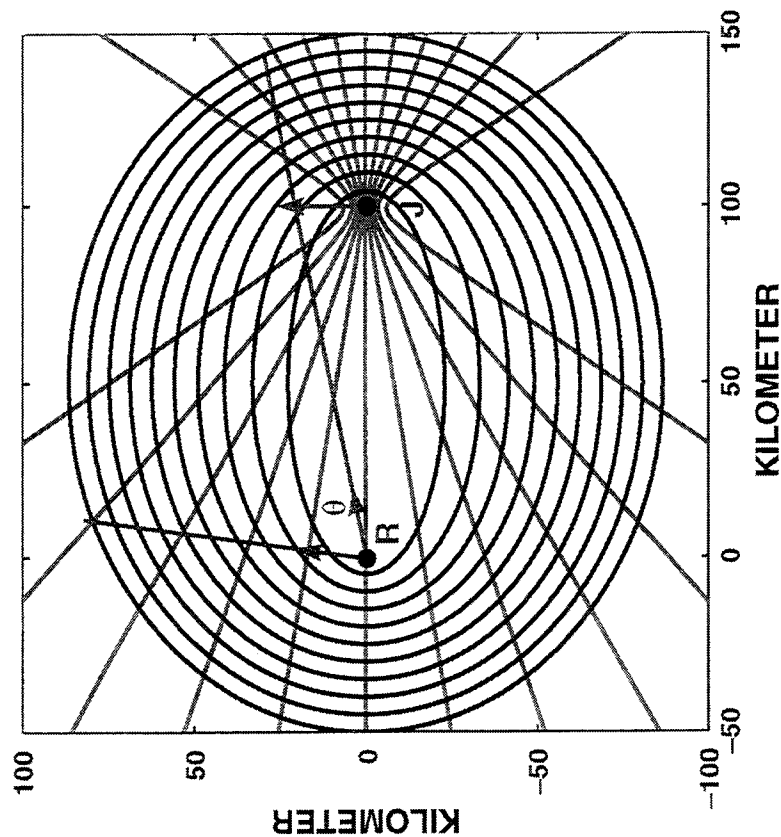
CRAMER-RAO LOWER BOUNDS



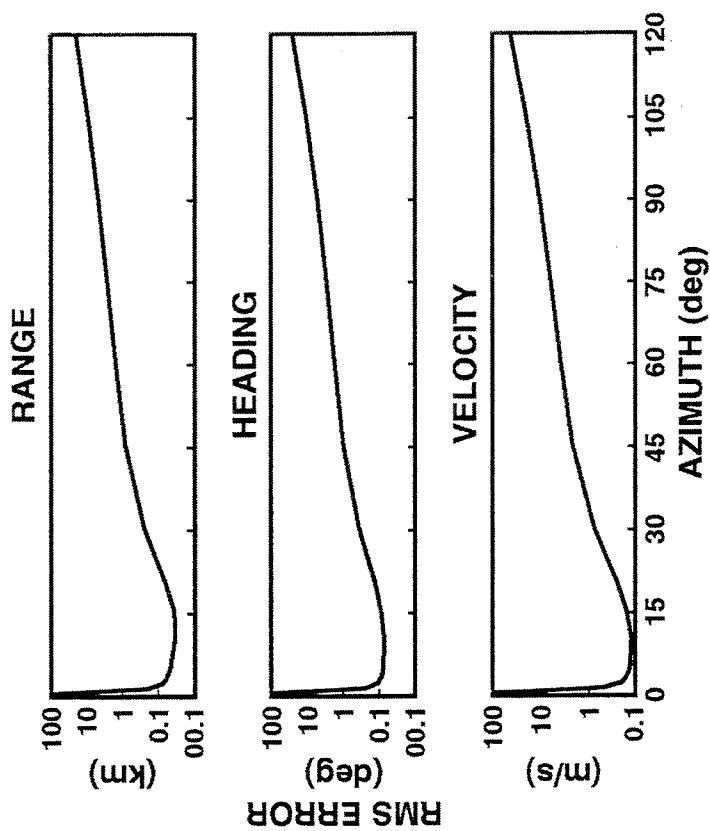
$R = 100 \text{ km}$, $V = 0 - 200 \text{ m/s}$,
 $H = 90 \text{ deg}$, $\theta = 30 \text{ deg}$,
 $\text{FILTER LENGTH} = 50$,
 $\text{JNR} = 15 \text{ dB / SAMPLE}$

LOWER BOUNDS vs RECEIVER AZIMUTH

GEOMETRY



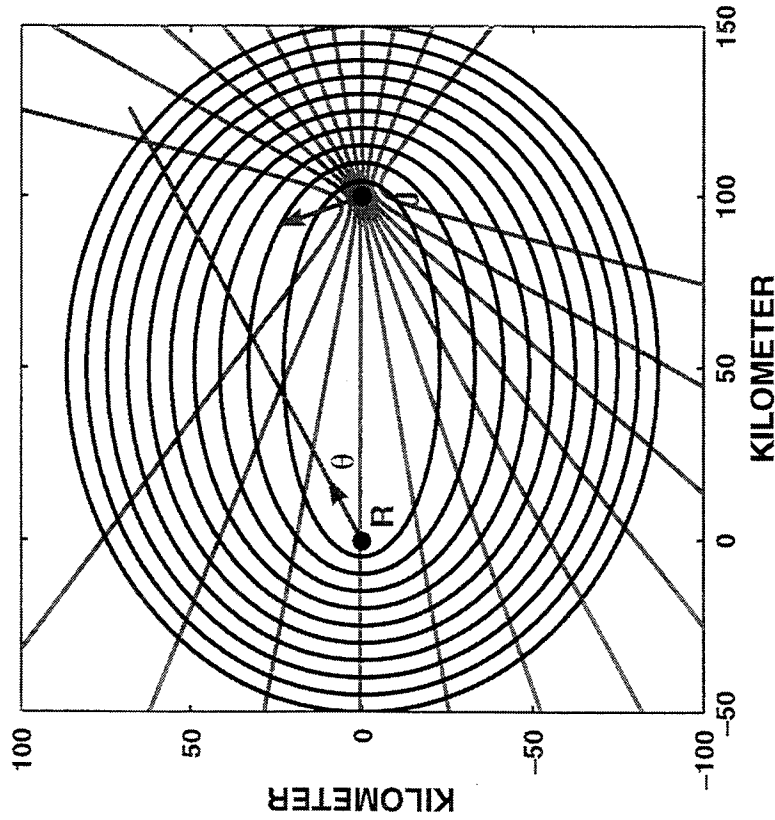
CRAMER-RAO LOWER BOUNDS



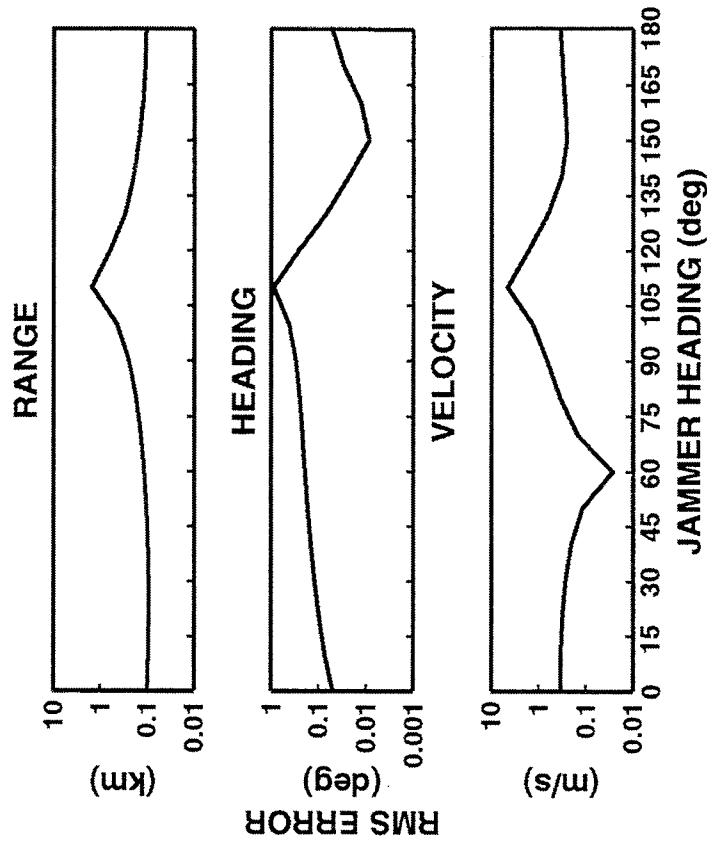
$R = 100 \text{ km}$, $V = 200 \text{ m/s}$,
 $H = 90 \text{ deg}$, $\theta = 0 - 120 \text{ deg}$,
 FILTER LENGTH = 50,
 $JNR = 15 \text{ dB / SAMPLE}$

LOWER BOUNDS vs JAMMER HEADING

GEOMETRY



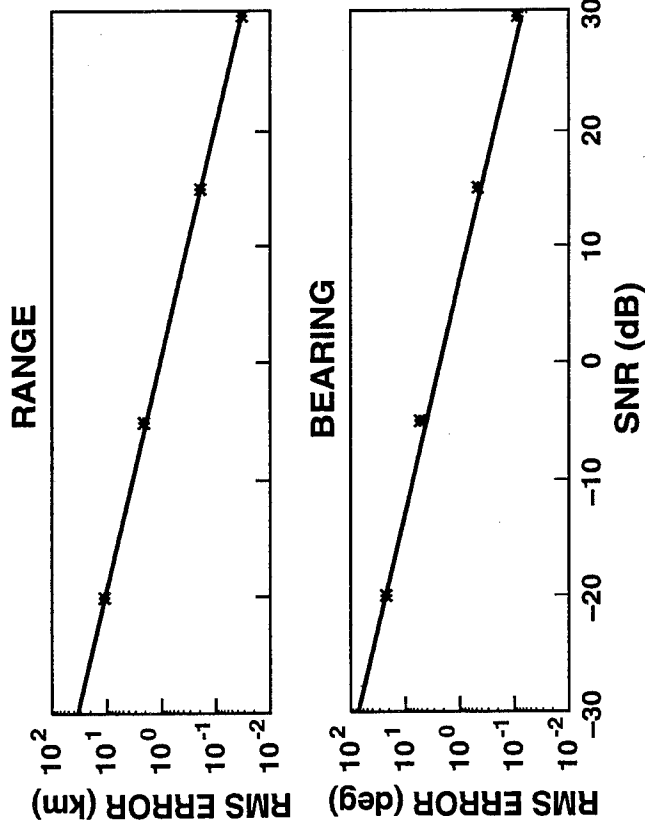
CRAMER-RAO LOWER BOUNDS



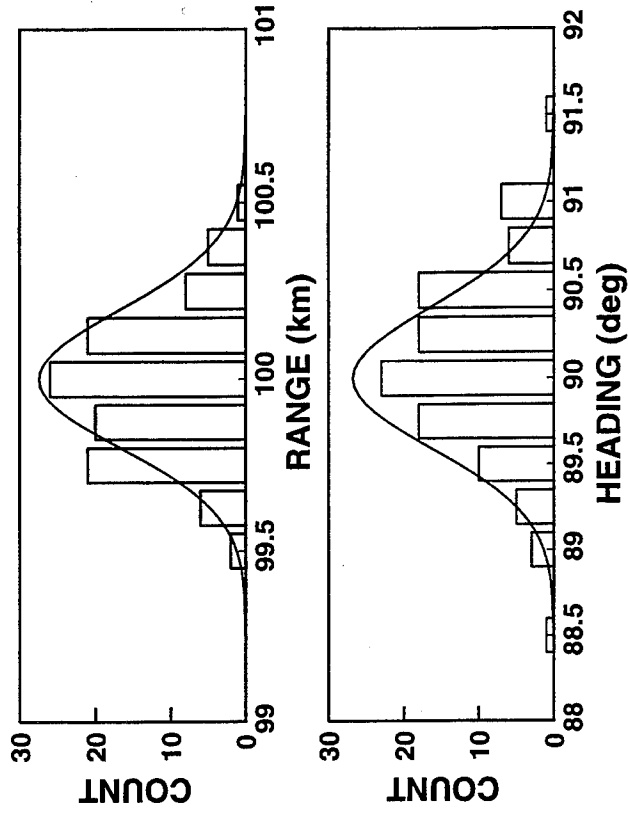
$R = 100 \text{ km}$, $V = 200 \text{ m/s}$,
 $H = 0 - 180 \text{ deg}$, $\theta = 30 \text{ deg}$,
 FILTER LENGTH = 50,
 JNR = 15 dB / SAMPLE

MONTE CARLO SIMULATIONS

CRLB vs SNR



ESTIMATE HISTOGRAMS

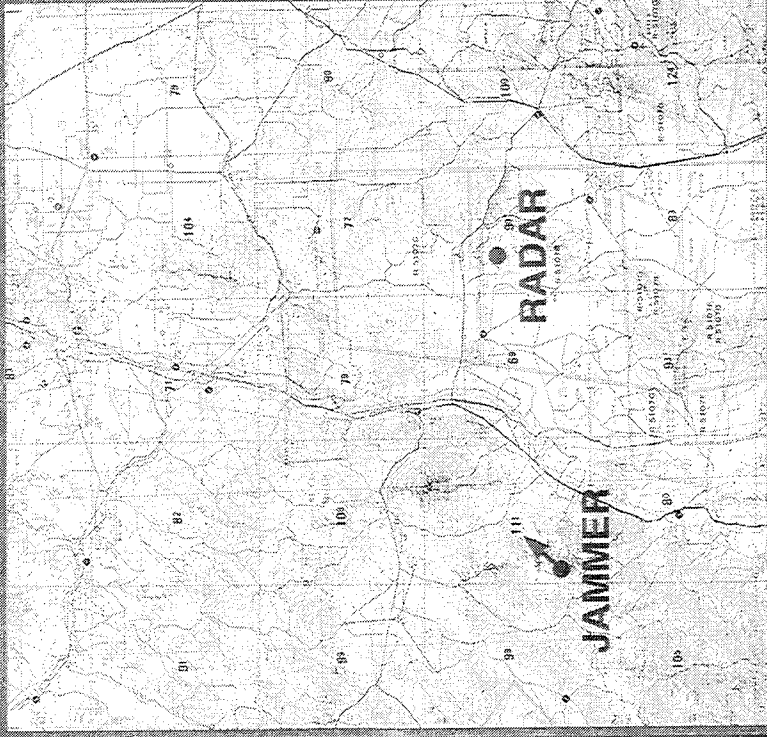


SIMULATION SCENARIO: $R = 100$ km, $\text{HEADING} = 90$ DEGREES, $V = 200$ m/s, FILTER LENGTH = 15, JNR = 15 dB FOR HISTOGRAMS, 2D SEARCH PERFORMED OVER RANGE AND HEADING

OUTLINE

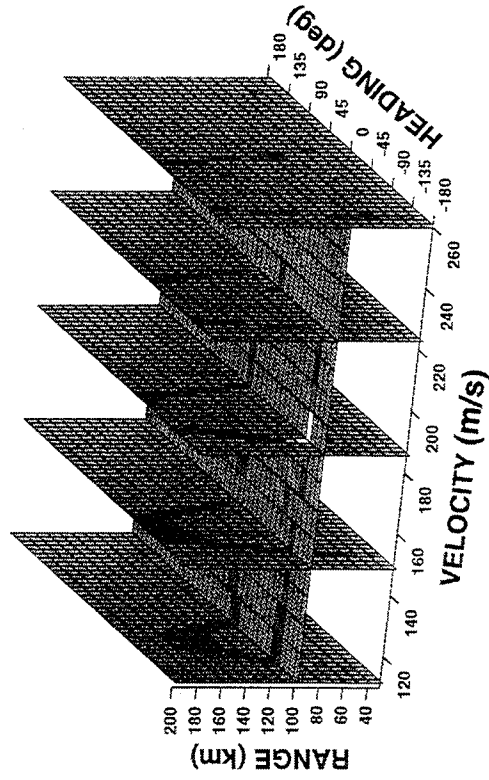
- **INTRODUCTION**
- **PROBLEM FORMULATION FOR MOVING JAMMERS**
- **JAMMER LOCALIZATION USING MOUNTAINTOP FIELD DATA**
 - **MAXIMUM LIKELIHOOD ESTIMATOR**
 - **SUBOPTIMUM ESTIMATOR**

MOUNTAINTOP RADAR AT WSMR

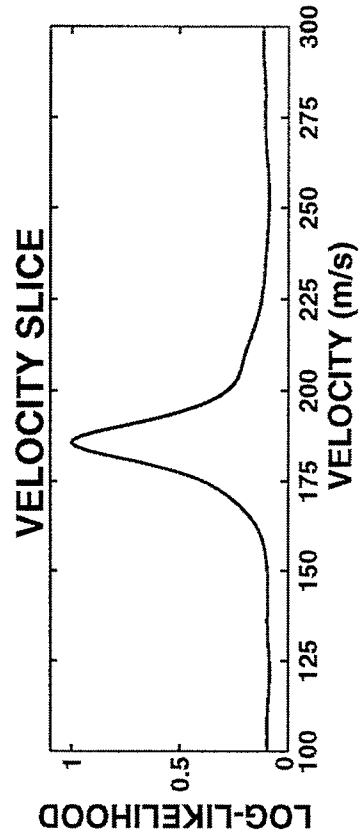
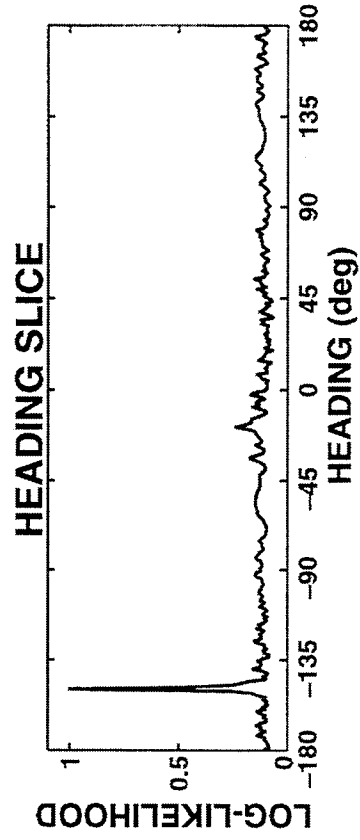
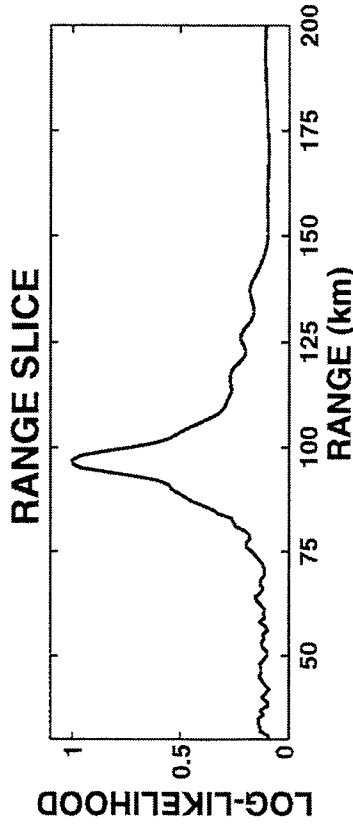
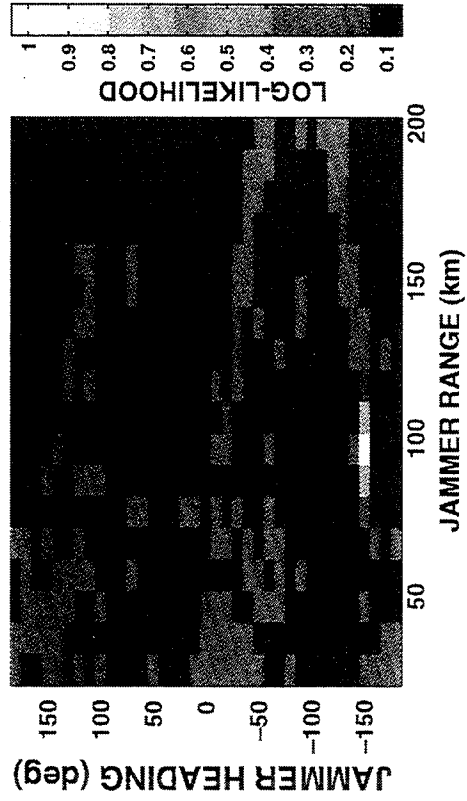


NORMALIZED 3D LOG-LIKELIHOOD FUNCTION

VELOCITY SLICES



RANGE-HEADING SLICE

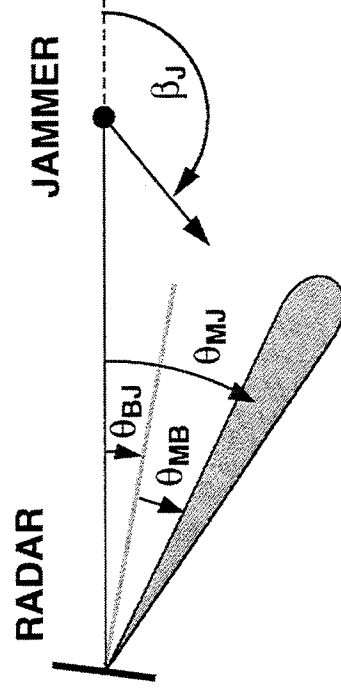
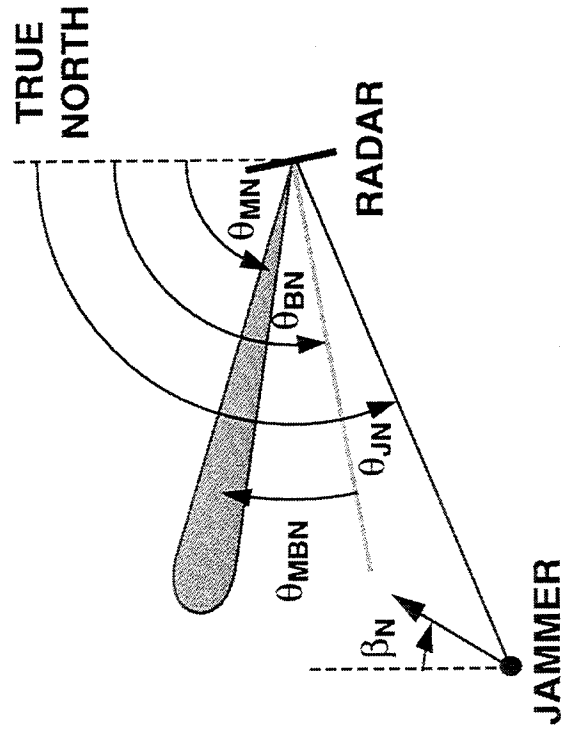


LOCALIZATION RESULTS

MOUNTAINTOP DATA SET HOT6067

MOUNTAINTOP COORDINATES

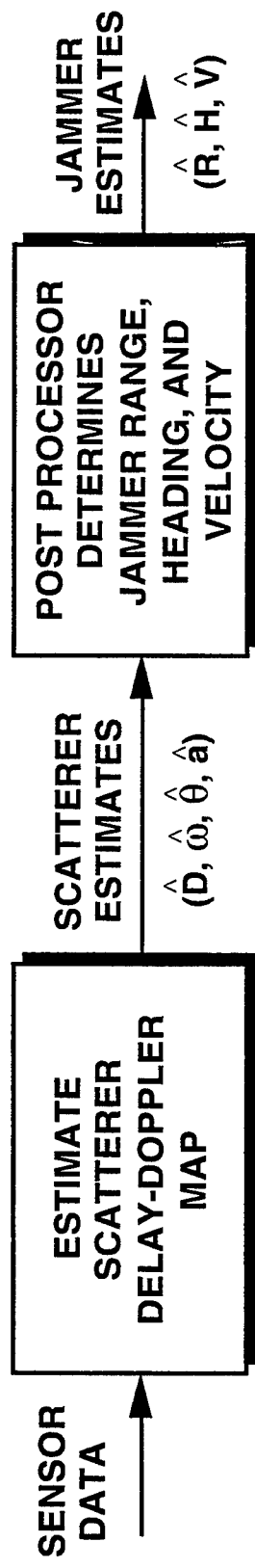
LOCALIZATION COORDINATES



PARAMETER	TRUE VALUE	ESTIMATED VALUE	ERROR
RANGE	101.7 km	97 km	4.6%
HEADING	148.8 deg	149.5 deg	0.47%
VELOCITY	184.5 m/s	185.5 m/s	0.54%
AZIMUTH	1.6 deg	1.3 deg	0.3 deg

FILTER PARAMETERS: 150 TAPS, 2 μ s SPACING, 600 SAMPLES SELECTED
FROM A 150 ms DATA INTERVAL

SUBOPTIMUM ESTIMATOR



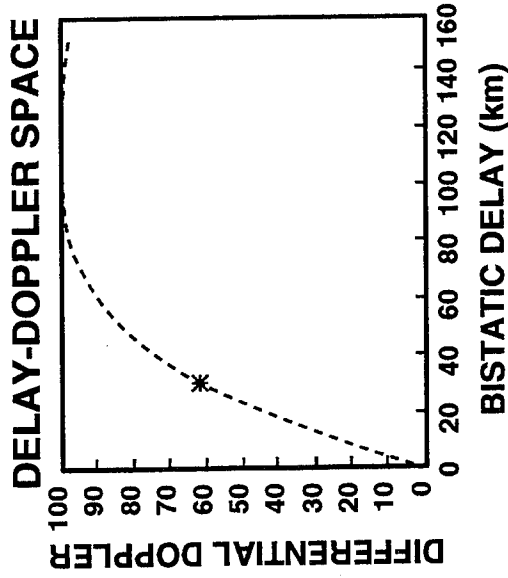
● TWO-PART APPROACH

1. ESTIMATE JAMMER DELAY-DOPPLER MAP FOR EACH BEAM
 - COMPUTE TIME INVARIANT LEAST SQUARE WEIGHTS AND FOURIER TRANSFORM
2. ESTIMATE JAMMER PARAMETERS
 - USE A BISTATIC HOUGH TRANSFORM
 - OTHER TECHNIQUES

LOCALIZATION USING THE HOUGH TRANSFORM

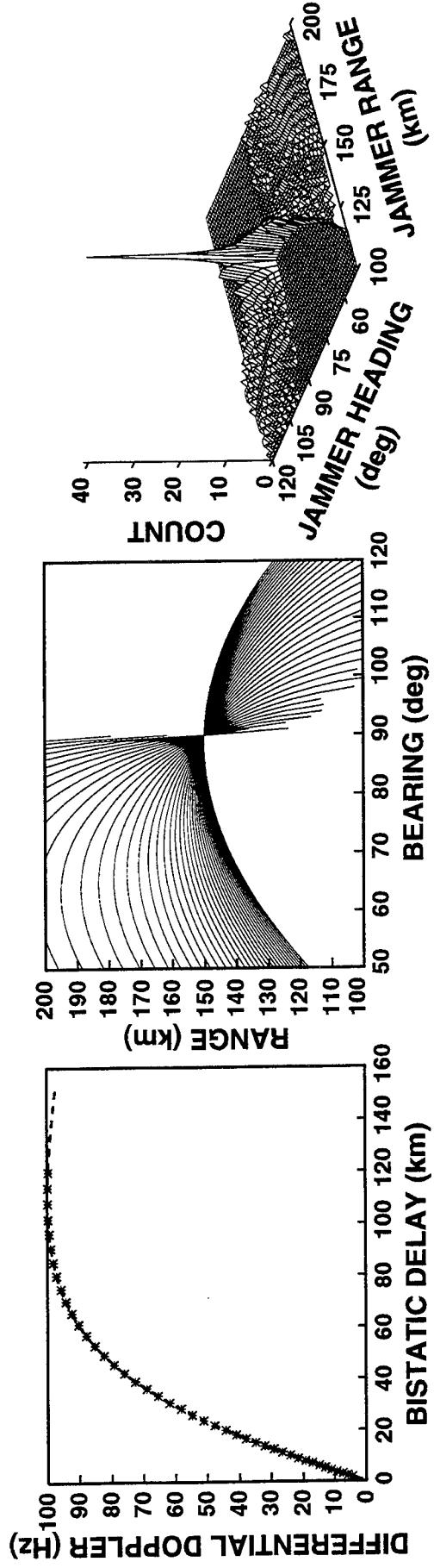
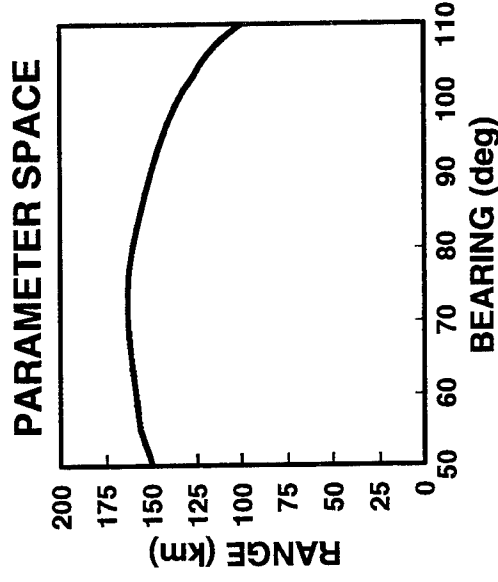
HT FOR LINES

$$H(p, \theta) = \iint I(x, y) \delta(p - x \cos \theta - y \sin \theta) dx dy$$



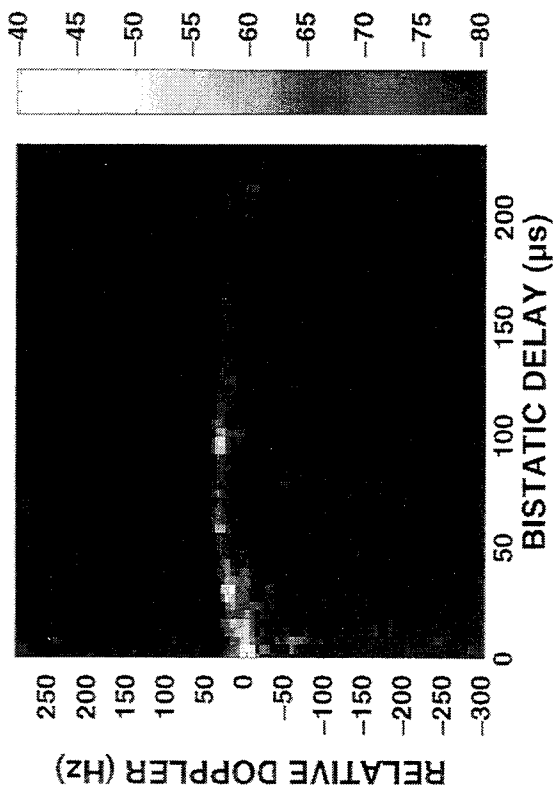
HT FOR DELAY-DOPPLER CONTOURS

$$H(\hat{R}, \hat{H}, \hat{V}) = \iint M(D, F) \delta \left(R - \frac{b}{\sin \phi(F, H, V)} + \frac{\sin \theta}{\sin \alpha} - 1 \right) dD dF$$

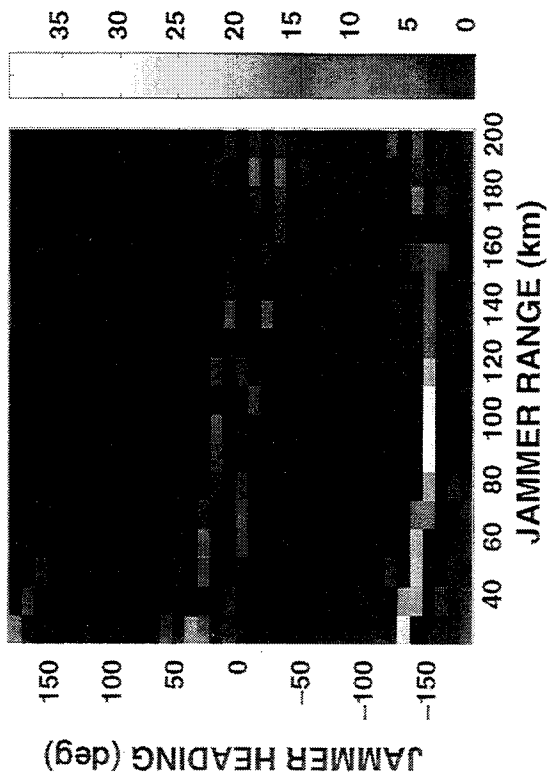


HOUGH TRANSFORM (Cont.)

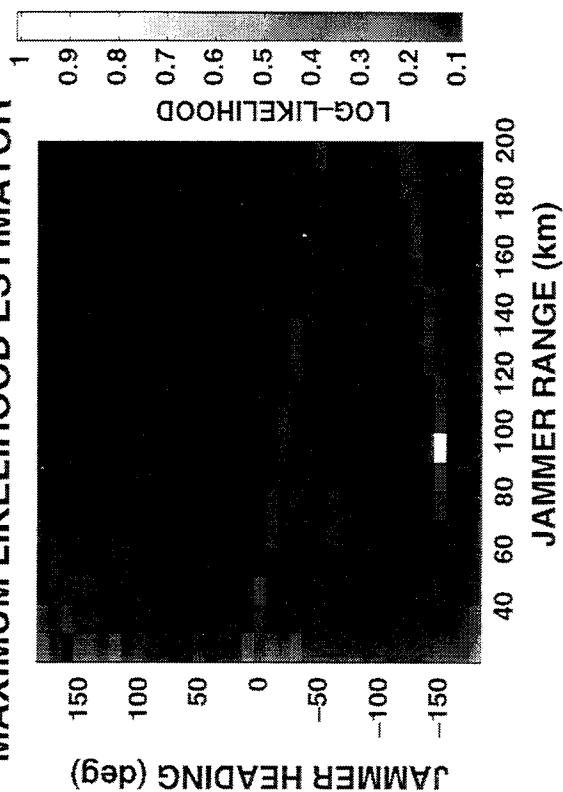
ESTIMATED DELAY-DOPPLER MAP



BINARY HOUGH TRANSFORM



MAXIMUM LIKELIHOOD ESTIMATOR



SUMMARY AND FUTURE WORK

- **PASSIVE LOCALIZATION USING OUT-OF-PLANE MULTIPATH MODEL PRESENTED**
 - MAXIMUM LIKELIHOOD ESTIMATOR
 - HOMOGENEOUS SCATTER AND 2-D GEOMETRY
 - CRAMER-RAO BOUNDS
 - MONTE-CARLO SIMULATIONS
- **CONCEPT VALIDATED USING MOUNTAINTOP FIELD DATA**
 - MAXIMUM LIKELIHOOD ESTIMATOR
 - SUBOPTIMUM TECHNIQUE
- **FUTURE WORK**
 - REFORMULATE PROBLEM USING 3-D GEOMETRY
 - ALTITUDE ESTIMATION POSSIBLE
 - DEVELOP FASTER MAXIMUM LIKELIHOOD SEARCHES
 - DEVELOP ADDITIONAL SUBOPTIMUM SOLUTIONS
 - DEVELOP SOLUTIONS FOR INHOMOGENEOUS CLUTTER
 - EXAMINE MORE MOUNTAINTOP DATA SETS

**CROSS-CORRELATION BASED ESTIMATION OF
MULTIPATH PROPAGATION CHANNELS**

Athina Petropulu, Haralambos Pozidis, and Kenneth Abend

Drexel University
Electrical and Computer Engineering Department
Philadelphia, PA 19104

tel: (215) 895-2358

fax: (215) 895-1695

email: athina@artemis.ece.drexel.edu

Gorca Systems, Inc.

P.O. Box 2325

Cherry Hill, NJ 08034

tel: (609) 273-8200

Abstract We propose a novel method for the reconstruction of an unknown signal that propagates in the presence of multipath. By oversampling the received sequence, or through spatial diversity, we first form a single input/two output problem. We then estimate the multipath effect by applying cross-correlation based operations of the two outputs, and recover the input signal via inverse filtering. The method is computationally attractive as compared to higher-order spectra based methods. It is not sensitive to errors in channel length estimates and performs better in low SNR's as compared to existing second-order statistics based methods. We show how the method can lead to a novel solution to the problem of estimating the propagation channels in radar applications.

CROSS-CORRELATION BASED ESTIMATION OF MULTIPATH PROPAGATION CHANNELS

Athina P. Petropulu, Haralambos Pozidis

*and Kenneth Aben^d**

Department of Electrical and Computer Engineering
Drexel University, Philadelphia, PA 19104

* GORCA Systems Inc. (GSI), Cherry Hill, NJ 08034

Literature Review

- Liu, Xu and Tong [1993]
Cyclic autocorrelation-based approach.
- Moulines et al. [1995]
SVD on previous approach. Exploitation of signal and noise subspaces structure.
- Petropulu and Nikias [1993] ,
Petropulu and Pozidis [1995]
HOS-based approach.

Problem

The system model is:

$$x_i(k) = h_i(k) * s(k) + n_i(k), \quad i = 1, 2$$

$h_1(k)$, $h_2(k)$: FIR channels (unknown)

$s(k)$: zero-mean stationary non-white random process
(unknown)

$n_1(k)$, $n_2(k)$: Noise processes uncorrelated to each other
and to $s(k)$.

Goal

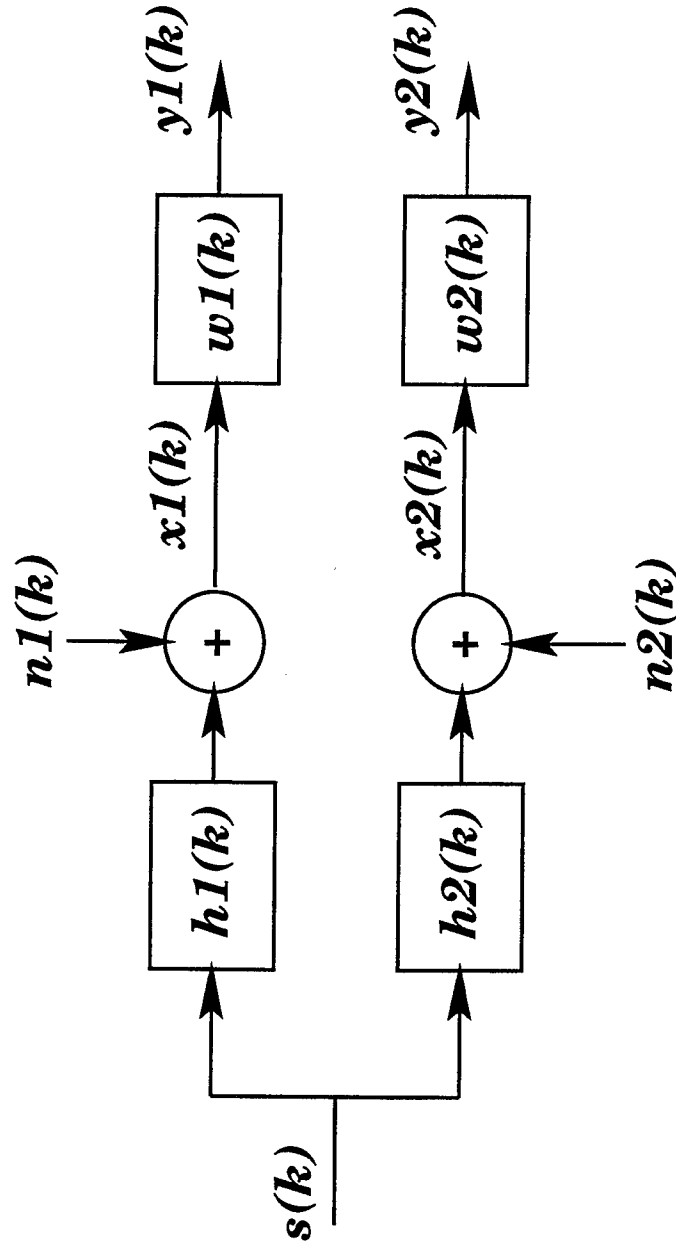
Derive an equalization scheme for $h_1(n)$ and $h_2(n)$.

Assumptions

- $h_1(k)$ and $h_2(k)$ have no common zeros,
- there are no zero-pole cancellations between $h_i(k)$ and convolutional components of $s(k)$.
- there are no common zeros between convolutional components of $s(k)$ and each of the channels.

Consider the filtered observations :

$$y_i(k) = x_i(k) * w_i(k), \quad i = 1, 2$$



$w_1(k), w_2(k)$: FIR channels.

Proposition 1

Let $E_{min}(\omega) = \arg\{Y_1^{min}(\omega)(Y_2^{min}(\omega))^*\}$,

$$E_{min}(\omega) = 0 \text{ for every } \omega$$

$$\iff$$

$$H_1^{min}(\omega) = W_2^{min}(\omega) \text{ and}$$

$$H_2^{min}(\omega) = W_1^{min}(\omega).$$

Proposition 2

Let $E_{max}(\omega) = \arg\{Y_2^{max}(\omega)(Y_1^{max}(\omega))^*\}$,

$$E_{max}(\omega) = 0 \text{ for every } \omega$$

$$\iff$$

$$H_1^{max}(\omega) = W_2^{max}(\omega) \text{ and}$$

$$H_2^{max}(\omega) = W_1^{max}(\omega).$$

Let

$$\begin{aligned} W_{min}(\omega) &= W_1^{min}(\omega)(W_2^{min}(\omega))^* \\ X_{min}(\omega) &= X_1^{min}(\omega)(X_2^{min}(\omega))^*, \end{aligned}$$

Setting $E_{min}(\omega)$ to zero we get:

$$\begin{aligned} &\sum_{n=-N_2, n \neq 0}^{N_1} w_{min}^R(n) \sin(\omega n - \psi(\omega)) \\ &- \sum_{n=-N_2}^{N_1} w_{min}^I(n) \sin(\omega n + \psi'(\omega)) = \sin(\psi(\omega)) \end{aligned}$$

where

$$\psi(\omega) = \text{Arg}\{X_{min}(\omega)\}, \quad \psi'(\omega) = \frac{\pi}{2} - \psi(\omega),$$

$$(\hat{w}_{min}(0) = 1.)$$

Repeating for different ω 's in the set $\{\omega = \frac{2\pi}{N}k, k = 0, \dots, N-1\}$, we can form the system of equations:

$$\Phi_{min} \mathbf{w}_{min} = \phi_{min},$$

Since there are $2L$ (L is the length of $w_{min}(n)$) unknowns to be estimated, N must be chosen so that $N > 2L$.

Solve adaptively or via least-squares.

Due to the structure of $w_{min}(n)$ we get:

$$\hat{w}_{min}(n) = \begin{cases} \hat{w}_1(n) = \hat{h}_2(n), & n > 0 \\ \hat{w}_2(-n) = \hat{h}_1(-n), & n < 0 \end{cases}.$$

In a similar way, we can get the non-causal cepstra of $h_1(n)$ and $h_2(n)$, $n < 0$.

The channels can then be reconstructed within a scalar and a time delay by using inverse cepstra operations.

On Estimating the phase of $X_{min}(\omega)$ (1)

Let $h(k)$ be an FIR sequence:

$$H(z) = cz^{-r_h} I_h(z^{-1}) O_h(z)$$

where

$$I_h(z^{-1}) = \prod_i (1 - c_i z^{-1}), \quad |c_i| < 1$$

(minimum phase part)

$$O_h(z) = \prod_i (1 - d_i z), \quad |d_i| < 1$$

(maximum phase part)

Minimum-phase equivalent

$$\tilde{H}(z) = I_h(z^{-1}) O_h^* \left(\frac{1}{z^*} \right)$$

Estimation of Minimum-phase equivalent

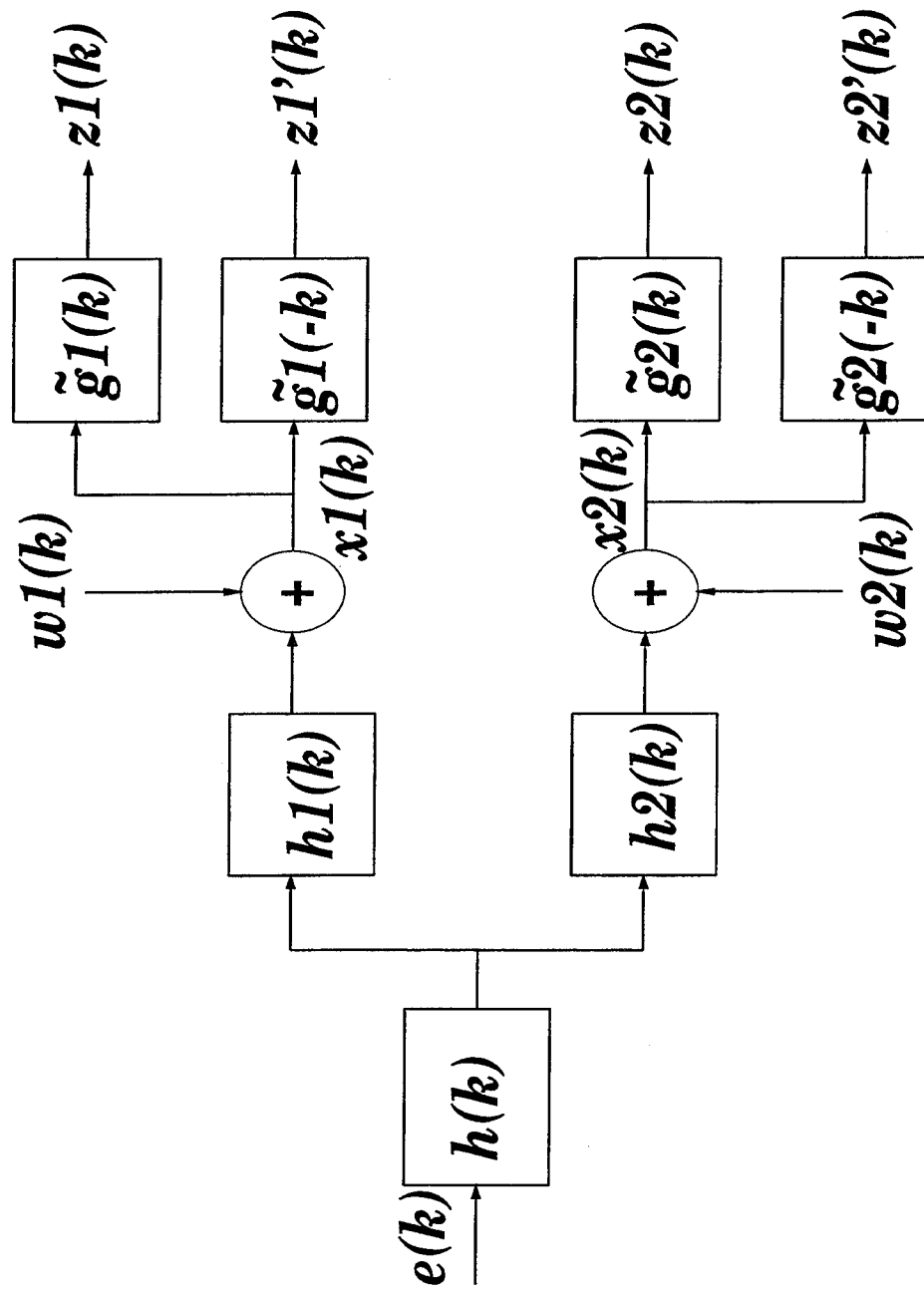
Power cepstrum approach :

$$\begin{aligned}\tilde{h}(n) &= F^{-1}\{\exp[C(\omega)]\} \\ c(n) &= F^{-1}\{\log|H(\omega)|^2\}u(n),\end{aligned}$$

where $u(n)$ is the unit step function, and $C(\omega)$ is the Fourier transform of $c(n)$.

If $h(n)$ is random, then $|H(\omega)|^2$ should be replaced by the power spectrum $S_h(\omega)$ of $h(n)$, obtained as the Fourier transform of its autocorrelation.

Let $\tilde{g}_i(k)$ be the minimum-phase equivalent of $x_i(k)$, $i = 1, 2$:



On Estimating the phase of $X_{min}(\omega)$ (2)

Cross spectrum of $z_1(k)$, $z_2(k)$:

$$S_{z_1 z_2}(z) = a z^{r_{h_1} - r_{h_2}} [I_{h_1}(z) I_{h_2}^*(1/z^*)]^2 P_1(z)$$

where

a : constant

$P_1(z)$: zero phase

$$\boxed{\text{Arg}\{S_{z_1 z_2}(\omega)\} = 2\psi(\omega) + (r_{h_1} - r_{h_2})\omega}$$

Taking one half of the phase of $S_{z_1 z_2}(\omega)$, we get:

$$\hat{\psi}(\omega) = \frac{1}{2} \arg\{S_{z_1 z_2}(\omega)\} + \frac{1}{2}(r_{h_1} - r_{h_2})\omega$$

Length of $w_{min}(n)$ is unknown

Knowledge or estimation of the true length, L and parameter N_2 can be bypassed. The solution can still be found if the length is over-estimated. This is illustrated in the following table, assuming true values of $L = 6, N_2 = 4$.

\hat{L}	$\hat{N}_1 = \hat{L} - \hat{N}_2$										
	1	2	3	4	5	6	7	8	9	10	11
6		X									
7		X	X								
8		X		X							
9		X			X						
10		X				X					
11		X					X				

The X's in the table indicate values of \hat{L} and \hat{N}_1 that result in a correct solution. It can be observed that a correct solution can be obtained whenever $\hat{N}_1 = N_1$ or $\hat{N}_1 = \hat{L} - N_2$, regardless of the length \hat{L} used.

Simulations

Set A:

$$\begin{aligned}h_1(n) &= [-0.306, 0.2446, 1, -0.237, -0.231], \\h_2(n) &= [-0.357, -0.25, 1, 0.327, -0.36]\end{aligned}$$

Set B:

The channel is generated from two delayed raised cosine pulses :

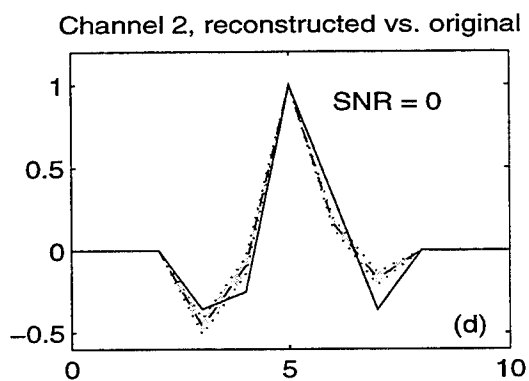
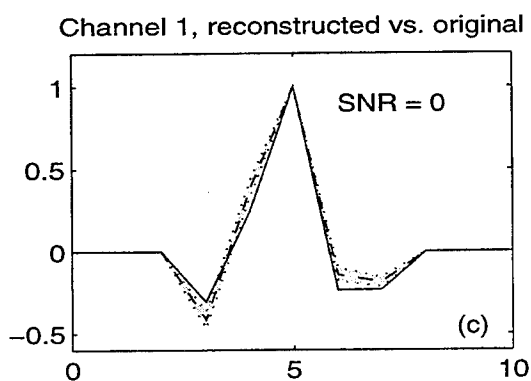
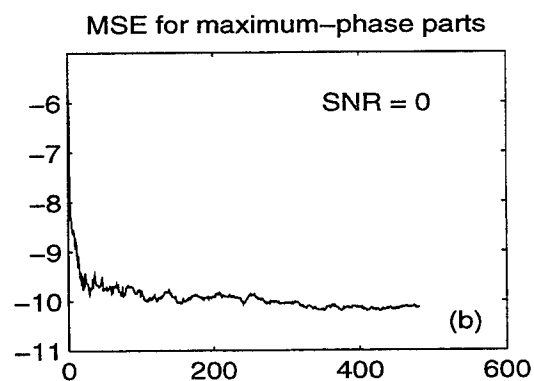
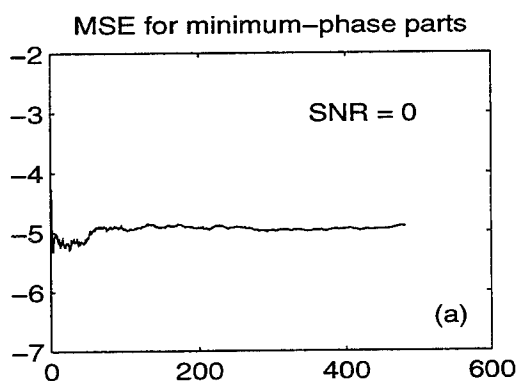
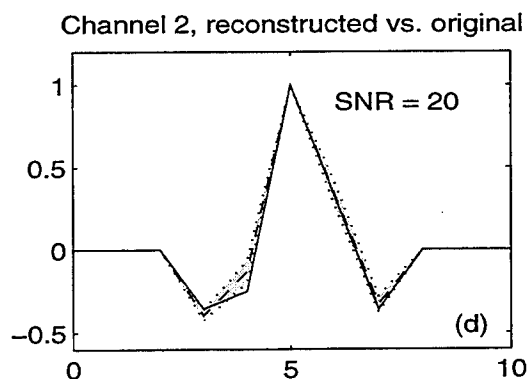
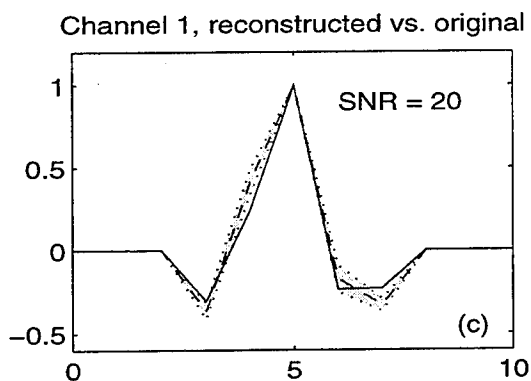
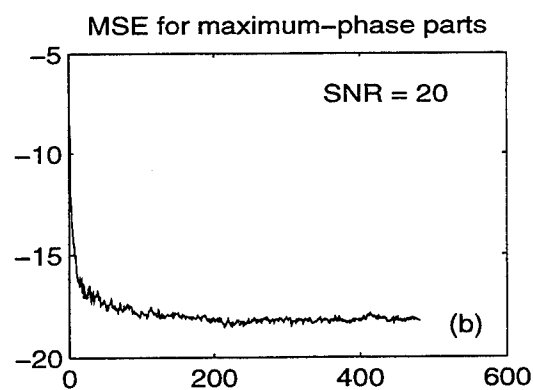
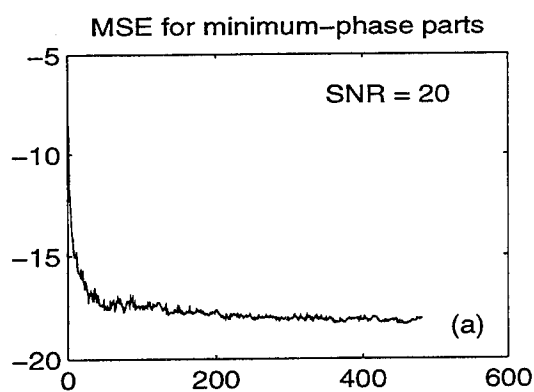
$$h(t) = 0.2c(t, 0.11) + 0.4c(t - 2.5, 0.11)$$

where $c(t, a)$ denotes a raised cosine pulse, and a the roll-off factor.

Two virtual channels $h_1(n)$ and $h_2(n)$ were generated by oversampling $h(t)$ by a factor of two.

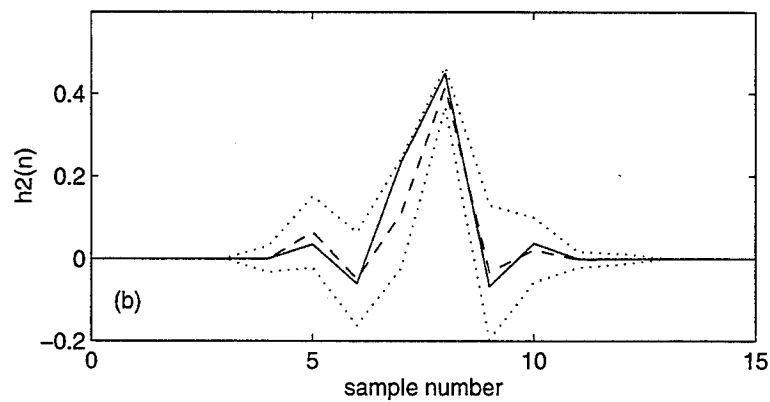
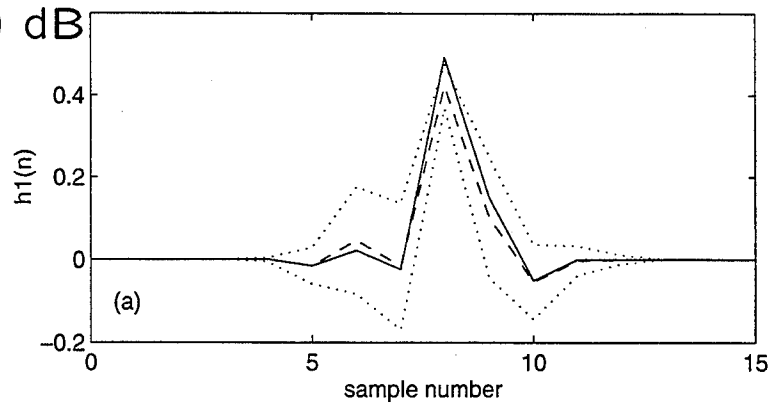
A) Non-white signals

Case 1: $s(n) = e(n) * h(n)$, where $h(n) = [1, 1.4, -4.8]$.

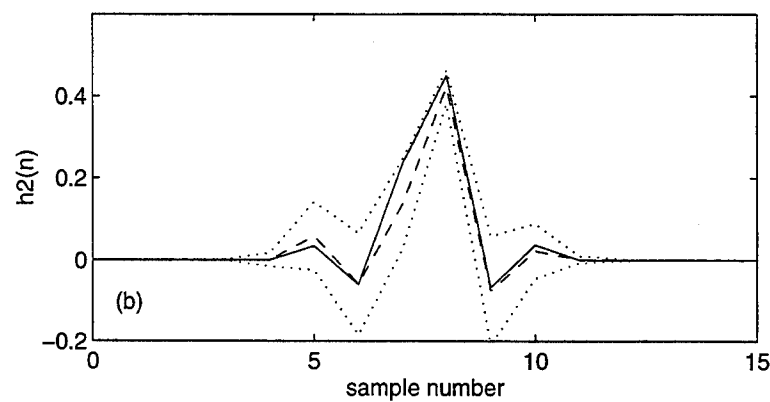
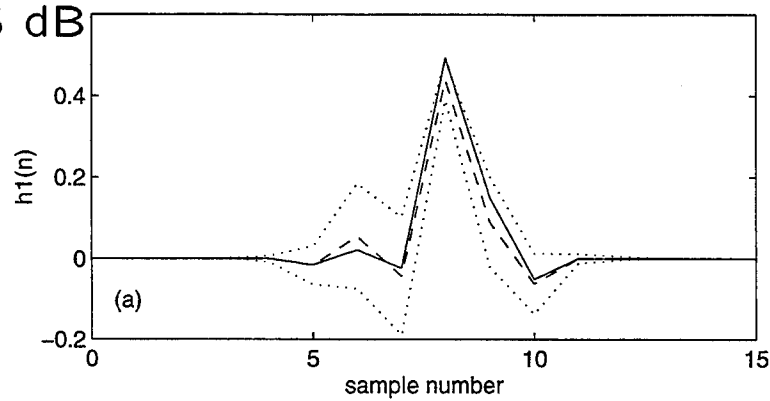


Case 2: $h(t)$ generated from two delayed raised cosine pulses.

SNR = 10 dB



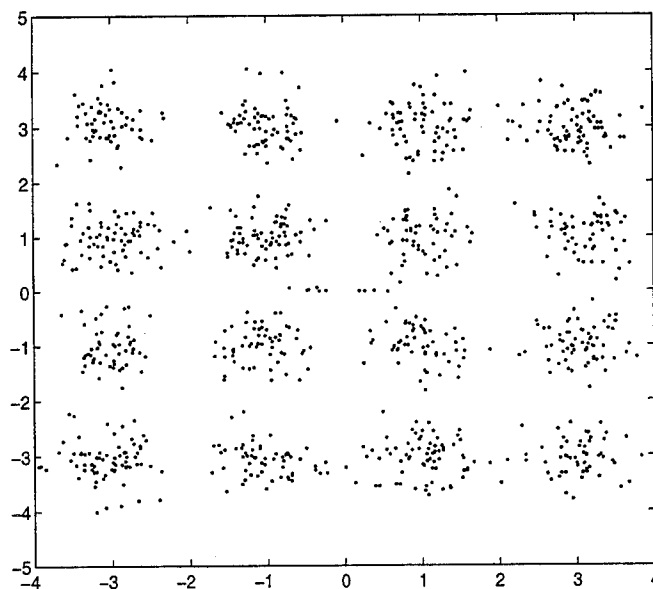
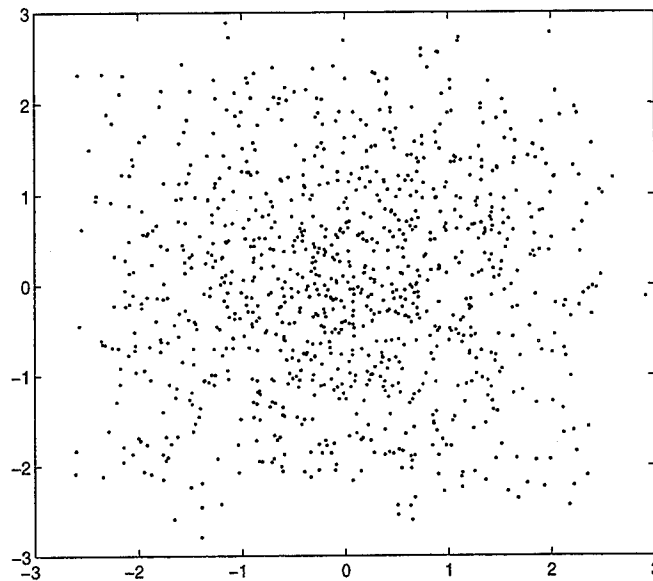
SNR = 15 dB



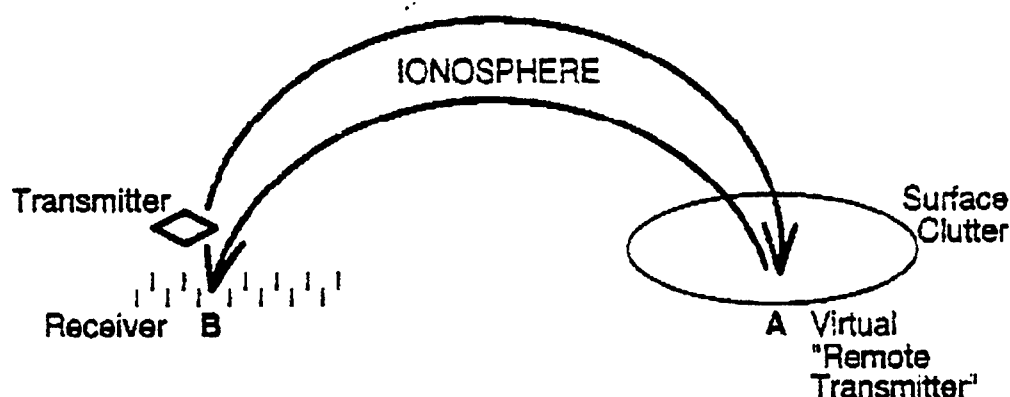
C) 16-level QAM communication signals

Input was taken to be a white i.i.d.

16-level QAM signal.



Application: Estimating OTH propagation channels without the need of an OTH transmitter



- Remote transmitter is replaced by ground or sea clutter. Its position is relocated by re-steering the beam.
- A patch of homogeneous clutter is illuminated and received array data are processed to form two beams within that illuminated region. These beams are equivalent to transmitters generating i.i.d. signals. The statistical equivalence of these signals allows for the blind estimation of the return channels (A to B).

Summary

- A novel cross-correlation based framework is proposed for the problem of blind equalization in communications.
- We assume that we have access to two observations obtained either by sampling at the symbol rate the outputs of two sensors, or by oversampling by a factor of two the output of a single sensor. In either case, the two observations correspond to the outputs of two channels excited by the same input. We estimate the channels using as a basic tool the phase of the cross spectrum of functions of the observations.
- The proposed method is computationally attractive as compared to higher-order spectra based ones. It is not sensitive to errors in channel length estimates, and performs better in low SNR's as compared to existing second-order statistics based methods.

References

- [1] W.A. Gardner, "Exploitation of spectral redundancy in cyclostationary signals," *IEEE Signal Processing magazine*, vol. 8, pp. 14-36, April 1991.
- [2] M. Gurelli and C.L. Nikias, "EVAM: An Eigenvector-Based Algorithm for Multichannel Blind Deconvolution of Input Colored Signals," *IEEE Trans. on Signal Processing*, vol. 43(1), pp. 134-149, January 1995.
- [3] D. Hatzinakos, C.L. Nikias, "Blind Equalization Using a Tricestrum Based Algorithm", *IEEE Trans. on Communications*, vol. 39, pp.669-682, May, 1991.
- [4] S. Haykin, *Adaptive filter theory*, second edition, Prentice Hall Inc., Englewood Cliffs, N.J., 1991.
- [5] H. Liu, G. Xu, and L. Tong, "A Deterministic Approach to Blind Equalization", *Asilomar Conference on Signals, Systems and Computers*, pp.751-755, November 1993, Pacific Grove, California.
- [6] E. Moulines, P. Duhamel, J.-F. Cardoso, and S. Mayrargue, "Subspace Methods for the Blind Identification of Multichannel FIR Filters", *IEEE Trans. on Signal Processing*, vol. 43, pp. 516-525, February 1995.
- [7] A.P. Petropulu, C.L. Nikias, "Blind deconvolution using reconstruction from partial Higher Order cepstral information", *IEEE Trans. on Signal Processing*, vol. 41(6), pp. 2088-2095, June 1993.
- [8] A.P. Petropulu, H. Pozidis, "Multichannel Blind Equalization of Colored Signals", *IEEE Signal Processing, Athos Workshop on Higher-Order Statistics*, pp. 35-38, Girona, Spain, June 1995.
- [9] L. Tong, "Blind Sequence Estimation", *IEEE Trans. on Communications*, vol. 43(12), pp. 2986-2994, December 1995.
- [10] L. Tong, G. Xu and T. Kailath, "Blind Identification and Equalization Based on Second-Order Statistics: A Time Domain Approach," *IEEE Trans. on Information Theory*, vol. 40(2), pp. 340-349, March 1994.
- [11] H. Attia, K. Abend and B. Fell, "Self-Cohering an OTH Radar on Clutter Returns," GORCA Systems Inc. Final Technical Report on Contract No. F19628-92-C-0024, for U.S.A.F. Rome Laboratory, ERCP, Hanscom AFB, MA, David S. Choi, COTR, January 1995.

EXPLOITING FREQUENCY DOMAIN MODELS IN ARRAY SIGNAL PROCESSING

A. Lee Swindlehurst

Brigham Young University
Electrical and Computer Engineering Department
Room 459CB

Provo, UT 84602

tel: (801) 378-4343

fax: (801) 378-6586

email: swindle@ee.byu.edu

Abstract This presentation describes several problems in array signal processing, and how they may be naturally cast in a frequency domain framework and solved. The problems considered all involve the reception of signals (of known or unknown shape) with various unknown delays. A delay in the time domain translates into a linear phase shift in the frequency domain, which amounts to scaling the signal spectrum by a Vandermonde vector for the evenly spaced FFT frequencies. Algorithms that exploit this idea are described for the following problems: 1) synchronization and spatial signature (or DOA) estimation for multiple users in a communication channel transmitting the same known (e.g., training) signal; 2) synchronization and spatial signature (or DOA) estimation for multiple users in a communication channel transmitting different but known (e.g., training) signals; 3) blind equalization of a multipath channel with one or more independent sources (blind here means without the use of training signals or array calibration data); and 4) resolution and pulse estimation for overlapping echoes of unknown shape using one or more sensors. This presentation shows how different variations of the same algorithm may be applied to each of the above problems, and a number of simulation examples are presented to illustrate performance.

Exploiting Frequency Domain Models in Array Signal Processing

A. Swindlehurst
Brigham Young University
Provo, UT 84602

Work supported by: NSF
 USC Center for Research on
 Applied Signal Processing

Presentation Outline

1. Problem Statement

- Applications
- Assumptions/Limitations

2. Current Approaches

3. New Model Based on Physical Parameters

- Mathematical model
- Why estimate physical parameters?
- Approximation in the frequency domain

4. Identifiability

5. Algorithms

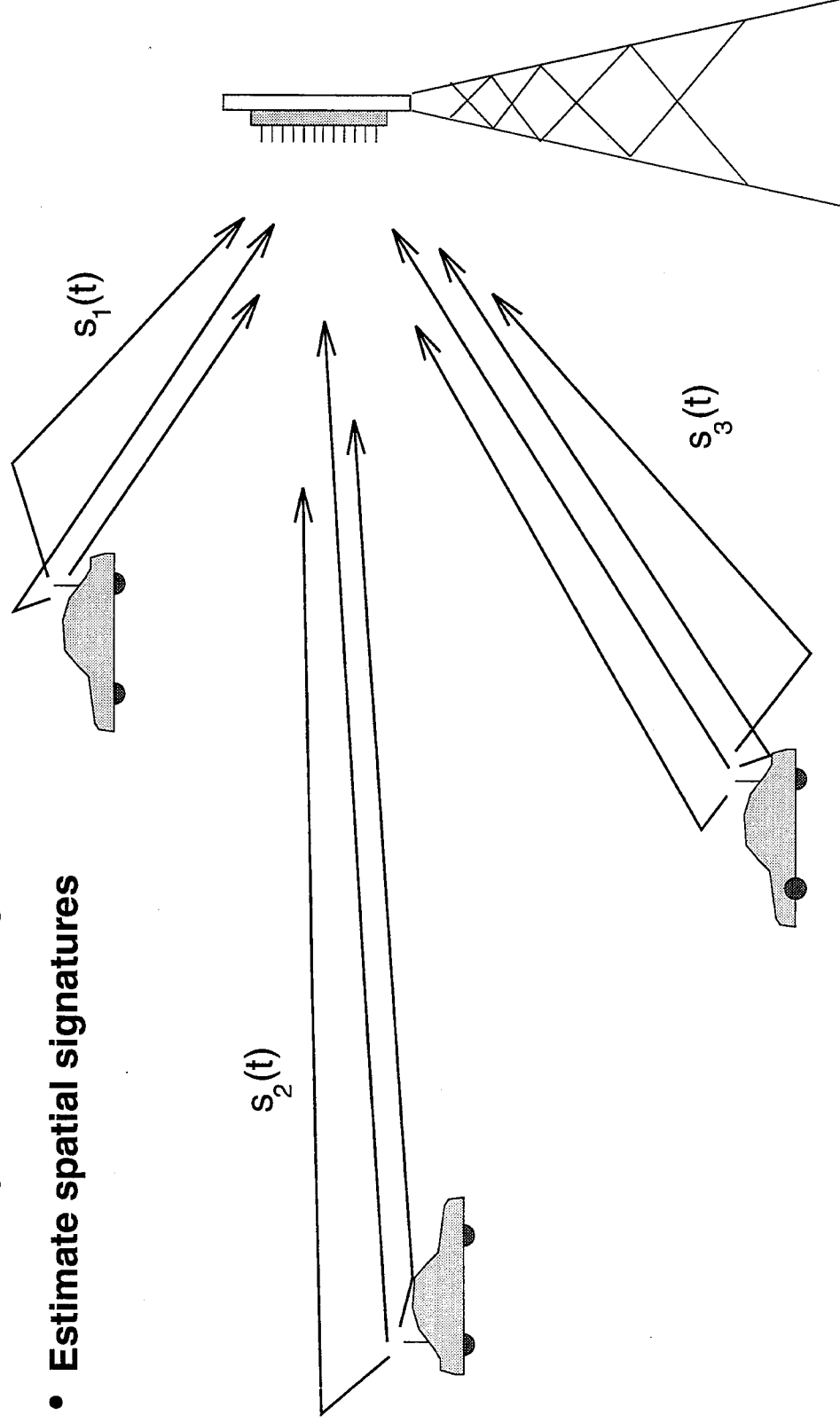
- Maximum Likelihood
- Iterative Quadratic ML
- ESPRIT

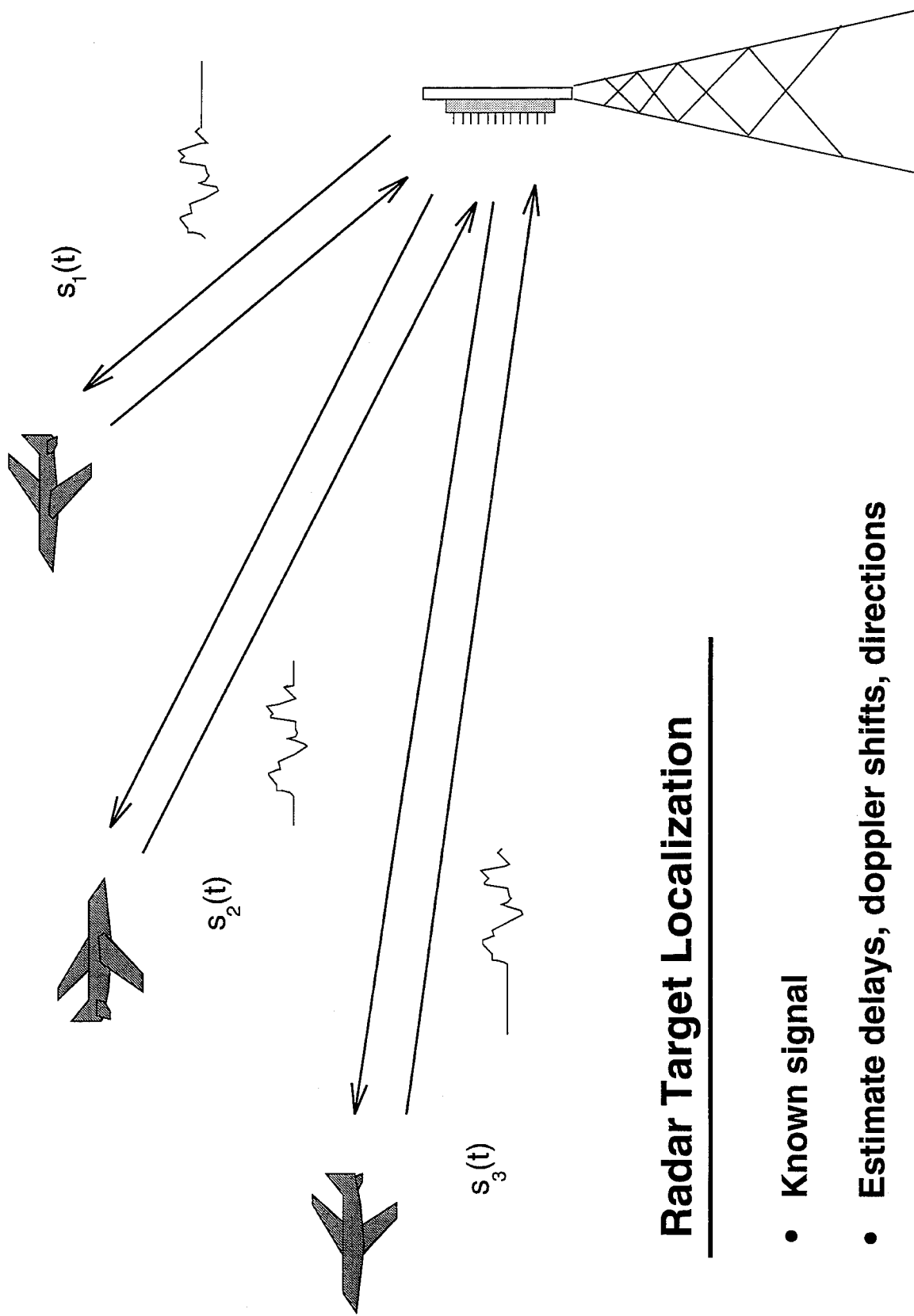
6. Simulation Examples

7. Future Work

Spatial Acquisition in Coherent Cellular Radio

- Known asynchronous signals
- Estimate spatial signatures



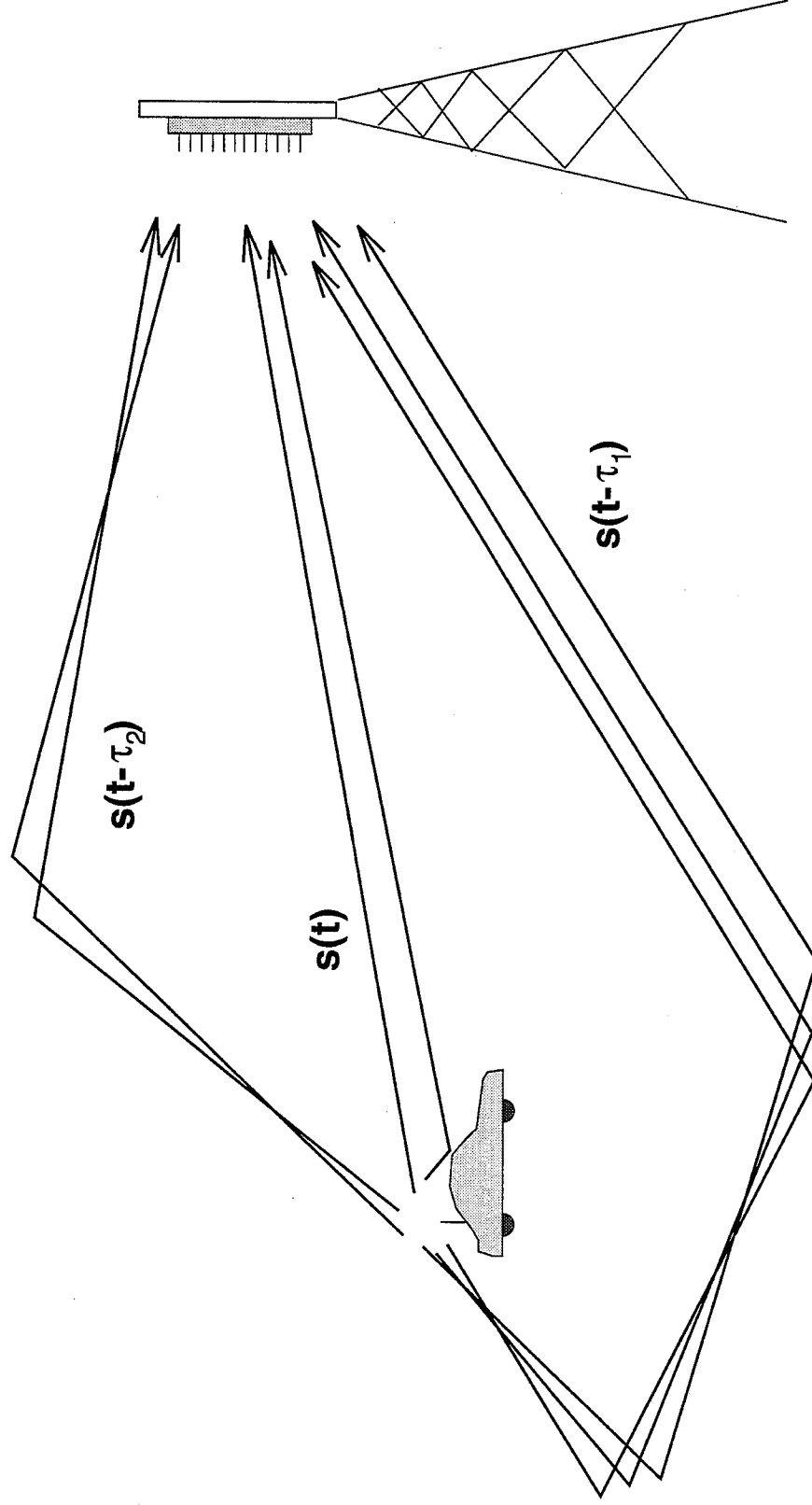


Radar Target Localization

- Known signal
- Estimate delays, doppler shifts, directions

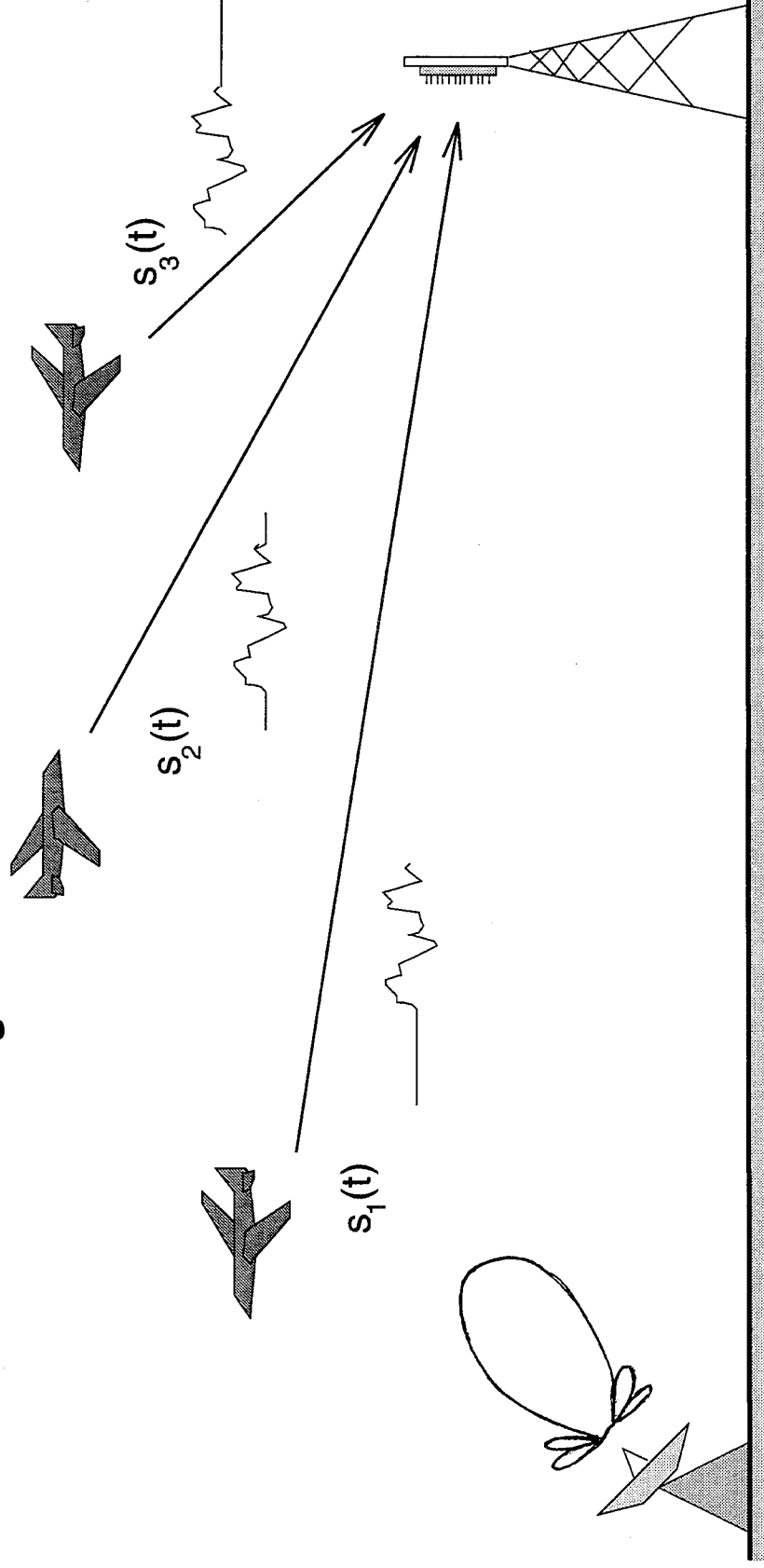
Blind Channel Equalization

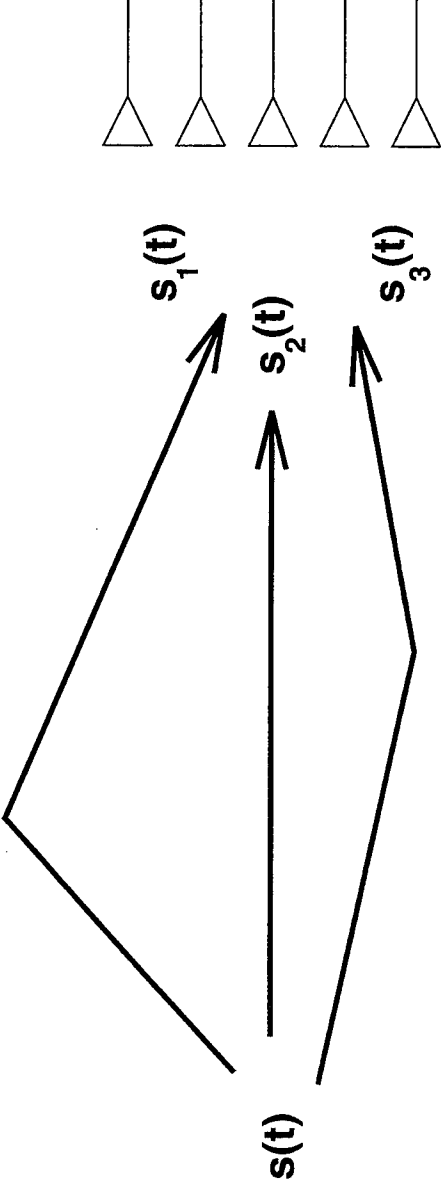
- Estimate unknown asynchronous signal
- Estimate spatial signatures



Bistatic Radar Localization

- Estimate directions, (relative) delays & doppler shifts
- Known or unknown signal





Scenario:

An array of antennas receives several copies of an unknown transmitted signal

Problem:

Recover $s(t)$ without the aid of

- array calibration or shape data
- channel geometry
- information about the signal

Assumptions & Limitations

- Single source
- Source is narrowband
- Array sampled at Nyquist rate (at least)
- Number of samples collected \gg longest multipath delay
- No appreciable doppler shift (for the moment)
- Can estimate number of (incoherent) multipath groups

Blind Equalization Methods

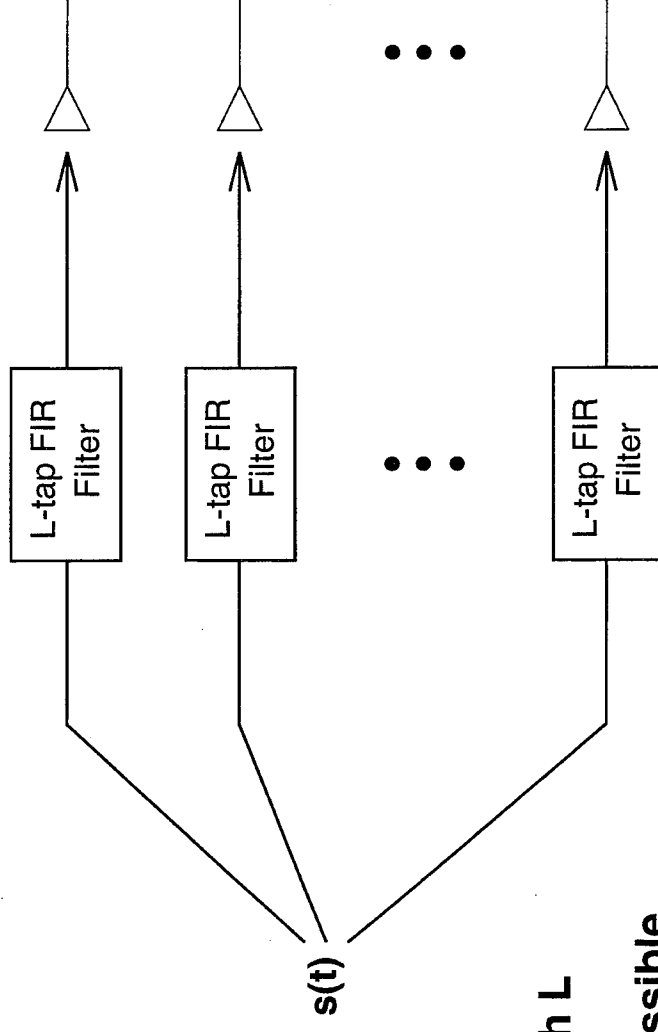
- **Adaptive LMS, MSE, CMA, HOS based**

- Sato, 1975
- Godard, 1980
- Benveniste & Goursat, 1984
- Foschini, 1985
- Tugnait, 1987
- Hatzinakos & Nikias, 1989, *etc.*

- **2nd Order Cyclostationarity, FSE**

- Gardner, 1991
- Tong, Xu, Kailath, 1991
- Li & Ding, 1993
- Liu, Xu, Tong, 1993
- Tugnait, 1993
- Moulines, 1995, *etc.*

2nd Order Cyclostationary Model



- Must determine filter length L
- “Closed form” solution possible
- Must estimate L filter coefficients for each antenna
- Can incorporate pulse shaping filter at source
- Channel parameters estimated directly
- Signal estimated indirectly

Subchannel Response Matching (SRM)

- Promising method based on work by

Baccala & Roy, 1993

Liu, Xu, & Tong, 1993

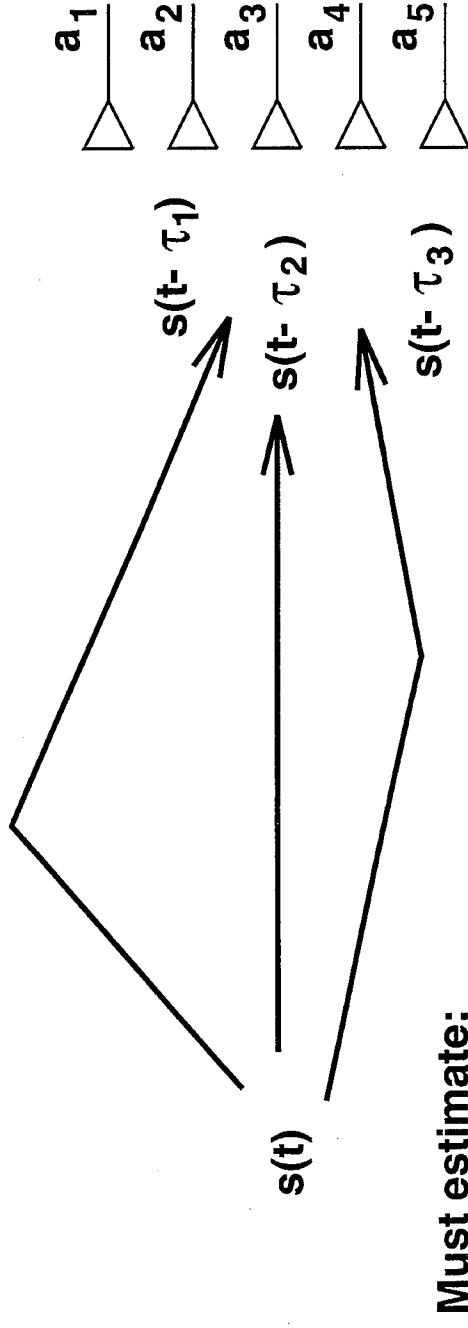
Schell & Smith, 1994

- Let $x_i(t)$ denote the output of antenna i , and $h_i(t)$ the impulse response of channel i . SRM based on the observation that

$$\begin{aligned} h_i(t) * x_k(t) &= h_i(t) * (h_k(t) * s(t)) \\ &= h_k(t) * (h_i(t) * s(t)) = h_k(t) * x_i(t) \end{aligned}$$

- All filter/sensor pairs are combined to form an overdetermined set of linear equations, which is solved via least squares.

Model Based on Physical Parameters



Must estimate:

τ_i = (relative) delay of multipath i

a_i = response vector for antenna i in the
direction of each multipath

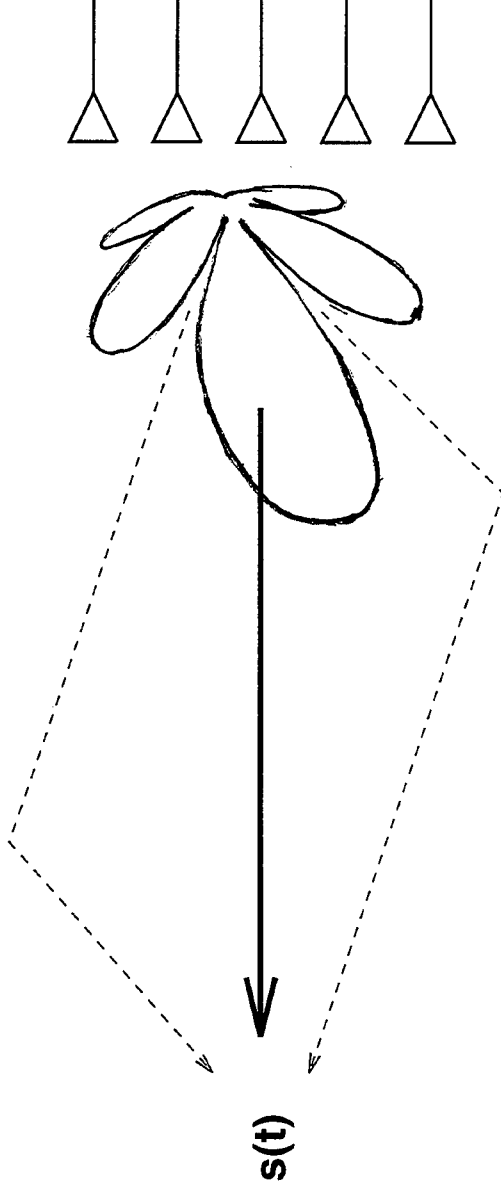
$$A = [a_1 \ a_2 \ a_3 \ a_4 \ a_5]$$

spatial signature matrix

$s(t)$ = transmitted signal samples

Why Estimate Physical Parameters?

- Fewer parameters (most filter taps = 0)
- Relative delays provide information about channel geometry (delay spread, coherence bandwidth), or target positions in overlapping echo problem
- Spatial signatures can be used to mitigate multipath fading in downlink transmission to remote



Frequency Domain Approach

- **Key idea: shift property of Fourier transforms**

If $s(t) \leftrightarrow s(\omega)$, then $s(t - \tau) \leftrightarrow \exp(-j\omega\tau)s(\omega)$.

- **Given N samples where $t_N - t_1 \gg \tau$, a DFT yields**

$$\begin{bmatrix} s(t_1 - \tau) \\ s(t_2 - \tau) \\ \vdots \\ s(t_N - \tau) \end{bmatrix} \leftrightarrow \underbrace{\begin{bmatrix} s(\omega_1) \\ s(\omega_2) \\ \dots \\ s(\omega_N) \end{bmatrix}} \underbrace{\begin{bmatrix} 1 \\ e^{-j2\pi\tau/N} \\ \vdots \\ e^{-j2\pi(N-1)\tau/N} \end{bmatrix}} = S_\omega \times v(\tau)$$

- **With d signals having distinct delays**

$$\begin{bmatrix} s(t_1 - \tau_1) & s(t_1 - \tau_d) \\ s(t_2 - \tau_1) & s(t_2 - \tau_d) \\ \vdots & \vdots \\ s(t_N - \tau_1) & s(t_N - \tau_d) \end{bmatrix} \leftrightarrow S_\omega \underbrace{[v(\tau_1) \dots v(\tau_d)]}_{V(\tau)}$$

Frequency Domain Approach (cont.)

- Let $x_i(\omega)$ denote the frequency domain output of sensor i :

$$\begin{bmatrix} x_i(\omega_1) \\ \vdots \\ x_i(\omega_N) \end{bmatrix} = \mathbf{S}_\omega \mathbf{V}(\tau) \mathbf{a}_i$$

where the elements of \mathbf{a}_i denote the array response in the direction of each multipath.

- Stacking all m antenna outputs together in \mathbf{X} yields:

$$\mathbf{X} = \begin{bmatrix} x_1(\omega_1) & x_m(\omega_1) \\ \vdots & \vdots \\ x_1(\omega_N) & x_m(\omega_N) \end{bmatrix} = \mathbf{S}_\omega \mathbf{V}(\tau) \mathbf{A}$$

- Mathematical restatement of the blind equalization problem:

Given noisy data $\mathbf{X} = \mathbf{S}_\omega \mathbf{V}(\tau) \mathbf{A} + \mathbf{N}$, estimate the delays τ , spatial signatures \mathbf{A} , and reconstruct the signal samples \mathbf{S}_ω .

Parameter Identifiability

Theorem:

Given an array of $m \geq 2$ sensors and $\mathbf{X} = \mathbf{S}_\omega \mathbf{V}(\tau) \mathbf{A}$, if

$$d < \frac{N + m - 1}{2},$$

then with probability 1,

- τ can be uniquely determined, and
- \mathbf{S}_ω and \mathbf{A} can be uniquely determined to within a complex scaling.

Implication:

$N \gg m$ implies the signal may be recovered when number of multipaths is far greater than number of sensors.

Maximum Likelihood

- Unlike SRM, use of physical parameters allows ML problem formulation
- For spatially & temporally white noise, ML is equivalent to following least squares problem:

$$\hat{S}_\omega, \hat{A}, \hat{\tau} = \operatorname{argmin} \|X - S_\omega V(\tau)A\|_F^2$$

- Separable in either A:

$$\hat{S}_\omega, \hat{\tau} = \operatorname{argmin} \|P_{S_\omega V(\tau)}^\perp X\|_F^2, \quad \hat{A} = [\hat{S}_\omega V(\hat{\tau})]^\dagger X$$

- or S_ω :

$$\hat{A}, \hat{\tau} = \operatorname{argmin} \sum_{i=1}^N x_k P_{A v_k(\tau)}^\perp x_k^*, \quad \hat{s}(\omega_k) = \frac{x_k \hat{A}^* v_k^*(\hat{\tau})}{v_k(\hat{\tau}) \hat{A} \hat{A}^* v_k^*(\hat{\tau})}$$

Alternative ML Formulation

- Define a polynomial

$$b(z) = b_0 z^d + b_1 z^{d-1} + \dots b_d$$

whose roots are $\exp(-j2\pi\tau_1/N), \dots, \exp(-j2\pi\tau_d/N)$

- Then the Sylvester matrix **B** satisfies $\mathbf{B}^* \mathbf{V}(\tau) = 0$:

$$\mathbf{B} = \begin{bmatrix} 0 & & & & & & & & \\ b_0 & & & & & & & & \\ b_1 & \cdots & & & & & & & \\ b_2 & b_1 & & 0 & & & & & \\ \vdots & b_2 & & b_0 & & & & & \\ b_d & \vdots & & b_1 & & & & & \\ 0 & b_d & & b_2 & & & & & \\ & 0 & & \vdots & & & & & \\ & & & b_d & & & & & \\ & & & 0 & & & & & \end{bmatrix}$$

Alternative ML Formulation (cont.)

- Thus

$$\mathbf{S}_\omega \mathbf{V}(\tau) \perp \mathbf{S}_\omega^{-*} \mathbf{B}$$

$$\mathbf{P}_{\mathbf{S}_\omega}^\perp \mathbf{V}(\tau) = \mathbf{P}_{\mathbf{S}_\omega^{-*} \mathbf{B}}$$

- ML criterion is then rewritten as

$$\hat{\mathbf{S}}_\omega, \hat{\mathbf{b}} = \operatorname{argmin} \left\| \mathbf{P}_{\mathbf{S}_\omega^{-*} \mathbf{B}} \mathbf{X} \right\|_F^2$$

where $\mathbf{b} = [\mathbf{b}_0 \ \cdots \ \mathbf{b}_d]$.

- This offers the possibility of an Iterative Quadratic ML solution
 - First used by Bresler & Macovski, 1986
 - Replaces search with a series of successive linear least squares problems

Exploiting Shift Invariances

- Suppose $m > d$, and define the following:

$$V_1, V_2 = \text{first, last } N - \delta \text{ rows of } V(\tau)$$

$$E = d \text{ principal left singular vectors of } X$$

$$\Phi = \begin{bmatrix} e^{-j2\pi\delta\tau_1/N} & & \\ & \ddots & \\ & & e^{-j2\pi\delta\tau_d/N} \end{bmatrix}$$

- Signal subspace ideas imply $E = S_\omega V(\tau)T$ for some $d \times d$ T
- With E_1, E_2, S_1, S_2 defined similarly, $DE_2 = E_1\Psi$ where $D = S_1S_2^{-1}$ and $\Psi = T^{-1}\Phi T$.
- Eigenvalues of Ψ are related to τ .
- Similar to standard ESPRIT algorithm, except $D \neq I$.

An ESPRIT-Like Approach

- Solve the least squares problem:

$$\hat{\mathbf{D}}, \hat{\Psi} = \operatorname{argmin} \|\mathbf{D}\mathbf{E}_2 - \mathbf{E}_1 \Psi\|_{\mathbf{F}}^2$$

- Separable in Ψ and $\mathbf{d} = \operatorname{diag}\{\mathbf{D}\}$:

$$\hat{\mathbf{d}} = \operatorname{argmin} \mathbf{d}^* [\mathbf{P}_{\mathbf{E}_1}^\perp \odot (\mathbf{E}_2 \mathbf{E}_2^*)^T] \mathbf{d}$$

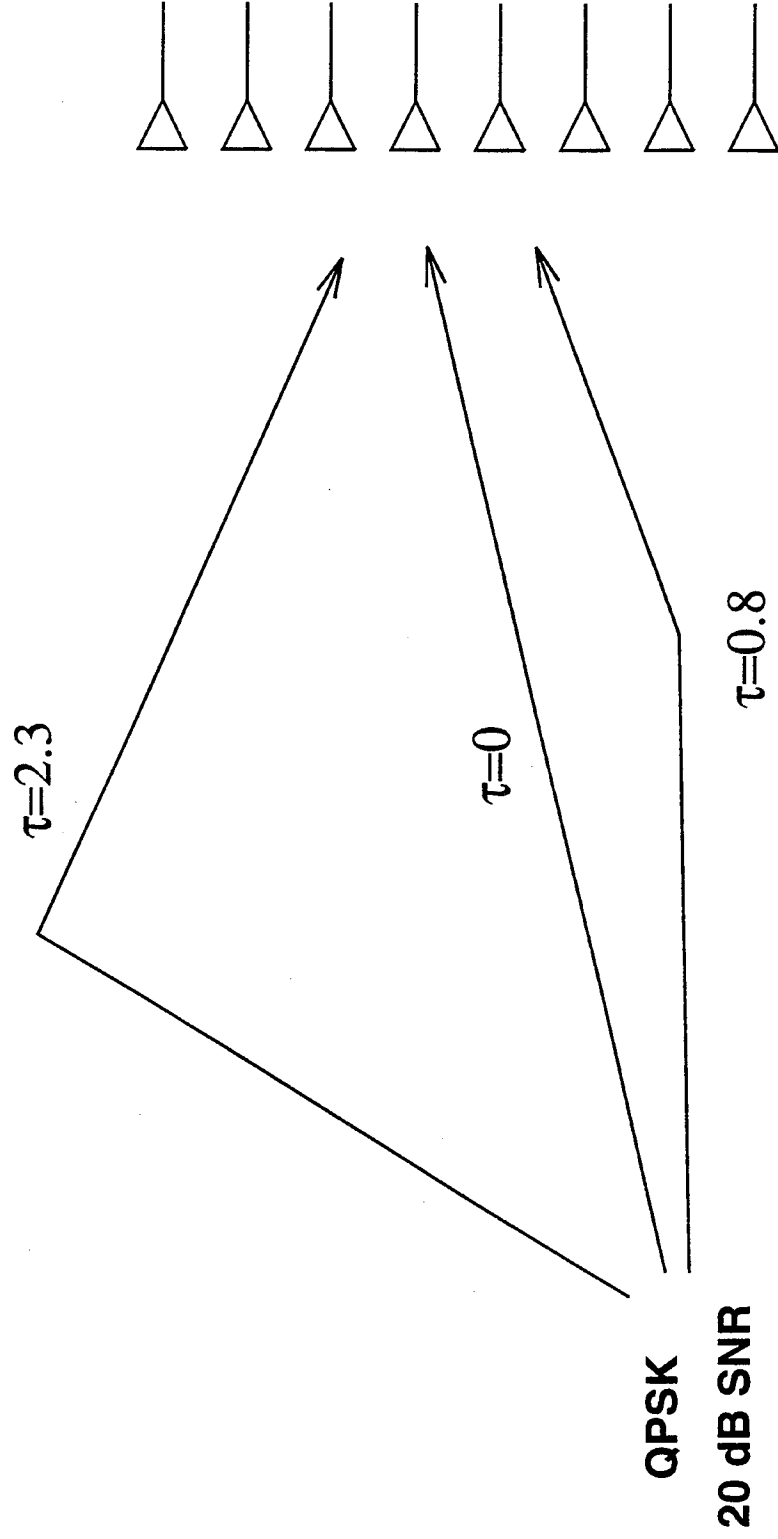
$$\hat{\Psi} = \mathbf{E}_1^\dagger \hat{\mathbf{D}} \mathbf{E}_2$$

- The algorithm:

1. Calculate \mathbf{E} and the matrix $\mathbf{Z} = \mathbf{P}_{\mathbf{E}_1}^\perp \odot (\mathbf{E}_2 \mathbf{E}_2^*)^T$
2. Find $\hat{\mathbf{d}}, \hat{\mathbf{D}}$ by computing singular vector of \mathbf{Z} with smallest σ .
3. Calculate the eigenvalues λ_i of $\hat{\Psi} = \mathbf{E}_1^\dagger \hat{\mathbf{D}} \mathbf{E}_2$
4. Set $\hat{\tau}_i = -N \angle \lambda_i / (2\pi\delta)$.

- Solving for S_ω from \mathbf{D} is impractical due to Vandermonde ambiguity. Use equation $\mathbf{E} = \mathbf{S}_\omega \mathbf{V}(\hat{\tau}) \hat{\mathbf{T}}$ instead.

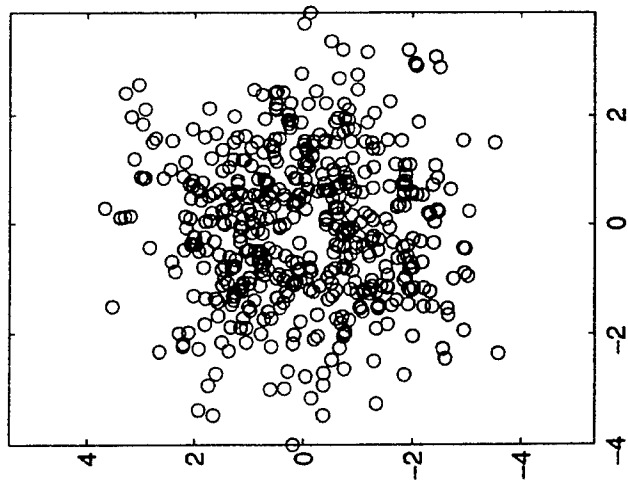
Simulation #1



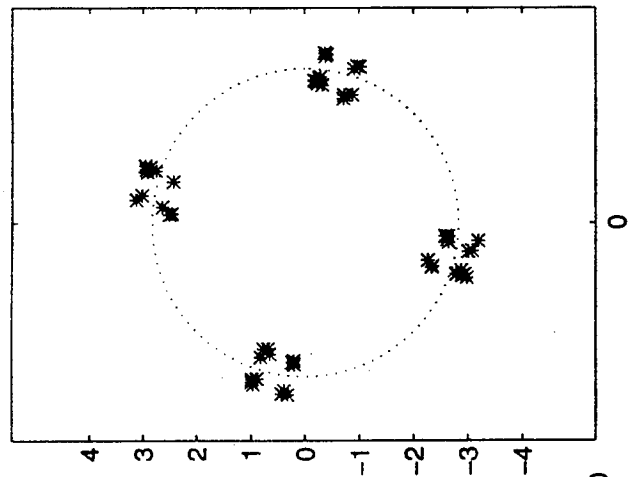
N=64 samples

random A

Received Symbols



ESPRIT Equalized Symbols



SNR = 20

$m = 8$

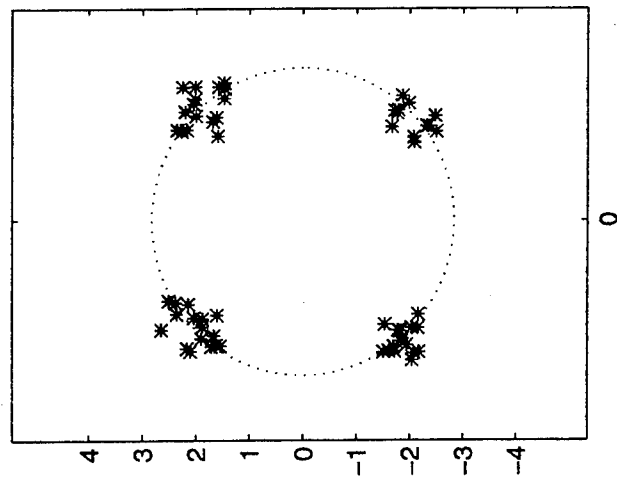
$N = 64$

$\tau_1 = 0$

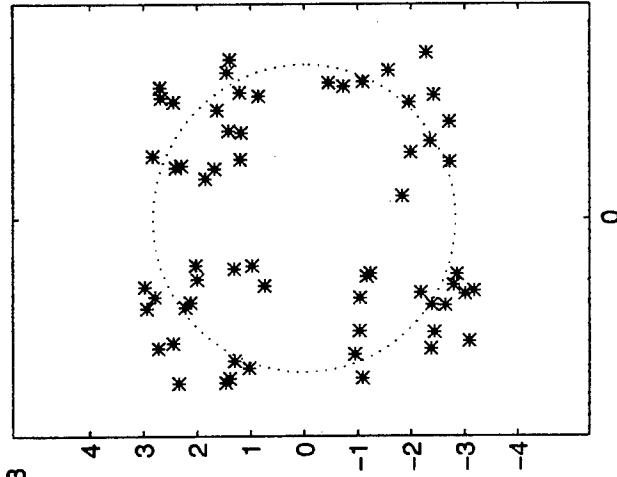
$\tau_2 = 0.8$

$\tau_3 = 2.3$

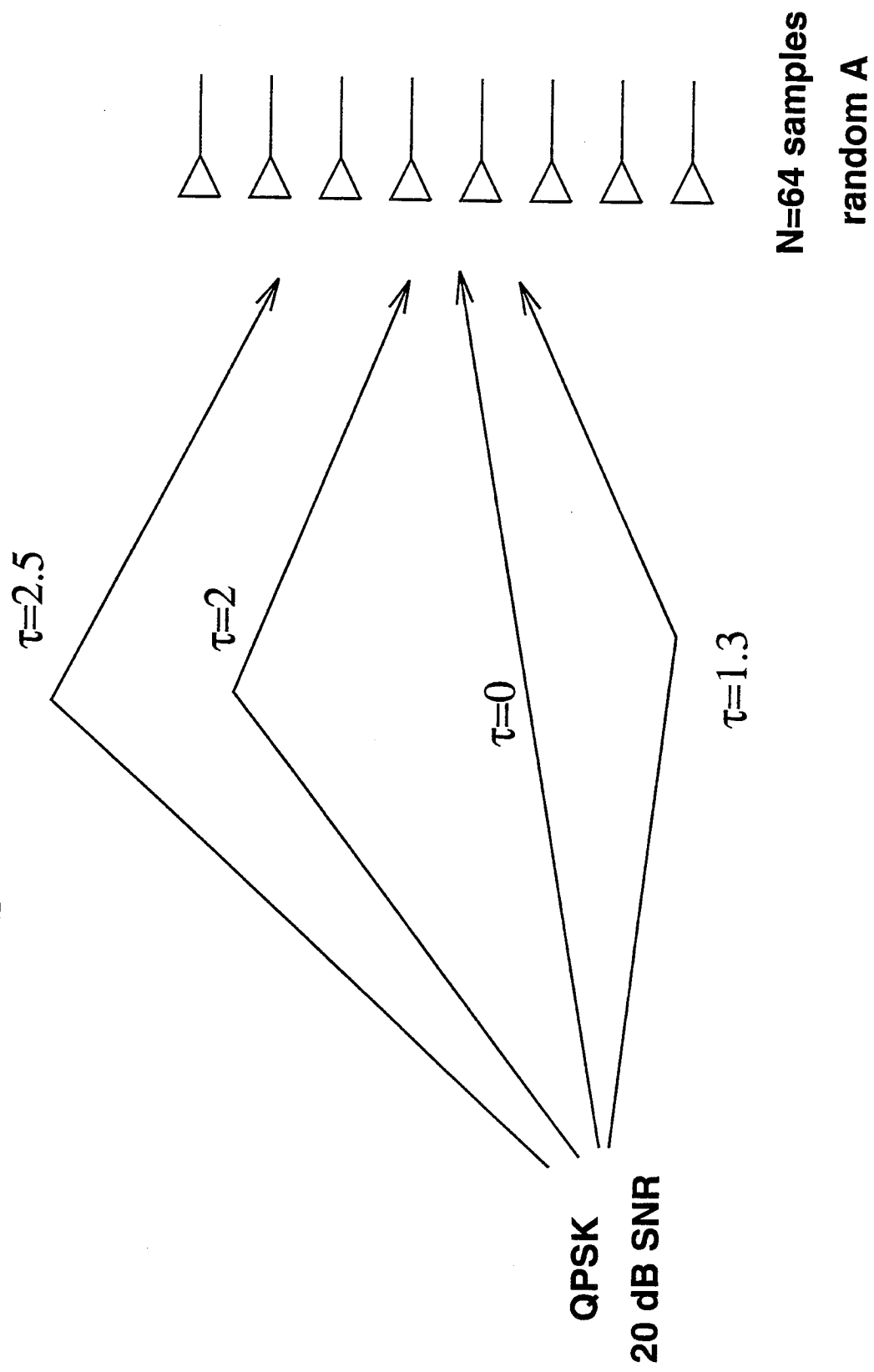
ML Equalized Symbols



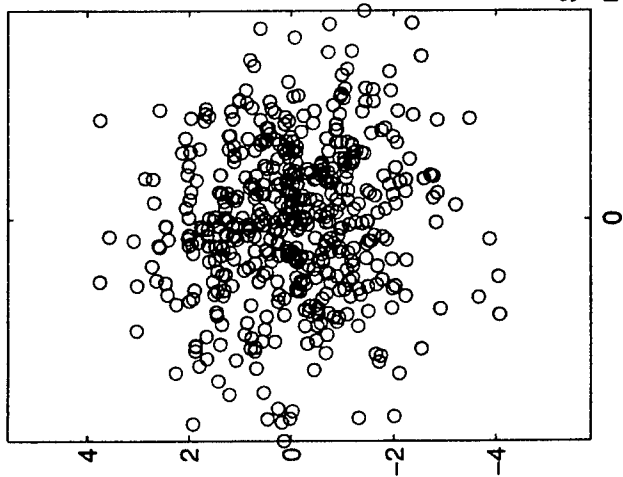
SRM Equalized Symbols



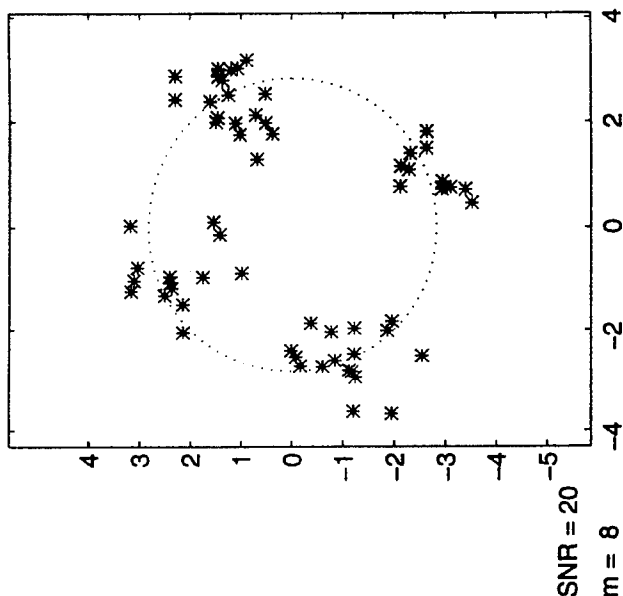
Simulation #2



Received Symbols



ESPRIT Equalized Symbols



SNR = 20

m = 8

N = 64

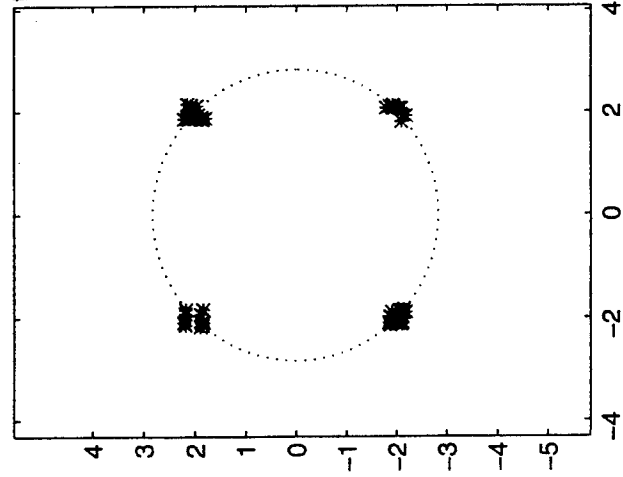
tau1 = 0

tau2 = 1.3

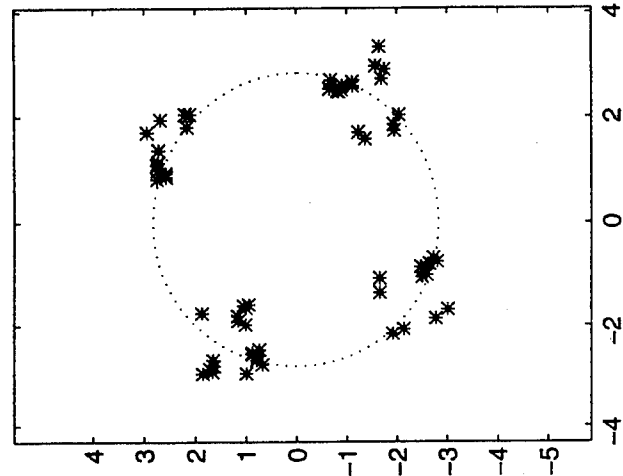
tau3 = 2

tau4 = 2.5

ML Equalized Symbols



SRM Equalized Symbols



Future Research

- **Incorporation of doppler into the model**

- Only relative doppler is identifiable
- SRM not suited for this case
- Model:

$$\mathbf{X} = (\mathbf{S}_\omega + \mathbf{D}_\omega \Omega) \mathbf{V}(\tau) \mathbf{A}, \quad \mathbf{D}_\omega = \partial \mathbf{S}_\omega / \partial \omega$$

$$\Omega = \begin{bmatrix} \Delta\omega_1 & & \\ & \ddots & \\ & & \Delta\omega_d \end{bmatrix}$$

- **Multiple independent sources**

- Individual signals not identifiable
- Must use information about signals to separate them
- SRM appears better suited to handle this case

- **Theoretical Performance Analyses**

REPORT DOCUMENTATION PAGE

Form Approved
OMB No. 0704-0188

Public reporting burden for this collection of information is estimated to average 1 hour per response, including the time for reviewing instructions, searching existing data sources, gathering and maintaining the data needed, and completing and reviewing the collection of information. Send comments regarding this burden estimate or any other aspect of this collection of information, including suggestions for reducing this burden, to Washington Headquarters Services, Directorate for Information Operations and Reports, 1215 Jefferson Davis Highway, Suite 1204, Arlington, VA 22202-4302, and to the Office of Management and Budget, Paperwork Reduction Project (0704-0188), Washington, DC 20503.

1. AGENCY USE ONLY (Leave blank)		2. REPORT DATE 29 April 1996	3. REPORT TYPE AND DATES COVERED Project Report ASAP-4, Volume 1	
4. TITLE AND SUBTITLE Proceedings of the Adaptive Sensor Array Processing (ASAP) Workshop			5. FUNDING NUMBERS C — F19628-95-C-0002 PE — 63326E, 63226E PR — 681	
6. AUTHOR(S) Patricia A. Netishen, Editor				
7. PERFORMING ORGANIZATION NAME(S) AND ADDRESS(ES) Lincoln Laboratory, MIT 244 Wood Street Lexington, MA 02173-9108			8. PERFORMING ORGANIZATION REPORT NUMBER ASAP-4, Volume 1	
9. SPONSORING/MONITORING AGENCY NAME(S) AND ADDRESS(ES) DARPA 3701 N. Fairfax Drive Arlington, VA 22203-1714			10. SPONSORING/MONITORING AGENCY REPORT NUMBER ESC-TR-96-062	
11. SUPPLEMENTARY NOTES None				
12a. DISTRIBUTION/AVAILABILITY STATEMENT Approved for public release; distribution is unlimited.			12b. DISTRIBUTION CODE	
13. ABSTRACT (Maximum 200 words) The 1996 Adaptive Sensor Array Processing (ASAP) workshop focuses on the uses of ASAP for advanced military radar systems, from a more developed perspective, with an emphasis on end-to-end systems issues and the user's perspective. New topics include the target detection and parameter estimation steps that typically follow clutter and jammer nulling. Several papers that describe algorithm mapping to parallel processors will also be presented.				
14. SUBJECT TERMS			15. NUMBER OF PAGES 666	
			16. PRICE CODE	
17. SECURITY CLASSIFICATION OF REPORT Unclassified	18. SECURITY CLASSIFICATION OF THIS PAGE Same as Report	19. SECURITY CLASSIFICATION OF ABSTRACT Same as Report	20. LIMITATION OF ABSTRACT Same as Report	